

DOCTOR OF PHILOSOPHY

Evaluating reactivity and sorptivity of fly ash for use in concrete construction

G Islam

2012

University of Dundee

Conditions for Use and Duplication

Copyright of this work belongs to the author unless otherwise identified in the body of the thesis. It is permitted to use and duplicate this work only for personal and non-commercial research, study or criticism/review. You must obtain prior written consent from the author for any other use. Any quotation from this thesis must be acknowledged using the normal academic conventions. It is not permitted to supply the whole or part of this thesis to any other person or to post the same on any website or other online location without the prior written consent of the author. Contact the Discovery team (discovery@dundee.ac.uk) with any queries about the use or acknowledgement of this work.

**EVALUATING REACTIVITY AND SORPTIVITY OF
FLY ASH FOR USE IN CONCRETE CONSTRUCTION**

By

G. M. Sadiqul Islam, M. Eng.

A thesis presented in application for the degree of Doctor of Philosophy
in the Concrete Technology Unit, University of Dundee,
Dundee, Scotland, UK
August, 2012

DECLARATION

I hereby declare that the following thesis has been composed by me, that the work of which it is a record has been carried out by myself, and that it has not been presented in any previous application for a higher degree.

G. M. Sadiqul Islam

CERTIFICATE

This is to certify that **G. M. Sadiqul Islam** has carried out this work under our supervision, and that he has fulfilled Ordinance 14 of the University of Dundee, so that he is qualified to submit the following thesis in application for the degree of Doctor of Philosophy.

Michael J. McCarthy

Senior lecturer

Concrete Technology Unit

University of Dundee

M. Roderick Jones

Professor

Concrete Technology Unit

University of Dundee

ACKNOWLEDGEMENTS

The author would like to express his heartiest gratitude and appreciation to Dr M J McCarthy under whose supervision the research was carried out. His devoted wise advice and sincere encouragement made the journey easier. Thanks extended to Professor R Jones for providing direction in crucial moments.

The financial support through the Dorothy Hodgkin Postgraduate Awards Scheme (EPSRC Grant Number EP/P503094/1) and the industrial partners, namely, United Kingdom Quality Ash Association, Cemex Ash UK and RWE Power International are gratefully acknowledged. Sincere thanks extended to the syndicate of Chittagong University of Engineering & Technology (CUET) for approving a study leave to carry out this work.

Thanks extended for the valuable supports provided by industrial committee members, namely, Dr L K A Sear, P Edwards and R Coombs for arranging range of materials and their active participation in critical discussion during committee meetings. Honest appreciation must be extended to Dr L J Csetenyi for all his technical support in experimental work and participation in critical discussions, which contributed towards the understanding and completion of this study. Sincere thanks goes to Dr T D Dyer for helping through few experimental process. Supports from Dr M D Newlands, Dr L Zheng and Dr J E Haliday are also acknowledged. Assistance from Bradley Pulverizer Company, International Innovative Technologies and Aggregate Industries, UK are thanked sincerely.

The friendly supports from CTU research colleagues, especially those from K Wilmoth, J Pang and K Kulkarni during experimental phase, are greatly appreciated. Thanks also extended to the technical staffs of this department for their willingness to numerous help during experimental program.

The author is greatly indebted to his parents and wife, who have always wished to see him flying high up at the skies of success. Their prayers, sacrifices and encouragements supplied energy to overcome hard moments, especially those provided by Dr Aysha Akter during lonely moments. Therefore, this thesis is dedicated to them.

ABSTRACT

This thesis describes research carried out to investigate techniques for (i) rapidly assessing the reactivity of fly ash; and (ii) evaluating its interaction with air-entraining admixtures (AEAs), both with regard to use in concrete. The materials considered for the project included, 54 fly ashes from 8 UK sources, and an additional three materials from Bangladesh, covering a range of fineness, loss-on-ignition (LOI) and production conditions (run-of-station, carbon removed, air-classified, co-combustion, oxy-fuel technology); Portland Cements (PCs) from five UK sources with various properties (strength classes 32.5 R, 42.5 N and 52.5 N); laboratory grade hydrated and quick limes; and three commercial AEAs and a standard laboratory grade reagent (surfactant).

The research examining fly ash reactivity considered activity index tests to BS EN 450 (BSI, 2005c) as the reference and investigated tests covering fly ash properties/providing measures of fly ash behaviour to rapidly assess this. These included (i) fly ash fineness (45 μm sieve residue, or LASER particle size distribution (PSD) parameters), LOI and flow properties; (ii) accelerated curing of PC and lime-based mortars (iii) lime consumption by fly ash when combined with PC in paste or suspension (Frattini) or from a saturated lime solution; (iv) various measures of fly ash chemical composition (based on oxide/mineralogical analysis); and (v) a quicklime slaking test. The test results were validated by strength tests with 100 mm concrete cube.

Results of the above indicated good correlations between fly ash fineness, mortar flow/water requirement and (pozzolanic) activity index (standard or accelerated curing). However, fly ash reactivity and fresh properties appeared to be influenced by the properties of the test PC (e.g. chemical composition and fineness) and there is a need to take this into account during assessment. Generally, finer fly ashes gave better flow; however, there is an optimum fineness ($d_{90} \sim 40 \mu\text{m}$) for best performance, and which is similar to the fineness of the test PC. Strong correlations between the accelerated and standard cured PC-based mortar indicate the latter can be used to estimate the former taking account of the fly ash properties. In view of eliminating the effect of PC properties on reactivity, mortar tests with laboratory grade hydrated lime suggested potential for this. However, for better assessment, this approach requires further work to address issues relating to slower rates of strength gain and increased time requirements, although high temperature conditions were used for curing. Measuring $\text{Ca}(\text{OH})_2$

consumption from fly ash/PC paste or suspension agreed with the behaviour in mortar, but needs special instruments (e.g. TGA or XRF). A similar approach with saturated lime did not work well, despite several measures being taken to try and improve this. The oxide and mineralogical analysis results of fly ash did not give good correlations with activity index, but improved when a factor combining them with fineness was considered. The test results were validated in concrete and with air-classified fly ashes from single sources which gave clear trend/behaviour. The lime slaking test was found to be ineffective for identifying fly ash reactivity. The reactivity assessment results were validated by carrying out concrete strength tests. In general, more consistent trends were obtained for fly ash from single source as noted with mortar earlier.

Methods adopted/developed to assess the interaction of fly ash with AEA included (i) the foam index test; (ii) acid blue 80 (AB80) dye adsorption test (spectroscopic method); and (iii) methylene blue test. High variability in foam index test results between different operators were noted, which reflected differences in the degree of shaking applied and difficulties in identification of the test end point. Adoption of an automatic shaker and determination of suitable test conditions reduced this by more than 50%. Reliable test procedures were also established for the AB80 dye adsorption method. The results obtained from these tests gave very good correlations with fly ash specific surface area and the AEA dose required (both with commercial AEAs and standard reagent) for achieving target air contents in mortar and concrete. The methylene blue dye test also gave good correlations with these parameters, but was less effective for low LOI fly ashes.

Between-laboratory tests were carried out at three UKQAA members and considered, LOI, fineness (45 μm sieve and LASER PSD), and activity index. The results gave good agreement with those obtained at the Concrete Technology Unit for this work and again emphasized the role of fly ash fineness on its reactivity.

Overall, fly ash fineness was found to be the best means of rapidly assessing its reactivity. Some of the other methods considered gave promising behaviour but require further refinements. Therefore, it is suggested that in addition to 45 μm sieve residue, other types of fineness measurement (e.g. sub 10 μm quantities, d_{50} and d_{90}) can be considered suitable alternatives to activity index. Similarly, foam index tests with the automatic shaker or the AB80 test method could both be used as fly ash physical requirement tests, or in production control for air-entrained concrete.

LIST OF PUBLICATIONS

McCarthy M J, Islam G M Sadiqul, Csetenyi L J and Jones M R (2012). Refining the foam index test for use with air-entrained fly ash concrete. *Magazine of Concrete Research*, In Press.

McCarthy M J, Islam G M Sadiqul, Csetenyi L J and Jones M R (2012). Colorimetric evaluation of admixture adsorption by fly ash for use in air-entrained concrete. *Materials and Structures*, In Press.

Concrete Technology Unit (2012) Rapid assessment methods to predict fly ash performance in concrete. *Final Project report*, Division of Civil Engineering, University of Dundee, UK, May 2012.

Islam G M Sadiqul, McCarthy M J, Csetenyi L J and Jones M R (2012). Investigating fly ash/air-entraining admixture behaviour and their use in concrete. *EUROCOALASH 2012 Conference*, Thessaloniki, Greece, 25-27 September, 2012, accepted.

GLOSSARY OF TERMS

AAS	Abietic Acid Sodium Salt
AB80	Acid Blue 80 reagent
AE	Acoustic Emissions
AEA	Air Entraining Admixture
AFIT	Automated Foam Index Test
ASTM	American Society for Testing and Materials
BET	Brunauer, Emmett and Teller Theory
BSI	British Standards Institution
Ca/Si ratio	Calcium to Silica ratio
C-S-H	Calcium-Silicate-Hydrate
d_{10}	Size to which 10% of the material is finer
d_{50}	Size to which 50% of the material is finer
d_{90}	Size to which 90% of the material is finer
DSC	Differential Scanning Calorimetry
DTA	Differential Thermal Analysis
EDX	Energy-dispersive X-ray spectroscopy
ESEM	Environmental Scanning Electron Microscope
FTIR	Fourier Transform Infrared spectroscopy
GGBS	Ground Granulated Blast-furnace Slag
ICP	Inductively Coupled Plasma optical emission spectroscopy
IR	Infrared Spectroscopy
LASER	Light Amplification by Stimulated Emission of Radiation
LOI	Loss-On-Ignition
MAS	Magic-angle spinning
MB	Methylene Blue

MBV	Methylene Blue Value
MIP	Mercury Intrusion Porosimetry
NMR	Nuclear Magnetic Resonance
NO _x	Mono-nitrogen oxides NO and NO ₂
PC	Portland Cement
PI	Pozzolanicity Index
PPI	Potential Pozzolanic Index
PSD	Particle Size Distribution
RHA	Rice Husk Ash
SDBS	Sodium Dodecyl Benzene Sulfonate
SDS	Sodium Dodecyl Sulfate
SEM	Scanning Electron Microscope
STA	Simultaneous Thermal Analyser
TEA	Triethanolamine
TGA	Thermogravimetric analysis
UV-Vis	Ultraviolet-Visible Spectroscopy
XPS	X-ray photoelectron spectroscopy
XRF	X-ray Fluorescence Spectrometry
XRD	X-ray Diffractometry

TABLE OF CONTENTS

Declaration.....	i
Certificate.....	ii
Acknowledgements.....	iii
Abstract.....	iv
List of Publications.....	vi
Glossary of Terms.....	vii
List of Figures.....	xiv
List of Tables.....	xxiv
CHAPTER 1: INTRODUCTION.....	1
1.1 Field of Study	1
1.2 Aim and Objectives of the Research	6
1.3 Scope of the Investigation.....	6
1.3.1 Pozzolanic reactivity of fly ash.....	7
1.3.2 Fly ash/AEA interaction study	8
1.4 Outline of Thesis	8
CHAPTER 2: STATE OF THE ART.....	11
2.1 Introduction	11
2.2 Pozzolanic Reactivity Assessment of Fly Ash	12
2.2.1 Empirical/analytical equations	13
2.2.2 Physical and chemical properties affecting reactivity	15
2.2.3 Accelerated test methods	27
2.2.4 Prediction of performance from early age properties	31
2.3 Air-Entraining Admixture Adsorption Assessment.....	37
2.3.1 Carbon content and characterisation.....	39
2.3.2 Test methods to assess fly ash/AEA interaction.....	45
2.4 Conclusions.....	56

2.4.1	Pozzolanic activity assessment.....	56
2.4.2	Carbon sorptivity/admixture adsorption assessment.....	58
CHAPTER 3: EXPERIMENTAL DETAILS		61
3.1	Programme of Work	61
3.1.1	Phase 0 – Literature review.....	61
3.1.2	Phase 1 – Materials characterisation and initial tests.....	61
3.1.3	Phase 2 – Evaluation of selected assessment methods using a range of materials.....	62
3.1.4	Phase 3 – Validation of assessment test methods with concrete.....	64
3.1.5	Phase 4 – Between-laboratory tests.....	64
3.1.6	Phase 5 – Practical implications.....	64
3.2	Characterisation of Materials	64
3.2.1	Fineness of fly ash samples.....	64
3.2.2	LOI and moisture content	67
3.2.3	Mineralogy by X-ray diffraction (XRD).....	68
3.2.4	Oxide composition by X-ray fluorescence spectroscopy (XRF).....	68
3.2.5	Morphology by scanning electron microscopy (SEM).....	69
3.2.6	Portland cement (PC) tests.....	69
3.2.7	Aggregates tests.....	70
3.3	Reactivity Assessment Tests.....	70
3.3.1	Activity index test (PC-based mortar).....	71
3.3.2	Porosity of PC-based mortars by MIP	71
3.3.3	Hydrated lime mortar.....	73
3.3.4	Measuring Ca(OH) ₂ content in paste by TGA.....	74
3.3.5	Frattoni test.....	76
3.3.6	Lime consumption and conductivity measurements.....	78
3.3.7	‘True’ glass content measurement	78
3.3.8	Heat of reaction with quicklime.....	79
3.4	Fly Ash/AEA Interaction Assessment Tests.....	79
3.4.1	Foam index test.....	79
3.4.2	Acid blue 80 test	81
3.4.3	Methylene blue test	82
3.4.4	Air entrainment in mortars	82
3.5	Concrete Tests.....	84
3.5.2	Fly ash/AEA interaction assessment.....	85
3.6	Regression Analysis	87

CHAPTER 4: CHARACTERISTICS OF MATERIALS	88
4.1 Characteristics Range of Fly Ashes	88
4.1.1 Fineness of fly ash samples.....	90
4.1.2 LOI.....	101
4.1.3 Specific surface area.....	105
4.1.4 Oxide and phase composition.....	107
4.1.5 Morphological properties.....	111
4.2 Characteristics of PCs	117
4.3 Properties of Aggregates	118
4.4 Characteristics of AEAs and Other Reagents	120
4.5 Summary of Findings	122
CHAPTER 5: REACTIVITY ASSESSMENT OF FLY ASH	125
5.1 Introduction	125
5.2 Activity Index Test Using PC-Based Mortar	126
5.2.1 Mortar fresh properties and strength development.....	138
5.2.2 Fly ash physical properties.....	152
5.2.3 Effect of finest fly ash level in mortar.....	172
5.2.4 Accelerated curing.....	173
5.3 Porosity of PC-Based Mortars by MIP	177
5.4 Hydrated Lime Mortar	178
5.5 Reactivity by Measuring Ca(OH)₂ Content in Paste using TGA	186
5.6 Frattini, Lime Consumption and Conductivity Test	188
5.6.1 BS EN 196 – 5 (Frattini test).....	188
5.6.2 Saturated lime test.....	195
5.7 Fly Ash Oxide Analysis	203
5.7.1 The pozzolanic potential index (PPI).....	203
5.7.2 Major oxide analysis.....	205
5.8 Glass/Amorphous/Others Content in Fly Ash	206
5.8.1 Source dependency of glass.....	206
5.8.2 ‘True’ glass content measurements.....	209
5.9 Heat of Reaction with Quicklime	210
5.10 Summary of Findings	212

CHAPTER 6: FLY ASH/AEA INTERACTION ASSESSMENTS.....	215
6.1 Foam Index Tests	215
6.1.1 Manual shaking	215
6.1.2 Automatic shaking	218
6.1.3 Fly ash property/AEA effect	223
6.2 Acid Blue 80 Tests.....	225
6.2.1 Equipment and calibration.....	226
6.2.2 Adjustment for AB80 adsorption by filter paper	227
6.2.3 Fly ash sample size.....	228
6.2.4 Contact time	230
6.2.5 AB80 adsorption for evaluating fly ash/AEA interaction.....	230
6.3 Methylene Blue Tests.....	234
6.3.1 MB value and foam index	237
6.4 Air – entrainment in Mortar.....	237
6.4.1 Foam index and mortar AEA dose	237
6.4.2 AB80 adsorption and mortar AEA dose	239
6.4.3 Methylene blue value and mortar AEA dose	242
6.5 Summary of Findings.....	244
6.5.1 Foam index tests	244
6.5.2 Acid blue 80 tests.....	245
6.5.3 Methylene blue tests	245
CHAPTER 7: VALIDATION OF REACTIVITY AND SORPTIVITY ASSESSMENT WITH CONCRETE	246
7.1 Reactivity Assessment in Concrete.....	246
7.1.1 Fresh properties	246
7.1.2 Strength development.....	249
7.1.3 Fly ash properties	252
7.1.4 Mortar activity index and concrete strength	252
7.1.5 Hydrated lime mortar test and concrete strength.....	254
7.1.6 TG analysis and concrete strength	255
7.2 Air – entrainment in Concrete	258
7.2.1 Foam index and concrete AEA dose.....	259
7.2.2 AB80 adsorption and concrete AEA dose.....	259
7.2.3 Methylene blue value and concrete AEA dose	261
7.2.4 Initial surface absorption test (ISAT) of concrete.....	262

7.2.5	Water penetration under pressure	264
7.3	Summary of Findings	265
CHAPTER 8: BETWEEN-LABORATORY TESTS		267
8.1	Introduction	267
8.2	Particle Size Distribution	267
8.3	Fineness by 45 μm Sieve	271
8.4	LOI and Moisture Content	271
8.5	Activity Index with PC Mortars	273
8.6	Activity Index and Fly Ash Fineness	276
8.7	Summary of Findings	279
CHAPTER 9: CONCLUSIONS, PRACTICAL IMPLICATIONS AND RECOMMENDATIONS FOR FURTHER STUDY		280
9.1	Conclusions	280
9.1.1	Characteristics of fly ash.....	280
9.1.2	Reactivity assessment	281
9.1.3	Fly ash/AEA interaction study	283
9.2	Practical Implications	285
9.2.1	Characteristics of fly ash.....	285
9.2.2	Reactivity assessment	285
9.2.3	Fly ash/AEA interaction study	288
9.3	Recommendations for Further Study	289
9.3.1	Materials properties	290
9.3.2	Reactivity assessment	290
9.3.3	Fly ash/AEA interaction study	290
REFERENCES		291
APPENDICES		307

LIST OF FIGURES

Figure 2-1. Examples of glass surrounded by carbon (Hower and Mastalerz, 2001).....	18
Figure 2-2. Effect of fly ash level on (a) degree of PC hydration and (b) pozzolanic reaction at various ages (based on Wang <i>et al.</i> , 2004).....	24
Figure 2-3. AEAs adsorption sites at air/water interface and carbon surface. (based on Hachmann <i>et al.</i> , 1998 and Pedersen <i>et al.</i> , 2008).....	38
Figure 2-4. Definition of foam index test end point reported in literature: (a) Dodson, 1990; (b) Grace, 2006; and (c) Sporel <i>et al.</i> , 2009.....	48
Figure 2-5. Schematic of UV-vis measurement and parameters in Beer-Lambert's law.....	51
Figure 3-1. Overview of the research programme.....	63
Figure 3-2. Wet sieve analysis using 45 µm mesh to BS EN 451-2 (BSI, 1995).....	65
Figure 3-3. Malvern MasterSizer2000 LASER particle size analyser.....	65
Figure 3-4. Fly ash surface area test using (a) N ₂ adsorption; and (b) Blaine apparatus.....	66
Figure 3-5. (a) Electric furnace for LOI test; and (b) OHAUS MB45 Moisture balance.....	67
Figure 3-6. (a) X-Ray Diffractometer (XRD) for mineralogical analysis; and (b) Bulk oxide composition determination using X-ray Fluorescence Spectroscopy.....	68
Figure 3-7. Scanning Electron Microscope for morphology and EDX.....	69
Figure 3-8. Mortar tests: (a) mortar mixing and flow test; (b) water bath for high temperature curing; and (c) prism compression test.....	72
Figure 3-9. PoreMaster33 used for mortar porosity measurement.....	73
Figure 3-10. Hydrated lime mortar tests; (a) high temperature and moisture curing; and (b). Instron machine used for testing compressive strength.....	74
Figure 3-11. TG-FTIR instrument for Ca(OH) ₂ determination in fly ash/PC paste.....	75
Figure 3-12. Vacuum filtration for Frattini and lime consumption tests to limit carbonation....	77
Figure 3-13. (a) automatic titrator for determination of OH ⁻ ion concentration; and (b) portable meter for filtrate conductivity measurements.....	77
Figure 3-14 Automatic shaker for foam index test.....	80
Figure 3-15. AB80 tests; (a) exposing fly ash to AB80 solution; and (b) concentration determination with colorimeter.....	81

Figure 3-16. (a) methylene blue test set up; and (b) appearance of blue halo around fly ash on filter paper indicating the end point of the test.	83
Figure 3-17. (a) Air meters used to test (a) mortar, and (b) concrete air content	85
Figure 3-18. Water penetration test under pressure in air-entrained concrete	87
Figure 4-1. Classification of main fly ashes (<i>Sample names are given in italics</i>).....	89
Figure 4-2. Codes of air-classified fly ash samples (<i>Sample names are given in italics</i>).....	90
Figure 4-3. 45 μm sieve fineness and LOI of (a) monthly fly ash samples from Source A; (b) monthly fly ash samples from Source C; and (c) fly ash samples from various sources. (<i>BD S sieve residue 66.5% and LOI 1.4%</i>)	96
Figure 4-4. Comparison of particle size distribution for selected samples from a) Source C; b) Source D; c) Source F (trial burned oxy-fuel samples); and (d) Bangladesh	98
Figure 4-5. PSD comparison of air-classified fly ashes from Sources C and L.....	99
Figure 4-6. Comparison of d_{90} of air-classified fly ashes with respect to PCs	100
Figure 4-7. Sub-10 μm quantity (by volume) of (a) monthly fly ash samples from Source A and Source C; and (b) fly ash samples from various sources.	101
Figure 4-8. Relationship between fineness measurement by 45 μm sieve (by mass) and PSD (by volume).....	102
Figure 4-9. Relationship between fineness measurements; 45 μm sieve residue (by mass) and d_{50} measured by LASER PSD (by volume)	102
Figure 4-10. LOI of fly ash fractions finer and coarser than 45 μm (shown as their contribution to the overall LOI).....	104
Figure 4-11. Comparison of (a) LOI and (b) d_{90} of air-classified fly ash samples from Sources C and L	105
Figure 4-12. Comparison of specific surface area of air-classified fly ashes from Sources C and L with respect to the parent samples.....	106
Figure 4-13. Relationship between LOI and surface area of fly ashes.....	107
Figure 4-14. Sum of major oxides (SiO_2 , Al_2O_3 and Fe_2O_3) and LOI of air-classified fly ash	110
Figure 4-15. Relationship between fineness and glass/amorphous content	111
Figure 4-16. SEM images of Fly Ash A N Jul	112
Figure 4-17. SEM images of Fly Ash C ROS.....	112
Figure 4-18. SEM images of Fly Ashes: (a) D STI, and (b) D NSTI.....	113
Figure 4-19. SEM images of Fly Ashes: (a) H, and (b) BD S.....	113

Figure 4-20.	SEM images of oxy-fuel fly ashes from trial burning	114
Figure 4-21.	SEM images of air-classified fly ashes from Source C	115
Figure 4-22.	SEM images of air-classified fly ashes from Source L.....	116
Figure 4-23.	Types of PCs used for this project and their codes.....	117
Figure 4-24.	Particle size distribution of PCs used in this study	119
Figure 4-25.	Grading comparison between CEN and laboratory sands	119
Figure 4-26.	Particle size distribution of limes and PC HR52 used in this study.....	121
Figure 5-1.	BS EN 450 activity index (PC, HR52) of (a) monthly fly ashes from Source A; (b) monthly fly ashes from Source C; and (c) fly ashes from various sources.....	133
Figure 5-2.	BS EN 450 activity index of fly ashes from various sources using PCs (a) HK42; (b) LD32; and (c) LD52.....	134
Figure 5-3.	BS EN 450 activity index of air-classified fly ashes using PC HR52	135
Figure 5-4.	Comparisons between BS EN 450 activity index using PCs HR52, HK42; LD32; and LD52. <i>(points in red not included in the regression analysis)</i>	137
Figure 5-5.	Comparison of BS EN 450 mortar flows for different PCs	139
Figure 5-6.	Relationships between fly ash properties and BS EN 450 mortar flow (PC, HR52): (a) 45 μm sieve residue; (b) multiple factor ($\text{LOI} \times 45 \mu\text{m}$ fineness); and (c) sub-10 μm quantity. <i>(points in red not included in the regression analysis)</i>	140
Figure 5-7.	Relationships between fly ash properties and BS EN 450 mortar flow (PC, HK42): (a) 45 μm sieve residue; (b) multiple factor ($\text{LOI} \times 45 \mu\text{m}$ fineness); and (c) sub-10 μm quantity. <i>(points in red not included in the regression analysis)</i>	141
Figure 5-8.	Relationships between fly ash properties and BS EN 450 mortar flow (PC, LD32): (a) 45 μm sieve residue; (b) multiple factor ($\text{LOI} \times 45 \mu\text{m}$ fineness); and (c) sub-10 μm quantity. <i>(points in red not included in the regression analysis)</i>	142
Figure 5-9.	Relationships between fly ash properties and BS EN 450 mortar flow (PC, LD52): (a) 45 μm sieve residue; (b) multiple factor ($\text{LOI} \times 45 \mu\text{m}$ fineness); and (c) sub-10 μm quantity. <i>(points in red not included in the regression analysis)</i>	143
Figure 5-10.	Relationships between air-classified fly ash properties and BS EN 450 mortar flow (PC, HR52): (a) d_{50} , (b) d_{90} ; and (c) sub 10 μm quantity.....	145
Figure 5-11.	Relationships between BS EN 450 flow and activity index for (a) PC HR52; (b) PC HK42; (c) PC LD32; and (d) PC LD52. <i>(points in red not included in the regression analysis)</i>	147

Figure 5-12.	Relationships between air-classified fly ash properties and BS EN 450 mortar flow (PC, HR52): (a) d_{50} , (b) d_{90} ; and (c) sub 10 μm quantity.....	149
Figure 5-13.	Relationship between BS 3892-1 (1982) water requirement and flow using PC HR52: (a) general fly ash; and (b) air-classified fly ash.....	150
Figure 5-14.	Relationship between BS 3892-1 water requirement and pozzolanic activity index: (a) main fly ash; and (b) air-classified fly ash. (<i>points in red not included in the regression analysis</i>).....	151
Figure 5-15.	Relationship between BS EN 450 flow and activity index (accelerated) (<i>points in red not included in the regression analysis</i>).....	151
Figure 5-16.	Strength development of mortar, effect of (a) fly ash; (b) PC type; and (c) processing by air-classification	153
Figure 5-17.	Relationships between fly ash property and BS EN 450 activity index (PC HR52): (a) 45 μm sieve residue; (b) multiple factor (45 μm sieve residue \times LOI); and (c) sub-10 μm quantity of fly ash. (<i>points in red not included in the regression analysis</i>)	155
Figure 5-18.	Relationships between fly ash property and BS EN 450 activity index (PC HK42): (a) 45 μm sieve residue; (b) multiple factor (45 μm sieve residue \times LOI); and (c) sub-10 μm quantity of fly ash. (<i>points in red not included in the regression analysis</i>)	156
Figure 5-19.	Relationships between fly ash property and BS EN 450 activity index (PC LD32): (a) 45 μm sieve residue; (b) multiple factor (45 μm sieve residue \times LOI); and (c) sub-10 μm quantity of fly ash. (<i>points in red not included in the regression analysis</i>)	157
Figure 5-20.	Relationships between fly ash property and BS EN 450 activity index (PC LD52): (a) 45 μm sieve residue; (b) multiple factor (45 μm sieve residue \times LOI); and (c) sub-10 μm quantity of fly ash. (<i>points in red not included in the regression analysis</i>)	158
Figure 5-21.	Relationships between air-classified fly ash sub 10 μm quantity and BS EN 450 activity index: (a) Source C; and (b) Source L	159
Figure 5-22.	Relationships between air-classified fly ash multiple factor ($d_{90} \times \text{LOI}$) and BS EN 450 activity index: (a) Source C; and (b) Source L	160
Figure 5-23.	Relationships between fly ash property and (pozzolanic) activity index (PC HR52): (a) 45 μm sieve residue; (b) multiple factor (45 μm sieve residue \times LOI); and (c) sub-10 μm quantity of fly ash. (<i>points in red not included in the regression analysis</i>).....	161

Figure 5-24.	Relationships between air-classified fly ash (a) sub-10 μm quantity and (b) multiple factor ($d_{90} \times \text{LOI}$) with BS 3892-1 pozzolanic activity index	162
Figure 5-25.	Relationships between PSD and BS EN 450 activity index (PC, HR52): (a) d_{10} ; (b) d_{50} ; and (c) d_{90} of fly ashes. (<i>points in red not included in the regression analysis</i>).....	164
Figure 5-26.	Relationships between PSD and BS EN 450 activity index (PC, HK42): (a) d_{10} ; (b) d_{50} ; and (c) d_{90} of fly ashes. (<i>points in red not included in the regression analysis</i>).....	165
Figure 5-27.	Relationships between PSD and BS EN 450 activity index (PC, LD32): (a) d_{10} ; (b) d_{50} ; and (c) d_{90} of fly ashes. (<i>points in red not included in the regression analysis</i>).....	166
Figure 5-28.	Relationships between PSD and BS EN 450 activity index (PC, LD52): (a) d_{10} ; (b) d_{50} ; and (c) d_{90} of fly ashes. (<i>points in red not included in the regression analysis</i>).....	167
Figure 5-29.	Relationships between PSD and BS EN 450 activity index. Air-classified fly ash from Source C: (a) d_{10} ; (b) d_{50} ; and (c) d_{90}	168
Figure 5-30.	Relationships between PSD and BS EN 450 activity index. Air-classified fly ash from Source L: (a) d_{10} ; (b) d_{50} ; and (c) d_{90}	169
Figure 5-31.	Relationships between PSD and accelerated activity index (PC, HR52): (a) d_{10} ; (b) d_{50} ; and (c) d_{90} of fly ashes. (<i>points in red not included in the regression analysis</i>).....	170
Figure 5-32.	Relationships between PSD and BS 3892-1 pozzolanic activity index. Air-classified fly ash from Source C: (a) d_{10} ; (b) d_{50} ; and (c) d_{90}	171
Figure 5-33.	Effect of fly ash level on fresh properties of air-classified material	172
Figure 5-34.	Effect of replacement level on strength (reactivity) of air-classified fly ash	173
Figure 5-35.	Relationships between BS EN 450 activity index (accelerated) and standard curing conditions (PC HR52)	174
Figure 5-36.	Relationships between BS 3892-1 pozzolanic activity index (accelerated) and BS EN 450 activity index at various ages.....	175
Figure 5-37.	Compressive strength development at equivalent ages, calculated using Sadgrove equation (top); and modified Sadgrove equation (bottom)	176
Figure 5-38.	Porosity of air-classified fly ash mortars: (a) Source C and (b) Source L	177
Figure 5-39.	Effect of curing temperature and age on compressive strength of hydrated lime mortar (fly ash C S Jan and 50 mm cube).....	180
Figure 5-40.	Water content adjustment for different fly ashes	181
Figure 5-41.	Strength development in lime mortar (at 50°C high humidity curing).....	182
Figure 5-42.	Effect of water content on compressive strength of hydrated lime mortar	182

Figure 5-43.	Relationships between fly ash properties and lime mortar strength: (a) 45 μm sieve residue; (b) multiple factor (45 μm sieve residue \times LOI); and (c) sub-10 μm quantity of fly ash. (<i>points in red not included in the regression analysis</i>)	184
Figure 5-44.	Relationships between lime mortar 56 day strength and fly ash fineness	185
Figure 5-45.	Relationships between lime mortar strength and pozzolanic activity index (<i>points in red not included in the regression analysis</i>)	185
Figure 5-46.	Ca(OH) ₂ content variation in fly ash/PC paste with time.....	186
Figure 5-47.	Relationships between fly ash properties and Ca(OH) ₂ content	187
Figure 5-48.	Relationships between fly ash fineness (PSD) and Ca(OH) ₂ content.....	189
Figure 5-49.	Relationships between Ca(OH) ₂ content in fly ash/PC paste and BS EN 450 activity index test.	190
Figure 5-50.	Assessment of fly ash using BS EN 196-5 after (a) 8 days, and (b) 15 days (in collaboration with Wilmoth, 2011)	191
Figure 5-51.	Relationships between conductivity, CaO and OH ⁻ concentration at: (a) 8 days; and (b) 15 days. (<i>points in red not included in regression analysis</i>)	192
Figure 5-52.	Relationships between fly ash properties and remaining CaO concentration at 8 days (<i>points in red not included in regression analysis</i>).....	193
Figure 5-53.	Relationships between fly ash properties and remaining CaO concentration at 15 days (<i>points in red not included in regression analysis</i>).....	193
Figure 5-54.	Fly ash fineness and conductivity of filtrate at: (a) 8 days, and (b) 15 days	194
Figure 5-55.	Relationships between CaO concentration and BS EN 450 activity index at: (a) 8 days, and (b) 15 days (<i>points in red not included in regression analysis</i>).....	194
Figure 5-56.	Variation in CaO level with various temperature and exposure periods: (a) 40 \pm 2 $^{\circ}\text{C}$; (b) 80 \pm 2 $^{\circ}\text{C}$; and (c) 80 \pm 2 $^{\circ}\text{C}$ (<i>shorter period with saturated lime</i>) (in collaboration with Wilmoth, 2011).	197
Figure 5-57.	Variation in conductivity at various exposure temperature and periods: (a) 40 \pm 2 $^{\circ}\text{C}$; (b) 80 \pm 2 $^{\circ}\text{C}$; and (c) 80 \pm 2 $^{\circ}\text{C}$ (<i>shorter period with saturated lime</i>) (in collaboration with Wilmoth, 2011).	198
Figure 5-58.	Conductivity of fly ashes exposed to de-ionized water at 40 and 80 $^{\circ}\text{C}$ for different periods	199
Figure 5-59.	Effect of alkali combination on conductivity of test solution.....	199
Figure 5-60.	Calibration of CaO concentration determination by conductivity.....	200

Figure 5-61.	Relationships between (a) CaO concentration; and (b) conductivity of filtrate and fly ash fineness (<i>points in red not included in the regression analysis</i>)	200
Figure 5-62.	Relationships between BS EN 450 activity index (90 days) and remaining CaO concentration of filtrate for different PCs: (a) HR52; (b) HK42; (c) LD32; and (d) LD52. (<i>points in red not included in the regression analysis; in collaboration with Wilmoth, 2011</i>)	201
Figure 5-63.	Remaining CaO level after exposure to fly ash for 2 and 5 days.....	202
Figure 5-64.	Effect of sucrose content on lime solubility and conductivity of solutions	203
Figure 5-65.	Relationships between PPI and BS EN 450 activity index.....	204
Figure 5-66.	Relationships between modified pozzolanic potential index (MPPI) and BS EN 450 activity index. ($MPPI = PPI/45 \mu\text{m sieve residue}$)	204
Figure 5-67.	Relationships between major oxides and BS EN 450 activity index	205
Figure 5-68.	Sum of major oxides (SiO_2 , Al_2O_3 and Fe_2O_3)/(45 μm sieve residue) and BS EN 450 activity index. (<i>points in red not included in the regression analysis</i>)	206
Figure 5-69.	Relationships between major oxides / d_{50} and BS EN 450 activity index	206
Figure 5-70.	Relationships between fly ash component other than crystalline and BS EN 450 activity index (<i>general fly ashes used in the project</i>)	207
Figure 5-71.	Relationships between fly ash component other than crystalline and BS EN 450 activity index: (a) Source C and (b) Source L (<i>air-classified fly ashes</i>)	208
Figure 5-72.	Calculation of 'true' glass in fly ash H by extrapolating to zero added glass	209
Figure 5-73.	Relationships between fly ash 'true' glass content and BS EN 450 activity index ..	210
Figure 5-74.	Relationship between heat release of slaking lime/fly ash and BS EN 450 activity index.....	211
Figure 5-75.	Temperature variations with time for selected fly ash/lime	211
Figure 6-1.	Relationships between foam index, specific surface area and LOI (manual shaking): (a).AEA S; (b) AEA C1; (c) AEA C2; and (d) AEA C3	218
Figure 6-2.	Influence of automatic shaker speed and duration on foam index (Fly Ash D STI and AEA S).....	219
Figure 6-3.	Various stages of the foam index test with manual shaking and automatic shaker (at 1300 rpm).....	220
Figure 6-4.	Influence of number of shaking revolutions (time) on foam index at 1300 rpm for different fly ashes and AEAs.....	221

Figure 6-5.	Comparison of foam index coefficients of variation for manual shaking and automatic shaker between operators.....	222
Figure 6-6.	Relationships between foam index (using automatic shaker), specific surface area and LOI of fly ashes: (a) AEA C1; (b) AEA C2; and (c) AEA S (<i>points in red not included in the regression analysis</i>).....	224
Figure 6-7.	Relationships between foam index of fly ashes (using automatic shaker) with standard reagent and commercial AEAs	225
Figure 6-8.	Wavescan of standard AB80 solution (after Zhang and Nielson Jr., 2007)	226
Figure 6-9.	Calibration curve of AB80 solution	227
Figure 6-10.	Estimation of AB80 adsorption by filter paper	228
Figure 6-11.	Effect of fly ash sample size on AB80 adsorption.....	229
Figure 6-12.	AB80 stock solution and filtrates after exposing to various fly ashes	229
Figure 6-13.	Effect of contact time on AB80 adsorption by fly ash	230
Figure 6-14.	Relationship between fly ash LOI and AB80 adsorption. (a) general fly ashes used in the project; and (b) air-classified fly ashes. <i>Points with empty rectangles are not included in the regression analysis.</i>	231
Figure 6-15.	Relationship between fly ash specific surface area and AB80 adsorption	232
Figure 6-16.	Relationships between AB80 adsorption and foam index (a) AEA S; (b) AEA C1; and (c) AEA C2.....	233
Figure 6-17.	Relationships between MB value (10.0 g/l), specific surface area and LOI of all fly ashes. (<i>points in red not included in the regression analysis</i>)	235
Figure 6-18.	Relationships between MB value (5.0 g/l), specific surface area and LOI of selected fly ashes. (<i>points in red not included in the regression analysis</i>).....	236
Figure 6-19.	Comparison between MB values using different (a) dye concentrations; and (b) operators.....	236
Figure 6-20.	Relationships between MB value and foam index (a) AEA S; (b) AEA C1; and (c) AEA C2	238
Figure 6-21.	AEA C2 dose and mortar air content relationships for selective fly ashes	239
Figure 6-22.	Relationships between mortar AEA dose, foam index and specific surface area of selective fly ashes: (a) AEA C1; (b) AEA C2; and (c) AEA S	240
Figure 6-23.	Relationships between AB80 adsorption and mortar AEA dose (a) AEA S; (b) AEA C1; and (c) AEA C2	241

Figure 6-24.	Relationships between MB value and mortar AEA dose (a) AEA S; (b) AEA C1; and (c) AEA C2.....	243
Figure 7-1.	Relationships between mortar fresh properties and concrete slump: (a) BS EN 450 flow; and (b) BS 3892-1 water requirements. (<i>main fly ash; PC HR52</i>).....	248
Figure 7-2.	Relationships between mortar fresh properties and concrete slump: (a) BS EN 450 flow; and (b) BS 3892-1 water requirements. (<i>air-classified fly ash; PC HK52</i>).....	249
Figure 7-3.	Compressive strength of fly ash concrete at different curing age (PC HR52).....	251
Figure 7-4.	Compressive strength of fly ash concrete at different curing age (PC HK52).....	251
Figure 7-5.	Relationships between fly ash properties and concrete cube strengths (PC HR52): (a) 45 μm sieve residue; (b) multiple factor; and (c) sub 10 μm quantities. (<i>points in red not included in the regression analysis; PC HR52</i>).....	253
Figure 7-6.	Relationships between fly ash fineness (d_{90}) and concrete cube strengths: (a) Source C; (b) Source L (<i>PC HK52</i>).....	254
Figure 7-7.	Relationships between air-classified fly ash fineness (sub 10 μm quantities) and concrete cube strengths: (a) Source C; (b) Source L (<i>PC HK52</i>).....	255
Figure 7-8.	Relationships between concrete cube strength and BS EN 450 activity index (at 28, 56 and 90 days) with the main fly ashes: (a) 28 days; (b) 90 days; and (c) 180 days. (<i>PC HR52</i>).....	256
Figure 7-9.	Relationships between mortar (pozzolanic) activity index and concrete cube strength (at 14, 28 and 56 days; PC HK52): (a) BS EN 450 activity index (at 14, 28 and 56 days; PC HR52) and (b) pozzolanic activity index (accelerated 7 days; PC HK52).....	257
Figure 7-10.	Relationships between concrete compressive Strength and hydrated lime mortar strength (<i>points in red not included in the regression analysis</i>).....	257
Figure 7-11.	Relationships between $\text{Ca}(\text{OH})_2$ content in fly ash/PC paste (PC HR52) and concrete cube strength (PC HK52) at 14 and 28 days.....	258
Figure 7-12.	Relationships between concrete AEA dose, foam index of selective fly ashes (using automatic shaker) and mortar AEA dose (a) AEA C1; and (b) AEA S.....	260
Figure 7-13.	Relationships between AB80 adsorption and concrete AEA dose with AEA S and C1.....	261
Figure 7-14.	Relationships between MB value and concrete AEA dose using AEA S and AEA C1.....	261
Figure 7-15.	Comparison of ISATs for concretes with (a) AEA C1; and (b) AEA S (in collaboration with Pang, 2012).....	262

Figure 7-16. Relationships between air-entrained concrete compressive strength and their ISAT using: (a) AEA C1 and (b) AEA S	263
Figure 7-17. Comparison of ISATs for concretes with (a) AEA C1; and (b) AEA S (28 days water cured; in collaboration with Pang, 2012).....	264
Figure 7-18. Relationships between air-entrained concrete compressive strength and their ISAT using: (a) AEA C1 and (b) AEA S	265
Figure 8-1. PSD curves (frequency) using Malvern: (a) CTU; and (b) Lab C	268
Figure 8-2. PSD curves (cumulative finer) using Malvern: CTU; and (b) Lab C.....	269
Figure 8-3. Comparison between PSD results obtained using Malvern: from the CTU and Lab C: (a) d_{90} and (b) d_{50}	270
Figure 8-4. Comparison between d_{10} (PSD) using Malvern from the CTU and Lab C.....	270
Figure 8-5. Comparison between 45 μm sieve residue (PSD) results using Malvern from the CTU, Lab C and Lab I.....	271
Figure 8-6. Comparison of 45 μm sieve residue obtained from between-laboratory tests (Note: Lab C and CTU: wet sieve analysis; and Lab I: air jet sieve analysis).....	272
Figure 8-7. Comparison of LOI data obtained from between-laboratory tests (Note: Lab I used oven drying before LOI test)	273
Figure 8-8. Comparison of EN 450 mortar compressive strength (28 days) between the CTU (four PCs) and Lab C	274
Figure 8-9. Comparison of EN 450 mortar compressive strength (28 days) between Labs.....	275
Figure 8-10. Comparison of EN 450 mortar compressive strength (90 days) obtained from between-laboratory tests by CTU (three PCs) and Lab C.....	275
Figure 8-11. Comparison of EN 450 mortar compressive strength (90 days) between Labs.....	276
Figure 8-12. Comparison of relationships between fly ash fineness and 28 day BS EN 450 activity index between CTU and Lab C	277
Figure 8-13. Comparison of relationships between fly ash fineness and 90 day BS EN 450 activity index between CTU and Lab C	278

LIST OF TABLES

Table 1-1. Historical development of the requirements of the major characteristics of fly ash in various specifications (based on Thomson, 2008).....	4
Table 2-1. Comparison of foam index test methods from literature	47
Table 2-2. Fly ash/AEA interaction tests by UV-Vis spectroscopic method.....	51
Table 3-1. Frattini test conditions	76
Table 3-2. Mix proportions of concretes used for reactivity assessment	84
Table 3-3. Mix proportions of air-entrained concretes (air content: $5.0 \pm 1.0\%$)	85
Table 4-1. Physical properties of monthly fly ashes received from Source A.....	91
Table 4-2. Physical properties of monthly fly ashes received from Source C	92
Table 4-3. Physical properties of other fly ashes received from various sources	93
Table 4-4. Physical properties of other fly ashes received from various sources	94
Table 4-5. Physical properties of air-classified fly ashes from Sources C and L.....	95
Table 4-6. Range of chemical composition of fly ashes used in this project.....	109
Table 4-7. Physical properties of PCs.....	117
Table 4-8. Oxide composition of PCs.....	118
Table 4-9. Phase composition of PCs	118
Table 4-10. Properties of commercial AEAs (C1, C2, C3) and standard reagent (AEA S).....	120
Table 4-11. Characteristics of hydrated and quick lime used in the project.....	121
Table 4-12. Characteristics of dye reagents (supplier's information unless noted otherwise) ...	122
Table 5-1. Number of mortar mixes prepared for activity index tests during the study	126
Table 5-2. (Pozzolanic) Activity index and fresh properties of monthly fly ashes received from Source A	128
Table 5-3. (Pozzolanic) Activity index and fresh properties of monthly fly ashes received from Source C.....	129
Table 5-4. (Pozzolanic) Activity index and fresh properties of fly ashes received from various sources	130
Table 5-5. (Pozzolanic) Activity index and fresh properties of air-classified fly ashes from Source C and L.....	132

Table 5-6.	Range of activity index obtained using various PCs.....	138
Table 5-7.	Mix proportions of hydrated lime mortar	180
Table 5-8.	Compressive strength (MPa) of hydrated lime mortar cubes	181
Table 5-9.	Initial test conditions for saturated lime and KOH solution.....	195
Table 5-10.	Test set up for saturated lime (in collaboration with Wilmoth, 2011).....	200
Table 5-11.	Test conditions for lime-sucrose-KOH solution.....	202
Table 6-1.	Operator variability of foam index* test results by manual shaking	217
Table 6-2.	Operator variability of foam index* tests with the automatic shaker	222
Table 7-1.	Fresh properties of concretes (main fly ash; PC HR52).....	247
Table 7-2.	Fresh properties of concretes (air-classified fly ash; PC HK52)	247
Table 7-3.	Cube strength of concrete at different ages (main fly ash; PC HR52)	250
Table 7-4.	Cube strength of concrete at different ages (air-classified fly ash; PC HK52)	250
Table 7-5.	AEA doses, fresh properties and strength of air-entrained concretes	259
Table 8-1.	Between-laboratory tests for fly ash particle size analysis by Malvern	269
Table 8-2.	Between-laboratory results of fly ash fineness (45 μ m sieve residue) and LOI.....	272
Table 8-3.	Between-laboratory tests of fly ash mortar activity index at 28 days	274

CHAPTER 1: INTRODUCTION

1.1 Field of Study

Although developed countries are emphasizing the need for adopting renewable energy (e.g. electricity production from solar, wind and geothermal energy) current statistics show that, in 2011 in the USA 42% (1734 of a total of 4105 million MW hours) of produced electricity was based on coal (USDOE, 2012). Similarly in the European Union (EU) data, in 2009 indicate that total electricity production from combustible fuel accounted for 55% (1686 million MW hours) for the 27 countries (EC, 2012). Statistics by the British Government (Department of Energy and Climate Change (DECC)) show that 28% of total electricity production was from coal combustion power stations and used a total of 40.1 Million tonnes in 2009 (DECC, 2009). Due to abundance and cost effectiveness, coal is almost the main source for electricity production in many countries e.g. Poland (96%), South Africa (90%) and Australia (86%) (Thompson, 2008) and this is likely to be the case for the foreseeable future.

Coal is generally formed from the decomposition of plant and vegetation in the earth's sub-surface under appropriate moisture, pressure and temperature conditions and in the absence of air (Vorres, 1979). According to the International Classification System (mainly used in Europe) coals are classified as Hard and Brown, based on their heating value, i.e. higher and lower than 23.9 MJ/kg, respectively (Thompson, 2008). The heating value principally depends on the elemental composition. Proximate analysis gives proportions of fixed carbon, volatile matter, ash (mainly minerals) and moisture along with heating value, while ultimate analysis is used to estimate specific elements (viz. carbon, hydrogen, sulfur, oxygen, nitrogen and ash) by the coal industry (Speight, 2005). The mineral matter which is mainly the inorganic part of coal, originates from the minerals extracted by the original plant for their growth, incorporation of discrete foreign inorganic materials (typically sand, silt or clay) during decomposition and percolation of mineral-laden water through coal seam (Thompson, 2008). The majority of this non-combustible part is composed of

aluminosilicate clay minerals and quartz (60 – 90%). Other minerals include feldspars, garnets, kaolinite, calcite, pyrite and gypsum (Helmuth, 1987; Thompson, 2008).

During combustion of pulverized coal (most common for power generation), coal mineral matter turns into fine powder ('fly ash' ~90%) and is removed in the flue gases. The other by-products of the combustion process are furnace bottom ash, gypsum and boiler slag. The furnace bottom ash is generally coarser and denser in nature and mainly settles down to the base of the furnace by fusing and agglomerating after formation. As per BS EN 450 (BSI, 2005c) fly ash is defined as follows,

"Fine powder of mainly spherical, glassy particles, derived from burning of pulverised coal, with or without co-combustion materials, which has pozzolanic properties and consists essentially of SiO₂ and Al₂O₃, the content of reactive SiO₂ as defined and described in EN 197-1 being at least 25 % by mass."

According to the American Coal Ash Association (ACAA) total production of fly ash in the USA was 67.7 million tonnes in 2010 (ACAA, 2011), while this was 34.3 million tonnes in Europe (EU-15 countries) (ECOBA, 2010) and 5.3 million tonnes in the UK (Sear, 2011). This massive production has forced scientists and producers to explore various means of using the material.

On the other hand, sustainability issue in the construction sector have received increasing attention over the last two decades due to concerns regarding the use of virgin materials and the emission of greenhouse gases from the production of raw materials (e.g. cement). Next to water, concrete is the most widely consumed material across the world. For example in 2002 data indicate that on average 3 tonnes of concrete per capita per year were required (WBCSD, 2002). Cement is the prime component of concrete and requires substantial energy in production. Indeed, the cement industry contributes approximately 5% of global man made CO₂, with 9 kg of CO₂ produced from every 10 kg of cement. Furthermore, 50% of this CO₂ produced is from chemical processes involved in making clinker, 40% from burning fossil fuel and the rest (10%) from electricity and transportation (WBCSD, 2002). Therefore, the need to manufacture construction materials (especially concrete) using less energy and primary materials is becoming ever more pressing.

Several sectors have identified the potential of fly ash from electricity generation. In 2010, 38% (25.7 million tonnes) of fly ash produced in the USA was used in various applications, of which 43% corresponded to concrete/concrete products/grout, 8% blended cement/raw feed for clinker, 18% structural fill/embankments, 9% mining applications and 13% waste stabilization/solidification (ACAA, 2011). In Europe (EU 15) the utilization of fly ash in 2009 was 44% (15.4 million tonnes). The majority of which was as raw cement materials/blended cement/concrete additions (69%) and in general engineering fill/structural fill (20%) (ECOBA, 2010). In the UK, the UK Quality Ash Association (UKQAA; Sear, 2011) statistics indicate that in 2010 fly ash use included 33% in various cementitious applications (Cement raw material/blended cement/concrete addition/non-aerated concrete blocks and precast/grouting/Aerated blocks), 31% for fill, ground remediation/land reclamation projects and other uses and 36% was land-filled. The suitability of fly ash for these applications depends on its properties and to date the cement sector remains the major application area since it was initially investigated by Davis *et al.* (1937) at the University of California, USA.

In recent decades, fly ash had been widely used in concrete and has established technical (e.g. improved fresh properties, reduced heat development, and enhanced long-term strength and aspects of durability), environmental and economic benefits (Mehta, 1986; Sear, 2001; Concrete Society, 2011). Since fly ash was identified as a potential material required for use in cementitious systems, requirements covering its properties have been specified by various authorities. Table 1-1 gives a summary of the historical development of fly ash specifications provided by various organizations/(inter)national bodies during the last eight decades, since the work by Davis and co-workers.

In addition to various properties, including fineness (in terms of 45 μm sieve residue) and loss-on-ignition (LOI), used to assess fly ash, most standards covering the material as an addition in concrete include a measure of its reactivity based on mortar strength measurements. In the former UK standard, BS 3892-1 (BSI, 1997) this used a 'strength factor' (variable water/equal flow; fly ash level 30%). This was changed to an 'activity index' (equal water ($w/c=0.5$)/variable flow; fly ash level 25%) in the current European standard BS EN 450 (BSI, 2005c). The ASTM standard C618 (ASTM, 2012) considers a 'strength activity index' (variable water/equal flow; fly ash level 20%).

Table 1-1. Historical development of the requirements of the major characteristics of fly ash in various specifications (based on Thomson, 2008)

Specification	LOI, (max, %)	Fineness		Water req. (max, %)	Pozzolanic activity index (min, %)	
		Specific surface, (min, m ² /kg)	45 µm sieve residue, (max, %)			
Davis <i>et al.</i> (1937)	7.0	250	12.0	103	Min. 5 N/mm ² with lime	
US Bureau of Reclamation (1951)	5.0	300	12.0	103	-	
Nebraska State (1952)	10.0	-	-	-	-	
ASTM C350 (1954)	12.0	280	-	-	100	
BS 3892 (1965)	Zone A	125-275	-	-	-	
	Zone B	7.0	275-425	-	-	
	Zone C	-	> 425	-	-	
ASTM C618 (1968)	12.0	650	-	105	85	
Tennessee Valley Authority G-30 (1968)	Class I	6.0	650	< 12.0	-	85
	Class II	6.0	500	12.0-22.0	-	75
	Class III	6.0	-	22.0-32.0	-	75
ASTM C618 (1969)	12.0	-	12.0	105	75	
ASTM C618 (1971)	12.0	-	34.0	105	75	
BS 3892 (1982)	7.0	-	12.5	< 95	85 (7 d ^a)	
EN 450 (1995)	5.0	-	40.0	-	75 (28 d) 85 (90d)	
BS 3892 (1997)	7.0	-	12.0	< 95	80 (28 d)	
EN 450 (2005)	Cat. A	0.0-5.0	-	< 12 (Cat S)	< 95	75 (28 d)
	Cat. B	2.0-7.0	-	< 40 (Cat N)	-	85 (90 d)
	Cat. C	4.0-9.0	-	-	-	-
ASTM C618 (2012)	Class N	10.0	-	34.0	115	75 (7 d)
	Class F	6.0 ^b	-	34.0	105	75 (28 d)
	Class C	6.0	-	34.0	105	-

^a 5 days in 20°C, following this 46 hours in 50°C and finally 2 hours in 20°C

^b can be approved by the user if it satisfies other requirements

All of these tests involve the measurement of fly ash mortar strengths over particular time periods (e.g. 7, 28 and 90 days) and comparison with those comprising Portland Cement (PC, reference). The approach takes account of the properties of fly ash and provides an indirect means of assessing its reactivity. However, from a practical point of view the time-scale to obtain meaningful results is too long after the material in question is produced. Other techniques which consider lime consumption (e.g. BS EN 196-5 (2011a)) by fly ash have received coverage in the literature, but appear to have had limited use.

Another issue that has often influenced fly ash use in concrete construction has been its interaction with air-entraining admixtures (AEAs). Indeed, with the carbon present in fly ash, high admixture dosage levels are often required, although this situation has improved with the development of specially formulated admixtures. Although no standard method exists on an inter(national) basis, techniques (in line with the LOI test) such as the foam index test (Dodson, 1990) have been used to provide an indication of how fly ash will interact with AEAs. However, the reliability of this test (given it depends on operator input and observations) is open to question.

Against this background, recent changes in fly ash combustion technology have seen the introduction of co-combustion, where secondary fuels along with hard coal are used in the furnace (BSI, 2005c; Scott and Thomas, 2007; Al-Mansour and Zuwal, 2010). In addition, low emission burning techniques have also been introduced to reduce the environmental impact of coal-fired electricity generation (Hower *et al.*, 1999b; Pedersen *et al.*, 2010). Other modern coal combustion processes in the power generation sector include, oxy-fuel (Normann *et al.*, 2008) and supercritical steam cycles (DTI, 1999) to improve both efficiency of fuel and to reduce emissions. Furthermore, various technologies are currently available to process fly ash such as air classification (to control fineness) and STI for carbon removal. All of these can influence or modify the properties of fly ash produced and their reactivity and interaction with PC and AEA, respectively.

Given the time required to undertake these tests, their reliability and the implications of new generation fly ashes, there is need to examine the methods for assessing the properties of the material with regard to its continued use as a cement component and likely impact

on concrete. The study described in this thesis was, therefore, set-up to investigate this range of issue.

1.2 Aim and Objectives of the Research

The overall aim of the research was to develop assessment methods to (i) rapidly test the reactivity of fly ash; and (ii) evaluate their interaction and sorptivity characteristics with AEA in relation to their use in concrete construction.

In order to meet this, the following specific objectives were set,

- I. Review available literature to identify the range of techniques available to rapidly assess reactivity and test sorptivity of fly ash (with regard to AEA).
- II. Obtain a range of fly ash samples from various sources to consider seasonal variations, effect of processing and modern combustion technology on their properties; PC from various suppliers and sources (considering variation in strength class, fineness and chemical compositions) to examine its effect on the reactivity test results and range of AEA to identify their interaction with fly ash.
- III. Characterisation of test materials to understand their properties and likely behaviour in the assessment tests.
- IV. Carry out a series of initial experiments to examine the techniques identified from the literature review with selective fly ashes in order to establish those with potential to reliably assess of the properties of interest.
- V. Use promising methods from the initial tests to examine their reliability over a wide range of fly ashes covering various sources and repeat samples from selected sources.
- VI. Carry out tests in mortar and concrete to validate the suitability of the assessment test methods identified in Objective II and evaluated in Objective III.
- VII. Identify the practical implications of the research.

1.3 Scope of the Investigation

Broadly the area of interest of this research includes development/evaluation of test methods to rapidly assess fly ash reactivity and its interaction with AEA in a cementitious

system. In connection with these, a range of materials from various sources, viz. fly ashes (57 in total: processed, run-of-station, co-combustion and oxy-fuel technology), PCs (five in total: to identify the influence of PC type on reactivity test results), AEAs (three, commercial) and laboratory grade standard reagents (e. g. sodium dodecyl benzene sulfonate (SDBS), acid blue – 80 (AB80), methylene blue (MB), hydrated lime) were considered. The intention of using laboratory standard reagents, hydrated lime and AB80 was to minimize the influence of PC and AEA characteristics on the reactivity and AEA interaction study, respectively. Tests were carried out to evaluate fly ash characteristic properties including, fineness, LOI, specific surface area, particle size distribution (PSD), morphology, chemical and phase composition. Following these, tests were carried out to assess fly ash reactivity and interaction with AEA as described in the following sections.

1.3.1 Pozzolanic reactivity of fly ash

This part of the research was concerned with identification of fly ash properties or tests which can evaluate its pozzolanic reactivity. This was assessed from various tests including,

- activity index test and mercury intrusion porosimetry (MIP) with PC-based mortar;
- strength test with hydrated lime mortar;
- Thermogravimetric analysis (TGA) with PC/fly ash paste to determine Ca(OH)_2 consumption;
- Ca(OH)_2 consumption from PC and hydrated lime in solutions to reduce effects of packing and properties of PC, respectively;
- oxide and glass content analysis; and
- heat of hydration by exposing fly ash to quick lime.

Fly ash mortar strength tests generally give the indirect measurement of reactivity, however, could be influenced by the PSD and thereby packing of materials. Therefore, MIP was conducted to evaluate porosity at early ages (indicate packing) of mortar samples. Hydrated lime was used for mortar test to minimize the effect of PC type in traditional (strength) activity index tests. TGA gives the quantity of Ca(OH)_2 remaining in fly ash/PC paste which can be considered as a measure of its reactivity, while packing influence is minimum. Chemical tests such as exposing fly ash to PC or hydrated lime suspensions

also minimize the influence of packing effects on test results; especially the latter, which was expected to minimize both packing and the effect of PC type on the test results. Attempts were made to relate fly ash chemical composition with the activity index. Heat evolution from fly ash/quick lime reaction was also considered as a means of assessing reactivity. Finally, strength tests on 100 mm standard concrete cubes were carried out to validate the test results. Correlations were sought between fly ash properties and pozzolanicity test results.

1.3.2 Fly ash/AEA interaction study

To identify suitable assessment method(s) for evaluating fly interaction with AEA (i.e. the quantity of AEA adsorbed by fly ash carbon) several tests were adopted/developed. These included,

- Foam index tests,
- AB80 adsorption, and
- MB adsorption tests.

To minimise the influence of operator effort and judgement, an automatic shaker was used to standardise shaking effort during the foam index test and a spectroscopic method was employed in the AB80 tests. Correlations were then examined between fly ash properties and assessment test results. Finally, the assessment test results were validated by examining the AEA dose required to entrain a target quantity of air in cementitious media including mortar and concrete. In addition to commercial AEAs, laboratory standard surfactant was used for the foam index test and air-entrainment in mortar and concrete as a forward standardising this.

1.4 Outline of Thesis

Chapter 2 reviews background literature relating to fly ash characterisation and available means of assessing its reactivity and interaction with AEA. Information on test methods covered in (inter)national standards, or provided by organizations was gathered. Relationships between fly ash characteristics and various test results were identified from the literature. This also covered various activation methods (e.g. thermal, chemical and

mechanical) which could be considered as potential methods for assessing pozzolanicity. Available means for evaluating fly ash/AEA interaction were also studied and focussed on fly ash property influences with regard to this.

Chapter 3 describes the procedures followed for the range of tests carried out during the project. These include characterisation of materials and descriptions of assessment test methods relating to fly ash pozzolanicity and its interaction with AEA. Procedures for mixing and testing fly ash mortars and concretes are also described in this chapter.

Chapter 4 give the characterisation of the materials used in the study, and includes fly ash, PC, aggregate, AEA and other reagents used. Physical properties including fineness (45 μm sieve residue and LASER PSD), specific surface area (N_2 absorption method, Blaine); chemical properties including Oxide (XRF) and phase composition (XRD) and LOI are reported. Scanning Electron Microscope (SEM) imaging is presented to characterize fly ashes morphologically. Sieve analysis of laboratory and standard sand, absorption and specific gravity of fine and coarse aggregates used in concrete were also evaluated.

Chapter 5 investigates pozzolanic reactivity of fly ash. Mortar tests with BS EN 450-1 (BSI, 2005c) gave activity index, while accelerated curing BS 3892-1 (BSI, 1982) gave pozzolanic activity index in 7 days and water demand. MIP was used to measure porosity of mortar prisms. To minimize effect of PC properties, laboratory standard hydrated lime was also considered for mortar tests. To minimize packing/aggregate effect (mortar tests), TGA analysis was carried out with fly ash/PC paste and fly ash was exposed to PC/hydrated lime in solutions and then levels of $\text{Ca}(\text{OH})_2$ determined. Changes in conductivity of test solutions were also measured. The chemical and phase composition of fly ash was examined to relate with pozzolanic reactivity. Heat evaluation from the reaction of fly ash with quick lime was also considered.

Chapters 6 examined the interaction of AEA with fly ash. Consideration was given to assess this by improvement/adoption of foam index, AB80 and MB tests (BS EN 933-9 for aggregates; BSI, 1999a), these included the use of a mechanical shaker, laboratory standard reagents (surfactant/dye) and spectroscope to reduce operator influence. The results obtained were related with fly ash properties and validated with tests in mortar.

Chapter 7 considers the validation of fly ash assessment test methods in concrete. Compressive strength results obtained from standard 100 mm cube were used to assess fly ash pozzolanic reactivity. AEA dose requirements to entrain a specific quantity of air in concrete were related to the assessment test method results. Initial surface absorption test (ISAT) and depth of water penetration under pressure were measured to assess effect of air-entrainment in fly ash concrete.

Chapter 8 dealt with analysis of between-laboratories test results. Activity index, PSD, LOI and sieve analysis were carried out at 3 other laboratories (members of UKQAA). This gave a range of reproducibility test results.

Chapter 9 provides a summary of the outcomes of the research including conclusions, practical implications and recommendations for further study.

An Appendix at the end of these provides tables and figures of test results, discussed in the main chapters.

CHAPTER 2: STATE OF THE ART

This Chapter provides state-of-art on fly ash characterisation and available means of assessing its reactivity and interaction with AEA. Information on test methods covered in (inter)national standards or provided by organization were gathered. Relationships between fly ash characteristics and test results were identified from literature. This also covered various activation methods (e.g. thermal, chemical and mechanical) could be considered as potential methods for assessing pozzolanicity.

2.1 Introduction

The need to manufacture construction materials (especially concrete) using less energy and primary materials is becoming ever more pressing. In terms of thermal requirements, current clinker making technologies are approaching their theoretical limits; hence other routes need to be taken towards achieving this. Blending PC with a readily available pozzolanic material such as fly ash has great potential (Davis *et al.*, 1937; Mehta, 1986; Helmuth, 1987; Malhotra, 1993; Menz, 1999; McCarthy and Dhir, 2005; Sear, 2011).

Notwithstanding, fly ash has been successfully used in concrete since 1937 to improve its durability, ultimate strength and cost effectiveness. The environmental credentials of fly ash have also become of increasing importance (Sear, 2001). However, new regulations to suppress NO_x emissions at power stations, obtaining coal from multiple sources and the use of co-fuels result in variations in fly ash properties (Hower *et al.*, 1999b; Thompson, 2008; Pedersen *et al.*, 2010). Fly ashes produced from the emerging coal combustion processes (e.g. oxy-fuel and supercritical steam cycle technology) also need to be assessed in order to ensure their applicability in concrete construction. These may affect utilisation of the material in future and highlight the need for (i) regular and rapid assessment of the material including its pozzolanic reactivity and compatibility with AEAs; and (ii) checks on the suitability of existing methods for these purposes.

In this regard, the duration of standard methods to evaluate pozzolanicity (at least 7 and 28 days for ASTM C618 (ASTM, 2012) and BS EN 450-1 (BSI, 2005c) respectively) is recognised as an obstacle and, indeed, there is a history of endeavours to find suitable alternatives (Hubbard and Dhir 1984; Sharma *et al.*, 1993; Institute of Technological Research of São Paulo, 1997; Yamamoto *et al.*, 2006).

This literature review aimed to investigate currently available methods to assess fly ash pozzolanic reactivity and interaction with AEA in a cementitious system. In relation to the reactivity assessment properties of fly influencing their reactivity and various activation methods were also included to examine whether they can provide means of assessing pozzolanicity. Approximately 200 related literatures were covered from the database of ISI Web of Knowledge (including Web of Science), Science Citation Index, Scopus, SCIRUS, SpringerLink, Construction Information Service, ICE Journal Archive, ZETOC Nexis, OPENSOAR, Science, OpenSIGLE, British Library Catalogue and Industrial data and Reports. In addition, relevant books, conference proceedings reports and materials and instrument manufacturers' webpages were also visited.

2.2 Pozzolanic Reactivity Assessment of Fly Ash

There are several textbooks describing the generation, nature and reactions of fly ash, including those by Swamy (1986), Helmuth (1987), Joshi and Lohtia (1997) and Sear (2001). Fly ashes contain a significant proportion of glassy phase (50-70%) and crystalline components such as quartz, mullite, hematite and magnetite. Mostly the glassy phase has pozzolanic value, although the crystalline part can also play some role in the reactivity of fly ash due to physical effects (e.g. as nucleation sites) (Helmuth, 1987). A combination of silicate and aluminate ion release from the glassy phase of fly ash on exposure to a calcium source (hydrating PC or lime) results in the formation of C-S-H and C-A-S-H gels, thereby, refining the microstructure and improving strength of the particular system. These reactions are slower than PC hydration.

Changes in fly ash quality in the recent past, i.e. more remaining carbon (Hower *et al.*, 1997; Pedersen *et al.*, 2010), less glassy phase and a general coarsening of particles (Hower *et*

al., 1999a) has given new impetus to the effort to maintain or improve the utilisation level of fly ash in construction work.

There is an increasing number of test methods that have been developed, or are being improved, to assess the material. Many (inter)national standardisation bodies, and research institutions have their procedures for fly ash and other additions/pozzolana, such as GGBS, metakaolin, and silica fume. These tests include,

- activity index (BS EN 450; BSI, 2005c), strength factor (BS 3892-1; BSI, 1997) or pozzolanic activity index (BS 3892-1; BSI, 1982) with accelerated curing,
- strength activity index (ASTM C311; ASTM, 2011a), ASTM C1240 (ASTM, 2011c),
- Brazilian standards NBR 5751 (NBR, 1992a) and NBR 5752 (NBR, 1992b),
- modified Chapelle method (Institute of Technological Research of São Paulo, 1997),
- *K*-value of Ferét's law, assessed pozzolanic-activity index (API by Yamamoto *et al.*, 2006), potential pozzolanic index (PPI by Hubbard and Dhir, 1984), or an empirical equation developed by Sharma *et al.* (1993).

Good reviews of available methods have also been published, e.g. by Mehta (1986), Sybertz (1989), Malhotra (1993), Swamy (1993), Manz (1999), Yamamoto *et al.* (2006), and Gava and Prudencio (2007a and 2007b). In the following sections, these are considered according to the mechanism by which pozzolanicity is assessed.

2.2.1 Empirical/analytical equations

Hwang *et al.* (2004) investigated the compressive strength of concrete containing fly ash and offered an equation to estimate this as follows:

$$f_c(t) = A(t) \left(\frac{\alpha FA + C}{W} \right) + B \quad (\text{Eq. 2-1})$$

Where, $f_c(t)$ compressive strength at t days (N/mm²),

$A(t)$ function of age (t days),

α fly ash's contribution to strength,

FA fly ash content (kg/m³),

C cement content (kg/m³),

W unit water content (kg/m³), and

B Constant

The coefficient, $A(t)$ indicates strength development of concrete over time and is defined as,

$$A(t) = \frac{t}{a+bt} \quad (\text{Eq. 2-2})$$

Where, a and b are experimental constants at time t . The term α depends on factors such as, age, fly-ash content, and Blaine specific surface area. This equation is claimed to be capable of estimating increases and decreases in early strength due to replacement of fine aggregate and cement by fly ash, respectively. It also covers the effect of fly ash level and fineness (Blaine specific surface area) on strength, as well as long-term reactivity.

Papadakis *et al.* (2002) proposed an experimental procedure based on pozzolanic activity index to estimate an efficiency factor (k value) for both natural pozzolanas (volcanic tuff and diatomaceous earth) and artificial pozzolanas (fly ash with low, medium and high calcium content and GGBS). The active silica content of the pozzolana was correlated with the estimated k value for equivalent strength through an analytical expression as follows:

$$k = (\gamma_s f_{s,p} / f_{s,c})(1 - \alpha W / C) \quad (\text{Eq. 2-3})$$

- Where, γ_s the ratio of active silica to the total silica in the SCM,
 $f_{s,p}$ the weight fraction of silica in pozzolana,
 $f_{s,c}$ the weight fraction of silica in cement,
 α parameter depending mainly on time and curing,
 W water content in the fresh concrete mix (kg/m^3),
 C cement content in the concrete (kg/m^3).

The expression was claimed to be valid for artificial pozzolanas (fly ash, GGBS) only, while, it overestimated the k value for natural pozzolana. This discrepancy could be attributed to either formation of weaker C-S-H in the case of natural pozzolana, or the procedure followed to estimate the active silica content being invalid for these types of materials.

Bijen and van-Selst (1993) investigated cement equivalence factors for fly ash in concrete. Factors such as water-cement ratio, age, type of cement and fly ash properties were identified as influencing strength development of fly ash concrete. Four fly ash samples

(including two low-NO_x materials) were studied. Three types of cements, e.g. PC, fast reacting PC and a cement combination containing GGBS were included. The cement equivalence factor was found to be inversely proportional to w/c ratio, while the influence was greatest for the fast reacting PC and least for the slag cement. In the case of the latter cement, the equivalence factor was inversely proportional with age and directly proportional for the PCs investigated.

2.2.2 Physical and chemical properties affecting reactivity

There is general agreement that both physical (e.g. fineness, PSD) and chemical (e.g. reaction with lime) aspects could be considered for estimating the reactivity of fly ash in concrete (Swamy, 1986; NBR, 1992a; Frias *et al.*, 2005).

Fineness, particle size distribution and shape

Adamiec *et al.* (2008) studied the pozzolanicity of various fly ash fractions (granulometric and densimetric). The global fly ash (density 2.24 g/cm³, particle size d_{50} 24 μm) was subdivided into 20 categories. The dimensional fractions included fly ash of: (a) > 80 μm, (b) 40 – 80 μm, (c) 25 – 40 μm, and (d) < 25 μm. The densimetric fractions were: (i) > 2.9 g/cm³, (ii) 1.8–2.9 g/cm³, (iii) 1.2–1.8 g/cm³, (iv) <1.2 g/cm³, and (v) magnetic fraction. The Chappelle test was used to determine the lime consumed (i.e. pozzolanicity). The neoformed phases were found to depend on particles sizes. C-S-H was formed in the largest granular fractions ($d > 40$ μm) and C₃AH₆ in the other smaller fractions.

Paya *et al.* (1995) studied the effect of fineness on strength development of air-classified fly ashes. It was found that sub-10 μm particles made a significant contribution to compressive and flexural strength development of mortars containing fly ashes. A good correlation between strength and mean particle size was observed at a fly ash level of 60%.

Paya *et al.* (2000) also studied the influence of reduction in fly ash particle size by grinding on strength development of fly ash/cement mortars. Higher reactivity of fly ash was found for ground material compared to unground. In a similar study, Aydin *et al.* (2010) also investigated the effect of fly ash grinding (fineness) on the mechanical properties of mortar. Using a ball mill, Blaine fineness increased by more than three times that of the original material (from 290 m²/kg to 907 m²/kg). Fly ash levels of 20, 40 and 60% were investigated.

Depending on the fly ash level, significant increases (34 - 46%) in compressive strengths of ground fly ash mortars were observed (cured in steam for 15.5 hours).

Benezet and Benhassaine (2009) investigated pozzolanic reactivity of four distinct size pure quartz powders. The reaction of these powders with lime at 20°C showed that this depended on particle size. In the first stage of a thermally non-activated reaction (at 20°C), the amorphisation of grain surfaces mostly depended on the absorption of fine particles on coarse particle surfaces. Particle sizes < 1 µm mainly initiated these reactions. In the second stage (between 28 and 90 days), the micropowders (1 and 10 µm) completed their reactions. Finally, the mesopowders reacted.

Tangpagasit *et al.* (2005) considered the effect of fly ash particle size on packing and pozzolanic reactions using mortar (20% fly ash level). Inert materials with particle size similar to PC were used to study these effects. In general, the compressive strength of fly ash mortar reflected (i) PC hydration reactions, (ii) packing effects and (iii) pozzolanic reactions, whereas for mortars with inert material, the compressive strength depended on (i) and (ii) only.

In this study, the strength contribution from pozzolanic reactions was determined from the difference in compressive strengths of mortars prepared using fly ash and inert material. The influence of both fly ash median particle size and curing age was noted in the strength activity index of fly ash mortar. The fly ash median particle sizes considered were 2.7, 16.0, 19.0, and 160.0 µm and those for inert materials 3.3, 19.0 and 200.0 µm. Packing effects dominated over pozzolanic effects at early ages (3-28 day). In the case of the former, the difference in strength activity index between mean particle size 2.7 and 160 µm was 22% at all test ages. For the latter, these were 3%, 20%, and 27% at ages of 3, 28, and 90 days, respectively, between median particle sizes of 2.7 and 160 µm. With the coarsest fly ash (median size 160 µm), the increase in strength activity index, due to pozzolanic effects was found to be as low as 2% at 90 days.

Agarwal (2006) compared pozzolanic activity (room temperature for 7 and 28 days and accelerated curing) based on mortar compressive strength using silica fume, fly ash (as-received and fine ground), quartz, precipitated silica, metakaolin and rice husk ash (of different fineness and carbon content). Finely ground rice husk ash (< 45 µm) gave

highest reactivity, followed by quartz and silica fume. Ground fly ash reactivity was comparable with silica fume, while fused quartz gave much higher reactivity than the latter.

Shi *et al.* (2005) studied the effect of glass powder fineness on its pozzolanic reactivity. Mortar samples were made with four glass powders (fineness varied by grinding with a ball mill) and fly ash. The reactivity of the glass powders was found to be greatly influenced by their fineness.

A study by Shvarzman *et al.* (2002) reported the early age (1 day) activity of pozzolana to be influenced by its specific surface area. However, this seemed to be a physical effect, due to the high fineness of the material considered.

Glassy phase quantity and composition

Ward and French (2006) presented a method to estimate the glass content in fly ash samples by X-ray diffraction (XRD) using the SIROQUANT software package, based on Rietveld quantitative analysis. Fly ash samples were spiked with synthetic corundum and zinc oxide (known quantities) and XRD analysis was carried out using the SIROQUANT process. Raw or unspiked samples were also analysed. It appeared that the mineral matter present in the feed coal influenced that of the fly ashes (proportions of quartz, iron oxide and glassy constituents). The chemical composition of the crystalline minerals was subtracted from the overall fly ash chemistry, which gave that of the amorphous part. The results indicate that fly ashes derived from lower-rank coals had different glass compositions (with lower percentages of SiO₂ and higher percentages of Fe₂O₃) than those of higher-rank materials. The variations in glass compositions could also be related to other fly ash properties, for example, particle density and surface area.

Antiohos and Tsimas (2005) studied the influence of active silica of high-calcium fly ashes (ASTM Class C) on their reaction mechanism. The two fly ashes contained similar levels of free lime, while their active silica levels were different. These were ground appropriately to give similar fineness. Mortar samples were prepared with fly ash levels of 10, 20 and 30% and PC. Several parameters including compressive strength, remaining calcium hydroxide, generation of hydration products and microstructure development were

examined. The soluble silica part in fly ash played a significant role in strength gain, especially after one month of curing. Additional cementitious compounds (principally a second generation C-S-H) was produced in the matrix by the increasingly dissolving silica. However, fly ash reaction rates seemed to be independent of their active silica content. It was suggested that additional factors for example glass content and fineness should be considered in predicting fly ash pozzolanic performance.

In further work (Antiohos and Tsimas 2006) the authors tested five fly ashes (two originally used in the previous work, and another three, by blending these in various proportions). In their work, a theoretical expression between amorphous silica and k -value of cementitious systems was proposed. It was claimed that the relationship could be applied to estimate the k -value of the respective blended cements, which would allow a rapid prediction of the quantity and properties of fly ash to be used in concrete mix design. It was also noted that in the first stage of hydration (up to one month), the amorphous silica remained confined to the inner part of fly ash and did not react critically within the system.

The study by Shvarzman *et al.* (2002) indicated that later age pozzolanic activity is mostly dependent on the chemical and mineralogical composition (amorphous phase quantity of fly ash). A petrographic study by Hower and Mastalerz (2001) reported that glass can be surrounded by unburned carbon (Figure 2-1) and thereby its reactivity is expected to be affected in this case.

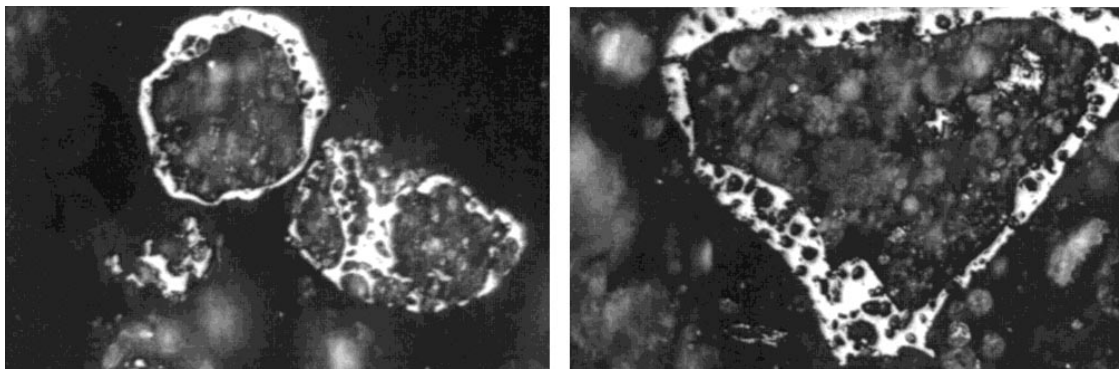


Figure 2-1. Examples of glass surrounded by carbon (Hower and Mastalerz, 2001)

Chemical, mechanical and thermal activation

Winnefeld *et al.* (2010) examined the effect of alkali activation (mixture of NaOH and Na₂SiO₃) on both low and high calcium (hard coal and lignite coal) fly ashes. Conduction calorimetry, XRD, thermal gravimetry analysis (TGA) and scanning electron microscope (SEM) were used to assess fly ash mortar and paste. Various doses of sodium silicate were used (with a constant molar SiO₂-to-Na₂O ratio of 1.0) for activation. Considering different curing protocols, 80°C for 24 h was found to be the optimum with regard to strength development of mortar. The results indicate that glass and calcium contents of fly ash were important factors affecting their reactivity and performance during alkali activation. A higher glass phase was found in low calcium fly ash, compared to that of high calcium content. With activation of the former, more alkali aluminate silicate hydrates and consequently a denser microstructure was found.

Li *et al.* (2002) studied activation of fly ash and GGBS using Ca(OH)₂, NaOH, NaSO₄, and water glass. A relationship between structure, composition, and activity of glassy cementitious materials was observed. SEM, XRD, TGA, differential scanning calorimetry-thermal gravimetry (DSC-TG), and pore structure analysis were carried out to examine the reactivity and hydration process of fly ash and GGBS. At room temperature, the reaction between fly ash and lime was found to be poor, however, the addition of alkali and sulfates accelerated the process. The effect of adding alkalis was found to be superior to sulfates. Although high alkalinity could improve the hydration properties of fly ash by dissolving the glassy phase, the formation of C-S-H gel was found to be comparatively lower than that of GGBS. This is because of the lower calcium present in fly ash, which leads to a relatively poor microstructure in the case of fly ash activation with other alkalis.

Lee *et al.* (2003) reported chemical activation of fly ash-cement systems. Three kinds of activators (Na₂SO₄, K₂SO₄, and triethanolamine) were used to try and improve the early strength and microstructure characteristics of fly ash mortar. All of the activators improved the early age strength characteristics, especially K₂SO₄. However, very minor differences in strength were noticed between the activated mortar and those without activators at 28 days. TGA and XRD analysis showed lower levels of Ca(OH)₂ in activated mortars than those without this at early ages. An increased level of ettringite was formed (especially for Na₂SO₄) by consuming the Ca(OH)₂, which gave a higher early strength.

The porosity reduced to the micro level, with lower total pore volume and this also influenced the early strength (K_2SO_4 was found to be most effective in reducing porosity).

Rowles and O'Connor (2003) investigated the effect of activation chemistry on the compressive strength of aluminosilicate geopolymers synthesised by Na_2SiO_3 (water glass) activation of metakaolin. Relative concentrations of Si, Al and Na in the polymer were found to be the primary influencing factors. Polymers with Si : Al molar ratios of 1.0 – 3.0 and Na : Al molar ratios of 0.5 - 2.0 were tested for compressive strength. These were cured for 24 h at 75°C. Compressive strengths were measured at 7 days. The maximum strength was found to be 64 ± 3 MPa (N/mm²) for a Si : Al : Na molar ratio of 2.5 : 1 : 1.3. XRD results indicated that the bonding network in the glassy alumina-silicate changed systematically with composition.

Qiao *et al.* (2006) compared the effect of chemical (K_2SO_4 , Na_2SO_4 , $CaCl_2$ and FGD sludge), thermal (20 and 60°C) and mechanical activation (grinding to reduce particle size < 75 µm) of rejected fly ash (coarse and high carbon part from classification). Lime reactivity was evaluated through compressive strength, differential scanning calorimetry-TG, XRD and MIP. Na_2SO_4 was found to be beneficial as it increased the solubility of Ca^{2+} . The addition of Na_2SO_4 could significantly increase the strength development both at 28 and 90 days, on the other hand K_2SO_4 and FGD sludge were only effective at 28 and 90 days, respectively. Elevating the curing temperature showed a slight increase in strength at 28 days; however, it reduced at 90 days. A higher porosity was observed due to steam curing, which might cause the effects noted for strength at the latter age. Mechanical grinding was found to have a slight influence on 28 days strength. However, at 90 days the effect was significant. The addition of $Ca(OH)_2$ with grinding was found to be a very effective activation method.

Shi and Day (2001) compared three activation methods to enhance the reactivity of volcanic ash (VA). Those were, (a) mechanical activation (prolonged grinding), (b) thermal activation (elevated temperature curing), and (c) chemical activation (using Na_2SO_4 and $CaCl_2$). Test samples were prepared using 80 and 20% hydrated lime and VA respectively. Comparisons were made in terms of $Ca(OH)_2$ consumption rate, strength development, ultimate compressive strength and cost. The chemical activation (addition of 4% Na_2SO_4 or $CaCl_2 \cdot 2H_2O$ by mass of lime-pozzolana blends) increased the ultimate strength

significantly, while the effect of mechanical and thermal activation was limited to very early ages (first 1-3 days). At latter ages, the influence of mechanical activation was not significant while thermal activation decreased the ultimate strength. Considering the cost and effects obtained, chemical activation was found to be the most efficient method for the activation of natural pozzolana.

Blanco *et al.* (2006) studied mechanical activation (wet milling) and chemical activation (leaching with sulfuric acid) of two Spanish fly ashes. Physico-chemical characterization, granulometry, density, Blaine, BET (Brunauer, Emmett and Teller Theory), XRD and SEM were used to evaluate the effect of activation. Mortar samples with different levels of silica fume and activated fly ash were prepared. These were tested for mechanical resistance (compressive and flexural strength) and porosity. Mortars with activated fly ash gave higher strength than that with silica fume (90 days strength of mortars with activated fly ash were greater than 180 days cured silica fume mortars). Mercury intrusion and SEM revealed that the increased strength of activated fly ash mortar was due to its reduced porosity, especially micro-porosity.

Fan *et al.* (1999) presented a chemical activation method for fly ash using $\text{Ca}(\text{OH})_2$ and Na_2SiO_3 . The effects of fly ash : $\text{Ca}(\text{OH})_2$ ratio (i.e. 3:1, 4:1 and 6:1) and temperature (i.e. 55, 70 and 90°C) were studied. An addition of 3.91% Na_2SiO_3 in solution was found to be effective in disintegrating the silica-alumina glass chain by raising the pH to 13.1 (by forming NaOH from the hydrolysis of Na_2SiO_3) from 12.6 (pH of saturated $\text{Ca}(\text{OH})_2$ solution). The sample was then wet ground for 40 minutes and dried at a temperature of 120°C to obtain activated fly ash. Using activated fly ash (up to a level of 15%) both initial and final setting times reduced by up to 50% compared to PC, indicating increased reactivity of the former. Strength tests with activated fly ash (up to 10%) gave higher results compared to PC mortars at 1, 3 and 28 days, suggesting effectiveness of the method.

Heinz *et al.* (2010) studied the effect of KOH (0.1 m/L, pH 13) and various quantities of triethanolamine (TEA) addition on fly ash dissolution. The concentration of dissolved elements in solution was analysed by inductively coupled plasma spectroscopy (ICP-OES) and it was found that TEA addition enhanced the dissolution of Al, Ca and Fe. However, the effects on Si and Na were minor. The addition of TEA prolonged the induction period

but the total heat evolution (recorded using isothermal calorimetry) was found to be slightly higher from tests without TEA. Mortar tests indicated higher early strength (1 day) with TEA addition (up to 0.04%).

Chun *et al.* (2006) tested the effect of adding a lithium-salt industrial residue (LSR) on the pozzolanicity of fly ash and found a significant influence on both pozzolanic activity and strength of concrete at various ages (7, 28, and 60 days).

Chemical reactions of fly ash with lime

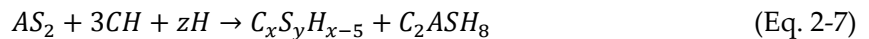
Several models exist in the literature describing the reaction between fly ash and $\text{Ca}(\text{OH})_2$. Bentz and Remond (1997) suggested the following pozzolanic reactions for fly ash:



According to Helmuth (1987) lime mainly reacts with the reactive silica part of fly ash. Equation 2-5 is the simplified form of this reaction.



In the process of reaching equilibrium, the lime : silica ratio (x to y) ranges from 0 - 2.0 depending on the concentration of the reaction materials. Fly ash reaction with lime can produce C-S-H and gehlenite hydrate. In the case of fully reacted lime, the equation may be expressed as shown in Equation 2-6,



Biernacki *et al.* (2001) investigated the kinetics of the reaction between $\text{Ca}(\text{OH})_2$ and fly ash at temperatures from 25 – 60°C. TGA was used to determine the production of hydrates (non-evaporable water) from $\text{Ca}(\text{OH})_2$ consumption, as a function of hydration temperature and time for different $\text{Ca}(\text{OH})_2$ /fly ash ratios (from 12.5 : 87.5 – 75 : 25). The reaction rate, stoichiometry, and activation energy were found to be dependent on the $\text{Ca}(\text{OH})_2$ /fly ash ratio. With test conditions of 60°C and a $\text{Ca}(\text{OH})_2$ /fly ash ratio of 75 : 25,

the Ca(OH)_2 consumption/g fly ash reached an asymptotic value at 16 day exposure period. Under these conditions, approximately 1.12 g Ca(OH)_2 was consumed by 1 g of fly ash.

Zhu and Yang (2006) dealt with the pozzolanic reactivity and reaction kinetics of fly ash. A kinetics model of the pozzolanic reaction was developed by considering the degree of reaction of fly ash- Ca(OH)_2 - H_2O systems, measured by the acid-dissolution method. The effect of the pozzolanic reactivity of fly ash on the strength of cement mortar was also investigated and it was found that variations in the former among fly ashes of low CaO had little effect on the latter.

de Rojas and Frias (1996) and Frias *et al.* (2005) proposed the use of laboratory grade lime (instead of cement) to evaluate pozzolanic reactivity. Fly ash (1.0 g) was placed in saturated lime solution (75 ml) in a double-sealed plastic container and kept at $40 \pm 1^\circ\text{C}$ for 1, 7, 28 and 90 days. At each test age, the concentration of CaO in solution was measured. The lower the value obtained (with respect to the original concentration) the greater the pozzolanic reactivity. Work by Donatello *et al.* (2010) compared pozzolanic reactivity assessment methods including strength factor (BSI, 1997), Frattini (BS EN 196-5; BSI, 2011a) and saturated lime tests (Frias *et al.*, 2005). A good correlation between results obtained from strength activity index (28 days) and Frattini tests (% CaO removed) was found. However, little or no correlation was observed between the former and saturated lime test results. A very low level of CaO present in a saturated lime solution was identified as an obstacle to accurate measurements, and it was suggested that an increased quantity of lime solution from 75 to 500 ml be considered for further testing.

Reactivity with PC

A test method is described in BS EN 196-5 (BSI, 2011a) to evaluate the reactivity of pozzolanic cement (blend of PC and pozzolanic materials). This involves the preparation of slurry by mixing 20 g cement in 100 ml de ionized water and storage at 40°C for a specified period in a sealed plastic container. The pozzolana consumes Ca(OH)_2 produced from cement hydration. The cement is considered sufficiently pozzolanic, if the resulting solution is not saturated by calcium ion (in terms of CaO) at 8 or 15 days.

Yamamoto *et al.* (2006) proposed the assessed pozzolanic activity index (API, an accelerated chemical test) for rapid evaluation of fly ash reactivity. The pozzolanic reaction was found to be primarily influenced by the diffusion kinetic, and the diffusion constant increased with water content used in mortar. A good correlation between the K -value from Feret's law (estimated from mortar strength and mix composition) and API was obtained. A linear relationship between the K -value and log of time was also noted. The effect of fly ash fineness was noted, with fine fly ash giving higher mortar compressive strength at all curing ages. A steeper gradient with higher water content mortar compared to when lower levels were used, suggests that water contents in mortar have a significant effect on the pozzolanic reaction of fly ash, as well as hydration of cement.

Wang *et al.* (2004) examined the degrees of cement clinker hydration and fly ash pozzolanic reaction (in fly ash/PC systems) at different fly ash levels (10-60%) and ages (7, 28, 90, 365 days). It was considered that fly ash reactions with $\text{Ca}(\text{OH})_2$ can promote the hydration of PC. Pozzolanic activity dominated at lower fly ash levels, but its role as a promoter of cement hydration was weaker. However, the opposite behaviour was noticed at higher fly ash levels. The results from that are summarized in Figure 2-2.

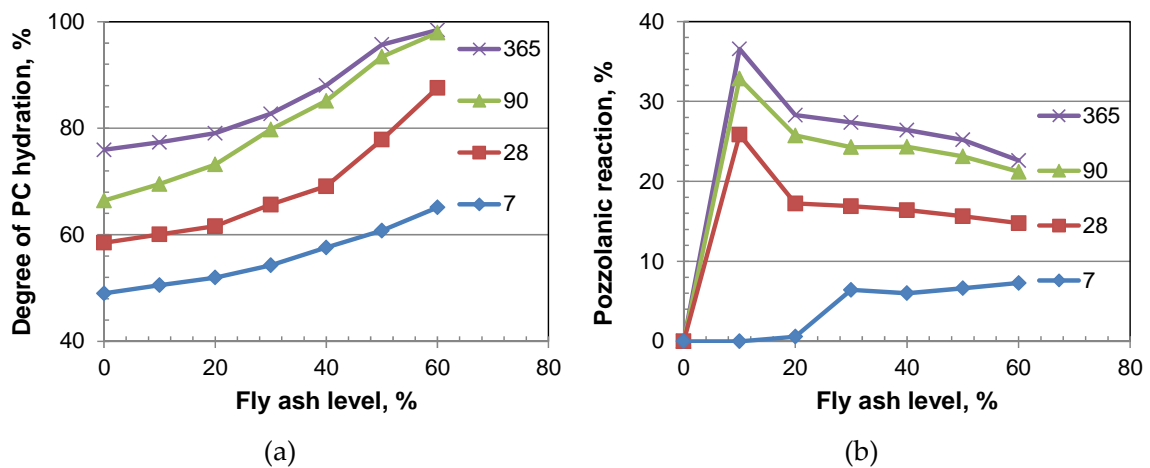


Figure 2-2. Effect of fly ash level on (a) degree of PC hydration and (b) pozzolanic reaction at various ages (based on Wang *et al.*, 2004)

Wang *et al.* (2009) proposed a kinetic model to simulate the hydration of low-calcium fly ash blended cement considering both PC hydration and pozzolanic activity. Properties such as fly ash reaction ratio, $\text{Ca}(\text{OH})_2$ content, heat evolution, porosity, and chemically

bound water of hydrating cement blends were estimated as a function of (reaction) time. The compressive strength development gave good agreement with experimental results.

Effect of acids/alkalis

Antiohos and Tsimas (2004) and Antiohos *et al.* (2006) investigated the effect of quicklime on the pozzolanic performance of three fly ashes with CaO contents of 13.8, 29.8 and 34.1%. Cement mortars containing 80% cement, approximately 20% fly ash and various quantities (0.6 – 1.2% for high lime fly ash and 1.0 – 3.0% for low lime fly ash) of quicklime were prepared. Strength development, hydration products, pozzolanic reaction rates, porosity and microstructure were evaluated. Linear correlations were obtained between the non-evaporable water contents (W_n) and the cementitious efficiency factor (k -values) of the activated systems. The addition of quicklime (0.6%) increased compressive strengths throughout the curing period (2 - 90 days) in case of both high-calcium fly ashes. In contrast, for the lower-lime fly ashes, this (1% quicklime addition) was found to be effective only at 2 days. Pore volume and distribution analysis and gel/space ratio calculations supported the strength results. A good linear correlation was obtained between the total porosity (%) and gel/space ratio.

Antiohos *et al.* (2008) studied the influence of quicklime addition (0.6 - 3.0%) on the mechanical properties and degree of hydration of blended cements containing two types of fly ash (CaO levels 34 and 14%). Compressive strength development in mortar (fly ash level approximately 20%) and lime depletion values were monitored. The morphology of reaction products was evaluated by SEM. Strength data showed that the addition of 0.6% lime in high lime fly ash mortars accelerated the reaction rate throughout the curing period (2-90 days), whereas in the case of lower-calcium fly ash, quicklime had a positive impact during the very early reactions (at 2 days) and thereafter inhibited the effect.

Feng *et al.* (2004) studied the pozzolanic properties of hydrochloric acid pre-treated rice husk ash (RHA). Methods including heat evolution, $\text{Ca}(\text{OH})_2$ content and pore size distribution of mortar were considered to estimate the pozzolanic activity. Additionally, the conductivity change of saturated $\text{Ca}(\text{OH})_2$ solution due to reaction with RHA was measured ($\text{RHA}/\text{Ca}(\text{OH})_2 = 1:1$, $W/C = 1.0$, 20°C). A significant increase in mortar strength was obtained by hot hydrochloric acid pre-treatment of rice husk ash. The presence of less

Ca(OH)₂ (after 7 days) and reduced pore size distribution (at 28 days) supported the strength results. Higher heat of hydration of treated RHA cement indicated its superiority over untreated material, but the difference was minor.

Leachability of fly ash

Panagiotopoulou *et al.* (2007) investigated the dissolution of aluminosilicate minerals (from kaolin, metakaolin, fly ash, natural pozzolana, zeolite and GGBS) in alkaline media. Study parameters included, the type of alkali metal (K, Na), the alkaline solution concentration (2.5, 5.0 and 10.0 M) and the dissolution period (5, 10 and 24 h). XRD and Fourier Transform infrared spectroscopy (FTIR) were used to examine the solid residue after leaching. The leachability of Al and Si were found to reduce in the following order: Metakaolin > Zeolite > GGBS > Fly Ash > Pozzolana > Kaolin. In addition, NaOH solution was more effective in dissolving these than KOH.

Panagiotopoulou *et al.* (2009) also studied the alkaline dissolution and geopolymerisation of fly ashes. In addition to the parameters investigated by Panagiotopoulou *et al.* (2007), to evaluate the dissolution rate of Al³⁺ and Si⁴⁺, the effect of curing conditions (50, 70 and 90°C, for 24, 48 and 72 hours) and the Si/Al ratio (Si/Al = 1.75 - 4.5) on the development of compressive strength was studied. Curing at 70°C for 48 hours was identified as optimal conditions. The geopolymers' compressive strength was found to depend systematically on the Si/Al ratio (A maximum of 45.5 ± 2 MPa was achieved with a Si/Al = 2.5).

Li *et al.* (2000a) investigated the alkalinity, chemical activator, temperature and microstructure of fly ash/cement systems. TGA, XRD and SEM analysis were conducted to evaluate the effects. The results indicated that the reaction of fly ash was slow in the fly ash/PC, due to the relatively lower pH in the system and Ca(OH)₂ being less effective as an activator on fly ash at room temperature. In the case of increased curing temperature or addition of alkali and sulfate, breaking of the fly ash glass structure was enhanced and stable hydrates formed (C-S-H and zeolites). Gypsum addition enhanced ettringite formation (needle crystals) and improved strength and other properties during the early stages of hydration by forming a framed structure.

2.2.3 Accelerated test methods

Accelerated curing techniques can in fact be adopted as rapid assessment methods to predict pozzolanicity of fly ashes. These tend to follow the normal course of pozzolanic activity tests, apart from modifying the conditions leading to a compression of the time-scale involved. Increasing the temperature is the most common of these options, although not all processes are enhanced by this. For example, the solubility of lime reduces at higher temperatures (Cameron and Patten, 1911), which is why proper validation of test results would be necessary for any emerging test method.

Mortar/Concrete cured at high temperature

BS 3892-1 (BSI, 1982) described a rapid test method to assess pozzolanicity of fly ash from strength results of mortars cured at high temperature. These had a fly ash level of 30% and varying water content to achieve the same flow/spread as a PC only mortar. The mortar was cured at 20°C for 5 days and 50°C for 2 days. The fly ash was considered to satisfy the standard criteria, if it achieved a strength of at least 85% of the control (cement only mortar) after the 7 days curing period.

Paya *et al.* (1995) compared the compressive and flexural strengths of fly ash mortar following curing at 20 and 40°C for 28 days. A fly ash level of 30% and varying water content was used to achieve the same flow. Approximately 25 – 30% and 40 - 50% enhancement in compressive and flexural strength, respectively, were achieved by high temperature curing. Among the 4 fly ash mortars cured at high temperature, 3 gave very similar behaviour as they contained similar levels of sub 10 µm particles and the other gave higher strength due to the increased proportion of this component.

In a further study Paya *et al.* (2000) observed a significant increase in compressive strength of fly ash mortars, even at early ages (3 days) at higher curing temperatures (40, 60 and 80°C). The greatest effect was noted with 28 days curing at 40°C. Plotting the compressive strength against curing time (on a logarithmic scale), and conducting regression analysis give similar slopes (linear lines) for the 20, 40 and 60°C curing temperature series, suggesting the temperature range 40 – 60°C could be used for accelerated curing to predict standard curing results. Relationships between compressive strengths obtained at different curing temperatures (20°C and 40°C) and times were found from strength data of mortars

containing various (15%, 30%, 45% and 60%) fly ash levels. A mathematical model for mechanical properties at early ages was also proposed from the mortar compressive and flexural strength data obtained with fly ash levels of 15-60% and cured at 20 – 80°C.

In the study by Shi *et al.* (2005), mortar curing at high temperatures was carried out to measure strength activity index (pozzolanic reactivity) of both glass powder and coal fly ash. The effect of curing temperature on fly ash mortar strength was noticeable in the results. At room temperature (23°C) fly ash mortars gave similar/lower activity index than glass powers at all ages (1, 3, 7 and 28 days), however, curing at 35°C for 28 days gave much higher activity index for fly ash mortar. Similarly, curing at 65°C always (up to 28 days) gave higher activity index values, suggesting sensitivity of fly ash to thermal activation and potential of the method to assess long-term strength from a short and accelerated curing method.

Aydin *et al.* (2010) also noticed an acceleration in strength gain for steam cured fly ash mortar. Test samples were prepared by replacing cement at levels of 20, 40 and 60%, with finer and coarser fly ashes. Heat treatment was applied between 3.5 - 14.5 hours following mixing. Testing the mortars in compression at 24 hours gave the highest strength value of 35.4 MPa at the 40% fly ash level.

Liu *et al.* (2005) tested the influence of steam curing on the compressive strength of concrete containing ultra – fine fly ash (UFA) and GGBS and chemical activators (CaSO_4 and $\text{Ca}(\text{OH})_2$). Heat treatment was applied at $60 \pm 5^\circ\text{C}$ for 13 hours and $\text{RH} > 90\%$. Results indicated that 13 h of steam curing on UFA-only concrete gave poor compressive strength compared to those using activator and GGBS combinations. The 28 days compressive strength of moist-cured concrete was approximately 10 – 15% higher than that of steam cured (13 h heat and then stored until 28 days in a standard curing room). UFA concrete activated by CaSO_4 or $\text{Ca}(\text{OH})_2$ had a high early strength but less improvement was noticed in 28 days strength, with the former having the greater effect.

Pheeraphan *et al.* (2002) used microwave energy to accelerate the hydration of cement. 7 and 28 days compressive strengths of concretes (PC and rapid-hardening cement) were predicted from microwave cured 3.5 and 5.5 hour strengths, respectively. The

relationships gave agreement between these with variations of less than 15% compared to the actual test results. The relationships obtained given in Equations 2-7 and 2-8.

$$S_{7d-NCC} = 9.3912 \times (S_{3.5h-MCC})^{0.522} \quad (\text{Eq. 2-8})$$

$$S_{28d-NCC} = 8.5459 \times (S_{5.5h-MCC})^{0.6003} \quad (\text{Eq. 2-9})$$

Where, S_{7d-NCC}	Strength of normal cured concrete at 7 days
$S_{28d-NCC}$	Strength of normal cured concrete at 28 days
$S_{3.5hd-MCC}$	Strength of microwave cured concrete at 3.5 hours
$S_{5.5hd-MCC}$	Strength of microwave cured concrete at 5.5 hours

Tumidajski *et al.* (2003) also used microwave techniques to predict 28 days concrete strength (standard curing) from 6 hour (accelerated microwave curing) compressive strength. The obtained relationships were as follows:

$$\log f_{28-day} = 1.31 + 0.351 \log f_{6-h} \quad (\text{Eq. 2-10})$$

$$f_{28-day} = 20.3 f_{6-h}^{0.35} \quad (\text{Eq. 2.11})$$

Where, f_{28-day}	Standard cured concrete strength at 28 days
f_{6-h}	Microwave cured concrete strength at 6 hours

Topcu *et al.* (CJCE 2008 and TD 2008) confirmed the observations made by both Pheeraphan *et al.* (2002) and Tumidajski *et al.* (2003) extending their work to fly ash concrete using microwave energy to accelerate the hydration of cement. Optimal test parameters were determined for microwave curing systems. Earliest times for the mortar strength prediction were found to be 6 and 8 hours for PC and fly ash, respectively. The error percentages for strength prediction of cement mortar at 7 and 28 days were $\pm 2.22\%$ and 2.91% , respectively. Those with fly ash mortar were $\pm 4.36\%$ and 5.20% for 7 and 28 days, respectively.

Thermal analysis methods

Amer (1998) studied the pozzolanic activity of hydrating fly ash-lime pastes ($w/s = 0.4$) by means of DTA. The effects of lime content (fly ash : $\text{Ca}(\text{OH})_2 = 90 : 10, 70 : 30$ and $50 : 50$)

and curing time were evaluated. These indicated that the rate of hydration (estimated from the residual lime) and hydrated compounds, increased with lime content and time.

Li *et al.* (2000b) used TGA, XRD and SEM to investigate the influence of curing temperature (60°C) and chemical activators (NaOH, Ca(OH)₂, CaSO₄ and Na₂SO₄) on the reactivity of low calcium fly ash. A slow reaction with fly ash/cement systems at room temperature was noticed due to the low pH value. Reaction of fly ash was enhanced by increasing the curing temperature and gypsum content. At the early stages, the effect of alkalinity was noticeable, while Na₂SO₄ was found more effective in accelerating hydration at later ages.

Autoclave

Ball and Carroll (1999) used an autoclave to accelerate the reactions of UK fly ashes with Ca(OH)₂. Fly ash/Ca(OH)₂ paste was kept at 184°C for 12 hours and then XRD was used to determine Ca(OH)₂ reduction and silicon, aluminium and alkali release. The presence of Ca(OH)₂ was not found after the 6 hour test period and its consumption rate was related to the fineness of the test fly ash. No particular correlation was noticed between Ca(OH)₂ consumption and fly ash glass content.

Jing *et al.* (2006) also used autoclave curing (150 – 250°C for 15 – 60 hours) under saturated steam pressure (0.47 – 3.98 MPa). The specimens were compacted at 20-50 MPa, prior to placing in the autoclave. The tensile strength determinations gave best results from 30% (by mass) Ca(OH)₂, 20MPa compaction pressure, 200°C curing temperature and 15 h curing. A tobermorite-like C-S-H was found to make an important contribution to the strength gain. Tobermorite was formed at a Ca/Si ratio of about 0.83 and was influenced by the autoclave curing temperature and time, and compaction pressure. The tensile strength increased proportionally with autoclave temperature; however, the effect of curing time after 15 h was minor when cured at 200°C.

Ma and Brown (1997) used isothermal calorimetry to evaluate the pozzolanic reaction of Class C and F fly ashes with Ca(OH)₂ and CaSO₄·2H₂O. A tubular pressure vessel was used to apply saturated steam pressure at 25, 60, 80, 100 and 180°C and calorimetric studies were performed. The rate of hydration determined from heat evolution and Energy-Dispersion X-ray (EDX) spectrometry analysis indicated the presence of C-S-H,

tricalcium aluminate hydrate and ettringite (in the presence of $\text{CaSO}_4 \cdot 2\text{H}_2\text{O}$ at 80°C or below) as the hydration products.

Goni *et al.* (2003) studied pozzolanic reactions by using a pressure reactor (hydrothermal method) to accelerate the reaction. Two Spanish fly ashes (Class F) were mixed with CaO at a Ca/Si molar ratio of 2 (water/solids ratio of 5.0). The mixture was hydrothermally treated at 200°C and 1.24 MPa for 4 hours. XRD, SEM and Infrared (IR) spectroscopy revealed $\alpha\text{-C}_2\text{SH}$, C-S-H gel, different solid solutions of katoites (the cubic crystallographic variety of the hydrogarnet series (C_3ASH_4)) and a mixed oxide (CaFe_2O_4) were present in the products formed.

2.2.4 Prediction of performance from early age properties

Estimating medium or long-term compressive strength values from early age properties might not always be valid at later ages, because the test could be influenced by other conditions at various stages (Majumdar and Larner, 1977). Nevertheless, they may offer simple and inexpensive tests and fast assessment, by measuring e.g. heat of hydration, or changes in electrical properties of mixes.

Calorimetric assessment methods

A study by de Rojas and Frías (1996) obtained good correlations between pozzolanic activity and hydration heat. The heat of hydration of mortars, as contributed by a range of pozzolanic materials (opaline rocks, fly ash and silica fume), was evaluated by a semi-adiabatic calorimeter method. The reactivity was tested by measuring the quantity of lime fixed with pozzolana from saturated lime solution/pozzolana reaction and its rate. Calorimetric evaluation indicated that silica fume and opaline rock mixes with cement increased the heat output during early hydration, while fly ash decreased early heat output, compared to the control cement.

Baert *et al.* (2008) correlated the remaining $\text{Ca}(\text{OH})_2$ content and total heat development from a fly ash/PC system. TG and isothermal calorimetry were used to measure the reactivity of fly ash in cement paste. A range of fly ash levels were used (i.e. 0, 35, 50 and 67%). The addition of fly ash decreased the acceleration period (early age) and a third hydration peak was noticed in isothermal calorimetry. At the early stages (1-7 days), the

level of chemically bound water and $\text{Ca}(\text{OH})_2$ content also increased with fly ash content. After 7 days of hydration, the total heat increased and the calcium hydroxide started to deplete with increasing fly ash level due to the pozzolanic reaction.

Pacewska *et al.* (2008a) studied pozzolanic and hydraulic properties of fly ashes (CaO and SO_3 ranging from 1.3 – 11.6% and 0.61 – 3.75%, respectively) originating from fluidized combustion of brown coal, and pulverized combustion of brown and hard coal. Calorimetry, thermal analysis (TG, DTG) and IR absorption were used to evaluate the reaction of water with fly ash and fly ash-lime pastes (water : solids = 0.70, with lime at 30% of solids, when used) at various ages (until 90 days). The results indicated that fluidized combustion fly ash exhibited higher reactivity (the majority of $\text{Ca}(\text{OH})_2$ was consumed by 28 days) compared to other fly ashes from pulverized combustion (the reaction continued until 90 days test). Pacewska *et al.* (2008b) also investigated the early hydration of cement paste with chemically activated (using CaCl_2 , Na_2SO_4 and NaOH) fly ash, using calorimetry and IR absorption. Chemical activators accelerated the hydration of cement pastes containing fly ash at early test ages (until 24 h) following water addition.

Roszczyński (2002) used the DTA-TG method to determine pozzolanic activity of materials (siliceous earth, diatomite, gaize, zeolite tuff and fly ash). Residual $\text{Ca}(\text{OH})_2$ in cement pastes containing pozzolanic materials (45% by mass) was determined at different ages (1, 3, 7, 28 and 90 days). Clear differences between various pozzolanic materials were noticed and this was suggested as a good method to determine differences in reactivity, but is cement-dependent.

Giergiczny (2004) used TG and DTA to investigate fly ash reactivity with $\text{Ca}(\text{OH})_2$ activated by different additives (CaSO_4 , CaCl_2 and silica fume). Acceleration in consumption of $\text{Ca}(\text{OH})_2$ in paste due to these additives was evaluated from TG measurements. DTA was found to be a good tool for evaluating the interaction between fly ash– $\text{Ca}(\text{OH})_2$ –additive systems.

Adonyi and Szécsényi (1996) distinguished the structural water from adsorbed or free in fly ash/water reaction products by TG. The reaction was found to be influenced by the fly ash chemical composition and the physical structure interaction period with water. Ubbriaco *et al.* (2001) studied reactivity of fly ash (from a municipal solid waste incinerator)

with lime using DTA/TG and XRD and evaluated hydrate phase formation (especially ettringite) from this.

Chaipanich and Nochaiya (2010) reported TGA results for binary and ternary cement combinations with fly ash and silica fume. With the same fly ash, a 10% level gave minor reactivity, however, at the 20% level, the $\text{Ca}(\text{OH})_2$ content was found to be 72% of the reference PC mix.

Shvarzman *et al.* (2002) investigated the influence of chemical and phase composition of various materials ((activated) kaolin clay, (activated) porcellanite, pumice, fly ash, silica fume and ground quartz) on pozzolanic activity. Mortars were prepared following ASTM C311 (ASTM, 2011a) and BS EN 450 (BSI, 2005c), cured in saturate limewater at 20°C for 1, 7, 28 and 90 days and then tested for compression to evaluate the pozzolanic reactivity. Thermal treatments were applied to activate standard kaolin, kaolin clay and porcellanite for 5 h in the temperature range 500 – 750°C. The phase transformation by thermal treatment was studied by XRD and DTA/TG. Pozzolanas containing amorphous aluminosilicates were found to be more reactive than those with amorphous silicate. Heat treatment increased pozzolanic activity of standard and local kaolin and porcellanite.

Moropoulou *et al.* (2004) evaluated the pozzolanic activity of natural pozzolana (earth of Milos) and artificial pozzolanas (ceramic powder produced by grinding handmade bricks and a metakaolin) by simultaneous DTA/TG analysis. Pastes were prepared by mixing pozzolanas with hydrated lime, in different ratios and cured under standard conditions (98% RH, 25°C) for 3, 7, 14 and 28 days. $\text{Ca}(\text{OH})_2$ consumption results indicated that lime/metakaolin paste was chemically stabilized at 14 days, however, the reaction of the two other pozzolanas with lime were not over, even at 28 days. Greatest reactivity was obtained for a lime/metakaolin ratio of 1 : 2, while this was 1 : 3 for a lime/ceramic power.

Heikal *et al.* (2003) studied the phase composition and hydration products from the pozzolanic activity of fly ashes using DTA and FTIR. The hydration of fly ash/lime mixes with fly ash levels of 60, 70, 80 and 90% were studied. Free lime, combined water contents and insoluble residue were measured up to 90 days. DTA results indicated the formation of C-S-H, C-A-H and C-A-S-H. A proportional relationship was found between the combined water and lime contents in the mix (especially between 7 and 90 days).

Electrical responses of reacting fly ashes

Majumdar and Lerner (1977) studied the applicability of fly ash pozzolanic activity assessment by dissolving it in hydrofluoric acid (HF) and recording the change in conductivity of the solution. Depending on the composition of fly ash, various ionic species (and of different concentrations) could dissolve in HF acid. It is also evident that the reaction of fly ash with PC will produce various ionic species in different concentrations. Therefore, it was concluded that conductivity measurements of this type of complex system may not reflect the pozzolanicity of the material accurately.

Luxan *et al.* (1989) proposed a rapid method to evaluate pozzolanicity by exposing the material to saturated lime solution and measuring the change in conductivity. A 200 ml saturated $\text{Ca}(\text{OH})_2$ solution was placed in a 600 ml polyethylene flask and stored in a water bath thermostatted at $40 \pm 1^\circ\text{C}$. Initial conductivity was measured and 5.0 g of pozzolanic materials added to the solution and mixed with an automatic stirrer. In 120 seconds, the conductivity was measured and based on the difference in conductivity measurements a ranking of pozzolanicity proposed (non-pozzolanic, variable pozzolanicity and good pozzolanicity ranges were, < 0.4 , $0.4 - 1.2$ and > 1.2 mS/cm respectively).

Paya *et al.* (2001) also followed Luxan *et al.* (1989) in evaluating the pozzolanic activity of low-lime fly ash by monitoring their conductivity in suspensions of $\text{Ca}(\text{OH})_2$ solution. Results were presented as a function of reaction times (100, 1000 and 10,000 s) and temperatures (40, 60 and 80°C). Loss in conductivity (%) of the suspension indicated pozzolanic activity. A hydrated lime/fly ash ratio of 0.04 : 1 was found to yield best results. Depending on fly ash properties, increasing the test temperature enhanced pozzolanic reactivity. However, the method was deemed unsuitable for high-lime fly ash.

Schwarz and Neithalath (2008) compared pozzolanic reactivity of fine glass powder, silica fume and Class F fly ash in cementitious systems by strength activity index (3, 7 and 28 days) and rapid electrical conductivity. Flame emission spectroscopy and electrical conductivity tests were carried out to evaluate alkali formation quantitatively. Both fly ash and glass powder were found to be moderate pozzolanic materials, whereas silica fume was classified as a highly pozzolanic material as per the classification by Luxan *et al.* (1989).

Sinthaworn and Nimityongskul (2009) developed a rapid technique to assess the reactivity of fly ash, silica fume, metakaolin, rice husk ash and river sand by measuring the electrical conductivity of cement suspensions at elevated temperature. Initially PC was mixed into water and kept undisturbed to enable suspended particles to settle and then the clear solution was transferred to another container to measure initial conductivity (10-11 mS/cm). 200 ml of this solution was poured into a flask and placed on a hotplate (maintaining $80 \pm 1^\circ\text{C}$) and mixed with a magnetic stirrer. 1.0 g of pozzolanic material was placed inside the solution and the change in conductivity was monitored for 4-28 hours (depending on the reactivity of the pozzolana) using a conductivity meter coupled with a personal computer. The reduction in normalized conductivity measurement correlated well with 28 days strength activity index (ASTM, 2011a) and indicated the potential of this method as a rapid pozzolanicity determination technique.

Zhang *et al.* (1998) investigated the early hydration of PC/fly ash blends (fly ash levels 20, 40 and 70%) and the effect of chemical activators (NaOH, $\text{Ca}(\text{OH})_2$ and Na_2SO_4) using microwave techniques (rate of change in dielectric constant) and conduction calorimetry. Fly ash was found to act mostly as an inert filler in the blends during the first 40 hours of hydration. To accelerate the early hydration of the blend, Na_2SO_4 was found to be more effective (at high fly ash content) than $\text{Ca}(\text{OH})_2$, whereas NaOH was not suitable for this.

McCarter and Tran (1996) developed a pozzolanicity index (PI) from conductivity measurements (over two days at ambient temperature) of pozzolana/ $\text{Ca}(\text{OH})_2$ mixtures. A range of pozzolanas including fly ash, metakaolin, micro-silica, calcined shale and GGBS were studied in two combinations, i.e. (i) exposing pozzolana in saturated lime solution; and (ii) blending pozzolana with $\text{Ca}(\text{OH})_2$ powder and then mixing with water (pozzolana/ $\text{Ca}(\text{OH})_2$ ratio 9 : 1 and water/solids ratio 0.45 – 1.2). The index considered the rate of pozzolanic reaction and time to setting as follows:

$$PI = \left(\frac{(d\sigma_t/dt)_{max}}{T} \right) \times 10^4 \text{ (S/m/h}^2\text{)} \quad (\text{Eq. 2-12})$$

Where, $\left(\frac{d\sigma_t}{dt} \right)_{max}$ maximum rate of change of conductivity
 T time to set from adding water

Wei and Li (2005) used an electrical resistivity method to study hydration in PC/fly ash systems (water/solids = 0.4 and fly ash levels 10 and 20%). A relationship between the

measured electrical resistivity, setting time and compressive strength of the paste at 1, 3, 7 and 28 days was found. The bulk electrical resistivity was also found to be dependent on the paste pore solution resistivity and porosity. The resistivity of the PC system was dominated by the change in solution ions and reduction in porosity during the early dissolution period and later ages respectively. PC/fly ash systems gave higher electrical resistivity than PC paste; however, the opposite occurred after setting.

Tashiro *et al.* (1994) evaluated pozzolanic activity by monitoring changes in electric-resistance (15 minutes intervals, up to 72 hours) and $\text{Ca}(\text{OH})_2$ consumption (by XRD) under accelerated curing conditions (70°C). Pastes (pozzolana : $\text{Ca}(\text{OH})_2 = 9 : 1$ or $8 : 2$ and $W/S = 0.5$ or 0.7) were made using fine ceramets (fine GGBS), fly ash, silica fume, kaolin, acid clay, zeolite and quartz activated by $\text{Ca}(\text{OH})_2$. In most cases, the electric resistances were found to be proportional to $\text{Ca}(\text{OH})_2$ consumption (except fly ash).

Special instrumental methods

Special instrumental methods, for example, Magic-angle spinning (MAS) nuclear magnetic resonance (NMR) of ^{29}Si , ^{27}Al and ^1H , inductively coupled plasma optical emission spectroscopy (ICP), X-ray photoelectron spectroscopy (XPS) and IR may provide valuable information on the kinetics of pozzolanic reactions. These may also help to evaluate the effect of certain chemicals added to accelerate the process in the method development stage of a research project. Nevertheless, due to their very high capital cost, techniques are not anticipated to be applicable to the fly ash production industry.

Yang *et al.* (2008) investigated the effect of mechanical grinding and/or alkali-activation on fly ash using NMR and SEM. The degree of polymerisation and structures of fly ash were compared before and after treatment. Mechanical grinding breaks Al–O networks and produces small symmetrical molecular structures. Alkali activation reduces the silicon monomer (Q^0 structure) and produces polymers (mainly Q^2). The polymerization degree of silicon-oxygen was found to be related to the potential activity of fly ash.

Rowles *et al.* (2007) also used ^{29}Si , ^{27}Al , ^1H and ^{23}Na Magic-Angle Spinning (MAS) NMR to study the bonding character of polymers originating from kaolinite, metakaolinite, silica fume and arbitrary samples prepared by mixing NaOH and silica fume (Si-to-Al and

Na-to-Al molar ratios between 1.08 – 3.0 and 0.57 – 2.0, respectively). The technique related composition, bonding character and compressive strength properties in alumina-silicate inorganic polymers. As with Yang *et al.* (2008), the systematic variation of the ^{29}Si chemical shift was correlated directly with strength properties.

Christensen *et al.* (1994) used impedance spectroscopy for testing the microstructure of hydrating cement-based materials. High relative dielectric constants (of the order of 10^5) measured just after set were related to the pore size distribution and C-S-H layer thickness between pores. Overall, conductivity was found to be related to the pore volume fraction, the conductivity of the pore solution and its interconnectivity. The normalized conductivity (to the pore solution) is a measure of pore interconnectivity and it was possible to use this for prediction of engineering properties (ionic diffusivity and water permeability).

Xu and Deventer (2003) studied the effect of structural and surface properties of source materials (kaolinite, albite, and fly ash) on geopolymerization. Characterisation of the source materials and geopolymers were conducted by using XRD, XRF, X-ray photoelectron spectroscopy, ^{27}Al and ^{29}Si MAS NMR spectroscopy, and SEM. Amorphous fly ash with lower structural binding energy gave highest reactivity during geopolymerization.

2.3 Air-Entraining Admixture Adsorption Assessment

Of the range of concrete durability issues arising, freeze/thaw attack typically accounts for about 10% of those in the UK and elsewhere (CIRIA, 2001). Entraining an appropriate quantity of air (approximately 5–6 vol%) with particular bubble size (less than 250 μm) characteristics is a well-established method of providing concrete with enhanced resistance to damage from this process. Several properties of concrete are also enhanced by entrained air. The inclusion of air bubbles improves workability and cohesion (Mielenz *et al.* 1958). However, with modern concretes the wider choice of constituent materials has made air-entrainment more difficult.

A considerable amount of research has examined changes in the required quantity of air-entraining admixture (AEA) to entrain a given quantity of air when coal combustion fly ash is used in combination with PC in concrete, since it is critical to performance and cost.

Studies have ascribed an observed increase in the level of AEA required in fly ash concrete to the quantity and nature of carbon present (Freeman *et al.*, 1997; Gao *et al.*, 1997; Dhir *et al.*, 1999; Sporel *et al.*, 2009; Folliard *et al.*, 2009; JolociEUR *et al.*, 2009). The AEAs are strongly adsorbed by this fraction of fly ash and tend to affect the stability of the air-water/cement interface, consequently reducing the quantity of entrained air achieved (Hachmann *et al.*, 1998; Pedersen *et al.*, 2008).

A schematic diagram of AEA adsorption by fly ash carbon is shown in Figure 2-3. The small circles of the AEAs correspond to the polar end and the tail corresponds to the hydrophobic end. Increasing the AEA dose can compensate this adsorption. However, depending on the other properties of fly ash (even where fly ash satisfies LOI requirements of standards), difficulties have still been encountered during air-entrainment in fly ash concrete (with LOI even less than 0.5%; Joshi and Lohtia (1997)).

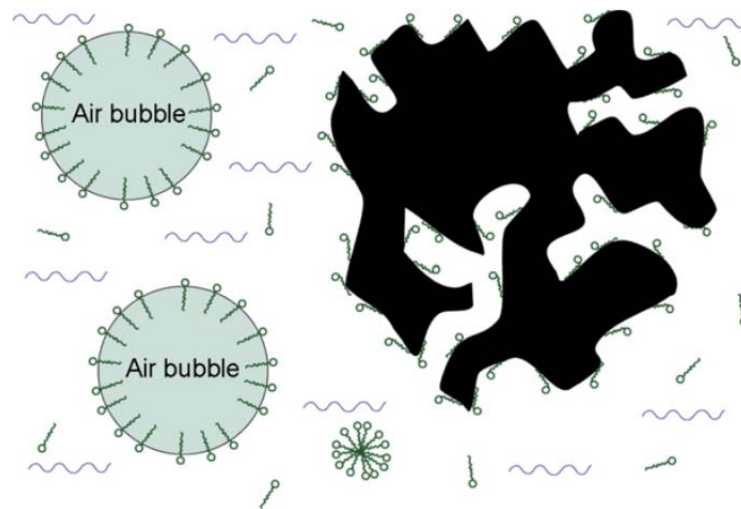


Figure 2-3. AEAs adsorption sites at air/water interface and carbon surface. (based on Hachmann *et al.*, 1998 and Pedersen *et al.*, 2008).

The degree of AEA adsorption by carbon in fly ash is especially important because many fly ashes contain increasing levels of carbon resulting from the use of low-NO_x burners to control emissions during coal combustion (Hower *et al.*, 1997) and also fluctuating load conditions (Clendenning and Durie, 1962). In the following sections, the literature relating to carbon content determination and its characterization are discussed. Thereafter, available techniques for estimating AEA adsorption by fly ash are evaluated.

2.3.1 Carbon content and characterisation

Studies have clearly demonstrated the influence of unburned carbon on AEA demand. However, oxidised fly ash (burned in a laboratory oven) was found to be not influenced by this (Clendenning and Durie, 1962; Hachmann *et al.*, 1998; Külaots *et al.*, 2003). The degree of AEA adsorption by fly ash depends on several factors including, (i) carbon content; (ii) carbon type (e.g. coarse particles or soot); (iii) specific surface area of fly ash (porosity); (iv) accessibility of AEA to particle surfaces (internal and external); and (v) chemical nature of these surfaces (polarity) (Gao *et al.*, 1997; Hill *et al.*, 1997; Maroto-Valer *et al.*, 2001, Külaots *et al.*, 2004; Pedersen *et al.*, 2008). LOI measurements can give an approximation of carbon content, while direct and more accurate measurements of unburnt carbon quantity can be carried out by controlled-atmosphere programmed-temperature oxidation.

Measurement of carbon content

The LOI test used in Europe and the UK is covered in BS EN 450-1 (BSI, 2005c) and BS EN 196-2 (BSI, 2005b). The fly ash samples are placed in a furnace at $950 \pm 25^\circ\text{C}$ for 1 hour. The loss by mass is considered a bulk estimate of carbon content. Similar procedures are also specified in ASTM C311 (at $750 \pm 50^\circ\text{C}$; ASTM 2011a). According to BS EN 450-1 (BSI, 2005c), fly ash could be used in concrete construction if they fall within the limits of the categories given below, while the maximum limit permitted by ASTM C618 (ASTM, 2012) is 6.0%:

- Category A: Not greater than 5.0 % by mass
- Category B: Between 2.0 % and 7.0 % by mass
- Category C: Between 4.0 % and 9.0 % by mass

During a LOI test, fly ash loses mass from the combustion of unburned carbon, decomposition of carbonates and sulfates and removal of water that is combined in clay minerals. While the first of these is the main contributor to this mass loss, there is a possibility of mass gain from the oxidation of Fe and S (Wesche, 2005). Dodson (1990) claimed LOI accounts for at least 99% of the carbon quantity. However, other studies have found significant differences from this and suggested LOI can only be used as an approximation of bulk carbon (Brown and Dykstra, 1995; Fan and Brown, 2001; Burris *et al.*, 2005).

As with the oxidation in an oven, modern instruments are available for rapid determination of LOI. The HOT FOIL LOI instrument (FERCo, 2012) is a bench-top analyzer which uses an electric current to burn a small quantity of fly ash (20-80 mg) and can provide results within 7-10 minutes. The instrument can be used to monitor and control fly ash LOI, enabling rapid decisions on sales/disposal. It is possible to use the real-time results for boiler tuning, mill optimization, burner and over-fire air (OFA) damper adjustments to achieve better carbon burnout.

In addition to LOI tests, the carbon content can also be determined by direct measurements. In BS EN 450-1 (BSI, 2005c), direct measurement of unburnt carbon is specified in accordance with ISO 10694 (ISO, 1995). During the test, the carbon is oxidised (in a closed chamber) to CO₂, by heating fly ash to at least 900°C in a flow of oxygen-containing gas. The quantity of CO₂ released can then be measured by titrimetry, gravimetry, conductometry, gas chromatography or using an infrared detection method.

Hill *et al.* (1997) used a LECO analyser (LECO Corporation, 2012) to quantify carbon, oxygen, hydrogen and sulfur in the high carbon fraction of fly ash. The instrument is traditionally used for the measurement of carbon and sulfur in metals, ores, ceramic and other inorganic materials. The sample is combusted in a stream of purified O₂, which produces CO₂ and SO₂ from carbon and sulfur respectively. These species are then detected and quantified by infrared application. The instrument is capable of detecting carbon and sulfur down to approximately 0.005% by mass. A similar apparatus, ELTRA model CS-800 (ELTRA, 2012) was used by Pedersen *et al.* (2007) for carbon content determination.

Studies (Gao *et al.*, 1997; Freeman *et al.*, 1997) showed a poor correlation between LOI and foam index, while Yu *et al.* (2000) reported a strong correlation between these parameters. An earlier study by Clendenning and Durie (1962) found a good correlation between AEA requirement and carbon content of fly ashes obtained from the same source; however, this was not valid for samples collected between sources. Differences in coal source (coal composition), boiler and burning conditions could cause this behaviour. Although carbon content (commonly estimated from LOI) is widely used as a limiting parameter for fly ash quality assessment, a number of studies have demonstrated that it is inadequate as an

indicator of air entraining performance of fly ash concrete (Hill *et al.*, 1997; Maroto-Valer *et al.*, 2001; Külaots *et al.*, 2004). Therefore, research has examined differing forms of unburned carbon present in fly ash, which are discussed in the following section.

Characterization of unburned carbon

Characterization of unburned carbon in fly ash and their effects on AEA adsorption have been widely studied (Hill *et al.*, 1997; Freeman *et al.*, 1997; Maroto-Valer *et al.*, 2001; Külaots *et al.*, 2004). These include the effect of coal type (co-fuel), active size fraction of carbon, its porosity, polarity and petrography.

Levels of carbon present in different size fractions of fly ash have been investigated in several studies. Dry-sieve size classification followed by measurement of the total mass and LOI of each size fraction have been performed (Yu *et al.*, 2000; Külaots *et al.*, 2004). Fly ashes tested under this system indicated increasing carbon content with particle size. However, as per Külaots *et al.* (2004), the relative AEA adsorption by the coarse fraction of fly ash was lower than that of the fine fraction. The study also explored the role of coal type on level and characteristics of unburned carbon. It was concluded that relatively lower rank coals leave less small fraction unburned carbon, while the opposite applies for higher rank coals.

Petrographic examinations of a number of high-carbon fly ashes have indicated that the unburned carbon is not visually uniform. Hower *et al.* (1995) reported three microscopically distinct carbon types, such as: (i) inertinite particles, which are relatively solid and considered unfused during the combustion process; (ii) isotropic coke or disordered carbon; and (iii) anisotropic coke or ordered carbon. The latter two are extensively reacted particles and indeed have passed through a molten stage. According to Hill *et al.* (1997) most commercial activated carbons (used as adsorbents) are isotropic by nature, whereas anisotropic carbon is adsorptive but to a lower degree than the former. Further work by Hower *et al.* (1997) reported that anisotropic type carbon mainly originates from higher rank coals.

ASTM D2799 (ASTM, 2011d) describes quantitative techniques for analysis of the maceral composition of coal, based on point counting. Hill *et al.* (1997) applied this to evaluate the

distribution of carbon forms within fly ash and their fractions using optical microscopy. Maroto-Valer *et al.* (2001) developed a method to isolate the three differing forms of unburned carbon. The process includes preliminary triboelectrostatic enrichment or acid digestion, followed by density gradient centrifugation (DGC) with a high-density lithium polytungstate media (2.85 g/cm³). The highest purity organic fractions from these separations were then examined using several techniques, including elemental and surface area analyses. The density of inertinite, isotropic coke and anisotropic coke particles were considered as <1650 kg/m³, between 1720 and 1780 kg/m³ and between 1880 and 1940 kg/m³. The surface area order of the different types of carbon was found to be inertinite < isotropic carbon < anisotropic carbon (Maroto-Valer *et al.*, 2001). The study also reported higher oxygen concentrations in amorphous type carbon.

Thermal analysis to characterize the carbon in fly ash was carried out in several studies (Hill *et al.*, 1997; Paya *et al.*, 1998). Hill *et al.* (1997) found two exotherms 540 and 590°C in DTA of which the lower one corresponded to a more easily-oxidized form of carbon (amorphous carbon) which adsorbs more AEA. Paya *et al.* (1998) reported the maximum carbon content in particle sizes > 80 µm in diameter. However, Spörel *et al.* (2009) indicated little or no influence of carbon particles of size > 80 µm in diameter on AEA demand in fly ash concrete.

Studies have also reported the effect of carbon surface polarity on AEA adsorption (Gao *et al.*, 1997, 2001 & 2002; Hill *et al.*, 1997; Hachmann *et al.*, 1998). Vapour-phase adsorption experiments on high-carbon fractions were conducted by Hill *et al.* (1997) with carbon tetrachloride (acetone as the adsorptive). It was indicated that inertinite or isotropic coke provided more polar sites on these carbons than anisotropic coke and tended to adsorb more AEA, which are also polar compounds. Hachmann *et al.* (1998) showed that modification to carbon surfaces can alter its surfactant adsorptivity. Post-combustion, air oxidation at temperatures above about 300°C reduced activity, whereas heat treatment at 900°C in argon increased this. The study by Gao *et al.* (2001) noticed significant reductions in AEA adsorption after ozone treatment in a fixed bed reactor, which was again confirmed in a further study by the same authors (Gao *et al.*, 2002).

Hill *et al.* (1997) carried out diffuse reflectance FTIR to characterize the carbon bands, however, no carbonyl functional group was found. The study then assumed that, the high oxygen content detected in some fly ash samples was present as heterocyclic compounds. Venter and Vannice (1987) reported that amorphous carbons (subjected to medium-to-high temperatures) are opaque to IR radiation and difficult to detect. However, Saperstein (1986) identified high-frequency bands of adsorbed toluene on carbon black using IR spectroscopy in his experiments.

The use of co-fuels in coal combustion also influences the surface characteristics of residual carbon and their AEA adsorption characteristics. Yu *et al.* (2000) found significantly lower AEA adsorption with pet-coke co-combustion fly ash, even when the level of unburned carbon present was significantly higher. This was attributed to the improved surface characteristics (relatively solid in nature) of co-combustion fly ashes. This tendency was confirmed in a later study by Scott and Thomas (2007), where it was comparatively easier to entrain an appropriate quantity of air in a pet-coke co-combustion fly ash concrete with significantly lower AEA doses than that with coal-only fly ash.

Specific surface area of fly ash (porosity)

The surface area of solids is generally and more precisely determined from physical adsorption of gas molecules on the surface, based on the BET (Brunauer *et al.*, 1938) method. This procedure has been applied in numerous studies for the determination of fly ash specific surface area in the last two decades (Hill *et al.*, 1997; Freeman *et al.*, 1997; Gao *et al.*, 1997; Yu *et al.*, 2000; Külaots *et al.*, 2004). BET theory provides an important analysis technique for the measurement of the specific surface area of a material. The BET equation is expressed as:

$$\frac{1}{v\left[\left(\frac{P_0}{P}\right)-1\right]} = \frac{c-1}{v_m c} \left(\frac{P}{P_0}\right) + \frac{1}{v_m c} \quad (\text{Eq. 2-13})$$

Where, P and P_0 are the equilibrium and saturation pressure of adsorbates at the temperature of adsorption; v is the adsorbed gas quantity (in volume units); v_m is the monolayer of adsorbed gas quantity; and c is the BET constant, which is expressed as:

$$c = \exp\left(\frac{E_1 - E_L}{RT}\right) \quad (\text{Eq. 2-14})$$

Where, E_1 is the heat of adsorption for the first layer; E_L is heat of adsorption for the second and higher layers and is equal to the heat of liquefaction; R is the gas constant; and T is the temperature in Kelvin

The active sites which are responsible for AEA adsorption are mainly found on the carbon surface (Pedersen *et al.*, 2008). Külaots *et al.*, (2004) found the surface area of the fly ash carbon part up to several hundred times (45 - 400 m²/g) higher than that of its mineral part (0.7 – 0.8 m²/g), which indicates that although the carbon proportion is relatively small in fly ash, its contribution to the specific surface area is substantial. The porosity of carbon is mainly responsible for the wide variation in specific surface area found between fly ashes. Being relatively solid in nature the mineral part makes a significantly lower contribution to surface area and is almost constant for different fly ashes.

Hachmann *et al.* (1998) studied the development of pore surface area from the burning of lignite and bituminous coals. At the initial stage of burning, devolatilization and early char combustion caused opening of pore space. However, further conversion at high temperature decreased the pore volume. In contrast to the latter, further combustion at low temperature (e.g. low-NO_x burning) lead to the continued development of more pores with higher active sites (Gao *et al.*, 2002).

A comparison test was carried out by Freeman *et al.* (1997) and claimed that a better correlation was obtained between BET specific surface area and AEA adsorption than with LOI, which was supported by Gao *et al.* (1997). Hill *et al.* (1998) observed similar behaviour with a less clear trend. However, a study by Yu *et al.* (2000) found completely the opposite effect with co-combustion fly ash. The carbon content correlated better with AEA adsorption than with specific surface area. More recent work suggests that N₂ gas adsorption by BET was the only fly ash parameter with a correlation to the AEA demand to entrain a certain air content in fresh concrete. Higher specific surface area was also found to be related to a greater loss in air content over a 45 minute period following mixing (Spörel *et al.*, 2009). However, in an earlier study (Dhir *et al.*, 1999) only minor losses in air content over time were reported.

The pore size distribution is another factor influencing AEA demand of fly ash concrete. The International Union of Pure and Applied Chemistry (IUPAC) classifies carbon pores in

three distinctive categories, e.g. micro pores (< 2nm), meso pores (2-50 nm), and macro pores (> 450nm). Studies (Gao *et al.*, 1997; Yu *et al.*, 2000; Külaots *et al.*, 2004) indicate that AEAs are not accessible to fine micropores, although this area can be covered by smaller N₂ gas (molecular size 0.43 nm) molecules during surface area measurements. This might cause lower AEA adsorption by larger carbon particles (especially > 80 µm size) of which a significant part of the inner micro pores remain unable to contribute to the adsorption process. Gao *et al.* (2002) applied Barrett Joyner Hallender (BJH) theory to N₂ adsorption isotherm data to estimate non-micro pores. From the fly ash produced in their pilot scale combustion of petroleum coke, a better correlation was obtained between the AEA adsorption and non-micro pores than with total pore space. Therefore, a fine carbon with higher surface area (soot) is potentially more active during the AEA adsorption process. However, Gao *et al.* (1997) indicated that the percentage of soot in a typical fly ash is low.

2.3.2 Test methods to assess fly ash/AEA interaction

The test used most often for indirectly measuring the relative adsorption of AEAs by fly ash is the foam index test (Dodson, 1990). Since the results of the foam index test may be influenced by modifications to the procedure and can be operator dependent, some alternatives have been developed, either as improved foam index test methods, or different means of evaluating fly ash/AEA behaviour. These include spectroscopic methods (Yu *et al.*, 2000; Baltrus and LaCount 2001) and a combination of tests (Stencel *et al.*, 2009). Surface tension measurements have also been proposed as an alternative to the foam index test (Pedersen *et al.*, 2007). Furthermore, an automated foam index test (AFIT) has been developed (Stencel *et al.*, 2009).

The sorptive nature of fly ash suggests that an alternative approach to establish fly ash/AEA interaction may be through the adoption of dye adsorption tests from other fields (e.g. Choy *et al.*, 2000; Hameed *et al.*, 2007).

Foam index test

Whilst other methods have enabled behaviour between materials to be investigated, arguably, the foam index test (a laboratory titration procedure, involving incremental additions of AEA to a PC/fly ash/water mixture until a stable foam is formed

(Dodson 1990)) given its relative simplicity, offers practical advantages. The foam index test was originally proposed by Dodson at an informal meeting of the Transportation Research Board in Washington D C (Dodson, 1980). As per Dodson (1990) it has four steps:

1. A 1 : 20 (by volume) dilute commercial AEA solution is prepared with water.
2. A 20.0 g fly ash/PC combination sample (or cement) is placed in a clean, dry 118.25 ml glass bottle. 50 ml of distilled water is added to the bottle, the cap closed, and this shaken for 1 minute to wet the fly ash/PC thoroughly.
3. Standard diluted AEA is added to the bottle in 0.2 ml aliquots from a burette. After each addition, the bottle is capped and shaken vigorously for 15 seconds. The foam stability in the bottle is observed by laying this on its side (or upright).
4. The quantity of dilute AEA (in ml), needed to produce a stable foam (i.e. no bubbles can be seen breaking for a period of 15 seconds), is the foam index.

The foam index is effective in determining if specific materials will require more or less AEA relative to others. The quantity of AEA required to obtain stable foam mainly depends on (i) fly ash properties; (ii) type of the AEA; and (iii) fly ash-PC interactions.

This can be a quality control test for fly ash to estimate the quantity of AEA required for achieving a stable foam (Pedersen *et al.*, 2008). The foam index test performed on the same materials gave a good correlation with the air content in mortar (Hill *et al.*, 1998; GRACE, 2006) or AEA requirements in mortar (Helmuth, 1987). Recent work by Spörel *et al.* (2009) indicates a very good relationship between foam index and AEA dose required to entrain a certain quantity of air in both mortar and concrete.

Although guidance on the foam index test is available (e.g. Dodson 1990; Gao *et al.*, 1997; GRACE 2006 and Taylor *et al.*, 2006 (US Federal Highway Administration)), there are currently no national/international standards for this. As a result, variations in test procedures have been noted in the literature as shown in Table 2-1. These include different use of (i) AEA and dilution factors; (ii) size of the vial (Folliard *et al.*, 2009); (iii) shaking durations; (iv) definitions of the endpoint; and (v) quantities of PC (Gebler and Klieger 1983; Gao *et al.*, 1997; LaCount and Kern 2005; Pedersen *et al.*, 2007). Figure 2-4 gives the definition of stable foam (i.e. test end point) reported in relevant studies.

Table 2-1. Comparison of foam index test methods from literature

METHOD	PC	FLY ASH	WATER	AEA AND PROCEDURE	DEFINITION OF END POINT AND CALCULATION
Dodson, 1990	20 g	-	50 ml (distilled) in a 118 ml glass bottle	1:20 by volume dilution, 0.2 ml increment. Shake vigorously for 15 s after each addition	Foam index = the amount of the dilute AEA, in ml, needed to produce a stable foam (i.e. no bubbles can be seen breaking for a period of 15 s).
Taylor <i>et al.</i> , 2006 (FHWA)	20 g (control)	-	50 ml (potable) in a 500 ml wide mouthed jar	AEA dilution and increment are not specified. Shake vigorously for 15 s after each addition.	Place the jar in an upright position for 45 s. The endpoint is that bubbles exist as continuous foam over the entire surface of the suspension in the jar. Foam Index = 100 (AEA required for test mixture) / (AEA required for control mixture)
	16 g	4g			
Gao <i>et al.</i> , 1997; Külaots <i>et al.</i> , 2003; Pedersen <i>et al.</i> , 2007	8 g (control)	-	25 ml (distilled) in a 70 ml bottle	10 vol % aqueous solution of Darex II added drop-wise from a 2 ml microburette. Shake vigorously for 15 s after each addition.	The endpoint is realized when a constant foam is maintained on the surface for at least 45 s. Foam index = the volume of diluted AEA required to produce stable foam. Effective foam index = foam index (fly ash/cement mixture) – foam index (control).
	8 g	2 g			
Hill <i>et al.</i> , 1997	PC : FA = 3 : 1		w/s = 5	Same as Dodson's	Same as Dodson's
LaCount and Kern, 2005	-	2 g	5 ml (distilled) in a 15 ml vial	1:40 Darex solution, 0.05 ml increment using a 2 ml microburette, shake vigorously for 15 s after each addition.	Foam index = the minimum amount of diluted AEA needed to produce a stable foam that persisted for 15 s and obscured all at the centre of the foam layer
GRACE, 2006	20 g (control)	-	50 ml in a 125 ml capacity glass jar.	1:1 to 1:10 AEA solution in increments of 2 to 5 drops at a time. Cap and shake the jar vigorously for 15 s after each addition.	Foam index = the minimum amount of diluted AEA needed to produce a foam that is stable (bubbles exist over the entire surface) for 45 s
	16 g	4 g			

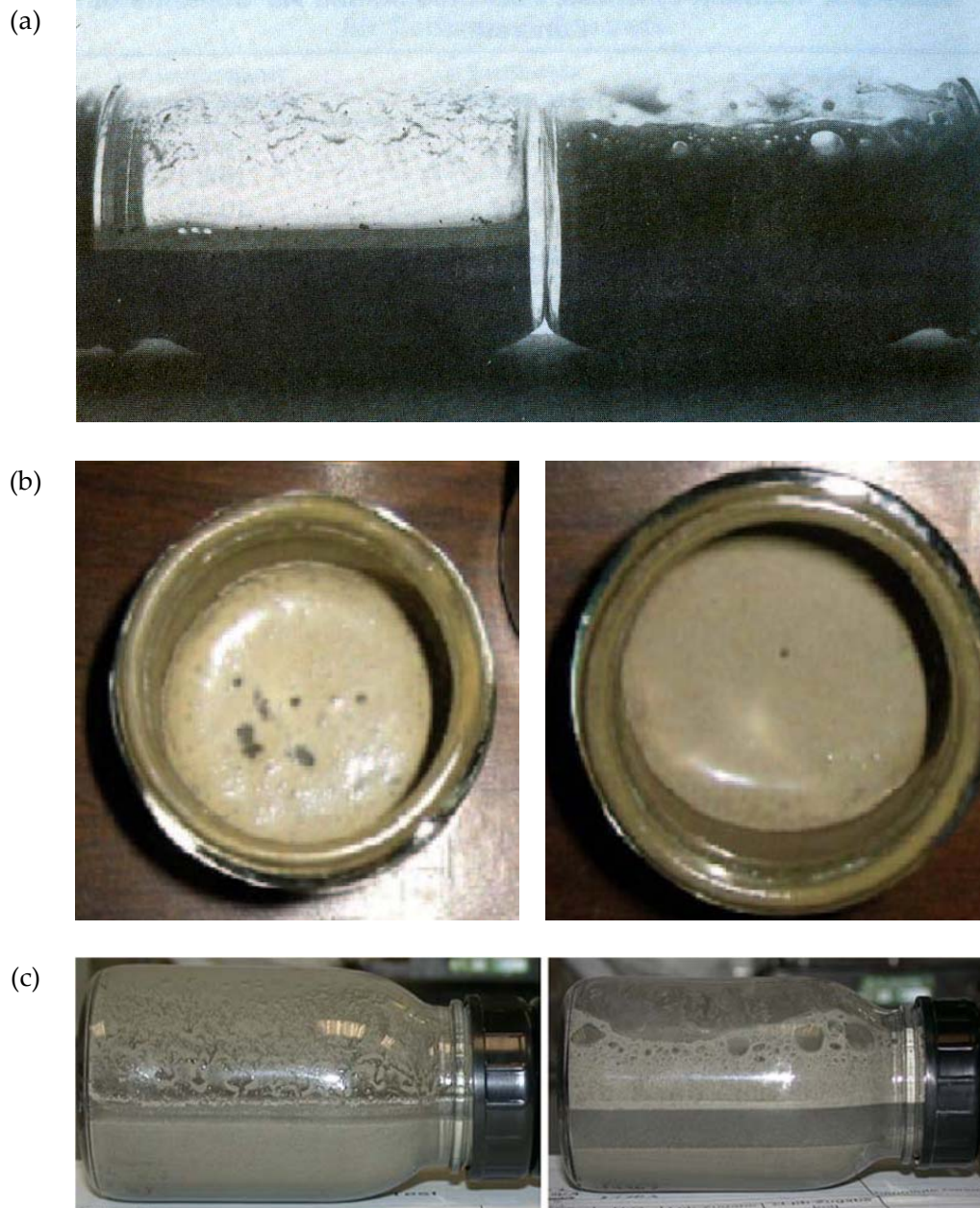


Figure 2-4. Definition of foam index test end point reported in literature: (a) Dodson, 1990; (b) Grace, 2006; and (c) Spörel *et al.*, 2009

A number of candidate commercial AEAs have been adopted in these procedures. Test results are sensitive to the strength of AEAs (differences in strength are influenced by the various natural or synthetic sources used) and this can degrade with time (Külaots *et al.*, 2003, Spörel *et al.*, 2009). Therefore, the results between labs (or even within a single lab) can be difficult to compare once the test AEA is changed (Külaots *et al.*, 2003). To develop a standardised foam index test, several approaches have been recommended, such as using

standard reagent instead of commercial AEAs and using spectroscopic methods instead of visual foam stability judgements (Manz 1999; Külaots *et al.*, 2003; Pedersen *et al.*, 2008).

Three standard reagents i.e. sodium dodecyl benzene sulfonate (SDBS), sodium dodecyl sulfate (SDS) and abietic acid sodium salt (AAS) were examined by Külaots *et al.* (2003). The concentrations of solutions used were 0.025 M, 0.035 M and 0.05 M for SDBS (MW = 348 g/mol), SDS (MW = 288 g/mol) and AAS (MW = 324 g/mol) respectively. The study indicated a good correlation between the adsorption behaviour of commercial anionic AEA materials and the three standard reagents.

It was also found that the uptake of AAS was over five times greater than that of SDS, while this was similar between SDS and SDBS. However, the uptake of different standard reagents correlated well with one another.

A better correlation with commercial AEA (Darex II) was obtained when the SDBS concentration was reduced to between 0.00625 - 0.001 M. It appeared that the SDBS might be a good choice for a pure surfactant-based standardised foam index test. Other studies used SDBS including 0.00287 - 0.00459 M by Hill *et al.* (1997) to examine the characteristics of the carbonaceous material in fly ash and 0.00172 - 0.00517 M by Pedersen *et al.* (2007) in UV-Vis spectroscopic tests and surface tension measurements (diluted to 0.00143 - 0.00287 M before the measurements).

Another issue exists with the degree of manual (hand) shaking that should be applied by operators during the test. Indeed, little information in the guidance is given on this, except that it should be carried out for a fixed time period (Folliard *et al.*, 2009). Similarly, identification of the end point of the test (i.e. a stable foam, maintained for 45 s, over the mixture surface) is made visually, and is likely to be influenced by the operator. If these aspects of the test could be improved and the procedure standardised, this would assist in the process of combining AEA and fly ash in concrete. Use of an automatic mechanical, shaker for example, could reduce the variation of this applied effort during the test.

UV-Vis spectroscopic measurements

UV-Vis spectroscopy is a technique to evaluate the properties of various technologically important materials for example pigments, coatings, windows, and filters from its

absorption, transmission, and reflectivity measurements (GmbH, 2012). During testing at least a portion of the UV-Vis spectrum is recorded to characterize the optical or electronic properties of materials. The attenuation of a beam of light after it passes through a sample or after reflection from its surface can enable a quantitative evaluation of the material's properties. Absorption measurements can be at a single wavelength, or over an extended spectral range. The UV-Vis spectral range is approximately 190 to 900 nm and spans the range of human visible acuity (400 -750 nm).

Absorbance spectroscopy is commonly known as *spectrophotometry* and is an analytical technique based on measuring the quantity of light absorbed by a sample at a given wavelength. Other available spectroscopic methods include *Transmission* and *Reflection Spectroscopy*, which can be widely used for solid, liquid or gaseous material. The concentration of an analyte in solution can be determined by measuring the absorbance at specific wavelengths and applying the Beer-Lambert Law. The law gives linear relationships between absorbance and concentration of an absorber of electromagnetic radiation. The general Beer-Lambert law is usually given as follows (Equation 2-14),

$$A = -\log_{10}(I_T/I_0) = -\epsilon_{\lambda} \times d \times c \quad (\text{Eq. 2-15})$$

Where, A is the measured absorbance; I_T is the monochromatic radiant power transmitted by the analyte; I_0 is the monochromatic radiant power incident on the medium; τ_i is the internal transmittance ($=I_T/I_0$); ϵ_{λ} is a wavelength-dependent absorptivity coefficient; d is the path length; and c is the analyte concentration.

A schematic of single-beam UV-Vis spectrometer measurement and its related parameters to the *Beer-Lambert Law* is shown in Figure 2-5. Single-beam spectrometers can utilize fixed wavelength light or continuous sources. Instruments with the latter have a dispersing element and aperture or slit to select a single wavelength before the light passes through the sample cell. A photodiode detector is used to measure the intensity of light. The instrument should be calibrated with a reference cell containing only a solvent for an absorbance measurement.

UV-Vis spectroscopic measurements have been used to evaluate fly ash/AEA behaviour in several studies including Hill *et al.* (1997), Yu *et al.* (2000), Baltrus and LaCount (2001) and

Pedersen *et al.* (2007). Table 2-2 compares the different approaches considered in the literature on this. As with the foam index test procedure, methodologies vary significantly in terms of AEA (including dilution factor), fly ash characteristics, test period and process.

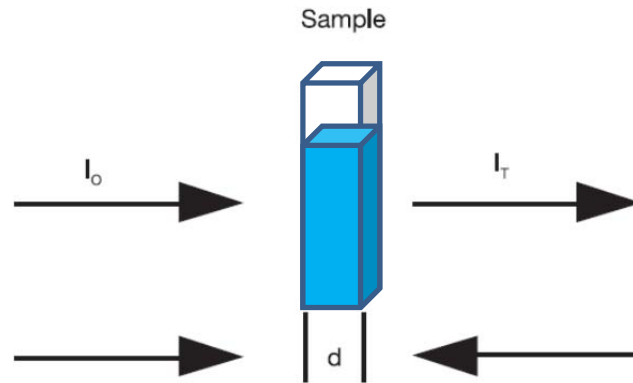


Figure 2-5. Schematic of UV-vis measurement and parameters in Beer-Lambert's law

Table 2-2. Fly ash/AEA interaction tests by UV-Vis spectroscopic method

METHOD	FLY ASH	WATER	AEA AND DILUTION	ABSORBANCE WAVELENGTH	PROCEDURE
Hill <i>et al.</i> , 1997	15 g	150 ml	1000 and 1600 ppm SDBS	Range of wavelength	Absorbance was recorded over period of time to create profile in a closed system
Yu <i>et al.</i> , 2000	20 mg	25 ml (distilled)	0.5 ml of 10% Darex II	233 nm	5 ml aliquot was tested at 1, 15, 30 and 60 minute(s). The relative absorbance, A/A_0 was
Baltrus and LaCount, 2001	5 mg	-	25 ml of 0.125% Darex II	195-300 nm (232.8 nm)	Absorbance tested at 0, 10 and 20 minutes in air, N_2 and CO_2 medium
Pedersen <i>et al.</i> , 2007	2 g (8 g PC)	-	25 ml 0.6 – 1.8 g/lit SDBS	223 nm	Ca^{2+} and Mg^{2+} in solution were considered. Test period of 3 days.

A/A_0 : The relative absorbance; ratio of optical absorbance (A) tested with fly ash sample and (A_0) without

In UV-Vis measurements carried out by Hill *et al.* (1997), fly ash was mixed with deionised water in a reaction vessel. The slurry was pumped through a pre-filter and then through a flow cell for absorbance measurements before returning to the vessel. A background scan was collected and then an aliquot of AEA was introduced. A profile of the concentration of AEA remaining in the solution with time was then recorded. This was a closed system and therefore the results were not affected by the environment air cover conditions.

Yu *et al.* (2000) mixed fly ash and diluted AEA (Darex II) with distilled water. Aliquots were extracted at different intervals using a filter syringe and transferred to cuvettes to measure the optical absorbance (A). Tests were also carried out on an aliquot taken from a solution without a fly ash sample (A_0). The relative absorbance, A/A_0 , indicated the concentration of UV-active compounds remaining in the solution with time.

A set of experiments focused on determining the optimal parameters for UV-Vis measurements was carried out by Baltrus and LaCount (2001). It was found that Darex gave a linear response with absorbance up to a concentration of 0.125%. Therefore, it was suggested that the procedure followed in a similar earlier study (Yu *et al.*, 2000) using a Darex concentration of 0.2% (approximately) could lead to miscalculation, unless the concentration of AEA remaining in solution after its interaction with fly ash fell below 0.125%. It was also found that 0.05 g of sample was an ideal quantity and the experiment should be carried out in nitrogen cover conditions.

With these established, better relative precision or less deviation (relative standard deviation (RSD) = 4.8%) was obtained than the foam index test (RSD = 7.2%). However, there was no correlation between the quantity of AEA adsorbed and carbon content of the fly ash. Correlations between the former and foam index were also found to be poor. Absorbance measurement are likely to be affected by the variation in quantity of soluble ions (Ca^{2+} and Mg^{2+}) and this was considered a possible cause of the lack of correlation.

Külaots *et al.* (2003) expressed concern about using commercial AEA for UV-Vis measurements. The light absorbance of different components of these AEAs is not same. Thus, significant differences in the interpretation of results may result, depending on the interaction of particular light sensitive components with fly ash. Therefore, it was

suggested that standard reagents (with known optical properties) should be used for spectroscopic tests.

As with the work of Baltrus and LaCount (2001), UV–Vis spectroscopic test results reported by Pedersen *et al.* (2007) were also poorly correlated to Foam index. It was suggested that the parameters affecting foam stability may complicate the development of spectroscopic assays. The method may only indicate a surfactant concentration in solution and not an overall contribution to foam stability. The study considered the effect of dissolved electrolyte such as, Ca^{2+} and Mg^{2+} from PC and fly ash (suggested in the earlier study of Baltrus and LaCount (2001)) on the absorbance of SDBS in water.

The foam index test usually requires approximately 5 to 20 minutes to complete a measurement. The UV–Vis test offers a more precise measurement of the behaviour between the AEA and fly ash/carbon components than the foam index test. However, it can be complicated by a number of factors. A better understanding of the nature of the interactions between AEA and cement/fly ash components (AEA with Ca^{2+} and Mg^{2+} ions, as well as precipitation of AEA from solutions exposed to air) that influence the foam index test is required to refine the UV–Vis method (Baltrus and LaCount, 2001). While Yu *et al.* (2000) found adsorption continued up to 60 minutes, Baltrus and LaCount (2001) reported that 20 minutes is sufficient to achieve equilibrium conditions. The former seemed to be because of interaction between AEA and atmospheric CO_2 , while the fly ash carbon active sites were saturated. Hill *et al.* (1997) used a test period as short as 10 minutes within a N_2 environment. Given these variations in test procedure and results, the method does not appear promising for assessment of fly ash/AEA interaction.

Surface tension measurements

Maximum bubble pressure measurements can be used to estimate the surface tension of a liquid. This has common use in evaluating liquids containing surfactants or other impurities by dynamic surface tension measurements. In general, the presence of AEA in an aqueous medium lowers the surface tension compared to water. The method offers advantages in terms of its accuracy and rapid nature, as it does not require contact angle measurement (Fainerman *et al.*, 1994). During tests, the capillary of the tensiometer (known radius) is submerged in the liquid sample. Air bubbles are produced at a constant

rate and blown through this. The pressure inside the gas bubble continues to increase until the bubble achieves a hemispherical shape whose radius corresponds to the radius of the capillary. It is possible to determine the surface tension using the Laplace equation (reduced form) for a spherical bubble within a liquid as follows,

$$\sigma = \frac{\Delta P_{max} \times R_{cap}}{2} \quad (\text{Eq. 2-16})$$

Where, σ = surface tension, ΔP_{max} = maximum pressure drop and R_{cap} = radius of capillary.

Surface tension measurements of test liquids can provide important information relating to the parameters (e.g. ionic strength, insoluble compounds, pH and concentration of surface active compounds) affecting fly ash/AEA interaction. There also exists a relationship between surface tension and foam stability. Pedersen *et al.* (2007) attempted to develop a test method to evaluate fly ash/AEA interaction from surface tension measurements. The sample preparation was similar to the foam index test. Initially, fly ash (2 g) and PC (8 g) were placed in a plastic beaker followed by a 25 ml of SDBS solution (0.5-1.0 g/l). The mixture was then sequentially shaken for 10 minutes, centrifuged for 1 minute and the supernatant filtrated. Surface tension measurements based on the maximum bubble pressure method were carried out on the filtrate. A good relationship was achieved between surface tension and foam index test results. The method gives advantages in eliminating individual operator judgement of foam stability and variations in chemical nature and concentrations of AEA (using SDBS). However, the difference in surface tension between two test fly ashes was found to vary between 58.8 – 61.5 mN/m (difference 2.7 mN/m), while the foam index gave differences of a factor of two (0.2 - 0.38 ml AEA) which question the reliability of the test. The test results also appear to be affected by the interaction between soluble ions released from PC/fly ash and the anionic AEA. Therefore, further development is necessary to standardize the test.

Another surface tension measurement with fly ash–water mixtures containing AEA was reported by Stencil *et al.* (2009). The approach used was simpler than that of Pedersen *et al.* (2007) and based on that described in Serway and Faughn (2011). The force required to pull an immersed needle from a liquid gives a measure of surface tension which can then be correlated with the concentration of AEA present in the system. Firstly, the required force to pull the immersed needle out of the mixture (either water or water-fly ash samples)

without AEA was measured. Diluted AEA (1:4 or 1:100 for water only and water-fly ash samples respectively) was then introduced into the liquid, followed by complete mixing (2-3 minutes) and equilibration (2-3 minutes), and then the force needed to pull the needle out was measured again. Relative surface tension values, i.e. force after AEA titration divided by that without AEA was reported. The absolute value of the force for fly ash/water mixtures cannot be obtained by this measurement because it was affected by floating fly ash particles, which attached to the needle as it was pulled from the mixtures. This is a drawback of the method and can affect measurements between fly ashes containing different levels of remaining carbon.

Automated foam index test

Stencel *et al.* (2009) proposed an automated foam index test (AFIT) to quantify the dynamics of fly ash/AEA interaction. No intrusion of a probe or device into a working environment was required. Appropriate foam stabilities are necessary for proper performance of the materials into which AEA's are applied. Stable foams have stable bubbles whereas their breakdown is likely where these are unstable. When bubbles break they produce unique acoustic signatures, the dynamic properties of which can be measured by detectors incorporated into the AFIT instrument. The outcome is quantitative, giving repeatable foam index values and foaming measurements.

A 20–80 g fly ash or cement-fly ash combination was added to 200 ml of water (using the automatic program of the device) to maintain a similar solid/water mass ratio with typical foam index tests. The mixture was agitated and the number of acoustic emissions (AE) recorded before AEA addition. Thereafter, AEA doses were introduced (at regular intervals) and agitated and following this AE data acquired until the foam index was established. A good correlation was observed between AEA dose required at peak AE events (AFIT) and visual metastable foam at the liquid surface (foam index). The total addition of AEA to produce peak AE is defined as the foam index. Good repeatability in the number of acoustic events was achieved. It was possible to estimate AEA dose required to produce a certain quantity of air in plastic concrete from the AFIT data.

Alternative dye adsorption tests from other fields

The sorptive nature of fly ash suggests that an alternative method for establishing fly ash/AEA interaction may be the adoption of dye adsorption tests from other fields (e.g. Choy *et al.*, 2000, Hameed *et al.*, 2007). Indeed, this quantitative approach has been used (with methylene blue) to determine the surface area and cation exchange capacity of clay minerals (Hang and Brindley 1970). Yool *et al.* (1998) attempted to evaluate harmful clay minerals in fine aggregate using methylene blue and cartasol dye. ASTM D3860 (ASTM, 2008) describes this type of test for evaluating the effectiveness of activated carbon. Research in this application has adopted a range of dyes including, Choy *et al.* (2000) (Acid Blue 80), Acid Red 114, and Acid Yellow 117), Valix *et al.* (2004) (AB80), Hameed *et al.* (2007) (methylene blue). Related work by Zhang and Nelson Jr. (2007) attempted to correlate foam index and AB80 adsorption of commercial activated carbon (with a spectroscopic method for the latter) and suggested this could be used with fly ash. A similar approach has been followed in Japan (JCAS, 2008) to assess the adsorption of methylene blue by fly ash. However, this uses a relatively short contact time and hand-shaking is required. The methylene blue (MB) test is traditionally used for the determination of levels of harmful fines in aggregates and described in BS EN 933-9 (BSI, 1999a). The test can be used for AEA sorptivity determination of fly ash instead of fine aggregate. Given the above it appears that there is potential of using standard dye reagents to investigate fly ash/AEA interaction.

2.4 Conclusions

2.4.1 Pozzolanic activity assessment

Although the literature covers mechanism of fly ash reactivity with PC and different methods of activation to improve its performance, there is a general lack of reliable assessment methods to predict the performance of fly ash in cementitious systems.

The phases formed during fly ash pozzolanic reactions appear to depend on particle sizes, with C-S-H present in larger fractions and C_3AH_6 smaller ones. Higher reactivity has also been found for ground material in research covering different levels of fly ash and curing conditions. Studies examining the effects of fly ash fineness on strength activity index

suggest little influence of this at early ages, 3 days, where physical packing was important, but greater differences at later ages due to pozzolanic activity. Various attempts have been made to examine reactivity in terms of equivalence factors and mathematical models have been developed to look at this. However, these appear to be specific to the materials used in the various investigations.

Several workers have examined the glassy phase of fly ash in relation to the feed coal. It has been found that those derived from lower-rank coals may have different glass compositions to those from higher rank materials (bituminous). These variations in glass composition also appear to correspond to factors including the particle density and surface area of the fly ash. Attempts have been made to relate the structure, composition and activity of fly ash, and on the basis of this, to explain differences in reactivity between pozzolanic materials. Other work has highlighted the importance of the reactive silica content of fly ash and the application of this as a method of estimating the k-value of the material.

Several studies have been carried out to examine chemical activation of fly ash. Various means of chemical activation have been followed, including the use of Na_2SO_4 , K_2SO_4 , KOH , triethanolamine, $\text{Ca}(\text{OH})_2 + \text{H}_2\text{O}$ and $\text{Ca}(\text{OH})_2 + \text{Na}_2\text{SiO}_3$. Several different techniques have been used to evaluate the effects of this including, calorimetry, TGA, XRD, Mercury Intrusion Porosimetry (MIP) and compressive strength. For alkali activation, the glass phase and calcium content of the fly ash have been identified as important factors influencing how the material behaved. In most cases, these various approaches indicated that activation gave improvements to mortar or concrete strengths, particularly at early ages, although longer-term benefits have also been noted.

Investigations have considered the reactive nature of fly ash by direct activation through exposure to various solutions and with tests then carried out on the resulting leachate and residue. These include fly ash/PC suspensions in water, fly ash/ $\text{Ca}(\text{OH})_2$ solutions and fly ash/alkaline solutions (K, Na). It has been suggested that the applicability of hydrofluoric acid for assessing pozzolanic activity by this approach may not be appropriate. Measurements carried out have included electrical conductivity of the leachate and X-ray

diffraction of the residue. It has been possible to relate these parameters obtained over a short period of time to the pozzolanic activity of fly ash.

Several techniques have been used which follow the normal course of pozzolanic activity tests, but change the conditions to enable results to be obtained earlier. These have included studies of fly ash under autoclaving and steam curing conditions. Other work has used differential analysis and thermo-gravimetric methods to determine $\text{Ca}(\text{OH})_2$ residues in hydrated pastes. These approaches have proved effective in contributing to the understanding of the chemical processes taking place with fly ash, how these can be modified, and in determining rates of pozzolanic reaction. Microwave assisted curing techniques have also been used to predict mortar strengths at 7 and 28 days. Slightly greater variability was noted with this method for fly ash mortars than those with PC only.

Calorimetric methods including heat of hydration of mortar containing fly ash have been used to establish good correlations with pozzolanic reactivity. Other work has demonstrated that it is possible to relate heat evolution with fly ash in cement paste and pozzolanic reactions as indicated by calcium hydroxide content through thermogravimetry. Electrical response techniques have also been found to offer potential in this area. Indeed, several studies have used fly ash pastes and fly ash/ $\text{Ca}(\text{OH})_2$ mixtures with measurements of electrical resistance/resistivity and conductance and capacitance carried out. These have proved useful techniques for rapid evaluation of pozzolanic activity.

Several other laboratory-based research techniques have been used to evaluate fly ash reactions including magic angle spinning nuclear magnetic resonance and applied impedance spectroscopy. While contributing to the understanding of fly ash, these are mainly research techniques and it is not anticipated that they will be used in practice.

2.4.2 Carbon sorptivity/admixture adsorption assessment

The degree of adsorption of AEA is not only dependent on the carbon content, but also on the characteristics of the carbon, such as its surface area, type and polarity. Carbon can be measured indirectly by LOI and techniques beyond the conventional method have been developed to carry this out. While LOI is widely used as a limitation on the residual

carbon in fly ash in international standards, a number of studies have demonstrated that it has limitations as an indicator of air-entraining performance of fly ash.

In addition to LOI, carbon content can be determined by direct means. BS EN 450-1 (BSI, 2005c) refers to ISO 10694 for this type of measurement. In the test, carbon is oxidised to CO₂ by heating to 900°C in a flow of oxygen-containing gas. The level of CO₂ is then determined using an appropriate analytical technique. This approach has been described in the literature for carbon content assessment by infrared detection.

Characterisation of differing forms of unburned carbon has been carried out in many studies. Three microscopically distinct phases have been identified namely, inertinite particles (entrained from the combustor prior to melting or combustion), isotropic coke and anisotropic coke (both are reacted particles that have passed through a molten stage). Distribution of carbon forms and their fractions have been investigated by optical microscopy using point counting techniques. It has also been found that inertinite and isotropic coke forms of carbon tend to adsorb more AEA than anisotropic coke.

The BET method, which is used in surface science to determine the surface area of solids, by N₂ adsorption, has been found to give a better correlation with foam index than LOI for fly ash. Work has also found that N₂ adsorption by BET gave a good correlation with the AEA dosage required to achieve a target air content in fresh concrete. The technique has also been used to examine the surface area of high carbon fractions.

The foam index test is that most often used for indirectly measuring the relative adsorption of AEAs by fly ash. Given the result can be influenced by the procedure used and operator carrying out the test, attempts to improve the test or to develop techniques which can be related to it, have been made. There is no standard test on a national or international basis, although guidance documents exist, mainly from the USA, describing the test.

To develop a standard test, several approaches have been recommended including the use of pure chemical surfactants and spectroscopic or other techniques which remove visual foam stability judgements. Various studies have examined these approaches.

Work examining different surfactants (standard chemicals) indicates these can be used as an alternative to AEAs, with SDBS representing a good candidate in this category for a

standardised foam index test. Indeed, this correlated well with AEAs and had a lower molar uptake than other surfactants considered at the test end-point.

Ultraviolet and visible (UV-Vis) absorption spectroscopy is the measurement of the attenuation of a beam of light after it passes through a sample, or after reflection from a sample surface. Attempts to use this approach to measure the adsorption of AEA by fly ash and carbon have been made by several workers. However, it appears that there are a number of difficulties associated with the test, and poor correlation with the foam index suggests that it is unlikely to offer advantages or achieve use as an alternative method.

Surface tension measurements have also been used as an alternative to foam index tests. Methods have included a similar approach to the foam index test in terms of sample preparation, with surface tension measurements, based on the maximum bubble pressure method, made using a tensiometer, following filtration of the PC/fly ash/surfactant. Good agreements have been obtained between this and foam index measurements. Other techniques, based on surface tension, involve removal of needles from mixtures with and without AEA and fly ash. These have been described in the literature, but appear unlikely to offer a realistic alternative to the foam index method.

An automated foam index device has been reported, which is based on the acoustic signatures associated with breaking bubbles in unstable foam. Measurements with the technique are made without intrusion of a probe into the working environment. It has been demonstrated that there is good agreement between the number of acoustic events occurring with regard to AEA addition and the visual observation of a metastable and uniform foam on top of solids/water mixtures.

Dye adsorption tests have been used in other fields to assess the effectiveness of commercial activated carbon. As the unburned carbon in fly ash has a similar adsorptive nature to commercial activated carbon, this approach could have potential as a test method to assess fly ash/AEA interaction in cementitious systems.

CHAPTER 3: EXPERIMENTAL DETAILS

This Chapter provides details of the experimental plan and procedures followed during the laboratory work. These including characterisation of materials and general descriptions of other assessment test methods related to fly ash pozzolanicity and its interaction with AEA. Procedures for mixing and testing fly ash mortars and concretes are also included in this chapter. These were developed in-house during the course of the project, or adopted from the literature.

3.1 Programme of Work

The programme of work comprised a literature review and four main stages, as indicated in Figure 3-1. The aim for this was to develop/adopt suitable test methods for assessing fly ash pozzolanic reactivity and its interaction with AEA. The steps carried out in each phase to accomplish these are described briefly in the following sections.

3.1.1 Phase 0 – Literature review

Initially, a survey was carried out of available information to examine the details of assessment test techniques, both standard, and those developed and reported in the literature, for (i) rapidly determining the reactivity of fly ash; and (ii) its interaction with AEA within a cementitious system. In this phase, approximately 200 documents were collected and examined. These included inter(national) standards, journal articles, books, technical reports published by various organizations, conference articles, technical bulletins and information from websites. From this Phase, potential techniques were identified for inclusion in the initial test phase of the experimental programme.

3.1.2 Phase 1 – Materials characterisation and initial tests

The fly ashes were characterised physically, chemically and morphologically. Tests were carried out on the other materials used during the study including physical and chemical properties of PCs; grading, absorption and specific gravity of fine and coarse aggregates.

Relevant information on characteristics of AEAs and standard reagents were also obtained from the suppliers.

Based on the work carried out during Phase 0, test methods were selected for initial consideration. The criteria for inclusion were (i) whether the method is covered in national standards, (ii) successful and reliable use as suggested by the literature and (iii) simplicity and relative cost associated with the method.

Several fly ash samples were tested during this stage including, coarse, medium and fine and those having a range of LOIs. Both commercial AEAs and a standard reagent were used to evaluate the influence of admixtures, on their interaction, with fly ash.

Tests were cross compared and considered with respect to the existing methods, i.e. activity index (BS EN 450 (BSI, 2005c); carried out over an extended test age range) to assess reactivity and air content/flow tests on mortar samples containing AEAs. This work enabled the selection of test methods for inclusion during the full evaluation stage.

3.1.3 Phase 2 — Evaluation of selected assessment methods using a range of materials

Fly ash was obtained from nine sources including, repeat sampling (over a year) from two of the power stations to identify seasonal variations. These also included processed fly ashes (air-classified and STI carbon removed), run-of-station, those from modern combustion technology (e.g. co-combustion and oxy-fuel burning technology). The materials were also fully characterised physically, chemically and morphologically.

The assessment tests were then carried out to evaluate (i) the effect of the typical range of properties likely to be encountered (i.e. from the samples used) in practice on the particular test, and (ii) its repeatability, where applicable.

The tests were again evaluated against activity index and mortars containing air-entraining admixtures. This led to the identification of test methods which were repeatable and best suited the range of practical material properties.



Figure 3-1. Overview of the research programme

3.1.4 Phase 3 – Validation of assessment test methods with concrete

Having established suitable methods to assess fly ash with regard to its use in concrete, the final experimental stage involved tests on concrete as a means of validating these. A range of concrete mixes using selected fly ashes with different properties were considered to determine fly ash reactivity and interaction with AEAs. This mainly focused on strength development, air contents in fresh concrete and permeation properties using water penetration under pressure tests and ISAT. Correlations between the assessment and concrete tests were then considered to evaluate the effectiveness of the former.

3.1.5 Phase 4 – Between-laboratory tests

Fly ash samples were sent to three laboratories of UKQAA members for between laboratory tests. Properties measured included, PSD, sieve analysis and LOI of fly ash and activity index (28 and 90 days) of mortar.

3.1.6 Phase 5 – Practical implications

Finally the outcomes of the work were evaluated and the practical implications associated with these examined.

3.2 Characterisation of Materials

3.2.1 Fineness of fly ash samples

Wet sieve analysis

Fly ash fineness was determined using wet 45 μm sieve analysis following BS EN 451-2 (BSI, 1995). The process is shown in Figure 3-2. A dry fly ash sample (1.0 g, weighed to the nearest 0.001 g) was sieved under a water pressure of (80 ± 5) kPa for (60 ± 10) seconds by swirling the sieve horizontally at about 1 rotation per second. The material remaining (on the sieve) was then oven dried (at 105 ± 5) $^{\circ}\text{C}$ and the proportion retained (by mass) was calculated and expressed as a percentage of the original material. The mean value from two consecutive tests (to one decimal place) was reported as the fineness of the fly ash. Where these differed by $> 0.3\%$, the test was repeated further until two values were obtained that differed by not more than this.

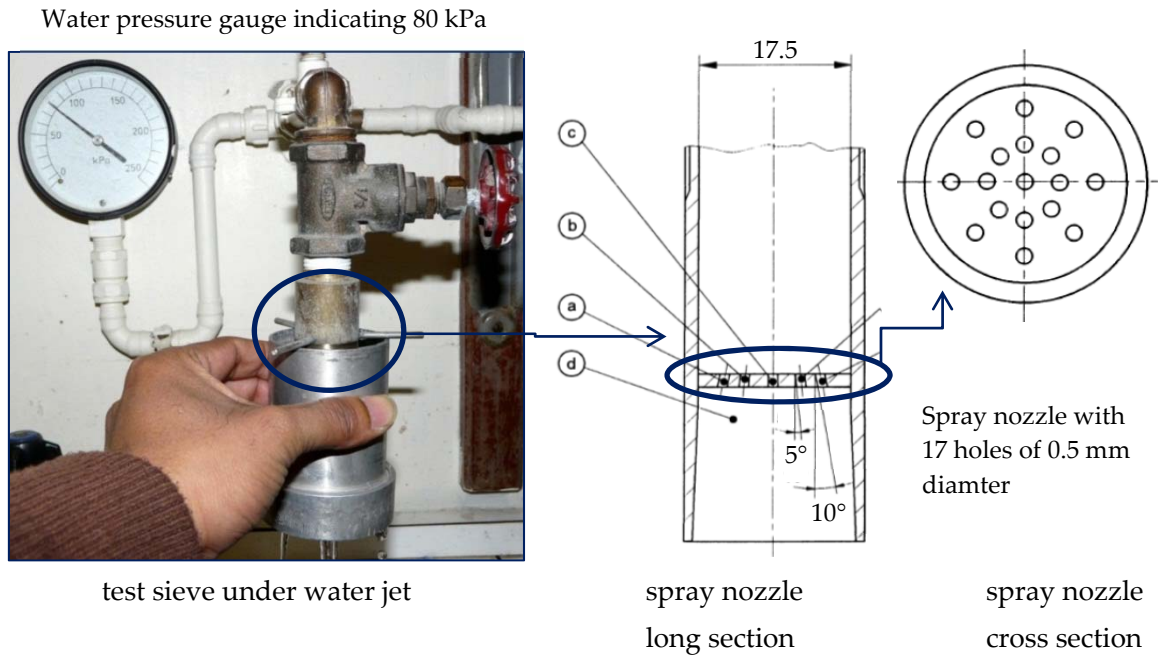


Figure 3-2. Wet sieve analysis using 45 μm mesh to BS EN 451-2 (BSI, 1995)

Particle size distribution

The particle size distribution (PSD) of fly ashes and PC were determined using a Malvern Mastersizer2000 LASER particle size analyser. Approximately 1.0 g of fly ash was dispersed in water using an ultrasonic attachment in the sample vessel of the equipment (Figure 3-3). In the case of PC and lime, these were dispersed in propanol (in a smaller dispersion unit to prevent reaction).



Figure 3-3. Malvern Masteresizer2000 LASER particle size analyser

Commercial software was used to create particle size distributions from the degree of scattering of a collimated, monochromatic, dual laser beam (red and blue) passing through the mixture of sample and solvent (de-ionized water for testing fly ash). This is based on the principle that the angle of deflection decreases proportionally with particle size. At least three measurements were carried out for each sample. Although repeated distributions were found to be similar for a given material, an average distribution result of these, created by the computer software, was reported.

Surface area by N₂ adsorption and Blaine

A Quantachrome Nova 3000e surface area analyser was used (Figure 3-4 (a)) for the measurement of fly ash and PC specific surface areas. This used N₂ which was adsorbed on samples and their pore surfaces as a single molecule layer and had a minimum pore volume detection level of less than 2.2 nanolitres. A very thin film of moisture can change the quantity of N₂ adsorbed, therefore, the samples were vacuum dried before testing. To do this, the test cells were attached to the dedicated terminals of the instrument under a vacuum pressure of 77 Pa and overnight temperature of 105°C. The quantity of N₂ involved in an adsorption and desorption cycle was automatically determined. The results can be expressed using a wide range of built-in calculations reflecting available surface area description theories (not only BET). The instrument can detect a surface area range of 0.01 to over 2000 m²/g, while the pore diameter range is 0.35 - 200 nm.

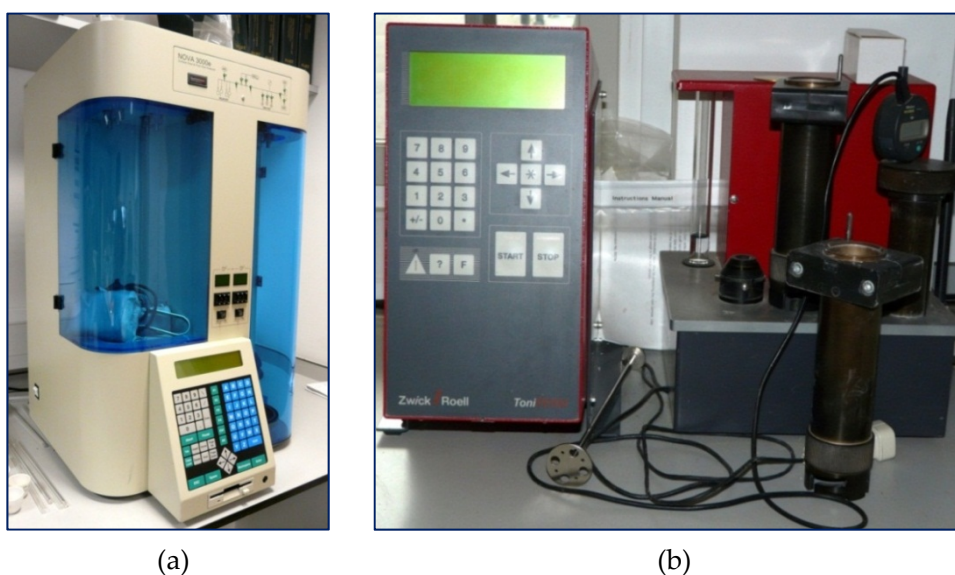


Figure 3-4. Fly ash surface area test using (a) N₂ adsorption; and (b) Blaine apparatus

Blaine fineness was determined by the air permeability method as per BS EN 196-6 (BSI, 2010a) using an automatic device (Figure 3-4 (b); *Zwick Roell*). The mean of three consecutive test results was reported where the variation between these was not more than 0.3%.

3.2.2 LOI and moisture content

LOI

Generally, the LOI is a measure of the level of unburnt carbon presents in fly ash. Approximately 1.0 ± 0.5 g (but accurately recorded) dry samples were ignited in an electric furnace (Figure 3-5 (a)) at 975°C for 60 minutes following BS EN 196-2 (BSI, 2005b) and BS EN 450-1 (BSI, 2005c). After ignition, the samples were removed from the furnace and left in a desiccator until cooling to room temperature before recording the weight. The LOI value was calculated by expressing the loss in mass as a percentage of the original mass of material and the mean of three results reported.

Moisture content

An OHAUS MB45 moisture balance (Figure 3-5 (b)) was used to measure the moisture content of samples at 105°C . The instrument is equipped with an infrared lamp and displays the moisture content when no further change in mass occurred.

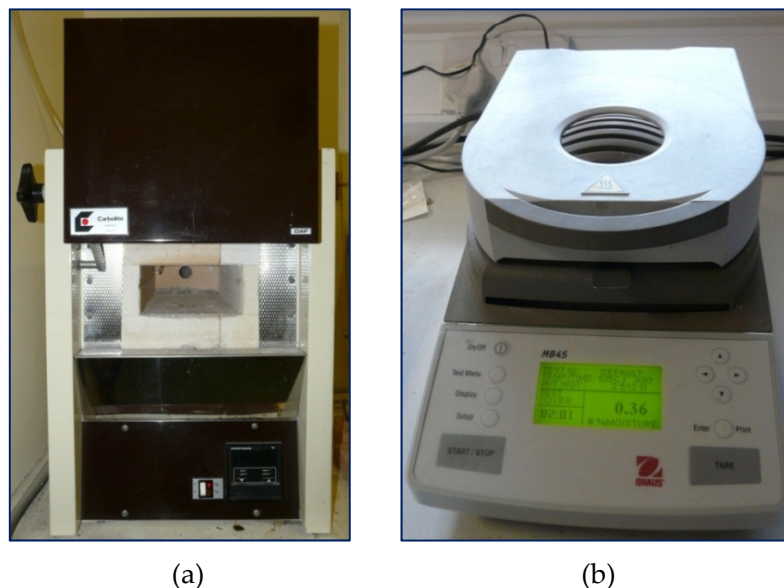


Figure 3-5. (a) Electric furnace for LOI test; and (b) OHAUS MB45 Moisture balance

3.2.3 Mineralogy by X-ray diffraction (XRD)

A Hilton-Brooks X-ray Diffractometer (Figure 3-6(a)) with monochromatic $\text{CuK}\alpha$ source and curved graphite, single crystal chrometer (40 kV, 30 mA) was used to test the phase composition of the materials. Dry fly ash is sufficiently fine for this test and hence samples were used without prior grinding. Sample was firmly compacted on the reverse side of a specimen holder, against a glass slide. Then the back steel cover was snapped into place and the glass slide removed from the front face.

Each sample was analysed over the 2θ range of $3\text{-}60^\circ$ at a scan rate of one degree/minute with 0.1 degree increments. XRD was used to determine crystalline phases (and hence glass/amorphous/others content) present in the samples of fly ash. The results can also be taken as an indication of the quantity of specific phases present in the materials. XRD pattern-fitting Rietveld refinement was considered to quantify the crystalline constituents, as described by Cheary and Coelho (1994). A 5% aluminium-oxide (corundum) was previously homogenised with the sample to identify a known reference peak. It should be noted that, the method gives only an estimate of the amorphous content of fly ash.

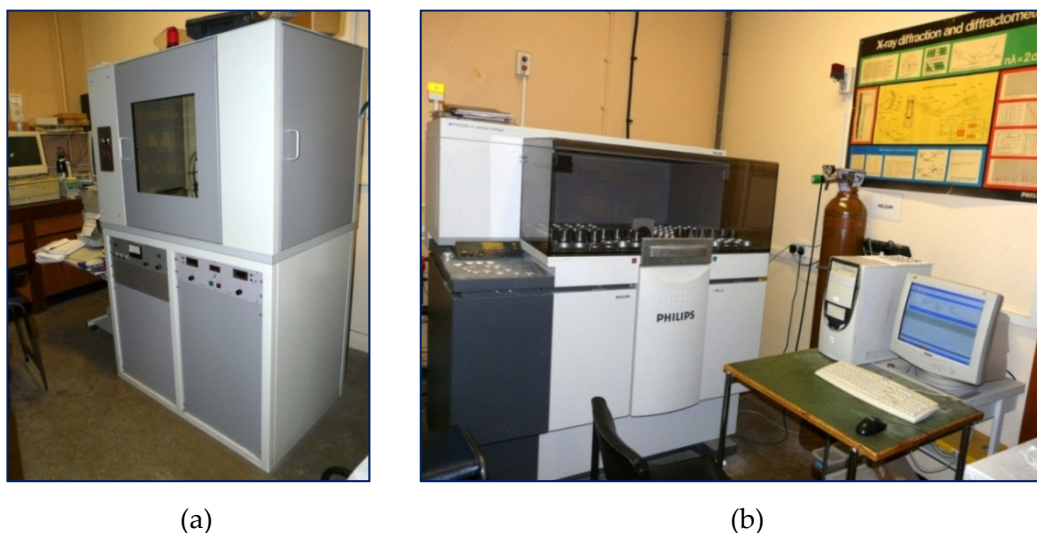


Figure 3-6. (a) X-Ray Diffractometer (XRD) for mineralogical analysis; and (b) Bulk oxide composition determination using X-ray Fluorescence Spectroscopy

3.2.4 Oxide composition by X-ray fluorescence spectroscopy (XRF)

A Philips PW2424 sequential X-ray Fluorescence Spectrometer (Figure 3-6(b)) with $\text{RhK}\alpha$ source was used to determine the oxide composition of the test materials. A few drops of a

2.0% Movoil water solution (organic type binder) was mixed with the fly ash sample using an agate mortar and pestle before placing in a $\text{Ø}27$ mm pellet mould. For PC samples, testing was carried out without the addition of binder. The pellet filled with sample was compacted under 75 kN load for the first 5 minutes and then at 150 kN for a further 10 minutes. Prepared samples were left overnight to dry out prior to testing. Certified standard materials were used to calibrate the instrument before testing the samples.

3.2.5 Morphology by scanning electron microscopy (SEM)

High magnification images Micrographs of test materials were obtain by SEM. A Philips XL-30 instrument (Figure 3-7) in SEM mode, at an accelerating voltage of 15 kV, in combination with a Links System Si(Li) X-ray detector was used. Selected samples were also analysed using the Energy-dispersive X-ray spectroscopy (EDX) mode to identify the nature of crystalline deposits on their surfaces. A 20 kV voltage was used for this. Double sided adhesive carbon tape was secured to a 10 mm diameter aluminium stub and the sample sprinkled on it. Specimens were coated by Pd-Au alloy vapour (applied layer thickness: 25 nm) to prevent charging during the test.

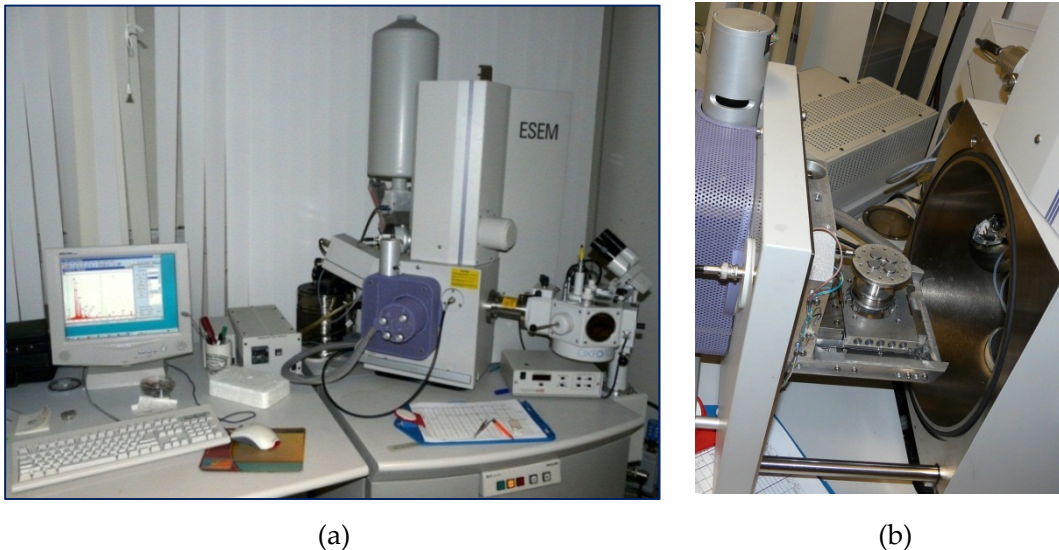


Figure 3-7. Scanning Electron Microscope for morphology and EDX

3.2.6 Portland cement (PC) tests

Five different PCs were used for the project. All of these were characterised physically and chemically for PSD, surface area (N_2 absorption and Blaine), LOI, and oxide compositions

following/slightly modifying the procedures described above. The phase composition of PCs was determined using the Bogue Equations.

3.2.7 Aggregates tests

Mortar tests were carried out with CEN standard sand as per BS EN 196-1 (BSI, 2005a). In the concrete tests, 10/20 and 4/10 mm fractions of natural gravel and a medium grade sand, all conforming to BS EN 12620 (BSI, 2002) were used. The particle density and absorption of these were tested as described in BS EN 1097-6 (BSI, 2000). The fineness modulus of the sands was tested as per BS EN 12620 (BSI, 2002).

3.3 Reactivity Assessment Tests

Reactivity of fly ashes was determined by a range of assessment methods including:

- a) the BS EN 450 (BSI, 2005c) method (reference);
- b) the accelerated test given in BS 3892-1 (BSI, 1982) i.e. 30% fly ash, mixes of the same flow, water cured for 5 days at 20°C and 2 days at 50°C;
- c) a combination of BS EN 450 mix proportions and BS 3892-1 (BSI, 1982) curing procedure;
- d) porosity of PC based mortars at early ages using MIP;
- e) a qualitative test method described in the ASTM C593 (ASTM, 2011b) standard, using hydrated lime in mortar (with CEN sand and BS EN 1015-3 (BSI, 1999b) flow measurements; variable water/same flow);
- f) Thermogravimetric analysis (TGA) for selected fly ash pastes.
- g) a qualitative method described in the BS EN 196-5 (BSI, 2011a) standard (Frattini test);
- h) lime consumption (Frias *et al.*, 2005) and conductivity measurements after exposing fly ash to saturated lime solutions of different compositions;
- i) a pozzolanic potential index (PPI) (Hubbard and Dhir, 1984) and the sum of the major oxides calculated from chemical analysis;
- j) chemical phase analysis and therefore, contents other than crystalline;
- k) the 'true' glass content determined from XRD analysis (Font *et al.*, 2010); and
- l) an approach measuring heat of reaction with quick lime; adopted from BS EN 459-2 (BSI, 2010b).

3.3.1 Activity index test (PC-based mortar)

BS EN 450 (BSI, 2005c) was the reference standard method for activity tests, measuring the contribution of fly ash to the compressive strength of mortar (comprising 75% PC (32.5R/42.5N/52.5N) and 25% fly ash), after 20°C water curing for 28 and 90 days. Selected samples were also tested at other ages (7, 14, 56 and 180 days). Three-gang moulds were filled with mortar following BS EN 196-1 (BSI, 2005a; PC (450 g), standard sand (1350 g) and water content (225 ml)) designated as the control mortar. Test mortars used fly ash at a level of 25%. The fly ash passes the test if its mortar achieves at least 75% of the compressive strength of the PC only counterpart at 28 days and 85% at 90 days. The mortar was prepared using an orbital mixer with a stainless steel bowl (about 5 litre capacity). Flow tests were conducted immediately after mixing and before casting mortar in the moulds (Figure 3-9 (a)).

The former British standard BS 3892-1 (BSI, 1982) recognised the potential water savings of high fineness fly ash and considered mortar with adjusted water contents to achieve similar flow to the PC reference. The composition of the test mortar was slightly different comprising 70% PC and 30% fly ash. An accelerated curing method was also given, which used water curing for 5 days at 20°C followed by 46 hours at 50°C (Figure 3-8 (b)) and finally 2 hours at 20°C. The criteria for passing the test were similar, i.e. comparison with the PC counterpart (minimum 85%) with the activity property designated a 'pozzolanic activity index'.

Both BS EN 450 (BSI, 2005c) and BS 3892-1 (BSI, 1982) procedures were considered in this project. In addition, a combined method with BS EN 450 mix proportions and BS 3892-1 (BSI, 1982) curing was also followed for selected mixes.

3.3.2 Porosity of PC-based mortars by MIP

Mercury Intrusion Porosimetry (using a Quantachrome PoreMaster33 instrument, Figure 3-9) was carried out to determine the pore structure of fly ash mortars. The device offers automated pore size analysis, achieving a maximum pressure of 33,000 psi (227.5 MPa) and pore size measurement (diameter) in the range 950 to 0.0064 µm. This consists of two low pressure stations and a high pressure one.

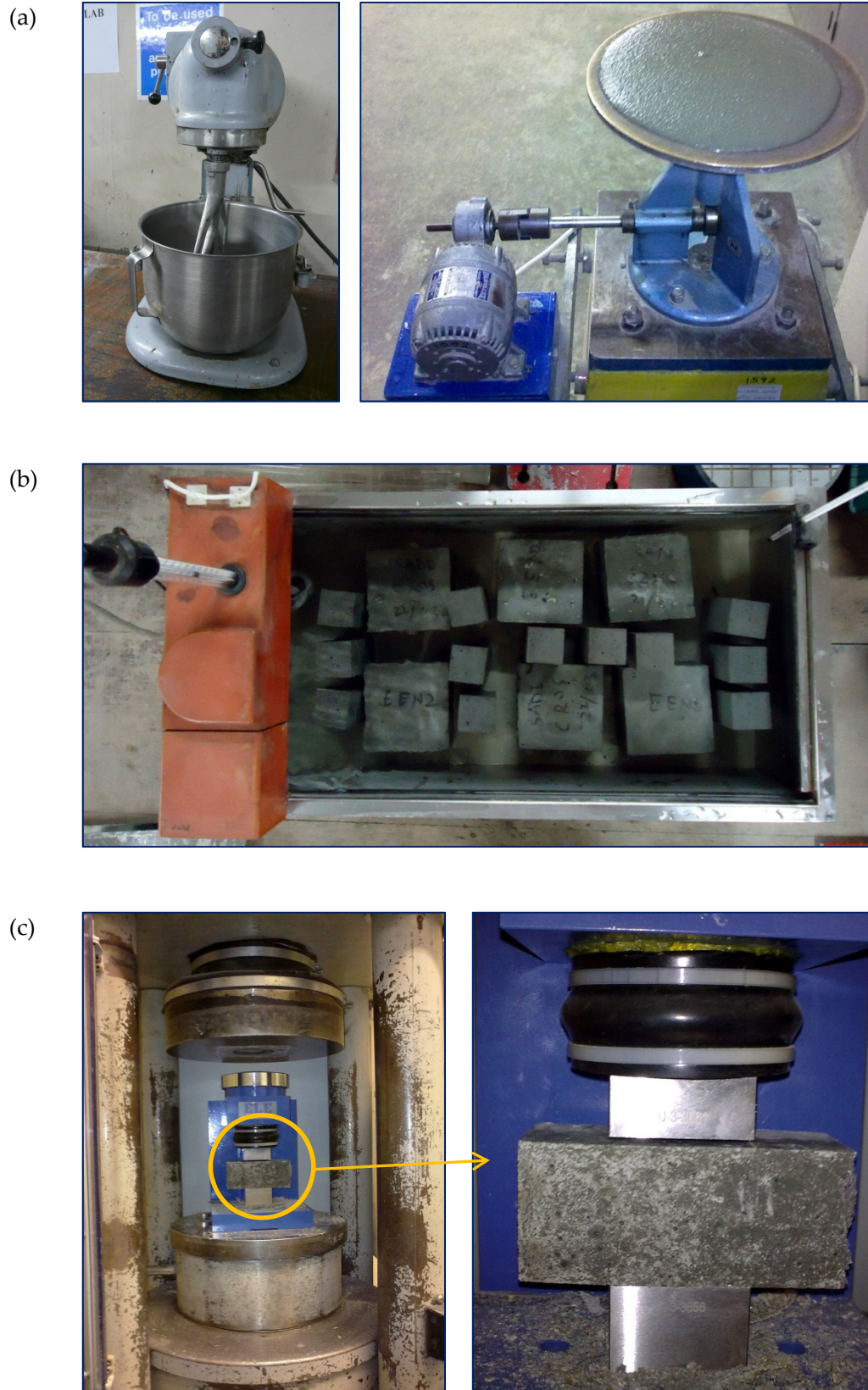


Figure 3-8. Mortar tests: (a) mortar mixing and flow test; (b) water bath for high temperature curing; and (c) prism compression test



Figure 3-9. PoreMaster33 used for mortar porosity measurement

Mortar samples were tested for porosity at the same ages as compressive strength. The size of cylindrical core drilled samples was approximately Φ 5 mm \times 20 mm. These were dried under a fan assisted infrared lamp at $< 50^{\circ}\text{C}$ temperature until constant weight, before placing into the test cell. The mass of the sample was recorded and the test initiated. During this automatic procedure, the test cell was evacuated and then gradually filled with mercury whilst recording the volume of its uptake (low pressure stage, characterising pore size distribution above 10 μm). The sample cell was then transferred to the second stage of the test where more pressure was applied by means of a hydraulic oil system and the volume of intruded mercury recorded as a function of the applied pressure (high pressure stage, for pores below 10 μm in size). At each step, the applied pressure was held until flow ceased (equilibrated) to ensure all pores were filled with mercury. Finally, the two pore size distribution curves were merged and the cumulative porosity estimated using the commercial software supplied by the instrument manufacturer.

3.3.3 Hydrated lime mortar

The ASTM C593 (ASTM, 2011b) test method was considered, which is normally used to determine the suitability of fly ash in lime-stabilized soils. It requires that 50 mm lime mortar cubes give at least 4.1 MPa compressive strength after 7 days curing at $54 \pm 2^{\circ}\text{C}$ and $> 95\%$ relative humidity. Initially local sand was used, but the tests did not give promising results. Therefore, much finer ASTM standard sand was obtained from the USA for

inclusion in the work. The feasibility of the test was evaluated with this material and the following work considered CEN standard sand as per BS EN 196-1 (BSI, 2005a). Water adjustment was made to achieve a consistency value of 65–75% (spread increase from the original dimensions of the cone base) for each mix. Immediately after casting, the samples (in the steel moulds) were placed in a sealed plastic container and the lid closed to prevent moisture loss. A small quantity of water was placed in the container (below the spacer) to ensure adequate moisture circulation (Figure 3-10 (a)).

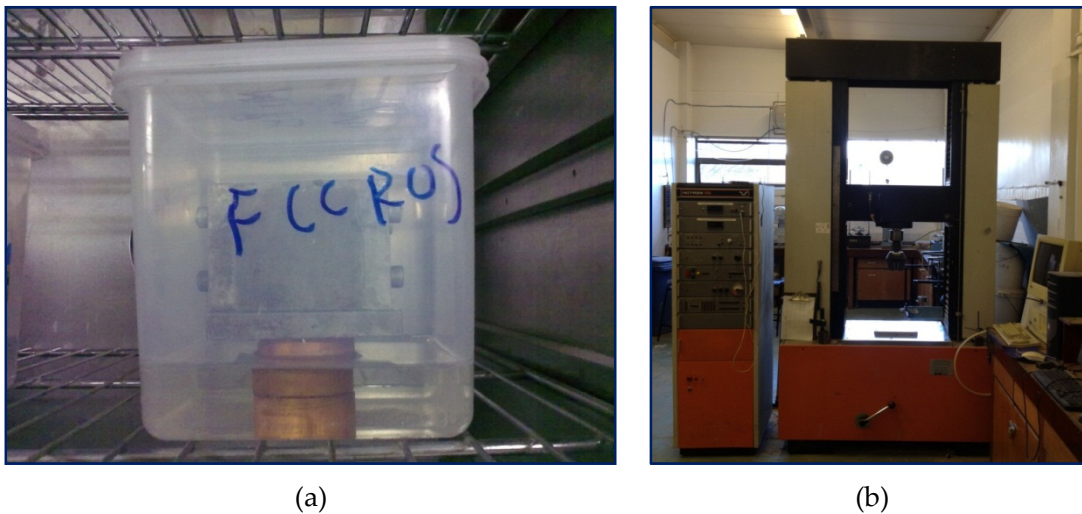


Figure 3-10. Hydrated lime mortar tests; (a) high temperature and moisture curing; and (b). Instron machine used for testing compressive strength

The container was located in an oven at a constant temperature of $54 \pm 2^\circ\text{C}$ for 14, 28 or 56 days. After this, the specimens were removed from the oven and left in a controlled high humidity chamber for at least two hours and then demoulded. These were then tested for compressive strength using an Instron testing machine (Figure 3-10 (b)). Tests with this equipment are strain controlled, with a rate of 0.5 mm/minute applied. A limited number of samples were also tested without water adjustment ($w/(fa+l) = 0.5$) and cured for a period of 7 days to check whether this could be related to the BS EN 450 active index.

3.3.4 Measuring $\text{Ca}(\text{OH})_2$ content in paste by TGA

TG analysis is based on mass loss of test samples with respect to temperature rise. The plot of sample weight against temperature gives important information regarding physical and chemical modification due to thermal decomposition. To avoid interference to the test

results from reactions between samples and atmospheric gases, the experiment is conducted with an inert atmosphere, nitrogen gas in the chamber. The TG equipment is capable of automatically evacuating evolved gases and volatile matter during the experiment. A computer with dedicated software is connected to the simultaneous thermal analyser (STA) fitted with a furnace (1500°C capacity) to automatically log and analyse the acquired data.

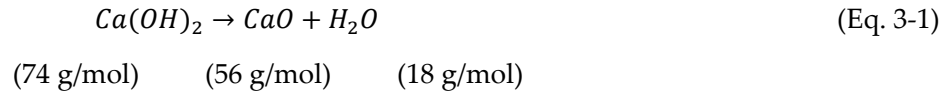
Paste specimens were prepared using PC/fly ash to test reactivity by measuring the consumption of $\text{Ca}(\text{OH})_2$, liberated from the primary reaction between water and PC. The mix proportions were kept similar to those in the mortar test, i.e. $w/c = 0.5$ and fly ash level of 25%. A reference PC only mix was also prepared. PC and fly ash were placed in double-sealed zipped air-tight plastic bags and blended together. Once a homogeneous condition was achieved, water was added and the bag sealed. The contents were then well mixed (inside the bag) and the sealed bag was kept under water at a controlled temperature ($20 \pm 1^\circ\text{C}$) until the test age.

At the respective test ages fragments from the sample's core were collected, and dried at low temperature (using the moisture balance at $\sim 50^\circ\text{C}$). This was left in a desiccator containing silica gel to cool at room temperature and ground into powder. Not less than 10 mg of this sample was then placed in a platinum crucible, inside the TG-FTIR instrument (TG system coupled with FTIR interface by Bruker's; Figure 3.11).



Figure 3-11. TG-FTIR instrument for $\text{Ca}(\text{OH})_2$ determination in fly ash/PC paste

The ground sample was heated in the platinum crucible up to 1000°C at a rate of 10°C/min. The Ca(OH)₂ quantity present in the samples was calculated from the TG plot as follows,



$$\% \text{Ca(OH)}_2 = \frac{\text{mass loss}}{18} \times 74 \quad (\text{Eq. 3-2})$$

Where, the mass loss was obtained from the dehydroxylation region (~420 - 500°C; Chaipanich and Nochaiya, 2010) of the first derivative graph.

3.3.5 Frattini test

A qualitative test method described in BS EN 196 – 5 (Frattini test; BSI, 2011a) was considered for the reactivity assessment of fly ash. The method is designed for evaluating pozzolanic cements and thus no mix proportions are specified. To match BS EN 450 (BSI, 2005) mix proportions, a fly ash level of 25% with PC was used for the tests carried out during the study. The general test conditions applied are summarized in Table 3-1.

Table 3-1. Frattini test conditions

MATERIALS	QUANTITY	UNIT
PC	15	g
Fly ash	5	g
De-ionized water	100	ml
Test temperature	40 ± 2	°C
Exposure period	8 and 15	d

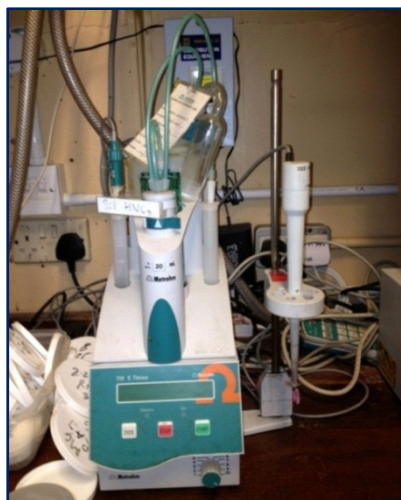
The procedure involves mixing 20 g of pozzolanic cement and 100 ml of deionised water, followed by storage of the slurry at 40 ± 2°C for 8 and 15 days. After this, the sample was filtered (Figure 3-12) and the remaining CaO and OH⁻ concentrations measured. The pozzolanic cement passes the test if this point lies below the saturation curve of CaO vs. OH⁻ ion concentration at the test temperature. Calcium levels were determined by XRF in liquid sample mode, under a He supporting atmosphere, while hydroxyl concentrations

were measured by titration, using HNO_3 , setting the end point of the process to a pH corresponding to that of methyl orange. An automatic Titrator (Metrohm Titrino 719, Figure 3-13 (a)), fitted with a standard pH electrode was used.

In addition to this, a portable type conductivity meter (Figure 3-13 (b)) was employed to measure the bulk conductivity of the filtrate. The presence of available ions (e.g. Ca^{2+} , OH^- , K^+ , Na^+ , Mg^{2+}) is likely to be reflected in the conductivity measurement.



Figure 3-12. Vacuum filtration for Frattini and lime consumption tests to limit carbonation



(a)



(b)

Figure 3-13. (a) automatic titrator for determination of OH^- ion concentration; and (b) portable meter for filtrate conductivity measurements

3.3.6 Lime consumption and conductivity measurements

It is well established that fly ash reacts with free lime present in a cementitious system. Given that the Frattini test described in BS EN 196 – 5 (BSI, 2011a) could be influenced by the type of cement used in the test, an attempt was made to carry this out with laboratory grade $\text{Ca}(\text{OH})_2$ (Frias *et al.*, 2005). Work by Rosell-Lam *et al.* (2011) described the evaluation of pozzolanic properties of zeolitic rock by conductivity measurement after exposure to saturated lime solution. This approach was applied to assess fly ash in the current study.

A series of initial tests was conducted to explore suitable test conditions, including temperatures of 40 and 80°C. Two types of laboratory prepared solutions were used for fly ash exposure. To raise the pH of the test solution above 13.0, a 100 mmol/l KOH stock solution was prepared and then laboratory grade $\text{Ca}(\text{OH})_2$ was dissolved in this up to saturation level. The other solution considered was a saturated lime solution. Both were filtered to ensure no suspended lime was present. A 20 g fly ash sample was exposed to 100 ml of these solutions in a water tight plastic container and kept in a temperature-regulated oven for different periods. After this, the slurry was filtered and the remaining CaO , OH^- ion concentrations and conductivity were measured, as in Section 3.3.5. The results obtained were then compared with various fly ash properties and BS EN 450 (BSI, 2005c) activity index.

3.3.7 'True' glass content measurement

XRD can be used for fly ash glass/amorphous content determination by quantifying its crystalline content and subtracting this from the total mass. However, it is arguably incorrect to count material other than crystalline as glassy (reactive) material. A novel method described by Font *et al.* (2010) claimed to give a more precise figure for the glass content of fly ash. It is also XRD based, but the fly ash sample is mixed with increasing quantities of glass (25, 50, 65, 75, and 90%) and the amorphous composition (balance of Rietveld mineral content; as described by Cheary and Coelho (1994)) extrapolated to zero glass addition to measure the 'true' glass content. This obtained glass content was then compared with the activity index of the fly ashes.

3.3.8 Heat of reaction with quicklime

The lime slaking test of BS EN 459-2 (BSI, 2010b) was adopted to compare differences in heat evolution during the reaction of CaO and water in the presence of different reactive fly ashes. A Dewar flask of 1000 ml nominal capacity was filled with 300 ml distilled water (20°C) and then 25 g of fly ash added. During constant stirring with the standard shape stainless steel paddle at a speed of 300 ± 50 rpm, 50 g of quick lime (CaO) were added and the temperature recorded at 30 s, every minute between 1-10 minutes and every 2 minutes after 10 minutes until it stabilised (usually at about 40°C higher than the start temperature). The area under the temperature curve, i.e. heat released until a certain cut-off point (20 minutes appeared to be suitable) was calculated to compare with the fly ash activity index.

3.4 Fly Ash/AEA Interaction Assessment Tests

Sorptivity of fly ash is important in the use of air-entrained concrete as the effective quantity of AEA may be reduced and therefore, lower air contents achieved correspondingly. Methods available in the literature and also those developed in the project were applied to assess this aspect of fly ash, including:

- Loss-on-Ignition (described in Section 3.2.2).
- Specific surface area by N₂ adsorption (described in Section 3.2.1).
- The foam index test using manual shaking and an automatic shaking device (to improve test reliability).
- Dye adsorption tests using
 - acid blue 80
 - methylene blue
- Air entrainment in mortars and concrete

3.4.1 Foam index test

Although there is currently no national/international standard for foam index measurements, the procedure is described in the literature (e.g. Dodson, 1990; Gao *et al.*, 1997; GRACE, 2006; Taylor *et al.*, 2006; Folliard *et al.*, 2009). The test involves incremental addition of AEAs to a PC/fly ash slurry and short vigorous shaking. This is

repeated until stable foam forms, indicating that adsorptive sites within/on fly ash carbon have become saturated with the surfactant AEA and the excess creates air-bubbles.

Preparations for the test included mixing 2.0 g of fly ash and 25.0 ml of deionised water in a centrifuge vial of $\text{Ø}40 \text{ mm} \times 110 \text{ mm}$ and ultrasonic dispersion for 5 minutes. Thereafter, 8.0 g of PC was added and the mix shaken for 1 minute.

Four different types of AEAs were used for this test including a standard reagent (hereafter AEA S) and three commercial AEAs (hereafter, AEA C1, AEA C2 and AEA C3). During manual shaking tests, small increments of AEA ($20 \mu\text{l}$ for AEA S) were added at a time and the slurry shaken for 15 s. The stage when the generated foam covers the whole liquid surface inside the vial and remains for 45 s is the end point of the test, and the results are expressed as the volume of AEA added, defined as the 'Foam index'.

To standardise the degree of shaking, a digital laboratory automatic shaker (IKA MS3 digital vortex mixer) was used as shown in Figure 3-14. The motion of the shaker was circular in a horizontal plane, with an agitation stroke of 4.5 mm, and allowed control of the rotational speed and period of application. A laboratory-prepared rectangular block of lightweight plastic was fitted to the head of the automatic shaker, where the vial was placed during testing.

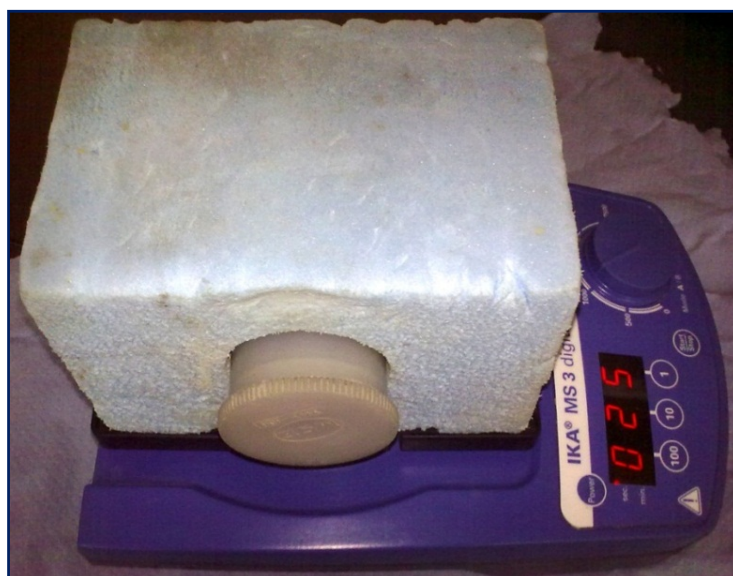


Figure 3-14 Automatic shaker for foam index test

Suitable test conditions were developed by considering the following effects i) degree of shaking; ii) shaking period; iii) AEA; and iv) fly ash and are discussed in the Section 6.1.2. The major benefits of the automatic shaker are the consistent degree of shaking and more uniform bubble size, making end point recognition more straightforward with uniform and larger bubble sizes.

3.4.2 Acid blue 80 test

The AB80 test is based on spectrophotometric determination of the absorbance of this dye in solution (i.e. concentration) at one of the three suitable peak wavelengths (626, 581 or 282 nm) and was originally developed for assessing the effectiveness of commercial activated carbon (Hameed *et al.*, 2007; Zhang and Nelson Jr., 2007; ASTM, 2008b). In principle, 2.0 g of fly ash is exposed to a 100 ml of AB80 solution (100 mg/l), and mixed by a magnetic stirrer at 400 rpm until there is practically no further dye uptake by fly ash (30 minutes, Figure 3-15 (a)).

The solution is then filtered with a cellulose filter paper of nominal pore size 11 μm . The difference between the original dye concentration in solution and that in the filtrate, expressed in mg per gram of fly ash, is defined as the AB80 adsorption. A Fisher Scientific digital colorimeter (*model 45*) capable of measuring the absorbance range from 0.00 – 1.99 with a resolution of 0.01 was used (Figure 3-13 (b)).



(a)



(b)

Figure 3-15. AB80 tests; (a) exposing fly ash to AB80 solution; and (b) concentration determination with colorimeter

The device has fixed wavelength filters, from which the 580 nm gave moderate sensitivity. Being highest peak, a 630 nm filter was found to give greater precision. The calibration curve using the 630 nm filter was found to be practically linear in the measurable range up to ~85 mg/l.

It was noted that the filter paper used during the test adsorbed a small quantity of AB80 from the mixture during the filtration process, thus reducing the concentration remaining in solution. Several known concentrations of AB80 solution were filtered and the absorbance values determined, to establish the necessary corrective adjustment, which was then applied during fly ash testing. At least three measurements were made with each fly ash sample and the average used to calculate the remaining concentration of AB80 in solution after adsorption by fly ash carbon.

3.4.3 Methylene blue test

The Methylene blue (MB) test is a dye test, traditionally used for the determination of potentially expansive constituents in fine aggregate and described in the European standard BS EN 933-9 (BSI, 1999a). The test was used in this study for determination of AEA sorptivity characteristics of fly ash carbon. This is similar in principle to the foam index test. A 200 g fly ash sample was mixed in 500 ml of de-ionised water and then the slurry stirred continuously using a propeller-type stirrer. After 5 minute of mixing, 5 ml of known concentration (10.0 g/l is recommended in the standard) methylene blue dye was added to the slurry and a stain test carried out on filter paper. Formation of a successive stable stain in the form of a halo (Figure 3-14) at 1 and 5 minutes indicates the end point of the test. The methylene blue value (MB value) of the sample was calculated from the total uptake to reach the end point.

3.4.4 Air entrainment in mortars

In order to investigate the effect of the reduced variability in the foam index test and the use of AB80 adsorption and methylene blue value with regard to estimating fly ash/AEA interaction, the study examined the behaviour of the materials (with selective fly ashes) in a cementitious system, initially mortar. The mix proportions adopted for this were those given in BS EN 450-1 (BSI, 2005c) for activity index, with a cement : sand ratio of 1 : 3 by

mass, a fly ash level in cement of 25% and a water/cement (PC + fly ash) ratio of 0.5. The target air content of the mortar in these tests was set at 5.0 to 6.0%.

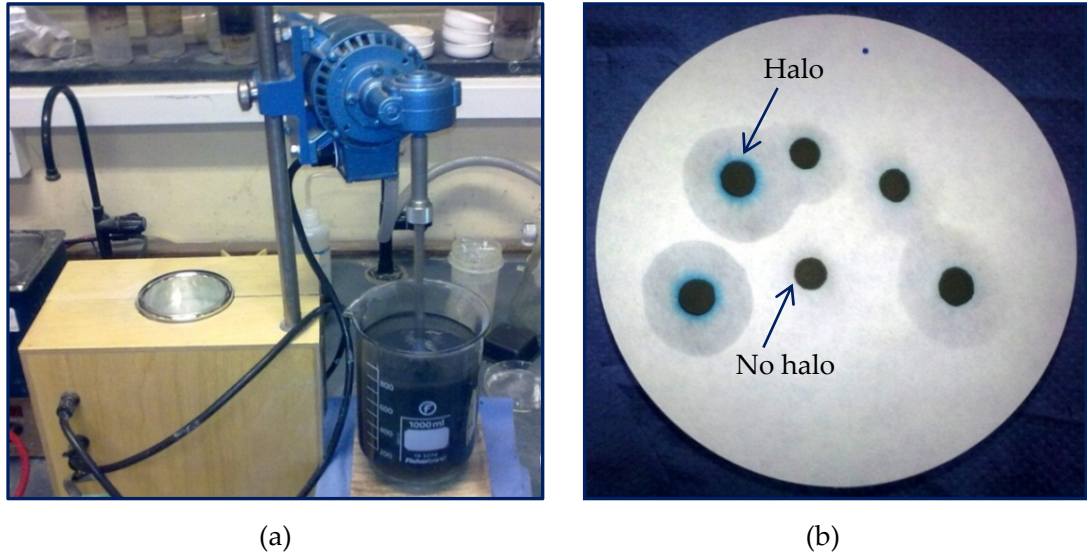


Figure 3-16. (a) methylene blue test set up; and (b) appearance of blue halo around fly ash on filter paper indicating the end point of the test

The mortar was prepared in a 5 litre orbital mixer of the type described in BS EN 196-1 (BSI, 2005a). The sand was placed in the bowl and half the water added gradually for 30 s, whilst mixing at low speed. PC and fly ash, blended together in a closed container, were then added over 30 s, while the mixer continued running at low speed. The required quantity of AEA was combined with the remaining mix water and these were then introduced over another 30 s under the same conditions. Mixing was then carried out at high speed for a total of 90 s, with a short break after 30 s to ensure all material was mixed in (adhering material scraped from the bowl wall).

Following this, the air content was measured as described in BS EN 1015-7 (pressure method; BSI, 1999c). The test with the equipment is shown in Figure 3-17(a). Initially, AEA doses were estimated based on the foam index of the particular fly ash. Following this, trials were made to determine required quantities of AEA to achieve the target air content.

3.5 Concrete Tests

Rapid reactivity assessment methods were validated by concrete tests carried out for compressive strength (of 100 mm cubes) at different ages. These were also carried out to examine the effectiveness of the foam index (using the automatic shaker), AB80 adsorption and MB value for estimating air-entrainment in concrete.

Concrete was mixed in a horizontal pan type mixer, of nominal capacity 0.035 m³. Initially, the laboratory-dry aggregates and half the water were added and mixed for 2 min. Following an eight minute rest period for aggregate absorption, the pre-blended PC/fly ash was added and mixed for one minute. The remaining water/AEA (where applicable) were introduced and mixing with all materials continued for a further two minutes. The slump and plastic density were then measured.

A 30% level of fly ash was used for both reactivity and sorptivity tests in concretes. The concretes had a fixed water/cement (fly ash+PC) ratio of 0.5, with the fine to total aggregate ratio of 0.42, based on Teychenné *et al.*, (1997) and allowance made for the volume of entrained air (where applicable).

3.5.1 Reactivity assessment

Following slump and plastic density measurements, 100 mm cube moulds were filled with concrete for strength tests. The mix proportions are given in Table 3-2. Results obtained at different ages (1, 7, 14, 28, 56, 90, 180 days) following standard water curing (20°C) were compared with the various other rapid test results.

Table 3-2. Mix proportions of concretes used for reactivity assessment

MIX	CONCRETE MIX PROPORTIONS ^a , kg/m ³								Total
	Free water	Cement/Addition			Aggregate ^b				
		PC	Fly ash ^c	Total	Sand	10 mm	20 mm	Total	
Reference	180	360	-	360	775	360	715	1850	2390
Fly ash	180	250	110	360	760	355	700	1815	2355

^a *w/c* = 0.50; ^b *sand/total aggregate ratio*: 0.42; and ^c *fly ash level*: 30%

3.5.2 Fly ash/AEA interaction assessment

Tests were carried out with AEA C1 and AEA S to entrain 5.0 ± 1.0 vol. % air in concrete containing fly ash (with the same materials used as in the mortar tests). The initial AEA doses were again estimated from the foam index test and then adjusted to entrain the target quantity of air by trial mixing. The mix proportions of the concretes are given in Table 3-3.

Table 3-3. Mix proportions of air-entrained concretes (air content: $5.0 \pm 1.0\%$)

MIX	CONCRETE MIX PROPORTIONS ^a , kg/m ³								Total
	Free water	Cement/Addition			Aggregate ^b				
		PC	Fly ash ^c	Total	Sand	10 mm	20 mm	Total	
Reference	175	350	-	350	730	340	670	1740	2265
Fly ash	175	245	105	350	715	330	655	1700	2225

^a $w/c = 0.50$; ^b sand/total aggregate ratio: 0.42; and ^c fly ash level: 30%

After measuring the slump and plastic density, the concrete was re-mixed for a further 30 s and the air content was measured to BS EN 12350-7 (pressure method, Figure 3-17 (b)) (BSI, 2009b). Once the air content target was met, 100 mm and 150 mm cubes were cast for compressive strength, ISAT and water penetration tests respectively, which were made following standard water curing at 28 days.

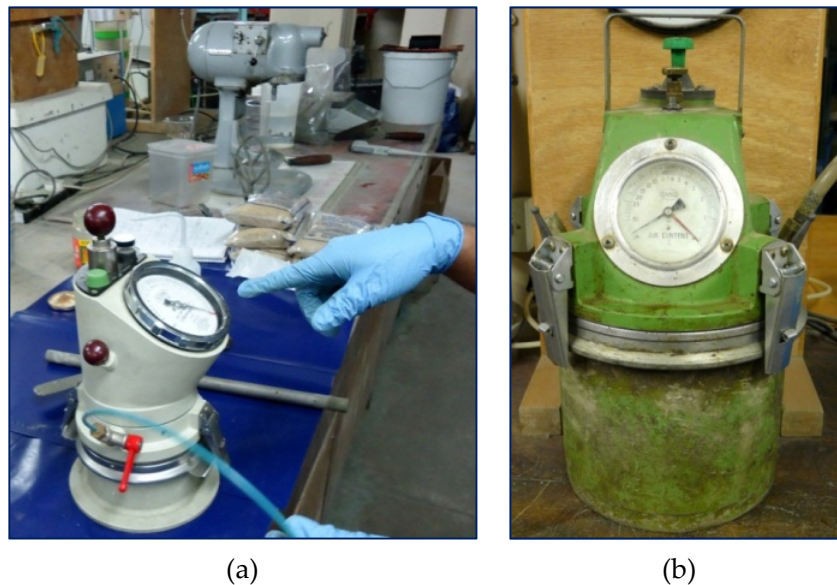


Figure 3-17. (a) Air meters used to test (a) mortar, and (b) concrete air content

Initial surface absorption test (ISAT)

The Initial surface absorption test (ISAT) gives uniaxial water absorption per unit surface area (i.e. the area immediately below the surface) under low pressure conditions. The test was carried out following BS 1881-208 (BSI, 1996) under a water head of 200 mm (slightly greater than might be applied by driving rain) at stated intervals of 10, 30 and 60 minutes. Two opposite faces of a 150 mm air-entrained concrete cube were tested.

Following 28 days of water curing, the cubes were oven dried (at $105 \pm 5^\circ\text{C}$) to a constant mass and kept in desiccator containing silica gel until cooling to room temperature. The specimen was then set up for testing (under a water head of 200 mm) and the distance of water movement (over 30 seconds) in the capillary tube was recorded at 10, 30 and 60 minutes following water contact with the specimen. The average of measurements on the two opposite faces was taken and the ISAT value calculated from Equation 3.3.

$$ISAT_t = N_t \times C_f \times 2 \quad (\text{Eq. 3-3})$$

Where, $ISAT_t$ = Initial surface absorption after time, t (minutes) in ml/(m².s)
 N_t = Number of scale division moved in 30 second
 C_f = Calibration factor of the capillary tube.

Calibration of the capillary tube was carried out with de-ionized water following BS 1881-208 (BSI, 1996).

Water penetration under pressure

Water penetration under pressure in concrete was carried out in accordance with BS EN 12390-8 (BSI, 2009c) and gives an indication of its permeability properties. The test face of 150 mm concrete cubes were scratched with a wire brush immediately after demoulding and then cured under water until the test age (28 days). The saturated test specimen's roughened surface was then set up in the test rig shown in Figure 3-18. A water pressure of 500 kN/m² was applied for 72 ± 3 hours on the scratched surface. The pressure was then released and excess water on the applied face wiped.

The cubes were split in half using a masonry splitter, perpendicular to the face on which water pressure was applied, immediately after the removal of water pressure. After

splitting, the samples were left in laboratory air for 2-3 minutes to allow the water front to become visible. This was marked and measurements were taken for maximum depth of penetration on both faces to the nearest mm. At least two cubes, prepared from the same batch of concrete, were tested and the average of these four values reported.

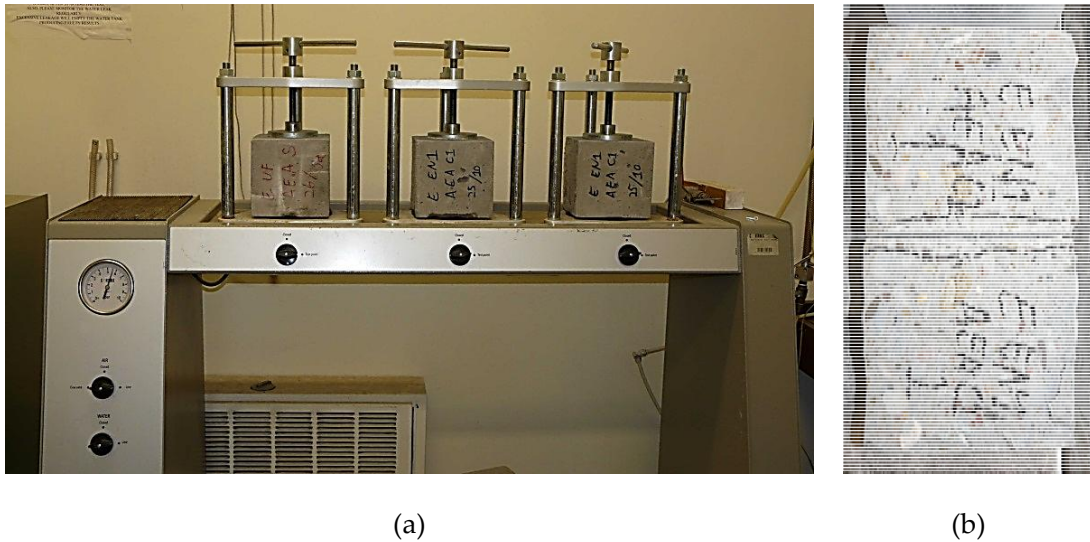


Figure 3-18. Water penetration test under pressure in air-entrained concrete

3.6 Regression Analysis

The nature of this research work is such that, relationships between test results using different methods, were examined. In most cases, linear regression analyses were carried out and relevant coefficients of correlation (R^2 values) given in figures, where applicable. In each case, null hypothesis for regression slopes were tested considering a significance level of 0.05. The null hypothesis states that the linear regression slope is zero and there is no significant correlation between the parameters under consideration. At a significance level of 0.05, obtaining a calculated P value < 0.05 indicates that the dataset can reject the null hypothesis and adopt the alternative hypothesis (i.e. a significant correlation exists between the parameters).

In Chapters 4 – 8, the P values are indicated (along with R^2 values) in the figures where the analysis failed to reject the null hypothesis. These were mainly found where R^2 values were relatively low or in some cases with moderate R^2 and a limited number of data points.

CHAPTER 4: CHARACTERISTICS OF MATERIALS

This Chapter give the characterisation results of the materials used in the study, and include fly ash, PC, aggregate, AEA and other reagents. Physical properties including fineness, specific surface area; chemical properties including, Oxide (XRF) and phase composition (XRD) and LOI are reported. SEM imaging is presented to characterize fly ashes morphologically. Sieve analysis of laboratory and standard sand, absorption and specific gravity of fine and coarse aggregates used in concrete were also reported.

4.1 Characteristics Range of Fly Ashes

Fifty four fly ashes were obtained from 8 sources in the UK for inclusion in the project. In addition, three run-of-station fly ash samples from Bangladesh were also considered. Tables A-1 and A-2 and Figures 4-1 and 4-2 give the details, coding and classification of the fly ash samples respectively. The sources of the fly ashes are designated alphabetically. The letter following the Source name in the coding indicates their fineness category in accordance with BS EN 450 (Category S, < 12% and Category N, > 12% and < 40% retained on a 45 μm sieve). Fly ashes from Bangladesh are designated BD W1, BD W2 and BD S. Air-classified fly ashes from source C and L are designated in terms of their source name followed by the separation target d_{90} . The parent fly ashes (feed for air-classification) are named as CFD and LFD, respectively. Detailed properties of the materials are given in Tables 4-1 to 4-4

Monthly fly ash samples (conforming to BS EN 450, fineness category S and with LOI < 7.0%) were obtained from Sources A and C over a one year period ($12 \times 2 = 24$ samples) to examine seasonal variation effects on their properties and with regard to the assessment tests being considered. However, it should be noted that these 24 samples were air-classified to give consistent properties to be acceptable to the market. Spot samples

(Category N, LOI < 7.0%) were also collected from Sources A and B, while spot run-of-station fly ashes were provided from Sources C and F to widen the property range.

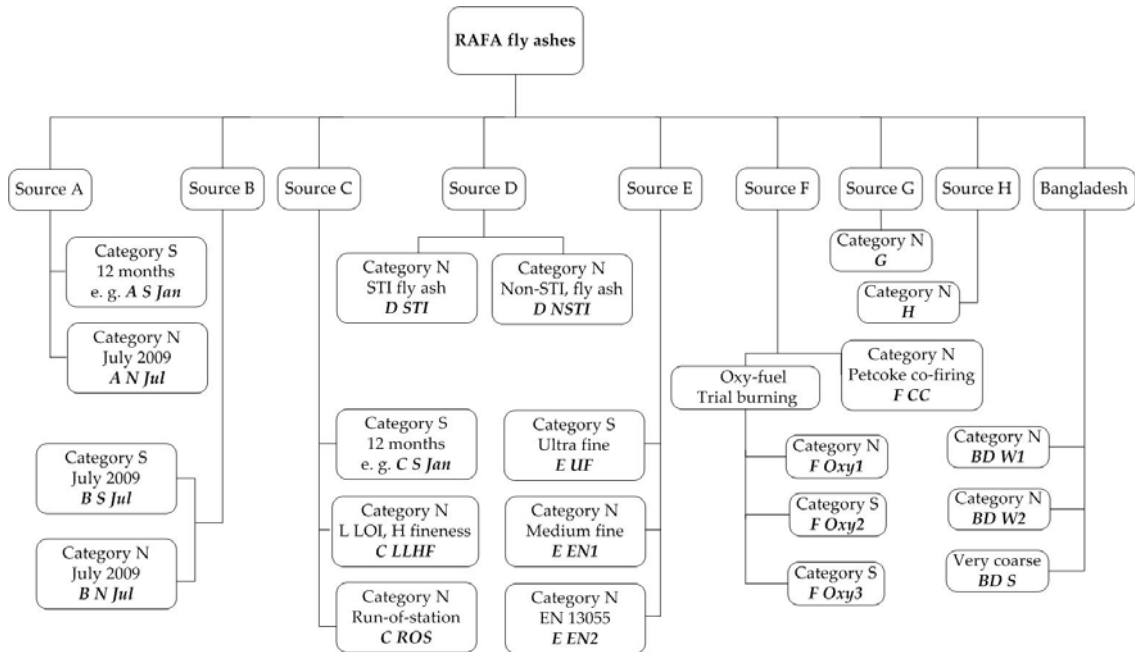


Figure 4-1. Classification of main fly ashes (*Sample names are given in italics*)

Source D used STI carbon removal to give low LOI fly ashes. Both STI and non-STI fly ashes were obtained from this source. Pet coke co-combustion fly ash was obtained from Source F to compare with coal-only fly ashes. Oxy-fuel combustion is a concept designed to enable the capture and subsequent sequestration of CO₂ from power stations. Given the limited use of the technique at full-scale, three oxy-fuel fly ashes from Source F were supplied from a 1 MW experimental power generation burner.

A high fineness (45 µm sieve retention 4.8%) and low LOI (3.0%) fly ash was obtained from Source E. Two other fly ashes were collected from the same source having higher LOIs and of Category N fineness. Fly ash with relatively high LOI (9.1%) and percentage of fine material (45 µm sieve residue 14.4% and 35.4% of the material finer than 10 µm) was obtained from Source H. A fly ash sample was also collected from Source G, which contained high levels of coarse carbon and was relatively coarse (fineness category N). Sample BD S had the lowest LOI, however, this was coarser than all of the other fly ashes used during the project.

Finally, two run-of-station fly ashes were obtained from Source C and L and air-classified at Bradley Pulveriser Company to give 6 different fine fractions. By air-classification, samples of particle size below a specific target d_{90} were obtained. The target d_{90} s were 5, 10, 20, 30, 40 and 50 μm and as shown in Figure 4-2, the 12 processed samples are designated with the source name and the target d_{90} size.

The samples were all dry, i.e. moisture contents were 0.1-0.2% by mass. Detailed properties of these are considered in detail in the following sections.

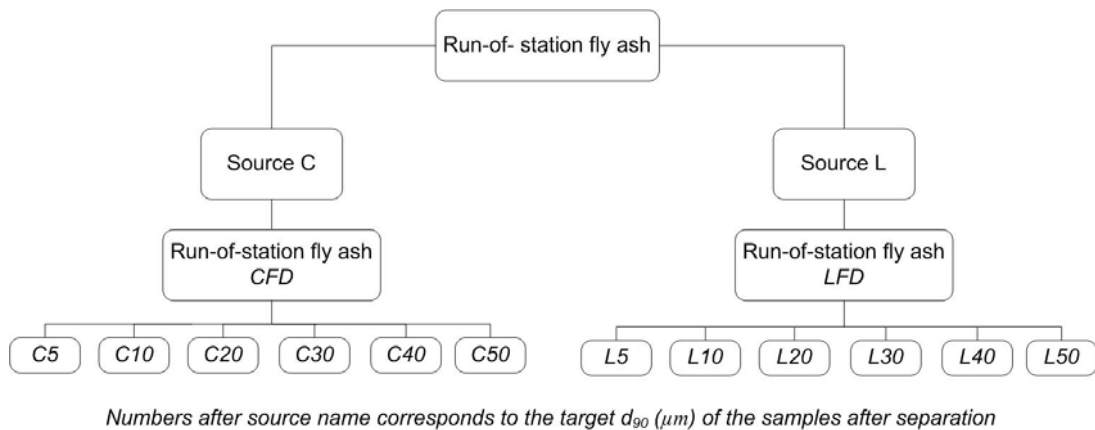


Figure 4-2. Codes of air-classified fly ash samples (*Sample names are given in italics*)

4.1.1 Fineness of fly ash samples

Wet sieve analysis

In general, monthly samples from Source A tended to be slightly coarser than Source C. The 45 μm sieve residues of the monthly samples from Sources A and C were between 9.6 - 11.7% and 9.2 - 11.3% respectively, while this was between 3.6 - 36.1% for the other fly ash samples. Fly ash F Oxy3 was found to be of lowest retention, 3.6% on the 45 μm sieve, while the highest was BD S at 66.5%. The 45 μm sieve residues of the fly ashes are given in Figure 4-3. The parent samples used for air-classification had retentions of 34.9 (CFD) and 22.6% (LFD) on the 45 μm sieve for Source C and L. Corresponding values for samples C50 and L50 were 1.3% and 1.6%. The other smaller size fractions were not tested for 45 μm sieve retention as there would be practically negligible/no retention.

Table 4-1. Physical properties of monthly fly ashes received from Source A

PROPERTIES	A-S Jul	A-S Aug	A-S Sep	A-S Oct	A-S Nov	A-S Dec	A-S Jan	A-S Feb	A-S Mar	A-S Apr	A-S May	A-S Jun
LOI ^a , %	4.9	4.6	5.1	4.1	4.5	4.4	3.8	4.7	4.3	4.5	4.2	3.9
<45 µm part	3.2	-	-	-	-	2.6	2.2	2.8	2.5	2.7	-	-
>45 µm part	1.7	-	-	-	-	1.8	1.6	1.9	1.8	1.8	-	-
BET area, m ² /g	2.45	1.93	1.70	1.70	2.13	2.05	1.55	2.17	2.31	1.68	1.80	2.20
45 µm sieve retention, %	10.6	10.3	10.0	10.6	9.9	10.1	9.6	11.7	10.4	9.8	11.3	9.9
PSD d ₁₀ , µm	2.8	2.9	2.0	2.1	1.9	1.8	2.0	2.2	2.0	1.9	2.4	2.1
PSD d ₅₀ , µm	17.6	17.1	16.5	16.3	16.1	15.3	15.2	17.7	16.3	15.7	17.6	16.8
PSD d ₉₀ , µm	66.1	66.1	64.7	60.9	59.5	62.2	60.2	72.6	67.2	63.4	66.0	64.3
Sub-10 µm quantity, %	32.8	33.1	35.6	35.4	35.9	37.7	37.5	34.0	36.0	36.7	33.3	34.4
Blaine fineness, m ² /kg	400	410	410	400	400	418	370	406	390	400	333	392

^a Loss-on-ignition carried out at 975°C, - Not detected/tested

Table 4-2 Physical properties of monthly fly ashes received from Source C

PROPERTIES	C-S Jul	C-S Aug	C-S Sep	C-S Oct	C-S Nov	C-S Dec	C-S Jan	C-S Feb	C-S Mar	C-S Apr	C-S May	C-S Jun
LOI ^a , %	4.4	3.7	4.4	4.1	5.0	4.2	4.3	3.8	3.8	3.9	4.4	5.1
<45 µm part	2.3	-	-	-	-	2.2	2.2	2	2	2	-	-
>45 µm part	2.1	-	-	-	-	2.0	2.1	1.8	1.8	1.9	-	-
BET area, m ² /g	2.52	1.67	2.41	2.22	2.40	2.61	1.88	2.28	2.33	2.13	2.10	2.80
45 µm sieve retention, %	10.5	10.4	10.1	10.5	10.4	9.2	9.9	10.3	10.4	10.5	11.3	11.2
PSD d ₁₀ , µm	1.9	1.8	1.9	1.4	1.4	1.7	1.9	1.7	1.7	1.6	2.0	1.9
PSD d ₅₀ , µm	13.0	12.5	12.8	11.7	11.8	11.6	11.5	11.9	12.0	12.0	14.0	14.5
PSD d ₉₀ , µm	61.9	60.7	63.9	61.8	59.7	67.1	67.3	66.0	63.9	63.2	73.3	75.9
Sub-10 µm quantity, %	42.2	43.4	42.9	45.6	45.1	45.6	45.7	44.9	44.6	45.2	40.7	40.4
Blaine fineness, m ² /kg	470	450	440	460	470	485	483	495	495	448	433	447

^a Loss-on-ignition carried out at 975°C - Not detected/tested

Table 4-3. Physical properties of other fly ashes received from various sources

PROPERTIES	A-N Jul	B-N Jul	B-S Jul	C LLHF	C ROS	D STI	D NSTI	E UF	E EN1	E EN2
LOI ^a , %	5.1	4.3	5.0	3.1	13.4	2.6	24.1	3.0	3.9	6.4
<45 µm part	2.8	1.2	0.9	0.6	3.8	0.7	9.2	0.7	0.9	1.4
>45 µm part	2.3	3.1	4.1	2.5	9.6	1.9	14.9	2.3	3.0	5.0
BET area, m ² /g	2.64	1.54	2.21	2.10	5.79	1.12	4.84	2.46	3.60	5.20
45 µm sieve retention, %	19.3	26.7	11.2	29.1	36.1	21.8	30.7	4.8	20.4	23.4
PSD d ₁₀ , µm	2.6	2.1	1.7	1.9	3.2	2.1	3.4	2.2	2.6	2.8
PSD d ₅₀ , µm	21.6	24.7	14.0	24.0	43.0	18.3	36.6	11.5	20.7	24.6
PSD d ₉₀ , µm	85.1	109.7	62.9	112.3	161.1	90.1	114.8	36.1	98.7	108.1
Sub-10 µm quantity, %	29.4	30.3	39.9	33.2	22.6	36.4	21.8	44.5	31.8	28.5
Blaine fineness, m ² /kg	370	350	410	489	439	554	325	547	519	494

^a Loss-on-ignition carried out at 975°C - Not detected/tested

(Continued on next page)

Table 4-4. Physical properties of other fly ashes received from various sources

PROPERTIES	F CC	F Oxy 1	F Oxy 2	F Oxy 3	G	H	BD W1	BD W2	BD S
LOI ^a , %	7.6	5.4	14.2	7.9	8.7	9.1	5.3	4.2	1.4
<45 µm part	2.5	1.8	1.8	0.7	1.8	5.3	-	-	-
>45 µm part	5.1	3.6	12.4	7.2	6.9	3.8	-	-	-
BET area, m ² /g	5.02	2.46	10.39	6.98	5.50	8.78	1.21	0.79	0.36
45 µm sieve retention, %	28.8	19.1	8.3	3.6	21.1	14.4	35.0	24.0	66.5
PSD d ₁₀ , µm	2.0	7.9	4.7	3.3	2.5	1.8	6.0	4.6	10.7
PSD d ₅₀ , µm	27.9	30.3	22.4	12.4	23.8	18.4	26.0	22.1	58.9
PSD d ₉₀ , µm	109.0	81.8	79.7	59.3	113.7	75.2	110.4	82.6	168.0
Sub-10 µm quantity, %	29.3	14.1	25.9	41.9	29.7	35.4	17.7	24.0	9.23
Blaine fineness, m ² /kg	517	248	418	309	437	611	235	270	167

^a Loss-on-ignition carried out at 975°C - Not detected/tested

(Continued from previous page)

Table 4-5. Physical properties of air-classified fly ashes from Sources C and L

PROPERTIES	C5	C10	C20	C30	C40	C50	CFD	L5	L10	L20	L30	L40	L50	LFD
LOI ^a , %	6.7	6.6	7.1	7.5	6.4	6.9	11.5	8.5	6.2	4.7	4.0	3.9	3.8	5.7
BET area, m ² /g	6.50	5.37	6.11	5.41	4.70	5.49	5.67	7.20	4.81	3.65	3.64	2.98	4.00	3.19
45 µm sieve retention, %	-	-	-	-	-	1.3	34.9	-	-	-	-	-	1.6	22.6
PSD d ₁₀ , µm	0.9	0.9	1.0	1.1	1.2	1.3	3.0	1.1	1.1	1.3	1.7	1.8	1.7	3.1
PSD d ₅₀ , µm	3.3	3.6	3.8	5.4	7.3	9.3	22.4	3.9	4.7	6.7	9.3	10.5	12.8	23.7
PSD d ₉₀ , µm	10.8	11.6	14.5	22.1	33.3	46.1	120.0	9.3	11.5	16.6	26.3	32.7	45.7	115.9
Sub-10 µm quantity, %	89.0	87.7	84.4	73.6	61.5	52.2	28.7	91.5	86.0	70.0	53.4	48.0	42.3	27.3
Blaine fineness, m ² /kg	706	693	717	630	620	597	408	766	613	547	522	507	504	434

^a Loss-on-ignition carried out at 975°C - Not detected/tested

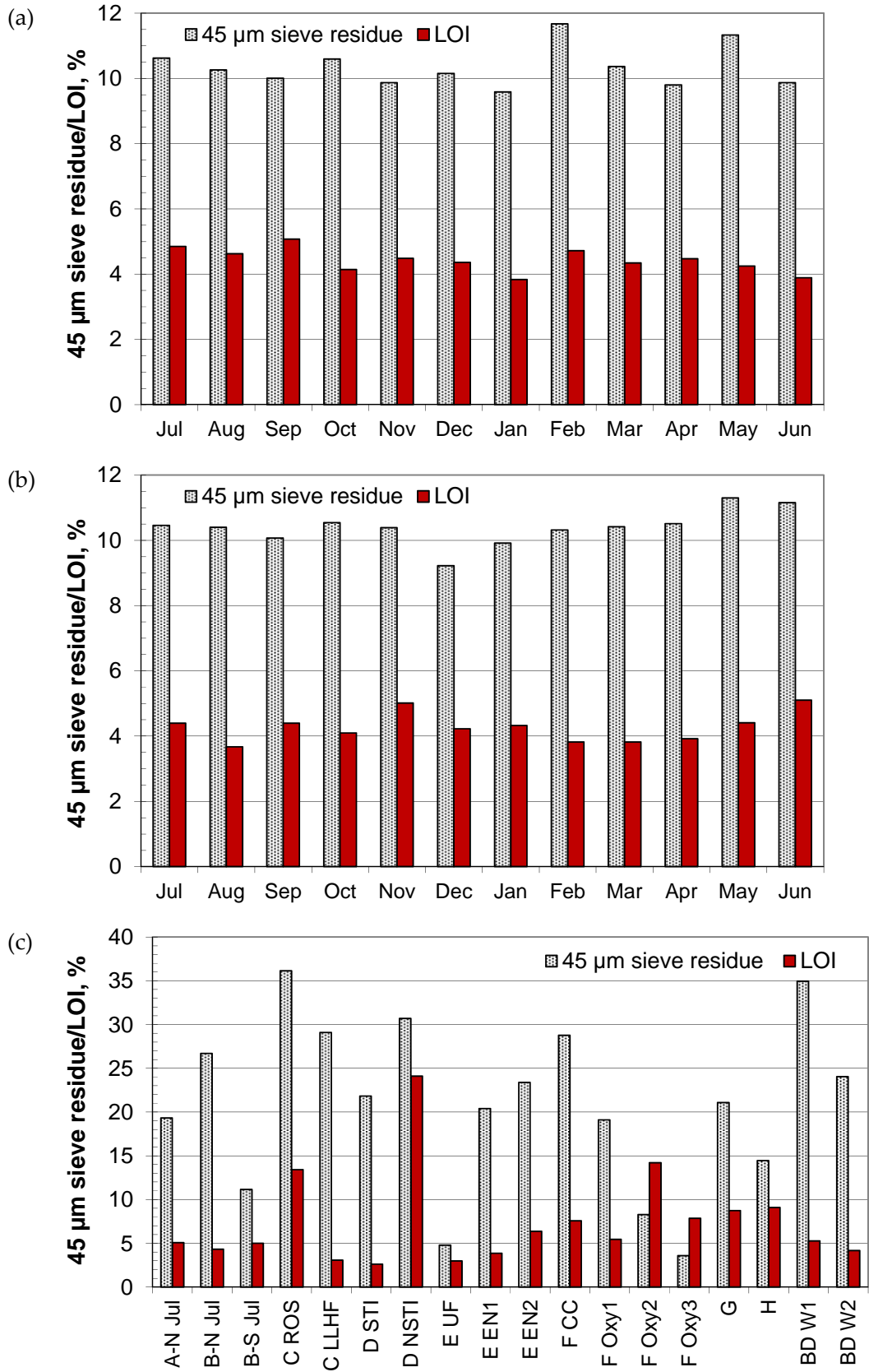
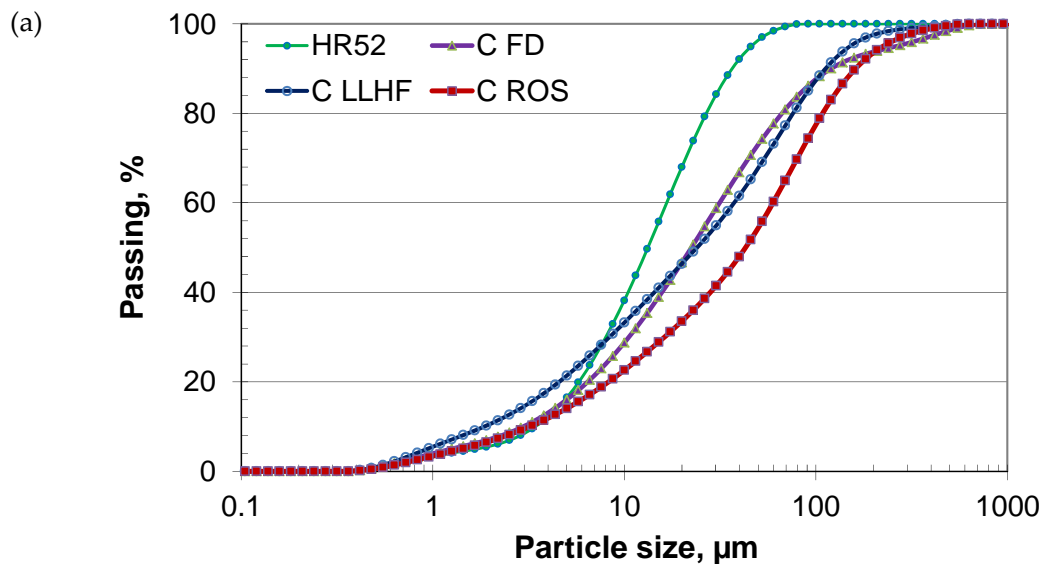


Figure 4-3. 45 µm sieve fineness and LOI of (a) monthly fly ash samples from Source A; (b) monthly fly ash samples from Source C; and (c) fly ash samples from various sources. (BD S sieve residue 66.5% and LOI 1.4%)

The run-of-station fly ash obtained from Source C during July 2011 (summer, C ROS, 36.1%) was found to be slightly coarser than that obtained during January 2012 (winter, CFD, 34.9%) as found elsewhere in the literature (Sear, 2011). The monthly samples from Source C are the result of air-classification used at this power station, which reduced the 45 μm sieve retention to $\sim 10\%$. Therefore, on average a quarter (coarsest part) of the material was removed (from the run-of-station fly ash) to be acceptable in the market. The fineness of samples from Source D improved by STI application, where 45 μm sieve retention reduced from 30.7% (D NSTI) to 21.8% (D STI) following this. The fineness of F CC obtained during February 2010 (co-combustion fly ash; winter, run-of-station) was 28.8%, while LFD obtained during January 2012 gave lowest retention (22.6%) on the 45 μm sieve of all run-of-station fly ashes used during the project.

Particle size distribution

Particle size distribution was obtained by LASER PSD analyser. Figure 4-4 shows the particle size distributions of samples from Sources C, D, F and Bangladesh, and, as with the 45 μm sieve residue, demonstrate the fineness range of the fly ashes. In order to make a comparison, the PSD of the main PC (HR52; detailed properties described later) is also included in these figures.



Continued to next page

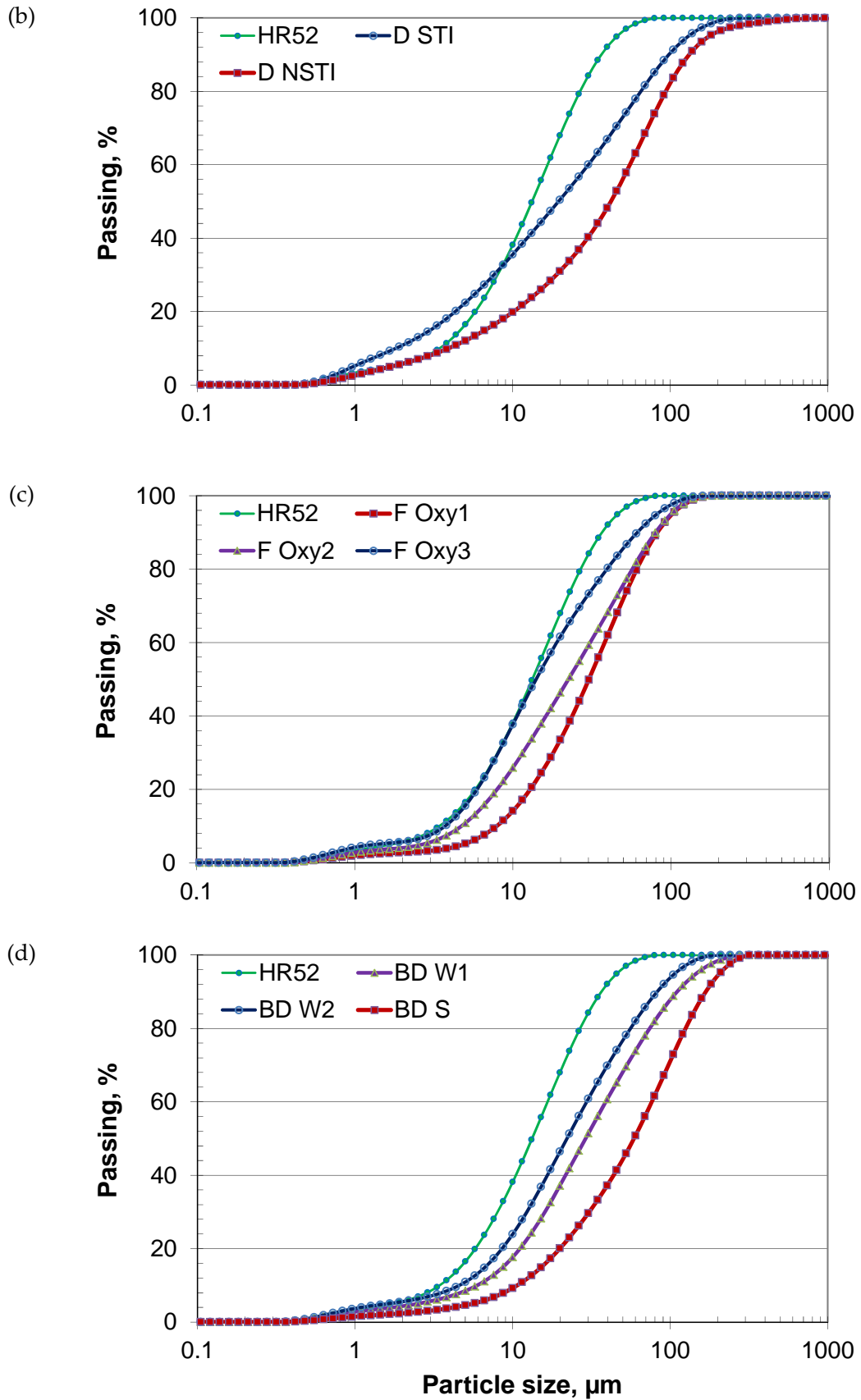


Figure 4-4. Comparison of particle size distribution for selected samples from a) Source C; b) Source D; c) Source F (trial burned oxy-fuel samples); and (d) Bangladesh

In general, the PC particles were found to be finer than the fly ashes. While in most cases the PSD curves for the fly ashes and PC were found to be parallel, difference were noted for two carbon removed fly ashes namely C LLHF and D STI. Clear differences in PSDs of run-of-station fly ashes C ROS and CFD (summer 2011 and winter 2012) were noted, as shown in Figure 4-4(a) and as found by 45 μm sieve retention.

Figure 4-5 gives PSD comparisons for air-classified fly ash samples from Sources C and L with respect to their parent sample and PCs (HR52 and HK52 for mortar and concrete respectively; detailed properties given later) used to test these. The parent fly ashes CFD and LFD were found to be coarser than the PCs. Among the classified fly ashes, L50 was close to PC HR52, while all others were finer than the PCs, which is in contrast to the other fly ashes described earlier.

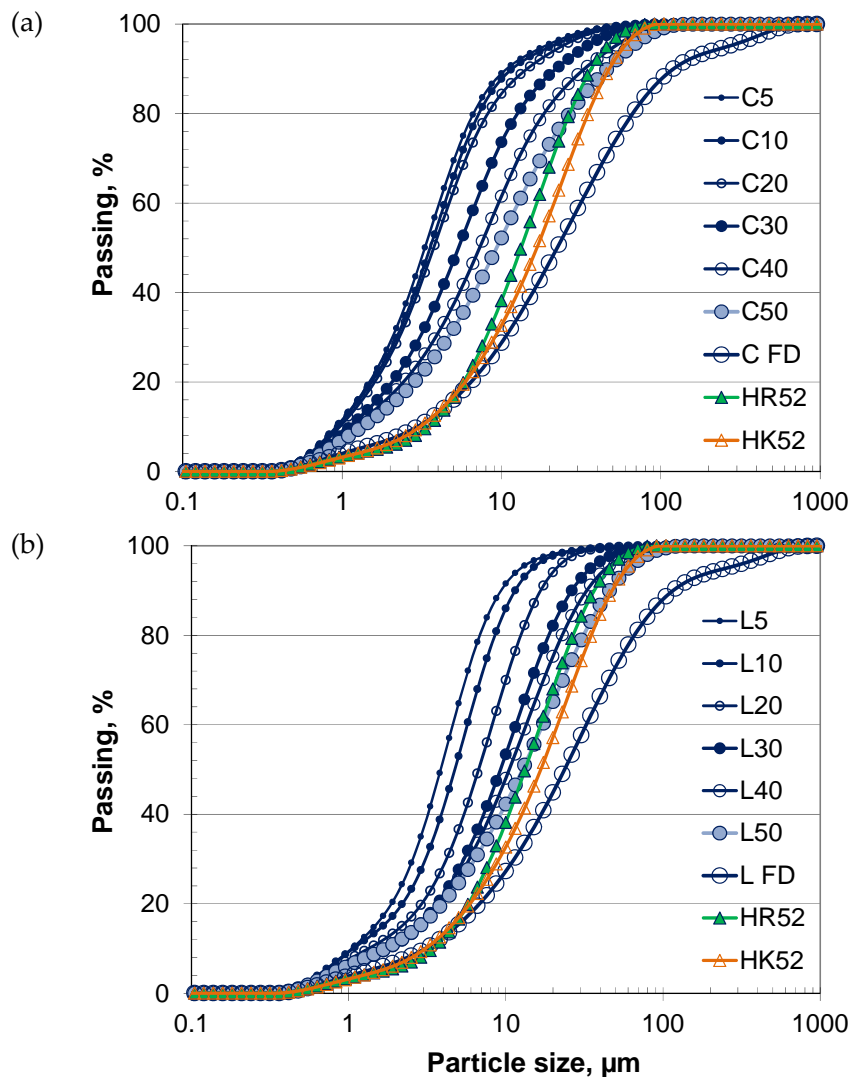


Figure 4-5. PSD comparison of air-classified fly ashes from Sources C and L

A comparison of the d_{90} of samples obtained by air-classification from Sources C and L is given in Figure 4-6. d_{90} of samples C40 and L40 was comparable with PC HR52 while this was similar between processed fly ashes C50 and L50 with PC HK52.

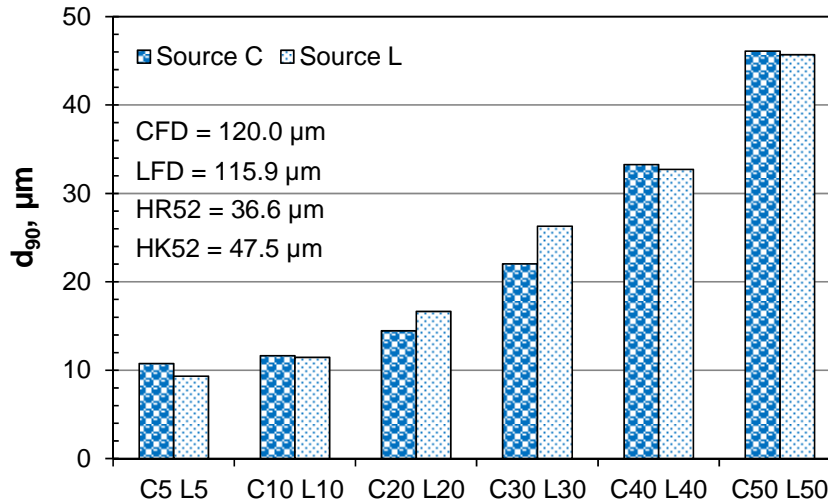


Figure 4-6. Comparison of d_{90} of air-classified fly ashes with respect to PCs

The sub 10 μm quantities of fly ashes from various sources are given in Figure 4-7. Variations in quantities were observed, depending on production season and sources. The fly ashes from the winter months gave higher percentages of sub 10 μm quantity. As shown in Figure 4-7 (a), Source C consistently gave higher quantities than Source A. Although the range of 45 μm sieve residues for monthly fly ashes from Sources A and C were close (between 9.6 – 11.7% and 9.2 – 11.3% respectively) a wider variation (32.8 - 37.7% and 40.4 – 45.7%) was observed in their sub-10 μm quantities. On the other hand, wider variations (9.2 – 44.5%) were observed for this between samples obtained from the various other sources.

The 45 μm sieve residue analysis is a weight basis measurement, while LASER PSD analysis is determined on a volume basis. Relationships between 45 μm sieve residue and fly ash quantity greater than 45 μm measured by LASER PSD are given in Figure 4-8. Although a very good correlation ($R^2 = 0.94$) was obtained, PSD results were consistently higher. The relationship between d_{50} measurements by LASER particle size analyser (PSD) and wet sieve analysis is given in Figure 4-9. Except for a few materials, a good correlation was achieved ($R^2 = 0.87$) between these. The materials that did not follow the general trend

either had carbon removed, or were from oxy-fuel trial burning, which, therefore, appeared to change the PSD from those obtained by normal means.

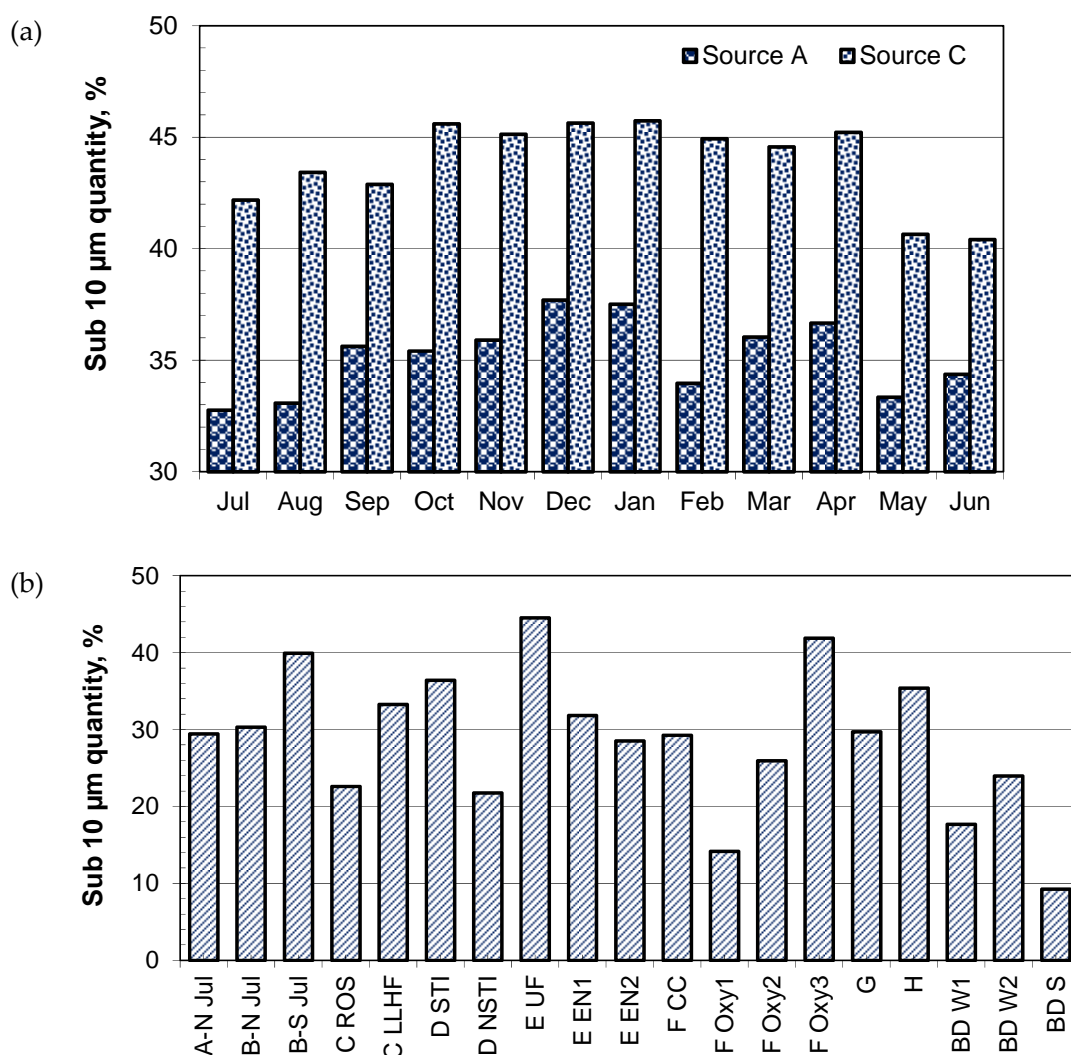


Figure 4-7. Sub-10 µm quantity (by volume) of (a) monthly fly ash samples from Source A and Source C; and (b) fly ash samples from various sources.

4.1.2 LOI

The LOI of monthly samples from Sources A and C were found to be very similar and ranged from 3.8 – 5.1% and 3.7 – 5.1% respectively, while this was between 1.4 - 24.1% for the other fly ashes (Figure 4-3). The two run-of-station fly ashes from Source C (C ROS and CFD) obtained during July 2011 (summer) and January 2012 (winter) had LOIs of 13.4% and 11.5%, respectively, indicating better burning during winter base-load conditions as

noted in the literature (Sear, 2011). The monthly sample's LOI was controlled by the air-classification system installed at Source C and reduced to ~4%.

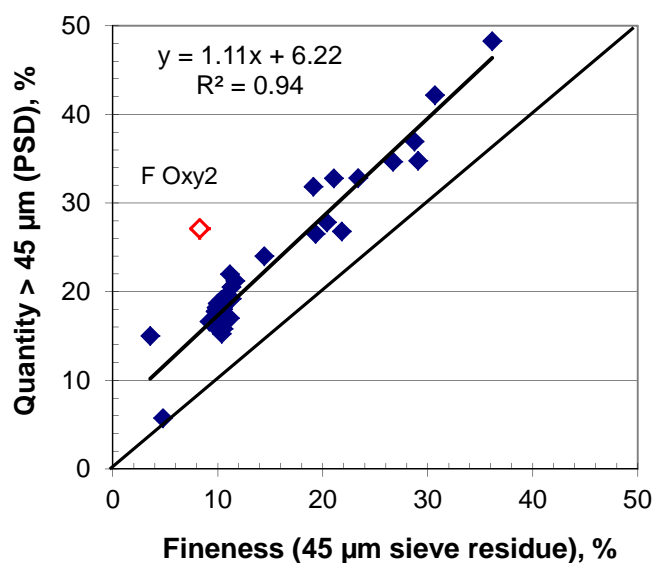


Figure 4-8. Relationship between fineness measurement by 45 µm sieve (by mass) and PSD (by volume)

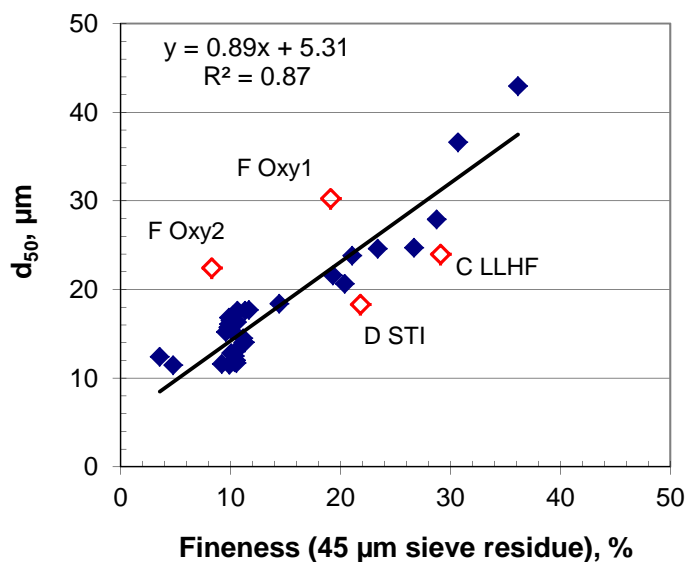


Figure 4-9. Relationship between fineness measurements; 45 µm sieve residue (by mass) and d_{50} measured by LASER PSD (by volume)

With the application of STI, the LOI of fly ash from Source D reduced to 2.6% from 24.1% and became lightest in colour of the UK materials. Fly ashes C ROS, CFD, F CC, F Oxy2, F Oxy3, G and H also gave high LOIs (>7.0%). The summer run-of-station fly ash, obtained

from Bangladesh had the lowest LOI (1.4%), though it gave highest retention on the 45 μm sieve (66.5%).

To further characterize the size of carbon, selected fly ashes were separated to obtain their portion greater and less than 45 μm , using wet sieving. The LOI of materials finer and coarser than 45 μm , for selected fly ashes, are shown in Figure 4-10. In the monthly samples from Sources A and C, the LOIs were found to have a similar contribution from both fractions, which indicates that coarse carbon ($> 45 \mu\text{m}$) is still dominant in these fly ashes, although a quarter of the materials had already been removed by classification. Wider variations were obtained for the other samples from various sources.

As shown in Figure 4-10 (c), coarse carbon was mainly responsible for the high LOIs in samples D NSTI, F CC and G, while the major portion of the LOI in fly ash H originated from its finer fraction. In general (except D NSTI and H), the LOI contribution from finer fractions was less than 5.0%. Although 62% of unburned carbon was present in the coarse fraction, the finer fraction still gave a LOI of 9.2% in fly ash D NSTI. Therefore, particle classification was not enough to reduce carbon content to an acceptable range, unlike STI technology, which reduced the LOI from 24.1% to 2.6%.

Figure 4-11 makes a comparison of the LOIs of air classified fly ash samples from Sources C and L. For Source C, with air-classification, LOI reduced to 55 - 66% of the parent sample, indicating the presence of significant quantities of coarse carbon particles with $d_{90} > 46.1 \mu\text{m}$. The lowest LOI was observed in the C40 sample. Indeed, the distribution of carbon was similar in all size fractions up to d_{90} of 46.1 μm . However, the opposite was noted in classified fly ash from Source L. In this case, although the parent fly ash had a comparatively lower LOI of 5.7%, this increased (up to 8.5%) as the particle fraction sizes reduced, indicating increased concentrations of carbon particles in finer fractions. Except for the finest fraction, fly ash from Source L always gave lower LOI than Source C in the similar size fractions. Although differences in d_{90} between finest samples L5 and L10 were minor (9.3 and 11.5 μm , respectively), their LOI varied significantly (8.5 and 6.2% respectively). This gives important information on the air-classification process. As indicated, the target d_{90} for C10 and L10 samples was 10 μm and after setting the air-classifier for this target, the d_{90} values achieved were 11.6 μm and 11.5 μm , respectively.

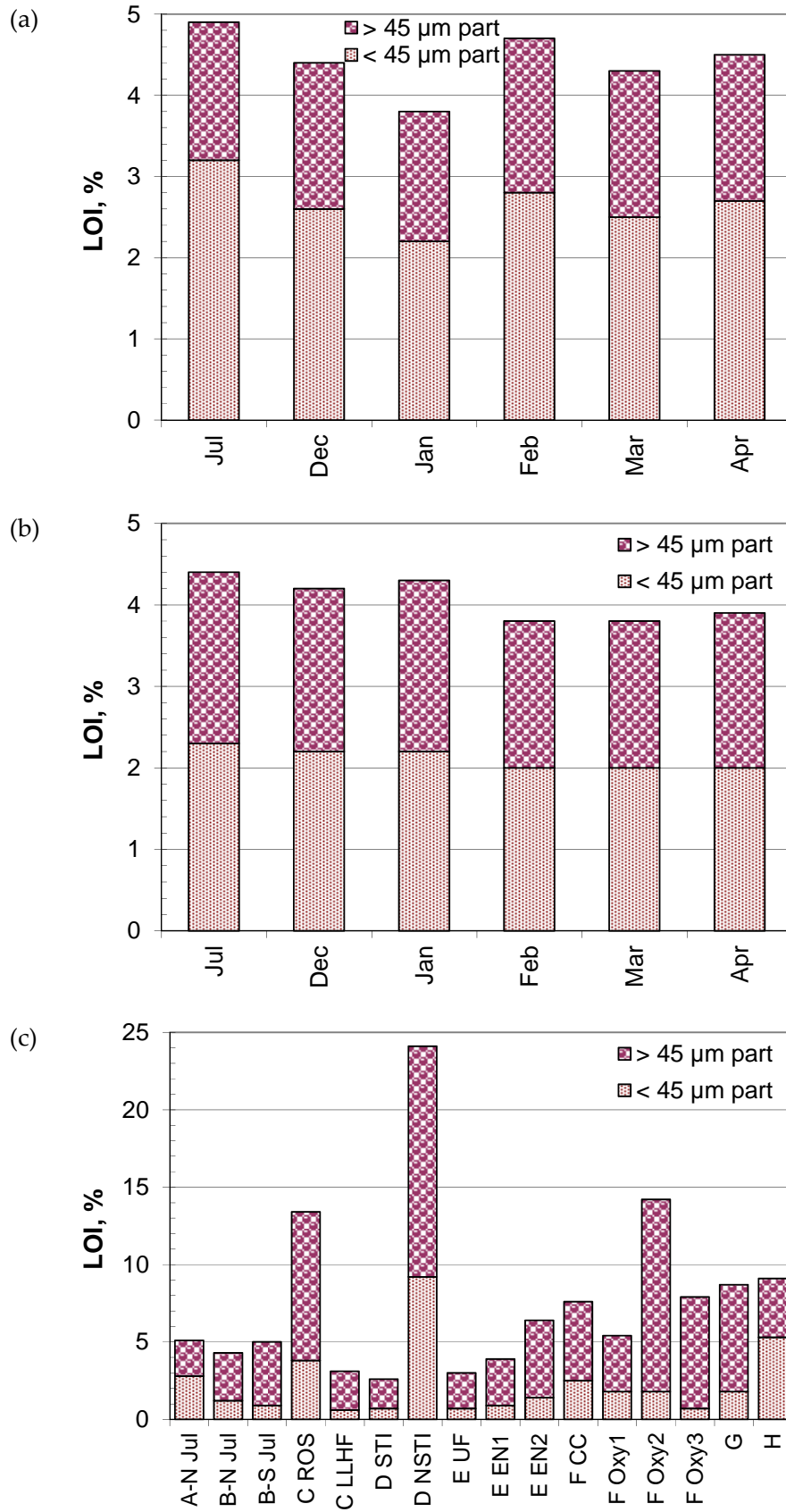


Figure 4-10. LOI of fly ash fractions finer and coarser than 45 µm (shown as their contribution to the overall LOI)

However, whilst the target 5 μm was set for C5 and L5 samples, the system only achieved 10.8 and 9.3 μm , respectively. As the carbon distribution in all fractions for Source C was similar, there was little difference between LOIs in C5 and C10 samples. However, due to the abundance of fine carbon, significant quantities accumulated in the L5 samples, while the target d_{90} was not achieved. This suggests that the current processing by air-classification was beneficial up to a target d_{90} of 10 μm .

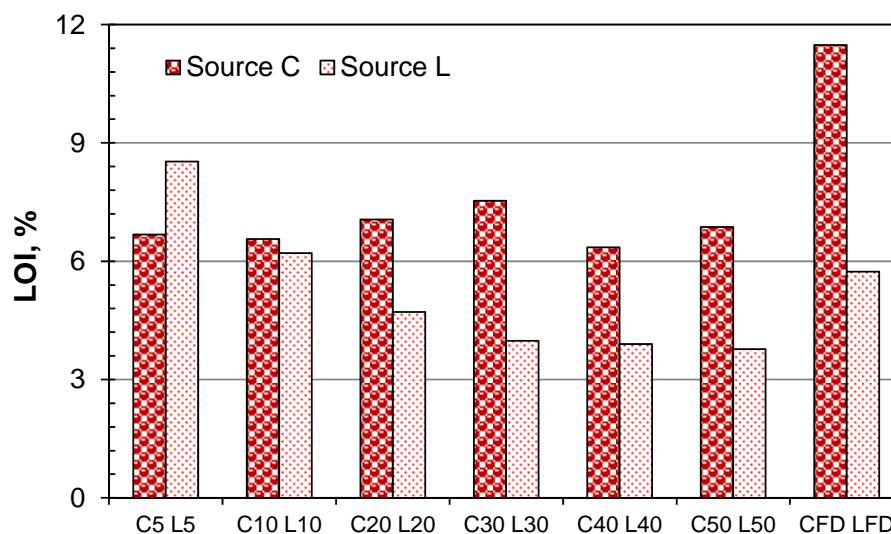


Figure 4-11. Comparison of (a) LOI and (b) d_{90} of air-classified fly ash samples from Sources C and L

4.1.3 Specific surface area

The specific surface area (by N_2 adsorption using BET theory) of monthly samples from Sources A and C ranged from 1.6 - 2.5 m^2/g and 1.7 - 2.8 m^2/g respectively, while the range for the other fly ashes was found to be 1.1 - 10.4 m^2/g . Although fly ashes from Source C gave slightly lower retentions on the 45 μm sieve, their N_2 specific surface areas were found to be slightly higher than those of Source A. In general, the specific surface area increased with LOI. However, exceptions were found, for instance fly ash C ROS, gave a lower specific surface area than expected given its LOI. In this case, the LOI appears to originate from relatively non-porous type carbon (see SEM images in Figure B-5 (b)).

Fly Ash BD S gave very unusual behaviour among the materials tested during the project. While it gave highest retention on the 45 μm sieve (66.5%), its LOI was lowest (1.4%). The

lowest LOI was also supported by its giving the lowest specific surface area of $0.36 \text{ m}^2/\text{g}$. Although other materials obtained from Bangladesh gave relatively lower specific surface area (0.79 and $1.21 \text{ m}^2/\text{g}$), the behaviour of Fly Ash BD S may be due to effects noted in its morphology. The SEM image B-11 (b) indicates the presence of relatively solid foreign materials in this fly ash, which might be impurities in the coal, which did not melt completely during the combustion process.

The specific surface areas of fractions coarser/finer than $45 \mu\text{m}$ of selected fly ashes were also measured and are shown in Table B-3. In general, the finer fractions made a higher contribution to the specific surface area but this was minor in the coarse fractions (relatively solid in nature) as indicated in the literature (Gao *et al.*, 1997).

A comparison between the specific surface areas of air-classified fly ashes with respect to their parent fly ashes is given in Figure 4-12. In general, finer fractions gave higher surface areas for both sources, with a clearer trend noted in the case of Source L. As with the LOI of the finest fractions, (C5, C10, L5 and L10), the specific surface area also indicates limitations of air-classification in targeting $d_{90} < 10 \mu\text{m}$.

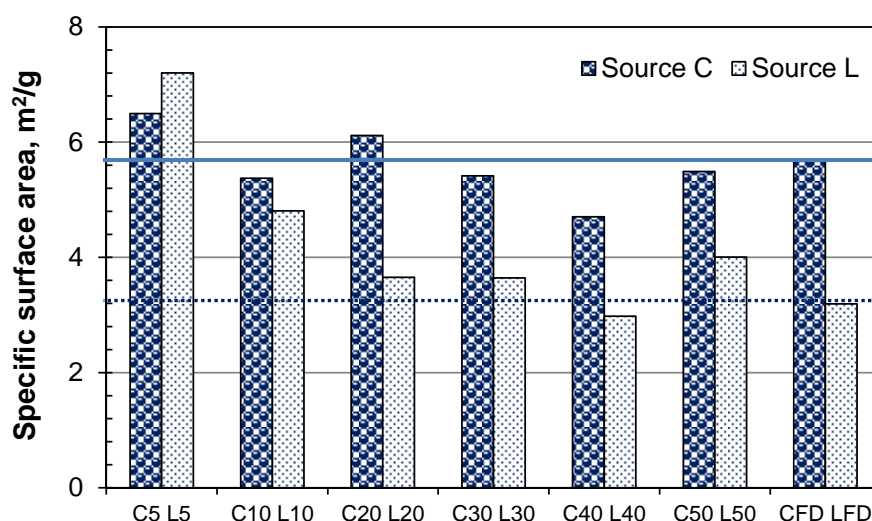


Figure 4-12. Comparison of specific surface area of air-classified fly ashes from Sources C and L with respect to the parent samples

Figure 4-13 gives the relationships between LOI and specific surface area of the fly ashes used. A general correlation was obtained except for fly ashes C ROS and D NSTI which gave relatively lower surface area compared to their high LOI values as run-of-station

samples. As noted earlier (Figure 4-10 (c)), the majority of the LOI of these two fly ashes originated from the relatively coarse portion, which was solid by nature. As given Figure 4-13 (b), a similar correlation was observed between LOI and specific surface area for different fractions of air-classified fly ashes. However, their parent samples (Fly Ashes CFD and LFD) did not follow the trend, as found earlier for run-of-station Fly Ashes C ROS and D NSTI.

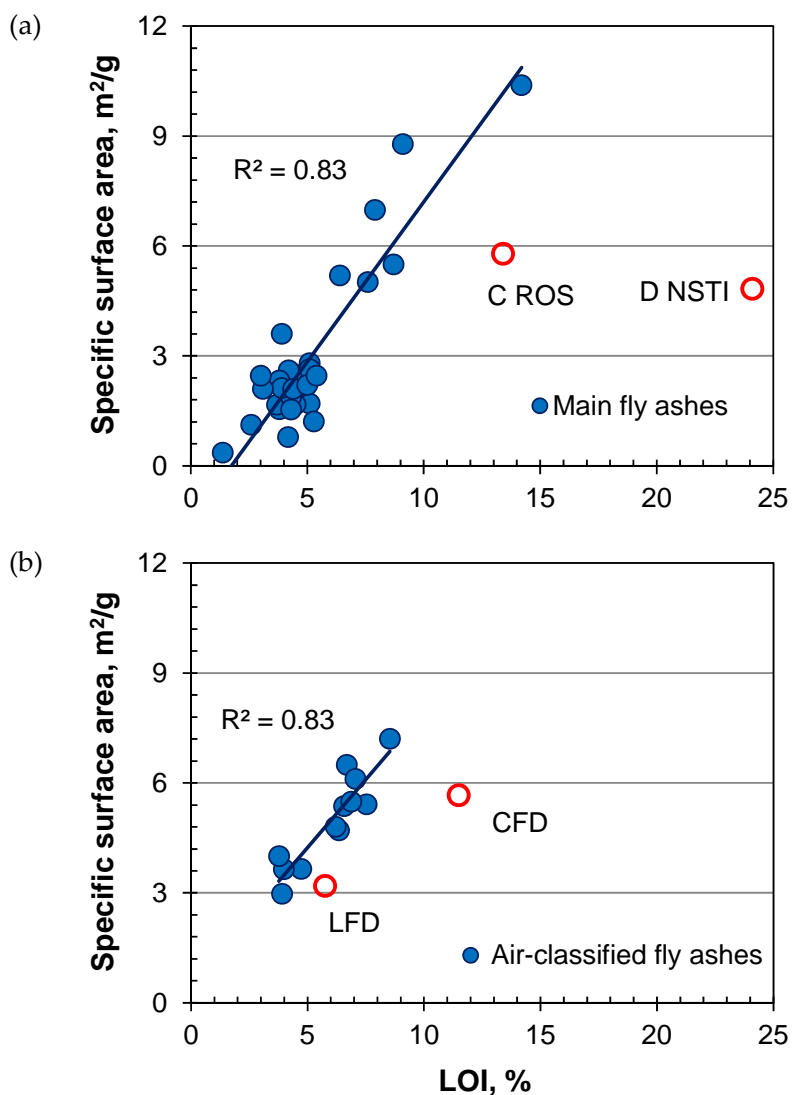


Figure 4-13. Relationship between LOI and surface area of fly ashes

4.1.4 Oxide and phase composition

The range of the chemical properties (Oxide and phase composition) of the fly ashes is given in Table 4-6, while the details are shown in Tables A-4 to A-8 (*Appendix A*). Monthly

fly ash from Source A was higher in calcium, iron, magnesium and sulfur, but contained less aluminium than that from Source C. Their silica and alkali contents were similar. The oxide and mineralogical composition of the other fly ashes obtained over a period of time, from various sources varied significantly. The sum of the major oxides (SiO_2 , Al_2O_3 and Fe_2O_3) was greater than 70% (BS EN 450 requirement) for all samples, except the non-STI fly ash from source D, which was 65% (LOI, 24.1%). The presence of chloride was found in the three oxy-fuel fly ashes only. A significantly higher level of Fe_2O_3 was also observed in these fly ashes compared to the other materials. Fly ashes from Bangladesh gave lowest CaO (0.7 - 1.1%) and Fe_2O_3 (2.8 - 2.9%) contents. Non-crystalline components were found to range from 69.9 - 76.5% and 69.8 - 81.4% for monthly fly ashes from Sources A and C respectively, while this had a wider range (34.0 - 88.2%) for fly ashes from the other sources. The coarsest Fly Ash (BD S, obtained from Bangladesh) contained the lowest quantity of materials other than crystalline with a significant contribution from crystalline Quartz (36.2%).

According to Helmuth (1987) factors influencing fly ash chemical and phase composition include (i) coal composition; (b) combustion conditions; and (c) collection system used. In this project, all of these factors could not be accounted for, since many of these were unknown. However, comparing the composition of the 12 air-classified fly ashes and their 2 parent feed samples gave important information. Figure 4-14 makes a comparison of the sum of major oxides and their LOIs.

In general, Source C gave lower oxide levels with increasing particle size, while the opposite was noted for Source L. However, considering the effect of LOI, it was noticed that there was a balance between the oxide content and LOI. As the 6 materials of varying fineness and LOI were obtained from the same parent samples and from two different sources, samples in each group were expected to have similar oxide compositions. For material from each source, the sum of major oxides increased with decrease in LOI (which was much clear in the case of Source L). As XRF does not detect LOI during analysis, the variation in oxide content appeared to be not because of its fineness, but as a result of its LOI.

Table 4-6. Range of chemical composition of fly ashes used in this project

Oxide composition	Monthly fly ashes				Other fly ashes		Air classified fly ashes			
	Source A		Source C		Min	Max	Source C		Source L	
	Min	Max	Min	Max			Min	Max	Min	Max
CaO	3.2	4.6	2.1	3.7	0.7	6.8	2.1	2.6	6.0	7.5
SiO ₂	43.9	50.8	44.3	49.6	39.0	59.2	46.1	50.1	45.5	49.9
Al ₂ O ₃	19.3	23.8	21.2	24.0	17.7	32.0	20.0	22.7	22.1	23.5
Fe ₂ O ₃	8.2	10.2	7.2	10.3	2.8	13.4	6.5	8.7	6.8	7.8
MgO	1.6	2.0	1.4	1.8	0.3	2.3	1.4	2.1	1.6	1.8
MnO	0.1	0.1	0.1	0.1	0.0	0.1	0.1	0.1	0.1	0.1
TiO ₂	1.0	1.2	1.0	1.2	0.9	3.1	1.0	1.1	1.1	1.2
K ₂ O	2.6	3.3	2.4	3.3	0.8	3.4	2.6	3.1	1.6	2.0
Na ₂ O	1.0	1.7	1.0	1.8	0.2	1.9	0.9	1.6	1.1	1.3
P ₂ O ₅	0.4	0.7	0.3	0.9	0.1	1.8	0.4	0.6	0.4	0.7
Cl	0.0	0.0	0.0	0.0	0.0	0.3	0.0	0.0	0.0	0.0
SO ₃	0.8	1.9	0.6	1.2	0.2	2.8	0.8	1.3	0.8	1.0
Mullite	9.7	15.4	6.8	16.7	5.1	43.5	9.3	11.6	13.8	16.7
Quartz	8.1	15.5	7.2	10.6	2.2	36.2	5.7	9.4	7.5	21.4
Hematite	2.7	4.9	2.0	4.7	0.0	4.5	1.1	2.8	1.7	4.1
Magnetite	0.1	0.4	0.1	0.4	0.0	0.4	0.0	0.2	0.0	0.1
Others	69.9	76.5	69.8	81.4	34.0	88.2	78.3	82.9	59.3	76.9

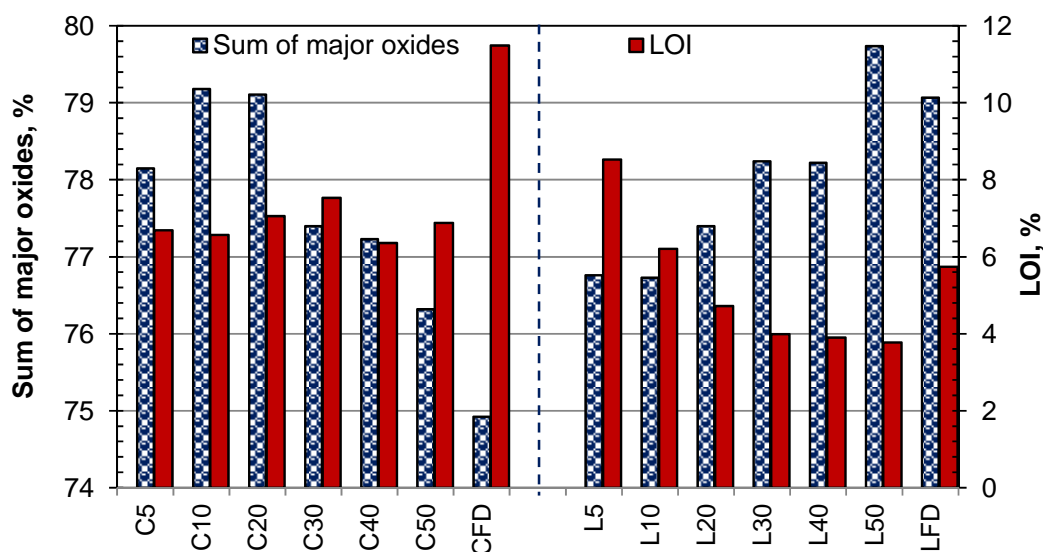


Figure 4-14. Sum of major oxides (SiO_2 , Al_2O_3 and Fe_2O_3) and LOI of air-classified fly ash

Fly ash glass/amorphous content generally increases with fineness (Helmuth, 1987; Hower *et al.*, 1997). As the other fly ashes obtained for this project are associated with various factors e.g. different source; coal composition and processing techniques, their glass/amorphous contents were not comparable with fineness or other properties. However, the influence of fineness on glass/amorphous content was noticed in the air-classified fly ashes from the two different sources, as shown in Figure 4-15. The fineness of fly ashes (d_{90}) was plotted against their contents other than crystalline in Figure 4-15(a). As XRD is also unable to detect carbon, this is included in the amorphous content. Therefore, the LOI was deducted from the content other than crystalline for each sample and again plotted against their fineness in Figure 4-15 (b). The relationships from this were improved, with a clearer trend.

Although the glass/amorphous content increased with fineness, the two sources gave significantly different behaviour. Source C consistently gave higher glass/amorphous content for similar fineness. Up to 14% (C5) and 30% (L10) increases in glass/amorphous content were achieved compared to the feed parent samples for Sources C and L respectively, from beneficiation by air-classification system.

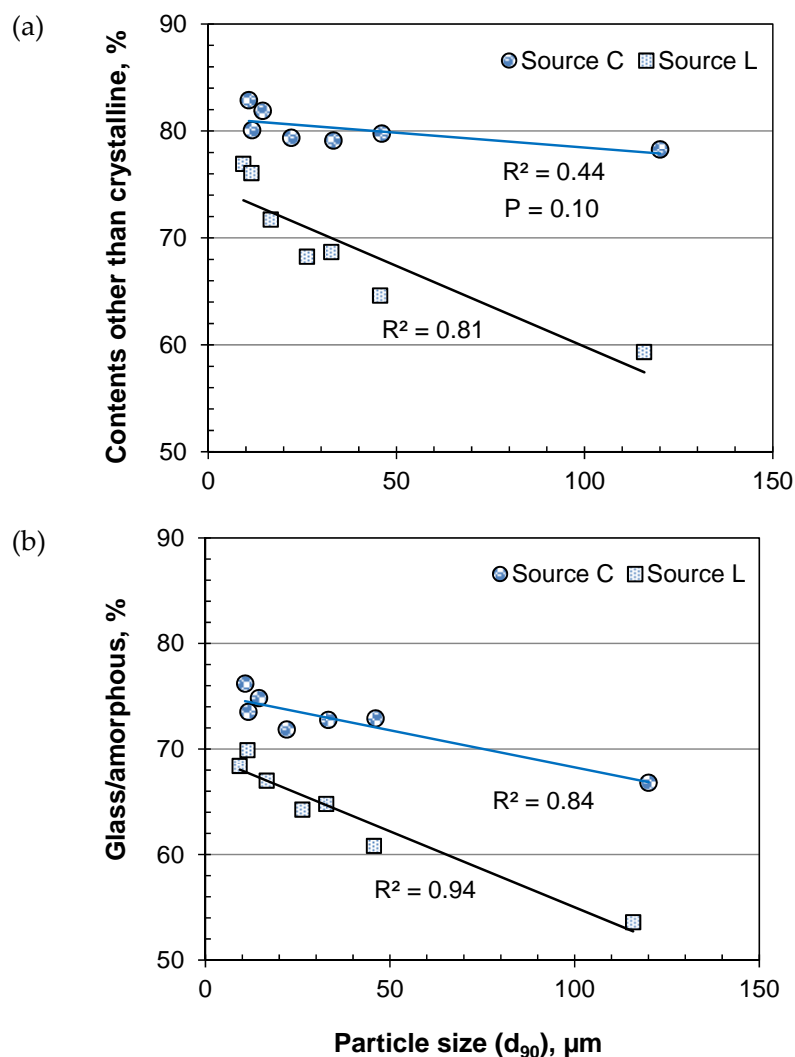


Figure 4-15. Relationship between fineness and glass/amorphous content

4.1.5 Morphological properties

SEM images of monthly (4 samples) and the other (19 samples) fly ashes are shown in Figures A-1 to A-11 (*Appendix A*) in alphabetical order of sources and BS EN 450 (BSI, 2005c) fineness categories. A few selected sample images are given in Figure 4-16 to 4-22. In general, the shape of the BS EN 450 Category S samples tended to be more spherical than Category N. Cenospheres were present in some fly ashes (e.g. A N Jul, Figure 4-16). Relatively solid type carbon was found in fly ash C ROS (Figure 4-17), which may be the reason for it giving comparatively lower specific surface area and consequently lower sorptive characteristics (discussed in Chapter 6) than expected given its LOI (13.4%).

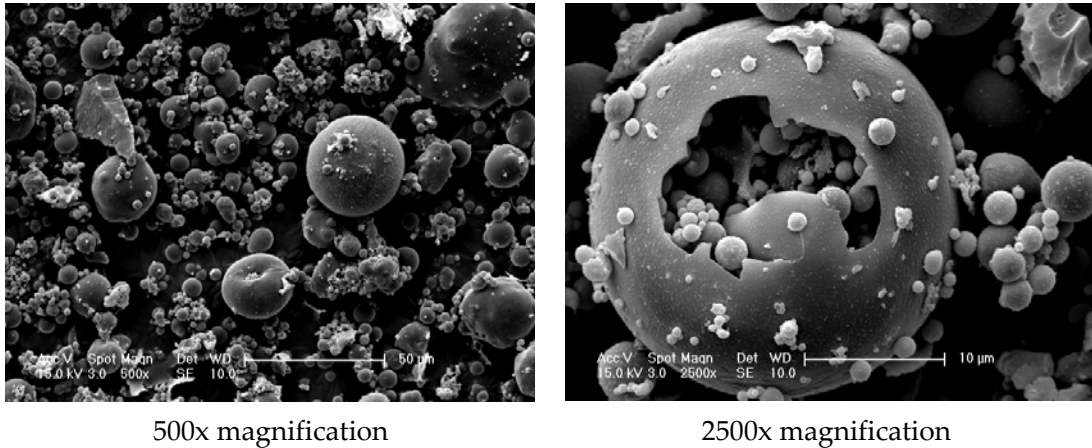


Figure 4-16. SEM images of Fly Ash A N Jul

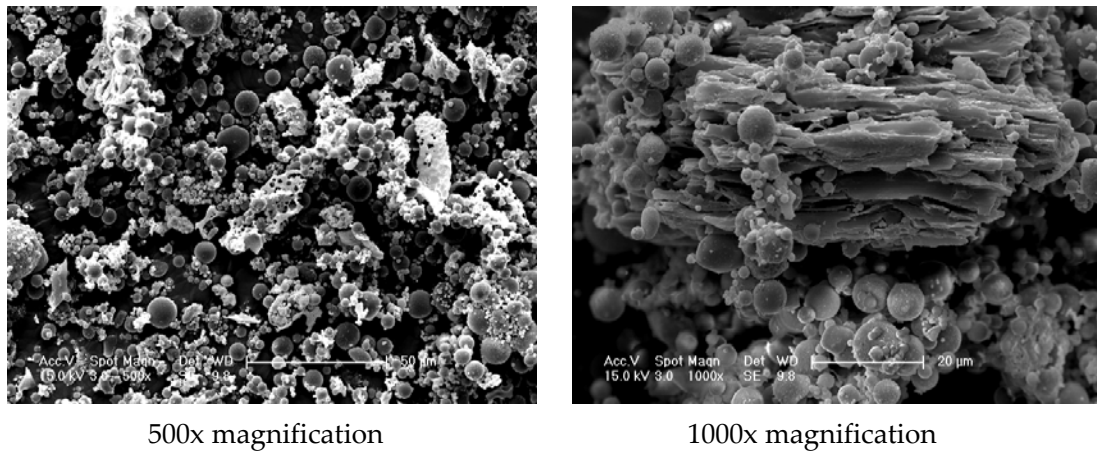
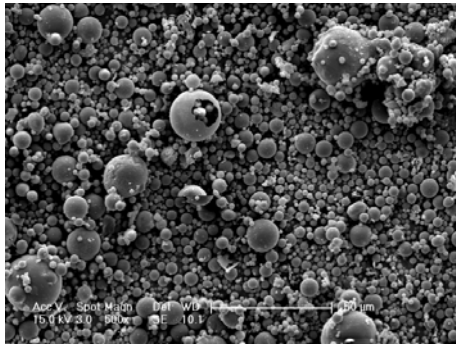
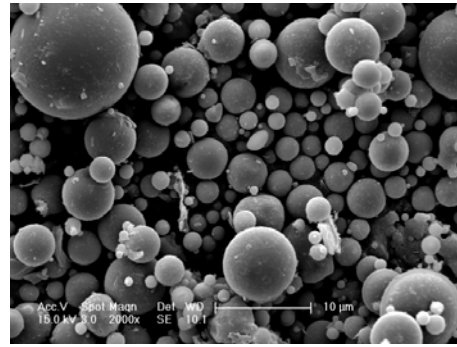


Figure 4-17. SEM images of Fly Ash C ROS

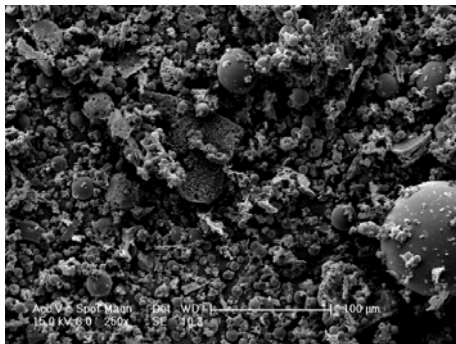
The STI sample from Source D (see Figure 4-18 (a)) appears to be the cleanest fly ash, with graded spherical particles. On the other hand, D NSTI (Figure 4-18 (b)), F Oxy2 (Figure 4-20 (b)) and H (Figure 4-19 (a)) fly ashes contained porous unburned carbon material. The surface characteristics of the oxy-fuel fly ashes were found to be rougher than the other samples (Figures 4-20 (a) and (c)). These fly ashes also gave lower mortar flow than expected from their fineness (discussed in *Chapter 5*). SEM images of fly ash samples collected from Bangladesh are shown in Figure A-11. These indicate the presence of very coarse and solid type particles in sample BD S (see Figure 4-19 (b)) which can be related to its higher retention on the 45 µm sieve.



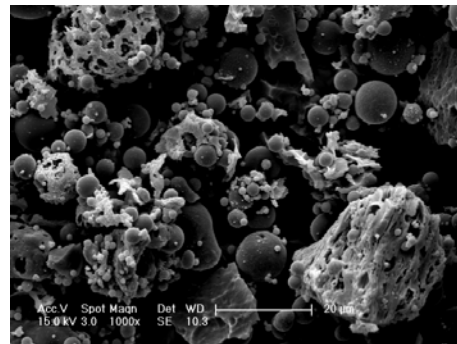
(a) D STI (500x magnification)



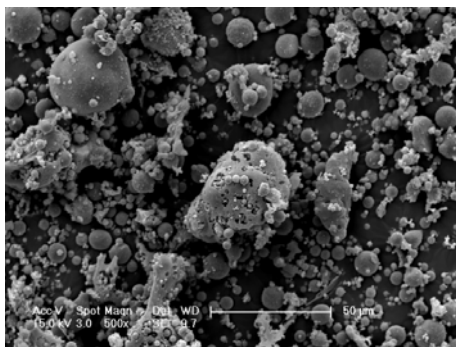
(a) D STI (2000x magnification)



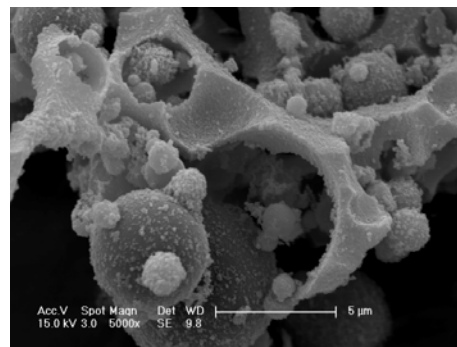
(b) D NSTI (250x magnification)



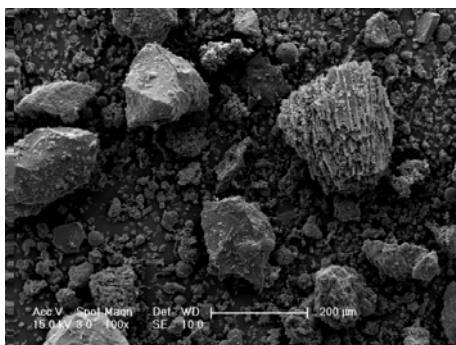
(b) D NSTI (1000x magnification)

Figure 4-18. SEM images of Fly Ashes: (a) D STI, and (b) D NSTI

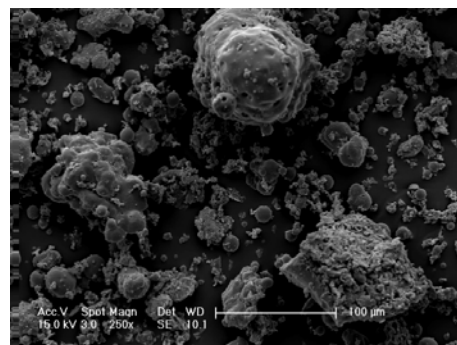
(a) H (500x magnification)



(a) H (5000x magnification)

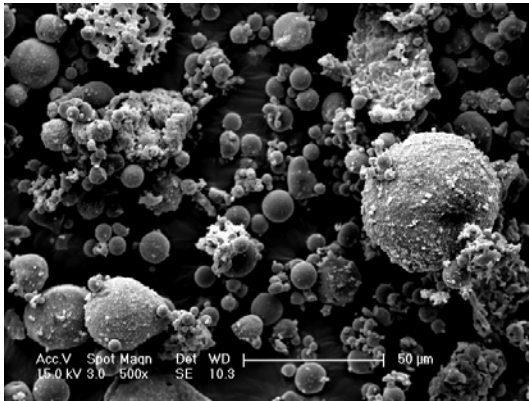


(b) BD S (100x magnification)

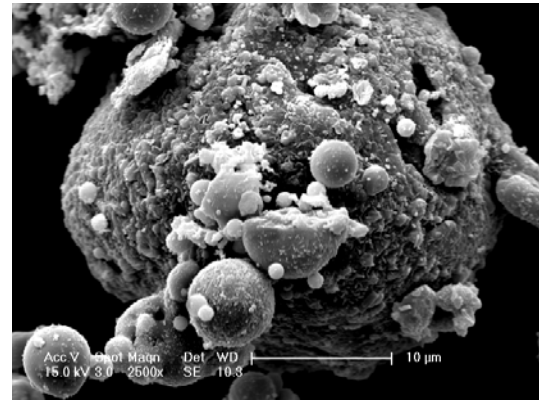


(b) BD S (250x magnification)

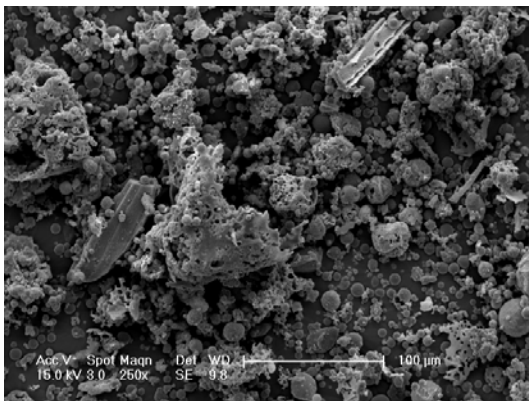
Figure 4-19. SEM images of Fly Ashes: (a) H, and (b) BD S



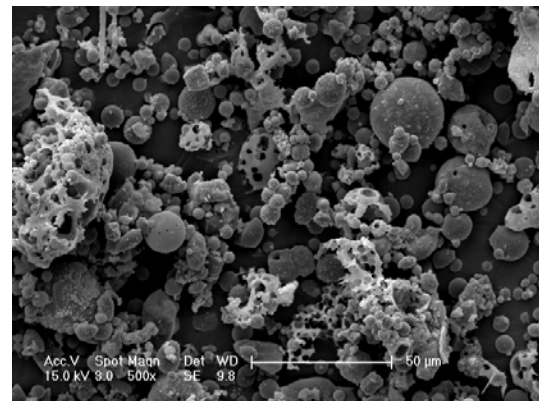
(a) F Oxy1 (500x magnification)



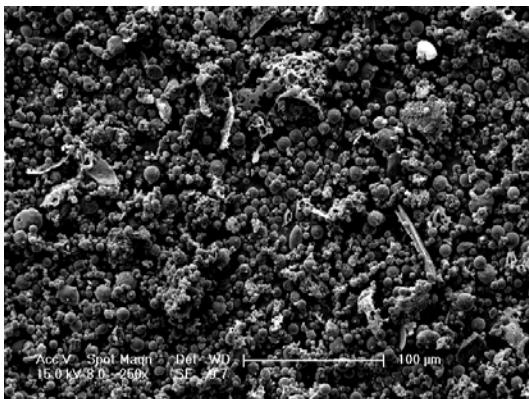
(a) F Oxy1 (2500x magnification)



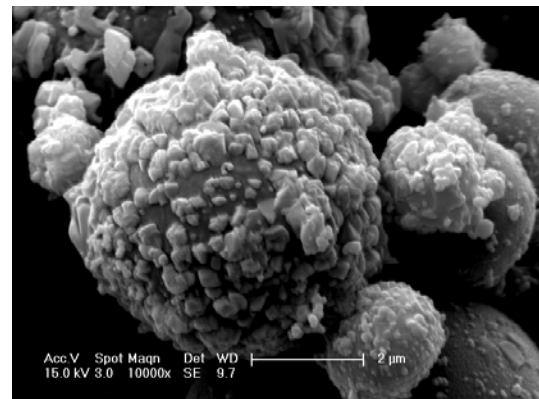
(b) F Oxy2 (250x magnification)



(b) F Oxy2 (500x magnification)



(c) F Oxy3 (250x magnification)

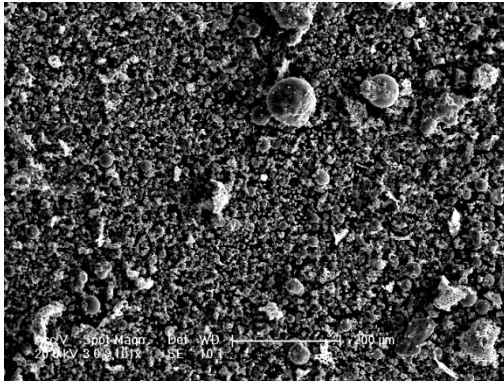


(c) F Oxy3 (10000x magnification)

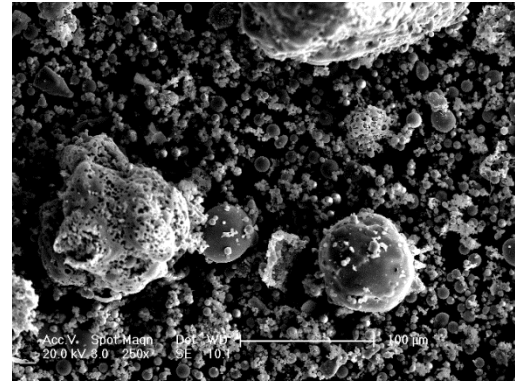
Figure 4-20. SEM images of oxy-fuel fly ashes from trial burning

The morphology of air-classified fly ashes along with their reference parent feed samples are shown in Figures 4-21 and 4-22 for Sources C and L, respectively (details in *Figures A-12 and A-13*). An abundance of carbon fractions were present in the feed sample CFD

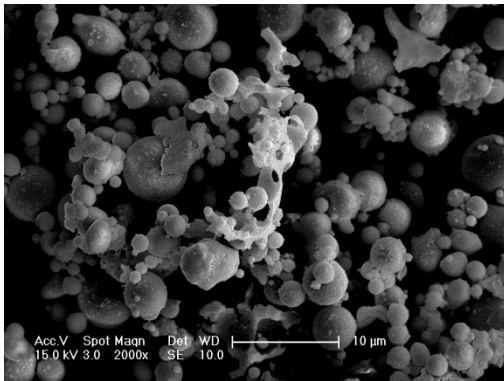
(Figure 4-21(a)) compared to LFD (Figure 4-22 (a)), as suggested from their LOI results. With air-classification spherical and solid small-sized fly ash particles were obtained, which were comparatively cleaner in nature for Source L (also indicated in their LOI).



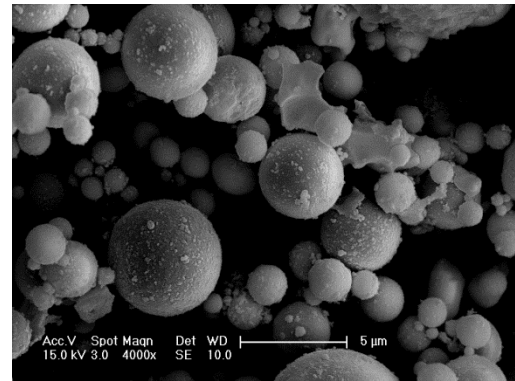
(a) CFD (101x magnification)



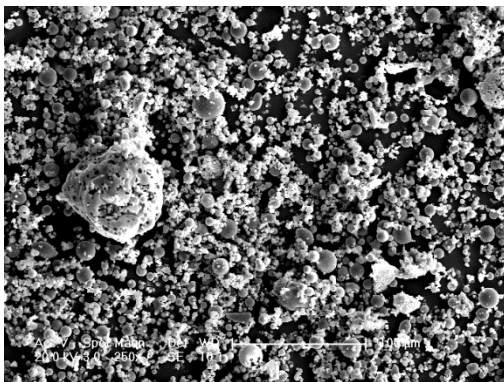
(b) CFD (250x magnification)



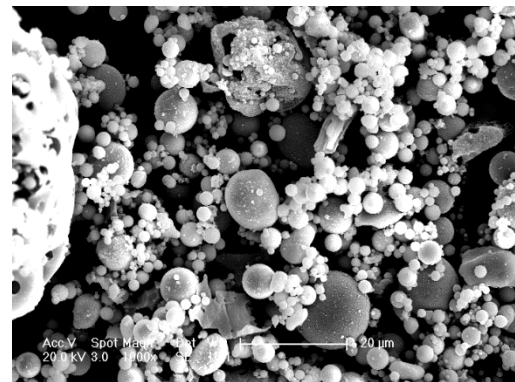
(c) C5 (2000x magnification)



(d) C5 (4000x magnification)



(e) C50 (250x magnification)



(f) C50 (1000x magnification)

Figure 4-21. SEM images of air-classified fly ashes from Source C

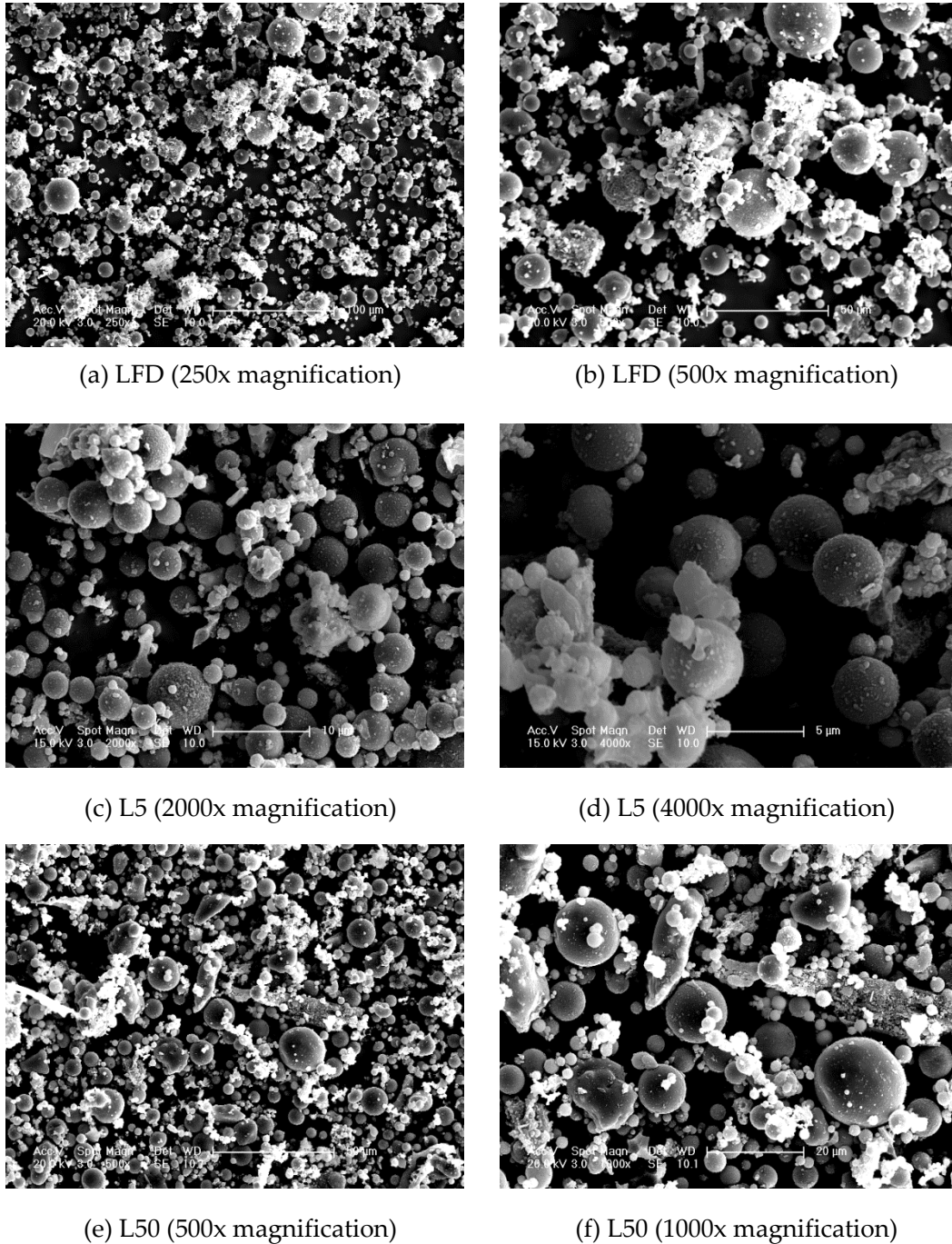


Figure 4-22. SEM images of air-classified fly ashes from Source L

Further tests using Energy-dispersive X-ray spectroscopy (EDX) were carried out on oxy-fuel fly ashes to identify the nature of deposits on their surfaces. As shown in Figure A-14 (*Appendix A*), crystals comprising Si, Al, C, O, K, Ca, Ti and Fe were identified in these deposits.

4.2 Characteristics of PCs

A total of 5 different PCs were used in the project as given in Figure 4-23. Unless otherwise indicated, a 52.5N (HR52) cement conforming to BS EN 197 – 1 (BSI, 2011b) was used for the experimental work. To evaluate the effect of PC type on the activity index of fly ashes, three additional PCs were obtained (strength class 42.5N (HK42), 52.5 N (LD52) and 32.5R (LD32) to BS EN 197 - 1). To test 100 mm concrete cubes with air-classified fly ashes, a 52.5N (HK52) was used.

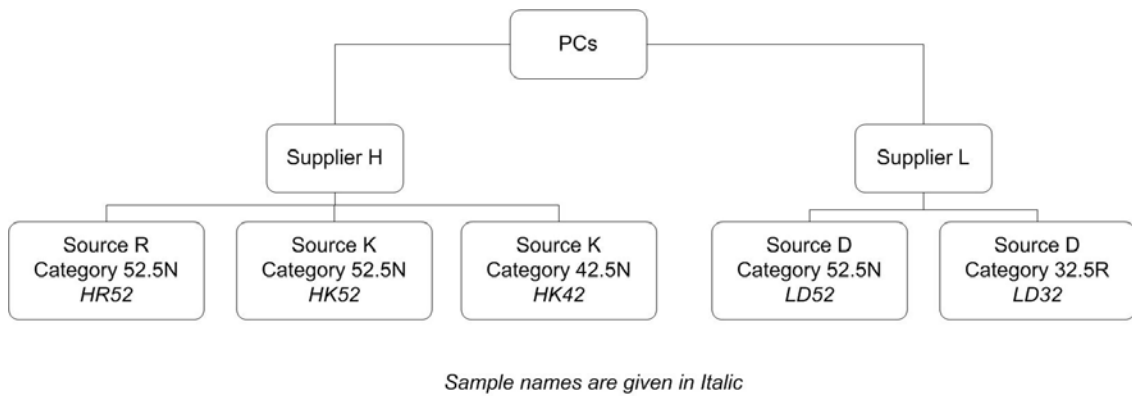


Figure 4-23. Types of PCs used for this project and their codes

The main physical, chemical and mineralogical properties of the cements are shown in Tables 4-7, 4-8 and 4-9. The PSD of the PCs are shown in Figure 4-24. PC HR52 was the finest cement. HK52 and LD52 (both 52.5 N) gave similar PSDs and were finer than PC HK42 (42.5 N) and LD32 (32.5 R), as expected.

Table 4-7. Physical properties of PCs

SAMPLE	Blaine fineness m ² /kg	LOI %	SSA ¹ m ² /g	d ₁₀ µm	d ₅₀ µm	d ₉₀ µm	Sub-10 µm %
HR52	550	1.9	1.60	3.4	13.3	36.6	38.2
HK52 ²	478	2.1	0.90	3.1	16.7	47.5	32.7
HK42	480	3.5	1.52	2.9	16.9	54.0	34.5
LD52	490	1.5	1.04	2.6	17.1	44.0	32.4
LD32	433	0.9	1.17	2.6	19.3	61.3	31.5

¹ SSA, specific surface area; and ² used for reactivity test in concrete for air-classified fly ashes

Table 4-8. Oxide composition of PCs

	HR52	HK52*	HK42	LD52	LD32
CaO	65.0	65.8	65.3	63.2	64.1
SiO ₂	21.0	20.2	19.9	20.6	20.2
Al ₂ O ₃	5.3	4.9	4.8	6.7	4.7
Fe ₂ O ₃	2.8	2.9	2.8	3.1	3.7
MgO	1.0	1.1	1.1	2.3	2.8
MnO	0.0	0.0	0.0	0.1	0.1
TiO ₂	0.5	0.5	0.4	0.3	0.2
K ₂ O	0.6	0.7	0.7	0.7	0.5
Na ₂ O	0.3	0.3	0.3	0.4	0.2
P ₂ O ₅	0.2	0.2	0.2	0.1	0.1
Cl	0.1	0.1	0.1	0.0	0.0
SO ₃	3.0	2.7	3.2	2.8	2.7

**used for reactivity test in concrete for air-classified fly ashes*

Table 4-9. Phase composition of PCs

	HR52	HK52*	HK42	LD52	LD32
C ₃ S	53.2	65.2	65.1	39.2	58.4
C ₂ S	20.1	8.8	8.0	29.5	14.1
C ₃ A	9.3	8.1	7.9	12.4	6.3
C ₄ AF	8.5	8.9	8.6	9.5	11.2
Gypsum	5.0	4.6	5.4	4.8	4.5

**used for reactivity test in concrete for air-classified fly ashes*

4.3 Properties of Aggregates

Tests on mortar were carried out with standard sand to BS EN 196-1 (BSI, 2005a). In the concrete tests, 10/20 and 4/10 mm fractions of natural gravel and a medium grade sand, all conforming to BS EN 12620 (BSI, 2002) were used. The particle density (SSD) and absorption (lab dry to SSD) of these were 2620, 2600, 2630 kg/m³ and 1.7, 1.8, 0.8%, respectively. The fineness modulus of the sand, to BS EN 12620, was 2.40. Figure 4-25 gives the grading comparison between the laboratory sand and CEN standard sand used during the project. The materials are similar in terms of their fineness; however, the CEN sand had slightly higher fineness at the coarse end.

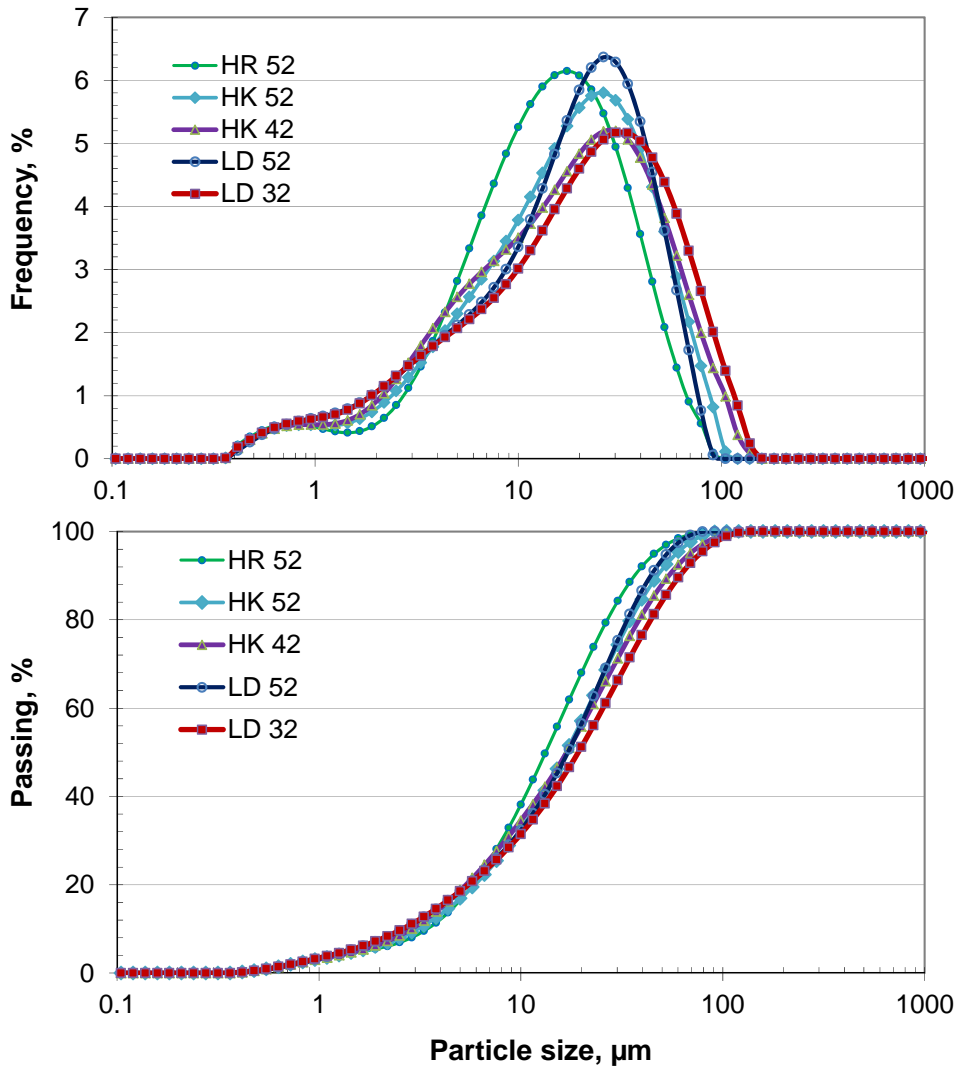


Figure 4-24. Particle size distribution of PCs used in this study

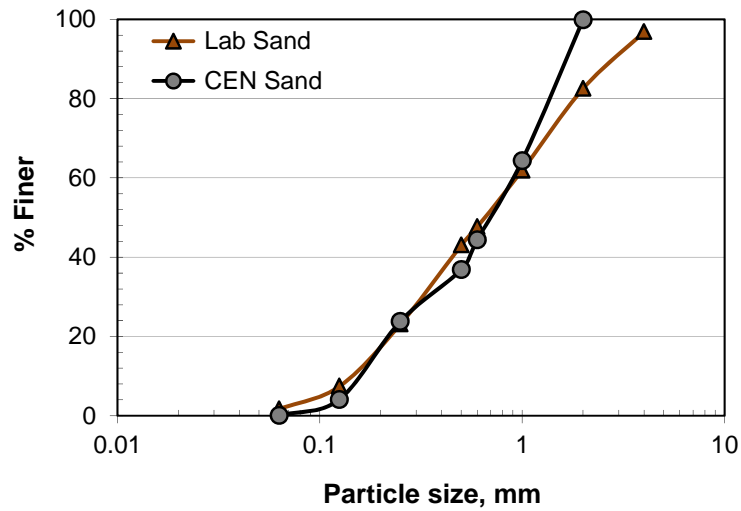


Figure 4-25. Grading comparison between CEN and laboratory sands

4.4 Characteristics of AEAs and Other Reagents

Three commercial AEAs and a standard chemical reagent (surfactant) were used. These cover materials currently adopted in the application, whilst also enabling their comparison with a long shelf-life reagent of known composition. Hereafter, the commercial AEAs are referred to as AEA C1 and AEA C2 and the standard reagent, sodium dodecyl benzene sulfonate (SDBS), as AEA S. AEA C1 was specially formulated for use with fly ash, while AEA C2 was a general purpose admixture, both conforming to BS EN 934-2 (BSI, 2009a) and ASTM C260 (ASTM, 2010). The main characteristics of the AEAs (as observed/given by the manufacturers) are shown in Table 4-10.

The characteristics of hydrated and quick lime used are given in Table 4-11. Their PSDs are shown in Figure 4-26. Hydrated lime ($d_{90} = 79.7 \mu\text{m}$) was found to be distinctively finer than quick lime ($d_{90} = 216.1 \mu\text{m}$). The hydrated lime was found to have a d_{90} more than double that of the PC HR52.

Table 4-10. Properties of commercial AEAs (C1, C2, C3) and standard reagent (AEA S)

CHARACTERISTIC	AEA C1	AEA C2	AEA C3	AEA S
Appearance	Dark brown liquid	Opaque green liquid	Opaque white liquid	White solid
Origin	Tall oil, fatty acids (CAS No: 61790-12-3) Polyethylene glycol (CAS No: 25322-68-3)	Tall oil, fatty acids (CAS No: 61790-12-3) Polyethylene glycol (CAS No: 25322-68-3)	–	Standard chemical (CAS No: 25155-30-0) MW348.48 g/mol
Specific gravity	1.03	1.00	–	–
pH-value	11.5	10.5	–	–
Alkali content, %	≤ 1.0	≤ 0.5	–	–
Chloride content, %	≤ 0.10	≤ 0.10	–	–
Suitability	Fly ash/PC concrete	PC concrete	Fly ash/ PC concrete	–
Dose for concrete, ml/kg cement	1.0	6.0	0.3–3.2	–

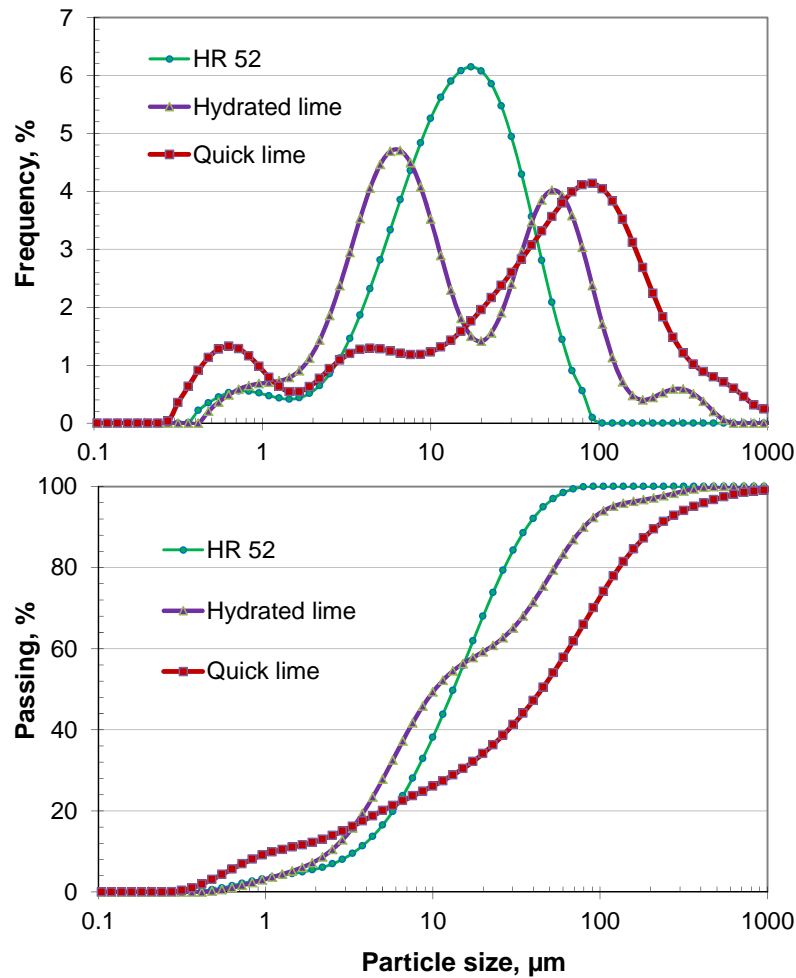


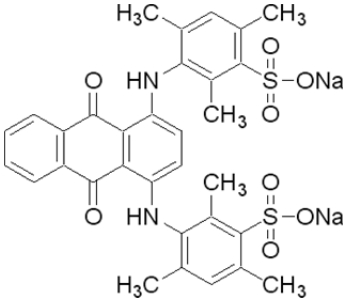
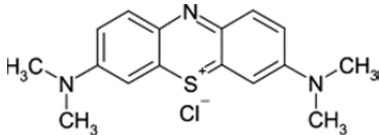
Figure 4-26. Particle size distribution of limes and PC HR52 used in this study

Table 4-11. Characteristics of hydrated and quick lime used in the project

CHARACTERISTIC	Hydrated lime	Quick lime
IUPAC name	Calcium hydroxide	Calcium oxide
Molecular formulae	Ca(OH) ₂	CaO
Molar mass	74.093 g/mol	56.0774 g/mol
CAS number	1305-62-0	1305-78-8
Specific gravity	2.21	3.35
Solubility in water	0.189 g/100 ml (0 °C) 0.173 g/100 ml (20 °C) 0.066 g/100 ml (100 °C)	1.19 g/l (25 °C), 0.57 g/l (100 °C)
Appearance	soft white powder/ colourless liquid	White to pale yellow/ brown powder
d_{10} , μm	2.4	1.1
d_{50} , μm	10.3	44.8
d_{90} , μm	79.7	216.1

The AB80 and methylene blue dyes were standard chemical reagents and their main characteristics are given in Table 3. These were selected as sorbates since their molecular structures and sizes are similar to those of active components used in AEAs and as noted above, they have been adopted to evaluate activated carbon (Zhang and Nelson Jr., 2007; Choy *et al.*, 2000; Environment Canada, 2008). Yang *et al.* (2007) also note the molecular size of AB80 to be of similar order to that of AEA S.

Table 4-12. Characteristics of dye reagents (supplier's information unless noted otherwise)

CHARACTERISTIC	AB80	Methylene blue
Appearance	Blue solid powder	Dark solid power
CAS No.	4474-24-2	7220-79-3
Molar weight,	678.68	373.9
Molecular size, nm	1.65×0.626^a	$1.43 \times 0.61 \times 0.4^b$
Molecular formula	$C_{32}H_{28}N_2Na_2O_8S_2$	$C_{16}H_{18}ClN_3S \cdot 2H_2O$
Molecular structure		
Melting point	$> 300^\circ C$	$190^\circ C$
UV absorption	λ_{max} 282, 581 and 626 nm	λ_{max} 668 nm
Colour index	61585	52015

^a Valix *et al.* (2004) ^b Lei *et al.* (2006)

4.5 Summary of Findings

The characteristics of the test materials and reagents used during the project are presented in this chapter. In most cases, tests were carried out to determine the properties of the materials; however, in a few cases the information reported here was supplied by the manufacturer.

Fly ashes were obtained from 8 UK sources and Bangladesh and had a wide range of properties. These were either run-of-station or processed. Variations may also occur due to (i) burning conditions and composition of the source coal; (ii) co-combustion; and (iii) introduction of modern combustion technology (oxy-fuel; trial burning).

Fineness of the run-of-station fly ashes were found to range from 22.6-36.1% (retention on the 45 μm sieve) depending on the source. By processing through air classification these decreased by more than 50% for the monthly samples obtained from two sources over a 1 year period. Fineness may also be dependent on the coal-pulveriser system.

The LOI of UK run-of-station fly ashes varied between 7.6 – 24.1%, while the range for materials obtained from Bangladesh was 1.4 – 5.3%. It was noted that among the run-of-station fly ashes, pet-coke co-combustion gave lowest LOI. To deal with these property ranges, many power stations have installed modern fly ash processing technology (e.g. STI carbon removal and air-classification systems). Material processed by STI reduced the LOI by 90% compared to the raw material and gave very clean fly ash, while the air-classification system reduced this by ~60-70%.

The monthly samples were all air-classified and gave LOIs ranging from 3.7-5.1%. Two run-of-station fly ashes were processed by air-classification at the Bradley Pulveriser Company. These gave different behaviour for the concentration of carbon in the various size fractions. Source C had a relatively higher carbon content, but this was mostly in coarse form, on the other hand the LOI of Source L fly ash was concentrated in the finer fractions, as found with Fly Ash H. Therefore, the distribution of carbon depends on the production conditions of the individual power station. Overall, processing by air-classification was found to be beneficial up to a d_{90} of 10 μm .

Fly ash LOI gave general agreement with specific surface areas up to a certain LOI range. However, the surface area varied between sources even when their LOIs were similar. With coarse particle size, the LOI of fly ashes gave relatively lower specific surface areas than those with finer particles.

The 57 fly ashes tested in the project conformed to the minimum composition of major oxides in BS EN 450-1 (BSI, 2005c) (SiO_2 , Al_2O_3 and Fe_2O_3), except D NSTI which was due to

its very high carbon content. The major oxide composition of the two run-of-station fly ashes and their classified fractions gave similar results, when the effect of their LOI contribution was considered. Wider variations in the glass/amorphous/others content of fly ashes obtained from various sources were noted. Considering the various size fractions of the two run-of-station fly ashes, it was found that the crystalline content decreased as the materials became finer.

SEM images gave important information. Cenospheres were noted in coarse fly ashes while their shape was also irregular. The finest fractions of fly ashes gave solid spherical-shaped particles.

Testing 5 different kinds of PCs gave variations in their properties, not only based on the supplier, but also their production source and strength class. These include differences in fineness, particle size distribution, chemical and phase compositions.

The grading of sands (CEN and local supply) was found to be similar, but CEN sand gave finer sizes at its upper end. The three commercial AEAs used in this project had various levels of effectiveness in cementitious systems as suggested from their manufacturer's worksheets.

From the PSD of limes, it was noted that the main test PC (HR52) exhibited half the fineness of the hydrated lime, while the quick lime was almost three times coarser than the hydrated.

CHAPTER 5: REACTIVITY ASSESSMENT OF FLY ASH

This Chapter investigates pozzolanic reactivity of fly ash. Mortar tests with BS EN 450-1 (BSI, 2005c) gave activity index while accelerated curing BS 3892-1: 1982 gave pozzolanic activity index in 7 days, and water demand. MIP was used to measure porosity of mortar prisms. To minimize the effect of PC properties, laboratory standard hydrated lime was also considered for the mortar tests. To minimize packing/aggregate effects in the mortar tests, TGA analysis was carried out with fly ash/PC paste, and fly ash was also exposed to PC or hydrated lime in solution and then the level of $\text{Ca}(\text{OH})_2$ was determined. Changes in conductivity of the test solutions were also measured. Chemical and phase compositions of fly ash were examined to relate with pozzolanic reactivity. Heat evaluation from the reaction of fly ash with quick lime was also considered.

5.1 Introduction

This chapter starts by reviewing activity index test results using PC-based mortars. Initially, a summary of the data obtained is presented and then a general discussion is provided on whether the tested fly ashes conform to the relevant requirements in the standard (BS EN 450; BSI, 2005c). Following this, activity index, obtained using various PCs, were compared to examine the effect of PC. Thereafter, the fresh properties of fly ash mortars were considered using the different PCs, and comparisons made between these and fly ash properties. MIP results for evaluating porosity at early ages were also related to the grading of fly ashes. The effect of fly ash physical properties was then examined with respect to activity index. These give correlations between fly ash physical properties and mortar fresh and hardened properties. The potential of accelerated curing methods for rapid assessment were evaluated by considering the BS 3892-1: 1982 curing method. Mortar test with hydrated lime to eliminate, effect of PCs on strength results are then presented. Pozzolanicity was also determined from TGA using fly ash/PC paste by considering remaining $\text{Ca}(\text{OH})_2$ after consumption by fly ash. The study then progressed to examine pozzolanicity determination, with a solution comprising fly ash/PC/water and

fly ash/saturated lime. Fly ash chemical properties and their heat of reaction with quick lime are then compared with activity index, to examine whether these can give an indication of reactivity. The results are discussed in the following sections, sequentially.

5.2 Activity Index Test Using PC-Based Mortar

Reactivity of fly ashes has been determined from mortar strength tests following: a) the BS EN 450 (BSI, 2005c) method (at 7, 14, 28, 56, 90 and 180 days); b) the accelerated test given in BS 3892-1 (BSI, 1982) i.e. 30% fly ash, mixes of the same flow, water cured for 5 days at 20°C and 2 days at 50°C; and c) a combination of BS EN 450 mix proportions and the BS 3892-1 (1982) curing procedure.

Four different types of cement were used for activity index testing. Table 5-1 provides a summary of the activity index tests carried out with these materials and the various fly ashes considered. Tables 5-2 to 5-4 give the activity index and mortar fresh properties for fly ashes from Source A (12 months), Source C (12 months), other sources (19 samples), and air-classified fly ashes (14 samples), respectively. Mortar activity test results with the 14 air-classified fly ashes using PC HR52 are given in Table 5-4.

Figures 5-1, 5-2(a), 5-2(b) and 5-2(c) show BS EN 450 activity index results at different ages using cements HR52, HK42, LD32 and LD52 respectively. With cement HR52 and LD32, all samples met the BS EN 450 (BSI, 2005c) criterion of at least 75% and 85% strength compared to the reference mortar at 28 and 90 days respectively.

Table 5-1. Number of mortar mixes prepared for activity index tests during the study

CEMENT	BS EN 450					BS EN 450 (A)	BS 3892-1: 1982
	7 days	28 days	56 days	90 days	180 days	7 days	7 days
HR52	37	40 + 14 ^a	10 + 14 ^a	40	40	20	36
HK42	-	15	-	15	-	-	-
LD32	-	15	-	15	-	-	-
LD52	-	15	-	15	-	-	-

BS EN 450 (A): following BS EN 450 mix proportions and BS 3892-1 (1982) curing (water for 5 days at 20°C and 2 days at 50°C)

^a *air-classified samples; 14 samples were also tested following 14 days water curing*

With cement HK42 fly ash C ROS did not exceed 75% of the control mortar strength at 28 days, while fly ash BD S did not pass either at 28 or 90 days. With cement LD52 all fly ashes passed the 90 days activity index criteria, except C ROS and F Oxy2. With a few exceptions (Cement HR52), monthly samples obtained from Sources A and C gave better strength than the control at 90 days. The fly ashes that did not meet the activity index criteria, either had high LOI, high retention on a 45 µm sieve, or a combination of the two. In general, the finest fly ashes E UF (4.8%) and F Oxy3 (3.6%) gave best strength results with all cements. Fly ash D STI did not give as high an activity index as expected, given its low LOI (2.6%) and good flow properties.

With the accelerated curing conditions following the BS 3892-1: (1982) standard, all fly ashes tested had strength of at least 85% of the control mortar, except fly ashes C ROS, D NSTI and F Oxy2. It should be noted that these fly ashes had very high LOIs of 13.4, 24.1 and 14.2%, respectively. For the same test, fly ashes E EN1 and G just exceeded this value. For the 20 fly ashes tested at 0.5 w/c ratio and following BS 3892-1: (1982) accelerated curing conditions, activity index values were lowest for Fly Ashes C ROS and F Oxy2.

Figure 5-3 gives activity index test results (14, 28 and 56 days) of air-classified fly ashes from Sources C and L. These samples were tested with PC HR52 and all (including feed raw samples) passed the criteria at 28 days (75% of control). A clear increase in activity index was obtained by processing the fly ashes. Given the similar fineness of feed samples CFD and LFD, the comparative higher activity index of LFD may correspond to its lower LOI value. By processing (air-classification) increases in activity index ranging from 4.6-14.7%, 8.1-17.4% and 13.7-26.1% were obtained at 14, 28 and 56 days respectively for Source C, while this was 2.3-8.9%, 8.8-15.6% and 5.3-20.1%, respectively for Source L.

The activity index given above is based on mean strength of 6 tests. Their mean, maximum and minimum of the BS EN 450 fly ash mortar strengths (28 and 90 days) using the four PCs are shown in Figures B-1 and B-2 (*Appendix B*). The range for air-classified fly ashes (28 and 56 days) is shown in Figure B-3. BS EN 450 activity index was also calculated using the minimum strength values obtained from the set of mortar prisms for each fly ash sample to examine whether this conforms to the minimum standard requirements.

Table 5-2. (Pozzolanic) Activity index and fresh properties of monthly fly ashes received from Source A

Properties	A-S Jul	A-S Aug	A-S Sep	A-S Oct	A-S Nov	A-S Dec	A-S Jan	A-S Feb	A-S Mar	A-S Apr	A-S May	A-S Jun
HR52												
Flow, %	101	102	103	105	105	103	104	104	102	101	104	102
7 d AI (BS EN 450), %	81	81	80	76	75	76	76	79	80	79	80	81
28 d AI (BS EN 450), %	91	93	94	89	90	89	91	90	93	91	92	94
56 d AI (BS EN 450), %	-	-	-	-	-	-	98	-	-	-	-	-
90 d AI (BS EN 450), %	108	106	108	107	107	106	108	108	110	109	109	109
180 d AI (BS EN 450), %	111	108	104	108	108	108	108	107	112	111	111	109
7 d ¹ AI (BS EN 450), %	98	-	-	-	-	-	97	-	-	-	-	-
Water requirement, %	96	-	96	95	94	93	93	95	94	95	95	-
7 d ² PAI (BS 3892), %	101	-	100	91	95	94	92	93	95	101	95	-
HK42												
Flow, %	-	-	-	-	-	-	105	-	-	-	-	-
28 d AI (BS EN 450), %	-	-	-	-	-	-	88	-	-	-	-	-
90 d AI (BS EN 450), %	-	-	-	-	-	-	109	-	-	-	-	-
LD32												
Flow, %	-	-	-	-	-	-	100	-	-	-	-	-
28 d AI (BS EN 450), %	-	-	-	-	-	-	103	-	-	-	-	-
90 d AI (BS EN 450), %	-	-	-	-	-	-	114	-	-	-	-	-
LD52												
Flow, %	-	-	-	-	-	-	103	-	-	-	-	-
28 d AI (BS EN 450), %	-	-	-	-	-	-	82	-	-	-	-	-
90 d AI (BS EN 450), %	-	-	-	-	-	-	93	-	-	-	-	-

¹BS EN 450 mix proportion and BS 3892 – 1: 1982 curing condition, ² Pozzolanic activity index as per BS 3892 – 1 (1982)

Table 5-3. (Pozzolanic) Activity index and fresh properties of monthly fly ashes received from Source C

Properties	C-S Jul	C-S Aug	C-S Sep	C-S Oct	C-S Nov	C-S Dec	C-S Jan	C-S Feb	C-S Mar	C-S Apr	C-S May	C-S Jun
HR52												
Flow, %	103	104	104	103	105	105	105	103	105	104	104	104
7 d AI (BS EN 450), %	81	81	79	77	76	76	77	77	75	75	79	80
28 d AI (BS EN 450), %	93	92	91	90	92	90	91	94	93	94	93	92
56 d AI (BS EN 450), %	-	-	-	-	-	-	101	-	-	-	-	-
90 d AI (BS EN 450), %	110	111	109	109	111	108	109	110	111	111	108	108
180 d AI (BS EN 450), %	110	110	109	111	108	114	116	113	111	111	106	113
7 d ¹ AI (BS EN 450), %	104	-	-	-	-	105	106	-	-	-	-	-
Water requirement, %	96	-	94	93	93	93	93	93	93	94	94	-
7 d ² PAI (BS 3892), %	103	-	107	96	98	98	108	96	106	103	102	-
HK42												
Flow, %	-	-	-	-	-	-	103	-	-	-	-	-
28 d AI (BS EN 450), %	-	-	-	-	-	-	88	-	-	-	-	-
90 d AI (BS EN 450), %	-	-	-	-	-	-	111	-	-	-	-	-
LD32												
Flow, %	-	-	-	-	-	-	101	-	-	-	-	-
28 d AI (BS EN 450), %	-	-	-	-	-	-	108	-	-	-	-	-
90 d AI (BS EN 450), %	-	-	-	-	-	-	117	-	-	-	-	-
LD52												
Flow, %	-	-	-	-	-	-	105	-	-	-	-	-
28 d AI (BS EN 450), %	-	-	-	-	-	-	82	-	-	-	-	-
90 d AI (BS EN 450), %	-	-	-	-	-	-	97	-	-	-	-	-

¹BS EN 450 mix proportion and BS 3892 – 1: 1982 curing condition, ² Pozzolanic activity index as per BS 3892 – 1: 1982

Table 5-4. (Pozzolanic) Activity index and fresh properties of fly ashes received from various sources

Properties	A-N Jul	B-N Jul	B-S Jul	C LLHF	C ROS	D STI	D NSTI	E UF	E EN1	E EN2
HR52										
Flow, %	101	99	104	106	91	108	89	103	99	100
7 d AI (BS EN 450), %	80	78	81	80	77	75	-	85	81	81
28 d AI (BS EN 450), %	88	86	91	85	80	89	80	94	92	88
56 d AI (BS EN 450), %	-	95	-	-	90	99	-	107	-	-
90 d AI (BS EN 450), %	107	100	108	102	93	103	91	110	106	100
180 d AI (BS EN 450), %	109	101	108	105	95	107	100	114	110	106
7 d ¹ AI (BS EN 450), %	91	92	97	92	84	93	-	105	-	91
Water requirement, %	100	99	97	92	105	92	107	96	99	99
7 d ² PAI (BS 3892), %	90	89	99	96	82	102	78	111	85	91
HK42										
Flow, %	99	-	104	103	92	110	87	103	-	96
28 d AI (BS EN 450), %	83	-	84	82	72	85	75	92	-	84
90 d AI (BS EN 450), %	101	-	108	103	95	104	99	112	-	99
LD32										
Flow, %	95	-	102	101	82	107	86	102	-	97
28 d AI (BS EN 450), %	96	-	98	96	79	100	90	109	-	98
90 d AI (BS EN 450), %	112	-	114	109	86	107	93	121	-	109
LD52										
Flow, %	98	102	104	103	87	108	-	105	-	99
28 d AI (BS EN 450), %	80	79	83	79	76	81	-	85	-	80
90 d AI (BS EN 450), %	92	90	93	90	84	90	-	98	-	88

¹BS EN 450 mix proportion and BS 3892 – 1: 1982 curing condition, ² Pozzolanic activity index as per BS 3892 – 1: 1982

(Cont'd over next page)

Table 5-4. (Pozzolanic) Activity index and fresh properties of fly ashes received from various sources

Properties	F CC	F Oxy1	F Oxy2	F Oxy3	G	H	BD W1	BD W2	BD S
HR52									
Flow, %	100	96	93	102	96	97	-	-	-
7 d AI (BS EN 450), %	76	79	-	-	78	75	-	-	-
28 d AI (BS EN 450), %	87	86	83	92	86	87	-	-	-
56 d AI (BS EN 450), %	97	-	-	103	96	96	-	-	-
90 d AI (BS EN 450), %	103	101	97	106	102	101	-	-	-
180 d AI (BS EN 450), %	106	101	97	113	106	103	-	-	-
7 d ¹ AI (BS EN 450), %	96	94	82	99	90	-	-	-	-
Water requirement, %	101	101	104	97	102	102	-	-	-
7 d ² PAI (BS 3892), %	90	92	83	104	85	94	-	-	-
HK42									
Flow, %	98	92	88	102	-	97	91	97	87
28 d AI (BS EN 450), %	82	83	78	88	-	86	77	83	69
90 d AI (BS EN 450), %	103	96	94	106	-	102	91	97	77
LD32									
Flow, %	90	86	81	97	-	90	-	-	-
28 d AI (BS EN 450), %	92	82	85	98	-	98	-	-	-
90 d AI (BS EN 450), %	106	100	101	117	-	112	-	-	-
LD52									
Flow, %	98	-	88	101	95	98	-	-	-
28 d AI (BS EN 450), %	80	-	77	82	78	77	-	-	-
90 d AI (BS EN 450), %	88	-	84	94	87	90	-	-	-

¹BS EN 450 mix proportion and BS 3892 – 1: 1982 curing condition, ² Pozzolanic activity index as per BS 3892 – 1: 1982 (cont'd from previous page)

Table 5-5. (Pozzolanic) Activity index and fresh properties of air-classified fly ashes from Source C and L

Properties	C5	C10	C20	C30	C40	C50	CFD	L5	L10	L20	L30	L40	L50	LFD
HR52														
Flow, %	100	101	102	104	106	106	94	100	101	101	102	102	103	98
14 d AI (BS EN 450), %	88	86	83			80	76	88	87	83	82		83	80
28 d AI (BS EN 450), %	94	92	90	89	88	86	80	95	92	91	90	89	89	82
56 d AI (BS EN 450), %	114	113	109	107	104	103	91	115	115	108	104	103	101	96
Water requirement, %														
7 d ¹ PAI (BS 3892), %	100	-	99	97	97	96	104		-	-	-	-	-	-

¹ Pozzolanic activity index as per BS 3892 – 1: 1982

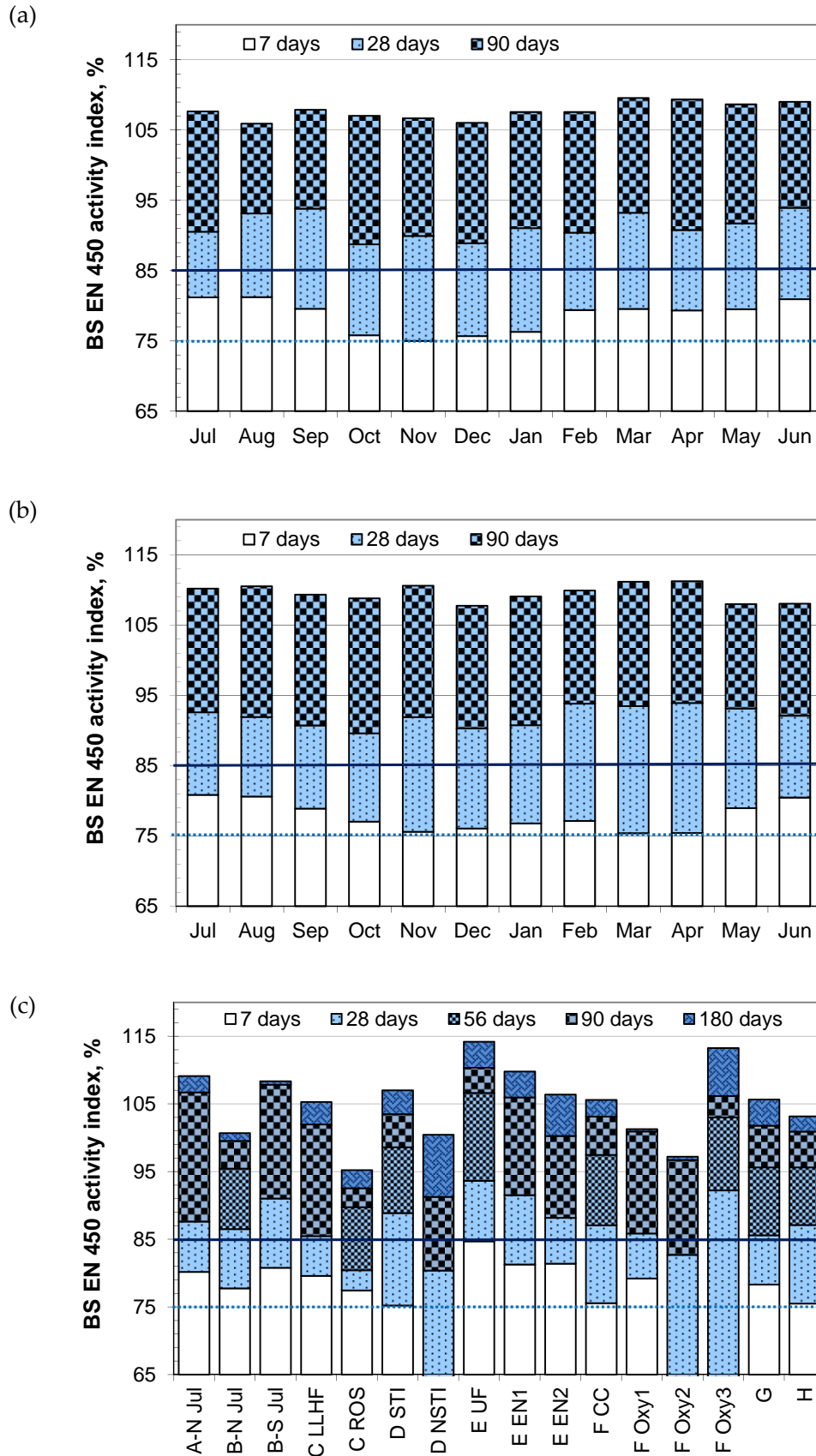


Figure 5-1. BS EN 450 activity index (PC, HR52) of (a) monthly fly ashes from Source A; (b) monthly fly ashes from Source C; and (c) fly ashes from various sources

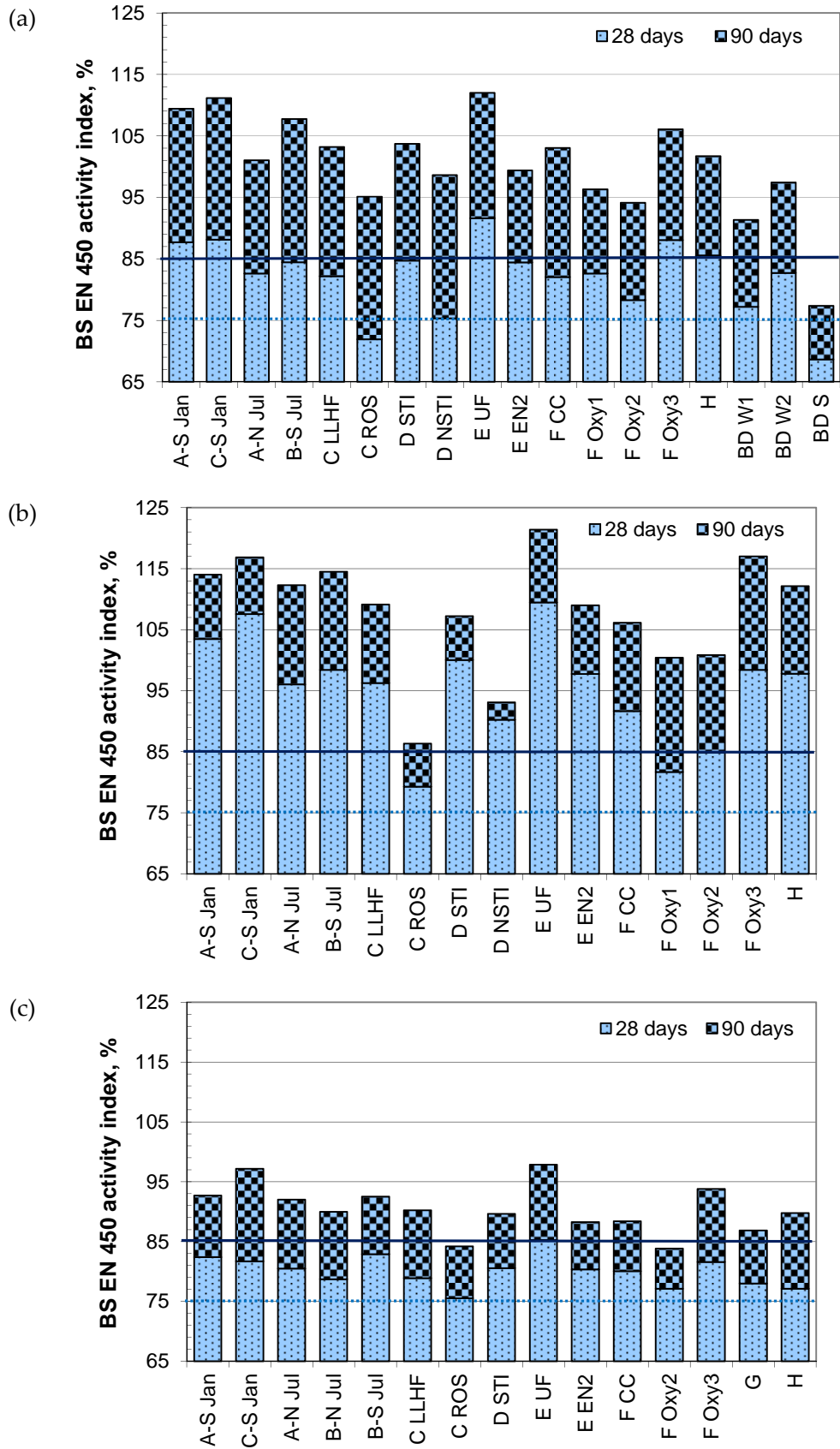


Figure 5-2. BS EN 450 activity index of fly ashes from various sources using PCs (a) HK42; (b) LD32; and (c) LD52

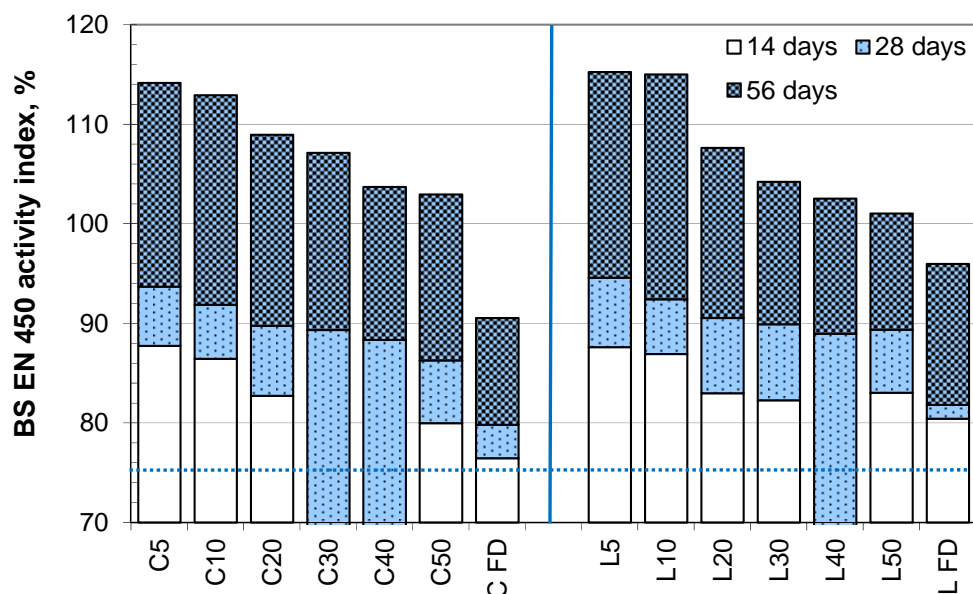
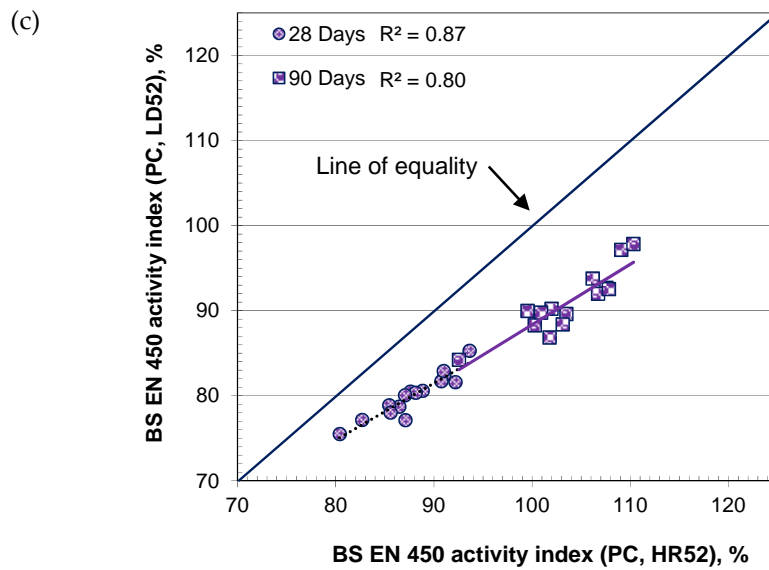
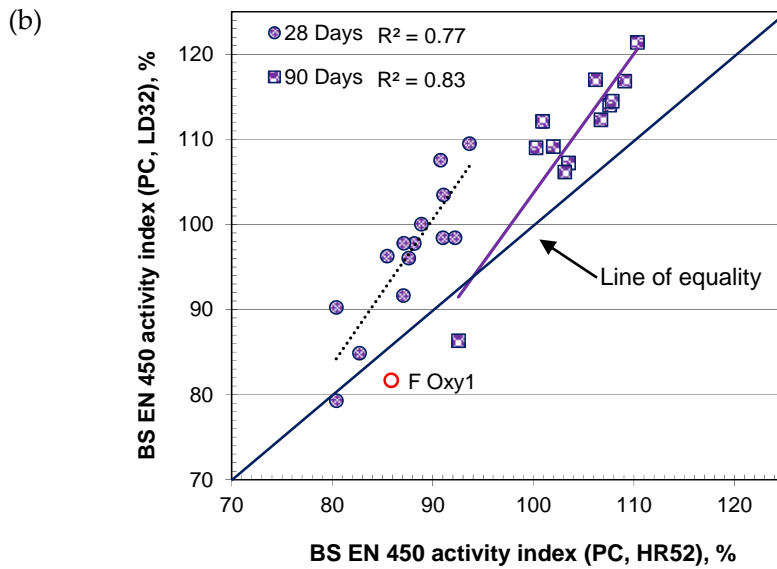
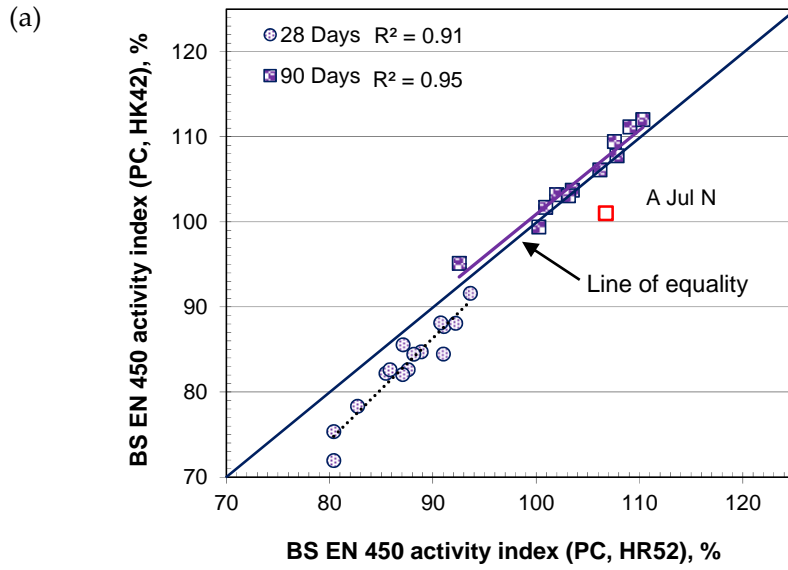


Figure 5-3. BS EN 450 activity index of air-classified fly ashes using PC HR52

Figures B-4, B-5(a), B-5(b) and B-5(c) (*Appendix B*) show the minimum activity index values at 28 and 90 days with cements HR52, HK42, LD32 and LD52, respectively. These indicate that fly ashes C ROS, D NSTI, F Oxy2, BD W1 and BD S at 28 days and BD S at 90 days did not meet the activity index criteria with cement HK42. The same effect was noted for C ROS with cement LD32 at 90 days and C ROS and G at 28 days and C ROS, F Oxy2 and G at 90 days with cement LD52. All these materials had either high LOI (> 7%) or coarse particle size (> 20% retention on the 45 μm sieve).

Figure 5-4 makes a comparison between activity indices obtained with the different cements at 28 and 90 days. Table 5-6 gives the range of activity indices obtained at the standard test ages (28 and 90 days) with four different PCs. It is clearly apparent that the same fly ashes gave a different activity index depending on the PC used; with more significant effect noted with finer/lower LOI fly ash. While the fly ash properties remain same the effect can be attributed to the properties of PCs. As shown, PC LD32 gave best activity index values following HR52, HK42 and LD52. The better performance of PC LD32 with fly ash appeared to relate its higher C_3S content (58.4%). PC HR52 (53.2%) and PC LD52 (39.2%) also followed the order of their C_3S content.



Continued on next page

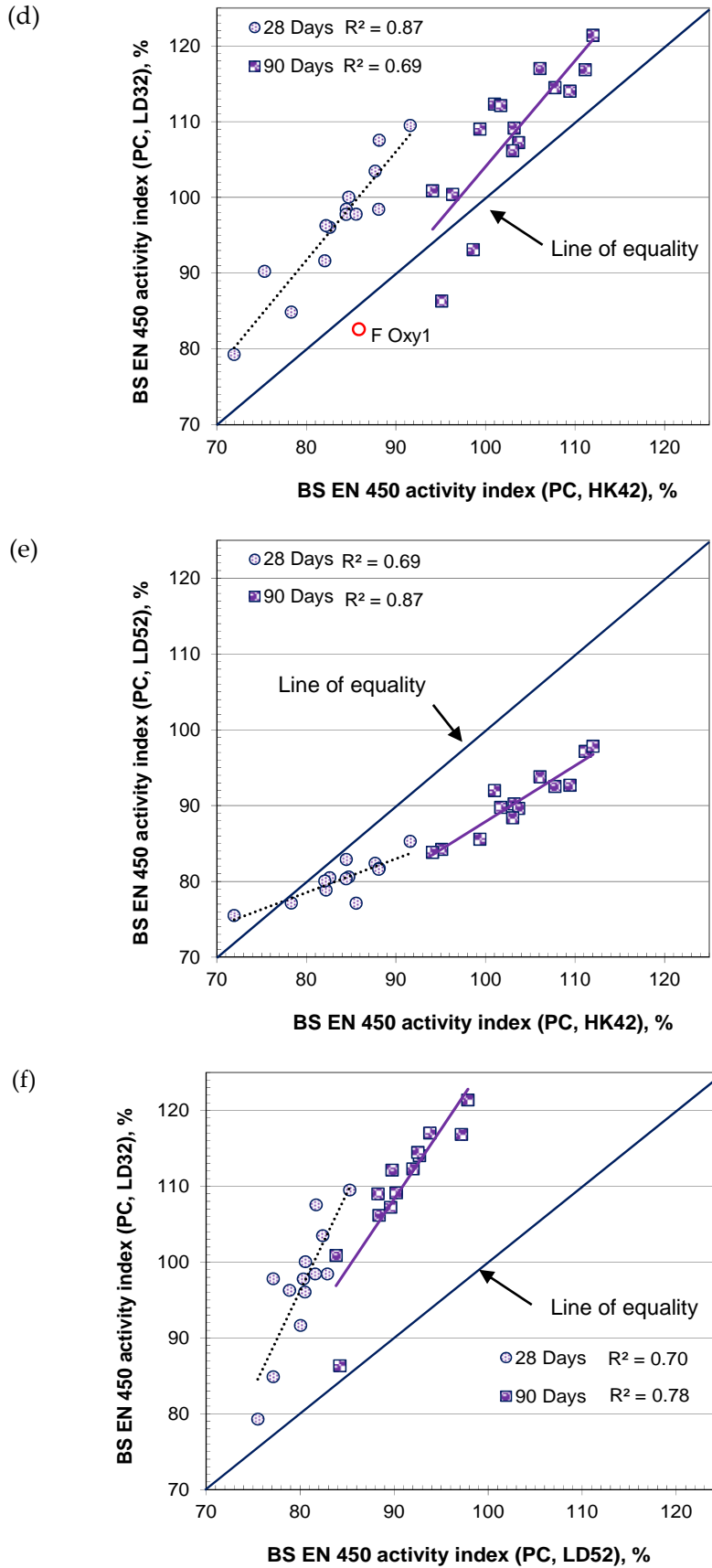


Figure 5-4. Comparisons between BS EN 450 activity index using PCs HR52, HK42; LD32; and LD52. (points in red not included in the regression analysis)

Table 5-6. Range of activity index obtained using various PCs

PC	28 day		90 days	
	Minimum	Maximum	Minimum	Maximum
HR52	80	94	91	111
HK42	69	92	77	112
LD32	79	109	86	121
LD52	76	85	84	98

Hydration of the C₃S phase in cement continues constantly with age and is approximately completed by 28 days, while the C₂S phase is slower in reaction and mainly takes place after 28 days. The quantity of lime released from C₃S is also higher than that of the C₂S phase (Neville, 2011). Therefore, the higher C₃S content in PC LD32 might release greater quantities of lime at an earliest age to create more favourable conditions for reaction of the aluminosilicate component of fly ash. The same applies for PCs HR52 and LD52 for their corresponding reactivity with fly ash. Although the C₃S content in HK42 appeared to be higher, its reactivity might reduce being relatively coarse in nature.

5.2.1 Mortar fresh properties and strength development

Flow values of fresh mortar samples were measured during preparation of BS EN 450 (BSI, 2005c) prism samples. Figure 5-5 makes a comparison between the flow (relative to the control) obtained with the different PCs. The relative flow ranking obtained with the fly ashes was similar to that for the various PCs and generally followed HR52 > LD52 > HK42 > LD32. This appeared to relate to the fineness of PCs. As given in Table 4-6 the order of d₉₀ was LD32 (61.3 µm) > HK 42 (54.0 µm) > LD 52 (44.0 µm) > HR52 (36.6 µm). Therefore, while the same fly ashes were used with different PCs, the variation in mortar fresh properties was inversely related to the fineness of PCs.

The flow values obtained with PCs HR52, HK42, LD32 and LD52 are plotted against corresponding fly ash properties (i.e. 45 µm sieve residue, sub 10 µm quantity and multiple factor (LOI × 45 µm fineness)) in Figures 5-6, 5-7, 5-8 and 5-9, respectively. The multiple factor is an optional physical requirement given in ASTM C618 (ASTM 2012). Samples plotted with empty circles (with names) did not follow typical behaviour and were not included in the analysis. In general, expected trends were obtained for each cement type.

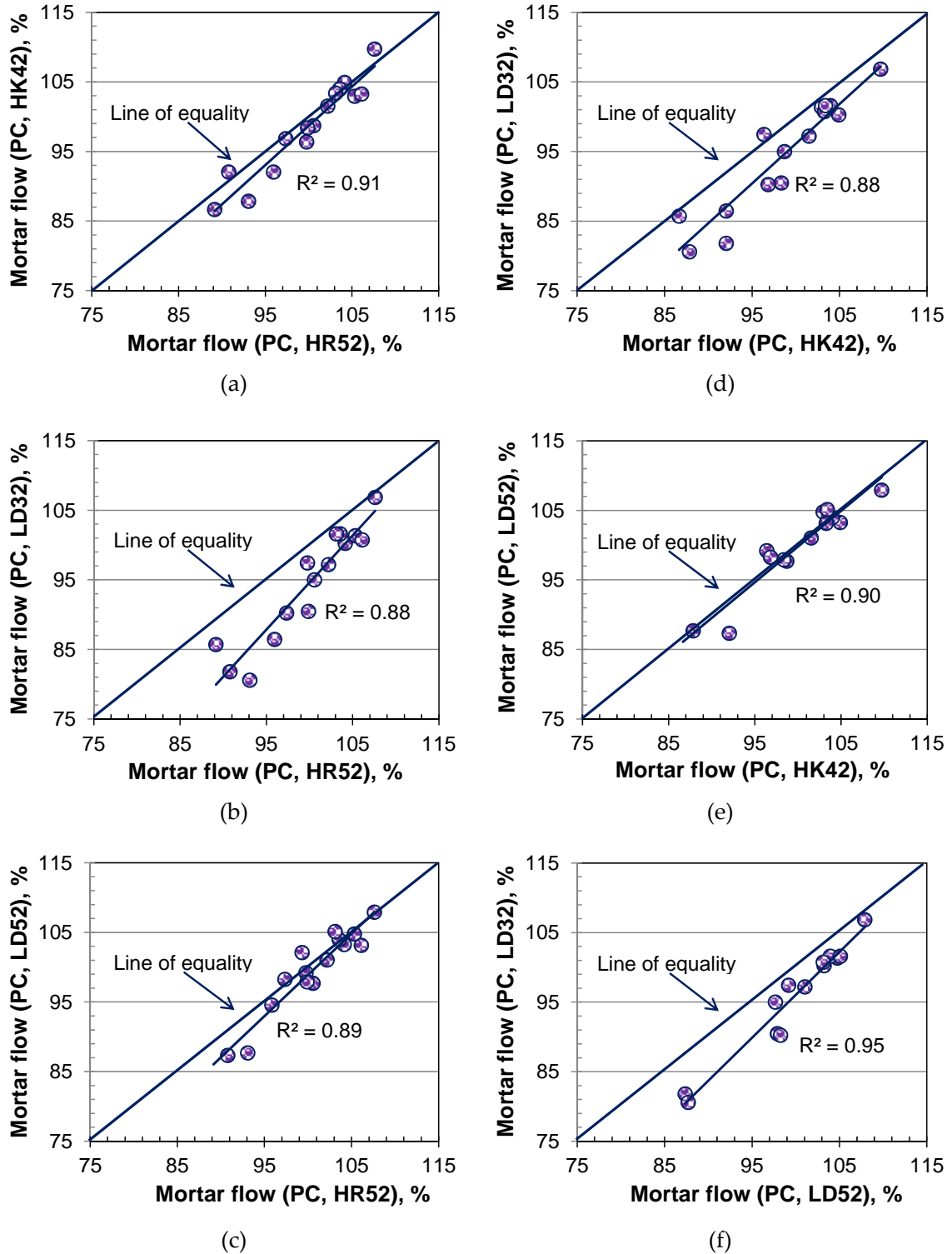


Figure 5-5. Comparison of BS EN 450 mortar flows for different PCs

The relationship of flow with sub 10 μm quantity was proportional, although inversely proportional behaviour was obtained with the 45 μm sieve residue and multiple factor. It was noted that while the relationship of flow with 45 μm sieve residue and sub 10 μm

quantities was linear, this was logarithmic with the multiple factor. Similar behaviour of fly ash in cementitious system has been noted elsewhere (Sear, 2001; Neville, 2011).

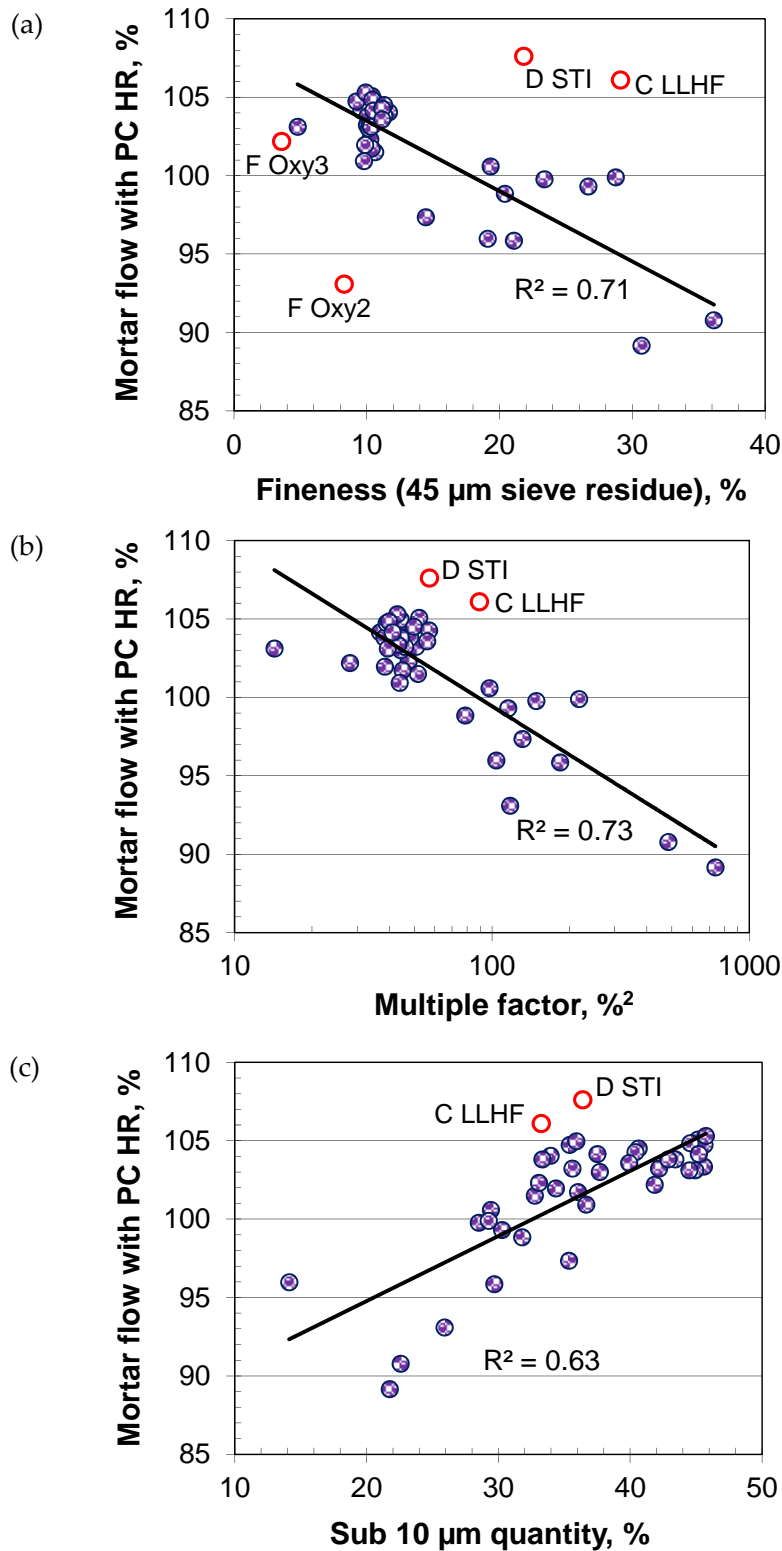


Figure 5-6. Relationships between fly ash properties and BS EN 450 mortar flow (PC, HR52): (a) 45 µm sieve residue; (b) multiple factor (LOI × 45 µm fineness); and (c) sub-10 µm quantity. (points in red not included in the regression analysis)

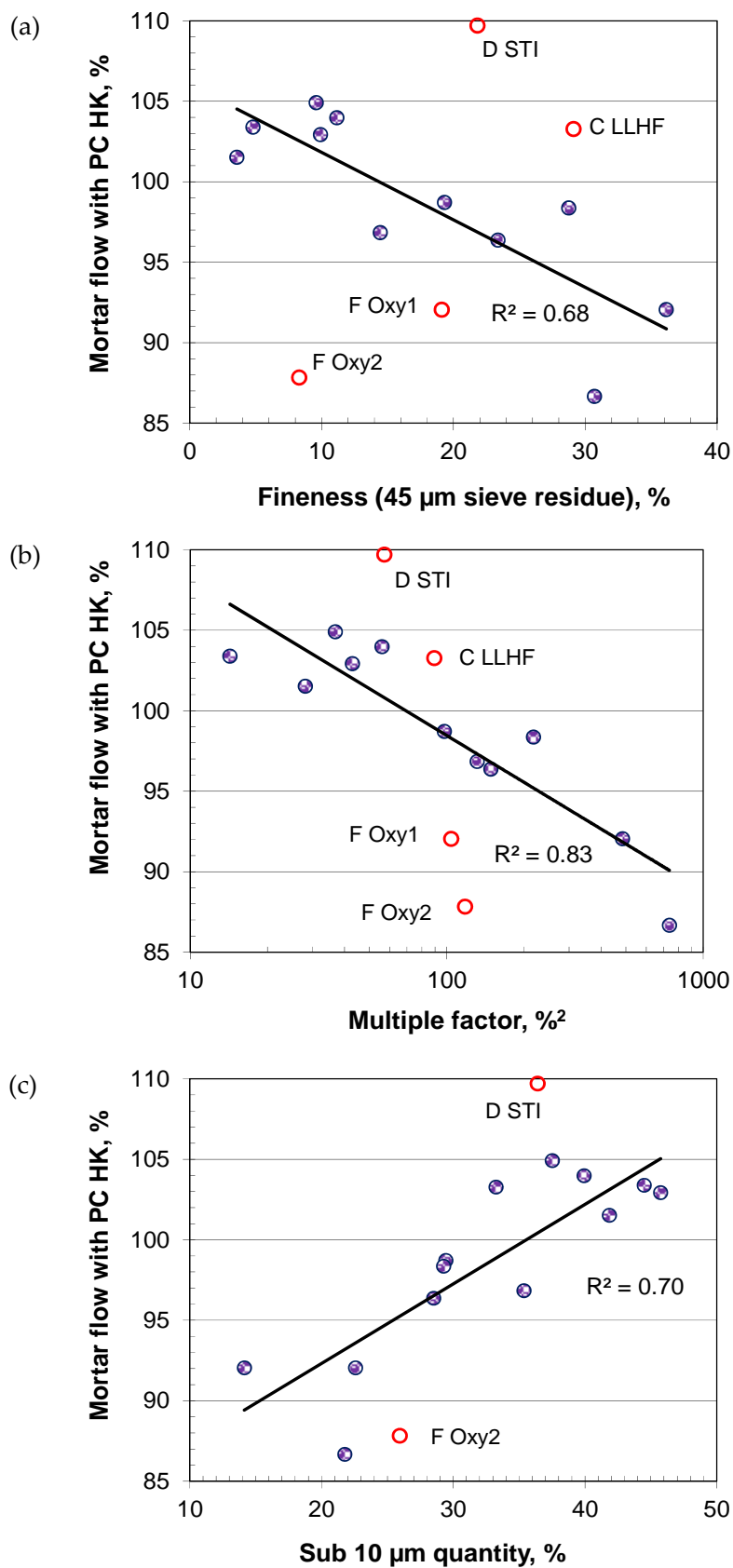


Figure 5-7. Relationships between fly ash properties and BS EN 450 mortar flow (PC, HK42): (a) 45 μm sieve residue; (b) multiple factor (LOI \times 45 μm fineness); and (c) sub-10 μm quantity. (points in red not included in the regression analysis)

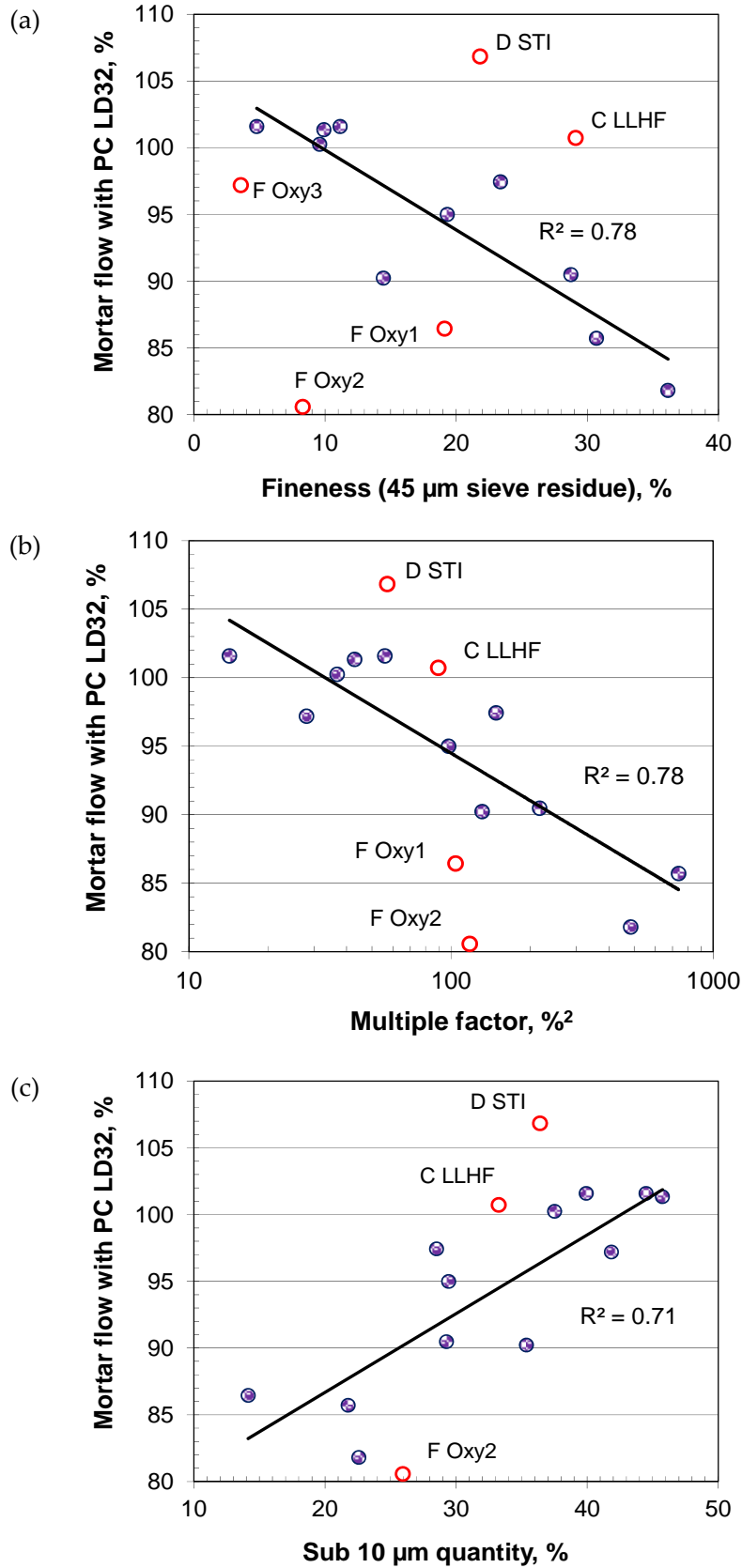


Figure 5-8. Relationships between fly ash properties and BS EN 450 mortar flow (PC, LD32): (a) 45 µm sieve residue; (b) multiple factor (LOI × 45 µm fineness); and (c) sub-10 µm quantity. (points in red not included in the regression analysis)

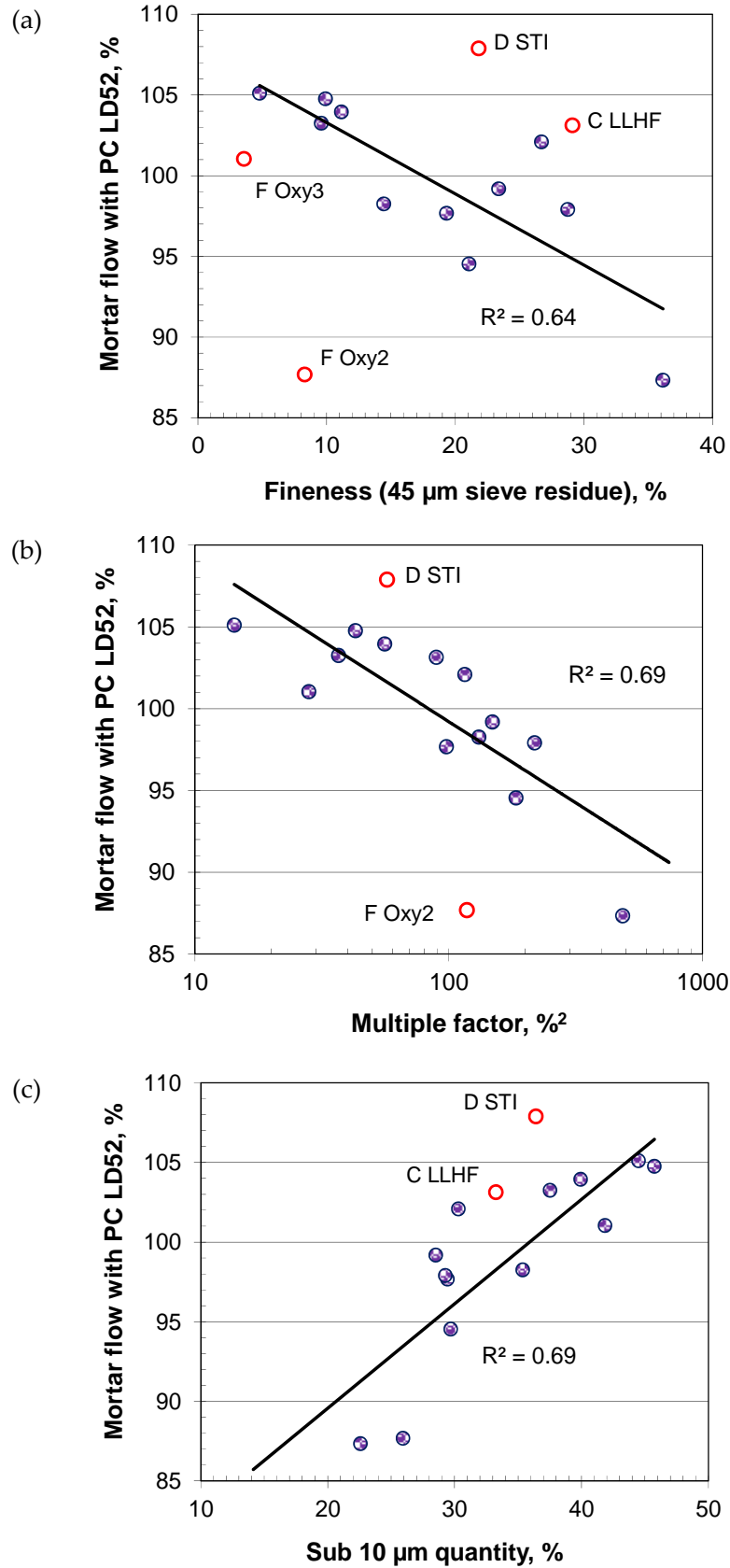


Figure 5-9. Relationships between fly ash properties and BS EN 450 mortar flow (PC, LD52): (a) 45 µm sieve residue; (b) multiple factor (LOI × 45 µm fineness); and (c) sub-10 µm quantity. (points in red not included in the regression analysis)

Considering the behaviour of the four cements, it was noticed that the multiple factor (considers both fineness and LOI) in general gave better correlations than the other two parameters. Fly ashes C LLHF, D STI, F Oxy1, F Oxy2 and F Oxy3 were mostly outwith the general trend and were not included in the regression analysis. The improved flows of fly ashes C LLHF and D STI correspond to their low LOI values, although their 45 μm fineness values were relatively high. On the other hand, although Fly Ash F Oxy2 gave low retention on the 45 μm sieve, it gave relatively low flow, probably due to its high LOI. SEM images of the oxy-fuel fly ashes (see Figure 4-20 (a) and (c)) also indicate rough particle surfaces with crystalline deposits. This could affect the ability of particles to move past one another and be a possible cause of the low flow, given its multiple factor value.

Figure 5-10 provides a comparison between properties of air-classified fly ashes and their flow using PC HR52. Being relatively coarser than the test PC ($d_{90} = 36.6 \mu\text{m}$), both feed raw samples CFD and LFD (d_{90} of 120.0 and 115.9 μm , respectively) gave less flow than the control mortar with PC. While the PSDs of the feed samples were comparable, significantly higher LOI in Fly Ash CFD (LOI = 11.5%) gave lower flow compared to that of LFD (LOI = 5.7%). With similar size fractions, Source C gave higher flow than Source L. As shown in Table 5-4 other fly ashes (E UF, E EN1 and E EN2) obtained from Source L always gave relatively lower flow despite their fineness and LOI and similar observation were made in other studies with fly ash from this source (Gayathri, 2008).

As shown in Figure 5-10 the air classified finer fly ashes gave the opposite trend compared to that observed with other general fly ashes noted above. The finest fly ashes (C5 and L5 with d_{90} of 10.8 and 9.3 μm) obtained from the classification process gave similar flow to the control mix and this increased with particle size for the other samples obtained from the process (C50 and L50 with d_{90} of 46.1 and 45.7 μm). In general, an increase in proportion of spherical shaped particles was noticed with a reduction in d_{90} of the air classified fly ashes from SEM images (see Figures A-12 and A-13). This may be expected to enhance ball-bearing effects and thereby the flow at the same water content. However, this was not achieved with the very fine components (e.g. C5, C10, L5 and L10). The relatively higher surface area in this case demands increased water, while still giving a ball-bearing effect and comparable flow to the control mix, suggesting their combined effect.

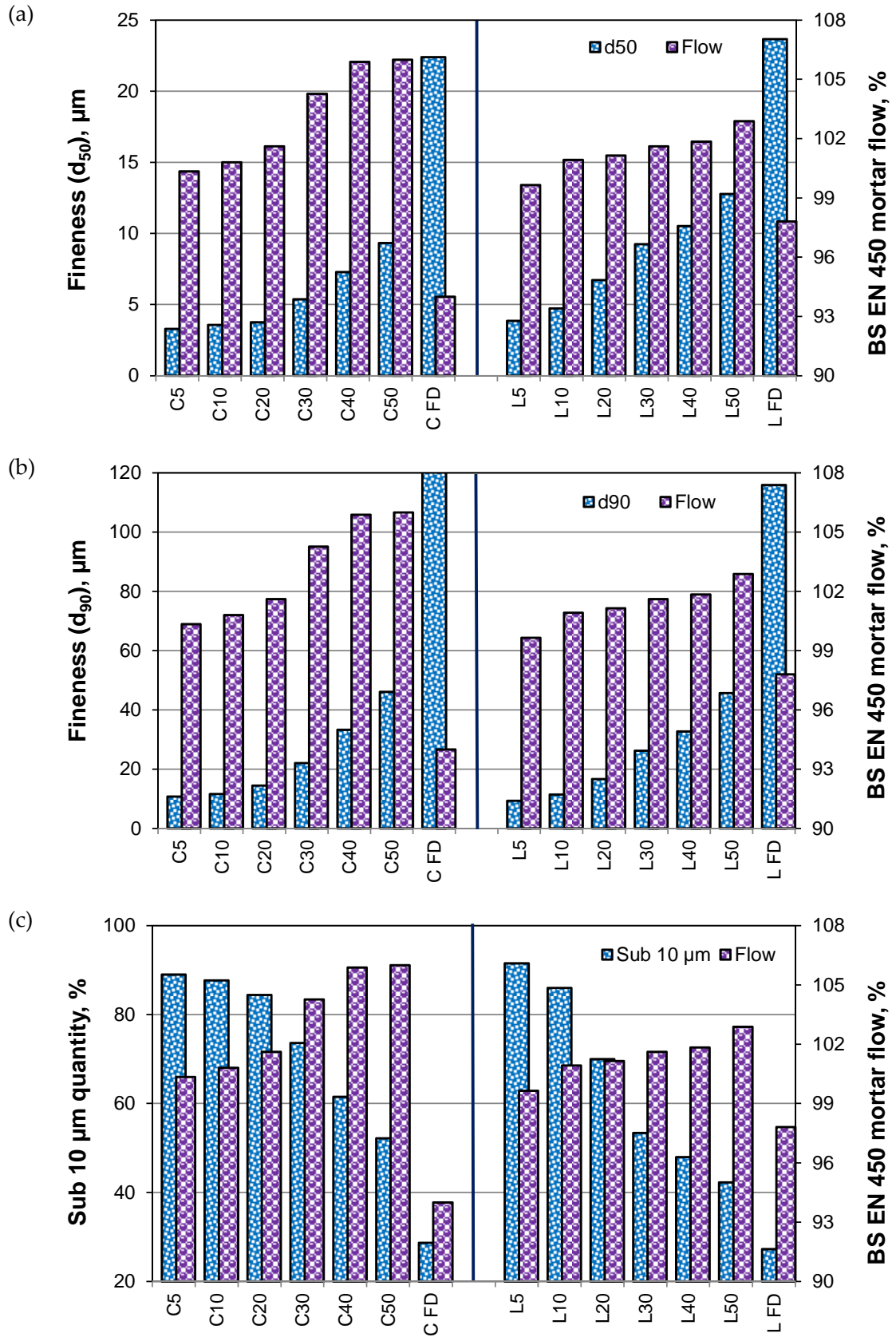
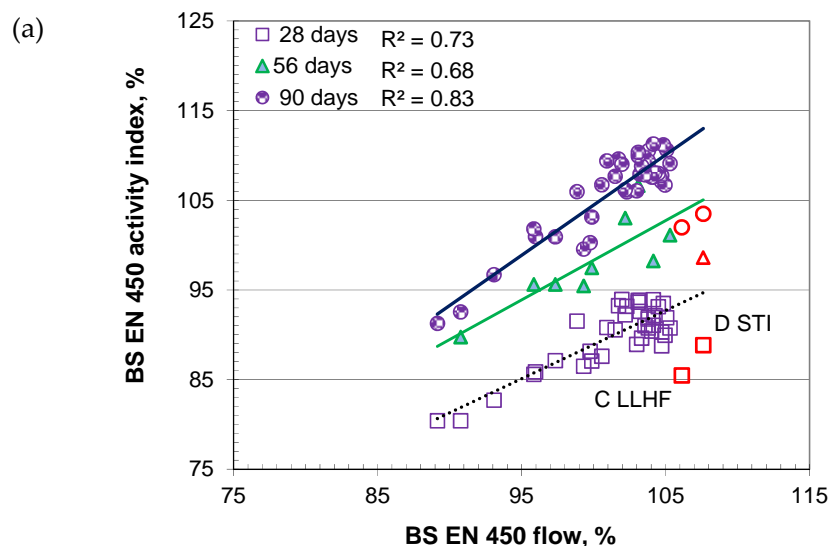


Figure 5-10. Relationships between air-classified fly ash properties and BS EN 450 mortar flow (PC, HR52): (a) d_{50} , (b) d_{90} ; and (c) sub 10 μm quantity

The sieve analysis of CEN sand indicates 99.9% material was coarser than 63 μm . During the mortar test it is expected that the cementitious (relatively finer than sand) part will comprise this 0-63 μm fraction to form a dense matrix. While 25% of the PC ($d_{90} = 36.6 \mu\text{m}$) was replaced by the fine component of fly ashes (mean particle size 3.3 and 3.9 μm), there appeared to be a grading gap (see Figures 4-5 and 4-6 for PSD and particle size comparison, respectively), which might also be responsible for this behaviour. As shown in Figure 5-10 with comparable particle sizes between PC and fly ashes, the effects were minimized and gave maximum flow. In these cases, the replacement of PC with similar size particles but spherical in shape gave better flow properties. Therefore, the relative increase in flow is not only dependent on fly ash fineness, it is also influenced by the fineness of PC and grading of fine aggregates used.

The relationship between BS EN 450 fly ash mortar flow and activity index using different cements at 28, 56 and 90 days are shown in Figure 5-11. With some exceptions (Fly Ashes D STI and C LLHF) good correlations were obtained between these. This is expected, in general, with finer fly ashes due to their better particle packing and greater reactivity (Sear, 2001). However, although by applying STI technology, Fly Ashes D STI and C LLHF gave relatively lower LOI, their particle size still remained relatively coarse, which did not give higher reactivity as expected from their flow.



Continued to next page

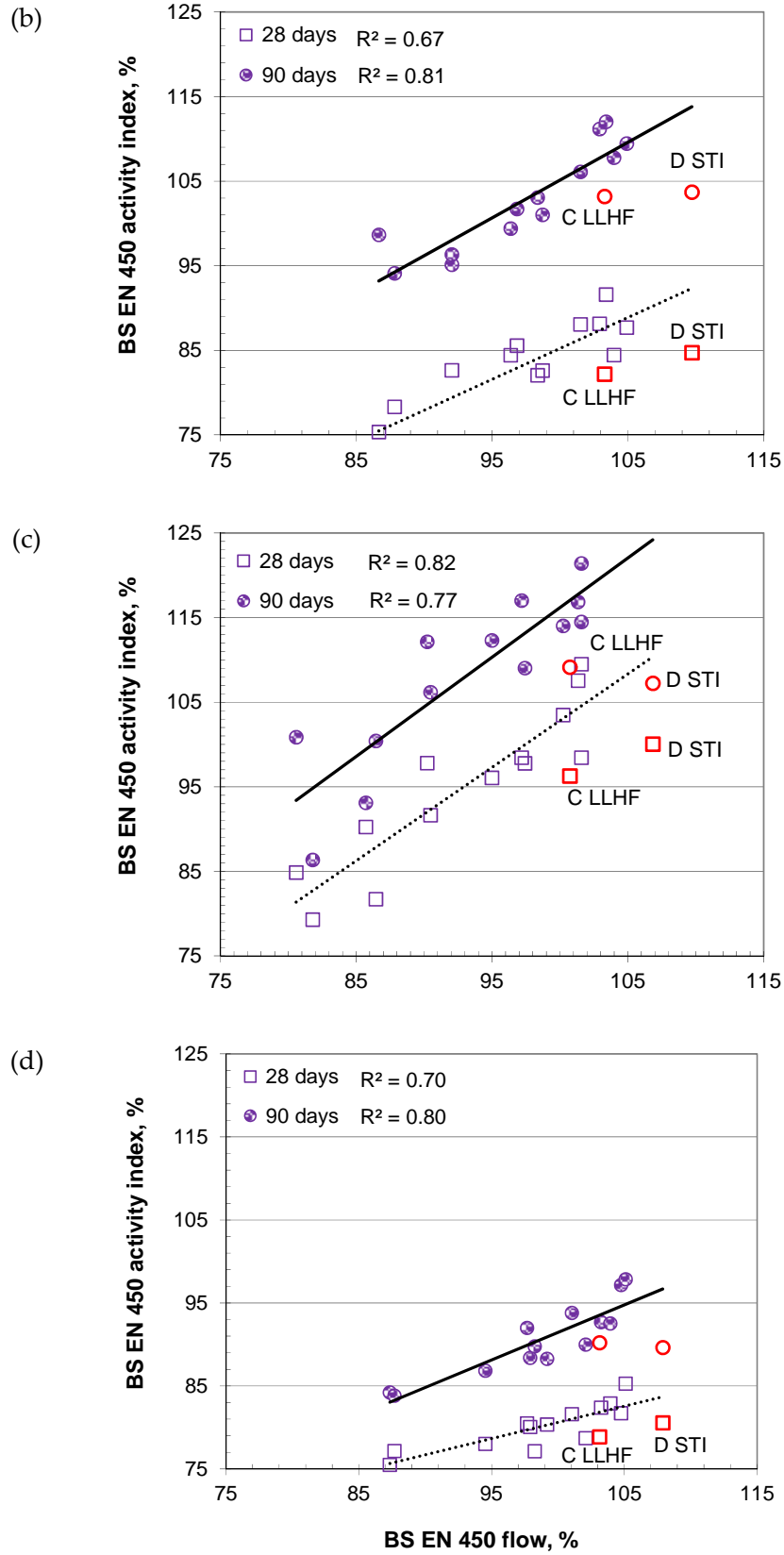


Figure 5-11. Relationships between BS EN 450 flow and activity index for (a) PC HR52; (b) PC HK42; (c) PC LD32; and (d) PC LD52. (points in red not included in the regression analysis)

The relationships of flow were reasonable with 28 days activity index and became stronger at 90 days. The coefficient of correlation (R^2) between activity index and flow ranged from 0.67 – 0.82 at 28 days and 0.77 – 0.83 at 90 days, depending on the cement used.

Figure 5-12 makes a comparison between the flow and activity index of air-classified fly ashes obtained at 14, 28 and 56 days. As with the behaviour obtained between fineness and flow for air-classified fly ashes, strength also did not follow the trend obtained with the other fly ashes used in this project. Although the increase in flow with the finest fraction of fly ashes was minor compared to the control mortar, they gave considerably higher activity index than the corresponding coarse fractions. Therefore, it appeared that the pozzolanic action was dominant compared to the packing of the finest fractions.

Figure 5-13 shows very good correlations between the water requirement (tested following BS 3892-1: 1982) and the flow (following BS EN 450) both using cement HR52. Results in Figure 5-13 (a) were obtained using fly ashes from various sources, while those in Figure 5-14 (b) were for different fractions (air-classified) and feed sample from Source C. The latter gave a higher co-efficient of correlation, which is likely to reflect the fact that the samples were obtained in a more controlled way and there was less chance of variations, which might occur due to individual burning conditions and coal chemistry from different sources.

The water requirements were compared with the pozzolanic activity index (accelerated) in Figure 5-14. As shown in Figure 5-14 (a) for the main fly ashes, it was noted that a higher flow/lower water demand was a good indicator of greater reactivity. However, the situation for the fine components of fly ashes obtained from air-classification was slightly different. As shown in Figure 5.14 (b), the water demand for the parent feed Fly Ash CFD was 104%, which is expected given its coarse particles (45 μm residue = 34.9%) and high LOI (11.5%).

The water demand for the classified fractions ranged from 96.5 - 99.5%. The trend obtained for flow with the same water content was confirmed here, with the finer fraction demanding relatively higher water due to its higher surface area. However, this almost levelled off for fly ash fractions C30, C40 and C50 having a relatively close PSD to the test PC and given their ball-bearing effect.

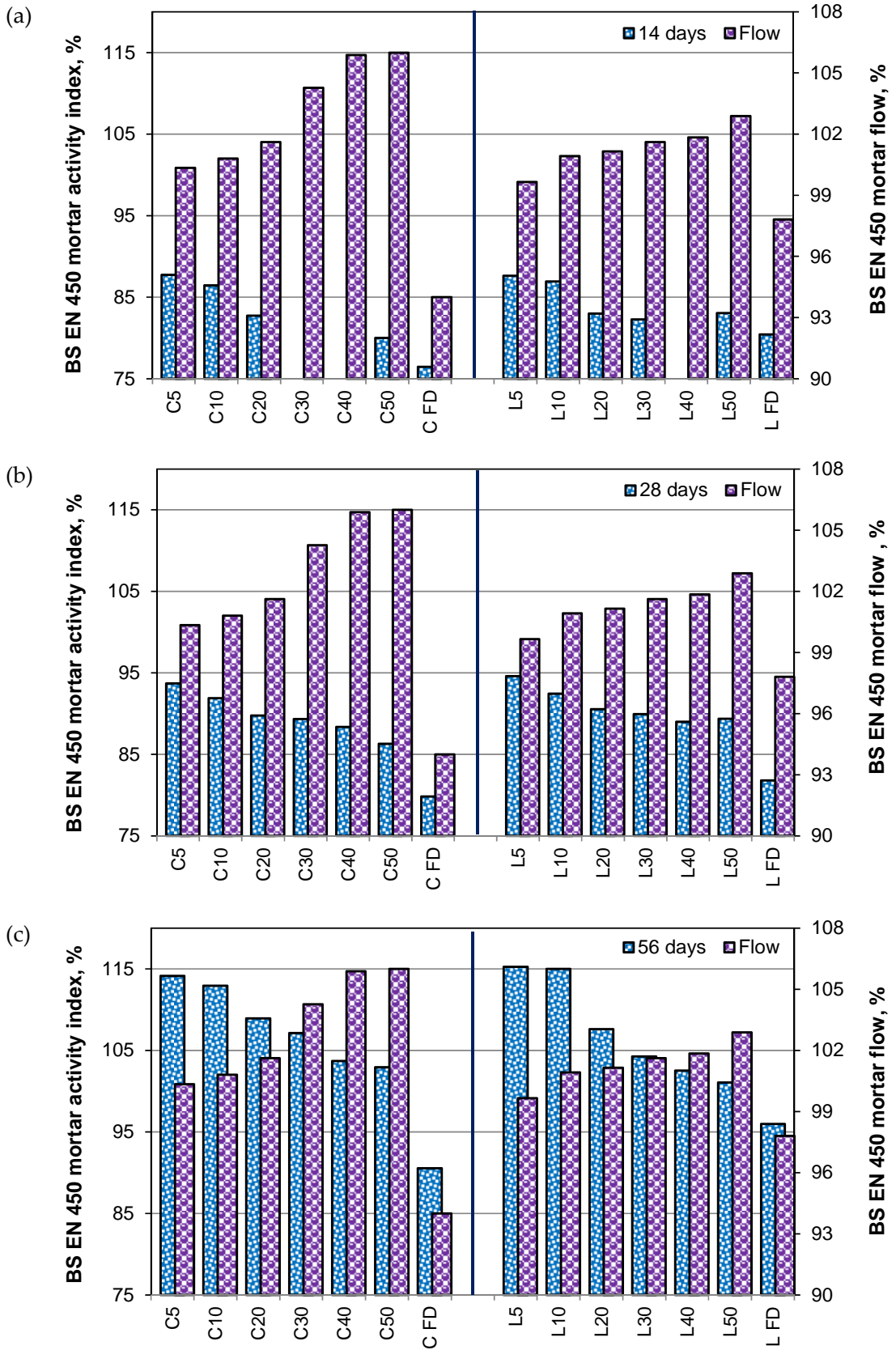


Figure 5-12. Relationships between air-classified fly ash properties and BS EN 450 mortar flow (PC, HR52): (a) d_{50} , (b) d_{90} ; and (c) sub 10 μm quantity

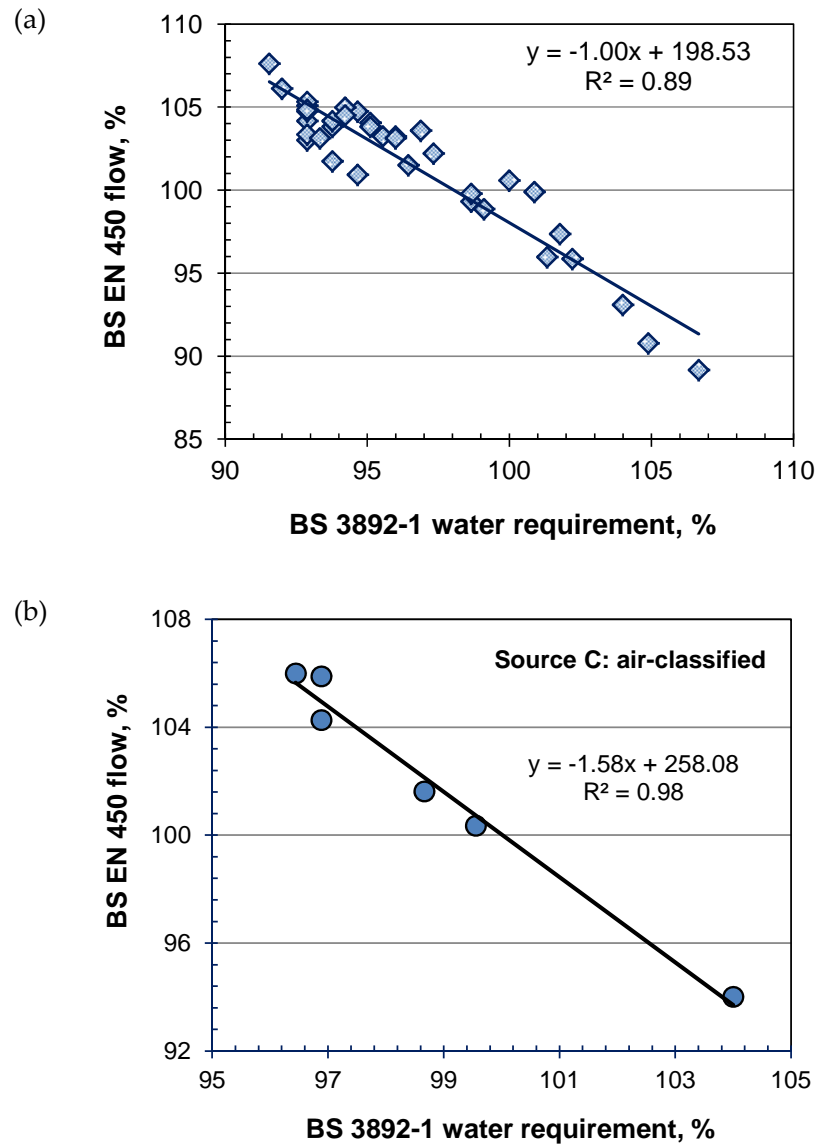


Figure 5-13. Relationship between BS 3892-1 (1982) water requirement and flow using PC HR52: (a) general fly ash; and (b) air-classified fly ash

Selected activity index test results using BS EN 450 mix proportions and BS 3892-1: (1982) accelerated curing conditions and their flows are related in Figure 5-15. As with the relationship between flow and activity index for standard curing conditions, a general agreement was obtained between these, except for Fly Ashes D STI and C LLHF. This was explained earlier where the two fly ashes obtained from STI carbon removal gave comparatively higher flow but their reactivity (compressive strength) in mortar was not as good as expected.

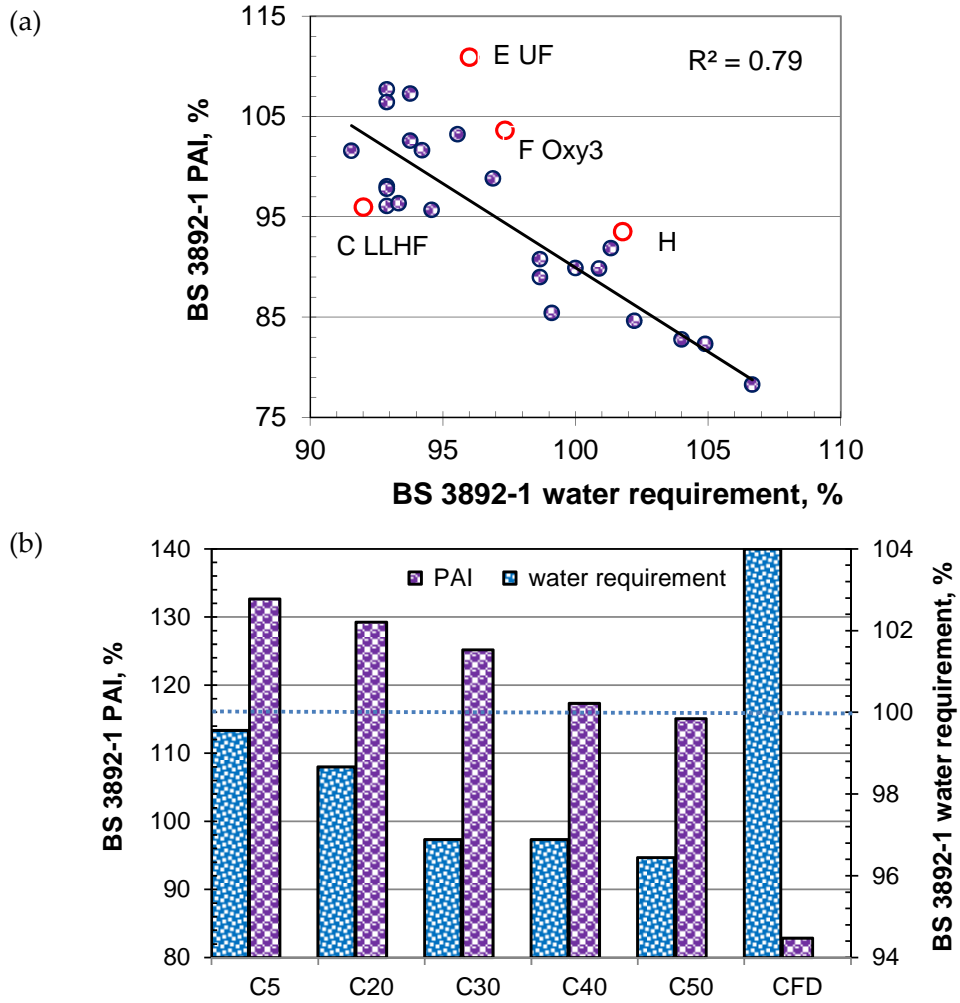


Figure 5-14. Relationship between BS 3892-1 water requirement and pozzolanic activity index: (a) main fly ash; and (b) air-classified fly ash. (points in red not included in the regression analysis)

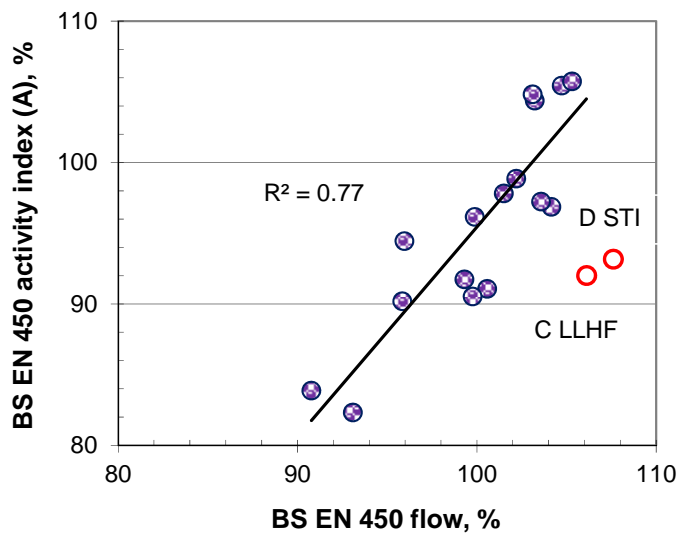


Figure 5-15. Relationship between BS EN 450 flow and activity index (accelerated) (points in red not included in the regression analysis)

Figure 5-16 shows the effect of fly ash (using cement HR52) and cement (using fly ash E UF) on the strength development of selected fly ash mortar samples. As shown in Figure 5-16 (a), in general, the control mortar strength was considerably higher than those with fly ash, at both 7 and 28 days. However, with some fly ashes, mortar strength at 90 and 180 days equalled or exceeded the control, indicating greatest reactivity after 28 days and mainly between 28 and 90 days. Figure 5-16 also indicates a good logarithmic relationship between curing age and strength development of the fly ash mortars.

Greater reactivity was obtained for the finer components obtained by air-classification. As shown in Figure 5-16 (c) higher reactivity was noticed at 28 days for the finest fractions from both Sources C and L. The control PC mortar strength was 2.7 and 1.7% higher than that with Fly Ashes C5 and L5. Paya *et al.* (1995) studied reactivity of air-classified material (mean size $\sim 12 \mu\text{m}$) in mortar at 28 days and obtained $\sim 95\%$ strength of control PC mortar at the 30% fly ash level, which is comparable with the results obtained in the current study using 25% fly ash and comparatively finer material ($d_{50} \sim 4 \mu\text{m}$).

By classification, 14.4 and 13.3% increases in strength were obtained for Fly Ashes C5 and L5 compared to their parent feed samples CFD and LFD, respectively, at 28 days. The mortar strengths with the finest classified Fly Ashes (14.1 and 15.3% respectively for C5 and L5) were well above the control mortar at 56 days. Increases in strength from the parent sample were 26.1 and 20.1% respectively at this age. This rapid strength gain (reactivity) of these fine fractions of fly ash may potentially solve the problems with early strength gain which might be frequently encountered using fly ashes for concrete.

5.2.2 Fly ash physical properties

Sub 10 μm quantity, 45 μm sieve residue and multiple factor

The effects of fineness (45 μm sieve residue), multiple factor and sub 10 μm quantity of fly ash on its reactivity (standard curing at 28, 56 and 90 days) are shown in Figures 5-17, 5-18, 5-19 and 5-20 using cements HR52, HK42, LD32 and LD52, respectively. With a few exceptions, fineness of fly ash was found to be a good parameter to estimate reactivity.

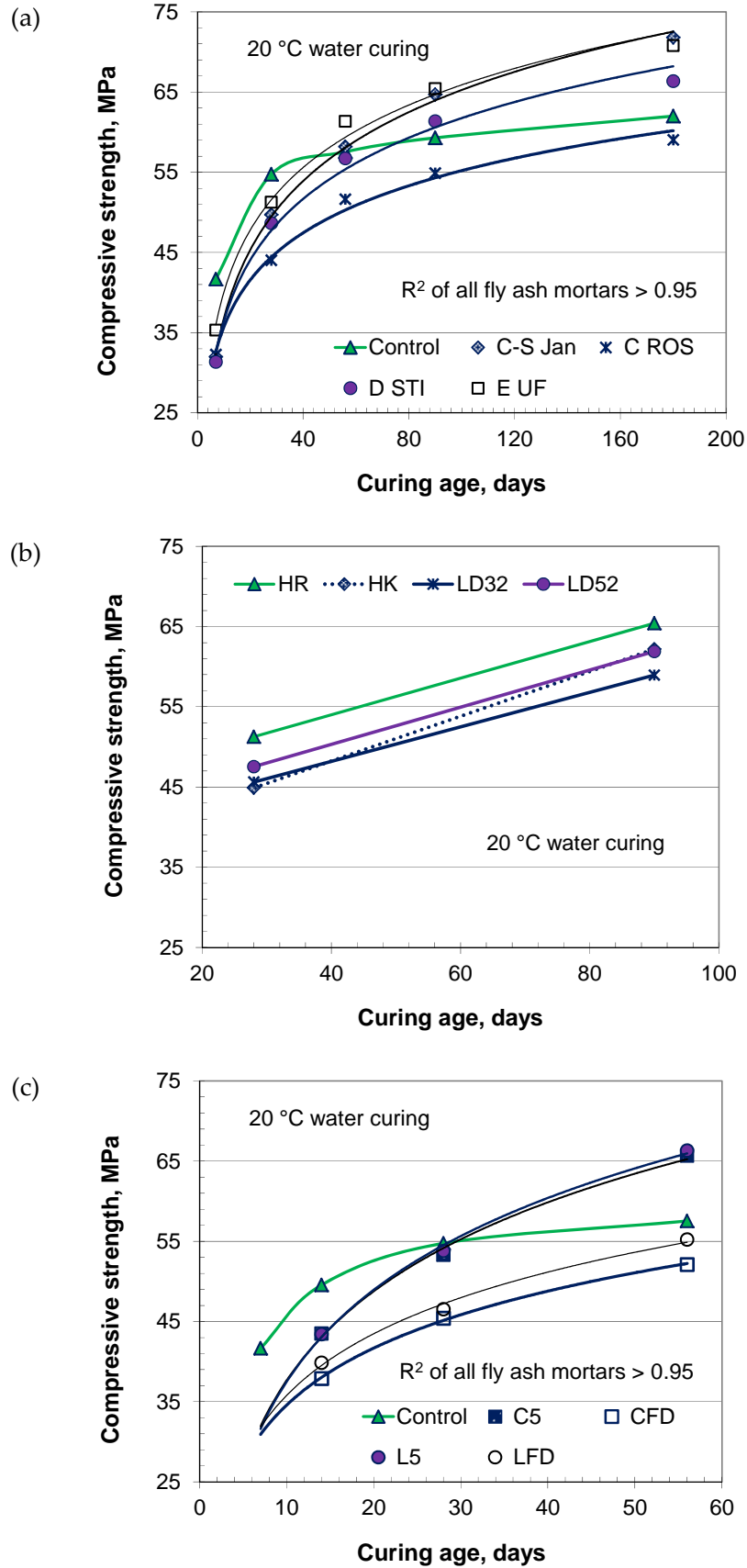


Figure 5-16. Strength development of mortar, effect of (a) fly ash; (b) PC type; and (c) processing by air-classification

The coefficient of correlation between the BS EN 450 activity index (using different cements) at 90 days and the multiple factor of fly ash ranged from 0.76 – 0.81, while this was between 0.69 – 0.79 with 45 μm sieve residue and 0.77 - 0.83 with the sub 10 μm quantity of fly ash. A few samples (10) were tested for activity index at 56 days with cement HR52. The coefficients of correlation of the 56 days activity index with 45 μm sieve residue, multiple factor and sub 10 μm quantity of fly ash were 0.71, 0.86 and 0.81 respectively. The correlations with 28 day activity index were also found to be good with all cements considered. In general, it was noted that sub 10 μm quantity tended to correlate slightly better with 28 day activity index than at the later test age (90 days).

Figure 5-21 indicates very good correlations between the sub 10 μm fractions of air-classified fly ashes from Sources C and L and their activity index at 14, 28 and 56 days as they contained a significant quantity of sub 10 μm particles. The relationships obtained were slightly different between the sources, which might be expected due to the variation in their chemistry originating from the burning conditions and composition of feed coal. As with the main fly ashes, discussed earlier, the relationships improved with test age.

It was noted that Fly Ash L50 gave higher activity index than L40 (finer) at 14 and 28 days, however, this changed at 56 days. As shown in Figure 4-5 (*Chapter 4*) the PSD of Fly Ash L50 was close to the test PC and, therefore, gave highest flow (see Figure 5-10) among the classified samples from Source L. Therefore, it appears that at early ages the packing effect governed, over pozzolanic action for this fly ash, however, at later ages (56 days) the pozzolanicity made a significant contribution to the strength development and therefore to activity index, with Fly Ash L40 exceeding that of L50.

Figure 5-22 gives relationships between the multiple factor ($d_{90} \times \text{LOI}$) and the activity index of air-classified fly ashes, at different ages. There relationships were good for Source C, but poor (except 56 days) for Source L.

It was noted earlier (Figure 4-11) that relative LOIs of air-classified fly ashes from Source C were similar, and considerably lower than the feed sample, however, the opposite occurred for Source L, with higher LOI in the finest fraction and then gradual decreases with increasing particle size. This behaviour may have been the main cause for the poor relationships obtained between the multiple factor and activity index for Source L.

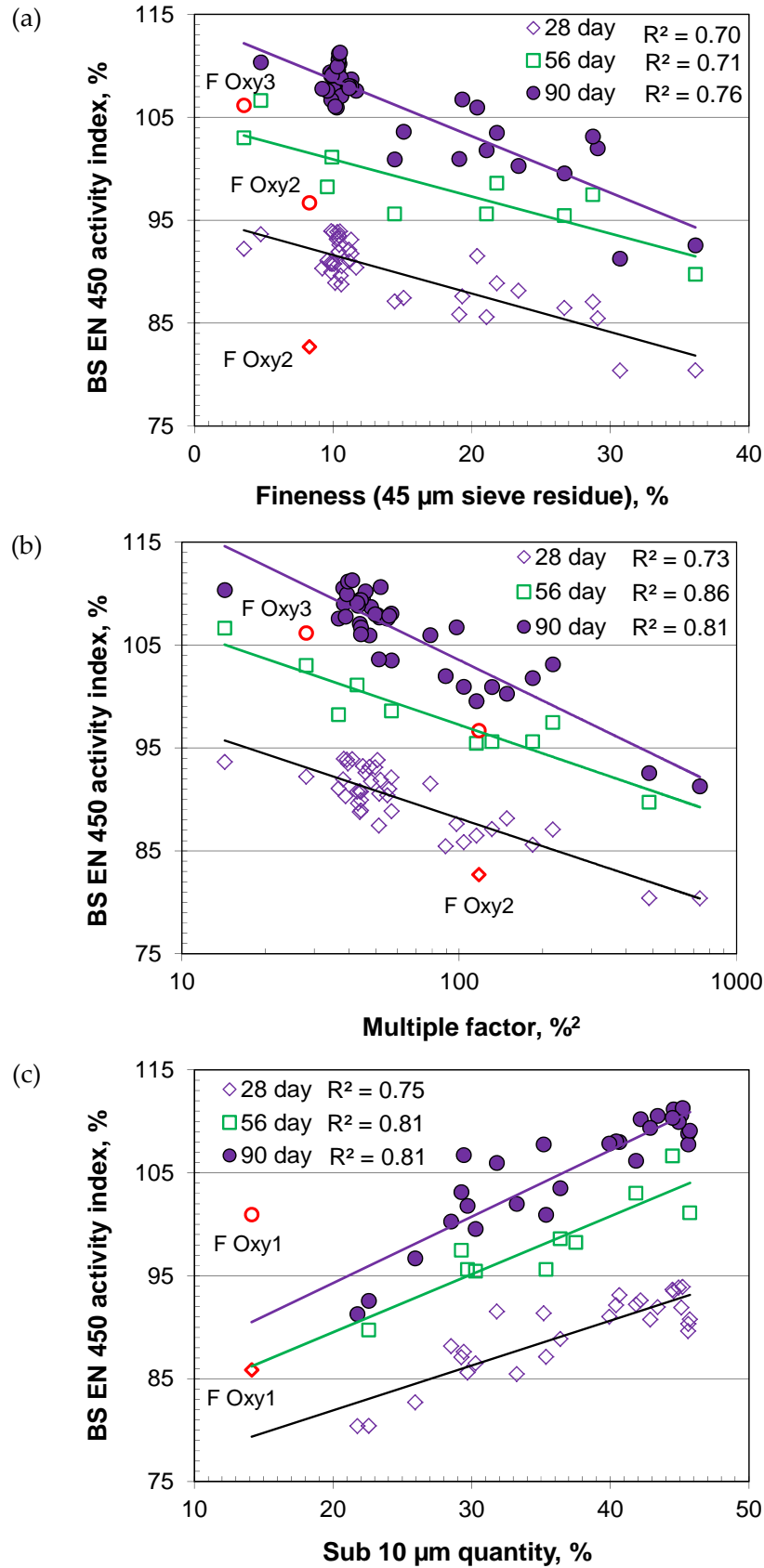


Figure 5-17. Relationships between fly ash property and BS EN 450 activity index (PC HR52): (a) 45 μm sieve residue; (b) multiple factor (45 μm sieve residue \times LOI); and (c) sub-10 μm quantity of fly ash. (points in red not included in the regression analysis)

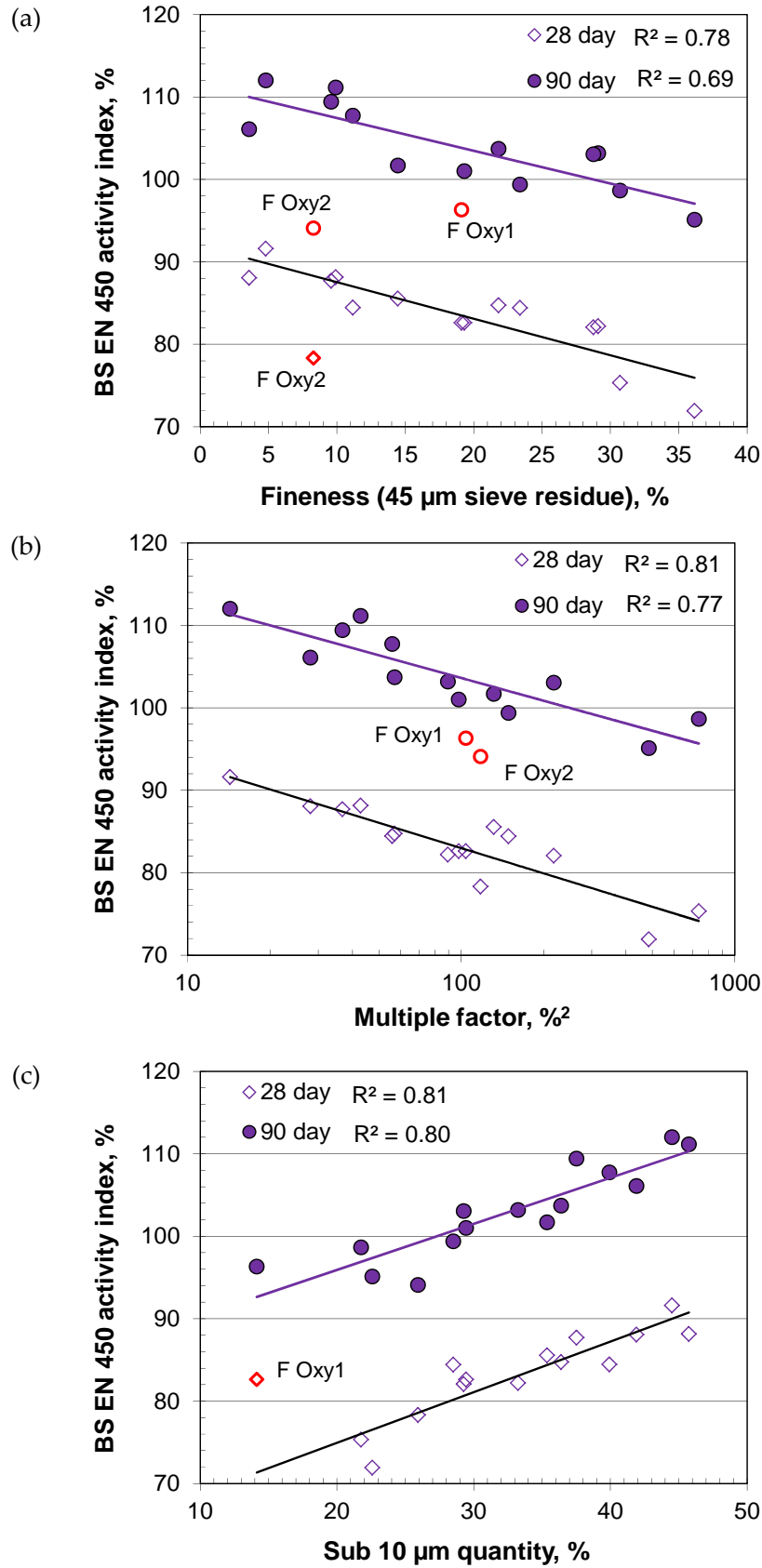


Figure 5-18. Relationships between fly ash property and BS EN 450 activity index (PC HK42): (a) 45 μm sieve residue; (b) multiple factor (45 μm sieve residue \times LOI); and (c) sub-10 μm quantity of fly ash. (points in red not included in the regression analysis)

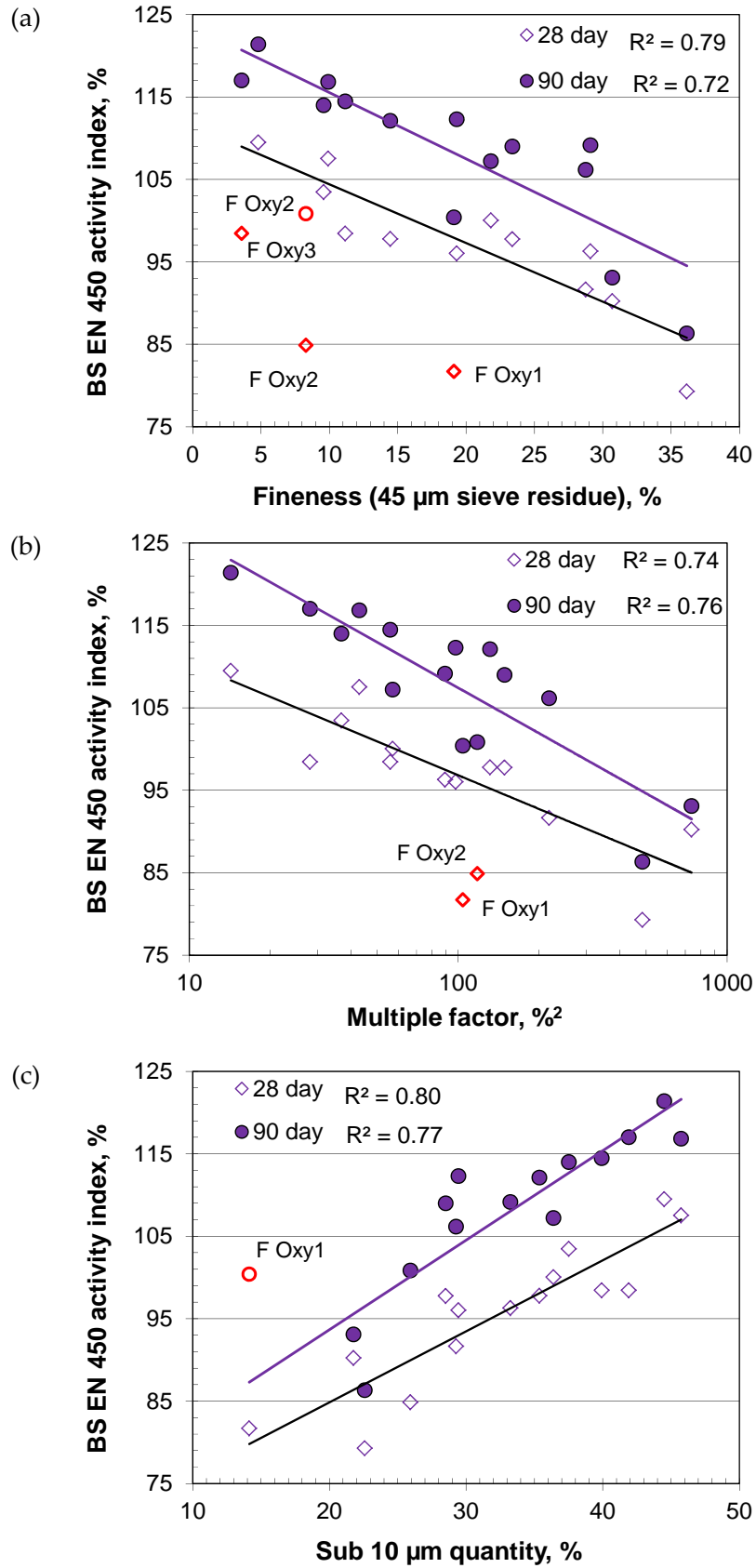


Figure 5-19. Relationships between fly ash property and BS EN 450 activity index (PC LD32): (a) 45 µm sieve residue; (b) multiple factor (45 µm sieve residue × LOI); and (c) sub-10 µm quantity of fly ash. (points in red not included in the regression analysis)

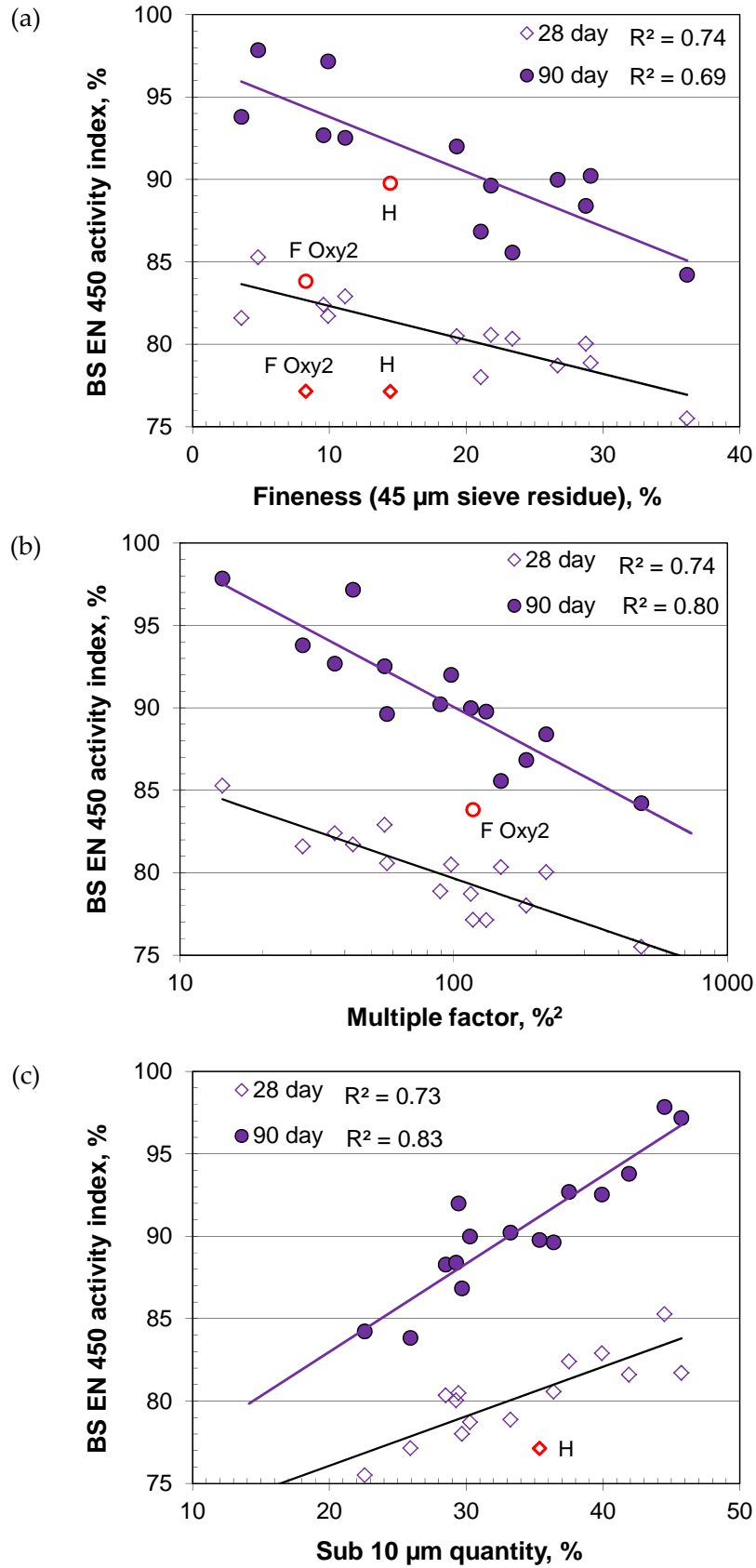


Figure 5-20. Relationships between fly ash property and BS EN 450 activity index (PC LD52): (a) 45 µm sieve residue; (b) multiple factor (45 µm sieve residue × LOI); and (c) sub-10 µm quantity of fly ash. (points in red not included in the regression analysis)

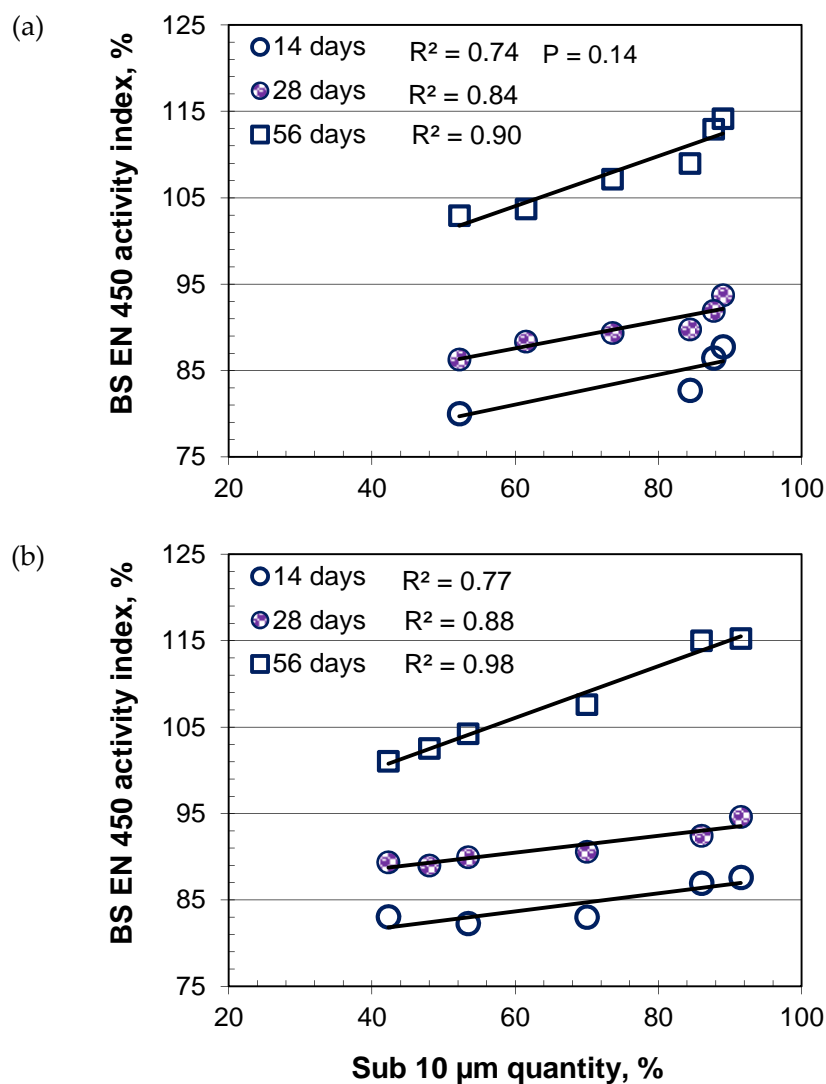


Figure 5-21. Relationships between air-classified fly ash sub 10 µm quantity and BS EN 450 activity index: (a) Source C; and (b) Source L

Figure 5-23 shows the correlation of activity index obtained with accelerated curing conditions and fly ash properties. As with the standard curing conditions, the 45 µm sieve residue, multiple factor and sub 10 µm quantity of fly ash gave a consistently good indication of reactivity, especially the sub 10 µm quantity, which tended to give better results than the other two parameters. There were a few exceptions, either associated with the processing technology (STI), or modern burning conditions (e.g. oxy-fuel).

Figure 5-24 gives relationships between the sub 10 µm quantities, multiple factor and the pozzolanic activity index of air-classified fly ashes from Source C. Very good correlations were obtained between these parameters indicating higher reactivity (PAI) for fly ashes

with high sub 10 μm quantities/low multiple factors as expected. The better correlation obtained compared to the main fly ashes (Figure 5-23) was attributed to the better control over the sample properties (chemistry, variation due to burning conditions), except fineness, as they were from the same source.

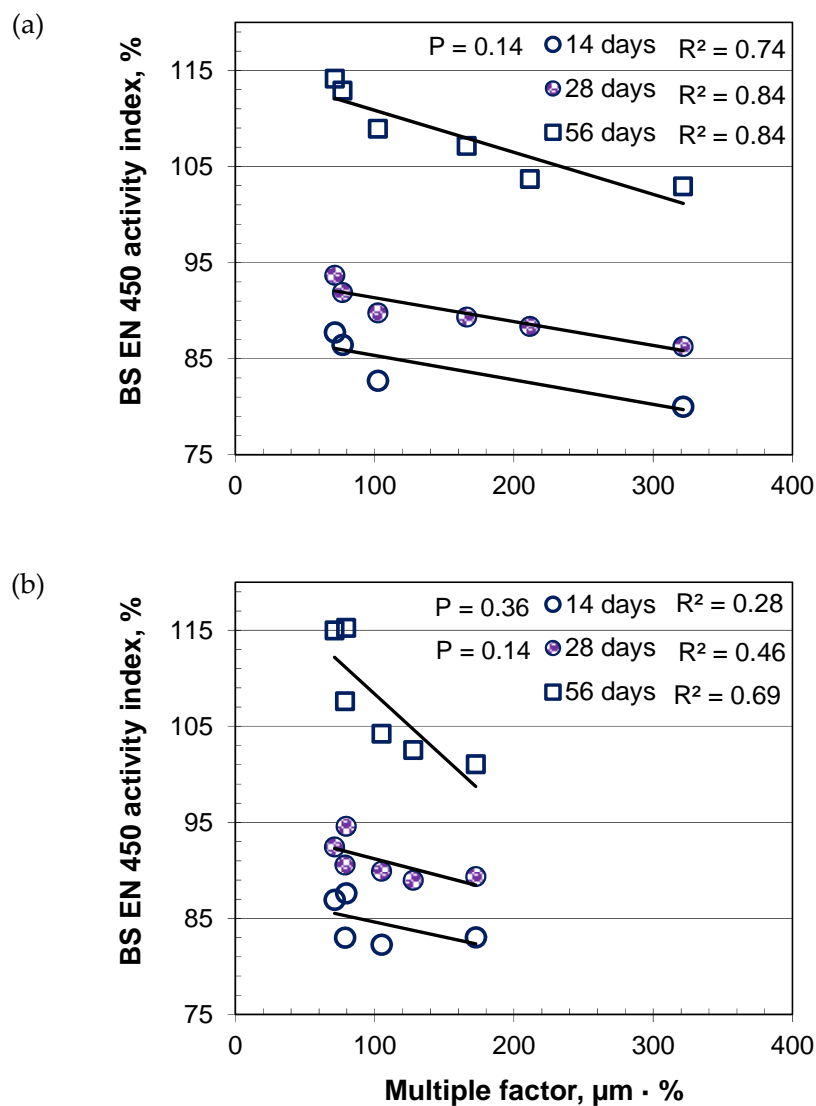


Figure 5-22. Relationships between air-classified fly ash multiple factor ($d_{90} \times \text{LOI}$) and BS EN 450 activity index: (a) Source C; and (b) Source L

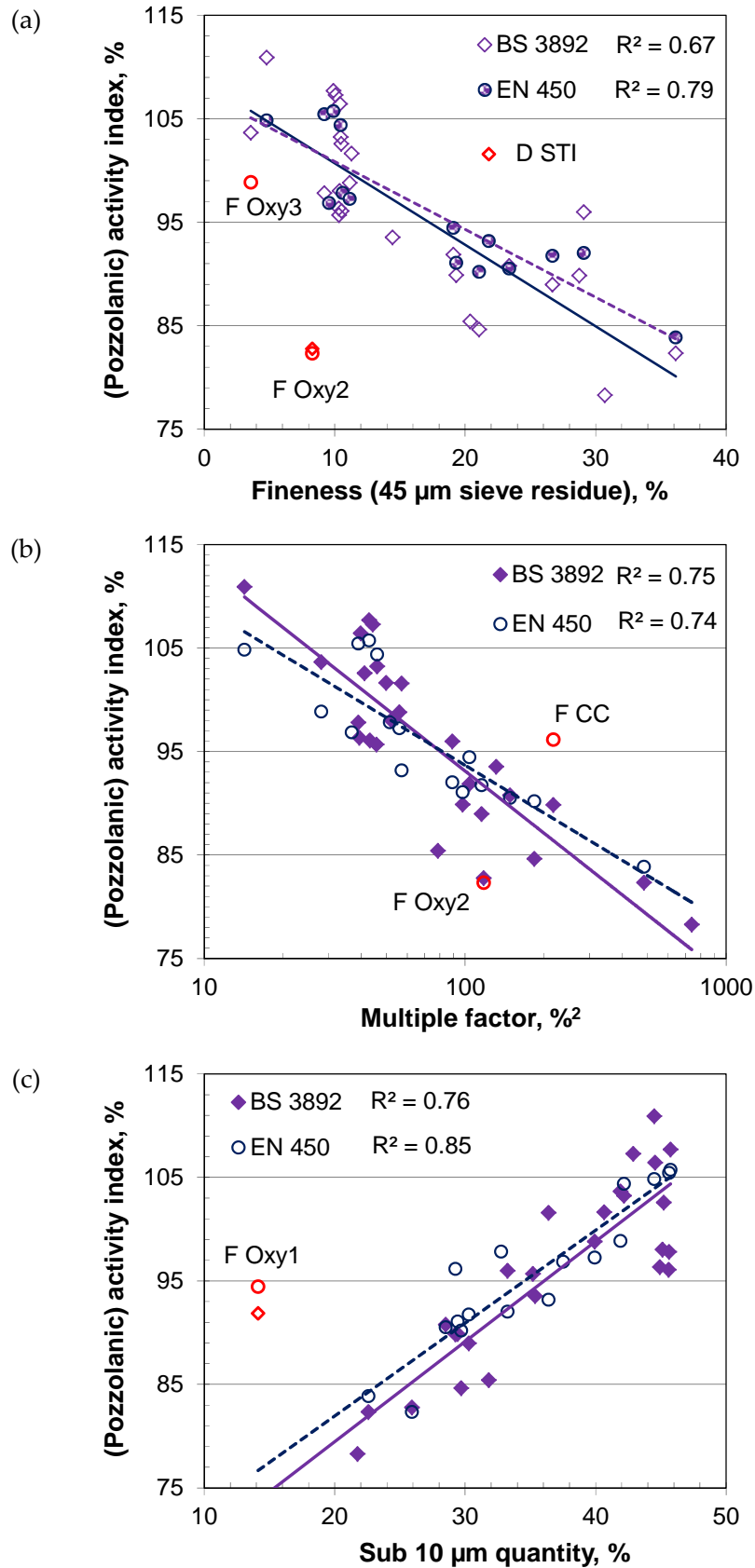


Figure 5-23. Relationships between fly ash property and (pozzolanic) activity index (PC HR52): (a) 45 μm sieve residue; (b) multiple factor (45 μm sieve residue \times LOI); and (c) sub-10 μm quantity of fly ash. (points in red not included in the regression analysis)

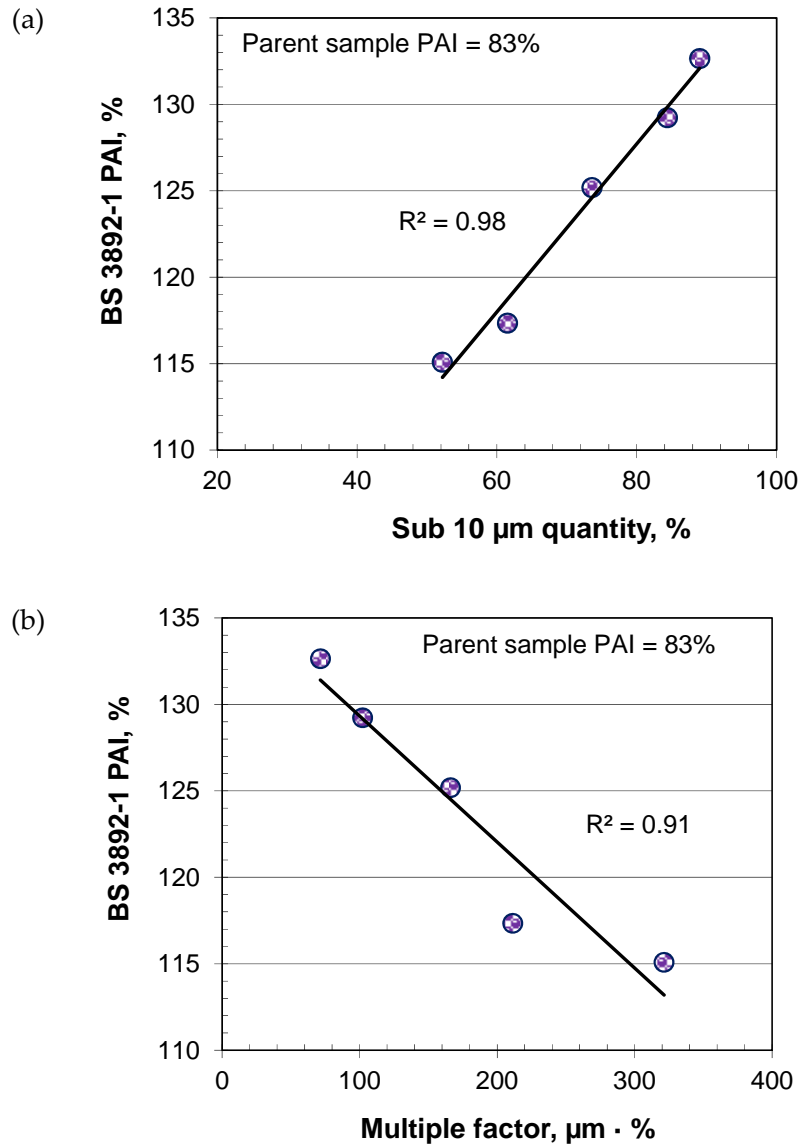


Figure 5-24. Relationships between air-classified fly ash (a) sub-10 μm quantity and (b) multiple factor ($d_{90} \times \text{LOI}$) with BS 3892-1 pozzolanic activity index

PSD analysis and activity index

Activity index is also compared with PSD in Figures 5-25 to 5-28 using cements HR52, HK42, LD32 and LD52 respectively. These follow generally expected behaviour, with finer fly ash giving greater reactivity. Comparing the 90 days activity index obtained using the different cements with d_{10} , d_{50} and d_{90} , the correlation was best with d_{50} , suggesting it has a significant influence on reactivity. The coefficients for these ranged from 0.75 - 0.89, while they were between 0.77 - 0.83 with d_{90} . These ranged from 0.75 - 0.90 and 0.66 - 0.92 with

d_{50} and d_{90} , respectively at 28 days. This suggests that the d_{90} , which represents the overall maximum particle size has a significant influence on how the material will behave in a cementitious system.

Apart from 90 days activity index with cement HK42, poor relationships were obtained between d_{10} and activity index for all cements and test ages. This suggests that d_{10} may be of limited value for assessing the reactivity of fly ash. The PSD of these fly ashes varied significantly (both at the finer and coarser ends). Therefore, a minor change in smaller size fraction due to production variation between sources influences the d_{10} significantly and therefore is not a good means of assessing fly ash reactivity.

In most cases, the relationships of d_{50} and d_{90} with activity index were improved at later ages (coefficient of correlation with activity index increased in the following order 28, 56 and 90 days). It should be noted that, in general, the oxy-fuel fly ashes were outwith the main trends. Similarly, the high LOI fly ashes C ROS and H did not always follow the effects commonly observed and were not included in the correlations. These samples are marked separately and noted in the Figures.

Figures 5-29 and 5-30 give relationships between the PSD parameters (d_{10} , d_{50} and d_{90}) and activity index of air-classified fly ashes at 14, 28 and 56 days from Sources C and L, respectively. With better controlled conditions, samples obtained from individual sources gave good correlations between their d_{10} , d_{50} and d_{90} and activity index. A slightly lower coefficient of correlation for d_{90} at Source L corresponds to the packing effect on activity index test results, as noted earlier.

As shown in Figure 5-31, activity index values obtained from accelerated curing also gave good correlations with d_{50} and d_{90} for the main fly ashes. As shown in Figure 5-32 the PSD parameters gave excellent correlations, with the air-classified fine fly ashes obtained in a more controlled way. Given the above discussions, the d_{50} and d_{90} values obtained from PSD analysis can be used to assess the likely behaviour of fly ash in cementitious systems. The estimation might be better for the samples obtained from the same source, as the feed coal and burning conditions would be similar.

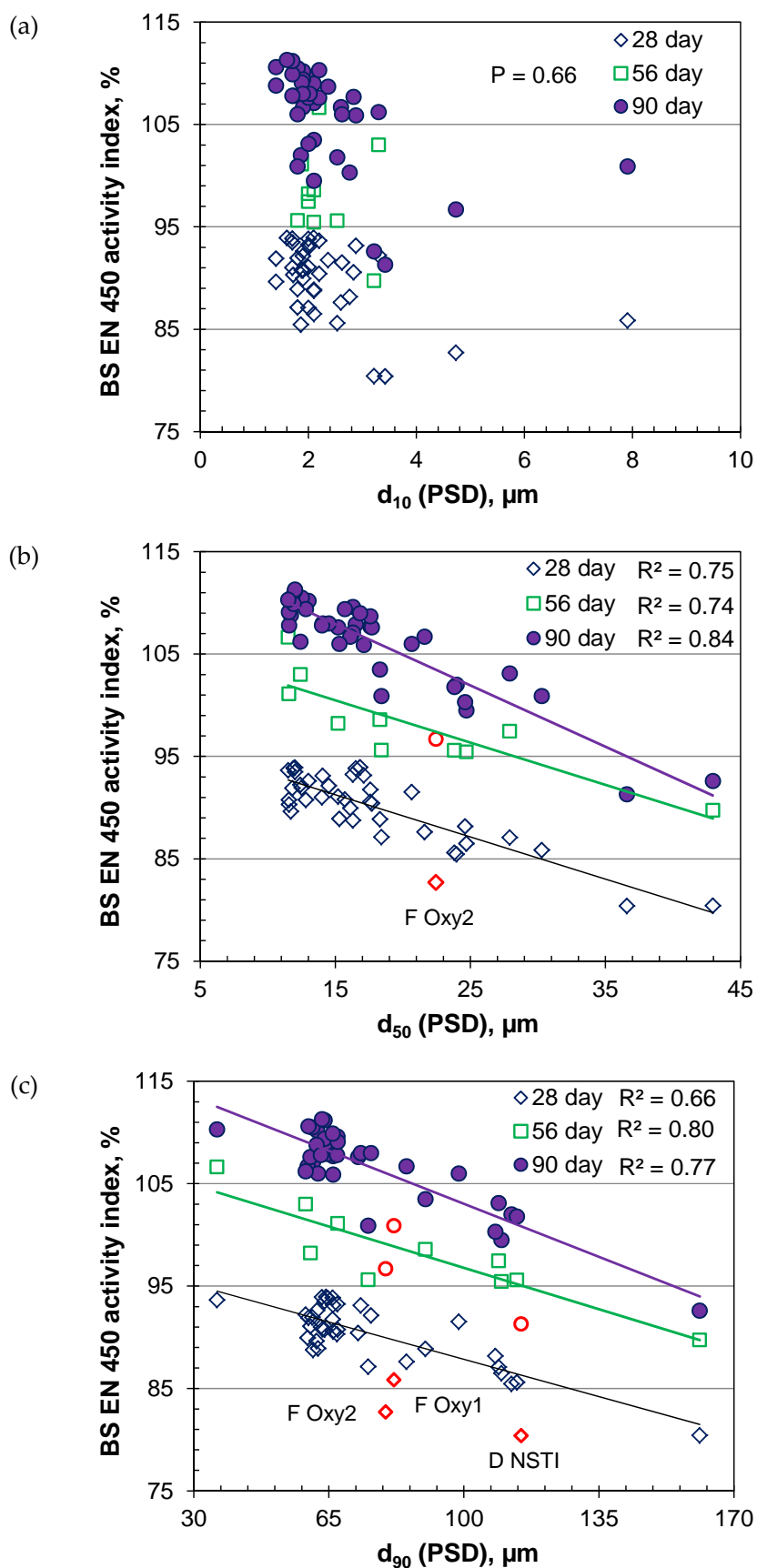


Figure 5-25. Relationships between PSD and BS EN 450 activity index (PC, HR52): (a) d_{10} ; (b) d_{50} ; and (c) d_{90} of fly ashes. (points in red not included in the regression analysis)

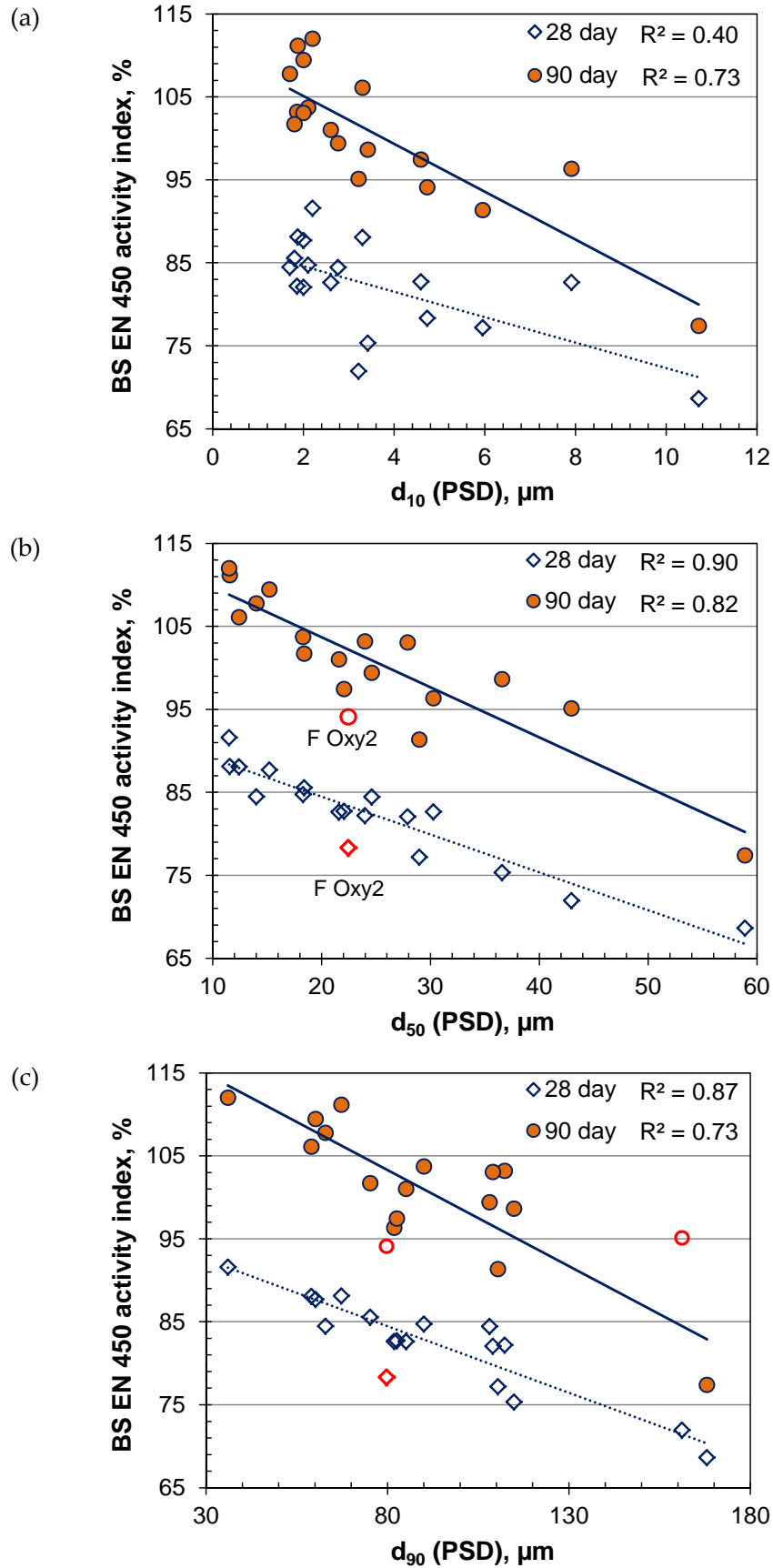


Figure 5-26. Relationships between PSD and BS EN 450 activity index (PC, HK42): (a) d_{10} ; (b) d_{50} ; and (c) d_{90} of fly ashes. (points in red not included in the regression analysis)

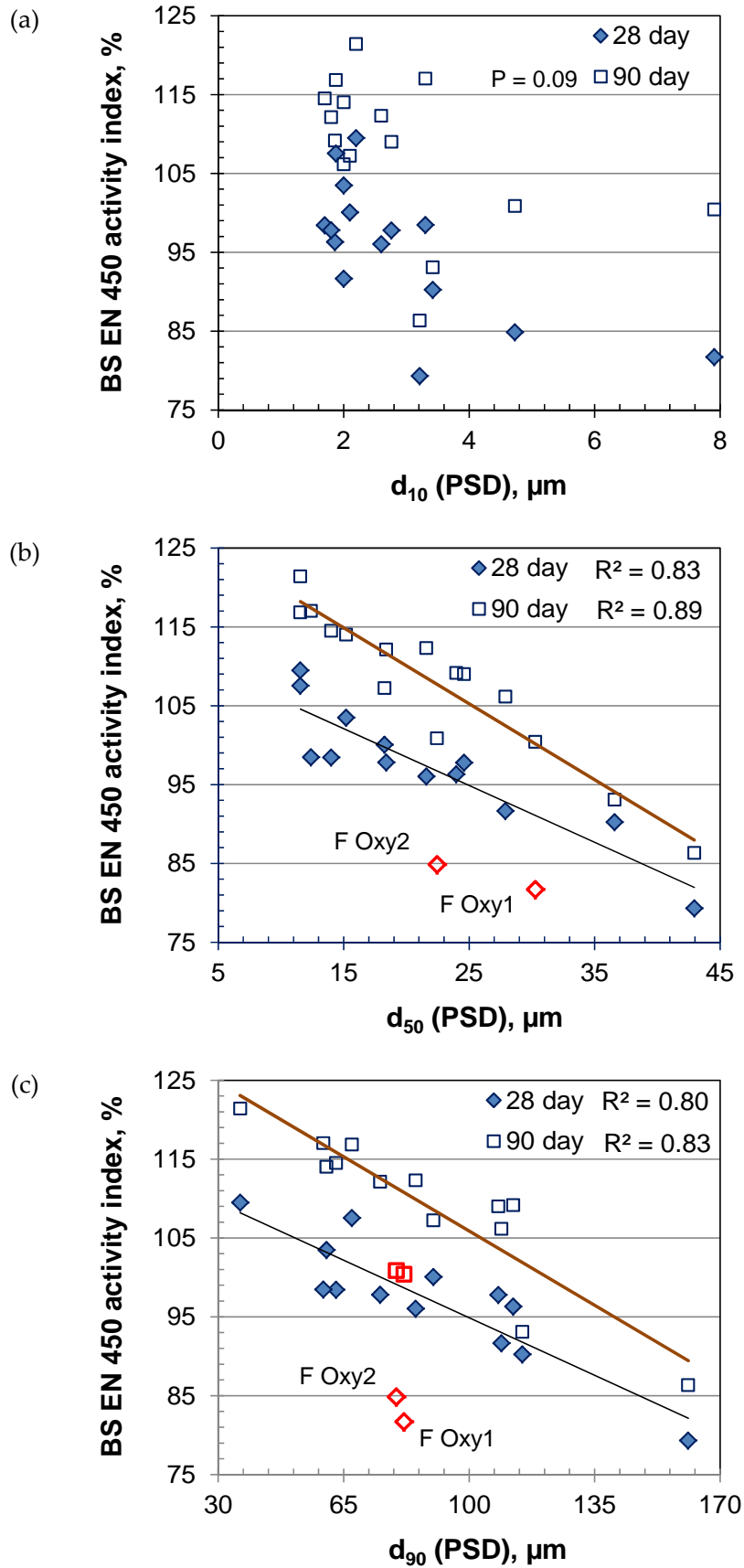


Figure 5-27. Relationships between PSD and BS EN 450 activity index (PC, LD32): (a) d_{10} ; (b) d_{50} ; and (c) d_{90} of fly ashes. (points in red not included in the regression analysis)

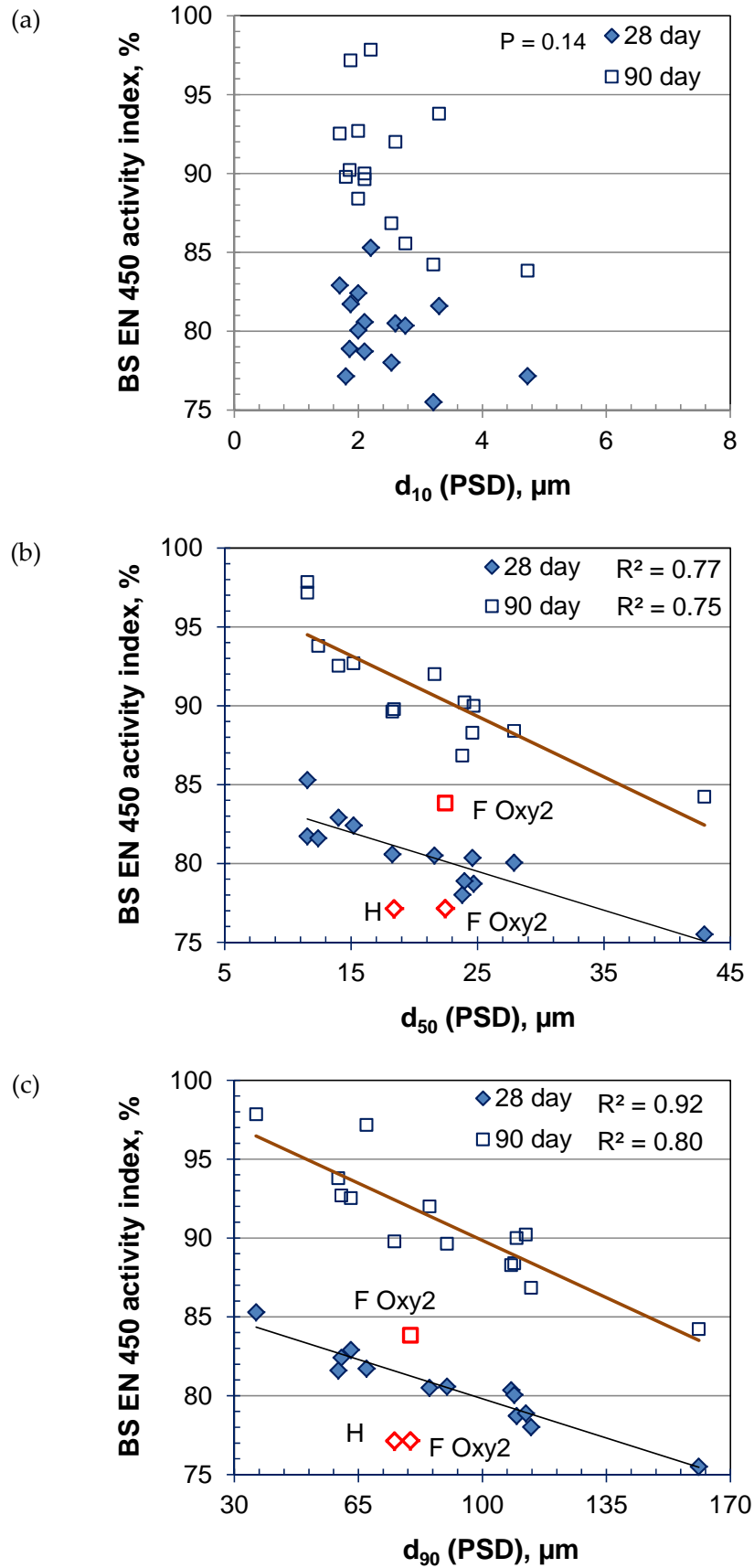


Figure 5-28. Relationships between PSD and BS EN 450 activity index (PC, LD52): (a) d_{10} ; (b) d_{50} ; and (c) d_{90} of fly ashes. (points in red not included in the regression analysis)

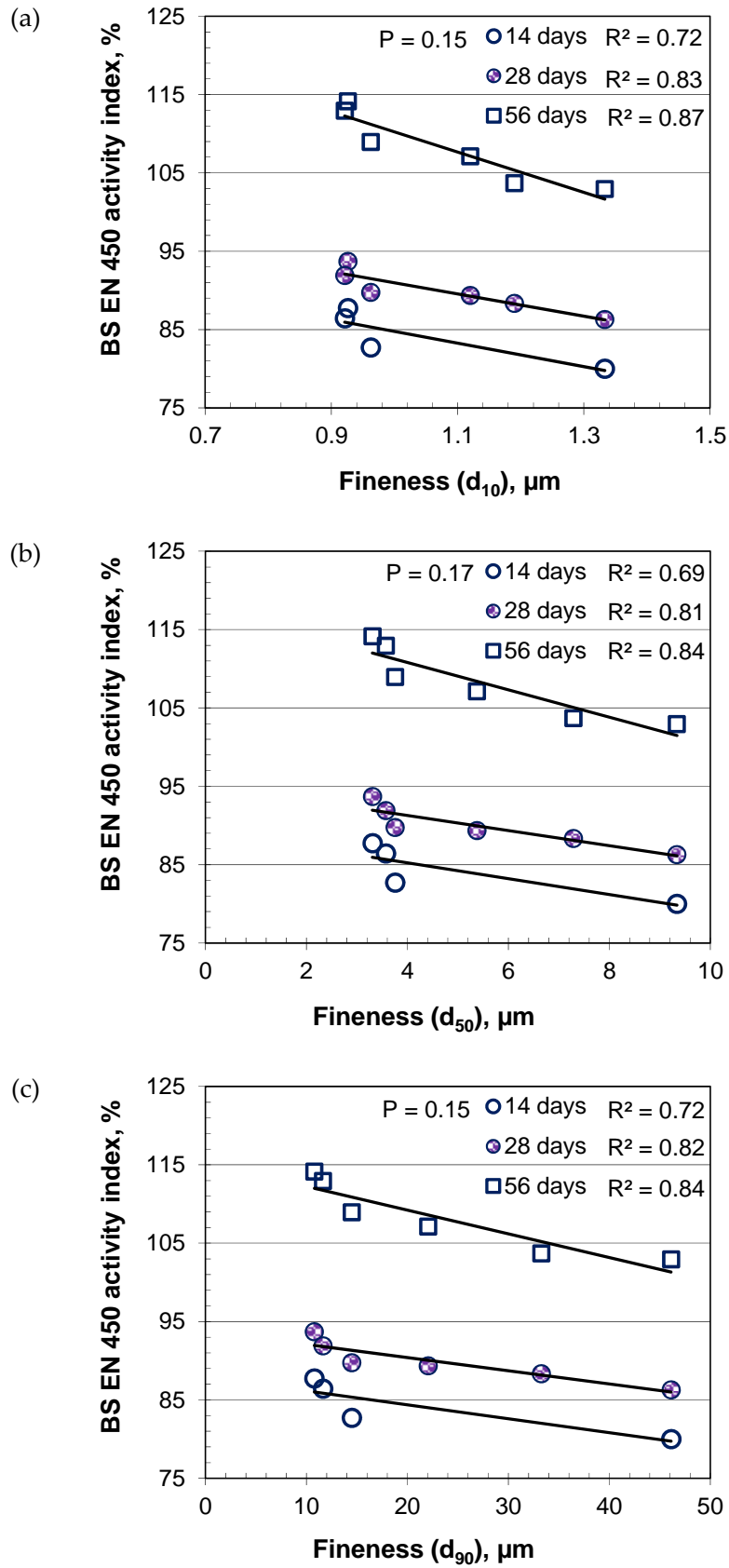


Figure 5-29. Relationships between PSD and BS EN 450 activity index. Air-classified fly ash from Source C: (a) d_{10} ; (b) d_{50} ; and (c) d_{90}

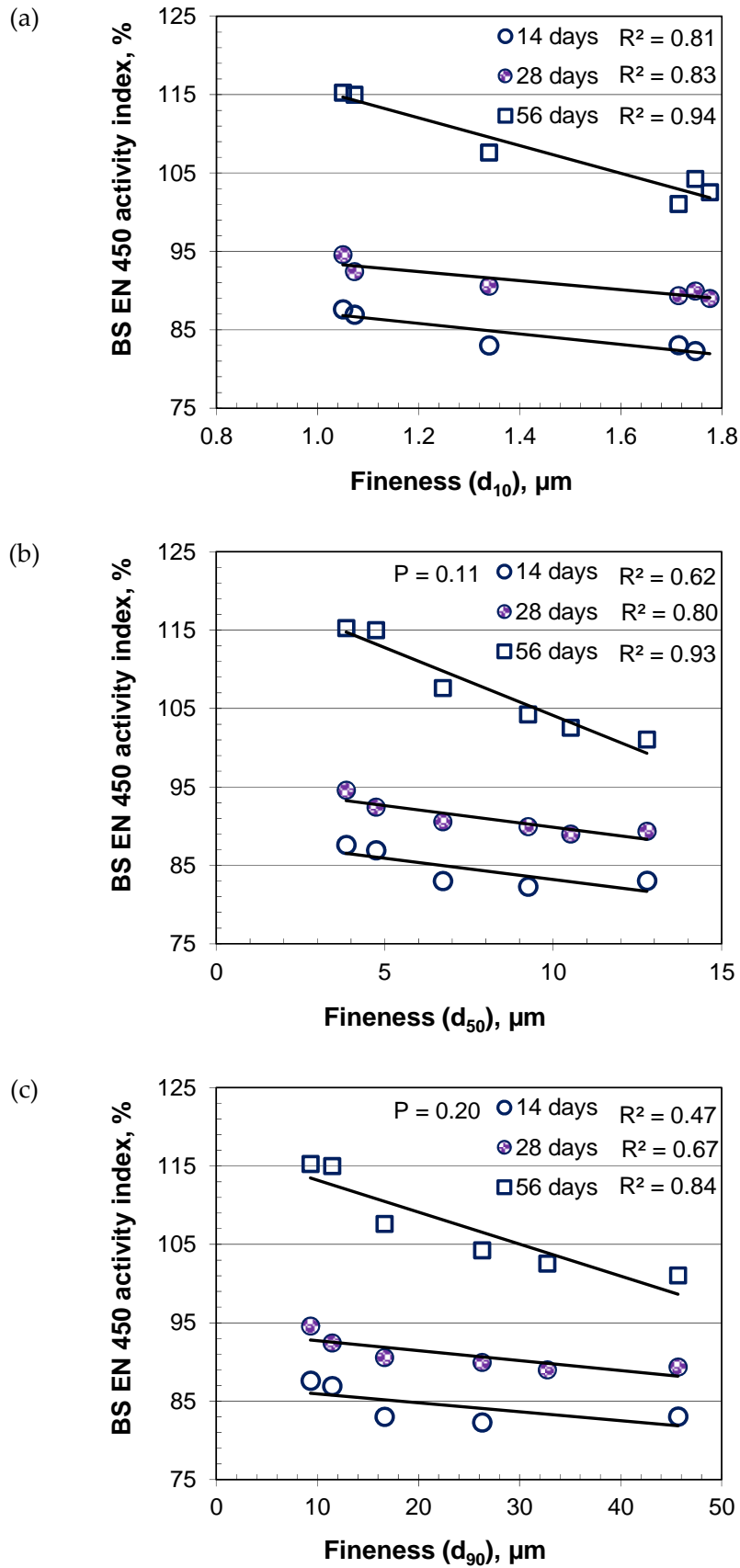


Figure 5-30. Relationships between PSD and BS EN 450 activity index. Air-classified fly ash from Source L: (a) d_{10} ; (b) d_{50} ; and (c) d_{90}

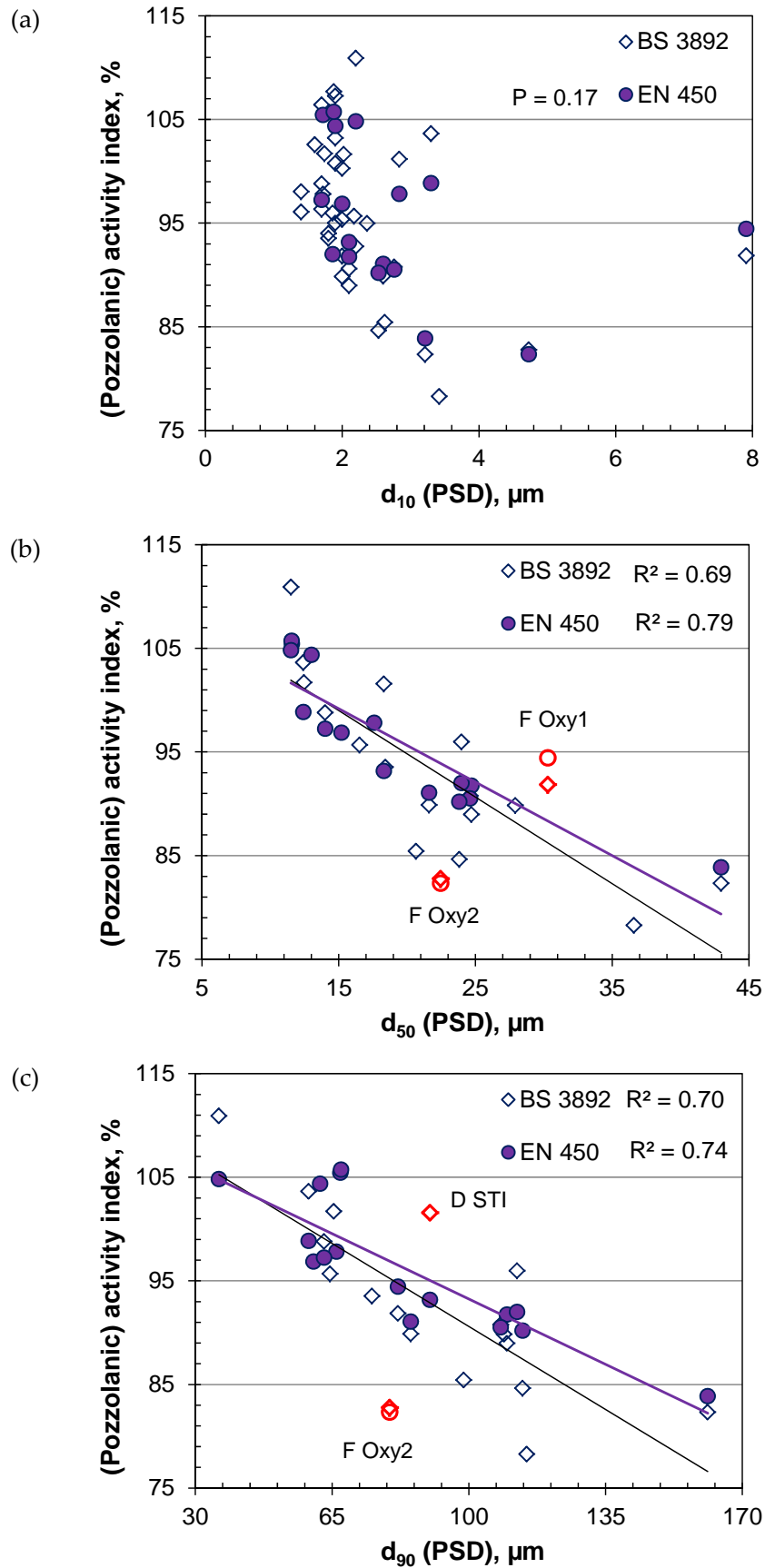


Figure 5-31. Relationships between PSD and accelerated activity index (PC, HR52): (a) d_{10} ; (b) d_{50} ; and (c) d_{90} of fly ashes. (points in red not included in the regression analysis)

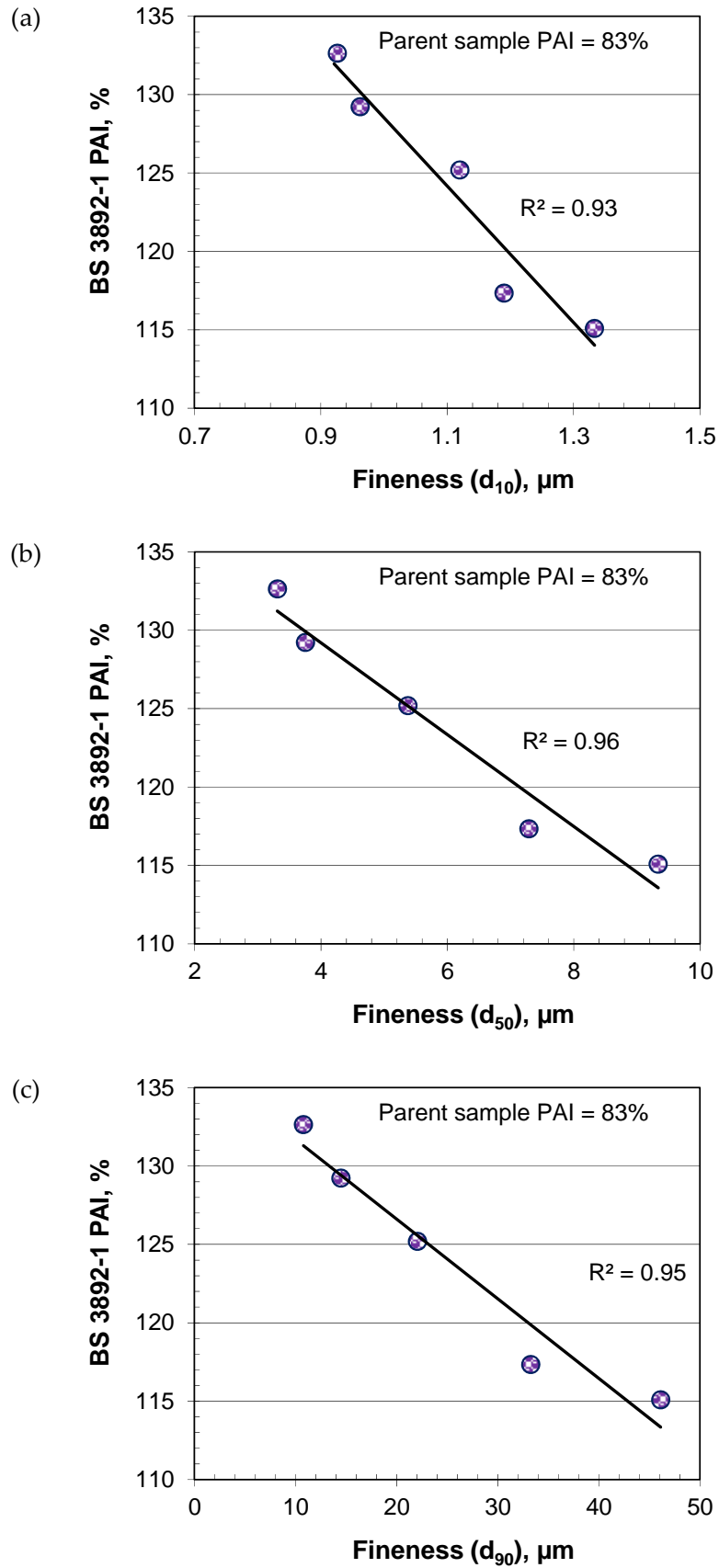


Figure 5-32. Relationships between PSD and BS 3892-1 pozzolanic activity index. Air-classified fly ash from Source C: (a) d_{10} ; (b) d_{50} ; and (c) d_{90}

5.2.3 Effect of finest fly ash level in mortar

As noted in the earlier discussion the fine component of fly ash (C5 and L5) gave very good reactivity, but their flow was very similar to that of the PC. Those mortar tests were with a constant fly ash level of 25% as per BS EN 450 (BSI, 2005c). To determine where the optimum replacement level, further mortar tests were carried out with the finest component C5 (Source C) using different levels (10, 15, 20, 25 and 30). The water content (225 ml) remained the same for each mix (i.e. w/c ratio was fixed).

As shown in Figure 5-33, with an increase in fly ash level, flow increased up to the 20% level and then decreased again. It appears that up to 20%, the 225 ml water was sufficient and in addition to the ball-bearing effect, the flow increased. However, with further increases in fly ash level, the proportion of the finest part in the matrix increased and flow decreased. This may also be caused from the grading effect, as noted earlier. Therefore, the 20% fly ash level appeared to be optimum in terms of water requirement and grading for utilizing fly ashes' ball-bearing effect, to achieve greatest flow with fine fly ash and thereby expected to give better packing.

The above mortar samples were tested at 28 days as it was noted earlier that with Fly Ash C5, it is possible to obtain meaningful results at this age. As shown in Figure 5-34, highest activity index was obtained at the 10% fly ash level at 28 days. An 11% increase in mortar strength was noted from the control at this level. The 20% level of fly ash gave the same mortar strength as the control. With further increases in fly ash level a 6% decrease in compressive strength was noted for both 25% and 30% fly ash level.

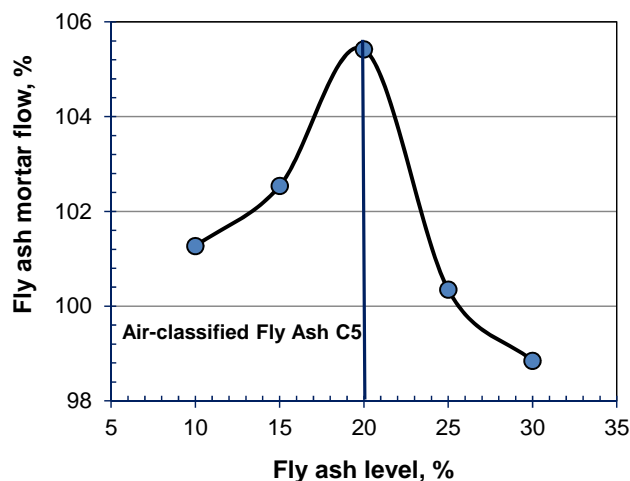


Figure 5-33. Effect of fly ash level on fresh properties of air-classified material

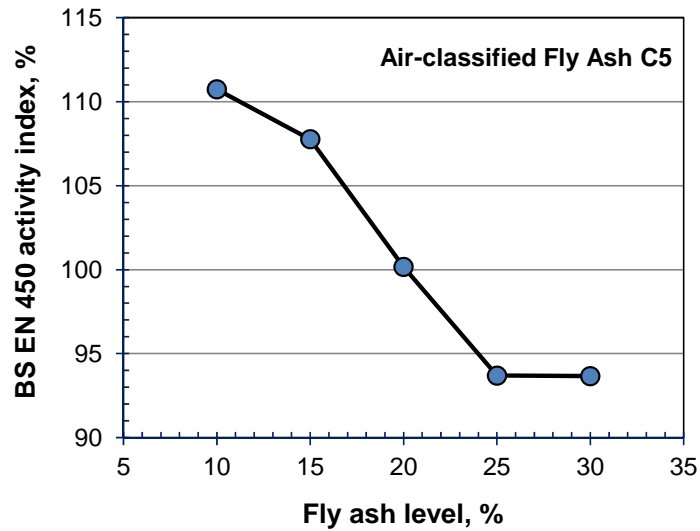


Figure 5-34. Effect of replacement level on strength (reactivity) of air-classified fly ash

Fly ash levels beyond 30% were not tested as a decrease (compared to the control PC mortar) in flow was noted at a fly ash level higher than 25%. In the study by Paya *et al.* (1995) a 20% decrease (with respect to the reference PC test) at 28 days mortar compressive strength was noted when fly ash level increased from 15% to 45%. Based on these results, it is suggested that with ultrafine fly ash, a 20% replacement level would give maximum flow and similar strength to PC mortar at 28 days. However, at later age, the activity index pattern is expected to change for the 25 and 30% fly ash level. It is likely that at higher fly ash levels (e.g. 25 and 30%), greater long-term strength development would be expected as noted in McCarthy and Dhir (2005).

5.2.4 Accelerated curing

An attempt was made to correlate the activity index following accelerated curing ($20 \pm 1^\circ\text{C}$ for the first day, and then water curing at $20 \pm 1^\circ\text{C}$ for 4 days, followed by $50 \pm 1^\circ\text{C}$ for 46 hours, and finally $20 \pm 1^\circ\text{C}$ for 2 hours) with that of 28, 56 and 90 day standard water curing. All tests were carried out using cement HR52. As shown in Figure 5-35, the activity index from accelerated curing (7 day test) and 28 day activity index (standard curing) gave similar results for the very high LOI/coarse fly ashes, however, increases of up to ~15% in activity index were noted with accelerated curing for fine fly ashes. These indicate significant effects of high temperature curing on the finer fly ashes.

The activity indices were similar at 56 days, with the accelerated test results greater by 90 days. Generally, good correlations were obtained between accelerated and standard curing activity index values at 28 ($R^2 = 0.73$), 56 ($R^2 = 0.82$) and 90 days ($R^2 = 0.85$). As noted earlier, the correlations were improved with longer-term standard curing.

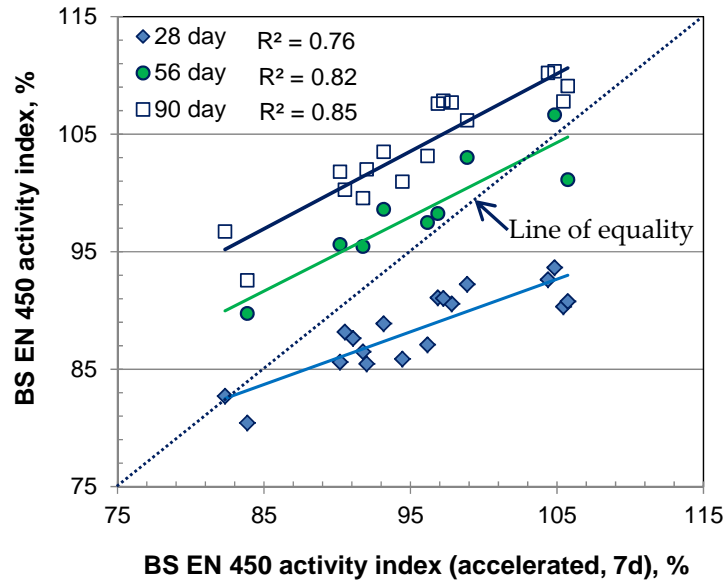


Figure 5-35. Relationships between BS EN 450 activity index (accelerated) and standard curing conditions (PC HR52)

The results obtained with air-classified fly ashes (Source C) following BS 3892-1: 1982 (accelerated curing and water adjustment; fly ash level 30%) and BS EN 450 (BSI, 2005c; standard curing and the same water content; fly ash level 25%) are plotted in Figure 5-36. A very good correlation between the accelerated curing and longer standard curing conditions was achieved. The improved relationships, compared to the main fly ashes discussed above, are again attributed to the control in sample production and that they were obtained from the same source (air-classified from Source C).

As with the main fly ashes discussed above, the activity index of the feed sample CFD was comparable between 7 days (accelerated) and 28 days (standard) curing, however, the finest component C5 gave ~38% higher activity index than the feed sample following accelerated curing, though the level of fly ash in accelerated curing was 30%.

The accelerated test results suggest this could potentially be applied to estimate long-term reactivity following standard curing conditions. However, the fly ash response to heat is

different from that of standard curing condition and depends on its properties. Therefore, both fly ash fineness and accelerated conditions should be considered together to apply this approach. Limited test were conducted to match curing ages (at different temperatures) with selected fly ashes, and are discussed in the following section.

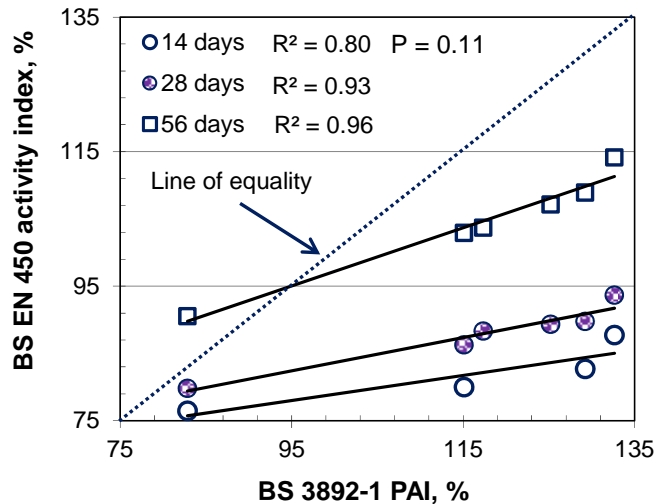


Figure 5-36. Relationships between BS 3892-1 pozzolanic activity index (accelerated) and BS EN 450 activity index at various ages

Maturity calculation using Sadgrove equation

It was noted in previous section that the behaviour of fly ash mortar under heat treatment depends on the properties of fly ash. The Sadgrove equation gives the equivalent curing age at 20°C to that of high temperature curing of PC concrete (Sadgrove, 1975). The intention of this part of the study was to check whether this equation can be used for fly ash-based mortar. The equation for PC concrete is as follows:

$$\text{Equivalent age at } 20^{\circ}\text{C} = \sum \left(\frac{\theta + 16}{36} \right)^2 \quad (\text{Eq. 5-1})$$

Where, θ is the curing temperature and the equation is valid for PC 42.5 and 52.5 concrete in the temperature range 1 to 45°C from 5 hour to 28 day (Harrison, 1995).

For this test, Fly ashes C S Jan and F CC were used. Mortar samples were cured following BS 3892-1 (BSI, 1982) for the first 5 days, and then high temperature curing at 50°C was

carried out for a further 2, 4, 6, 8 and 10 days. Then the results obtained by standard curing (20°C) until 180 days were compared with this.

Figure 5-37 (top) shows the compressive strength development in fly ash mortar from standard and high temperature curing. The slope of the strength gain curve at high temperature was found to be much steeper than for the standard curing conditions. The power of the Sadgrove equation was set to 3.75 by trial and error to match the slopes and the equivalent age recalculated. This gave a similar slope at both high temperature and standard curing for the fly ashes under consideration. Therefore, with an equation similar to that given in Figure 5-37, it may be possible to estimate fly ash mortar compressive strength, considering the curing conditions and other properties of fly ash. However, this was only considered for a limited number of fly ashes and represents an area where further work would be required.

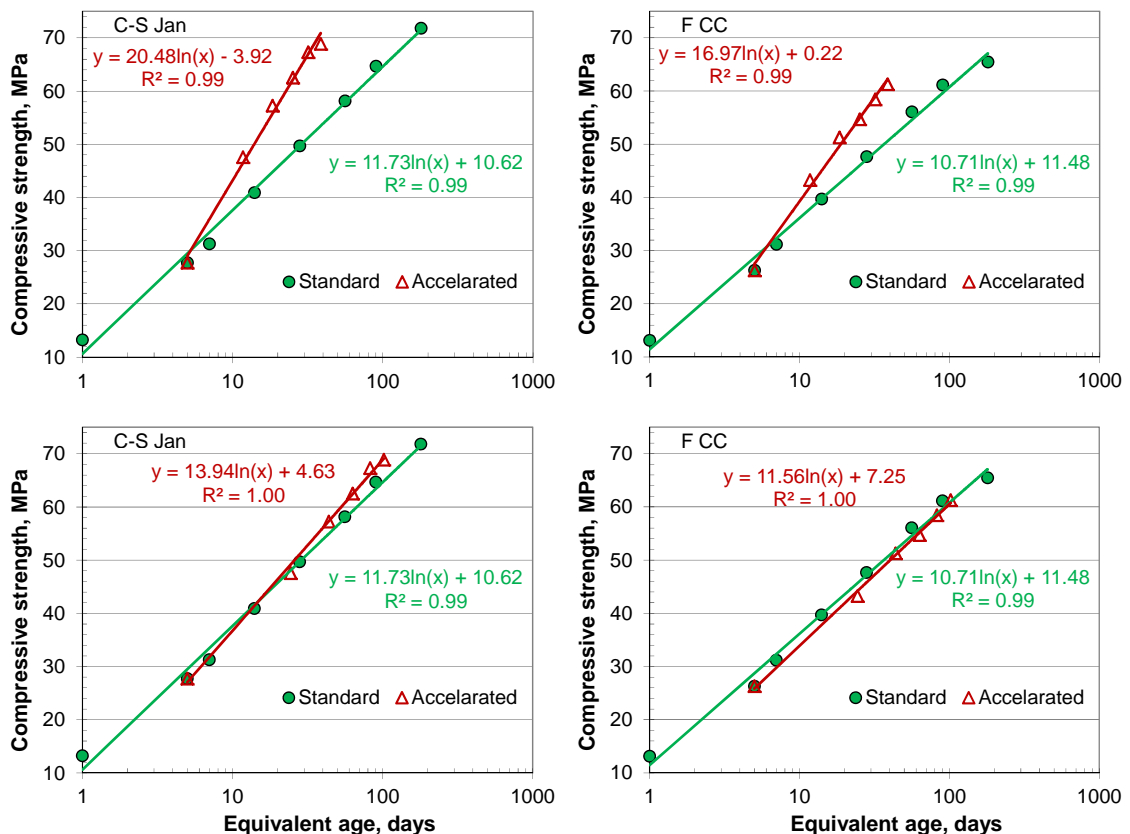


Figure 5-37. Compressive strength development at equivalent ages, calculated using Sadgrove equation (top); and modified Sadgrove equation (bottom)

5.3 Porosity of PC-Based Mortars by MIP

Selected mortar samples prepared with air-classified fly ashes from Source C and L were tested for porosity at 14 days. Figure 5-38 makes a comparison between cumulative intrusions of mercury in the fly ash mortar samples. As the tests were carried out at a relatively early age, this was most likely to reflect packing effects rather than pozzolanicity, unless the fly ash is very reactive (Tangpagasit *et al.*, 2005).

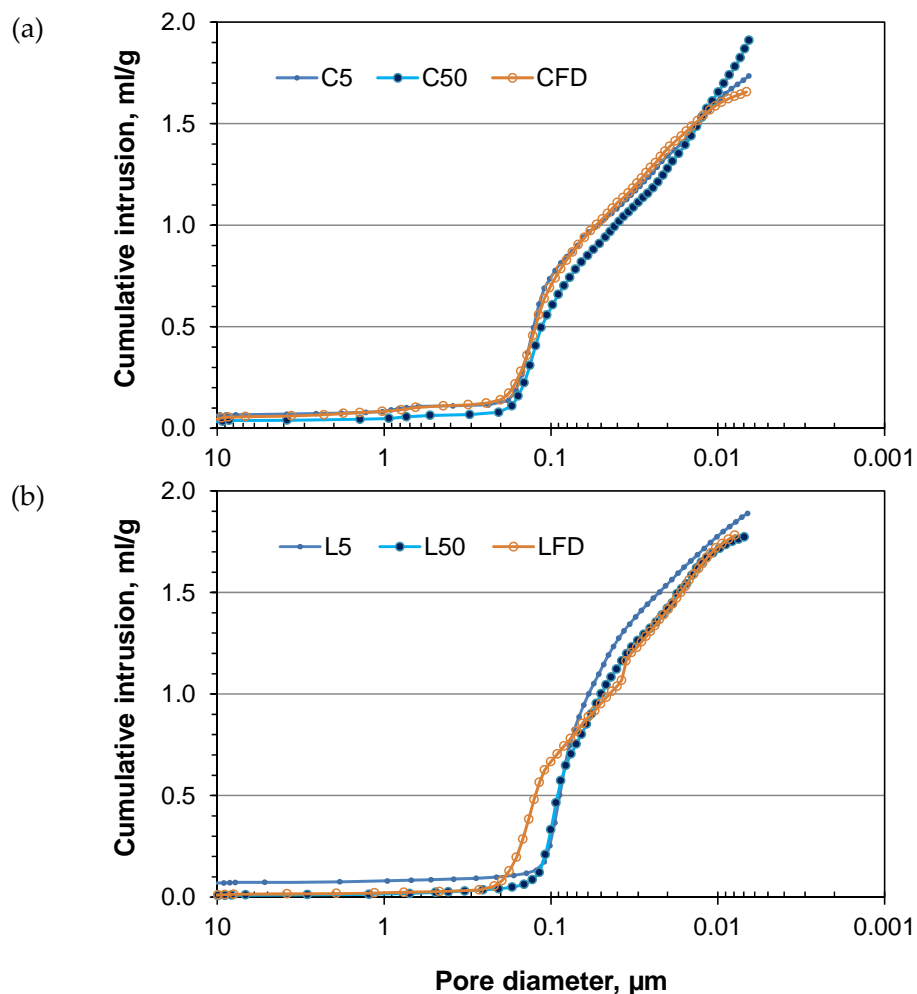


Figure 5-38. Porosity of air-classified fly ash mortars: (a) Source C and (b) Source L

As shown in Figure 5-38 the pore distribution of Fly Ash C50 and L50 were comparatively finer than their parent feed samples (CFD and LFD) and the finest fractions (C5 and L5). This observation agrees with the flow of the corresponding mortar. As shown earlier in Figure 5-12, with same water content Fly Ashes C50 and L50 gave the highest flow in their respective group and, therefore, were expected to give better packing.

The study by Tangpagasit *et al.* (2005) indicated no change in activity index by packing, while the particle size of PC (mean size = 11 μm) and accompanying materials were comparable in mortar. However, up to a 12% decrease in strength was noted by using a 200 μm mean size PC replacing inert material. Results from the current study indicate that packing of both finest (d_{90} of C5 = 10.8 μm and L5 = 9.3 μm) and coarse run-of-station (d_{90} of CFD = 120.0 μm and LFD = 115.9 μm) fly ashes were affected and gave relatively higher porosity, which may be caused by their differences in grading compared to the test PC (d_{90} = 36.6 μm). It also appeared that the fly ashes (d_{90} for C40, C50, L40 and L50 are 33.3, 32.7, 46.1 and 45.7 μm , respectively) with similar grading to the test PC (see Figure 4-5) gave best performance in terms of flow and, therefore, packing.

5.4 Hydrated Lime Mortar

The ASTM C493 test method is used to determine the suitability of fly ash for use in soil stabilization with lime. In accordance with the standard, 50 mm lime mortar cubes should have a compressive strength of at least 4.1 MPa after 7 days curing under the specified high temperature and humidity conditions. Laboratory grade hydrated lime was used for preparation of fly ash lime mortars following the ASTM C593 (ASTM, 2011b) standard, to investigate whether this could provide a means of assessing reactivity of fly ash by reducing the possible test variability due to variations in PC properties. Initially, using local sand, the test method did not give promising results. Therefore, ASTM standard sand was obtained from the USA for inclusion in the work. Using sealed high humidity and temperature conditions, and the ASTM standard sand, Fly Ash E UF and F CC were tested to assess feasibility of the test.

After mixing the mortar samples, flow test was carried out and if they satisfied the target flow range, the material was placed in cube mould and then compacted using the vibrating table. The compacted material with mould was placed in a sealed container. A small quantity of water was placed in the container beforehand and the mould was placed on a spacer as described in Section 3.3.3, and the container then located inside an oven, set to a constant temperature of $54 \pm 2^\circ\text{C}$. After specific periods of high temperature and moisture curing, the samples were tested for compressive strength.

The w/c ratios to maintain the same flow with Fly Ash E UF and F CC were 0.49 and 0.52, respectively, while their compressive strengths (at 7 days) were 6.6 and 5.7 MPa, respectively. This was promising considering the low LOI and 45 μm sieve retention Fly Ash E UF gave lower water demand and higher strength compared to Fly Ash F CC.

A further 5 fly ash samples (C S Jan, D STI, D NSTI, E UF and F CC) were then tested without water adjustment ($w/(fa+l) = 0.5$) and cured for a period of 7 days, to check if a test comparable with BS EN 450 (BSI, 2005c) could be developed by modifying the original ASTM C593 (ASTM, 2011b) procedure. The consistency of lime mortars varied between the fly ashes, as it does in the activity index test. Finer/low LOI fly ashes gave higher consistency and were easier to compact. In contrast, the opposite was experienced with coarse and high LOI fly ashes, which resulted in poor compaction in some cases (very high LOI Fly Ash D NSTI).

In general, finer/lower LOI fly ash gave higher strength; however, there were minor differences in cube compressive strength between the four fly ashes after 7 days (results not presented), while Fly Ash D NSTI gave significantly lower compressive strength, probably because of its poor compaction. This suggests that the test conditions followed (i.e. use of fixed water content for all fly ash) were not suitable to assess the difference in reactivity of fly ashes and could be affected by the degree of packing. It was concluded that the use of a longer time with the specified temperature of $54 \pm 2^\circ\text{C}$, or a higher temperature could allow fly ash behaviour to be more clearly observed. It was noted that the ASTM C1240 (ASTM, 2011c) test for pozzolanicity determination of silica fume uses $65 \pm 2^\circ\text{C}$ for 6 days and is based on a strength test with PC.

From these initial findings, it was decided to carry out further tests, with modification to the original test procedure. The main changes included i) the use of CEN standard sand instead of ASTM graded sand; ii) flow measurements following BS EN 1015 – 3; and iii) a change in curing temperature and duration. To fix a suitable combination of temperature and test period, an initial series of tests was carried out using fly ash C S Jan at $50 \pm 2^\circ\text{C}$ and $65 \pm 2^\circ\text{C}$ for test periods of 7, 14 and 28 days. The mix proportions of the hydrated lime mortar samples are given in Table 5-7. As shown in Figure 5-39, initially at 7 days and $65 \pm 2^\circ\text{C}$, higher strength was obtained compared to that at $50 \pm 2^\circ\text{C}$. However, the

opposite behaviour was observed at 14 and 28 days. The strength values at $50 \pm 2^\circ\text{C}$ were higher by approximately 15 and 25% respectively than at $65 \pm 2^\circ\text{C}$. Therefore, further tests were carried out at $50 \pm 2^\circ\text{C}$, mainly at 14 and 28 days, with a wider range of fly ashes. Selective samples were also tested at 56 days.

Table 5-7. Mix proportions of hydrated lime mortar

MATERIALS	QUANTITY	SOURCE/TYPE
Hydrated lime, g	150	Lab supplier
Fly ash, g	300	-
Standard sand, g	1350	CEN
Free water, ml	to achieve flow of 215 ± 5 mm (BS EN 1015 – 3)	

Note: Quantity for 2 No. 75 mm cubes or 6 No. 50 mm cubes

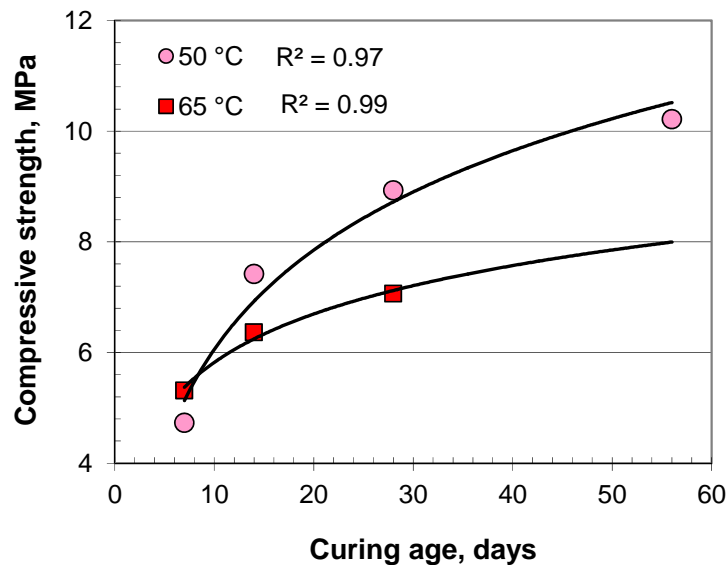


Figure 5-39. Effect of curing temperature and age on compressive strength of hydrated lime mortar (fly ash C S Jan and 50 mm cube)

Trials were required to adjust the water content to achieve similar flow values. Figure 5-40 shows the change in flow values with water content for selected fly ashes. As expected, coarse/high LOI fly ashes demanded considerably higher water to achieve the target flow. Table 5-8 and Figure 5-41 give the compressive strength of hydrated lime mortar at different test ages. It should be noted that both 50 and 75 mm cubes were used for compression testing and minor variation in the results were noted due to specimen size.

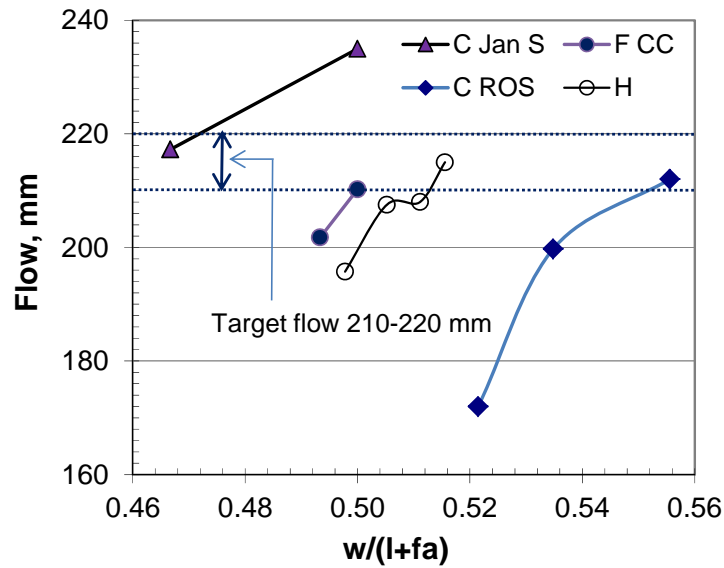


Figure 5-40. Water content adjustment for different fly ashes

Table 5-8. Compressive strength (MPa) of hydrated lime mortar cubes

SAMPLE	14 DAYS	28 DAYS	56 DAYS
A-S Jan	6.1	-	-
A-N Jul	6.5	7.4	8.7
C-S Jan	7.4	8.9	10.2
C LLHF	5.1	6.3	7.2
C ROS	5.9	7.5	-
D STI	7.1	9.4	-
E UF	7.1	9.8	-
F CC	5.8	6.2	7.4
F Oxy3	7.7	-	-
H	6.7	7.6	-

Note: 14 day strength using 75 mm cubes; 28 and 56 day tests using 50 mm cubes

Tests carried out at 14 days were with 75 mm cubes, while 50 mm cubes were used at 28 and 56 days. At 28 days tests, Fly Ash E UF gave highest compressive strength of the 10 materials assessed, which was expected given its fineness (finest). Although with the same water content Fly Ash D STI did not give expected strength with PC, given its lower LOI values, it showed considerable reactivity with hydrated lime. This may be due to the effect of water adjustment and thereby greater level of packing. The coarse/high LOI fly

ashes (C ROS and F CC) on the other hand, gave considerably lower strengths. The Fly Ash C LLHF gave unusual behaviour, with very low strength given its fineness and LOI values.

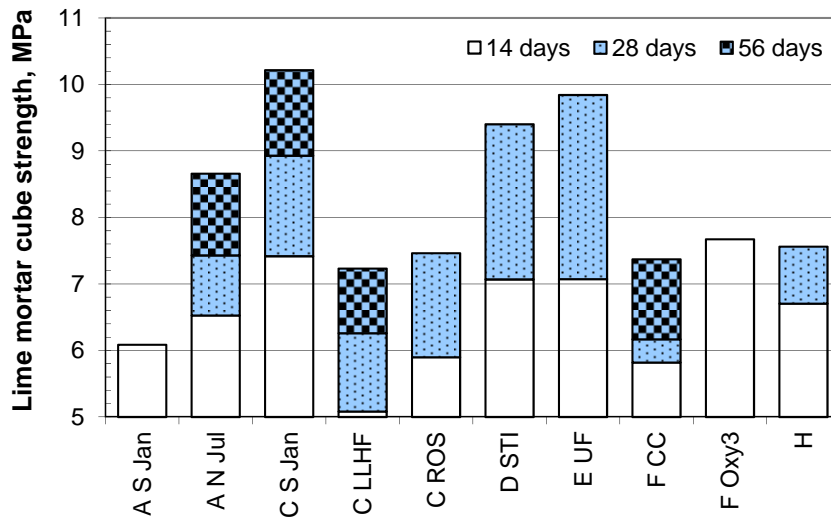


Figure 5-41. Strength development in lime mortar (at 50°C high humidity curing)

As shown in Figure 5-42, inverse relationships were obtained between water demand and compressive strength at both 14 and 28 days. However, the correlation was not strong, as found for tests with PC-based mortar. Therefore, water demand tests with hydrated lime might give misleading results. Although the mean particle size of hydrated lime (10.3 μm) was comparable with the test PC (13.3 μm) as shown in Figure 4-26, their PSDs were different which may affect flow properties of the mix.

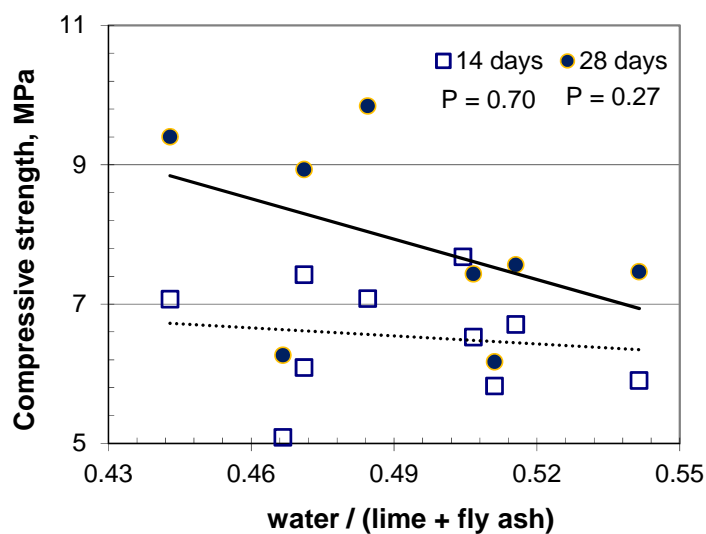


Figure 5-42. Effect of water content on compressive strength of hydrated lime mortar

Figure 5-43 shows relationships between the physical properties of fly ash and compressive strength of hydrated lime mortar at 14 and 28 days. In each case, the correlation was better at 28 days, in particular with 45 μm sieve residue and the multiple factor, with a few exceptions. The latter in this analysis were either fly ash with very high LOI (e.g. C ROS) or with very low LOI, but considerably higher 45 μm sieve retention (e.g. D STI and C LLHF).

The 56 days compressive strength of the 4 fly ash samples are plotted against their 45 μm sieve retentions and sub 10 μm quantities in Figure 5-44. The coefficient of correlation between the compressive strength and 45 μm sieve retention was found to be 1.00. A good correlation between the sub 10 μm quantity and compressive strength at 56 days was also obtained. This again indicates the influence of fly ash fineness on its reactivity, as found earlier with PC-based mortar tests (Section 5.2). Another possible factor that could influence the water requirement is that with PC-based mortar the fly ash level was 30%, while in the hydrated lime mortar test, the lime : fly ash ratio was 1 : 2.

The compressive strength values obtained at 14 and 28 days were compared with the pozzolanic activity index obtained following BS 3892-1: 1982 (at 7 days). Both hydrated lime mortar and PC-based mortar used water adjustment to maintain the same flow and were cured under high temperature conditions. However, it should be noted that the fly ash level in PC-based mortar was 30%, but the ratio of fly ash to lime was 2:1 in the case of hydrated lime mortar tests. As shown in Figure 5-45, the correlation of PC-based accelerated activity index was good with both 14 and 28 day hydrated lime mortar strength. Fly ash C LLHF did not appear in the correlation (its LOI value gave lower water demand but its coarseness meant that it did not seem to be particularly reactive in lime-only systems).

As noted earlier the ASTM C593 (ASTM, 2011b) test method is recommended for assessing the suitability of fly ash for lime stabilisation purposes and is a qualitative type test. Examining the approach for assessing reactivity of fly ash for use in cementitious systems it showed potential but several factors associated with the test would need to be resolved to develop its use for assessment purposes. These include rate of strength gain and accuracy of the measurement.

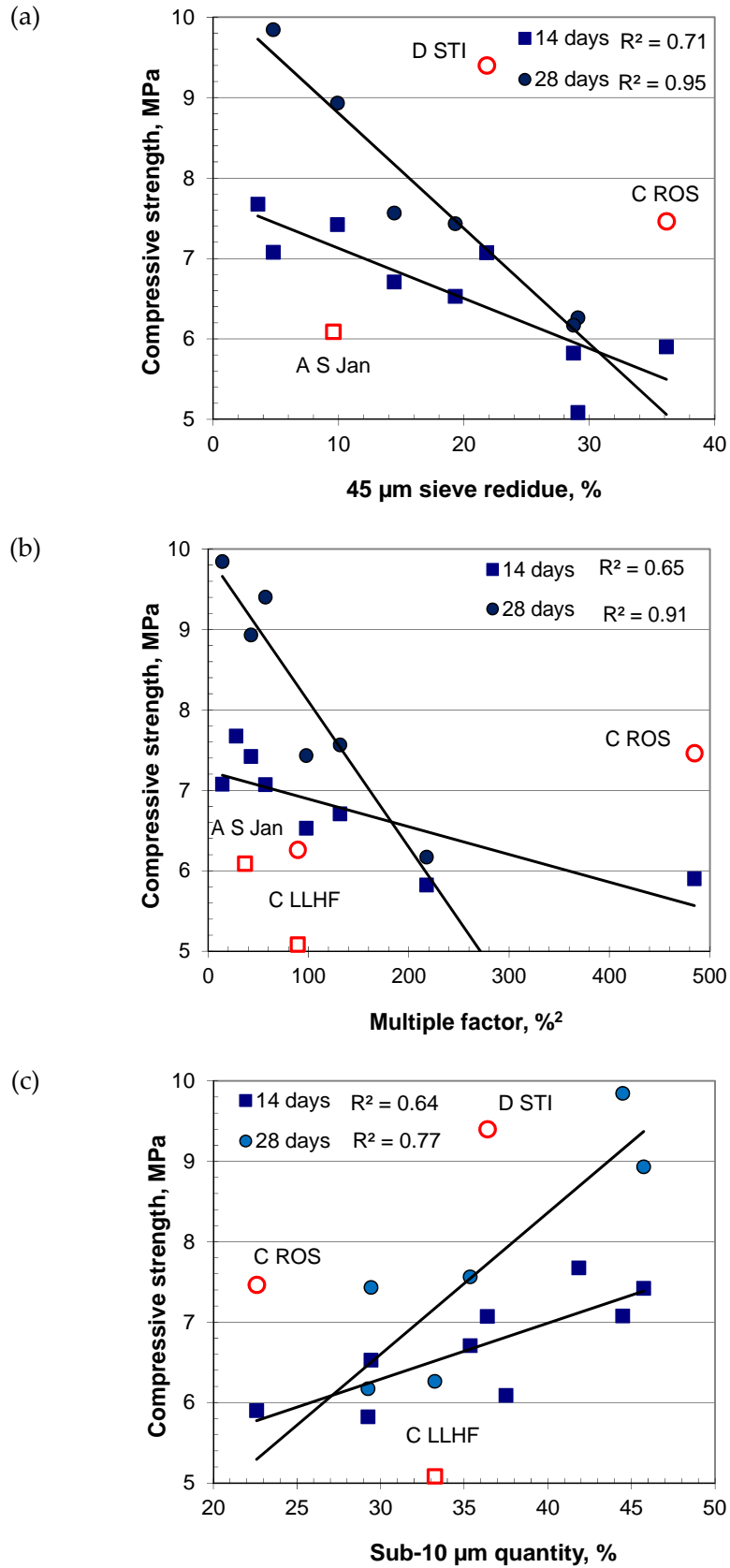


Figure 5-43. Relationships between fly ash properties and lime mortar strength: (a) 45 μm sieve residue; (b) multiple factor (45 μm sieve residue \times LOI); and (c) sub-10 μm quantity of fly ash. (points in red not included in the regression analysis)

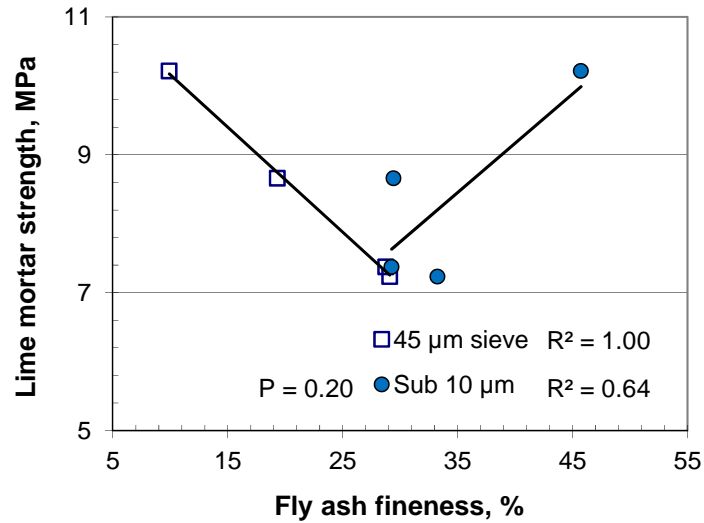


Figure 5-44. Relationships between lime mortar 56 day strength and fly ash fineness

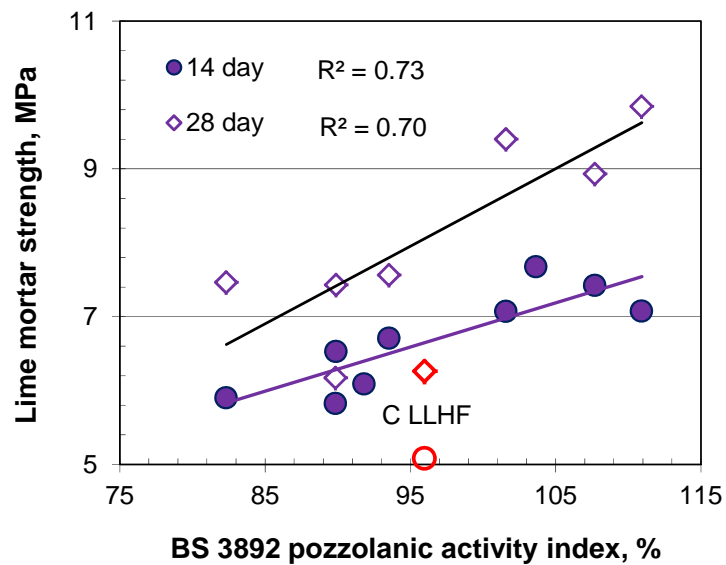


Figure 5-45. Relationships between lime mortar strength and pozzolanic activity index (points in red not included in the regression analysis)

Curing in water is deemed to be the best method to enable hydration and therefore further studies could be carried out with high temperature water curing. In addition to this, the matrix needs to achieve sufficient strength before demoulding. A potential loss of lime might occur during underwater curing by leaching, therefore, saturated lime solution could improve this situation and thereby promote strength gain and enable a better assessment.

5.5 Reactivity by Measuring Ca(OH)_2 Content in Paste using TGA

The reactivity of selected air-classified materials was assessed by TGA using fly ash/PC pastes. Tests with paste sample are expected to reduce the possible influence of sand, which might occur in mortar tests. PC liberates Ca(OH)_2 during the hydration process and fly ash is expected to react further with this. Therefore, the remaining Ca(OH)_2 level in fly ash/PC paste would indicate the reactivity of fly ash. Tests were carried out at 14 and 28 days. The samples included the finest components from each source (d_{90} of C5 = 10.8 μm and L5 = 9.3 μm). The medium fineness (d_{90} of C50 = 46.1 μm and L50 = 45.7 μm) and feed parent fly ashes (d_{90} of CFD = 120.0 μm and LFD = 115.9 μm) were also considered. To compare the reactivity test results with mortar, the same w/c ratio (0.5) and fly ash level (25%) was used.

Figure 5-46 gives the change in Ca(OH)_2 content in fly ash/PC pastes with time. At 14 days, the lime content of the parent fly ashes CFD and LFD were found to be 77 and 75% respectively, indicating little or no consumption of Ca(OH)_2 at this early age. The processed fly ashes from Source C gave 4% (C50) and 9% (C5) less Ca(OH)_2 content than their parent fly ashes, while these were 1% (L50) and 8% (L5) indicating superior reactivity of the processed fly ashes.

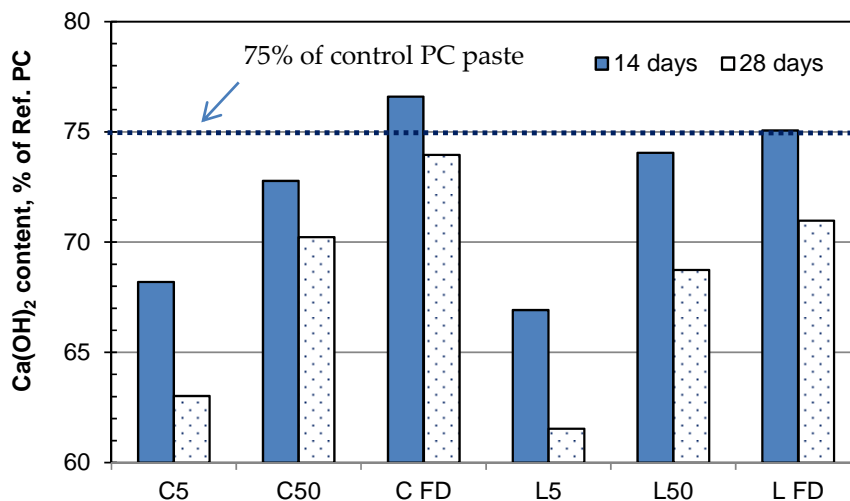


Figure 5-46. Ca(OH)_2 content variation in fly ash/PC paste with time

The Ca(OH)_2 level in all fly ashes under consideration were reduced at 28 days compared to that found at 14 days. The consumption rate for finest components was significant,

indicating accelerated reactivity of these. The other fly ashes also gave minor reductions in $\text{Ca}(\text{OH})_2$ content. A study by Roszczynialski (2002) reported the presence of ~40% (of the reference PC) $\text{Ca}(\text{OH})_2$ in fly ash/PC paste (45% fly ash level) after 28 days. A recent study (Chaipanich and Nochaiya, 2010) also reported ~88% and ~72% $\text{Ca}(\text{OH})_2$ in fly ash/PC paste with fly ash levels of 10% and 20% respectively, at 28 days.

Figure 5-47 gives the relationships between the fly ash properties and $\text{Ca}(\text{OH})_2$ level in air-classified fly ash/PC paste. As shown in Figure 5-47 (a), a strong correlation was obtained between the sub 10 μm quantity and remaining $\text{Ca}(\text{OH})_2$ level in fly ash/PC pastes under consideration. The multiple factor considering both fineness and LOI also gave a good logarithmic relationship with the $\text{Ca}(\text{OH})_2$ level, however, these were weaker than that obtained with sub 10 μm quantity. The results indicate greater influence of fineness on the reactivity in a fly ash/PC system than LOI of the material.

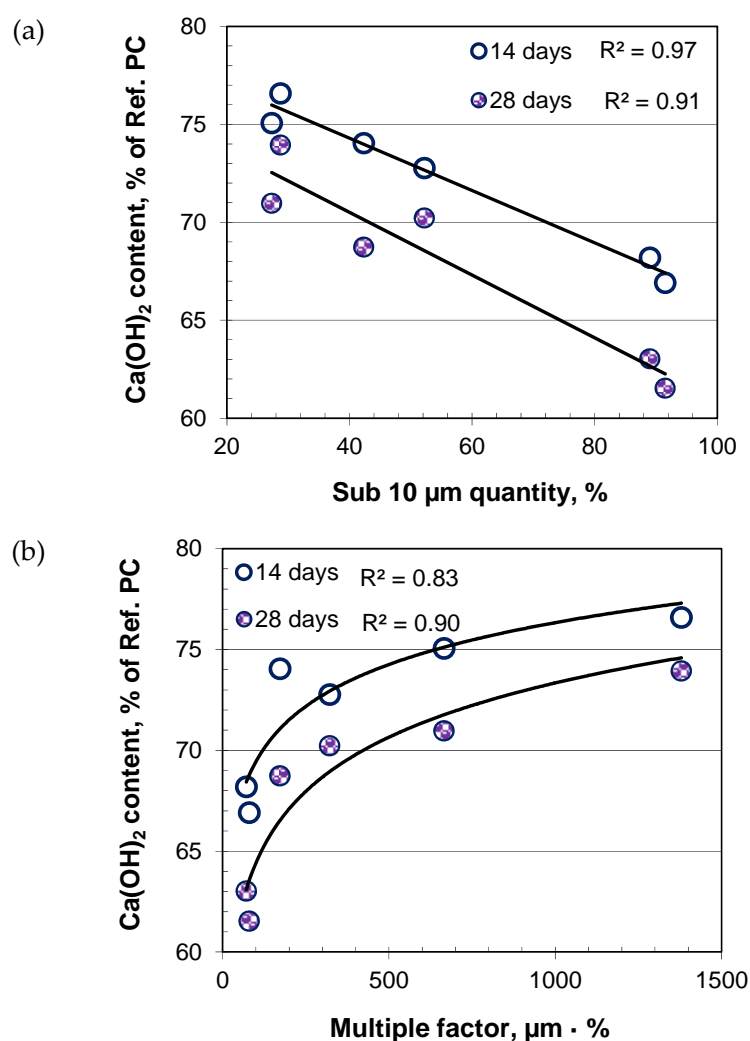


Figure 5-47. Relationships between fly ash properties and $\text{Ca}(\text{OH})_2$ content

Figure 5-48 gives the relationship between fly ash fineness (PSD parameters) and their reactivity in terms of Ca(OH)_2 content obtained from TGA analysis. At both 14 and 28 days, generally with coarsening of fly ashes, reactivity was found to decrease. However, the correlations with either of these parameters were not as strong as found earlier with sub 10 μm quantity. In both cases, fly ashes from Source C and L were considered together. Therefore, it appears that the reactivity assessment from fly ash quantity finer than a particular size (10 μm) gives better results than their PSD parameters, as these parameters depend on the distribution of material over the entire size range.

Figure 5-49 indicates strong relationships between the Ca(OH)_2 obtained from TGA and the corresponding fly ash activity index, both at 14 and 28 days. Results obtained from both test methods at same age, were considered for comparison. As expected, the relationship became stronger with age (coefficient of correlation, $R^2 = 0.92$). As mentioned, the tests were carried out with the same materials (PC and fly ash), mix proportion and age. Therefore, their behaviour was comparable.

Overall, the finest fly ashes (d_{90} of C5 = 10.8 μm and L5 = 9.3 μm) from air-classification gave very good reactivity (even at early ages, 14 days) which was confirmed by activity index and TGA, while their LOI (d_{90} of C5 = 6.6% and L5 = 8.5%) had only a minor effect on this. With the physical properties, sub 10 μm quantities were found to show most reactivity and can be used as a property for assessing this.

5.6 Frattini, Lime Consumption and Conductivity Test

5.6.1 BS EN 196 – 5 (Frattini test)

Given the fly ash reactivity assessment using mortar strength tests can be influenced by the properties of aggregate (e.g. packing of material can affect strength), a qualitative test method described in BS EN 196 – 5 (BSI, 2005a; Frattini test) was considered, which uses a slurry of PC and fly ash in water. Similar to the TGA analysis, the Ca(OH)_2 level remaining in solution after consumption by fly ash was determined to evaluate their reactivity. To match BS EN 450 (BSI, 2005c) mix proportions, a fly ash level of 25% was used with PC. The control sample consisted of 20 g of PC without any fly ash. Part of the work described in this section was carried out in collaboration with Wilmoth (2011).

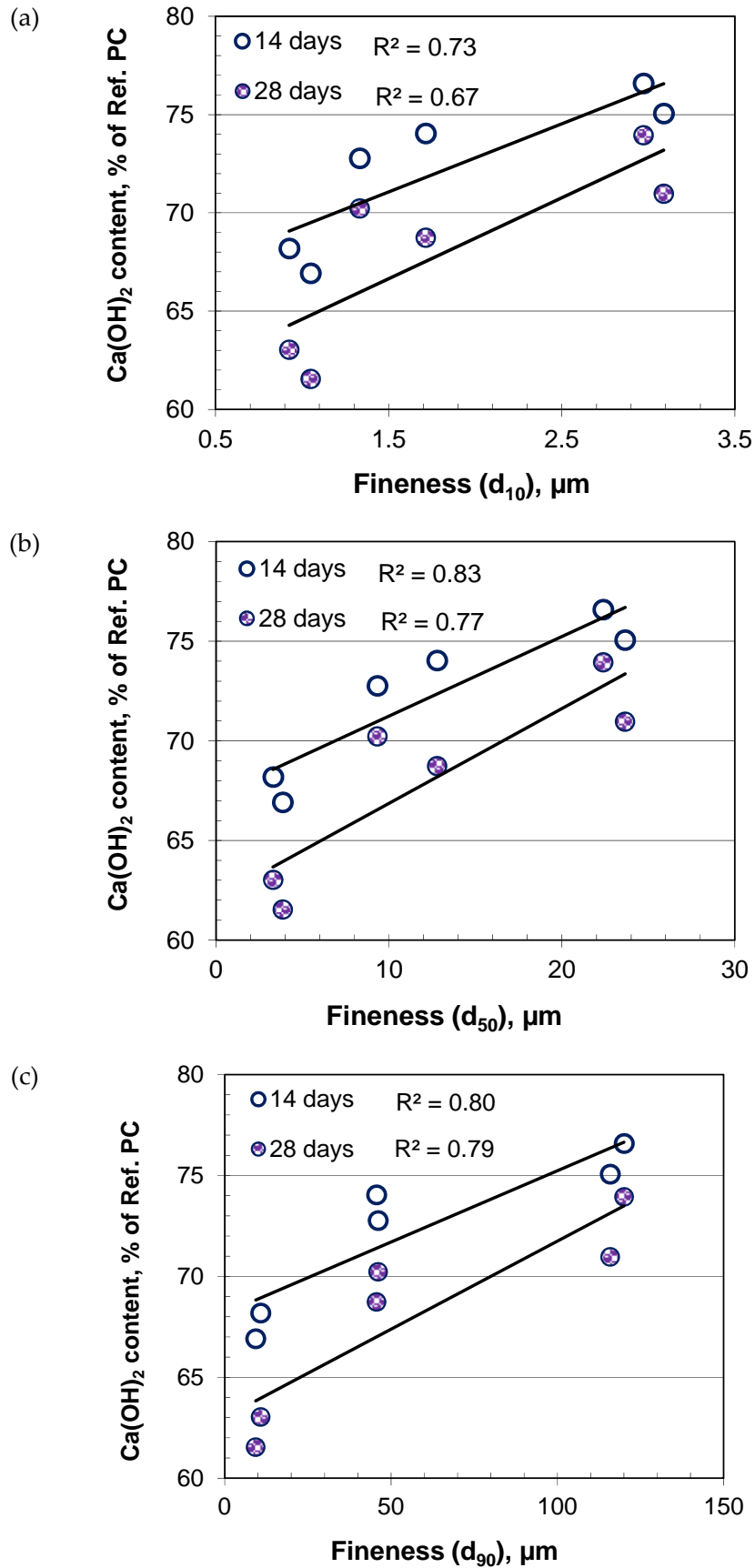


Figure 5-48. Relationships between fly ash fineness (PSD) and Ca(OH)_2 content

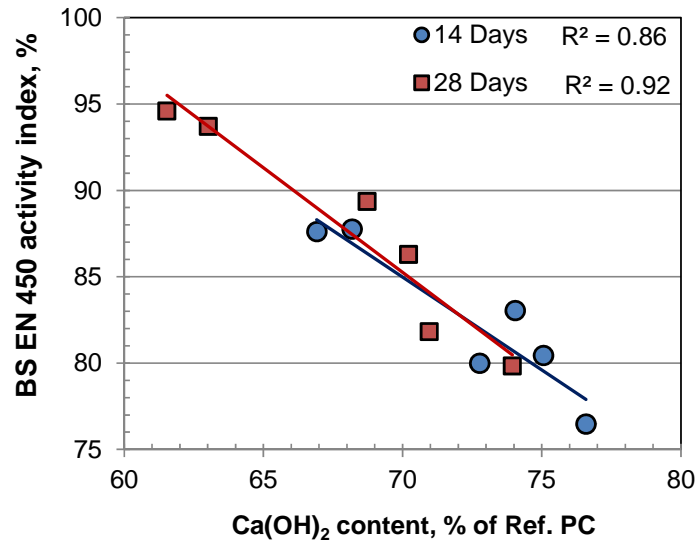


Figure 5-49. Relationships between $\text{Ca}(\text{OH})_2$ content in fly ash/PC paste and BS EN 450 activity index test.

As per the standard, the required quantity of materials were mixed to prepare a slurry and stored at the specified temperature ($40 \pm 2^\circ\text{C}$) for 8 and 15 days. After this, the sample was filtered and the remaining CaO and OH^- concentrations measured to check whether the fly ash meets the standard criterion. The material was considered as satisfying this if the point lies below the saturation curve of calcium ion on a plot of OH^- ion concentration against CaO concentration remaining in the test solution.

A series of fly ash samples with a range of physical properties were tested for 8 and 15 days. Figure 5-50 shows the test results at the two storage periods, as specified in the standard. At 8 days 6 out of 10 fly ashes met the standard criterion. The remaining 4 fly ashes that failed to meet this had fineness $> 20\%$ (retention on the $45 \mu\text{m}$ sieve). However, the 9 fly ashes tested at 15 days all met the criterion specified in the standard. This highlights a wide variation in the rate of their pozzolanic reaction, but also indicates the relative insignificance of the time effect from the test conformity point of view. It should be noted though that BS EN 196-5 (BSI, 2005a) is a pass-fail type of assessment and is not intended to provide an expected strength contribution ranking between the fly ashes when used in concrete. Other more sensitive aspects of the test method are discussed below.

The filtrate solution retained after exposing fly ash to PC (in solution) was also investigated by measuring its bulk conductivity with a view that this might reflect the change in free ion

concentration and thereby reactivity of the material. This was plotted against the remaining CaO and OH⁻ ion concentration and is shown in Figure 5-51 at 8 and 15 days. At 8 days, the conductivity increased with both CaO and OH⁻ ion concentration in the filtrate solution. However, at 15 days, although the OH⁻ ion concentration maintained the same type of relationship, CaO concentration gave the opposite trend with conductivity, and there was a stronger correlation between them.

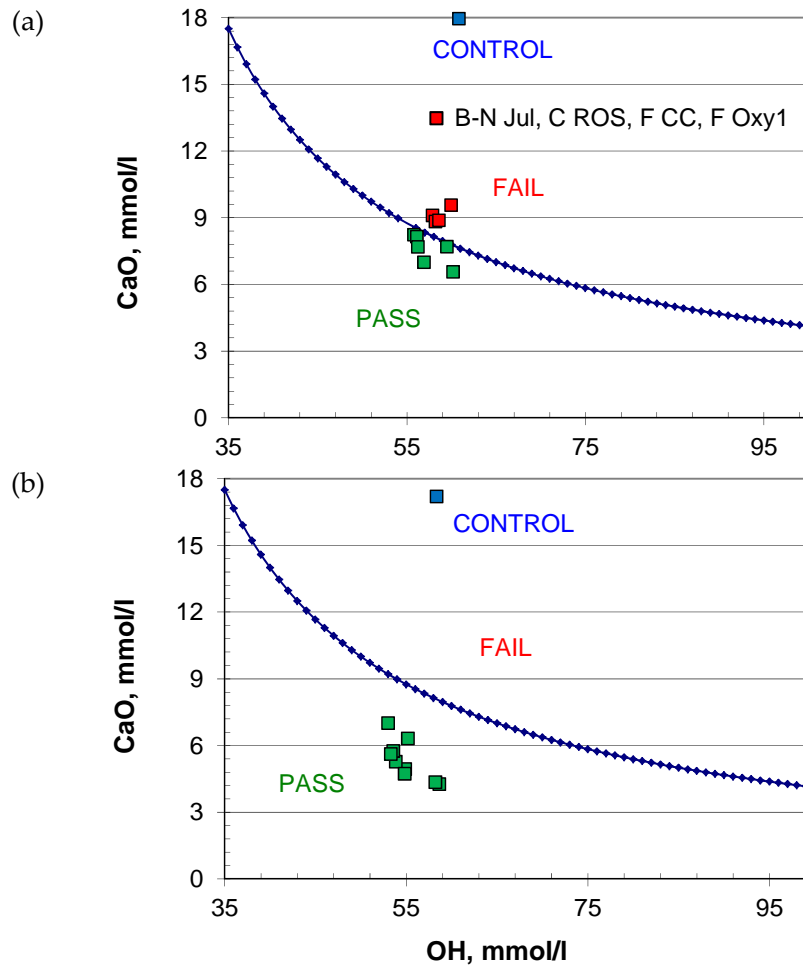


Figure 5-50. Assessment of fly ash using BS EN 196-5 after (a) 8 days, and (b) 15 days (in collaboration with Wilmoth, 2011)

Some of the tested fly ashes did not follow the general trend although the test conditions were same (see Figure 5-51 (a)) and excluded from the regression analysis. This might be caused by their different level of ion contribution in the solution and thereby in conductivity measurements. Shehata and Thomas (2006) reported that there is a balance of alkalis in a hydrating PC/pozzolana system. Calcium being the major component in PC means that an abundant amount released at initial phase of hydration, and with continued

reactions, and consequent consumption of $\text{Ca}(\text{OH})_2$ by the fly ash, other alkali ions are released. The result in current study indicate that the alkali contribution in solution at the early age (8 days) was mostly from CaO , however, with consumption of $\text{Ca}(\text{OH})_2$ from the solution, other alkalis were released which contributed to the conductivity to a greater extent than that from the CaO level and, therefore, with decreasing CaO level, the conductivity increased by contribution from other ions.

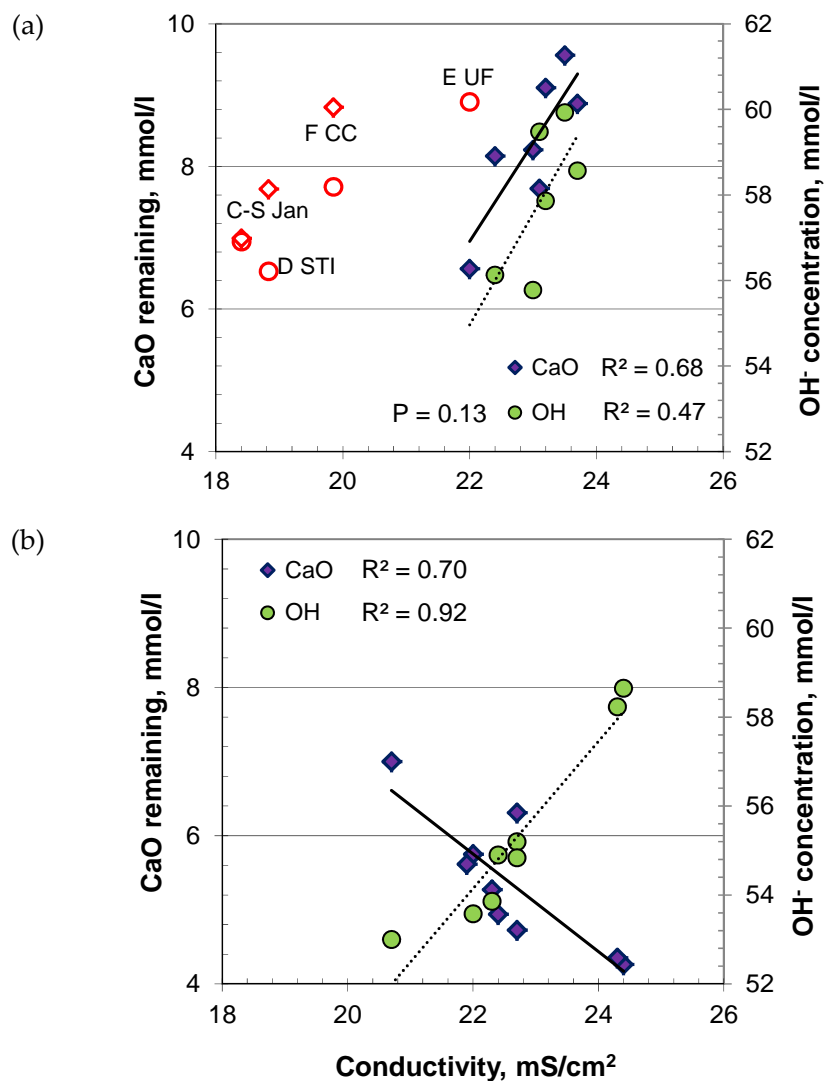


Figure 5-51. Relationships between conductivity, CaO and OH^- concentration at: (a) 8 days; and (b) 15 days. (points in red not included in regression analysis)

Further analysis was carried out to correlate properties of the filtrate solution with those of fly ash properties influencing the activity index (discussed earlier). Figures 5-52 and 5-53 show relationships between fly ash properties and the remaining CaO concentration at

8 and 15 days, respectively. The remaining CaO concentration in solution gave good correlations with fly ash fineness (especially at 8 days). Finer/higher sub 10 μm quantity fly ash consumed more CaO from the solution and hence showed greater reactivity. However, the multiple factor did not give good agreement with the remaining CaO concentration, except for a general trend at both 8 and 15 days.

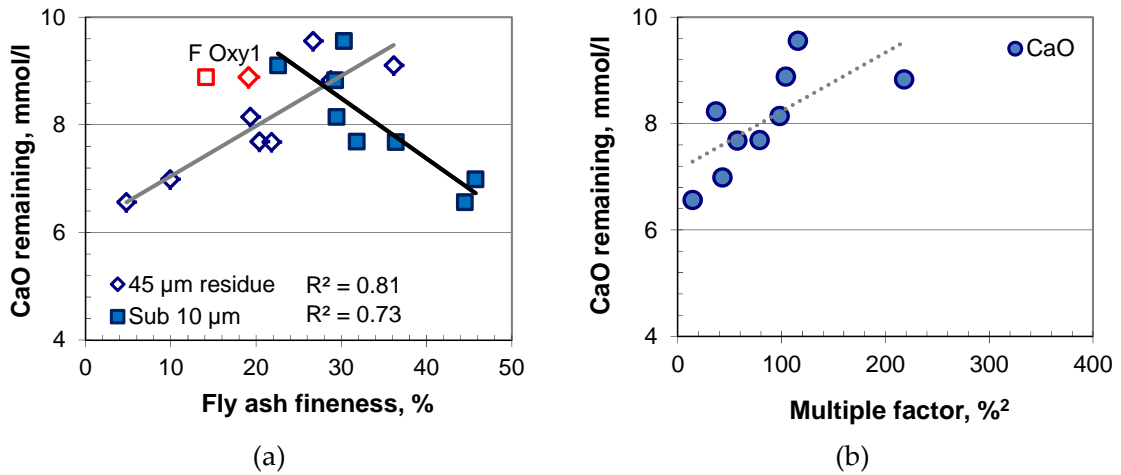


Figure 5-52. Relationships between fly ash properties and remaining CaO concentration at 8 days (points in red not included in regression analysis)

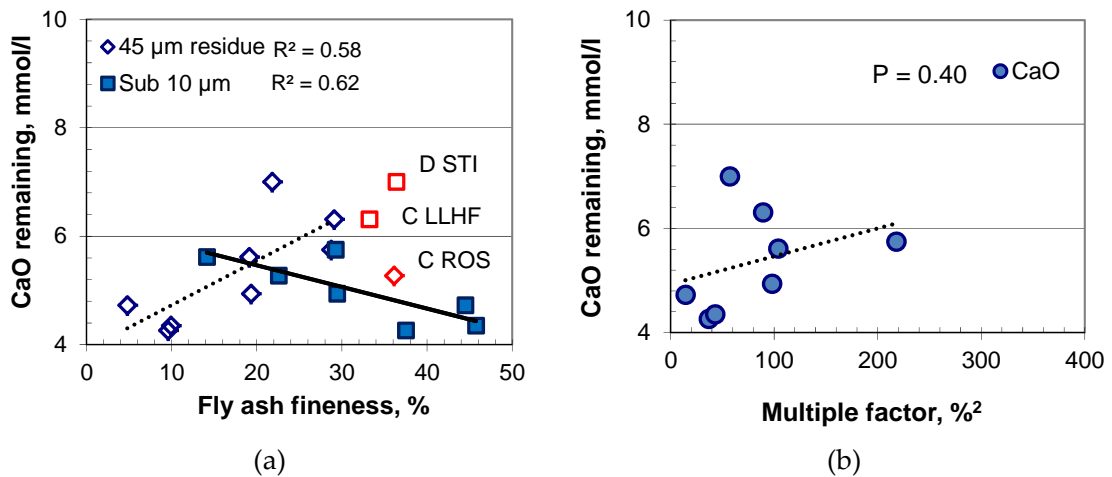


Figure 5-53. Relationships between fly ash properties and remaining CaO concentration at 15 days (points in red not included in regression analysis)

The conductivity of the solution, which is an indicator of free ions present, did not correlate well with fly ash fineness (Figure 5-54). This might be caused by the presence of other ions (liberated during PC hydration) in addition to $\text{Ca}(\text{OH})_2$ in the test solution. Fly ash soluble component dissolution rates in the solution are also likely to affect these relationships.

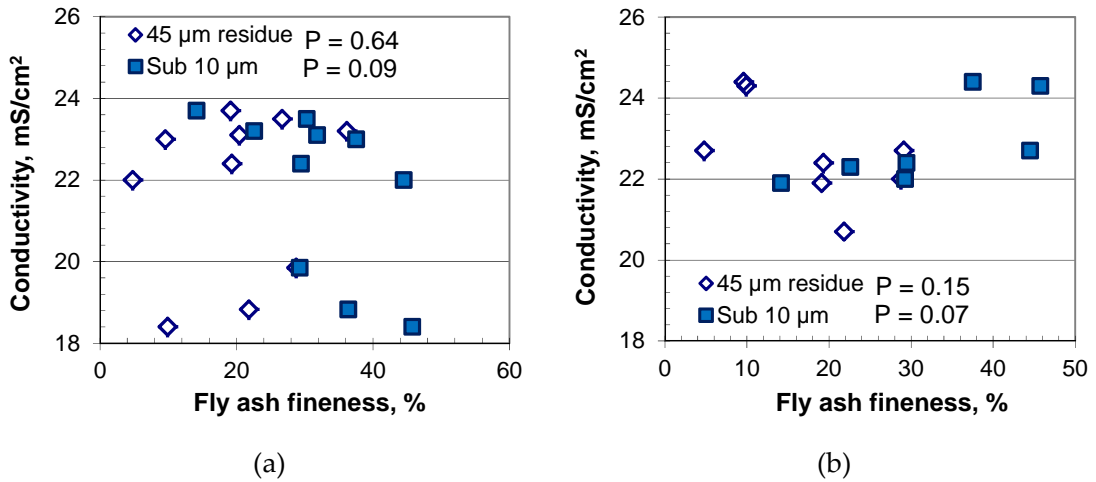


Figure 5-54. Fly ash fineness and conductivity of filtrate at: (a) 8 days, and (b) 15 days

BS EN 450 activity index at 28 and 90 days, (using the same cement HR52) is plotted against the remaining CaO in the filtrate solution at 8 and 15 days in Figure 5-55. With a few exceptions (high LOI, C ROS and carbon removed fly ash D STI), the remaining CaO concentration in the filtrate solution correlated well with the BS EN 450 activity index. As with the fly ash properties (noted earlier), the relationship was also good at 8 days. Given relatively higher CaO consumption, the relatively lower activity index of fly ash C ROS may be attributed to the packing effect in fly ash mortar. With higher LOI, this gave low flow and thus the strength of the mortar was affected by its packing. While this did not affect in this test, and Fly Ash C ROS gave better reactivity compared to its activity index.

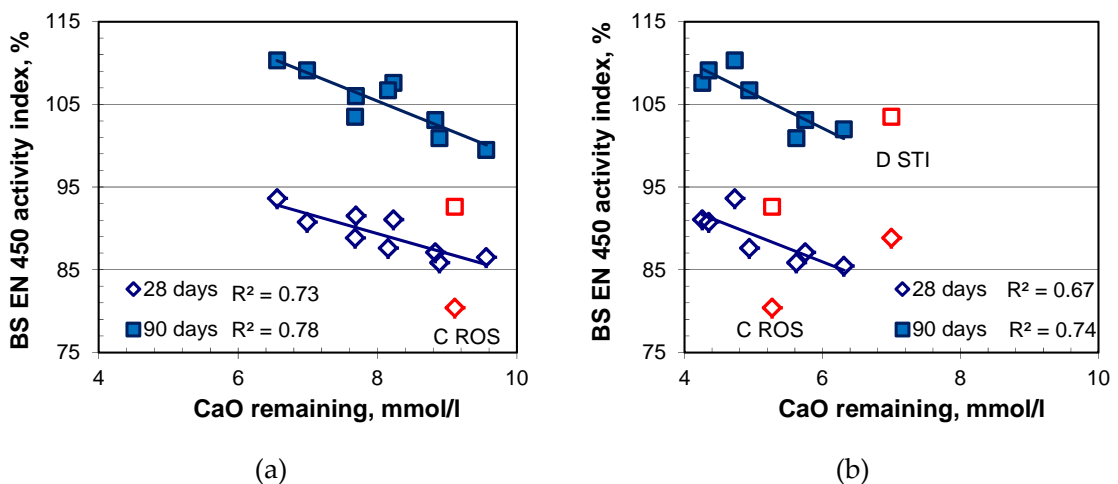


Figure 5-55. Relationships between CaO concentration and BS EN 450 activity index at: (a) 8 days, and (b) 15 days (points in red not included in regression analysis)

On the other hand, the opposite was noted for Fly Ash D STI. Being relatively cleaner by nature, it always gave highest flow in mortar at the same w/c ratio. Therefore, its relatively higher activity index, compared to the CaO consumption, may be attributed to better packing. Although Fly Ash D STI followed the general trend at 8 days it was outwith at 15 days. Having low LOI, the overall rate of reaction was comparable with other fly ashes at 8 days, but this did not follow at 15 days.

5.6.2 Saturated lime test

Initial test set up

It is well established that fly ash reacts with free lime present in a cementitious system. Given that the Frattini test described in BS 196 – 5 could be influenced by the PC type used for this, an attempt was made to carry out the test with laboratory grade Ca(OH)₂. Work by Rosell-Lam *et al.* (2011) described the evaluation of pozzolanic properties of zeolitic rock by conductivity measurement of solutions after exposing to saturated lime solution. It was intended to apply this approach to fly ash in the study. A series of initial test were conducted to explore suitable test conditions. Table 5-9 shows the key parameters used in the initial experiments.

Table 5-9. Initial test conditions for saturated lime and KOH solution

TEST CONDITION	SATURATED LIME	KOH AND LIME
KOH	-	100 mmol/l
Ca(OH) ₂	Saturation level	Saturation level
Temperature	40 ± 2°C and 80 ± 2°C	40 ± 2°C and 80 ± 2°C
Fly ash	E UF and C ROS	E UF and C ROS

Note: Each set tested at 1, 2, 3 and 4 days at 80 ± 2°C and 2, 4, 6 and 8 days at 40 ± 2°C

Two types of laboratory prepared solutions were used for fly ash exposure. To raise the pH of the test solution above 13.0 a 100 mmol/l KOH stock solution was prepared and then laboratory grade Ca(OH)₂ was dissolved in this up to saturation level. The other solution considered was saturated lime. Both were filtered to ensure no suspended-lime was present. A 20 g fly ash sample was exposed to 100 ml of these solutions in a water-tight plastic container and kept in a temperature controlled oven for different periods. After this the slurry was filtered and the remaining CaO, OH⁻ ion concentration and conductivity

measured. Initially, the ultra-fine and coarsest fly ashes E UF and C ROS were considered during this test series.

Figures 5-56 and 5-57 show the change in remaining CaO and conductivity measured after exposing the fly ashes to the two types of solution for different exposure periods. In all cases, a drop in CaO level with time was observed. It should be noted that only a very low level of Ca(OH)₂ (3.04 mmol/l) could be diluted in the solution, as it was suppressed by the KOH (which will be discussed later). Most of this lime was consumed by fly ash at around 96 and 24 hours from the lime + KOH solution when exposing the fly ashes to 40 and 80°C respectively. The CaO level also decreased with time from the saturated lime solution, where the effect of temperature was noticeable (see Figure 5-56 (a) and (b)). This was also confirmed by the reduction in conductivity of saturated lime solution with time and reflects the lower CaO concentration and corresponding pozzolanicity of fly ash. It was also noticed that the finer fly ash was more reactive than that with high LOI and coarse particle size.

The conductivity change in solution containing lime + KOH proved to be misleading. The possible cause of this could be interference from a very high level of KOH (100 mmol/l) compared to CaO (3.04 mmol/l) in solution. The fly ashes C ROS and E UF were also exposed to de-ionized water for a period of 1 and 4 days at different temperatures and their contributions to conductivity are shown in Figure 5-58, which indicate that fly ash type and temperature had a minor effect.

Tests with saturated lime

In order to further investigate the effect of lime/KOH solutions on lime solubility and conductivity, stock solutions were prepared with 0, 25, 50 and 100 mmol/l KOH and then Ca(OH)₂ was diluted in these up to saturation level. The conductivity of these solutions was also measured. As shown in Figure 5-59, the conductivity increased with KOH level which was expected; however, with increasing KOH level, the quantity of lime that could be dissolved in the solutions reduced as the higher KOH content suppressed their solubility. As with the earlier tests, it was also noticed that the conductivity measurements after exposing fly ashes to the solutions with lime + KOH were difficult to interpret. Therefore, it was decided to use saturated lime-only solution in subsequent work.

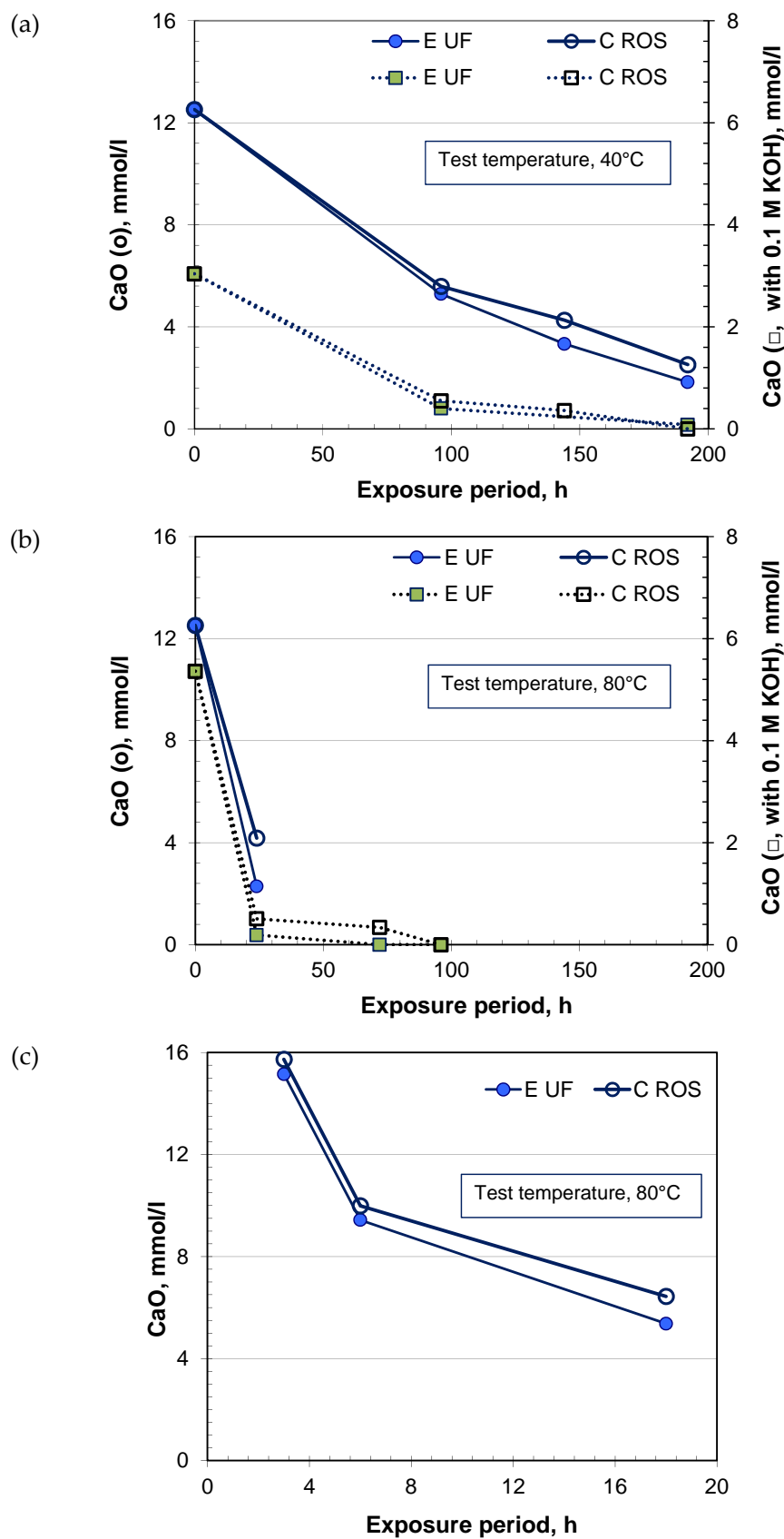


Figure 5-56. Variation in CaO level with various temperature and exposure periods: (a) $40 \pm 2^\circ\text{C}$; (b) $80 \pm 2^\circ\text{C}$; and (c) $80 \pm 2^\circ\text{C}$ (shorter period with saturated lime) (in collaboration with Wilmoth, 2011).

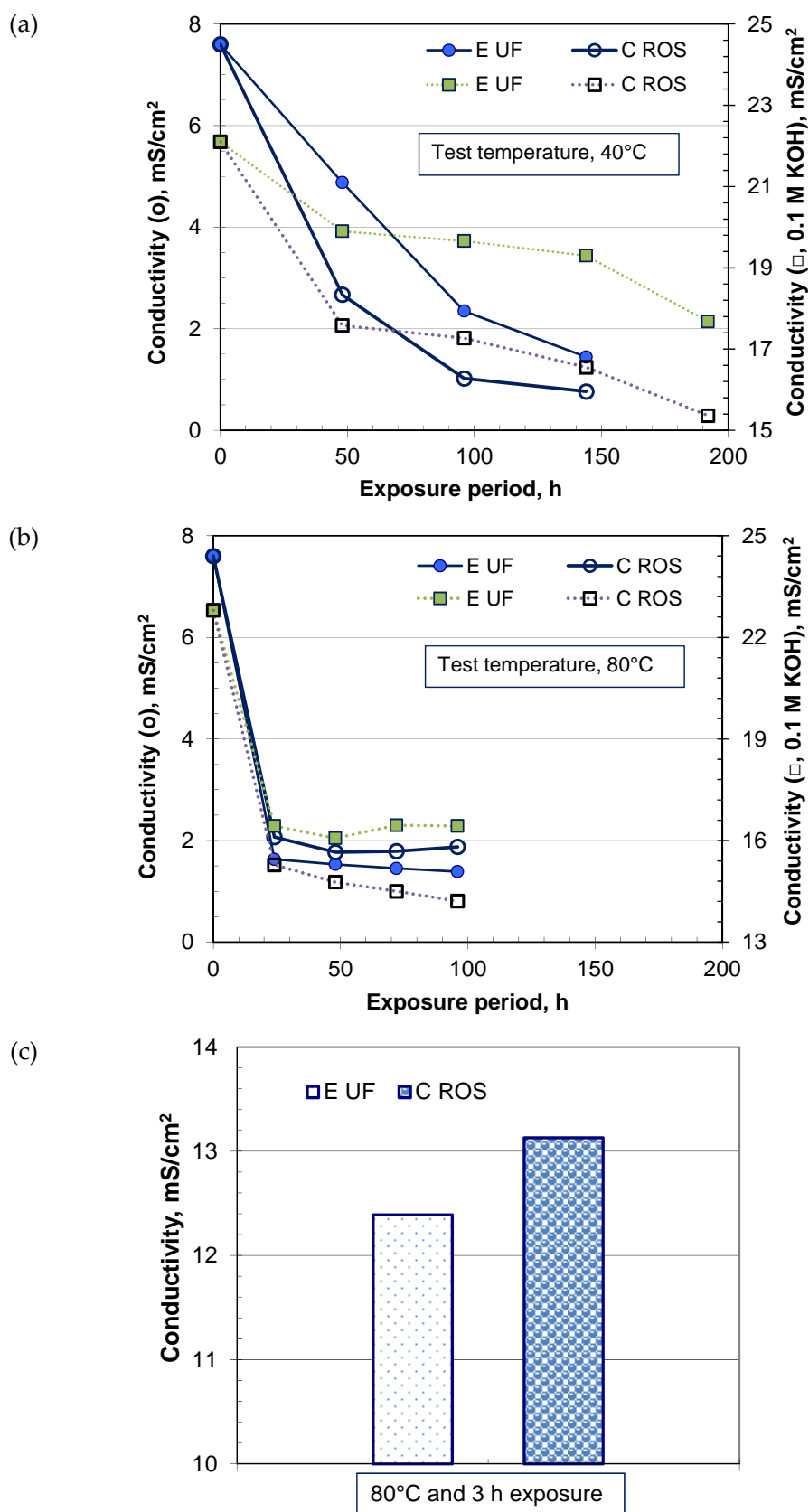


Figure 5-57. Variation in conductivity at various exposure temperature and periods: (a) $40 \pm 2^\circ\text{C}$; (b) $80 \pm 2^\circ\text{C}$; and (c) $80 \pm 2^\circ\text{C}$ (shorter period with saturated lime) (in collaboration with Wilmoth, 2011).

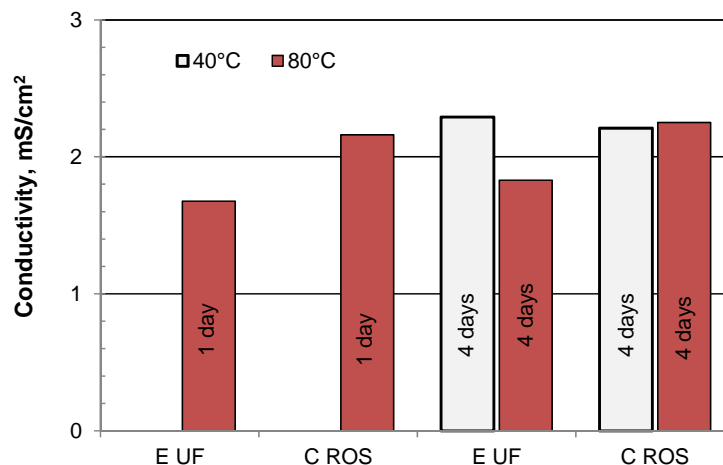


Figure 5-58. Conductivity of fly ashes exposed to de-ionized water at 40 and 80°C for different periods

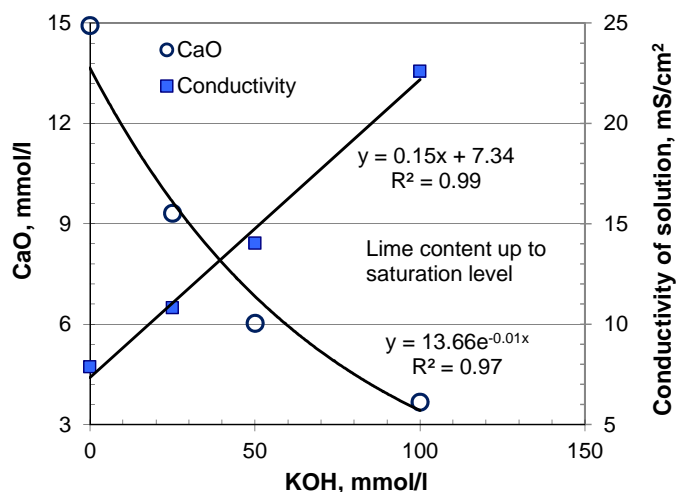


Figure 5-59. Effect of alkali combination on conductivity of test solution

An attempt was made to calibrate the lime concentration with solution conductivity. As shown in Figure 5-60, a very good correlation was obtained between these. Following these tests, 7 fly ashes with a wide range of properties, were exposed to saturated lime solution at $40 \pm 2^\circ\text{C}$ for 2 days. The s/l ratio of 1 : 5 (used for the initial tests) was maintained. Detailed test parameters are shown in Table 5-10.

The results obtained are plotted against fly ash fineness in Figure 5-61. As expected, finer fly ashes gave a greater reduction in CaO than coarse fly ash. No definite correlation between fly ash fineness and conductivity measurements was obtained and this needs to be studied further, with a wider number of fly ashes.

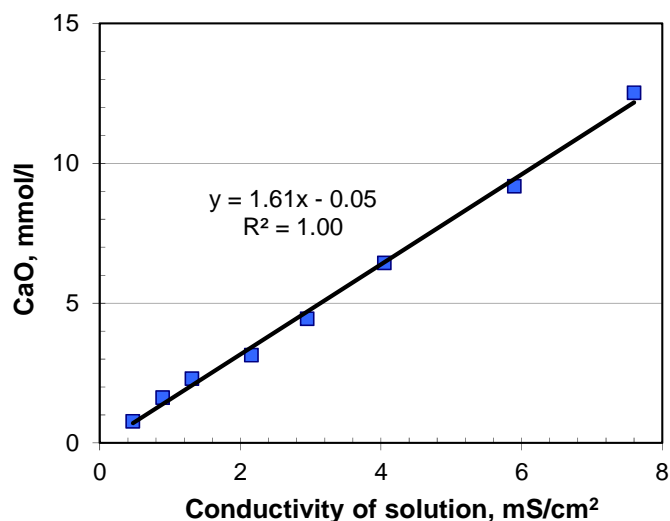


Figure 5-60. Calibration of CaO concentration determination by conductivity

Table 5-10. Test set up for saturated lime (in collaboration with Wilmoth, 2011)

TEST CONDITION	SATURATED LIME
Ca(OH) ₂	Saturation level (14.27 mmol/l)
Temperature	40 ± 2°C
Exposure period	2 days
Fly ashes	A S Jan, A N Jul, C ROS, E UF, E EN1, F Oxy3 and G

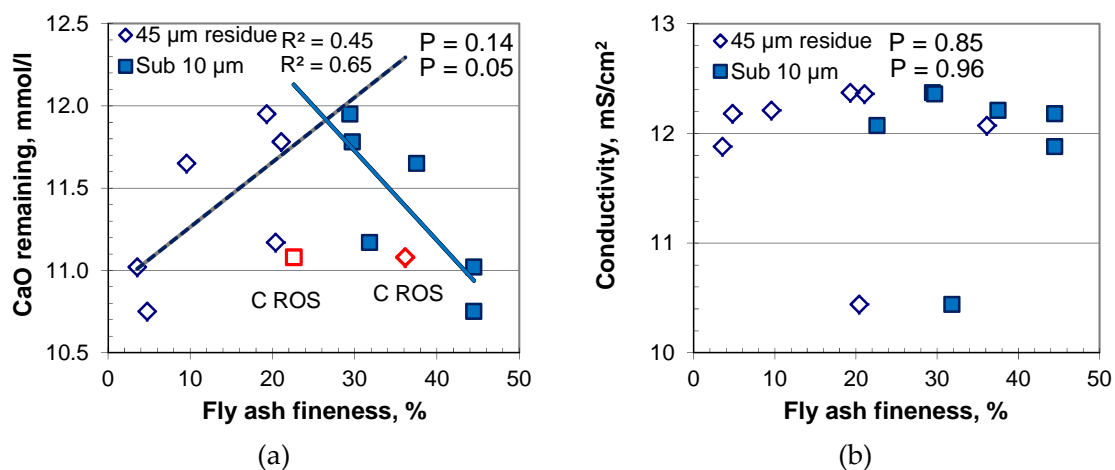


Figure 5-61. Relationships between (a) CaO concentration; and (b) conductivity of filtrate and fly ash fineness (points in red not included in the regression analysis)

CaO showed inverse relationships with BS EN 450 activity index (Figure 5-62) where good correlations were obtained for cements LD32 and LD52, however, these were poor with cements HR52 and HK42. The correlation with conductivity was poor with all test PCs. The reason for this is not clearly known.

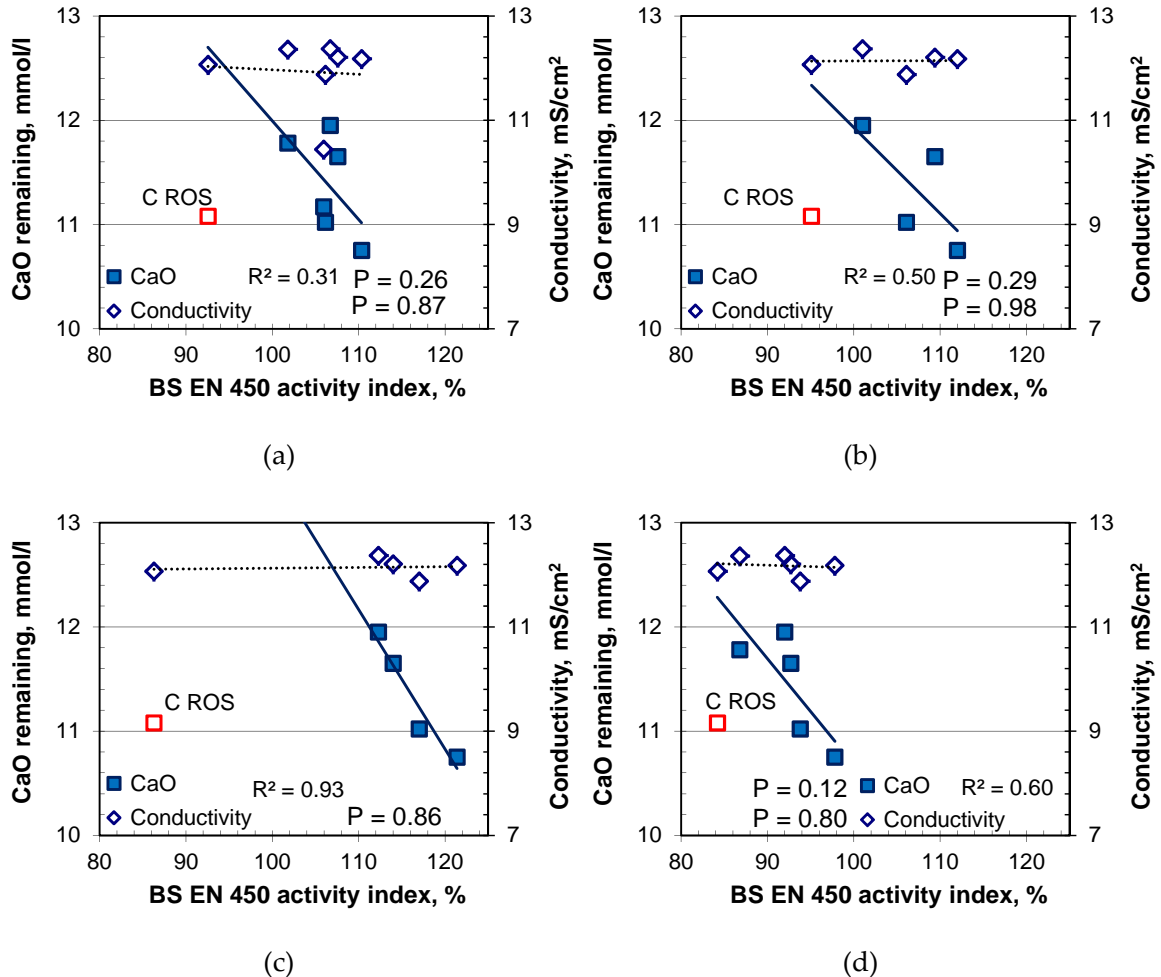


Figure 5-62. Relationships between BS EN 450 activity index (90 days) and remaining CaO concentration of filtrated for different PCs: (a) HR52; (b) HK42; (c) LD32; and (d) LD52. (points in red not included in the regression analysis; in collaboration with Wilmoth, 2011)

Test with lime – sucrose – KOH solution

It was noted that the use of additional alkali (KOH) with lime could accelerate the pozzolanic reaction. However, the use of KOH suppressed the solubility of lime. Literature (Stone and Scheuch, 1894) was found describing techniques for increasing the solubility of lime using sucrose in solution. At this point, an arbitrary solution was prepared with the mix proportions shown in Table 5-11. Three fly ashes were exposed to

the solution and the level of CaO was measured at 48 and 120 hours. As shown in Figure 5-63 no specific conclusion was reached as the level of CaO measured in the control solution was significantly lower (45%) than that introduced. Therefore, suspended lime appeared to be present, which may have interfered with the test.

Table 5-11. Test conditions for lime-sucrose-KOH solution

TEST CONDITION	LIME-SUCROSE-KOH
KOH	100 mmol/l
Ca(OH) ₂	10 g/l
Sucrose	10%
Temperature	40 ± 2°C
Exposure period	2, 24, 48, 120 h

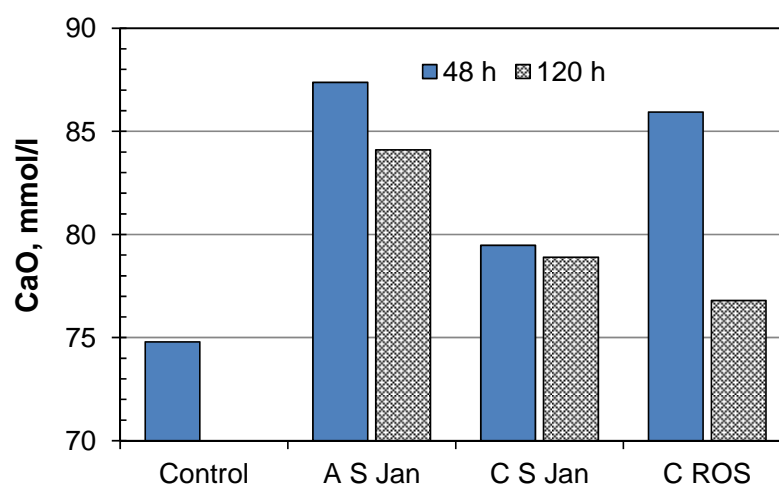


Figure 5-63. Remaining CaO level after exposure to fly ash for 2 and 5 days

Attempts were made to check how the sucrose enhanced the solubility of lime and properties of the solution. A stock solution was prepared with 0.1 M KOH and then 1, 2, 5 and 10% sucrose dissolved in this. Excess lime was then added and brought to saturation level. After this, the solution was filtered and CaO and conductivity measured as shown in Figure 5-64. It was observed that with the increase in sucrose level the solubility of lime in 0.1 M KOH solution was enhanced significantly. However, with the use of sucrose, the conductivity of solution appeared to be affected. As per Asadi (2007) the solubility of lime

in sucrose solution is enhanced by forming calcium saccharate ($\text{Ca}(\text{C}_{12}\text{H}_{22}\text{O}_{11})$), which does not reflect the calcium level in the solution from conductivity measurements. This suggested that the assessment with conductivity measurements may not be possible with this type of solution. It was also difficult to filter the thick solution with sucrose because of its viscosity. Indeed, this blocked the filtering system and it was decided not to proceed further with this combination of materials.

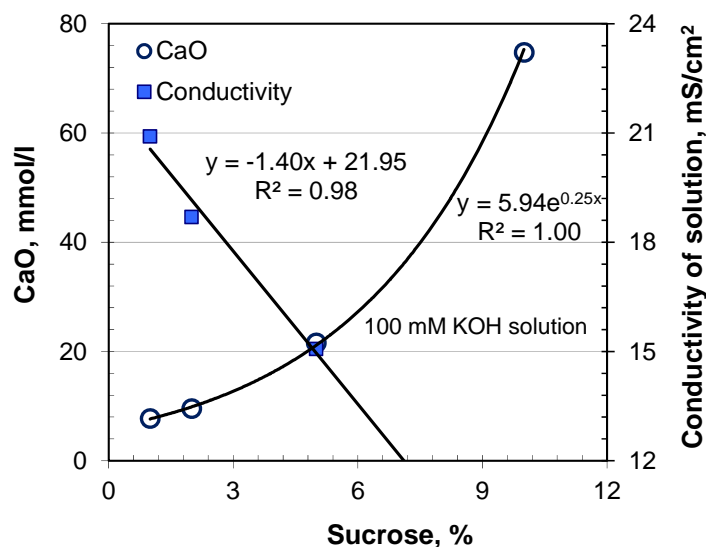


Figure 5-64. Effect of sucrose content on lime solubility and conductivity of solutions

5.7 Fly Ash Oxide Analysis

5.7.1 The pozzolanic potential index (PPI)

The pozzolanic Potential Index (PPI) was proposed by Hubbard and Dhir (1984). This work found that the oxide composition of fly ash reflects the proportions of illite and kaolinite in the clay impurities of the coals burnt. The fluxing action of K_2O , leads to silicate glass (pozzolana) production from illite rather than kaolinite. The molar ratio of potash to alumina (K/A) should therefore reflect the relative proportions of illite and kaolinite and hence be directly proportional to the concentration of reactive component in fly ash. The $(\text{K}/\text{A}) \times 10$ was defined as a pozzolanic potential index (PPI), which might allow compositional characterisation of fly ash for use in concrete. Figure 5-65 shows the correlation of PPI with BS EN 450 activity index. There seemed to be no definite trend for

PPI with activity index at 28, 56 and 90 days. However, it was noted earlier that finer fly ashes gave higher activity index values, even when PPI values were lower, for example Fly Ash E UF. In light of this, a modified PPI (MPPI) was explored by dividing the PPI by the 45 μm sieve residue.

Figure 5-66 shows some correlation between MPPI and activity index values. However, it should be noted that the coefficient of correlation did not improve from what it was originally between 45 μm fineness and activity index values ($R^2 = 0.69-0.79$) at 90 days. Hubbard and Dhir (1984) noted that PPI did not correlate with short-term/accelerated test activity values. However, neither short nor long-term activity index values in this research correlated well with either PPI or MPPI.

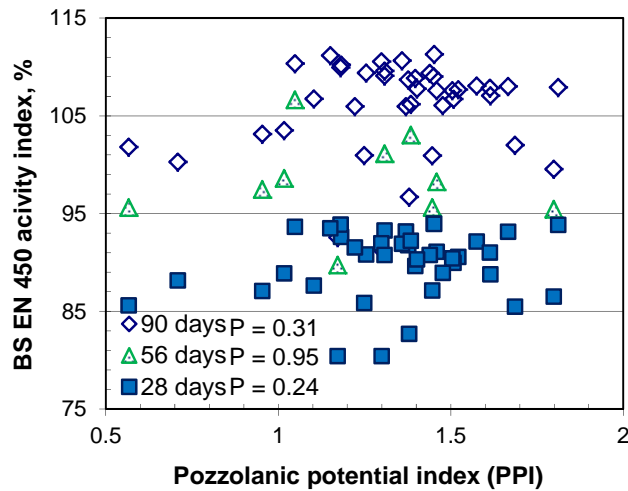


Figure 5-65. Relationships between PPI and BS EN 450 activity index

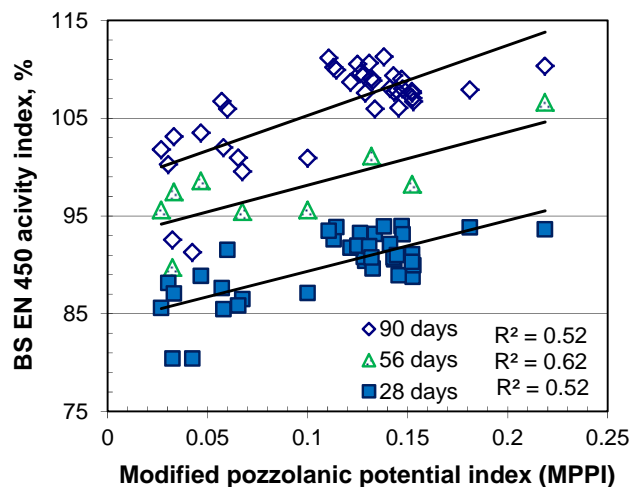


Figure 5-66. Relationships between modified pozzolanic potential index (MPPI) and BS EN 450 activity index. ($MPPI = PPI/45 \mu\text{m}$ sieve residue)

5.7.2 Major oxide analysis

BS EN 450 requires that the sum of the major oxides (SiO_2 , Al_2O_3 and Fe_2O_3) in fly ash should be more than 70% by mass, in order to ensure its suitability for use in concrete. The same is also required by ASTM C618 (ASTM, 2012) for Class N and F fly ashes. This sum of major oxides was calculated from the x-ray fluorescence (XRF) analysis data and attempts were made to correlate these with BS EN 450 activity index values. As shown in Figure 5-67, activity index increased with the sum of major oxides (i.e. mineral proportion); however, the correlation was poor.

Improved relationships were observed, as with the PPI analysis, by dividing the sum of major oxides by the 45 μm sieve residue, as shown in Figure 5-68. The coefficients of correlation ranged from 0.68-0.74 at different ages of activity index testing. The oxy-fuel fly ashes F Oxy2 and F Oxy3 were not considered in this section.

A Similar attempt was made to correlate BS EN 450 activity index and the sum of major oxides/ d_{50} . As shown in Figure 5-69 the R^2 values were found to improve and ranged from 0.71 – 0.82 at different ages. All fly ashes tested were included in this correlation. These results also indicate that the major oxides inversely followed fineness. Therefore, with coarse fly ash, relatively higher LOI was expected and thus the oxides decreased and due to this, good relationships were found between the fineness and major oxides.

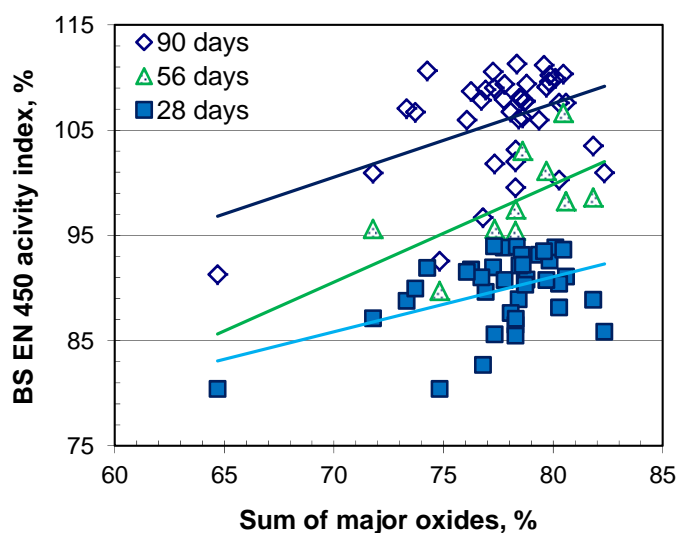


Figure 5-67. Relationships between major oxides and BS EN 450 activity index

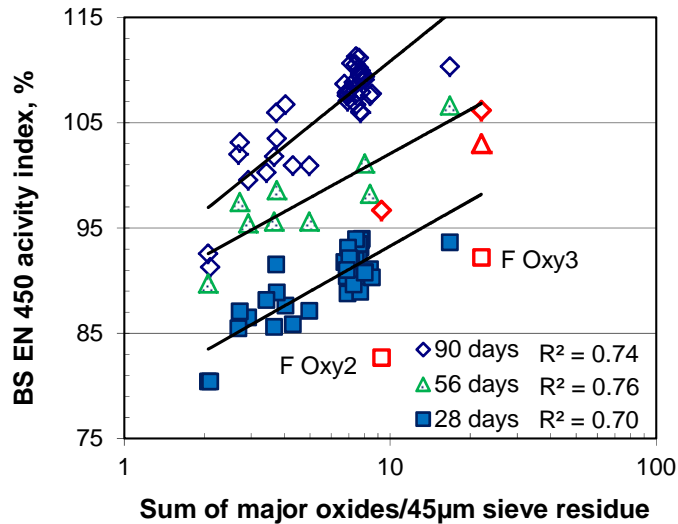


Figure 5-68. Sum of major oxides (SiO_2 , Al_2O_3 and Fe_2O_3)/(45 μm sieve residue) and BS EN 450 activity index. (points in red not included in the regression analysis)

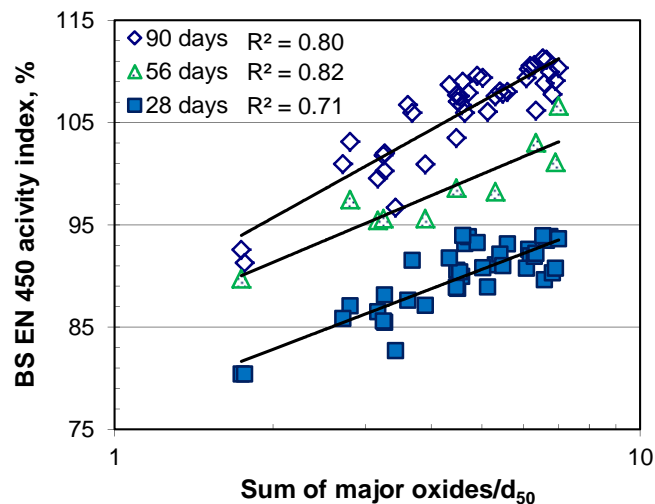


Figure 5-69. Relationships between major oxides / d_{50} and BS EN 450 activity index

5.8 Glass/Amorphous/Others Content in Fly Ash

5.8.1 Source dependency of glass

Fly ash is principally composed of glassy and crystalline components. Having disordered atomic structures, by nature, the glass proportion is mainly deemed to give the pozzolanic reactivity within a cementitious system (Font *et al.* 2010). From XRD analysis, the crystalline components of fly ash were measured and the portion other than crystalline was

estimated by subtracting the total crystalline part from 100. It was intended to relate this property with mortar activity index as shown in Figure 5-70, however, no specific correlations were found for this comparison.

As mentioned in Section 4.1, the fly ashes assessed in this project had a wide range of properties due to variations in: (i) source, (ii) season of collection, (iii) classification or carbon removal process and (iv) introduction of modern combustion technology (e.g. oxy-fuel burning technology or co-combustion).

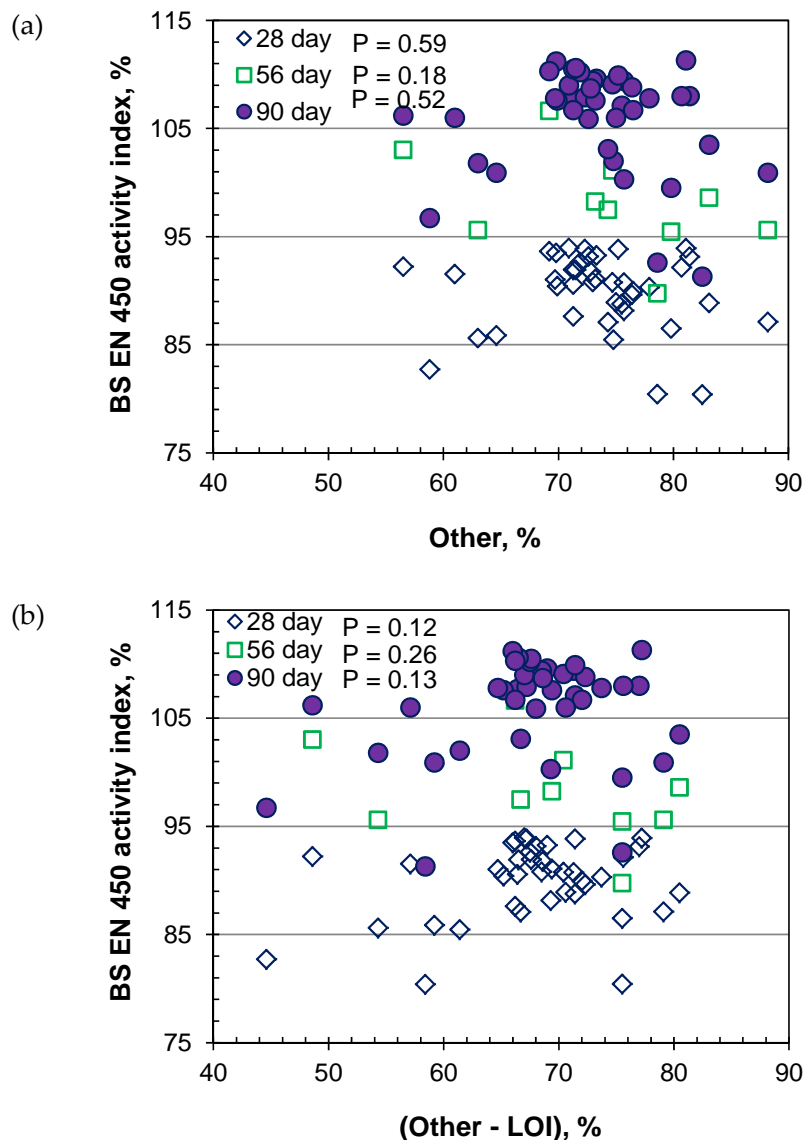


Figure 5-70. Relationships between fly ash component other than crystalline and BS EN 450 activity index (*general fly ashes used in the project*)

As XRD does not consider LOI during analysis, this quantity was deducted from the components other than crystalline, and further attempts made to correlate this with mortar activity index (see Figure 5-70 (b)). No improved relationships were found and it was concluded that due to the range of variations in production, the material is likely to contribute in different ways and the glass/amorphous content does not always indicates how they will react in a cementitious system, as mentioned earlier in Swamy (1986).

As noted above, attempts were made to reduce the effects associated with production of fly ash by separating run-of-station pulverised coal fly ashes (from Sources C and L) into various size fractions by air-classification. The results from tests following this approach are shown in Figure 5-71. Positive correlations between fly ash components, other than crystalline and BS EN 450 activity index were obtained (14, 28 and 56 days) for both sources. Activity index at later ages gave relatively acute slopes with stronger correlations than at the early age.

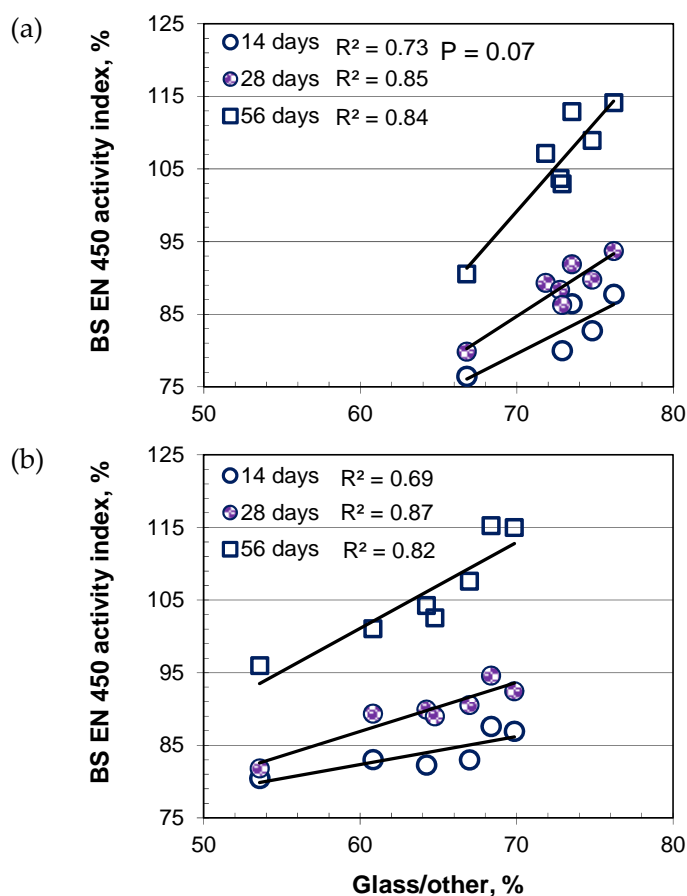


Figure 5-71. Relationships between fly ash component other than crystalline and BS EN 450 activity index: (a) Source C and (b) Source L (*air-classified fly ashes*)

Although glass content of fly ashes from single sources gave good correlations with their corresponding activity index at various ages, the behaviour noted was not the same for each source under consideration. As given in Figure 5-71, although, fly ashes from Source C gave relatively higher glass contents in similar size fractions, their activity index followed the opposite trend. Therefore, it appeared that the reactivity of fly ash not only depends on the glass content, other factors for example (i) coal chemistry; (ii) burning conditions; and (iii) collection system at individual power stations significantly influence this. In general, fly ash from a single source gave high glass contents with increasing fineness (noted in Section 4.1.4) and thus greater reactivity.

5.8.2 'True' glass content measurements

X-ray diffraction (XRD) can be used for fly ash glass content determination by quantifying its crystalline content and subtracting from the total mass. However, it is arguably incorrect to count material other than crystalline as glassy (reactive). A novel method described by Font *et al.* (2010) may give a more reliable assessment for the glass content of fly ash based on XRD. Figure 5-72 shows an example of data (Fly Ash H) using this method. Fly ash was mixed with glass material ($d_{90} < 50 \mu\text{m}$; at level of 25, 50, 65, 75, and 90%) and the amorphous compositions (balance of Rietveld mineral content) extrapolated to zero glass addition to measure the 'true' glass content.

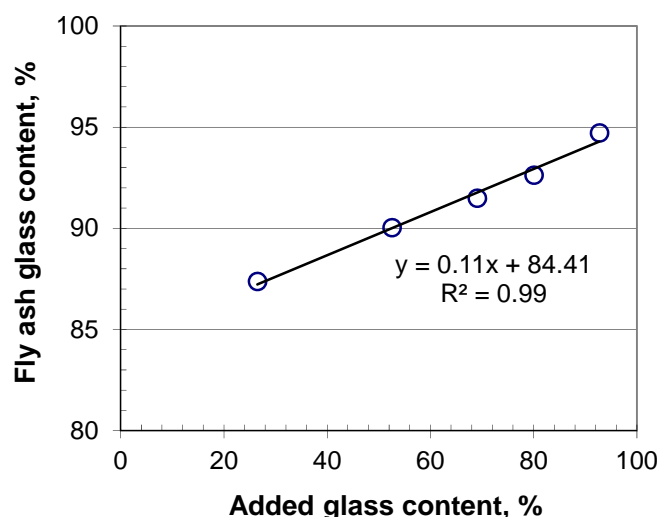


Figure 5-72. Calculation of 'true' glass in fly ash H by extrapolating to zero added glass

The obtained glass content was then compared with the activity index of the fly ashes. As shown in Figure 5-73 (a), it is apparent that there was no correlation between the 'true' glass content and activity index both at 28 and 90 days. This is very similar to the data presented earlier in Figure 5-70 with fly ashes from various sources and considering different production conditions. A closer examination revealed that finer fly ashes gave higher reactivity even though their true glass content was found to be less than some coarse fly ashes. The determination of the crystalline content in D NSTI was not good enough to predict its true glass content, probably due to its high LOI.

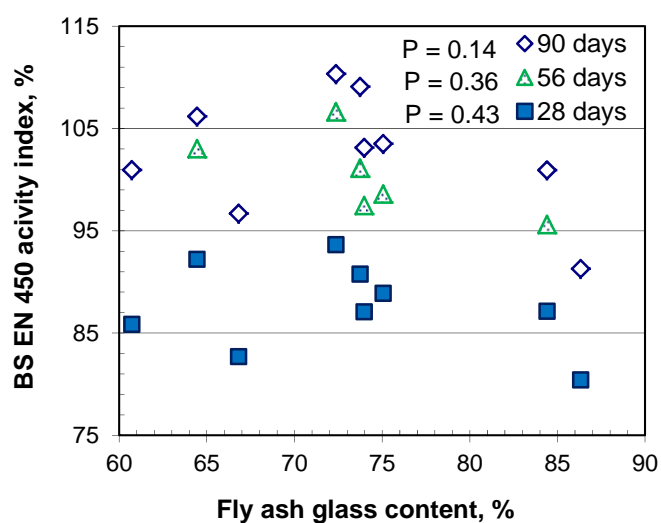


Figure 5-73. Relationships between fly ash 'true' glass content and BS EN 450 activity index

5.9 Heat of Reaction with Quicklime

The European standard BS EN 459-2 (Section 5.10; BSI, 2010b) describes a test method for assessing the reactivity of building lime. A modification of this test method was considered for measuring that of fly ash. The approach compared the heat released from 50 g of lime and 25 g of fly ash added to 300 ml of de-ionized water in a heat insulated vessel to that of a 75 g lime only sample (reference). Figure 5-74 shows test results of 18 fly ash samples. No correlation was observed between the BS EN 450 activity index and heat release (percentage of the reference lime-only test). To check the validity of this test method, repeat measurements were made using limestone powder instead of fly ash.

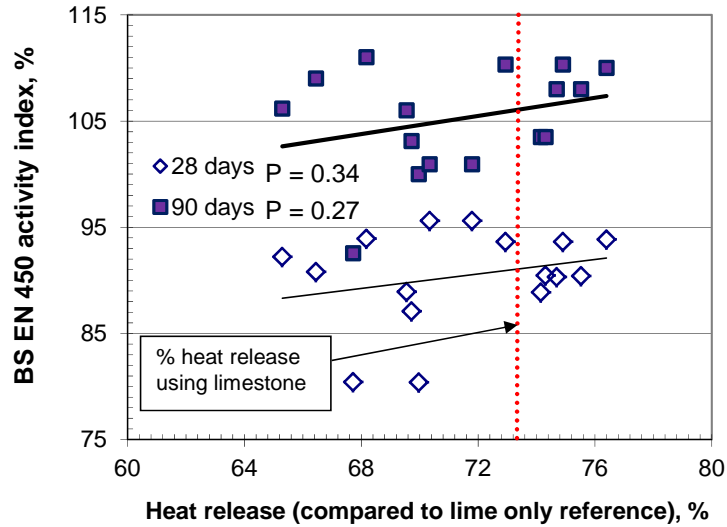


Figure 5-74. Relationship between heat release of slaking lime/fly ash and BS EN 450 activity index

Figure 5-75 shows the time – temperature curve for reference lime only and where part of this was replaced with limestone (very fine fly ash (E UF) and coarse (D STI)). Minor differences were observed between the tests with limestone and the fly ashes. The heat release with limestone is shown as a dotted line in Figure 5-74. It was observed that few fly ashes gave higher levels of heat release than that of the test with limestone powder. This test therefore appears unlikely to be sensitive enough to give differences in fly ash reactivity.

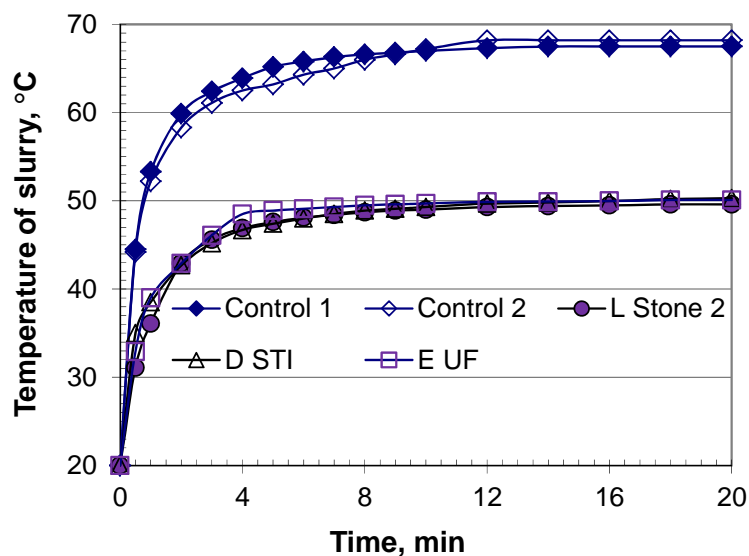


Figure 5-75. Temperature variations with time for selected fly ash/lime

5.10 Summary of Findings

This Chapter dealt with pozzolanic reactivity assessment of fly ashes. Tests were carried out to evaluate the effectiveness of various test methods for this. Pozzolanicity test results were compared with relevant material properties.

The carbon-removed and oxy-fuel fly ashes gave different behaviour than the other materials tested in this project. Although the fresh properties of carbon-removed materials were improved, their reactivity still depended on their fineness. The oxy-fuel fly ashes were obtained from trial burning and therefore, might not represent the conditions at full-scale. During these trials, the degree of coal pulverisation and burning conditions were expected to vary producing 3 distinctive types of materials.

Both physical and chemical properties of the PCs influenced how the material behaved in a cementitious system. Fresh properties of fly ash mortars varied with the fineness of PCs, while tests were carried out with the same set of fly ashes and other test conditions remained same. Although the particle size of carbon-removed fly ash was relatively larger, those gave higher flow with all PCs tested. The water requirement of fly ashes gave very good correlations with their corresponding flow.

Tests with the main fly ashes gave increases in flow with decreasing particle size and LOI. The opposite was found in the case of air-classified finer components, although the finest sub 10 μm fraction gave comparable flow with the control PC mortar. There appeared to be an optimum fineness ($d_{90} \sim 40 \mu\text{m}$) to give maximum flow considering the grading of PC, standard sand and fly ash. This was confirmed by MIP tests and suggested an optimum fineness range gave lower porosity than the finest component and feed raw fly ash at early ages, where porosity is mainly dominated by packing action. Mortar tests with different levels of the finest fly ash indicated 20% of the material in the matrix would give best fresh property.

Activity index test results with PC-based mortars showed dependency on the properties of the test PC. The reactivity of fly ash alumino-silicate components in mortar systems appeared to depend on the rate of lime release by hydration and, therefore, PC with higher

C₃S content gave higher activity index, although fineness of PC is another influencing factor on this process.

Fly ash fineness gives a good indication of its reactivity, regardless of its fresh properties. Various means of fineness measurements (viz. 45 µm sieve residue, sub 10 µm quantity and PSD parameters) correlated well with the activity index in PC-based mortars. Using various levels of the finest fly ash component in mortar, it was found that 20% of the material gives similar strengths to the PC control mortar, while 10% gives 11% higher strength at 28 days. These suggest that 20% of the finest fly ash can potentially deal with early strength gain issues and also give better flow than PC control samples, although the strength is expected to increase at later ages.

Tests with accelerated curing suggested that being sensitive to temperature, fly ash reactivity can be enhanced greatly and therefore, this approach can be used for reactivity assessment in a relatively short time period. It is possible to estimate longer-term results with standard curing from accelerated short-term curing. It was also noted that the effect of temperature was more prominent on finer fly ashes. To match the strength gain rate in standard and accelerated curing conditions, a limited number of tests were carried out and suggest that Sadgrove's equation for maturity can be applied to these with a modification. Further work would be necessary to establish this for a wider range of fly ashes.

To try and reduce the variability of test result with PC-based mortar, hydrated lime was used in mortar tests. Several modifications to the original ASTM C593 (ASTM, 2011b) test procedure including test temperature, period and fine aggregate type were considered. This gave good relationships between fly ash properties and strength of mortars, however, the strength gain rate remained comparatively slower than PC-based mortars.

Reactivity analysis from mortar strength tests could be affected by properties of the materials used (e.g. sand and fly ash grading), therefore, tests were carried out with fly ash/PC paste. Levels of Ca(OH)₂ were determined using TGA and the results gave a good inverse correlation with the fly ash fineness and also good proportional correlations with activity index in mortar tests with the same PC.

Given fly ash reactivity tests with mortar can be influenced by the type of PC and packing, two alternative approaches were tested. The Frattini test traditionally gives a qualitative pass-fail type assessment of fly ash. Further analysis showed good correlations of the remaining CaO with fly ash properties and their activity index, with few exceptions. Therefore, this approach can be considered for quantitative assessment of the material. Attempts were made to reduced test variability that can originate from the type of PC used by using laboratory grade saturated lime. Use of high temperature gave some promising results, but it did not correlate well with activity index, indicating unsuitability of this method for pozzolanicity determination.

Fly ash chemical compositions were analysed in various ways (PPI, sum of major oxides, components other than crystalline) and correlated these with activity index. These gave some indication of how the materials could behave in a cementitious system but the relationships were not very strong with the corresponding activity index in mortar. Considering the effect of fineness of fly ash, the relationships improved and among these the sum of major oxides/d₅₀ consistently gave the best correlations with 28, 56 and 90 days activity index.

Heat release from the reaction between quick lime and fly ash was considered and found to be unsuitable for assessing the reactivity of the material.

CHAPTER 6: FLY ASH/AEA INTERACTION ASSESSMENTS

This Chapter is concerned with the sorptivity properties of fly ash with regard to air-entrainment in concrete. In particular, it is focussed on establishing reliable test techniques for distinguishing behaviour between different fly ashes. Foam index test reliability was improved by employing an automatic shaker to standardise the effect of shaking effort on test results and thereby operator judgement. Acid blue 80 (AB80) dye tests using spectroscopic determination thereby eliminating operator influence and the Methylene blue (MB) dye test was also considered. The results are compared with fly ash properties (e.g. LOI, specific surface area) related to sorptivity of AEA and also between tests. Finally, the reliability of these results was compared with mortar tests (AEA dose required to obtain target air-contents).

6.1 Foam Index Tests

6.1.1 Manual shaking

The initial part of the study was concerned with evaluating the foam index test procedure, and essentially followed that described in FHWA-HRT-06-080 of the US Department of Transportation (Taylor *et al.*, 2006). The mixture was prepared with 8.0 g, 2.0 g and 25.0 ml of PC, fly ash and de-ionized water respectively, i.e. half the proportions described by Taylor *et al.* (2006), with a $\varnothing 40$ mm \times 110 mm (round bottom) centrifuge vial being used.

Initially, water and fly ash were combined in the vial, and ultrasonic dispersion applied for 5 minutes to minimize agglomeration. PC was then added and the vial shaken vigorously by hand for 1 minute. Following this, AEA was introduced, but rather than applying by 'dropper', as described in guidance (e.g. GRACE, 2006; Taylor *et al.*, 2006), a calibrated variable volume pipettor (10-100 μ l) was used to dispense precise quantities. The mixture was then similarly shaken for 15 s following the addition of each AEA increment. In the early stages, the admixture is adsorbed by the unburned carbon present in fly ash. With

increasing doses and continued shaking, the active sites of carbon become saturated by the AEA and then a stable foam is formed. The end point of the test is reached when the foam covers the whole surface of the liquid in the vial for 45 s.

Three commercial AEAs (AEA C1, AEA C2 and AEA C3) and a standard reagent (AEA S) were used during the study. To fix the AEA dose increment, initial experiments were carried out with various concentrations of the AEAs and the fly ashes of lowest and highest LOI. Based on this, appropriate dilution factors were established such that at least 3 – 4 and 20 – 22 doses were required to achieve the end point during testing. A 0.01 mol/l solution of AEA S was used, while dilution factors of 1%, 10% and 10% were adopted for those with AEA C1, AEA C2 and AEA C3 respectively. The foam index was then expressed with respect to their original concentration, enabling comparisons of the effect of the AEAs on fly ash to be made.

As noted above, little guidance on shaking during the test is given, other than it should be applied for a fixed period of time (Dodson, 1990; Folliard *et al.*, 2009). A series of tests were, therefore, initiated in which 10 operators carried out foam index tests (with 15 s of manual shaking) for fly ashes D STI, E UF and F CC, with a 20 µl increment of AEA S (0.01 mol/l, using a freshly prepared sample). The operators were all familiar with laboratory testing of cement-based materials and received basic training with the method. The principal (single) operator also determined the foam index of fly ash E UF daily over a 10-day period, to quantify the variation associated with an individual carrying out the test.

Table 6-1 shows the results and statistical parameters from these tests. These indicate that each operator always gave the same ranking for the fly ashes in terms of their AEA demand. However, the range varied from 60 to 380 µl for D STI and F CC (i.e. differences of 3 to 19 increments) to achieve the end-point between operators. The corresponding coefficients of variation were 27.0 and 19.6%. The test conditions were the same for each operator, except for the degree of shaking applied, which is likely to have been different. As noted above, judgement of the end point is based on visual assessment and could also have contributed to these results. When the single operator tests were considered with fly ash E UF, the range was 60 µl and the coefficient of variation was reduced by approximately 50%, to 11.6%.

Table 6-1. Operator variability of foam index* test results by manual shaking

TEST NUMBER	DIFFERENT OPERATORS			SINGLE OPERATOR
	D STI	E UF	F CC	E UF
1	80	200	560	200
2	80	180	380	220
3	100	220	560	180
4	60	160	480	200
5	60	180	480	200
6	120	260	760	160
7	60	140	480	200
8	100	240	660	220
9	120	220	620	220
10	80	280	620	160
Mean	86	208	560	196
Range	60	140	380	60
SD	23	45	110	23
COV, %	27.0	21.4	19.6	11.6

*Values are in μl (AEA S concentration 0.01 mol/l)

SD: standard deviation; COV: coefficient of variation

Note: All operators were experienced in testing cement-based materials and received basic training with the method.

This series of tests demonstrates the influence of the operator and materials on the foam index and highlights why this may be unreliable. However, the more consistent conditions and greater experience of the single operator indicate that improved precision is likely to be achievable.

In order to use the method for evaluating AEA/fly ash interaction, initial foam index tests were carried out by manual shaking by the single operator on selective fly ashes. The results obtained from the standard reagent AEA S and commercial AEAs (AEA C1, AEA C2 and AEA C3) are shown in Table C-1 (Appendix C). These were then compared against fly ash markers of AEA adsorption (e.g. LOI, specific surface area). Figure 6-1 shows the relationships between the foam index, fly ash specific surface area (measured by N_2 adsorption (Brunauer *et al.*, 1938); *Quantachrome Nova 3000e*) with foam index using AEA S and the other commercial AEAs. The results indicate that a better correlation of foam index was obtained with specific surface area than LOI of the fly ashes. Overall these

confirm suitability of the test for assessing AEA/fly ash interaction given the test would be carried out by the same operator. However, using different operators the test gave higher variability and therefore, an automatic shaker was considered and the results are discussed in the following section.

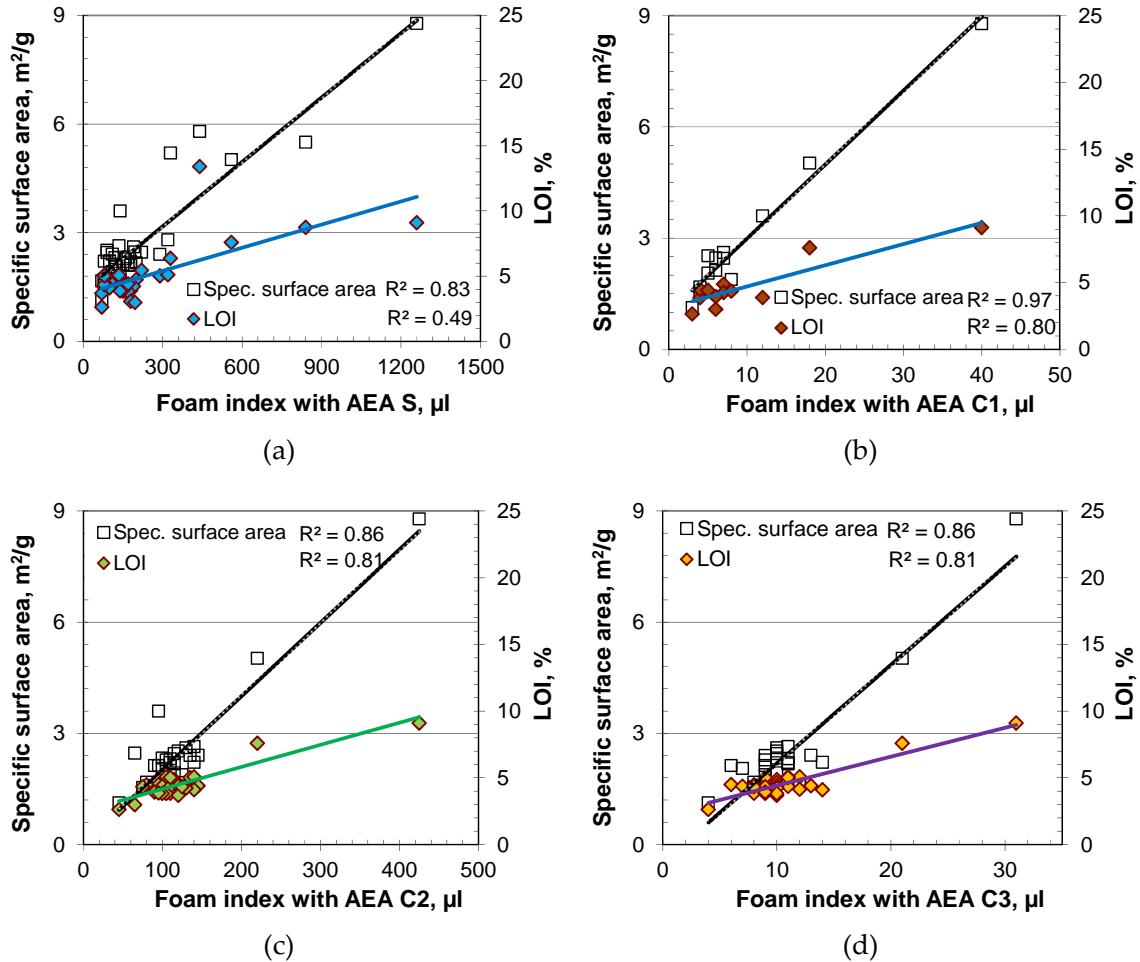


Figure 6-1. Relationships between foam index, specific surface area and LOI (manual shaking): (a).AEA S; (b) AEA C1; (c) AEA C2; and (d) AEA C3

6.1.2 Automatic shaking

A digital laboratory automatic shaker (IKA MS3 digital vortex mixer) was considered for this work. The motion of the shaker was circular in a horizontal plane, with an agitation stroke of 4.5 mm, and allowed control of the rotational speed and period of application. A laboratory-prepared rectangular block of lightweight plastic was fitted to the head of the automatic shaker, where the vial was placed during testing. In order to examine the

behaviour of the automatic shaker, trials were carried out on selected materials (D STI and AEA S) at various speeds (1000, 1300 and 1500 revolutions per minute, rpm) and shaking times (mainly 13 to 35 s). During these, initial ultrasonic dispersion was applied as described earlier and mixing of PC/fly ash/water carried out at the above speeds for a fixed number of revolutions (1300). As with manual shaking, AEA increments were added until a stable foam was formed.

The results shown in Figure 6-2 indicate that the foam index was influenced both by speed of shaking and number of revolutions applied (shaking time). In all cases, reductions in foam index were achieved by extending the shaking time. At 1000 rpm, the foam index tended towards a limiting value of 120 μl after 850 revolutions. In contrast at 1300 and 1500 rpm, a limiting value of approximately 80 μl was achieved at about 550 revolutions.

The results, therefore, highlight the effect of the shaking speed and its duration on the foam index. These suggest that the variability noted between operators carrying out the test manually, as indicated in Table C-1 (*Appendix C*), was likely to be, at least in part, the result of their shaking at different speeds. This then brings into question the prescription of a fixed time period for shaking, although beyond a certain minimum speed and time, there was less effect on the results. Differences were also noted with regard to the visual appearance of samples, depending on the shaking method used, as shown in Figure 6-3.

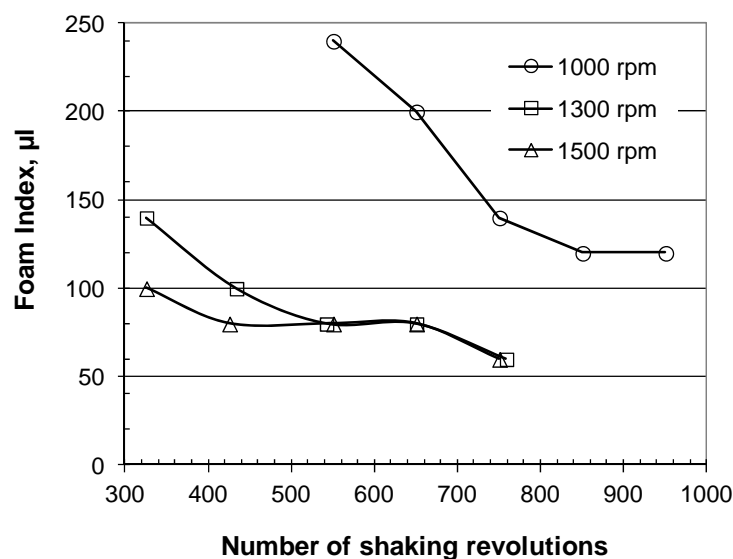
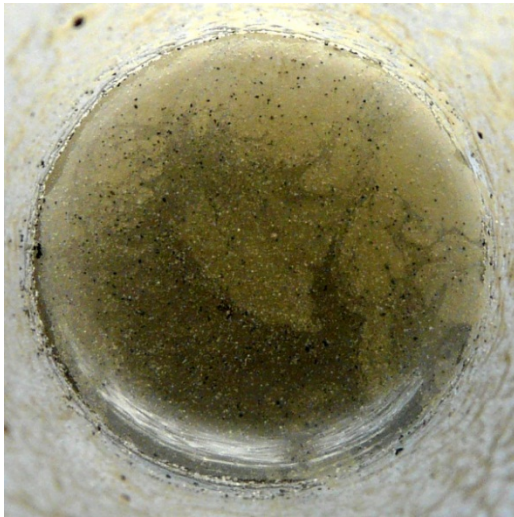
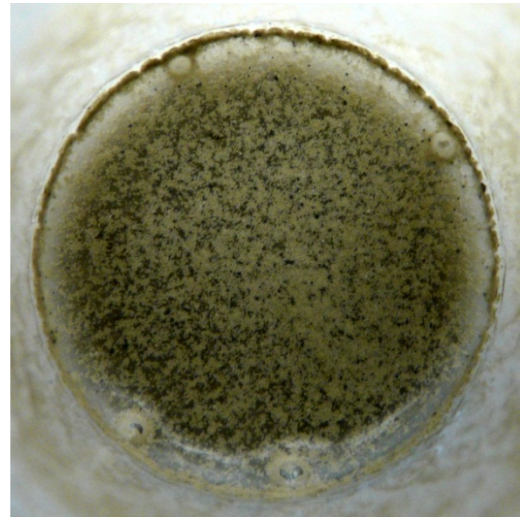


Figure 6-2. Influence of automatic shaker speed and duration on foam index (Fly Ash D STI and AEA S)



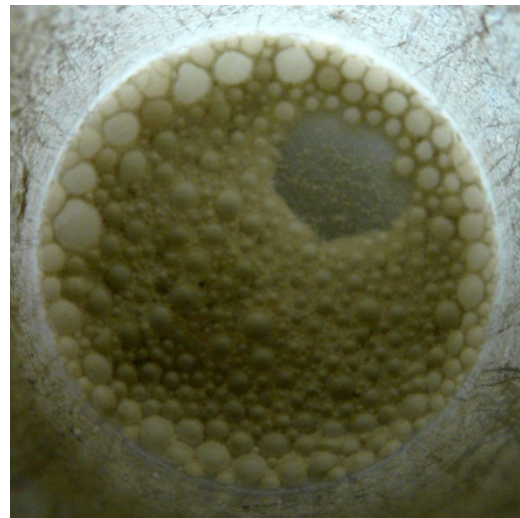
(a) PC/fly ash/water/before adding AEA



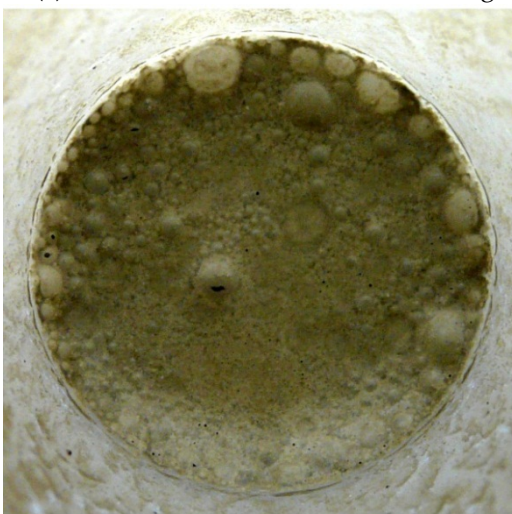
(b) after first AEA dose and shaking



(c) unstable foam with manual shaking



(d) unstable foam with automatic shaker



(e) stable foam with manual shaking



(f) stable foam with automatic shaker

Figure 6-3. Various stages of the foam index test with manual shaking and automatic shaker (at 1300 rpm)

This highlights the more variable appearance following manual shaking of the samples, compared to the uniform and larger bubble foam at different stages of the test with the automatic shaker. The requirement for the end point was therefore more easily identified with the automatic shaker, and hence likely to reduce operator influence.

Having identified the role of the shaking parameters and influence of the automatic shaker on the end point observation, tests were carried out with different fly ashes (D STI and F CC) and AEAs (AEA S and AEA C1) at 1300 rpm. The results are shown in Figure 6-4 and indicate a reduction in foam index with increased shaking time and that beyond 25 s (542 revolutions) the effect was minor, with similar type behaviour noted for the different materials. Therefore, further foam index tests with the automatic shaker were made at 1300 rpm, with shaking time steps of 25 s.

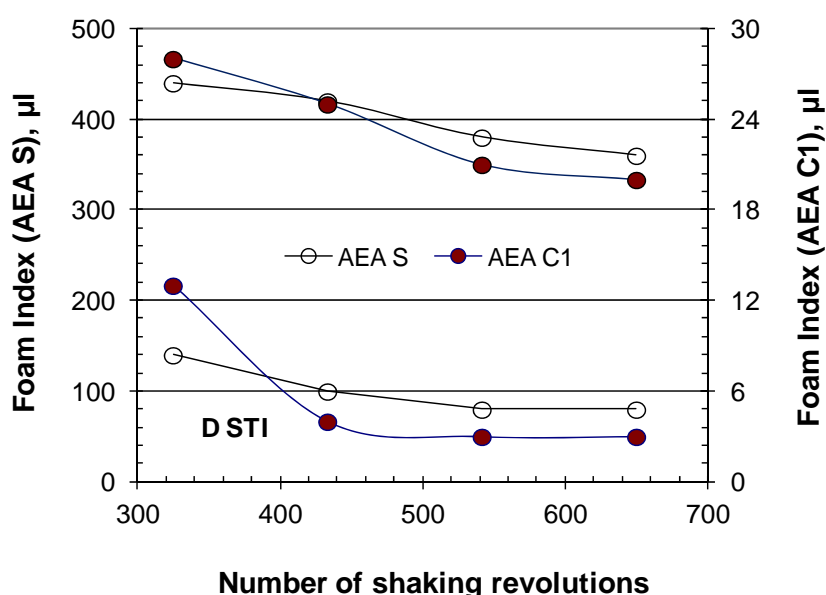


Figure 6-4. Influence of number of shaking revolutions (time) on foam index at 1300 rpm for different fly ashes and AEAs

With suitable working conditions for the automatic shaker established, tests with the same 10 operators and materials used during the manual shaking series were repeated with this device. The principal operator also carried out the test 10 times following the same procedure. Table 6-2 shows the data from these measurements, while Figure 6-5 makes a comparison of the coefficients of variation obtained for manual shaking and automatic shaker between operators.

Table 6-2. Operator variability of foam index* tests with the automatic shaker

TEST NUMBER	DIFFERENT OPERATORS			SINGLE OPERATOR
	D STI	E UF	F CC	E UF
1	80	152	380	160
2	80	200	380	140
3	100	160	420	160
4	80	160	420	140
5	100	160	400	140
6	80	160	300	180
7	80	140	320	140
8	80	140	340	160
9	80	140	420	160
10	80	140	320	140
Mean	84	155	370	152
Range	20	60	120	40
SD	8	18	46	14
COV, %	10.0	11.8	12.5	9.2

*Values are in μl (AEA S concentration 0.01 mol/l)

SD: standard deviation; COV: coefficient of variation

Note: All operators were experienced in testing cement-based materials and received basic training with the method.

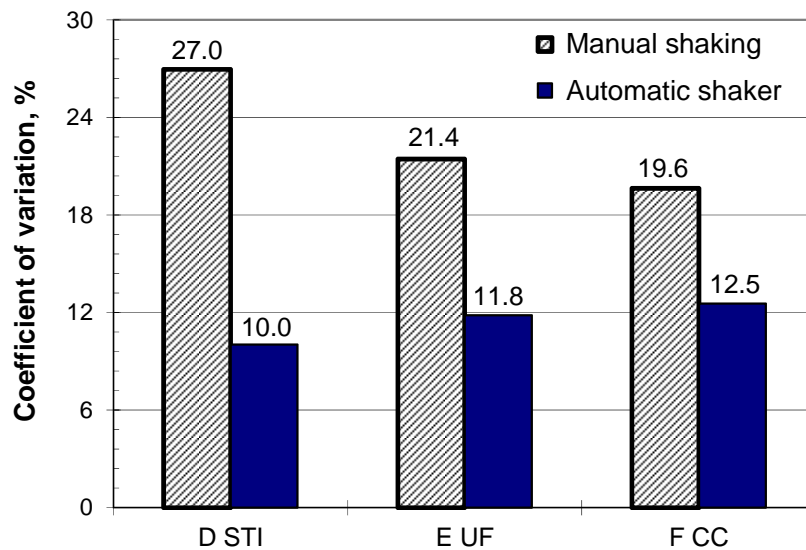


Figure 6-5. Comparison of foam index coefficients of variation for manual shaking and automatic shaker between operators

In this case, the foam index ranges to achieve the end point between operators were 20 and 120 μl for D STI and F CC (i.e. differences of 1 to 6 increments). The foam index with the automatic shaker also reduced the corresponding coefficients of variation by approximately 50% on average compared to manual shaking. For the single operator this reduced from 11.6 to 9.2% between manual and automatic shaking.

Comparing the variation between the different and principal operators, some benefits were obtained by the latter, as might be expected. Overall, however, the automatic shaker significantly reduced operator influence on the test results. It is possible that further improvements in the variability of the foam index test could be achieved by, for example, modifying the AEA concentration and/or size of increments added.

6.1.3 Fly ash property/AEA effect

Given the reduced variability established with the foam index test, the study progressed to examine this, using the automatic shaker for the wider range of fly ashes and AEAs. Figure 6-6 shows relationships between the foam index, fly ash specific surface area and LOI.

A strong correlation was noted consistently between the specific surface area and foam index for each AEA and the 20 fly ashes considered, where the values of R^2 ranged from 0.91 – 0.95. The correlation of foam index with LOI was less ($R^2 = 0.78 - 0.79$). Fly Ashes C ROS and D NSTI were excluded from the correlation as they did not follow the general trend due to the presence of a significant portion of relatively coarse carbon. The results, therefore, highlight the role of the characteristics of carbon, as reflected by the specific surface area, in relation to foam index measurements, rather than the more general indication of this given by LOI, as noted elsewhere (Külaots *et al.*, 2003; Spörel *et al.* 2009).

With the manual shaking process (Section 6.1.1, single operator) the corresponding range of R^2 values obtained between foam index (using different AEAs) and specific surface area ranged from 0.83 – 0.97. In contrast, to the results obtained with the automatic shaker, the relationships were not consistent with all AEAs under consideration. It is also noted that the tests with manual shaking were carried out with different operators, which might cause variations in the degree of shaking applied and this again highlights the benefit of the foam index test with the automatic shaking device.

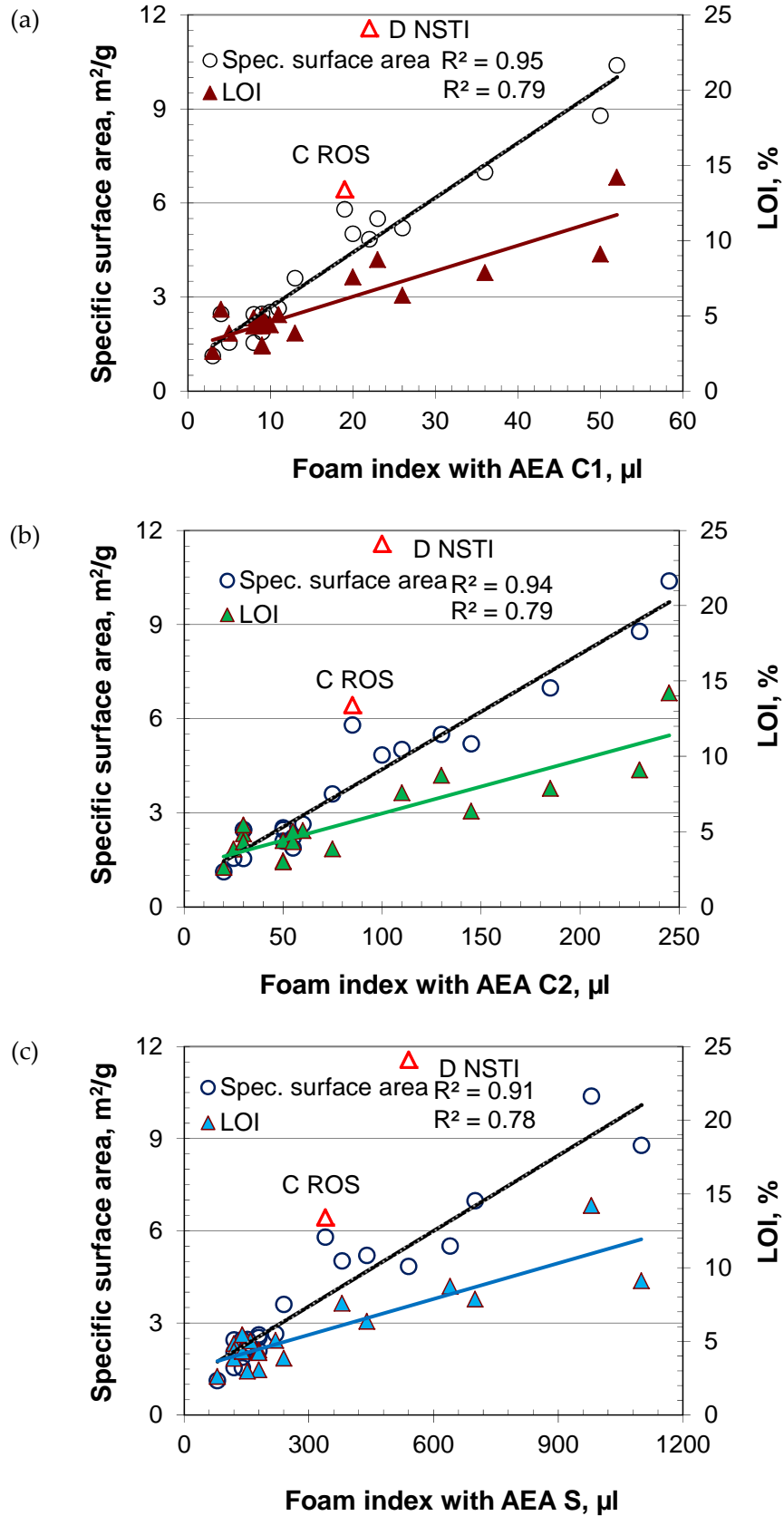


Figure 6-6. Relationships between foam index (using automatic shaker), specific surface area and LOI of fly ashes: (a) AEA C1; (b) AEA C2; and (c) AEA S (points in red not included in the regression analysis)

The results shown in Figure 6-7 indicate that the uptake of AEA C2 was approximately 5 to 6 times higher than that of AEA C1, reflecting the formulation of the latter for use with fly ash. On the other hand, the foam index with AEA S (at 0.01 mol/l) was approximately 4 times that of AEA C2. Overall, the results indicate consistent behaviour with regard to the ranking of fly ashes between AEAs using the automatic shaker and that there is potential for using a standard reagent during the test as an alternative to commercial AEAs, as suggested previously (Külaots *et al.*, 2003; Pedersen *et al.*, 2008; Spörel *et al.*, 2009).

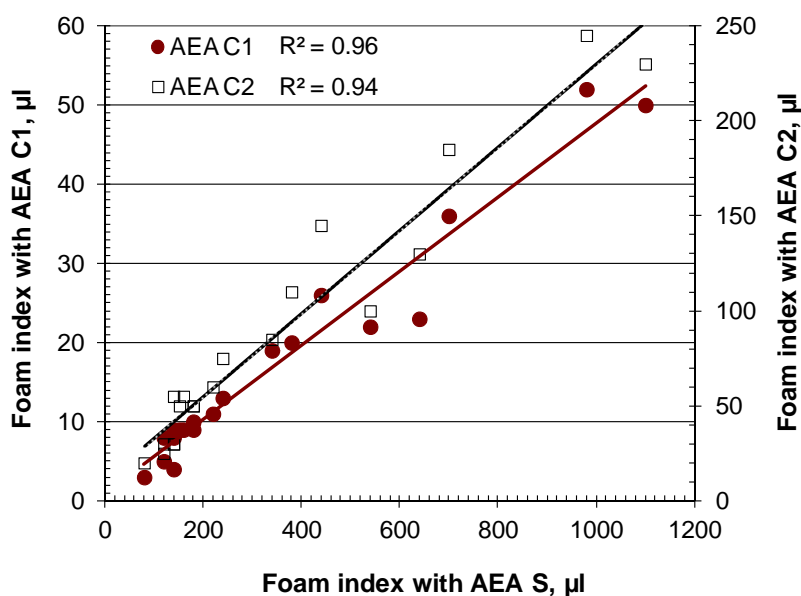


Figure 6-7. Relationships between foam index of fly ashes (using automatic shaker) with standard reagent and commercial AEAs

6.2 Acid Blue 80 Tests

The sorptive nature of fly ash suggests that an alternative method for establishing fly ash/AEA interaction may be possible through the application of dye adsorption tests from other fields (Section 2.3.2; e.g. Choy *et al.*, 2000, Hameed *et al.*, 2007; Zhang and Nelson Jr., 2007). According to Choy *et al.* (2000), adsorption of a single sorbate follows the Langmuir sorption isotherm, providing (i) adsorption energy between the sorbate and adsorption surface is equal for each site; (ii) no interaction between the sorbates; and (iii) equal competition between sorbate species for each sites. Given the instrumental basis of the dye adsorption approach, which eliminates operator influence, this section describes a

study carried out to investigate its feasibility (using a simple spectroscopic method) to establish fly ash/AEA interaction for use in air-entrained concrete.

The AB80 test adopted is based on spectrophotometric determination of the absorbance of this chemical reagent in solution (Hameed *et al.*, 2007; Zhang and Nelson Jr., 2007; ASTM, 2008b). In principle, a certain quantity of fly ash was exposed to an AB80 solution of known concentration. This was mixed (by magnetic stirrer at 400 rpm) for a suitable time period to achieve equilibrium conditions (i.e. no further dye uptake by fly ash) and then filtered with a cellulose filter paper of nominal pore size 11 μm . At least three measurements were made and the average used to calculate the remaining concentration of AB80 in solution after adsorption by fly ash carbon. Assuming that the active sites of fly ash are saturated by AB80, the difference between the original dye concentration in solution and that in the filtrate, expressed in mg per gram of fly ash, is defined as the AB80 adsorption.

6.2.1 Equipment and calibration

The absorption spectrum of an AB80 aqueous solution is given in Figure 6-8. The dye solution gives peak absorbance values at three different wavelengths (cf. 626, 581 and 282 nm). A digital colorimeter (*Fisher Scientific, Colorimeter Model 45*) with an absorbance measurement range from 0.00 – 1.99 and a resolution of 0.01 was considered for these measurements. The device used fixed wavelength filters.

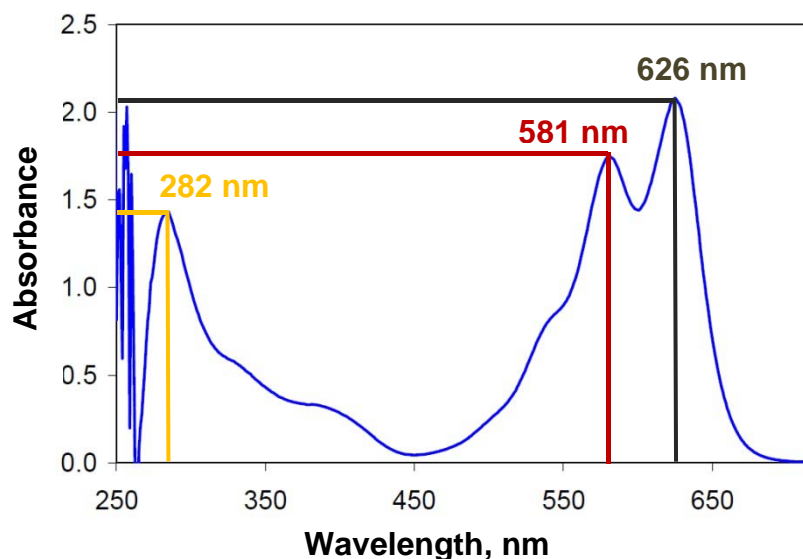


Figure 6-8. Wavelength scan of standard AB80 solution (after Zhang and Nielson Jr., 2007)

Given the wavelength spectrum, suitable filters for absorbance measurements were 580 nm and 630 nm (closest to the two main peaks). Initial tests using a range of known solutions indicated that 630 and 580 nm filters could measure a concentration range up to approximately 85 and 200 mg/l, respectively. Overall, however, the sensitivity at 580 nm was poorer than that at 100 mg/l. Hence, subsequent tests used an initial concentration of 100 mg/l AB80 and the 630 nm filter. According to Zhang and Nelson Jr. (2007), the alkalinity of the test solution has little effect on absorbance test results ($\pm 2\%$ variation), therefore, this was not considered in this study.

A calibration curve was constructed, using the 630 nm filter, and was found to be practically linear in the measurable range up to 85 mg/l. The relationship, shown in Figure 6-9, was then used to calculate the concentration of AB80 remaining in solution from the absorbance measurements by the colorimeter.

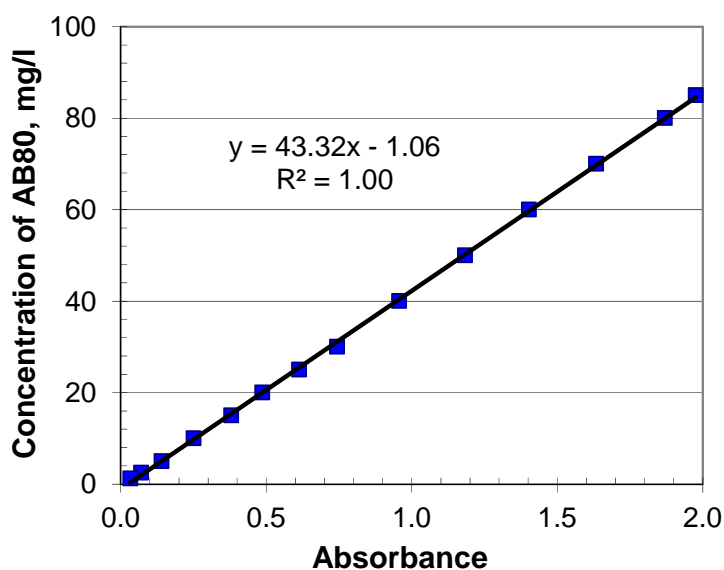


Figure 6-9. Calibration curve of AB80 solution

6.2.2 Adjustment for AB80 adsorption by filter paper

It was noted that the filter paper used during the test adsorbed a small quantity of AB80 from the mixture during the filtration process, reducing the remaining concentration. Therefore, several known concentrations of AB80 solution were filtered and the absorbance values determined using the relationship given in Figure 6-9. The necessary adjustment for adsorption by the filter paper was established by relating the AB80 concentration before

and after filtration, as shown in Figure 6-10, and this equation applied during subsequent tests.

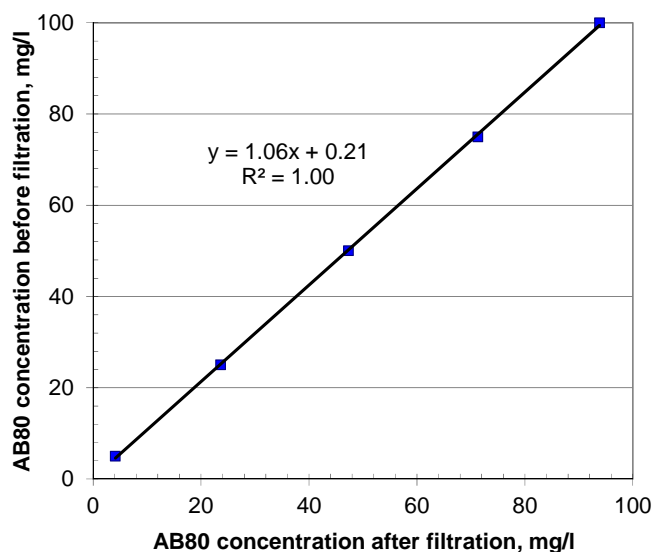


Figure 6-10. Estimation of AB80 adsorption by filter paper

6.2.3 Fly ash sample size

To set the test sample size, Fly Ashes D STI and H (lowest and highest LOI in the material range for this test) were considered. Initially, 2.0 g of fly ash were exposed to 100 ml dye solution (100 mg/l) for 30 minutes and indicated minimal adsorption by Fly Ash D STI, while the filtrate from Fly Ash H had a very low concentration of AB80. Therefore, to further examine this, tests were carried out using different sample sizes with Fly Ashes D STI (2.0, 3.5 and 5.0 g), F CC (1.0, 2.0 and 3.0 g) and H (0.5, 1.0 and 2.0 g).

The adsorption results from these tests are shown in Figure 6-11. In the case of Fly Ash H, the 2.0 g sample size (concentration of filtrate: 1.8 mg/l) gave a significantly lower AB80 adsorption than those of 0.5 and 1.0 g. Similar results were found for the 3.0 g sample of F CC (remaining concentration 5.2 mg/l). However, there was little change in results between 1.0 and 2.0 g samples. These effects did not occur with D STI, where only minor changes in adsorption were obtained between 2.0, 3.5 and 5.0 g.

Given the above, it appears that there is an optimum sorbate concentration range that should be attained following exposure to fly ash, i.e. approximately 10 – 85% of the original

solution concentration. It was, therefore, decided to generally adopt a fly ash sample size of 2.0 g. However, in cases where the remaining concentrations were less than 10 mg/l (10% of the original solution) the test was repeated with half the sample size (1.0 g). For very low adsorption fly ash (remaining concentration in filtrate > 85 mg/l), a follow-up test was made by doubling the fly ash quantity (i.e. with 4.0 g). This ensured that a reasonable reduction in concentration of the AB80 solution occurred. A colour comparison between the original stock solution and those after exposure to different sorptive fly ashes (with de-ionized water (DIW-blank) also shown) is given in Figure 6-12.

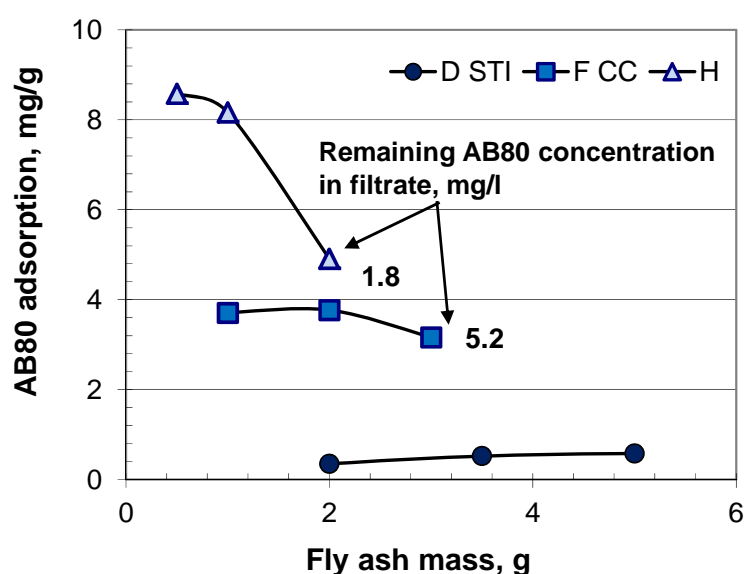


Figure 6-11. Effect of fly ash sample size on AB80 adsorption

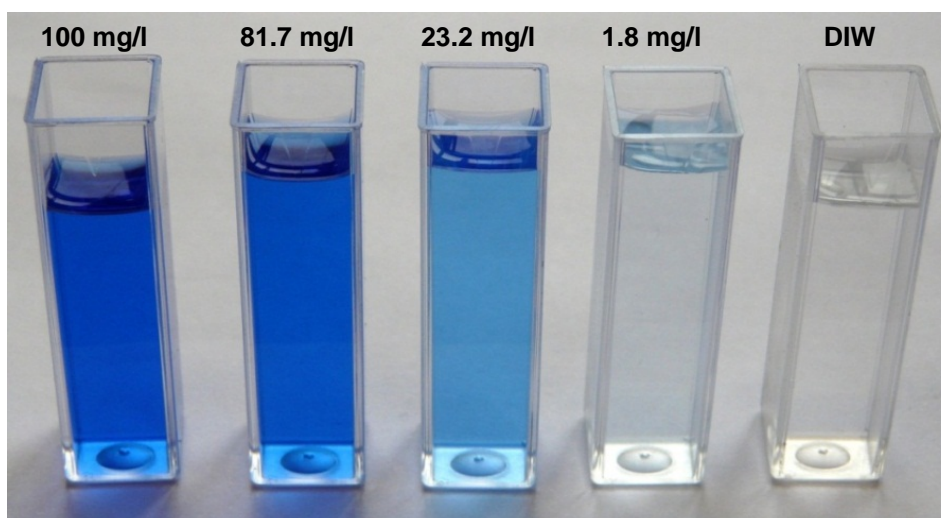


Figure 6-12. AB80 stock solution and filtrates after exposing to various fly ashes

6.2.4 Contact time

In order to examine variations in adsorption with contact time, the same set of fly ashes (D STI, F CC and H) was exposed to AB80 solution for 10, 20, 30 and 60 minutes. As shown in Figure 6-13, clear differences between materials were apparent at 10 min. It was also noted that very minor changes in adsorption occurred for low LOI Fly Ash D STI over the test period. However, where this was higher (Fly Ashes F CC and H), up to 30 minutes were required before reaching a constant value (equilibrium). A contact time of 60 minutes was used during subsequent tests to ensure equilibrium conditions and saturation of active fly ash carbon by the AB80 dye was achieved.

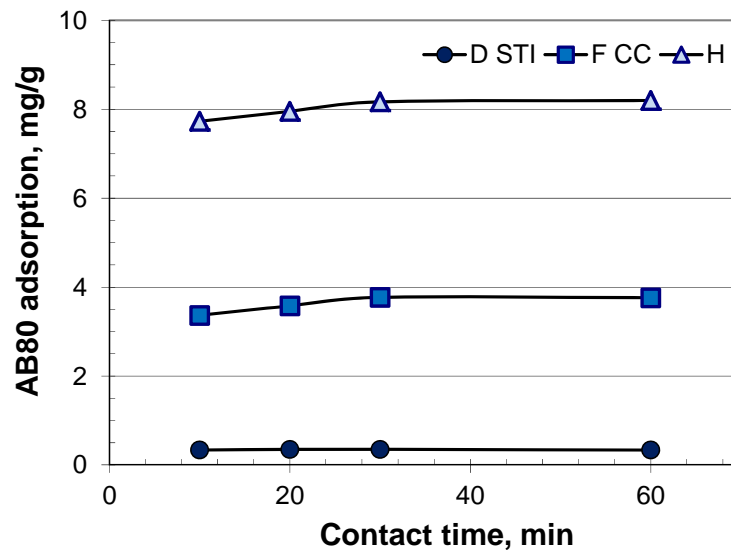


Figure 6-13. Effect of contact time on AB80 adsorption by fly ash

6.2.5 AB80 adsorption for evaluating fly ash/AEA interaction

From the initial tests, suitable conditions were identified, as described above, for carrying out measurements and the study progressed to investigate the potential of the AB80 adsorption technique as a means of evaluating air-entrainment in fly ash concrete. During this, comparisons were made between AB80 adsorption and parameters recognised as markers of fly ash/AEA interaction (including LOI, specific surface area (measured by N₂ adsorption) and foam index; using 15 general and 14 air-classified fly ashes) and admixture doses necessary to achieve target air contents in mortar and concrete (using 6 fly ashes, with LOIs ranging from 2.6 to 7.6%).

LOI

The correlation between AB80 adsorption and the LOI of the fly ashes is shown in Figure 6-14 and indicates general agreement between properties. The parent feed sample did not follow the general trend of air-classified samples and are indicated separately (see Figure 6-14 (b)). The parent fly ashes gave relatively lower sorptivity as expected from their LOI because they included a significant portion of coarse carbon which was not as adsorptive as the fine part. This was also noted earlier (Section 3.1.3, Figure 3-13) where the parent fly ashes gave lower specific surface area compared to their classified samples and in relation to their LOI. Similar effects of LOI were noted on foam index test results earlier, and this again highlights that estimation of sorptivity of fly ash from LOI could be misleading, especially for fly ashes with coarse carbon.

Although ASTM C618 (ASTM, 2012) and BS EN 450-1 (BSI, 2005c) permit the use of fly ashes of LOI up to 6.0% and 9.0% (Category C) respectively in concrete, difficulties associated with air-entrainment using fly ash have been noted even for LOI as low as 3.0% (Freeman *et al.*, 1997). Indeed, several studies suggest that LOI is not an effective means of estimating the adsorption characteristics of fly ash during air-entrainment (Hill *et al.*, 1997; Freeman *et al.*, 1997; Külaots *et al.*, 2004).

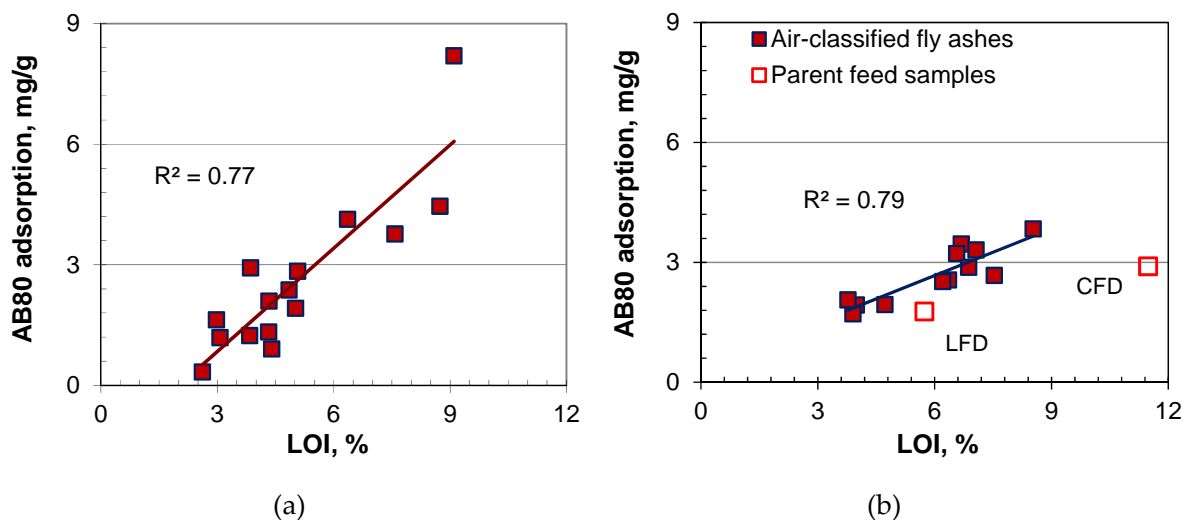


Figure 6-14. Relationship between fly ash LOI and AB80 adsorption. (a) general fly ashes used in the project; and (b) air-classified fly ashes. Points with empty rectangles are not included in the regression analysis.

While LOI provides a measure of carbon present in fly ash, as noted in the literature review, it is factors including a) the specific surface area; b) accessibility to this; and c) its chemical nature (Gao *et al.*, 1997; Freeman *et al.*, 1997; Yu *et al.*, 2000; Külaots *et al.*, 2004) that affect adsorption. Recent research by Spörel *et al.* (2009) suggests that, of these, the specific surface area of carbon has greatest influence on adsorption.

Relationships with specific surface area and foam index

The relationships of AB80 adsorption with specific surface area and foam index (with standard and commercial AEA's), i.e. all involving adsorption measurements on solid surfaces are shown in Figures 6-15 and 6-16, respectively. These represent the quantity of AB80 or AEA required to saturate the active carbon sites/N₂ to form a monolayer on fly ash.

In the case of N₂ adsorption, Külaots *et al.* (2004) have reported that the surface area of the carbon part (30 - 400 m²/g) is up to several hundred times higher than that of the mineral part (0.7 - 0.8 m²/g) of fly ash, which indicates that although the carbon is present in relatively small quantities, its contribution to the specific surface area is substantial. In addition, depending on the porosity of carbon, its specific surface area varies significantly, while the mineral part is almost constant for different fly ashes.

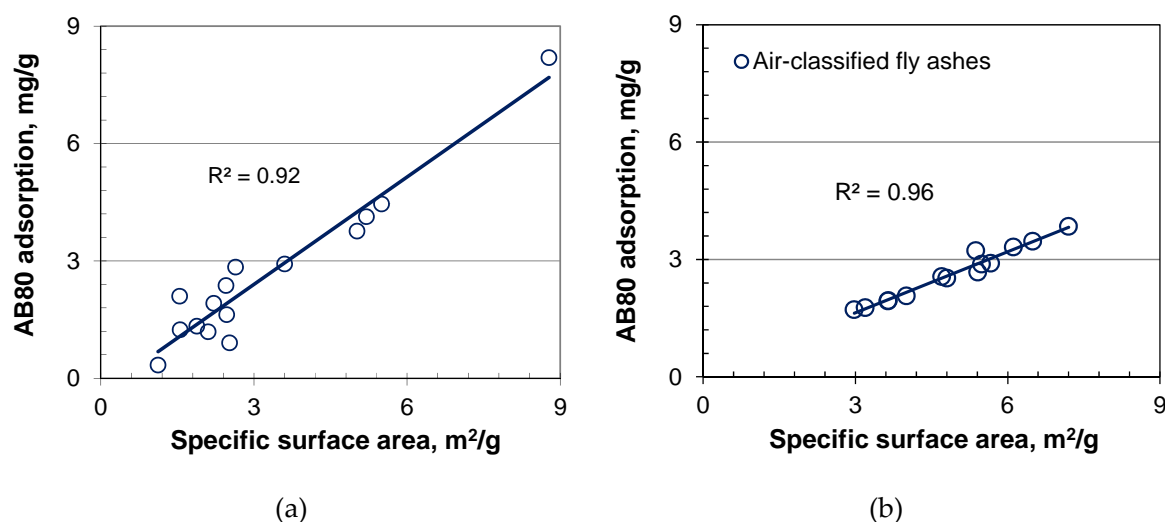


Figure 6-15. Relationship between fly ash specific surface area and AB80 adsorption

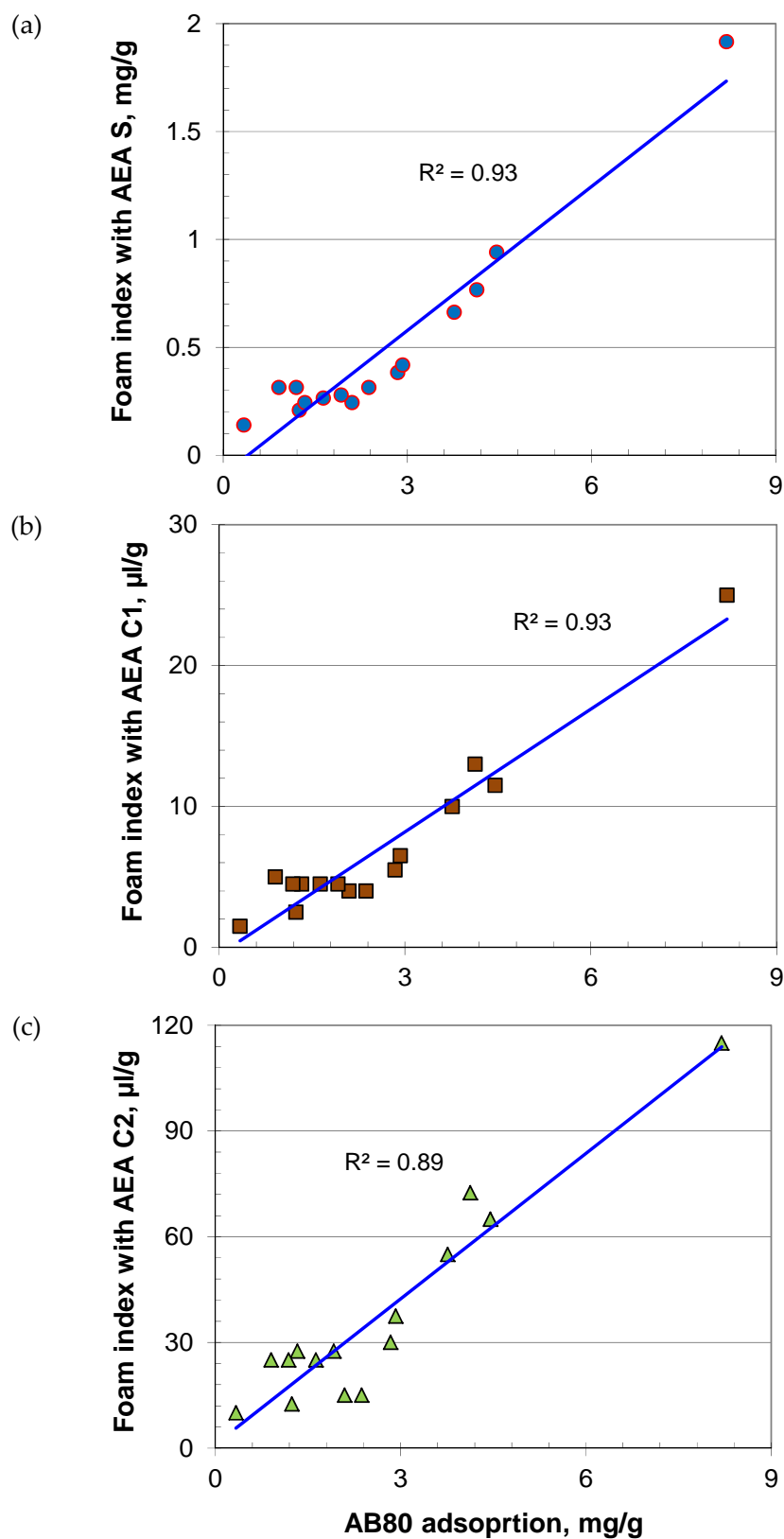


Figure 6-16. Relationships between AB80 adsorption and foam index
(a) AEA S; (b) AEA C1; and (c) AEA C2

Strong correlations ($R^2 = 0.92$ and 0.96 for general and air-classified fly ashes, respectively) were obtained between the AB80 adsorption and N_2 specific surface area of fly ash. Although the LOI of the parent feed sample of the air-classified fly ashes did not reflect their adsorption properties, those fitting very well in the regression analysis with AB80 adsorption and specific surface area, indicate the significant role of the later in the adsorption process. These also suggest that it is possible to estimate the surface area of fly ash from AB80 adsorption for a particular set of materials.

By removing coarse carbon particles ($> 80 \mu\text{m}$) from the original fly ash, Sporel *et al.* (2009) found a minor effect on foam index results. This suggests that coarse carbons are relatively solid in nature and make minor contributions to the specific surface area and thus adsorption process, while they still contributes to the overall LOI. This is why the parent feed fly ashes (especially CFD where coarse carbon is almost 55-66% as indicated in Section 4.1.2) LOIs did not give good correlations with their specific surface area and AB80 adsorption.

Similar correlations ($R^2 = 0.89 - 0.93$) were also obtained (Figure 6-16) between the AB80 adsorption and foam index as it was between the specific surface area and the former (with the main fly ashes). These results suggest some insensitivity of the foam index test at low AB80 adsorption for AEA C1 and AEA S, which may be due to the increment size used during the former test. However, these gave a slightly better correlation than AEA C2, reflecting greater variability of this general purpose admixture in the foam index test. Overall, the results indicate the potential of the AB80 adsorption to evaluate fly ash/AEA interaction.

6.3 Methylene Blue Tests

The Methylene blue (MB) test is a dye test traditionally used for the determination of levels of harmful fines in aggregates and described in European standard BS EN 933-9 (BSI, 1999a). The test is used here for AEA sorptivity determination of fly ash carbon. This is similar in principle to the foam index test. A 200 g fly ash sample was mixed in 500 ml of de-ionized water and then the slurry stirred continuously using a propeller-type stirrer. After 5 minutes of mixing, 5 ml of known concentration (10.0 g/l is recommended in the

standard) methylene blue dye is added to the slurry and a stain test carried out on filter paper. Formation of successive stable stains in the form of a halo (see Figure 3-16) at 1 and 5 minute indicates the end point of the test. The methylene blue value (MB value in g/kg of fly ash) of the sample is calculated from the total uptake of the dye to reach the end point.

A set of 40 fly ashes were tested with this method. The relationships between methylene blue value with specific surface area and LOI are shown in Figure 6-17. A very good correlation between MB value and specific surface area was obtained. However, as found from earlier tests (foam index and AB80 adsorption) it did not correlate so well with the LOI of the fly ashes.

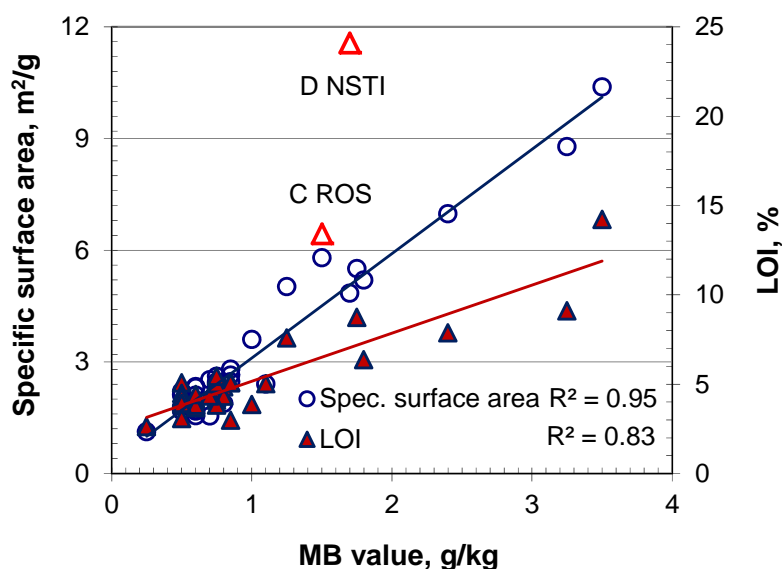
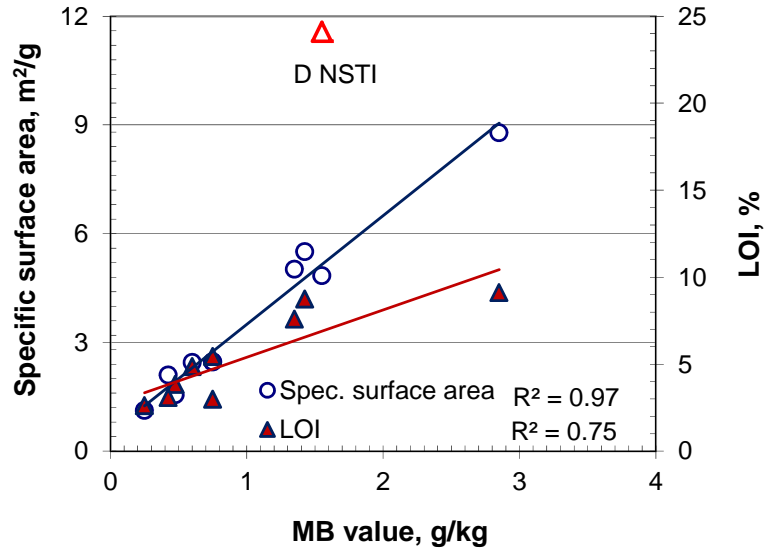


Figure 6-17. Relationships between MB value (10.0 g/l), specific surface area and LOI of all fly ashes. (points in red not included in the regression analysis)

The concentration of methylene blue dye (10.0 g/l) specified by the standard seemed to be too high to determine relative differences in the adsorption of fly ashes precisely, especially those with low adsorption. Therefore, a set of 10 fly ashes were tested with 5.0 g/l methylene blue dye solution. As shown in Figure 6-18, a minor improvement in correlation between the MB value and specific surface area was found with the lower concentration dye. As shown in Figure 6-19, with a 5.0 g/l solution a lower MB value was obtained in most cases, with greater accuracy. Another factor that could influence the results with the test is operator judgement, but this should not have a significant effect, as detection of the endpoint is reasonably clear.



6.3.1 MB value and foam index

As with AB80 adsorption, the MB dye test also supported the results obtained from the foam index test with the automatic shaker (using both standard and commercial AEAs) as shown in Figure 6-20. Results obtained with 20 fly ashes were compared. A very good correlation ($R^2 = 0.96 - 0.98$) between the MB value and foam index was obtained, with the commercial AEA C1 giving the best results. These data indicate the potential of this test method for evaluating fly ash/AEA interaction.

6.4 Air – entrainment in Mortar

In order to investigate the foam index test (with the automatic shaker) and the use of AB80 adsorption and MB value with regard to estimating fly ash/AEA interaction, the next stage of the study examined the behaviour of the materials considered above (selectively, A-S Jan, C-S Jan, D STI, E UF, E EN1 and F CC; and AEA S, AEA C1 and AEA C2) in a cementitious system, initially mortar. Tests were carried out to determine the required AEA dose to entrain a target air content (5-6%).

Initially AEA doses were estimated based on the foam index of the particular fly ash. Following this, trials were made to determine required quantities of AEA to achieve the target air content. Figure 6-21 shows the variation in mortar air content in relation to AEA C2 dose for the fly ash mortars. This indicates that the effect of a change in admixture dose reduced with increasing LOI of fly ash. For AEA C1 and C2, their original (as-supplied) concentrations were used. However, with AEA S (0.01 mol/l) significantly higher doses were required than with the commercial AEAs. Therefore, to avoid changes in water/cement ratio, the same quantity (by mass) of water was taken out of the mix as AEA S added.

6.4.1 Foam index and mortar AEA dose

Figure 6-22 shows the relationship between the AEA dose required to achieve the target air content (5-6%) in mortar, the foam index of the fly ashes and their specific surface area, for the three AEAs. Both foam index and specific surface area gave very good correlations with the AEA dose required to entrain the target level of air in mortar, with the former generally giving slightly better coefficients of correlation.

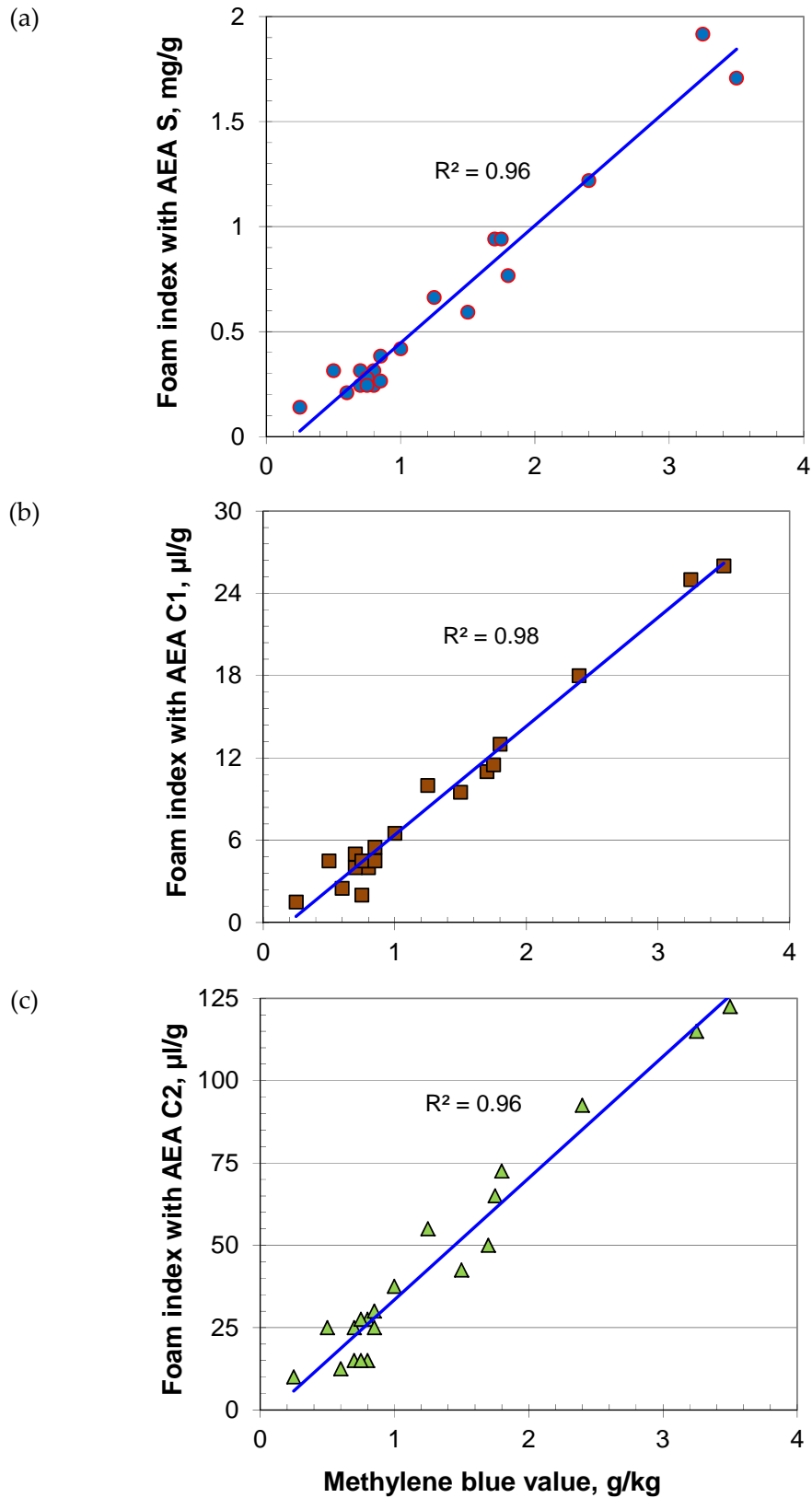


Figure 6-20. Relationships between MB value and foam index (a) AEA S; (b) AEA C1; and (c) AEA C2

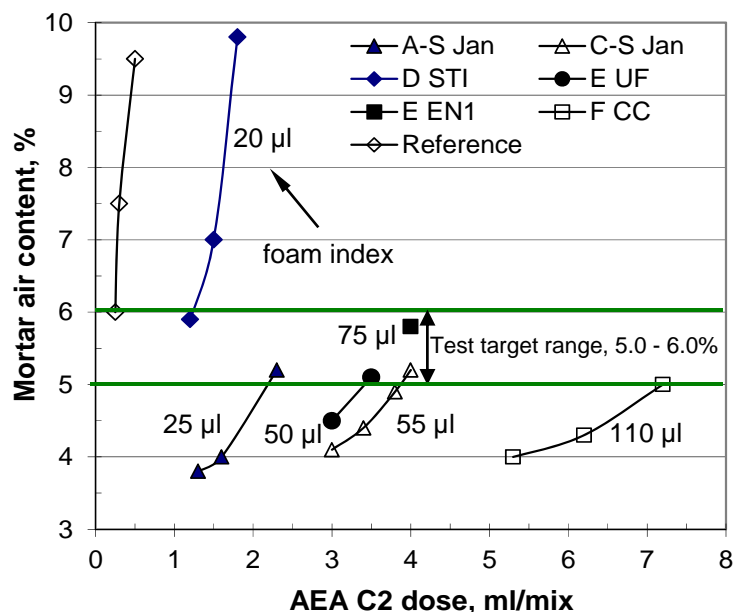


Figure 6-21. AEA C2 dose and mortar air content relationships for selective fly ashes

As discussed above, there are several factors that influence air-entrainment in fly ash mortar and while the specific surface area has an important role on the process, the foam index is also likely to reflect some of the other effects noted (e.g chemical nature of the surface) and hence provides a better evaluation of their air-entrainment characteristics.

6.4.2 AB80 adsorption and mortar AEA dose

Figure 6-23 shows the relationship between admixture doses required to achieve the target air content (5 – 6%) in mortar and their AB80 adsorption. The dose for AEA S and AEA C1 gave very good correlations with AB80 adsorption, while this was slightly poorer for AEA C2. This generally agrees with the relationships noted for these admixtures with the foam index.

A closer examination of the data illustrates several issues associated with the air-entrainment process in fly ash mortar. Indeed, with fly ash, a component of the admixture is adsorbed in addition to the entrainment of air. Given the AB80 test is a measure of adsorption capacity, the ordinate intercepts in Figure 6-23 indicate the quantity of admixture necessary to entrain the target air content if no adsorption occurs.

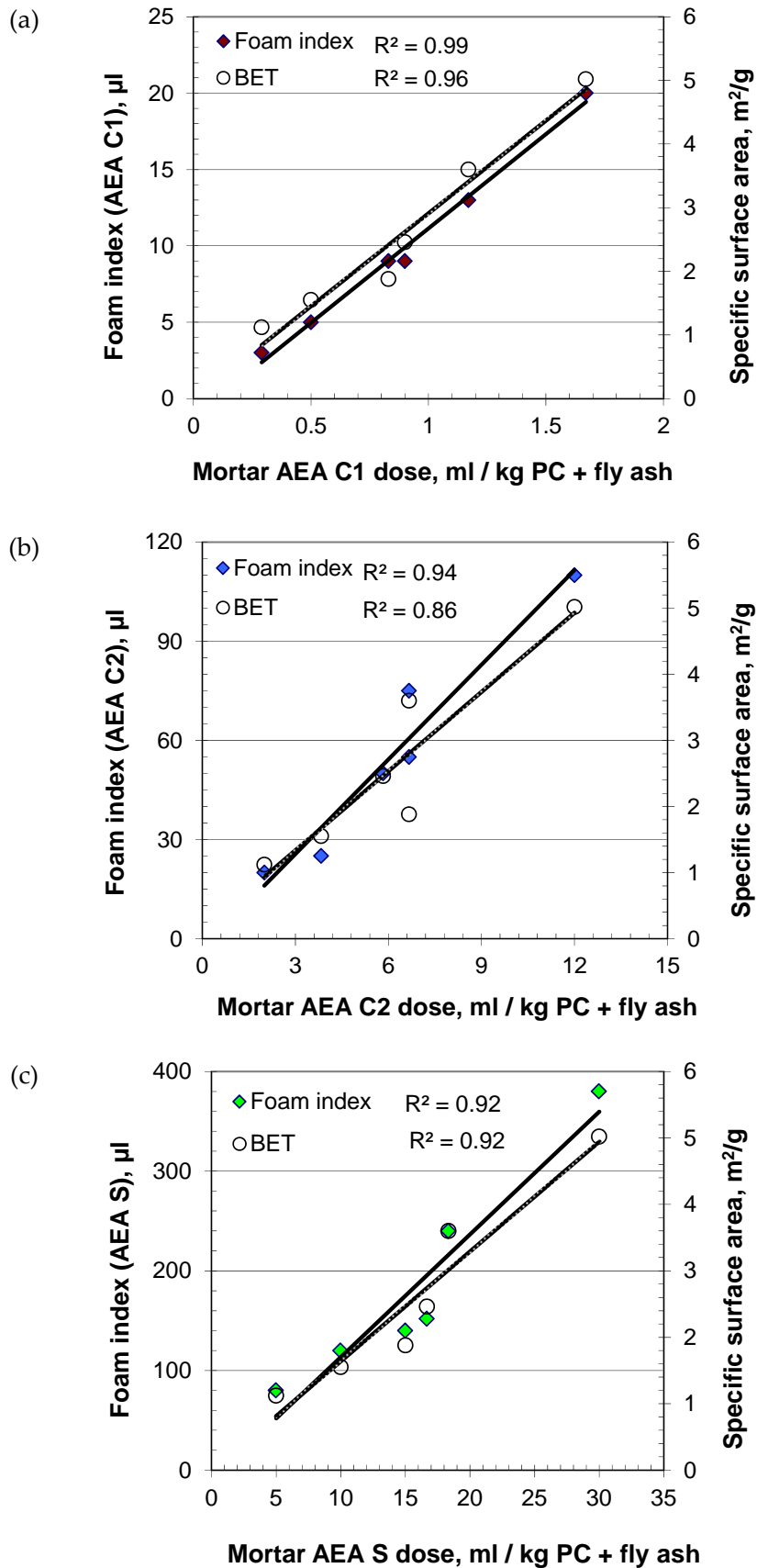


Figure 6-22. Relationships between mortar AEA dose, foam index and specific surface area of selective fly ashes: (a) AEA C1; (b) AEA C2; and (c) AEA S

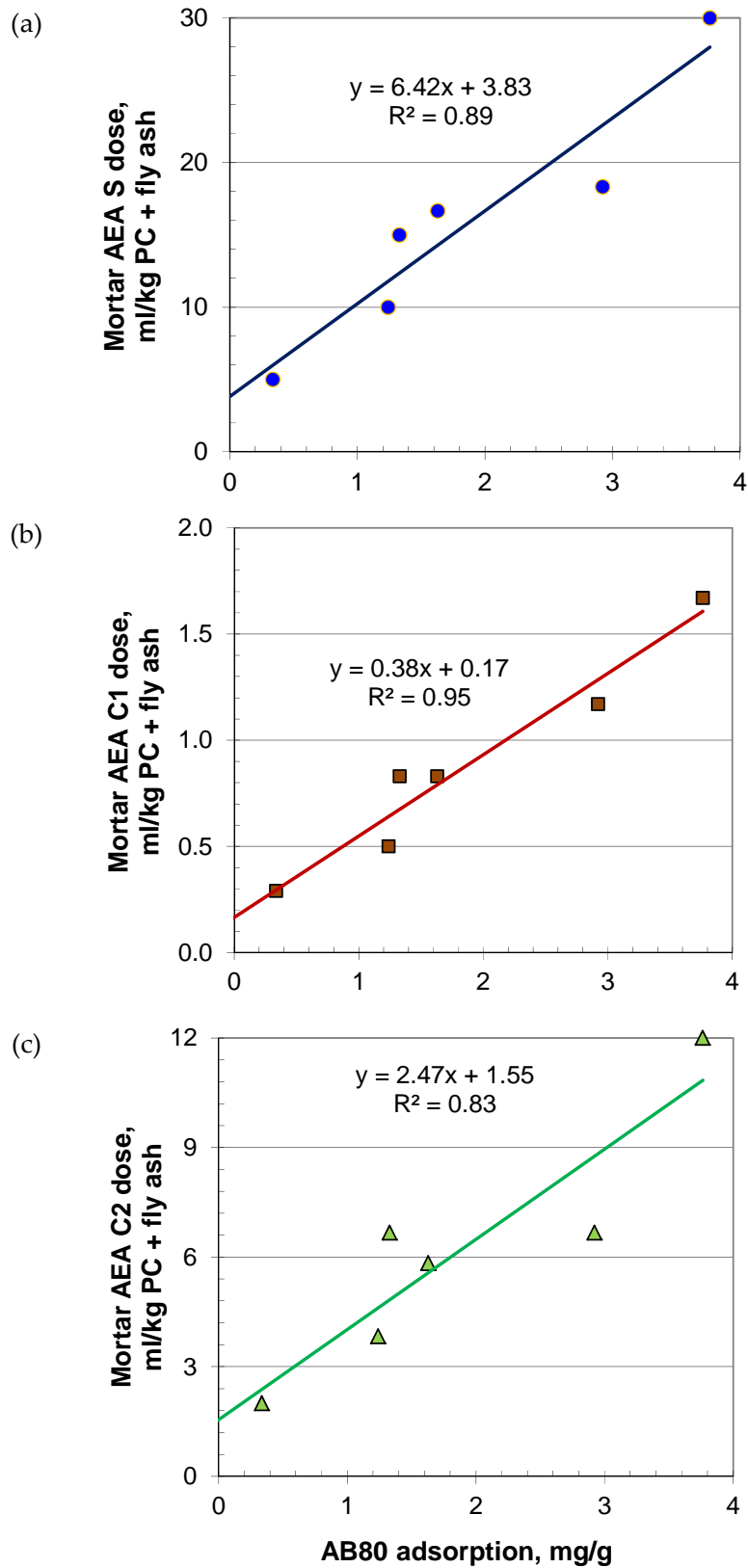


Figure 6-23. Relationships between AB80 adsorption and mortar AEA dose (a) AEA S; (b) AEA C1; and (c) AEA C2

The gradients of the lines in the figure represent the quantity of AEA necessary to achieve the target air content with changing adsorption components (due to fly ash) in the mix. It is also apparent that in some cases, the part adsorbed by carbon in fly ash is several times that required to entrain the target air content.

The differences in doses required between AEAs for the fly ashes and air content are likely to depend on the concentration of active chemical components in the admixtures and their molecular size. It is expected that with an increasing or decreasing target air content in the mortar mix, the ordinate intercept would change accordingly, but the gradient of the line would remain essentially unchanged (for a given set of fly ashes and AEA).

6.4.3 Methylene blue value and mortar AEA dose

Figure 6-24 shows the relationship between AEA dose required to achieve the target air content (5 – 6%) in mortar and their MB value. With all three AEAs very good correlations were obtained. Again, the relationship with AEA C2 was slightly poorer than with the other admixtures.

Compared to the AB80 adsorption relationship with AEA dose, a significant difference was noted with regard to the axis intercept. The relationship intercepted the abscissa rather than the ordinate found for AB80 adsorption. This highlights the necessity of adjusting the dose increment to ensure the minimum quantity of dye is present in the mixture for end point identification compared to that required to saturate the carbon surface. The test otherwise indicates potential for evaluation of fly ash/AEA interaction.

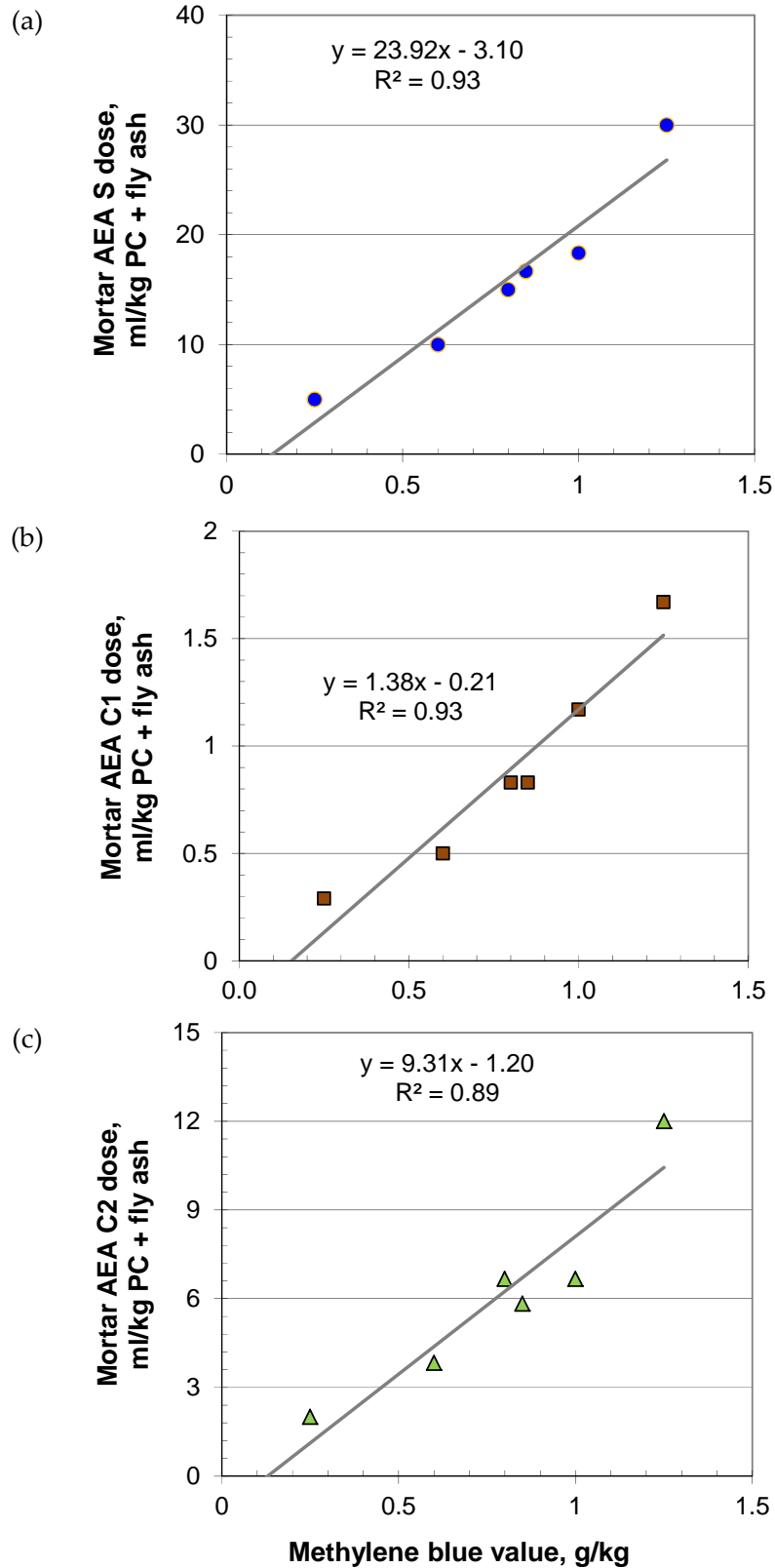


Figure 6-24. Relationships between MB value and mortar AEA dose
(a) AEA S; (b) AEA C1; and (c) AEA C2

6.5 Summary of Findings

6.5.1 Foam index tests

- Following a typical foam index test procedure by manual shaking, the coefficients of variation between test results of ten operators using 3 fly ashes with LOIs up to 7.6% were found to range between 19.6 – 27.0% for the same conditions, while that for a single operator was 11.6%. This suggests that the foam index test could be used as a means of evaluating interaction between AEA and fly ash in cementitious systems, but different operators can give inconsistent results.
- Using an automatic shaker it was found that changing the shaking speed over a fixed time period can give significant differences in foam index. This also applied when extending the shaking time at a fixed speed. However, there appeared to be a minimum shaking speed and time (1300 rpm and 25 s in the tests carried out) beyond which there was little change in foam index.
- With the automatic shaker, the foam produced during the test was more uniform in appearance and of larger bubble size than by manual shaking, making visual judgement of the end point easier.
- When applying the test conditions established, the automatic shaker reduced the coefficients of variation for the foam index, between operators, by around 50% compared to those of manual shaking, with slight reductions also noted for the single operator.
- The foam index obtained using the automatic shaker was found to give a very good correlation with fly ash specific surface area (N_2 adsorption), which was better than that with the bulk LOI of the material. Similar effects were noted for the two commercial AEAs and standard reagent considered.
- Tests carried out on fly ash mortars indicate that the foam index determined using the automatic shaker gave very good correlations with the dosage requirements to entrain a target quantity of air. Again the effects noted were similar between the commercial AEAs and standard reagent used.

6.5.2 Acid blue 80 tests

- From the colorimetric test, a very good linear relationship was found between the concentration of AB80 solution (approximately 0-85 mg/l) and absorbance value (0.00-1.99) with a 630 nm filter. Therefore, it was possible to use this to determine the concentration of AB80 in solution.
- Initial tests indicate that a balance of AB80 quantity and fly ash sample size needs to be established to ensure an appropriate concentration of dye (10-85 mg/l) remains after exposure, particularly in the case of high / low sorptive material. In general, a combination of 2.0 g fly ash in 100 ml of 100 mg/l AB80 solution was satisfactory. However, in some cases, it was necessary to modify the quantity of fly ash used to achieve the target range and hence improve the reliability of the test.
- Contact times as short as 10 minutes could give the relative ranking of fly ash adsorption between samples. In the case of high carbon fly ash, 30 minutes was necessary to reach equilibrium. No difference in AB80 adsorption was found between 30 and 60 minutes exposure.
- Applying the test conditions identified, the AB80 adsorption was found to give general agreement with LOI. However, very good correlations were obtained with fly ash specific surface area (by N₂ adsorption) and foam index. On average, 1 mg AB80 was adsorbed per m² surface area of fly ash.
- The results from tests on fly ash mortars gave very good correlations between AB80 adsorption and the dose required to entrain target quantities of air. Furthermore, the data could be used to identify the air entraining/adsorption components of the AEA when used with fly ash in these systems.

6.5.3 Methylene blue tests

The test results provided very good relationships with foam index and the AEA dose required to entrain a target quantity of air in fly ash mortar. Refining the dose increment could improve the potential of this test as a method for evaluating fly ash/AEA interaction.

CHAPTER 7: VALIDATION OF REACTIVITY AND SORPTIVITY ASSESSMENT WITH CONCRETE

This Chapter covers validation of fly ash assessment test methods in concrete. Compressive strength results obtained from standard 100 mm cube were used to assess fly ash pozzolanic reactivity. AEA doses required to entrain specific quantities of air were related with sorptivity test results. Initial surface absorption test (ISAT) and depth of water penetration under pressure were measured to assess effect of air-entrainment in fly ash concrete.

7.1 Reactivity Assessment in Concrete

7.1.1 Fresh properties

The fresh properties of concretes using the main fly ashes and air-classified fly ashes are shown in Tables 7-1 and 7-2 respectively. It should be noted that tests with the main fly ashes were carried out with PC HR52, while PC HK52 was used for those with air-classified fly ashes (both 52.5 N category from the same supplier, but different source) but with the same mix proportions. A relatively wide variation in slump (20-90 mm) was noticed with the main fly ashes, compared to that of air-classified samples (25-65 mm). This may be due to the relatively low slump for the reference sample with PC HK52 (40 mm) than PC HR52 (65 mm). The cause of these may be the higher fineness of PC HR52 ($d_{90} = 36.6 \mu\text{m}$) than PC HK52 ($d_{90} = 47.5 \mu\text{m}$), as found earlier during the mortar tests (Section 5.1.1).

For the main fly ashes, slump increased with fly ash fineness and decreasing LOI, as found during the mortar tests. Carbon removed Fly Ash D STI (LOI = 2.6%) gave highest slump, while run-of-station Fly Ash C ROS (LOI = 13.6%) gave lowest. As with mortar flow, at the same w/c ratio, the slump of air-classified fly ash gave the opposite trend with fineness, but this was within a relatively narrow range.

Table 7-1. Fresh properties of concretes (main fly ash; PC HR52)

SAMPLE	SLUMP, mm	PLASTIC DENSITY, kg/m ³
Reference	65	2385
A N Jul	30	2355
C S Jan	85	2340
C ROS	20	2340
D STI	90	2355
E UF	60	2370
E EN2	55	2345
F CC	50	2330
F Oxy1	25	2350
F Oxy3	55	2360
H	30	2365

Note: Estimated density for control and fly ash mix were 2390 and 2350 kg/m³, respectively

Table 7-2. Fresh properties of concretes (air-classified fly ash; PC HK52)

SAMPLE	SLUMP, mm	PLASTIC DENSITY, kg/m ³
Reference	40	2375
C5	50	2355
C20	55	2355
C30	65	2355
C40	60	2360
C50	65	2355
CFD	25	2330
L5	40	2350
L20	40	2365
L30	40	2345
L40	45	2355
L50	50	2350
LFD	30	2335

Note: Estimated density for control and fly ash mix were 2390 and 2350 kg/m³, respectively

As shown in Figures 7-1 and 7-2 with both sets of fly ashes, concrete slump values agreed well with mortar flow (BS EN 450) and water requirements (BS 3892-1; BSI, 1982). Higher slump values were obtained for fly ashes with lower water requirements/higher flow values. However, as with the mortar tests (Section 5.1.1), the trend for the main and air-classified fly ashes was opposite, i.e. the main fly ashes gave higher slump with increasing fineness and the opposite occurred with the air-classified fly ashes.

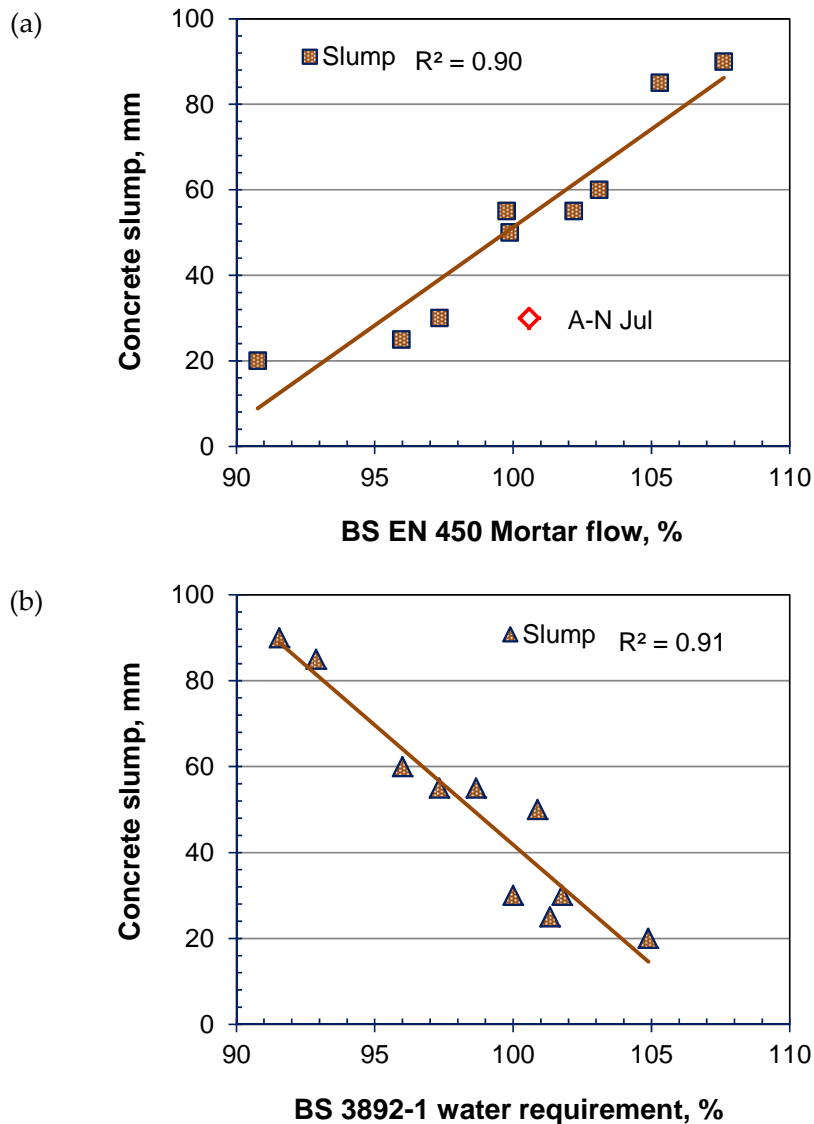


Figure 7-1. Relationships between mortar fresh properties and concrete slump: (a) BS EN 450 flow; and (b) BS 3892-1 water requirements. (*main fly ash; PC HR52*)

With both sets of fly ashes, the plastic density was found to be within $\pm 20 \text{ kg/m}^3$ of the estimated density, therefore the mix design was not revised. For the main coarse fly ashes,

being 'lighter' by nature, concrete gave lower density, while the opposite was found for the finer samples. The plastic density of the air-classified fly ashes concretes was found to be similar for each classified size fraction, but being coarse, in size, both the parent feed fly ashes gave $\sim 20 \text{ kg/m}^3$ lower density than was estimated.

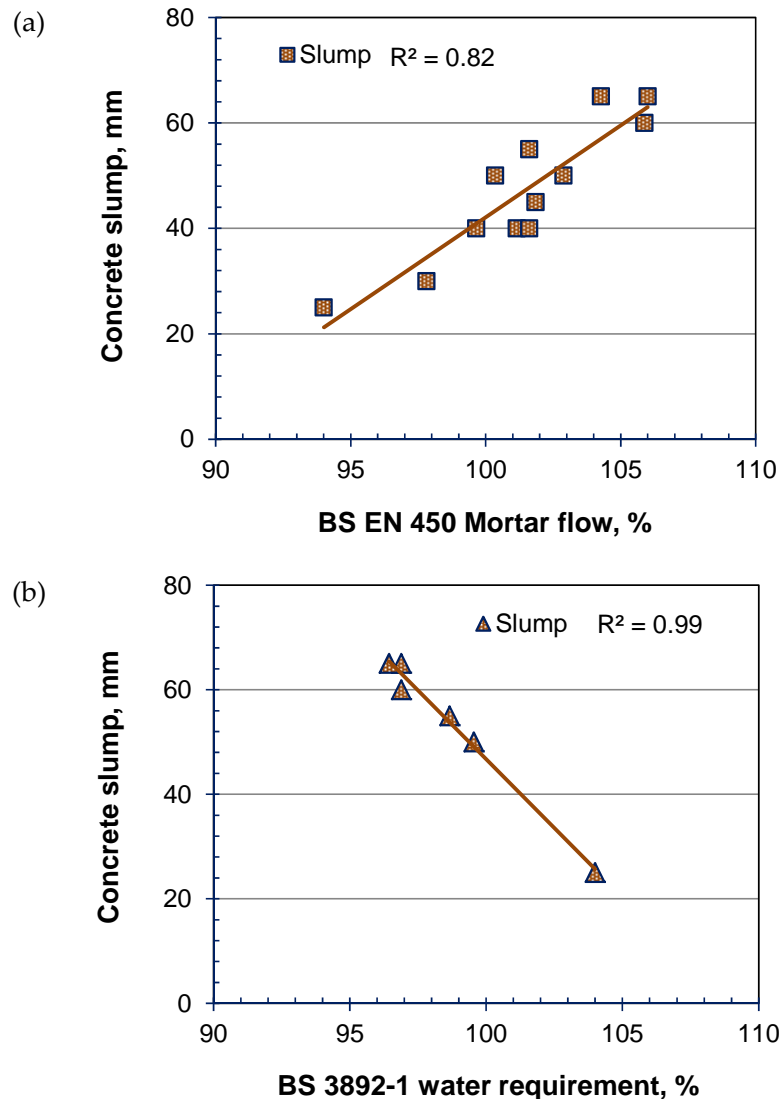


Figure 7-2. Relationships between mortar fresh properties and concrete slump: (a) BS EN 450 flow; and (b) BS 3892-1 water requirements. (*air-classified fly ash; PC HK52*)

7.1.2 Strength development

Concrete tests were carried out for compressive strength (of 100 mm cubes) at different ages. The results for the main and air-classified fly ashes are given in Tables 7-3 and 7-4, respectively.

Table 7-3. Cube strength of concrete at different ages (main fly ash; PC HR52)

SAMPLE	COMPRESSIVE STRENGTH, MPa					
	1 day	7 day	28 day	90 day	180 day	7 days (A) ^a
Reference	16.5	36.5	49.0	51.5	56.5	43.5
A N Jul	10.0	23.0	37.0	45.0	47.5	40.5
C S Jan	9.0	20.5	35.0	45.5	49.0	41.5
C ROS	8.5	20.5	33.5	42.0	43.0	37.0
D STI	9.0	22.0	35.5	43.5	46.0	39.0
E UF	9.5	22.0	35.5	45.0	50.5	39.5
E EN2	8.0	20.5	35.0	43.5	46.5	39.0
F CC	9.0	22.5	36.0	42.5	45.0	36.0
F Oxy1	8.6	22.5	36.5	44.0	46.5	35.0
F Oxy3	9.5	21.5	36.0	45.5	47.0	37.5
H	8.5	23.0	35.0	44.5	47.5	38.0

^a Curing at 50°C following de-moulding 24 h after mixing

Table 7-4. Cube strength of concrete at different ages (air-classified fly ash; PC HK52)

SAMPLE	COMPRESSIVE STRENGTH, MPa		
	14 day	28 day	56 day
Reference	46.0	49.0	51.0
C5	32.0	39.5	47.0
C20	30.5	39.0	46.0
C30	29.5	37.5	45.0
C40	28.0	37.0	44.0
C50	28.5	36.0	44.0
CFD	27.0	35.0	40.0
L5	34.0	42.0	49.5
L20	32.0	40.5	48.0
L30	31.5	38.0	47.0
L40	31.5	37.5	46.5
L50	31.5	37.0	44.5
LFD	28.0	35.5	43.5

The strength development of fly ash concretes with the main and air-classified fly ashes at various curing ages is given in Figures 7-3 and 7-4, respectively. Differences in rate of strength increase were noted between the main and air-classified fly ashes. The highest strengths with the main fly ashes (lowest $d_{90} = 40.6 \mu\text{m}$) were lower by 24 and 12% than the reference PC mix at 28 and 90 days respectively, while these were lower by 26, 15 and 3% for air-classified fly ash (lowest $d_{90} = 9.3 \mu\text{m}$) at 14, 28 and 56 days respectively. This not only indicates the influence of fly ash fineness on reactivity in concrete, but also the benefits of classification.

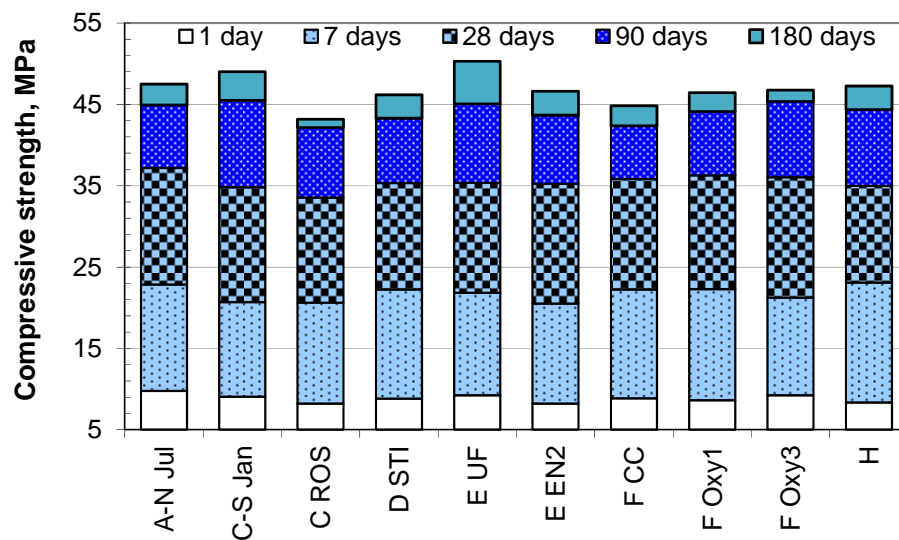


Figure 7-3. Compressive strength of fly ash concrete at different curing age (PC HR52)

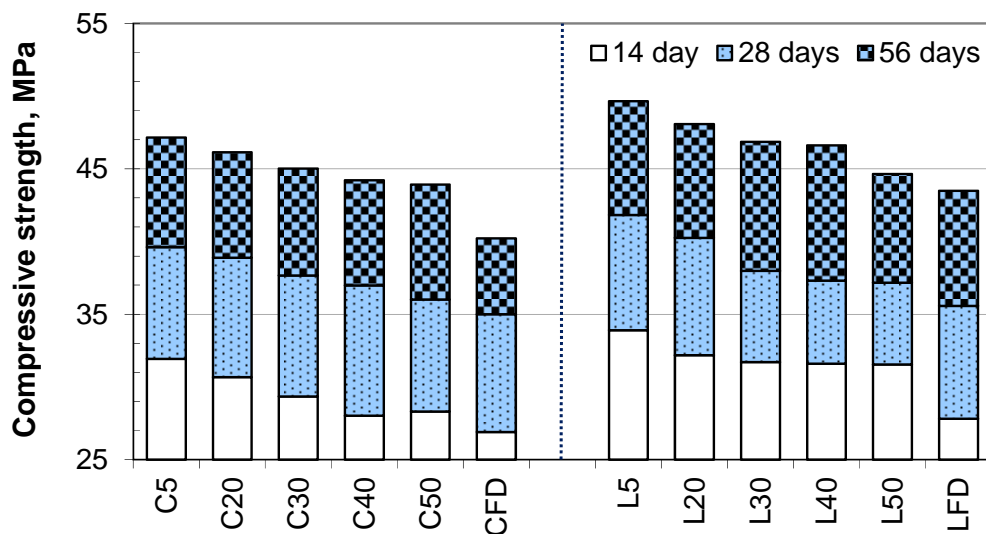


Figure 7-4. Compressive strength of fly ash concrete at different curing age (PC HK52)

7.1.3 Fly ash properties

Fly ash properties (45 μm sieve residue, multiple factor and sub 10 μm quantities) are compared with compressive strength of concrete in Figure 7-5. For the main fly ashes, at 28 days the concrete strength did not give any particular trend. In general the 45 μm sieve residue correlated well with the compressive strength at 90 and 180 days, while the other two parameters, gave somewhat lower R^2 values.

Air-classified fly ash fineness (d_{90} and sub 10 μm quantity) is plotted with their corresponding strengths at various ages in Figures 7-6 and 7-7. In general, sub 10 μm quantities gave better linear correlations, while a logarithmic type best fit was found with d_{90} . As mentioned earlier, discrepancies might occur from variations in particle size distribution, even though their d_{90} s are comparable.

7.1.4 Mortar activity index and concrete strength

Figure 7-8 shows a plot of concrete cube strength values obtained at 28, 90 and 180 days, with BS EN 450 (BSI, 2005c) activity index at 28, 56 and 90 days using the main fly ashes and PC HR52. With a few exceptions, there was good agreement between the mortar activity index (28, 56 and 90 day) and concrete strengths obtained at 90 and 180 days. However, poor relationships were found between 28 days concrete strength and BS EN 450 activity index (28, 56 and 90 days). It appears that 28 days is not sufficient to assess PC/fly ash reactivity in concrete, as it contains relatively lower proportions of cementitious components than mortar systems.

The behaviour was clearer with air-classified fly ashes. Figure 7-9 gives relationships between mortar activity index and concrete cube strength. As shown in Figure 7-9 (a), comparing these for standard curing at the same age gave good correlations. It was noted that the rate of strength gain in mortar was higher than concrete. The correlations were similar starting from 14 days to 56 days, suggesting that these ultrafine fly ash components gave considerable reactivity, as found earlier with mortar and TGA tests. Therefore, the reactivity test duration to produce meaningful results depends on the fineness of fly ash. As given in Figure 7-9 (b), the relationship between accelerated mortar tests was better with concrete strength at 56 days. As noted earlier, finer fly ashes are more sensitive to temperature and are therefore, able to indicate likely longer-term reactivity.

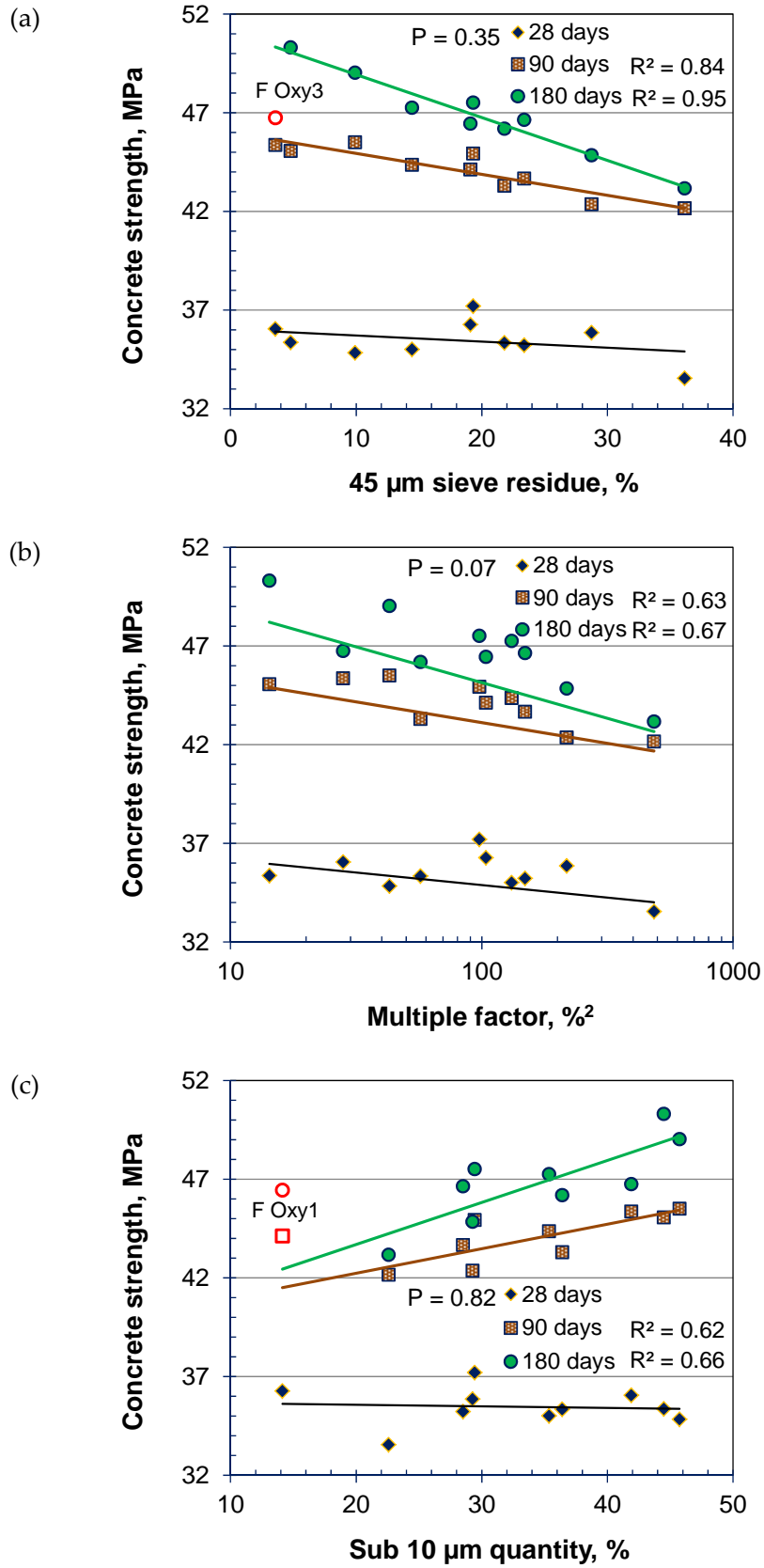


Figure 7-5. Relationships between fly ash properties and concrete cube strengths (PC HR52): (a) 45 µm sieve residue; (b) multiple factor; and (c) sub 10 µm quantities. (points in red not included in the regression analysis; PC HR52)

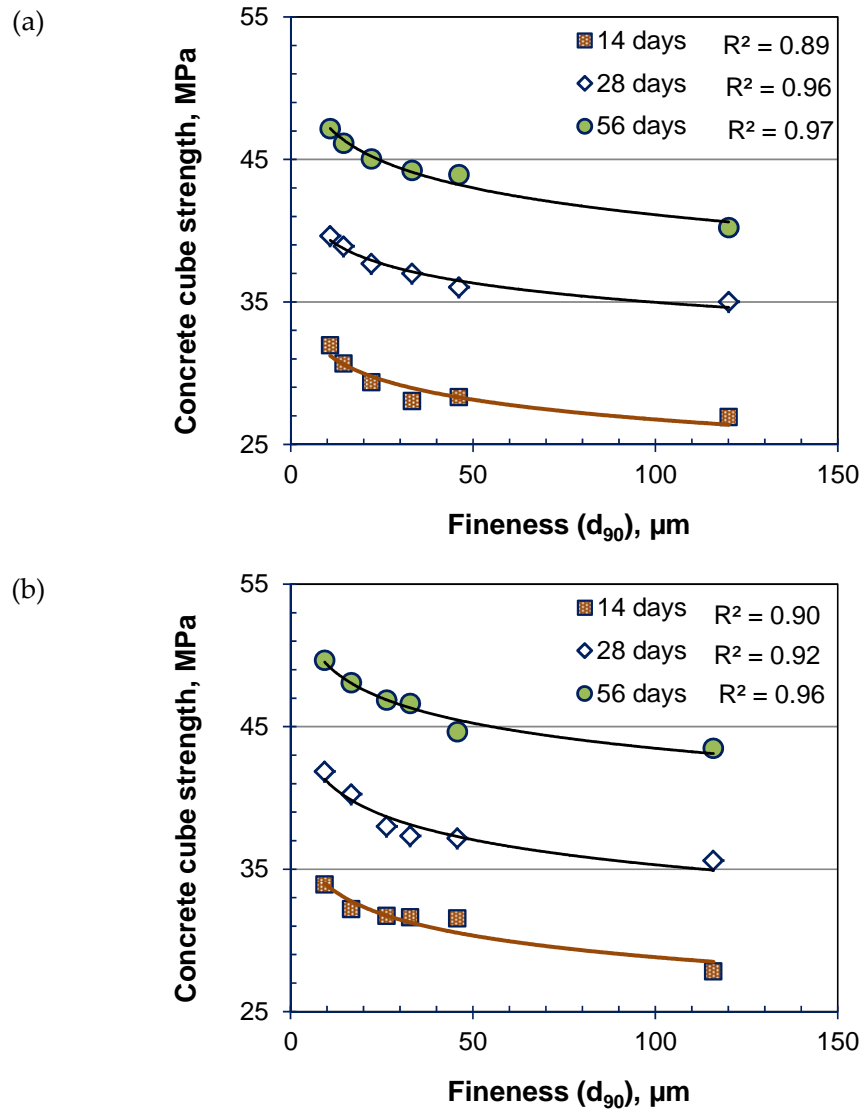


Figure 7-6. Relationships between fly ash fineness (d_{90}) and concrete cube strengths: (a) Source C; (b) Source L (PC HK52)

7.1.5 Hydrated lime mortar test and concrete strength

As shown in Figure 7-10, the compressive strength development trend in hydrated lime mortar also followed that for concrete strength. As with earlier relationships between fly ash properties and hydrated lime mortar strength (Section 5.3), Fly Ash D STI was excluded from the relationship between concrete compressive strength (90 days) and lime mortar compressive strength at 28 days. It appeared that D STI reacted better in a lime mortar system than with PC, or this might simply be the result of the water adjustment. This material gave highest flow and lowest water requirement in PC-based mortar,

therefore, a comparison using the same w/c ratio (i.e. higher water content than required for optimum packing) might affect the strength.

7.1.6 TG analysis and concrete strength

TG test results with selected air-classified fly ashes were compared with corresponding concrete strength using these materials at the same ages (14 and 28 days). As shown in Figure 7-11, at 14 days the relationship was good but it became strong at 28 days, indicating that 28 days might be sufficient to assess reactivity for ultrafine air-classified fly ashes. The mortar tests with these materials also gave meaningful results at this age.

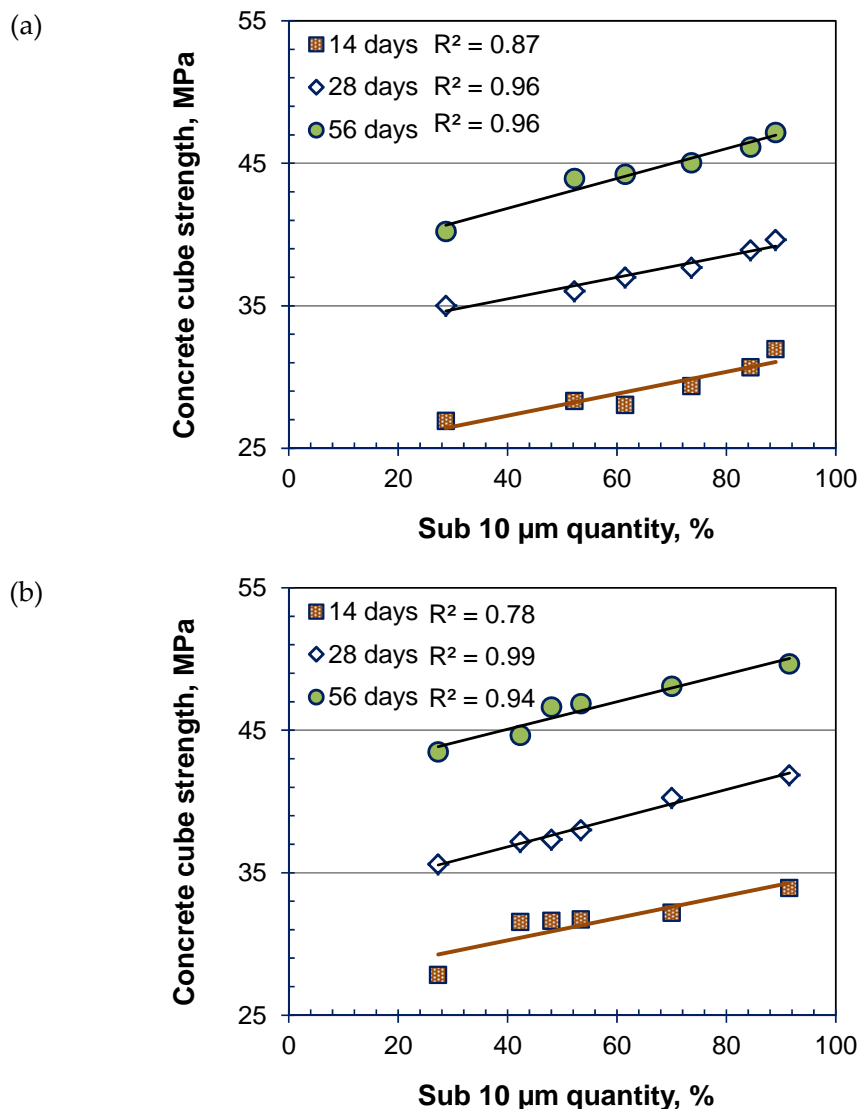


Figure 7-7. Relationships between air-classified fly ash fineness (sub 10 µm quantities) and concrete cube strengths: (a) Source C; (b) Source L (PC HK52)

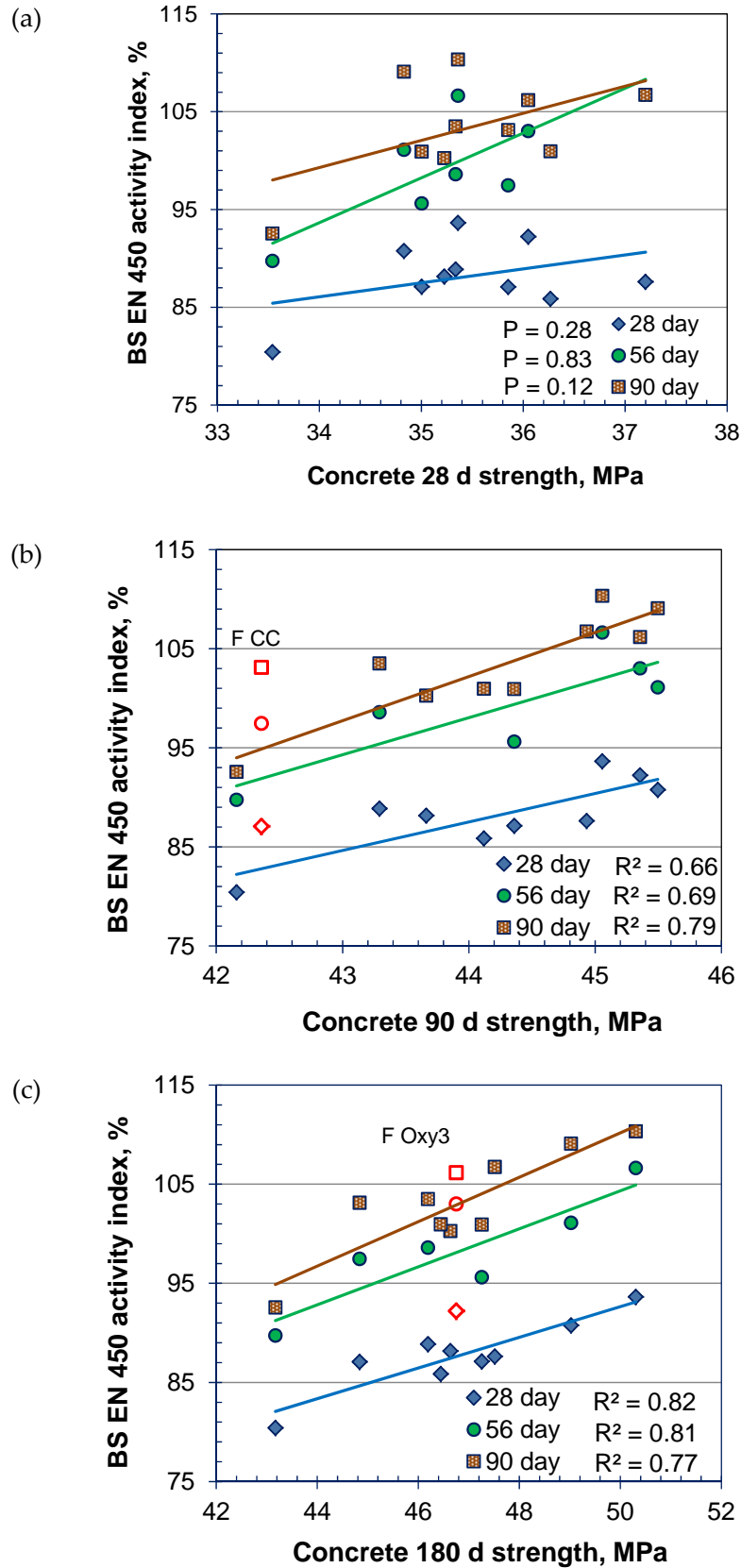


Figure 7-8. Relationships between concrete cube strength and BS EN 450 activity index (at 28, 56 and 90 days) with the main fly ashes: (a) 28 days; (b) 90 days; and (c) 180 days. (PC HR52)

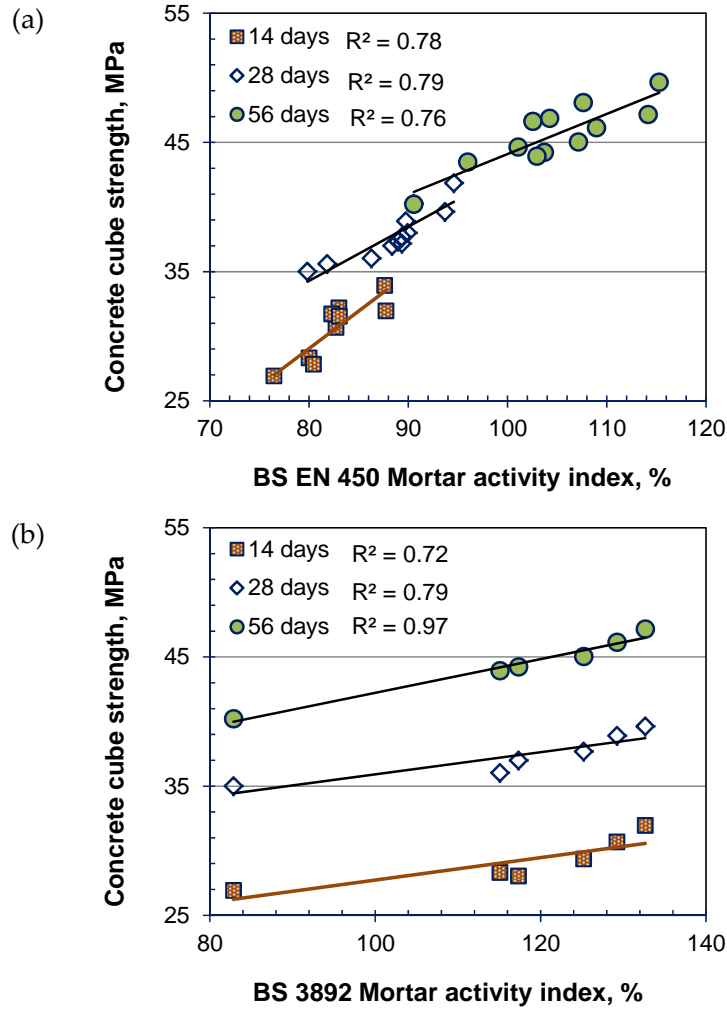


Figure 7-9. Relationships between mortar (pozzolanic) activity index and concrete cube strength (at 14, 28 and 56 days; PC HK52): (a) BS EN 450 activity index (at 14, 28 and 56 days; PC HR52) and (b) pozzolanic activity index (accelerated 7 days; PC HK52)

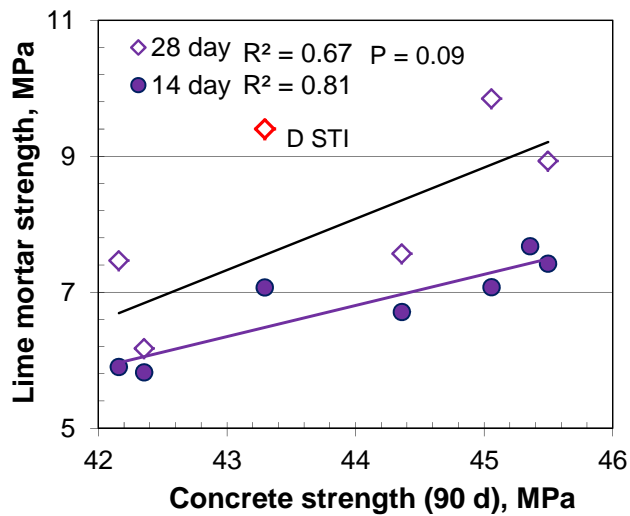


Figure 7-10. Relationships between concrete compressive Strength and hydrated lime mortar strength (*points in red not included in the regression analysis*)

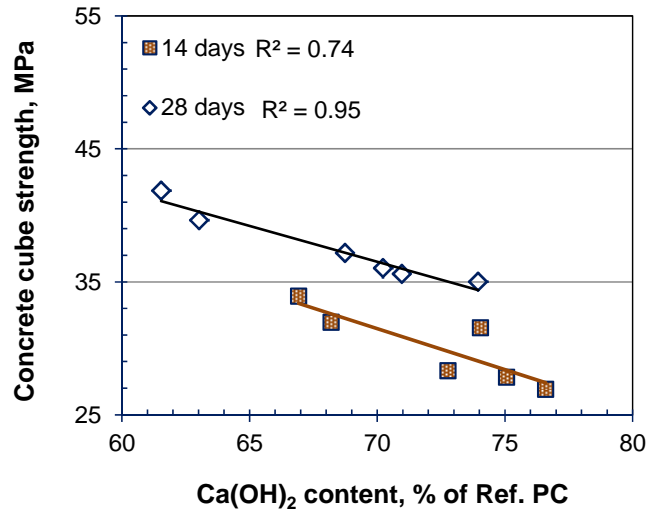


Figure 7-11. Relationships between Ca(OH)_2 content in fly ash/PC paste (PC HR52) and concrete cube strength (PC HK52) at 14 and 28 days.

7.2 Air – entrainment in Concrete

The final part of the sorptivity study was concerned with examining the effectiveness of the foam index (using the automatic shaker), AB80 adsorption and MB value for estimating air-entrainment in concrete. Tests were carried out with AEA C1 and AEA S, to entrain 5.0 ± 1.0 vol. % air in concrete containing fly ash (with the same materials used in the mortar tests described in Section 6.4) at a level of 30% in PC. The initial AEA doses were estimated from the foam index and mortar tests, and then adjusted to entrain the target quantity of air by trial mixing. As for the mortars considered earlier in the Section 6.4, water content adjustments were made for the concrete with AEA S to maintain the water/cement ratio.

The results of concrete fresh properties and compressive strength tests are given in Table 7-5 and indicate slightly higher slump values for the finer/lower LOI (lower specific surface area) fly ash concretes compared to the reference, and those of greater coarseness/higher LOI, despite the latter having increased AEA doses. This is likely to reflect differences in water-reducing properties of and AEA adsorption by fly ash and plasticizing effects of the admixture. F CC concrete also gave slightly lower plastic densities than the other fly ash concretes (probably relating to the coarseness/higher LOI of this material). For the narrow air content target range, there were relatively minor

differences in cube strength between the various concretes and there appeared to be little influence of fly ash properties on this.

Table 7-5. AEA doses, fresh properties and strength of air-entrained concretes

SAMPLE	AEA DOSE, ml/kg		SLUMP, mm		PLASTIC DENSITY, kg/m ³		AIR CONTENT, %		CUBE STRENGTH, MPa	
	AEA C1	AEA S	AEA C1	AEA S	AEA C1	AEA S	AEA C1	AEA S	AEA C1	AEA S
Reference	0.8	19.0	110	105	2270	2275	5.2	4.9	38.5	37.5
A-S Jan	2.2	55.2	120	115	2230	2225	5.6	4.9	23.0	23.5
C-S Jan	2.5	66.7	130	130	2240	2235	5.0	4.5	28.0	24.0
D STI	1.0	21.0	135	130	2225	2240	5.8	4.0	23.5	28.5
E UF	2.7	66.7	115	105	2240	2225	5.2	4.9	25.0	26.0
E EN1	3.1	74.3	100	80	2215	2225	6.0	5.0	24.0	26.5
F CC	5.3	123.8	115	95	2205	2205	5.5	4.6	25.5	24.0

Note: Estimated densities for reference and fly ash mixes were 2265 and 2225 kg/m³, respectively.

7.2.1 Foam index and concrete AEA dose

A comparison of the AEA doses to achieve the target air content ($5.0 \pm 1.0\%$) in concrete and the foam index of the fly ashes is shown in Figure 7-12. This indicates very good correlations between these, both for AEA C1 ($R^2 = 0.95$) and AEA S ($R^2 = 0.89$). There were also very good relationships between the doses used to entrain air in concrete and mortar.

7.2.2 AB80 adsorption and concrete AEA dose

A comparison of the AB80 adsorption and the AEA doses to achieve the target air content is shown in Figure 7-13. This again indicates very good correlations between these parameters, both for AEA C1 ($R^2 = 0.91$) and AEA S ($R^2 = 0.87$). The general behaviour noted between AB80 adsorption and the dose required to entrain air was very similar between mortar and concrete, as noted for these and foam index.

As with mortar, the ordinate intercepts were considered to estimate the active AEA component contributing to the air-entrainment in fly ash concrete. These were found to be 21.3 and 0.8 ml/kg of PC + fly ash for AEA S and AEA C1 respectively, which agrees well with the dose required for the reference concrete mix without fly ash (19.0 and 0.8 ml/kg

PC for AEA S and AEA C1 respectively) and is similar to the initial trial mix dose suggested by the admixture supplier for AEA C1, i.e. 1.0 ml/kg. These tests, again confirm the potential of this spectroscopic method for estimation of AEA dose required to entrain a specific quantity of air in cementitious systems containing fly ash.

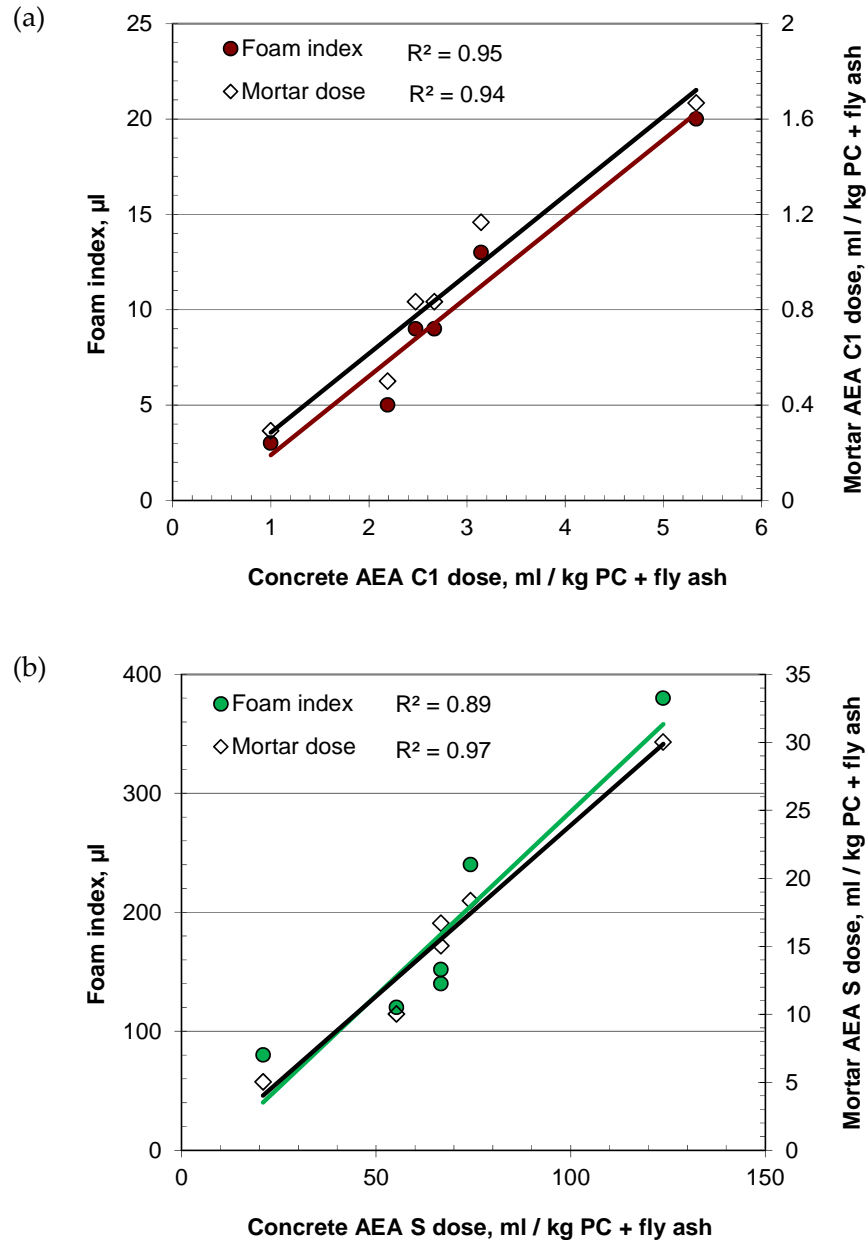


Figure 7-12. Relationships between concrete AEA dose, foam index of selective fly ashes (using automatic shaker) and mortar AEA dose (a) AEA C1; and (b) AEA S

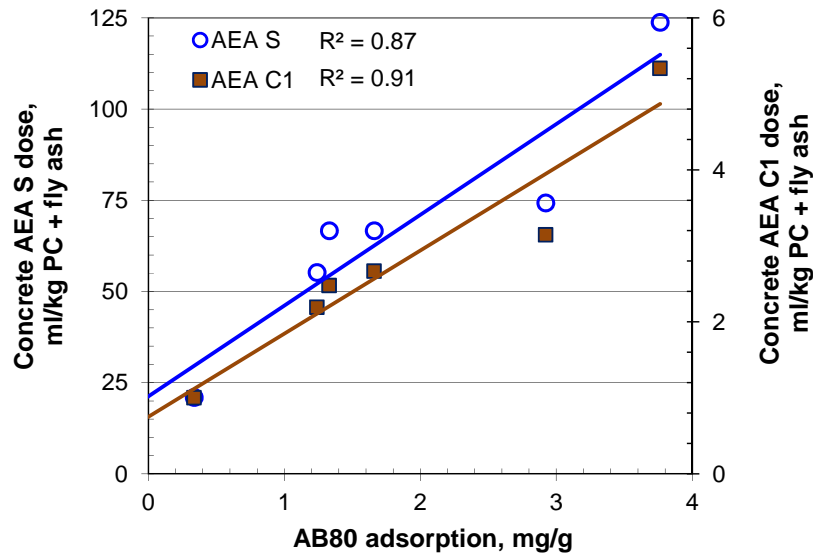


Figure 7-13. Relationships between AB80 adsorption and concrete AEA dose with AEA S and C1

7.2.3 Methylene blue value and concrete AEA dose

Figure 7-14 shows the relationship between AEA dose required to achieve the target air content in concrete and their MB value. As with the foam index and AB80 adsorption tests these gave very good correlations, i.e. 0.92 and 0.89 with AEA S and AEA C1 respectively. Again the line intercepting the abscissa rather than the ordinate reflects the necessity to refine the dose increment.

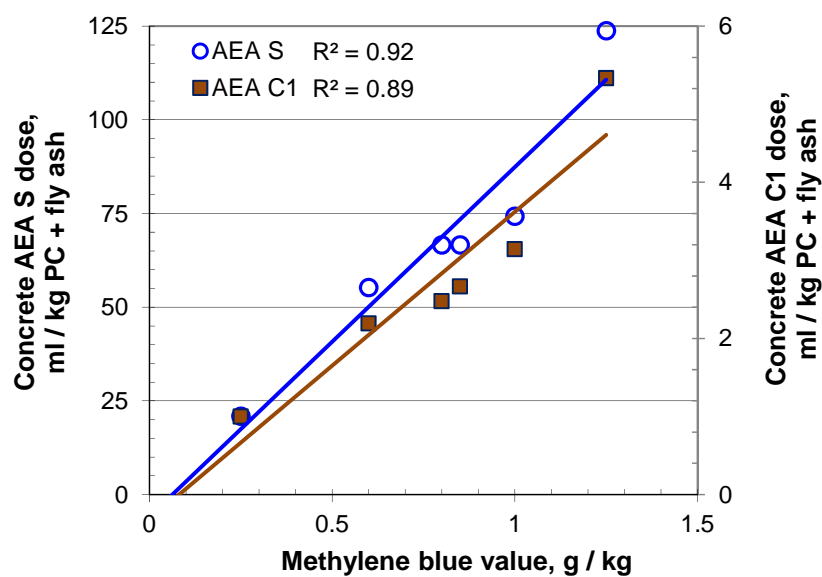


Figure 7-14. Relationships between MB value and concrete AEA dose using AEA S and AEA C1

7.2.4 Initial surface absorption test (ISAT) of concrete

The initial surface absorption test (ISAT) gives an indication of surface quality of concrete, which is important in relation to the protection of reinforcement. ISAT tests were carried out on air-entrained hardened concrete at 28 days to examine the effect of air entrainment. Part of the work described in this section was carried out in collaboration with Pang (2012). ISAT 10, 30 and 60 of selected air-entrained concrete cubes (150 mm) with AEA C1 and AEA S are shown in Figure 7-15.

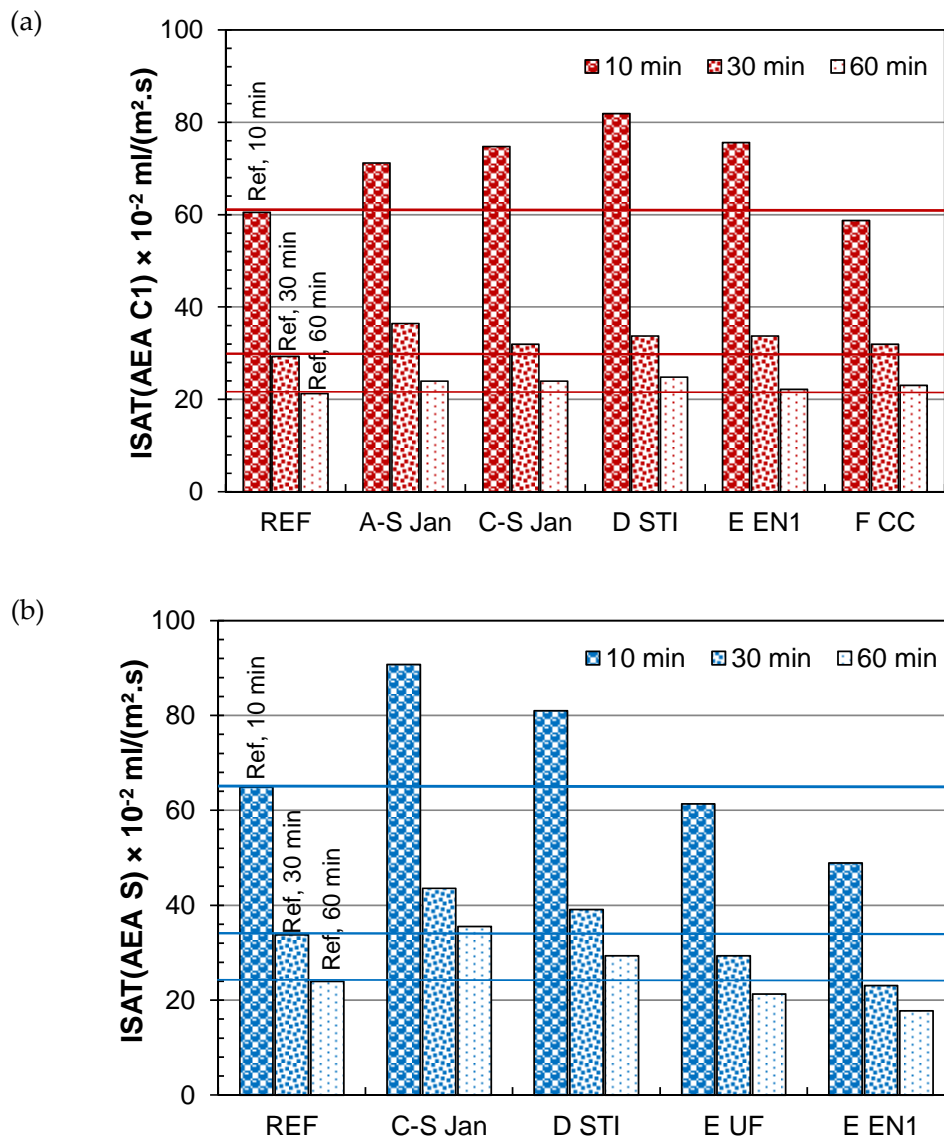


Figure 7-15. Comparison of ISATs for concretes with (a) AEA C1; and (b) AEA S (in collaboration with Pang, 2012)

Given the test was carried out at 28 days, in most cases ISAT of fly ash concrete was higher than that of reference PC concrete as noted previously (Folagbade, 2011) for equal w/c ratio concrete. Comparing between the two AEAs in concrete, the ISAT of the reference PC mix was similar in both cases, while there was more variation with the fly ash mixes. Folagbade (2011) obtained ISAT 10 and 60 results for fly ash non-air-entrained concrete with w/c = 0.5 and a fly ash level of 35%. Similar type behaviour between reference and fly ash concretes was noticed in that study. The ISAT values at 60 minutes were similar at 28 days, although the fly ash level was 5% higher in that study. Comparing ISAT 10 values the current study gave slightly higher values than Folagbade (2011), which might be the effect of 5% air-entrainment. According to Neville (2011) this test is good for relative comparisons, but might not provide exact information in many cases. It was also noted in Chapter 5 that the reactivity of the main fly ashes was limited at 28 days which might cause misleading results for any tests carried out at this age.

Air-entrained fly ash concrete strength was plotted against their respective ISAT values in Figure 7-16. With AEA C1, a general inverse trend was noted between the compressive strength and ISAT at different test periods, while this was not clear with AEA S. The slope of the line for 10 minutes ISAT was steeper than the other two indicating that the influence of strength on ISAT is more prominent initially, but with time the effect was no longer apparent.

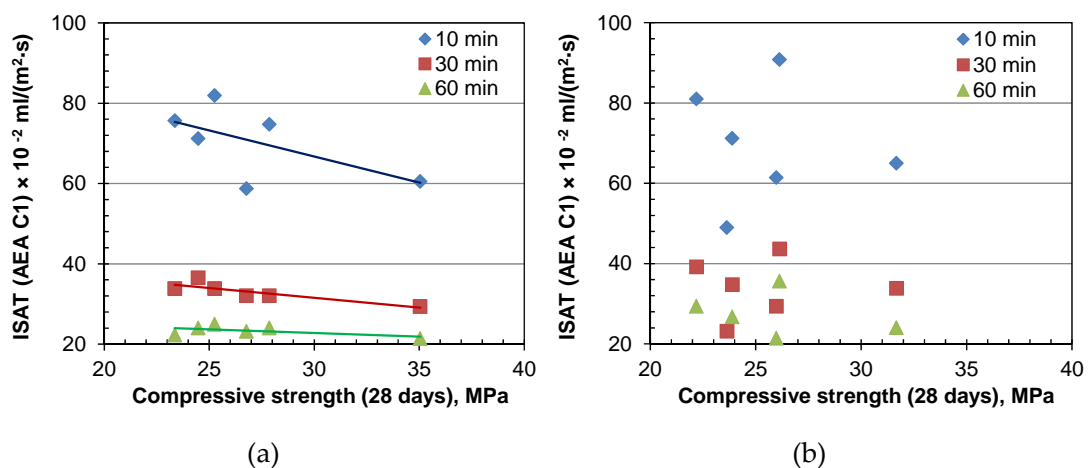


Figure 7-16. Relationships between air-entrained concrete compressive strength and their ISAT using: (a) AEA C1 and (b) AEA S

7.2.5 Water penetration under pressure

The permeability of concrete mainly depends on its porosity (both in cement paste and aggregate/paste interfacial zones), pore sizes, their continuity and tortuosity. This is further influenced by the degree of hydration, w/c ratio, fineness of cement and reactivity of pozzolana, where used. Therefore, it is a measure of likely ingress of potential aggressive chemicals (e.g. chloride, sulfate) in concrete under a pressure head. Part of the work described in this section was carried out in collaboration with Pang (2012). Figure 7-17 gives a comparison of depth of water penetration in air-entrained concretes under pressure. As per Neville (2011) the concrete is classified as ‘impermeable’ where the depth of water penetration is less than 50 mm and ‘impermeable under aggressive environments’ in cases where this is less than 30 mm.

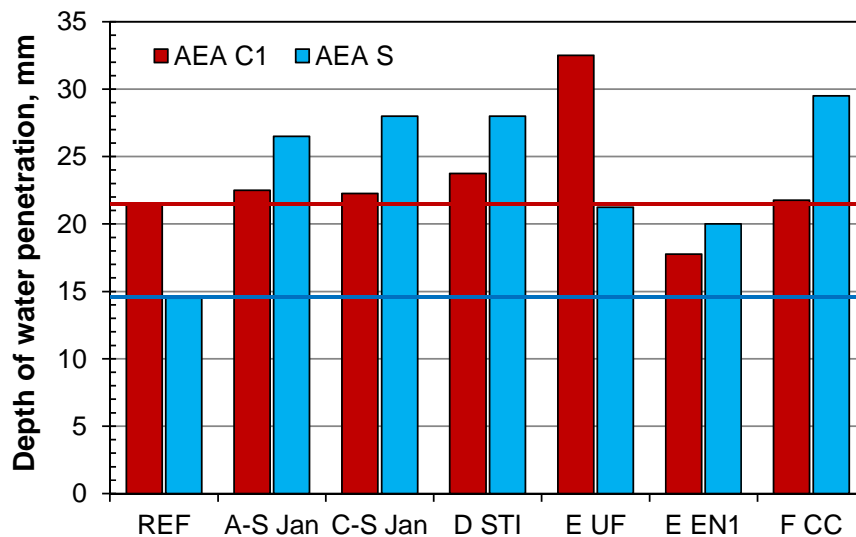


Figure 7-17. Comparison of ISATs for concretes with (a) AEA C1; and (b) AEA S (28 days water cured; in collaboration with Pang, 2012)

Therefore, all of the tested concrete gave very low permeability and would be classified as ‘impermeable under aggressive environments’. As with ISAT, water penetration of both reference mixes was lower than the fly ash mixes (except E EN1 with AEA C1). These again suggest incomplete pozzolanic reaction at 28 days for the fly ash mixes. However, comparing the guidelines provided by Neville (2011), these concretes are sufficiently impermeable at this stage. Comparing with Folagbade (2011; non-air-entrained) water penetration depths of concrete in the current study were found to be lower, which indicates

that uniformly distributed micro air-voids have little/no influence on water penetration (permeability) of concrete.

Finally, a comparison between two different permeation properties is plotted in Figure 7-18. Generally they agreed with each other but as mentioned earlier, fly ash has minor contributions in the microstructural development of concrete at the test age and therefore these might not show any strong correlations.

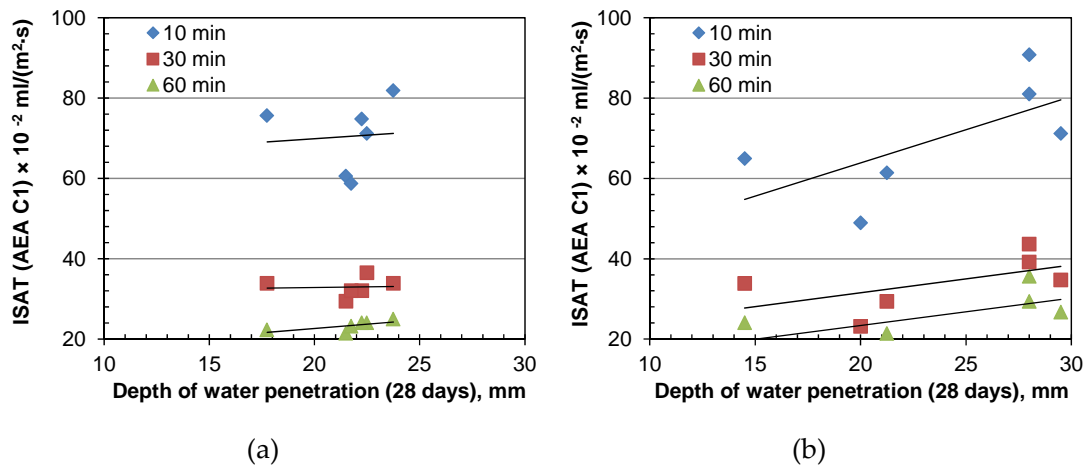


Figure 7-18. Relationships between air-entrained concrete compressive strength and their ISAT using: (a) AEA C1 and (b) AEA S

7.3 Summary of Findings

To validate the assessment test methods described in the earlier chapters, concrete tests were carried out for compressive strength and required AEA dose to entrain target quantities of air.

As with the mortar tests at the same w/c ratio, the slump increased with fineness for the main fly ashes, however the opposite was noted for air-classified finer components. Both the water requirements and flow from mortar tests gave good correlations with concrete slump. Entraining target quantities of air gave relatively higher slump and lower plastic density than non-air-entrained concrete.

As with Mortar, concrete strength results gave good correlations with fly ash properties. Activity index results from mortar tests gave better correlations with concrete strengths for

air-classified finer fly ashes. However, this gave lower coefficients of correlation in the case of the main fly ashes. This appeared to be due to the variation in fly ash production processes between individual sources. It was also noted that with higher proportions of cementitious components, strength gain rate in mortar was greater than that in concrete.

As with the mortar, TGA results for Ca(OH)_2 level in selected fly ash/PC pastes gave good correlations with concrete strengths, even at early ages (14 days). This also suggests higher reactivity of very fine components at early ages.

Tests carried out on fly ash concretes indicate that the foam index determined using the automatic shaker gave very good correlations with the dosage requirements to entrain a target quantity of air in this medium. The effects noted were similar between the commercial AEAs and standard reagent used.

The results from tests on fly ash concretes gave very good correlations between AB80 adsorption and the dose required to entrain target quantities of air. Furthermore, the data could be used to identify the air entraining/adsorption components of the AEA when used with fly ash in these systems. The methylene blue test results also gave very good relationships with AEA dose required to entrain a target quantity of air in fly ash concrete.

Tests on hardened concrete for absorption properties (ISAT) and permeation (depth of water penetration under pressure) were carried out. These suggested that fly ash concrete at equal w/c ratio was not as effective as PC concrete at 28 days. However, the results obtained appeared to be comparable with non-air-entrained concrete data published in the literature, which suggests no significant effect of air-entrainment on the permeation properties of concrete and appears to relate how the air-void distributed in air-entrained concrete (i.e. discrete and note contributing to continuity of capillary pores) (Dhir *et al.*, 1987). The relationships of ISAT with both compressive strength and depth of water penetration were not strong.

CHAPTER 8: BETWEEN-LABORATORY TESTS

Chapter 8 deals with the analysis of between-laboratory tests results. Activity index, PSD, LOI and sieve analysis were carried out at 3 other laboratories (members of UKQAA). This gave a measure of the reproducibility of the test results.

8.1 Introduction

Fly ash samples were sent to the laboratories of three UKQAA members (Viz. Lab A, Lab C and Lab I) for between-laboratory tests. Seven fly ashes (Viz. A S Jan, C S Jan, C ROS, D STI, E UF, FCC and H) were selected for this work. Tests at the Concrete Technology Unit (CTU) of the University of Dundee indicated that the fineness of fly ash is a key parameter influencing its reactivity. Therefore, different means of measuring this, i.e. (i) PSD by LASER using Malvern; (ii) traditional wet 45 μm sieving; and (iii) air-jet sieving were considered. In addition to these, LOI and mortar activity index were measured following BS EN 450 (BSI, 2005c) and BS EN 196-2 (BSI, 2005b) at two of the laboratories. The results obtained are discussed in the following sections.

8.2 Particle Size Distribution

A full range of PSD of the fly ash samples were obtained at the CTU and Lab C using LASER technology from Malvern. At the CTU, the Malvern was set to analyse particles between 0.01 - 10000 μm , while this was 0.1 - 2000 μm for Lab C, however, the particle size was never greater than 725 and 502 μm in the measurements at the CTU and Lab C, respectively. The frequency of results was obtained at intervals of 12.9 and 20.6% from the minimum particle size at the CTU and Lab C, respectively. A comparisons between the PSDs obtained from these tests are shown in Figures 8-1 and 8-2. The relative rankings of fly ash fineness were similar between laboratories. The frequency distribution curve from Lab C was similar to a normal distribution, while a second peak was noticed in each case

for the CTU results. The wider range of measurement sizes (0.01 - 10000 μm) with a relatively smaller step (12.9% increment) in the CTU tests may have given the second peak. The discrepancy could also be due to differences in software program algorithm.

A comparison between the PSD parameters (d_{10} , d_{50} and d_{90}) obtained are shown in Figures 8-3 and 8-4, with relevant data given in Table 8-1. Good correlations were obtained between test results for d_{50} and d_{90} . Compared to Lab C, the CTU gave higher d_{90} values for fine fly ash and d_{50} for coarse. The d_{10} results did not show good agreement (see Figure 8-4), probably because of different starting particle sizes (0.01 and 0.1 μm for the CTU and Lab C respectively).

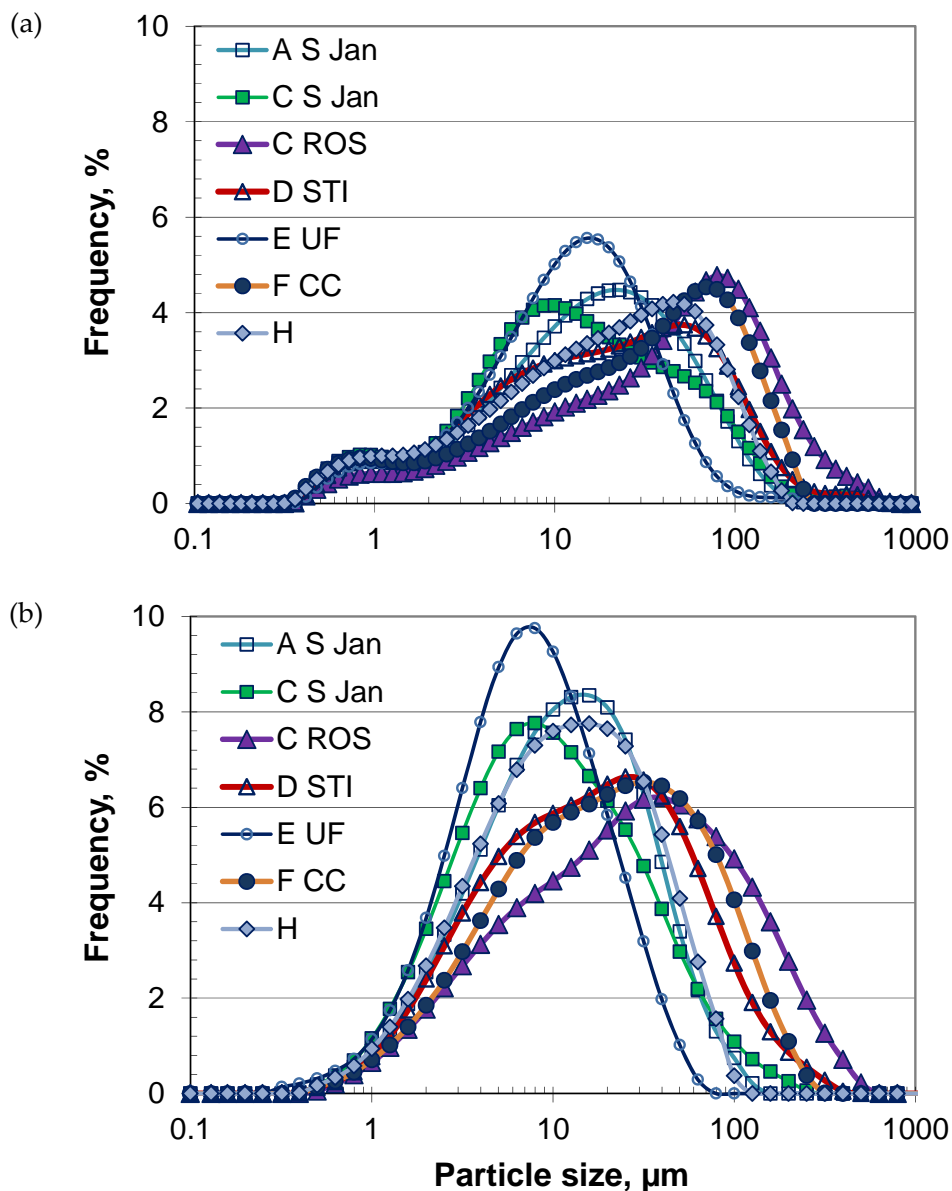


Figure 8-1. PSD curves (frequency) using Malvern: (a) CTU; and (b) Lab C

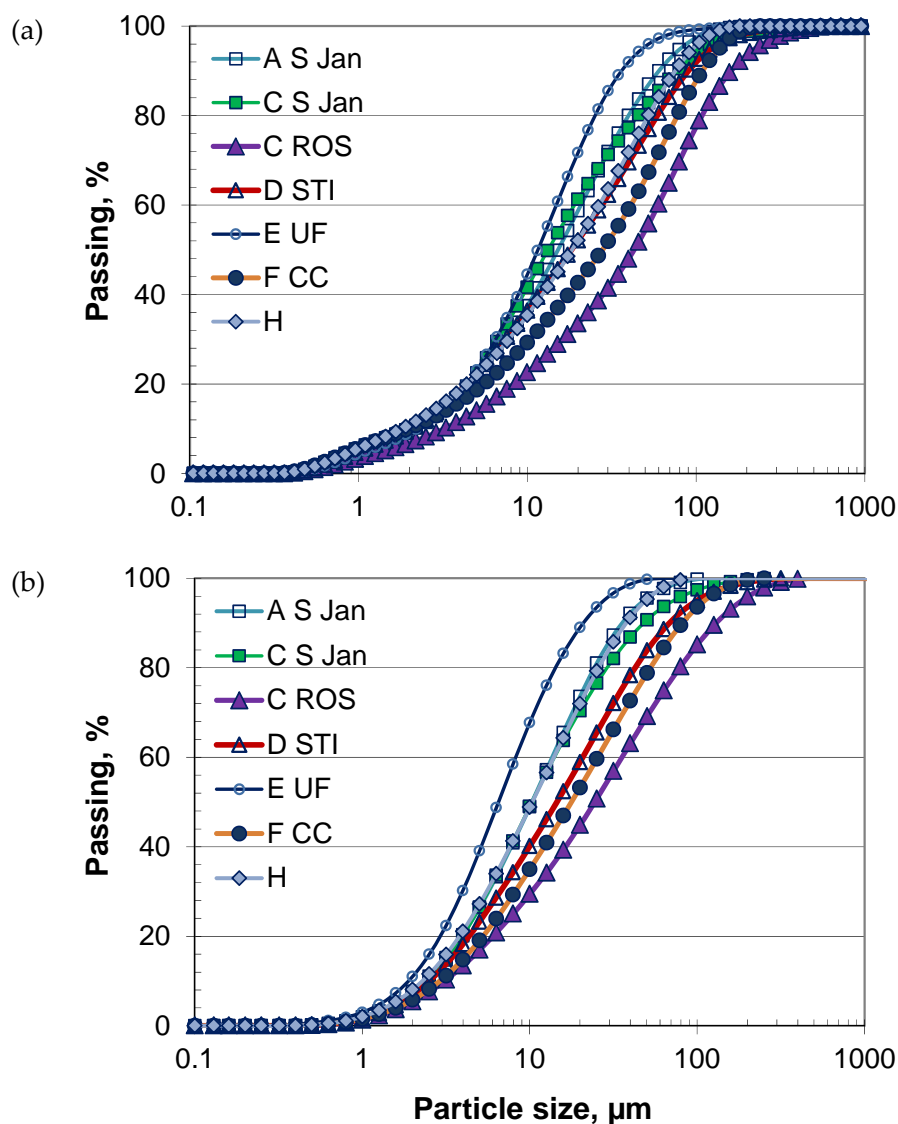


Figure 8-2. PSD curves (cumulative finer) using Malvern: CTU; and (b) Lab C

Table 8-1. Between-laboratory tests for fly ash particle size analysis by Malvern

SAMPLE	PSD d_{10}		PSD d_{50}		PSD d_{90}		Sub 10 μm	
	CTU	LAB C	CTU	LAB C	CTU	LAB C	CTU	LAB C
A S Jan	2.0	3.0	15.2	13.0	60.2	44.9	37.5	40.8
C S Jan	1.9	2.5	11.5	10.3	67.3	48.0	45.7	49.0
C ROS	3.2	3.9	43.0	30.9	161.1	163.6	22.6	24.9
D STI	2.1	3.2	18.3	18.3	90.1	86.1	36.4	34.2
E UF	2.2	2.4	11.5	8.2	36.1	26.3	44.5	58.4
F CC	2.0	3.7	27.9	22.4	109.0	102.7	29.3	29.3
H	1.8	2.9	18.4	13.1	75.2	47.5	35.4	41.2

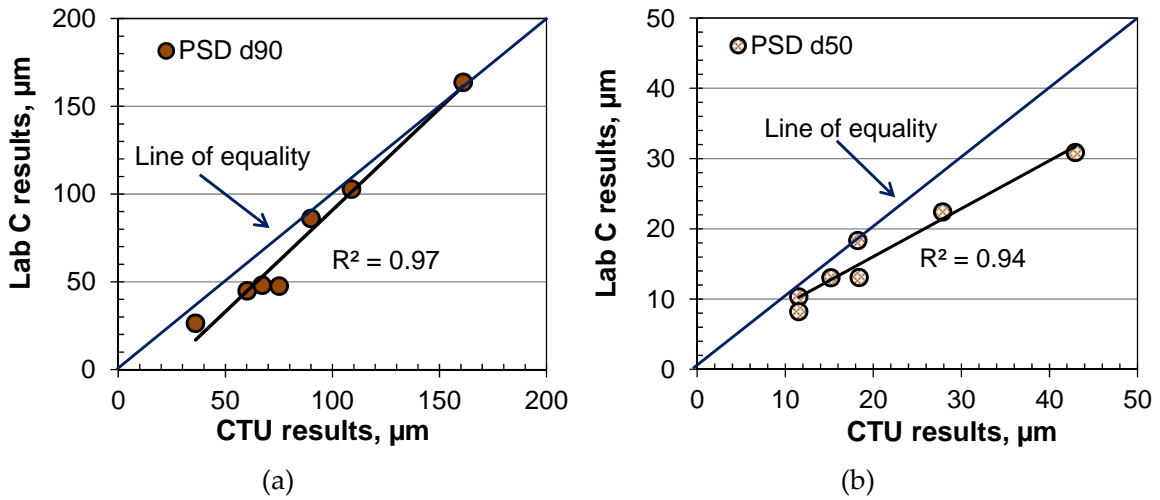


Figure 8-3. Comparison between PSD results obtained using Malvern: from the CTU and Lab C: (a) d₉₀ and (b) d₅₀

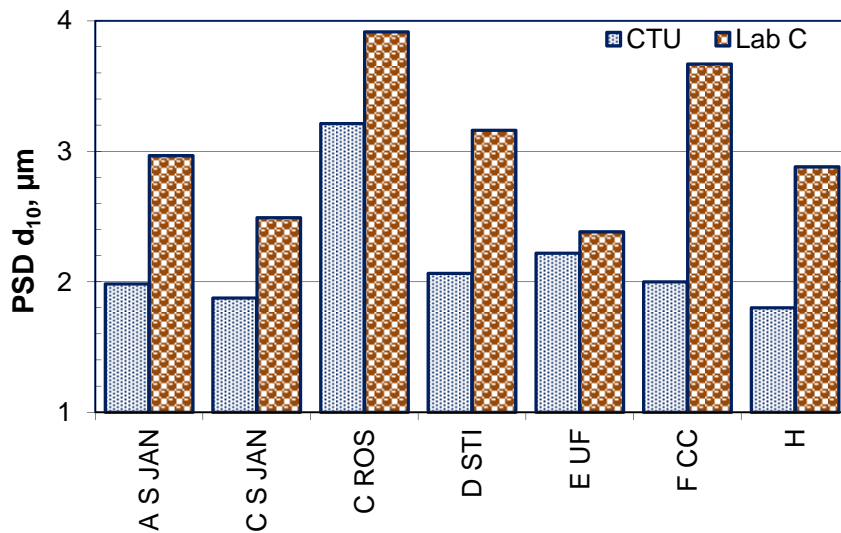


Figure 8-4. Comparison between d₁₀ (PSD) using Malvern from the CTU and Lab C

Traditionally the fineness of fly ashes is measured by wet 45 μm sieve analysis (on a mass basis). Hence, the % of materials coarser than 45 μm were calculated from Malvern PSD data (by volume) for the CTU and tests at Lab C and Lab I. Figure 8-5 shows a comparison between those obtained from the three laboratories. Both Lab C and Lab I test results correlated very well with the CTU data, especially Lab I data, which gave a R² value of 0.99, and was probably achieved because of the similar test conditions. It was also noticed that Lab C tests gave consistently lower results than the CTU, while these were consistently higher for Lab I.

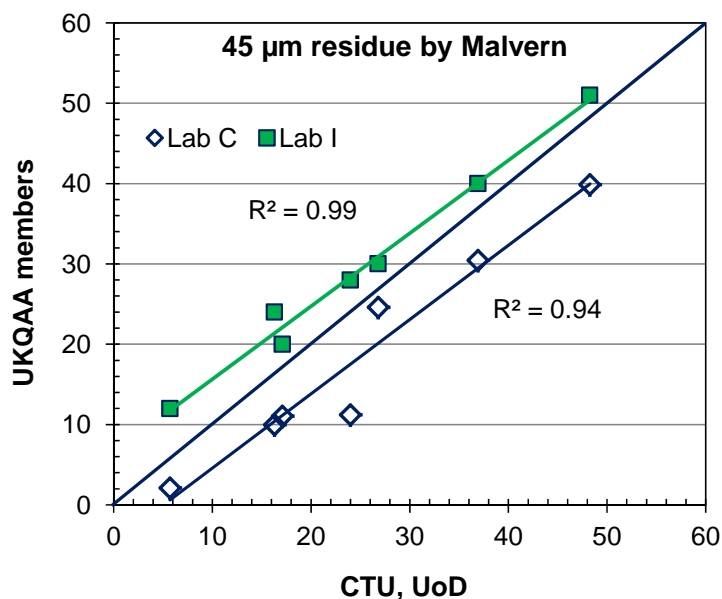


Figure 8-5. Comparison between 45 µm sieve residue (PSD) results using Malvern from the CTU, Lab C and Lab I

8.3 Fineness by 45 µm Sieve

Wet sieve analysis with water sprinkler following BS EN 451-2 (BSI, 1995) was carried out at the CTU and Lab C, while Lab I used air jet sieve analysis. A comparison of results is given in Figure 8-6 (data given in Table 8-2). With most samples, the CTU results were in the middle of the other two. The Lab I results gave higher retention on the 45 µm sieve because of the dry conditions used. During wet sieving there is a possibility of reducing agglomeration (where applicable) which may give lower retention on the 45 µm sieve, as noted in the case of the CTU and Lab C. As given in Table 8-2, the variation in test results were less for finer fly ash (e.g. for E UF, 3.7-4.8%) while this was more with coarse materials (e.g. for C ROS, 31.8-41.0%).

8.4 LOI and Moisture Content

The fly ash samples considered in this project are dry and the moisture contents from the CTU tests were found to be < 0.5%. Lab I determined moisture contents (< 0.5%, except Fly Ash H) and then used the dry samples for LOI determination. Lab C and the CTU LOI results are based on the as-supplied condition. A comparison between results obtained

from these three laboratories is given in Figure 8-7 (data given in Table 8-2). Moisture content data from Lab I are given on the top of the respective sample's LOI column in Figure 8-7. Minor variations (coefficients of variations from 1.1 – 4.8%) were obtained between the test results.

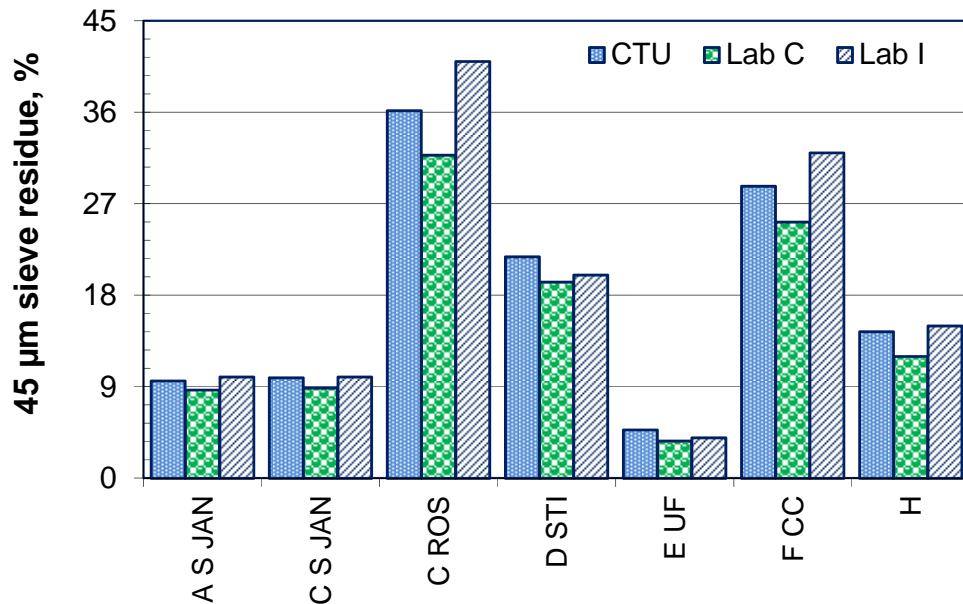


Figure 8-6. Comparison of 45 µm sieve residue obtained from between-laboratory tests (Note: Lab C and CTU: wet sieve analysis; and Lab I: air jet sieve analysis)

Table 8-2. Between-laboratory results of fly ash fineness (45 µm sieve residue) and LOI

SAMPLE	45 µm sieve residue			LOI		
	CTU ¹	LAB C ¹	LAB I ²	CTU	LAB C	LAB I ³
A S Jan	9.6	8.7	10.0	3.8	4.2	3.5
C S Jan	9.9	8.9	10.0	4.3	4.5	3.8
C ROS	36.1	31.8	41.0	13.4	13.7	13.1
D STI	21.8	19.3	20.0	2.6	2.5	2.2
E UF	4.8	3.7	4.0	3.0	3.0	2.4
F CC	28.8	25.2	32.0	7.6	7.3	6.8
H	14.4	12.0	15.0	9.1	9.5	8.7

¹ wet sieving; ² air jet sieving; and ³ oven drying before measurement

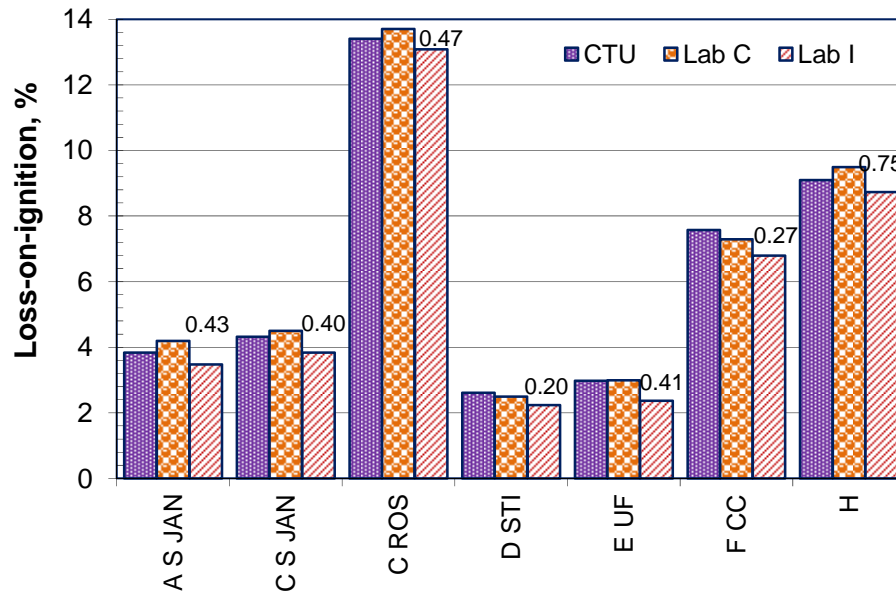


Figure 8-7. Comparison of LOI data obtained from between-laboratory tests
(Note: Lab I used oven drying before LOI test)

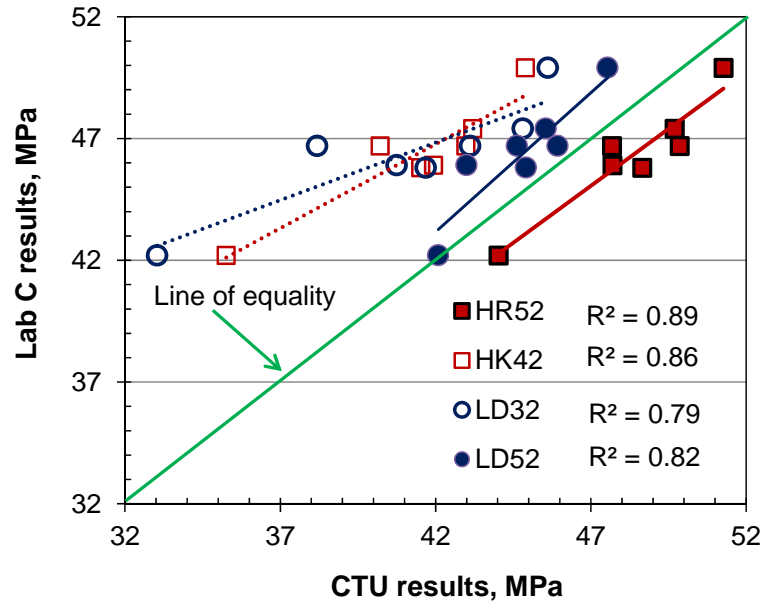
8.5 Activity Index with PC Mortars

Activity index of fly ash mortar was tested at Lab C and Lab I, following BS EN 450 (BSI, 2005c) at 28 and 90 days and compared with those obtained at the CTU using 4 different types of PC. The test results are given in Table 8-3. As shown in Figure 8-8 the compressive strength test results between the two laboratories at 28 days gave good correlations ($R^2 = 0.79 - 0.89$). Figure 8-9 makes a comparison of activity index values obtained from the 3 different laboratories.

Although control CEM I strength (59.9 MPa) from Lab C was higher than those used in the CTU; the fly ash mortar strength with PC HR52 in the CTU gave higher strengths than Lab C. Compressive strength with the other three PCs (CTU) gave lower values than Lab C. Therefore, it is not necessarily the case that higher grade PC will always give higher strengths (reactivity) in fly ash mortars.

Table 8-3. Between-laboratory tests of fly ash mortar activity index at 28 days

SAMPLE	MORTAR COMPRESSIVE STRENGTH, MPa					
	LAB A	LAB C	CTU			
	-	-	HR52	HK42	LD32	LD52
Control	63.6	59.9	54.8	49.5	41.3	55.7
A S Jan	49.9	46.7	49.9	46.7	43.1	45.9
C S Jan	50.4	47.4	49.7	47.4	44.8	45.5
C ROS	48.6	42.2	44.0	42.2	33.0	42.1
D STI	48.5	45.8	49.5	45.8	41.7	44.9
E UF	52.4	49.9	51.3	49.9	45.6	47.5
F CC	49.3	46.7	47.7	46.7	38.2	44.6
H	49.1	45.9	47.7	45.9	40.7	43.0

**Figure 8-8.** Comparison of EN 450 mortar compressive strength (28 days) between the CTU (four PCs) and Lab C

Figures 8-10 and 8-11 make a comparison between 90 days mortar strength data obtained at the CTU (using two 52.5 N and a 42.5 N PC) and those from Lab C. The data from these tests are given in Table 9.4. As indicated, very good correlations were observed between these ($R^2 = 0.91 - 0.95$). It should be noted that the strengths (control strength 69.5 MPa) obtained at Lab C were always higher than those found at the CTU (with any of the PCs).

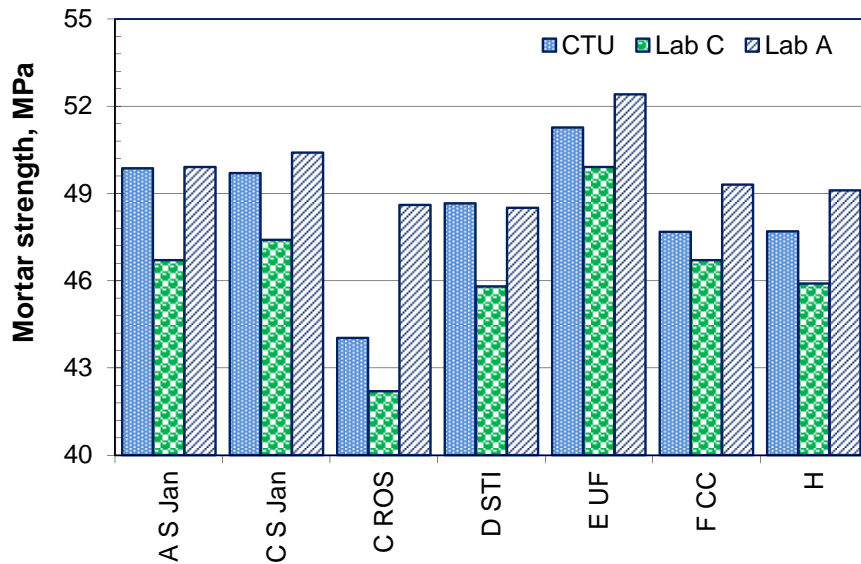


Figure 8-9. Comparison of EN 450 mortar compressive strength (28 days) between Labs

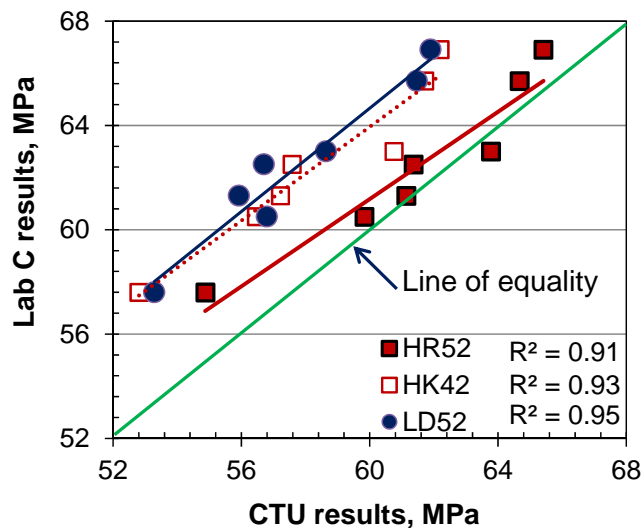


Figure 8-10. Comparison of EN 450 mortar compressive strength (90 days) obtained from between-laboratory tests by CTU (three PCs) and Lab C

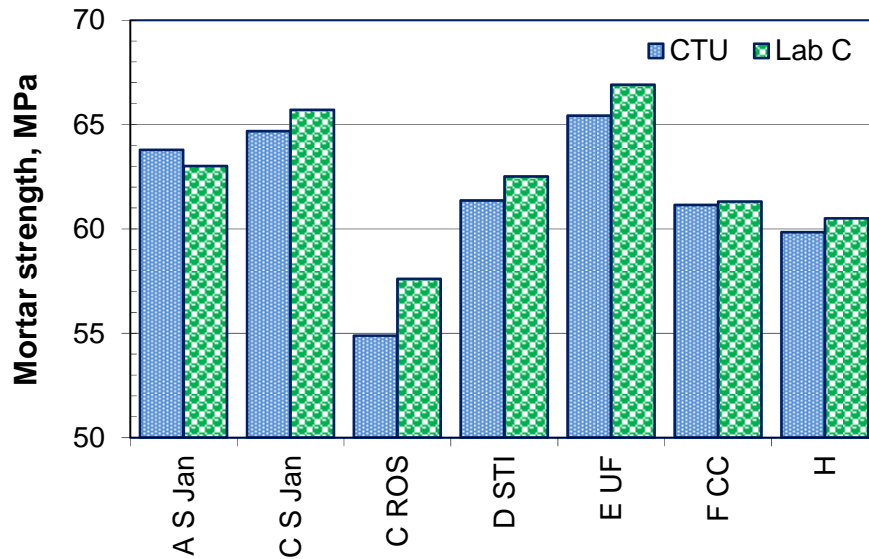


Figure 8-11. Comparison of EN 450 mortar compressive strength (90 days) between Labs

8.6 Activity Index and Fly Ash Fineness

Figure 8-12 gives relationships between the BS EN 450 (BSI, 2005c) activity index (PC HR52; 28 days) obtained from the three laboratories and corresponding fly ash fineness. With the limited number of samples and data obtained, both the CTU and Lab C results gave good correlations with fly ash fineness (45 μm sieve residue, d_{50} and sub 10 μm quantity). These were poorer for the data from Lab A.

Figure 8-13 gives correlations between activity index (90 days) obtained from Lab C and the CTU (PC HR52) and corresponding fly ash fineness (45 μm sieve residue, d_{50} and sub 10 μm quantities). For both laboratories, the best correlations were observed with d_{50} . The 45 μm sieve residue and sub 10 μm quantities also gave good correlations. This again indicates that the d_{50} of fly ash provides a good measure of its potential reactivity. Overall, at both 28 and 90 days, the correlations using LASER PSD were better than those with the 45 μm sieve.

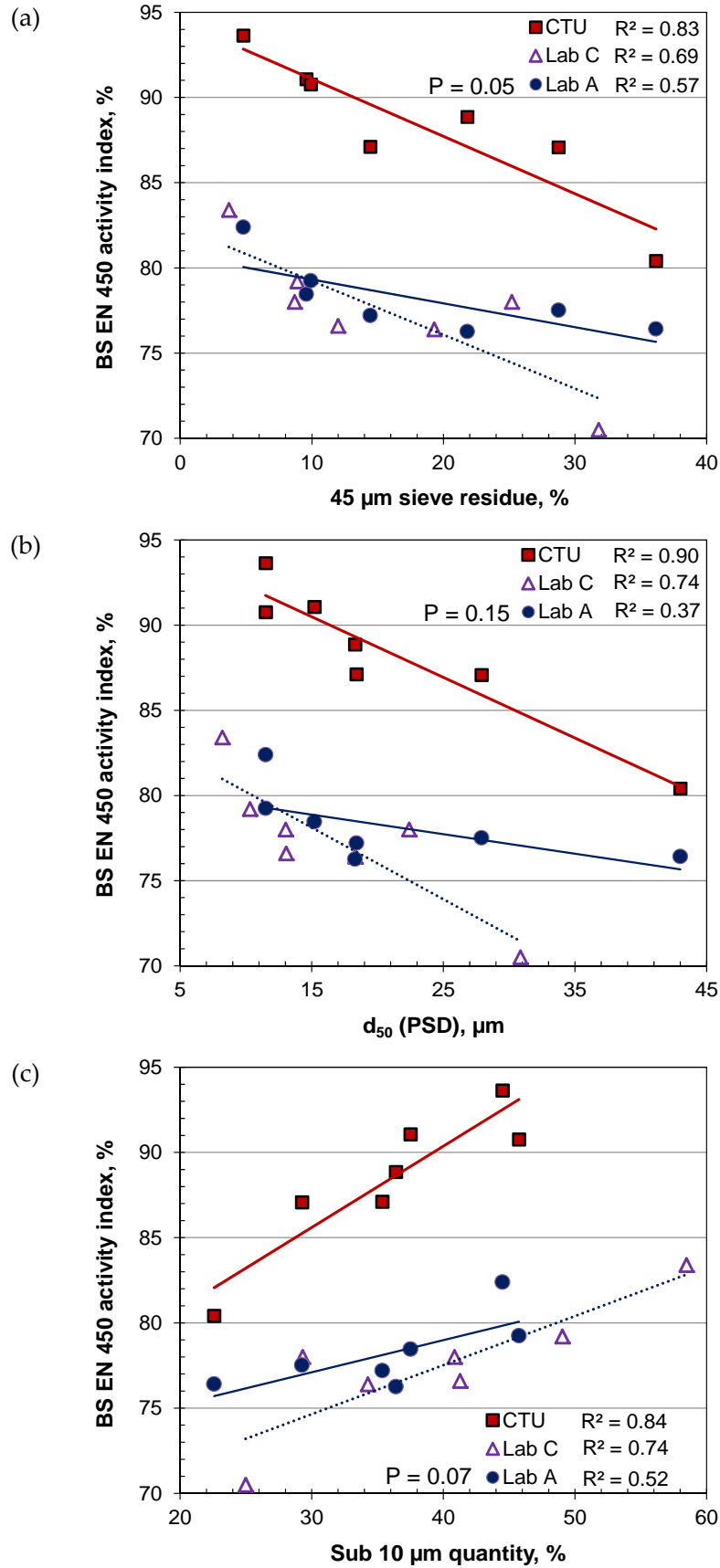


Figure 8-12. Comparison of relationships between fly ash fineness and 28 day BS EN 450 activity index between CTU and Lab C

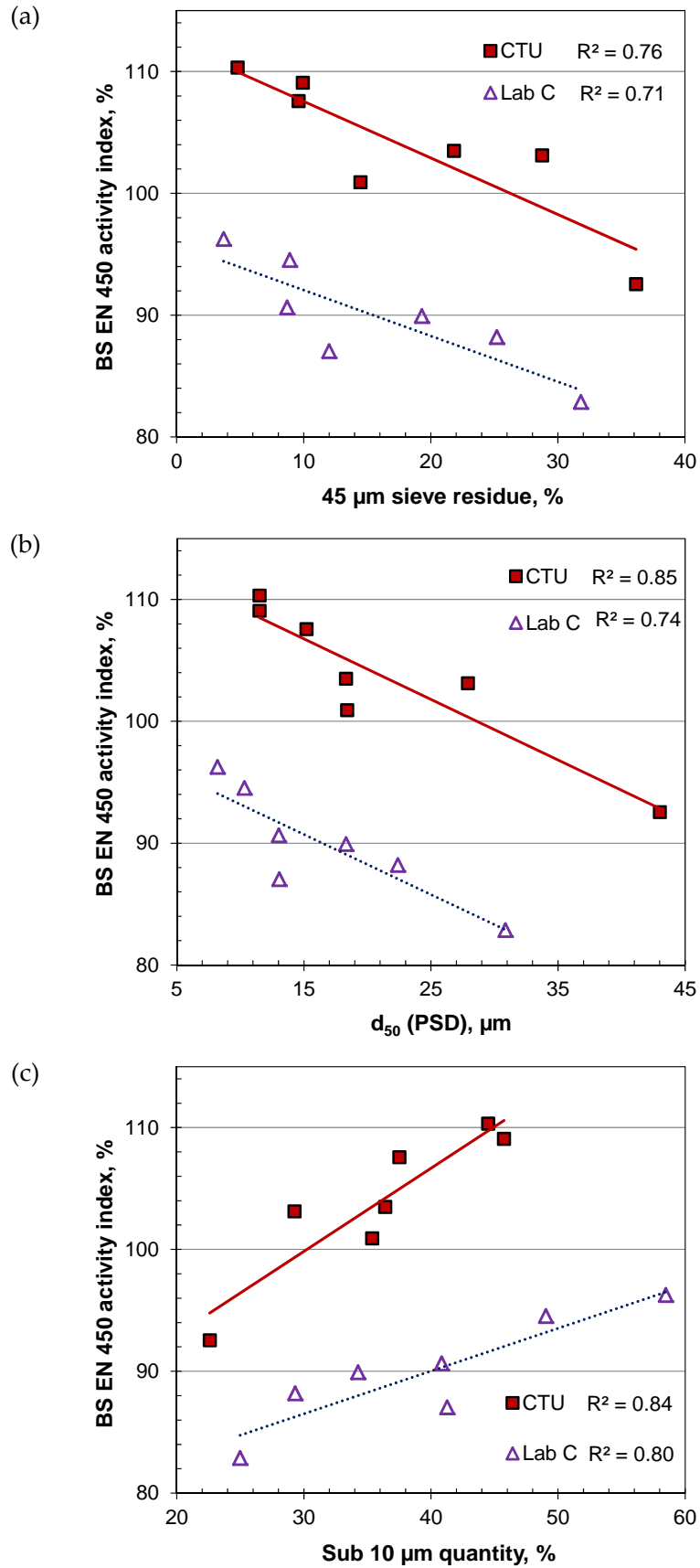


Figure 8-13. Comparison of relationships between fly ash fineness and 90 day BS EN 450 activity index between CTU and Lab C

8.7 Summary of Findings

Results from between-laboratory tests are presented in this Chapter. Seven fly ash samples with a range of properties were sent to three member laboratories of the UKQAA. These were tested for (i) fineness (PSD and 45 μm sieve residue), (ii) LOI and moisture content, and (iii) activity index at 28 and 90 days age.

The pattern of PSD curves obtained depended on the sensitivity of the test condition. However, generally good agreement was noted between the PSD parameters d_{50} and d_{90} in two of the laboratories. Given the difference in smallest particle size considered, there was no agreement between the d_{10} values. Particles coarser than 45 μm were calculated from PSD and very good correlations were obtained between the tests carried out at 3 laboratories.

Sieve analysis with 45 μm mesh also gave good agreement between tests carried out at the three laboratories. It was noted that air jet sieve analysis gave higher retention than water sprinkling analysis, because of reductions in possible agglomeration in the case of the latter. The LOI tests of between-laboratories also agreed with each other. As noted, the fly ashes were generally dry and had moisture content $< 0.5\%$.

Good agreement between activity index testing at different laboratories was noted. The slopes of trend lines were comparable when tests were carried out with similar strength class PCs, however, the rate of strength gain with lower strength grade PC was higher, which was also noted in Chapter 5. Having identified the role of fly ash fineness on its activity index (in *Chapter 5*) the individual laboratories test results were plotted using these two parameters. Two of these laboratories gave similar correlations, with the rest relatively poorer when tested at 28 days. This indicates that the activity index, in general, may not follow fly ash properties at early ages in all cases.

CHAPTER 9: CONCLUSIONS, PRACTICAL IMPLICATIONS AND RECOMMENDATIONS FOR FURTHER STUDY

This Chapter summarizes all of the findings of the study, its practical implications and recommendation for further work. Conclusions from individual Chapters are essentially summarized here and those practical aspects of the study are discussed and recommendation made for further research.

9.1 Conclusions

9.1.1 Characteristics of fly ash

A full characterisation was carried out covering various properties of the fly ashes. The summary of main findings is as follows:

- In general, the fly ashes tested during the project conformed to the fineness requirements (< 40% retention on the 45 µm sieve) of BS EN 450-1 (BSI, 2005c). However, with the introduction of low-NO_x and other modern combustion technology, the LOI of run-of-station materials did not comply with the standard requirement (< 9.0%).
- To deal with these, power stations adopted various processing systems including, carbon removal (e.g. Carbon from Source D had ~90% removed) and air-classification (overall LOI reduced by up to ~60-70%). The air-classification also top slices coarse materials from the run-of-station fly ashes.
- The carbon concentration was found in various size fractions, depending on the source.
- In general, the finer fly ash gave spherical shape particles with lower crystalline contents.

9.1.2 Reactivity assessment

Fly ash reactivity was assessed by various methods and attempts were made to correlate these with its properties. Relationships between test results to assess reactivity were also examined. The carbon-removed and oxy-fuel fly ashes gave different behaviour to the other materials (run-of-station/air classified) tested in this project. The following is a summary of the main findings from the work carried out,

- Fly ash/PC mortar gave higher flow with comparatively finer PCs. In general, the flow increased with fly ash fineness, however, there appears an optimum fineness ($d_{90} = \sim 40 \mu\text{m}$; similar to the test PC) below which it decreases with fineness. Minor/no variation was noted between PC (control) and fly ash mortar where the latter was of high fineness ($d_{90} = \sim 10 \mu\text{m}$). MIP tests with early age mortars indicated packing behaviour which is related to the flow.
- Concrete tests supported the fresh behaviour observed in mortar, i.e. fly ash with high flow/low water demand gave higher slump in concrete with the same w/c ratio.
- Activity index test results with PC-based mortars showed dependency on the properties of the test PC. The reactivity of fly ash alumino-silicate components in mortar systems appeared to depend on the rate of lime release by hydration and therefore, PC with higher C₃S content gave greater reactivity, although fineness of PC is another influencing factor on this process.
- Fly ash fineness gave a good indication of its reactivity. Good correlations of activity index (standard curing for 28 and 90 days and accelerated curing for 7 days) were found with fly ash 45 μm sieve residue and sub 10 μm quantities. PSD parameters (d_{50} and d_{90}) also correlated very well with fly ash activity index. Fly ash d_{10} of various size fractions from individual sources also gave a good indication of reactivity, but this was poor between materials from different sources. Tests with concrete also showed dependency of compressive strength on the fly ash fineness.
- Good correlations between strengths following 7 days accelerated curing and standard curing at 28, 56 and 90 days were found. This suggested that the accelerated activity index test has potential for use as a pozzolanicity assessment

test. From a limited number of data sets, a modification in Sadgrove's equation for equivalent curing age was established to match standard and high temperature curing. This suggests potential, but further work would be required.

- Hydrated lime/fly ash mortar tests carried out by modifying the ASTM C593 (ASTM, 2011b) test procedure indicated potential for assessing pozzolanicity. Due to slow strength gain, tests were carried out at 14, 28 and 56 days at $50 \pm 2^\circ\text{C}$. Lime mortar compressive strength correlated with fly ash fineness (both $45 \mu\text{m}$ sieve residue and sub $10 \mu\text{m}$ quantity), especially at later test ages and with PC-mortar test results (by water adjustment and accelerated curing). However, the water requirement test results with hydrated lime/fly ash mortar were not promising due to differences in PSD of the former from both PC and fly ash.
- Reactivity assessment with fly ash/PC paste and TGA gave good indications of its reactivity, indicating decreases in $\text{Ca}(\text{OH})_2$ content over time. The results also gave very good correlations for the respective air-classified fly ashes with activity index using the same PC.
- The Frattini test using a PC, fly ash and water mixture could assess the reactivity of fly ashes (by measuring the lime present in the liquid phase after consumption by fly ash). The level of lime consumed also correlated with fly ash properties and the BS EN 450 (BSI, 2005c) activity index (with the same PC).
- Several approaches were tried to assess fly ash reactivity with saturated lime solution (instead of PC) by measuring lime consumption and change in conductivity of the solution. Although initial tests gave promising results, tests with a wider range of materials were disappointing. The main obstacle noted was very low solubility of lime in water and thereby low pH of the test solution.
- Fly ash chemical analysis such as PPI, sum of the major oxides and glass/amorphous/others/'true' glass content generally agreed with activity index. By considering fineness as a factor with these, better correlations were observed. Among these, the sum of major oxides/ d_{50} consistently gave the best correlation with activity index at 28, 56 and 90 days.
- Heat release from fly ash reaction with quick lime was found to be unsuitable for assessing fly ash reactivity.

- The rate of strength gain in PC-based mortar was higher than concrete due to a relatively higher proportion of cementitious material in the former.
- Fly ash pozzolanicity depended on the origin of the material, therefore, a better correlation between the fly ash properties, mortar, paste and concrete test results was obtained for the material from the same source (air-classified) than different sources.

9.1.3 Fly ash/AEA interaction study

The effectiveness of test methods to assess fly ash/AEA interaction were evaluated by refining existing methods/adopting test methods from other fields. Various aspects of these test parameters (e.g. optimum shaking duration and speed, effects of AEAs in foam index, and the effect of contact time and fly ash mass/AB80 ratio in tests) were studied to find suitable test conditions for carrying them out. Test results were validated in cementitious systems (mortar and concrete). A summary of the main conclusions is as follows:

- Following a typical foam index test procedure by manual shaking, the coefficients of variation between test results of ten operators using 3 fly ashes with LOIs up to 7.6% were found to range between 19.6 – 27.0% for the same conditions, while that for a single operator was 11.6%. This suggests that the foam index test could be used as a means of evaluating interaction between AEA and fly ash in cementitious systems, but different operators can give inconsistent results.
- Using an automatic shaker it was found that changing the shaking speed over a fixed time period, can give significant differences in foam index. This also applied when extending the shaking time at a fixed speed. However, there appeared to be a minimum shaking speed and time (1300 rpm and 25 s in the tests carried out) beyond which there was little change in foam index.
- With the automatic shaker, the foam produced during the test was more uniform in appearance and of larger bubble size than by manual shaking, making visual judgement of the end point easier.
- When applying suitable test conditions, the automatic shaker reduced the coefficients of variation for the foam index, between operators, by around 50%

compared to those of manual shaking, with slight reductions also noted for the single operator.

- From the colorimetric test, a very good linear relationship was found between the concentration of AB80 solution (approximately 0-85 mg/l) and absorbance value (0.00-1.99) with a 630 nm filter. Therefore, it was possible to use this to determine the concentration of AB80, in solution.
- Initial tests indicated that a balance of AB80 quantity and fly ash sample size was required to ensure an appropriate concentration of dye (10-85 mg/l) remained after exposure, particularly in the case of high/low sorptive material. In general, a combination of 2.0 g fly ash in 100 ml of 100 mg/l AB80 solution was satisfactory. However, in some cases, it was necessary to modify the quantity of fly ash used to achieve the target range and hence improve the reliability of the test.
- Contact times as short as 10 minutes could give the relative ranking of fly ash adsorption between samples. In the case of high carbon fly ash, 30 minutes was necessary to reach equilibrium. No difference in AB80 adsorption was found between 30 and 60 minutes exposure.
- The foam index obtained using the automatic shaker was found to give a very good correlation with fly ash specific surface area (N_2 adsorption), which was better than that with the bulk LOI of the material. Similar effects were noted for the two commercial AEAs and standard reagent considered. AB80 adsorption and methylene blue tests also gave similar behaviour with specific surface area and LOI of fly ash. On average, 1 mg AB80 was adsorbed per m^2 surface area of fly ash. Foam index test results generally agreed with the AB80 adsorption and methylene blue test results.
- Tests carried out on fly ash mortars and concretes indicate that the foam index determined using the automatic shaker, AB80 adsorption and methylene blue gave very good correlations with the dosage requirements to entrain a target quantity of air with both (cement-based) systems. The effects noted were similar between the commercial AEAs and standard reagent used, as noted with foam index tests.
- It was possible to use AB80 adsorption data to identify the air entraining/adsorption components of the AEA when used with fly ash in these

systems; however, this did not work for methylene blue tests and suggests further work is required to refine the dose increment for this test.

- Tests with hardened concrete indicated little/no effect of air-entrainment on the permeation properties (ISAT and water penetration under pressure) of the material. These appears to relate how the air-void are distributed in air-entrained concrete (i.e. discrete and note contributing to continuity of capillary pores).
- The practical implications of the study were examined. It is suggested that with the reductions in variability (foam index), instrumental nature (AB80 adsorption), material effects observed and relationships noted with mortar and concrete, the refined foam index, and AB80 adsorption method could be used both as a physical requirement test for fly ash, or in concrete production control.

9.2 Practical Implications

9.2.1 Characteristics of fly ash

With the introduction of environmental regulations (e.g. low-NO_x burning) and modern combustion technologies (e.g. co-combustion and oxy-fuel) fly ashes, properties may deteriorate. In most cases, fineness requirements of the material conformed to that specified in the standard; however, this did not always follow for LOI. Techniques such as carbon removal and air-classification reduce LOI and coarse particles of the material, so they are acceptable to the market. Air-classification of two selected run-of-station fly ashes indicates that this system was very effective in yielding the finest particles (i.e. up to a d_{90} as low as $\sim 10 \mu\text{m}$) with low carbon.

9.2.2 Reactivity assessment

The general coarsening and higher unburnt carbon of fly ash influences fresh properties and reactivity in cementitious system, therefore, the research carried out investigated a range of methods to assess these. The approach considered activity index tests to BS EN 450 (BSI, 2005c) as the reference and investigated tests covering fly ash properties/providing measures of fly ash behaviour. These included (i) fly ash properties (fineness, LOI, and other chemical compositions); (ii) mortar fresh properties (flow and water requirement); (iii) mortar hardened properties (porosity and strength); (iv) accelerated curing of cement

and lime mortars (v) reactivity studies of fly ash/PC or fly ash/lime systems by measuring remaining $\text{Ca}(\text{OH})_2$ in paste (TGA), or suspension (Frattini/saturated lime test; using XRF); and (vi) a quicklime slaking test. The test results were also compared with 100 mm concrete cube strength tests.

There appears an optimum fineness ($d_{90} = \sim 40 \mu\text{m}$) for fly ash to achieve best fresh properties in mortar which is close to the fineness of the test PC, although the flows with the finest fly ashes were comparable with the control flow of the test PC. The relative flow increases with fineness of test PC. This also depends on the fly ash source (for similar fineness materials).

Good correlations between fly ash fineness (PSD parameters or $45 \mu\text{m}$ sieve residue), multiple factor (product of $45 \mu\text{m}$ sieve residue and LOI) and activity index were found. It should be noted that although PSD parameter d_{10} gave an indication of the reactivity of fly ashes from the same source, this was not valid for materials from different sources due possible variations in production conditions.

Activity index tests with different PCs can give significant differences in results, although the relative ranking of the fly ashes remains the same. These depend on both the physical and chemical properties of the test PCs. Mortar tests with laboratory grade hydrated lime can eliminate these variations, but needs a sophisticated low strength test device (Instron) and special curing arrangements.

Relationships between activity index using accelerated and standard curing, suggests the potential of the former for rapid reactivity assessment. The response of fly ash to thermal treatment is influenced by the fineness of the material, therefore, to estimate long-term reactivity from accelerated curing, the properties of fly ash also need to be considered. Limited work using maturity concepts suggests this may have potential for incorporation in the reactivity estimation process.

Given fly ash reacts with the liberated lime in a cementitious system, tests for the remaining $\text{Ca}(\text{OH})_2$ content in fly ash/PC paste, or suspensions can provide a measure of its reactivity. Although these can eliminate aggregate effects in tests, they require special/expensive instruments such as TGA. Tests with saturated lime solution could

eliminate possible influences of test materials, but due very low solubility and limited reactivity in relatively lower pH solution, this method was not found to be promising for the reactivity assessment of fly ash.

Approaches considering oxide and mineralogical composition of fly ash can provide a general indication of the material's reactivity, and combining with fly ash fineness, the assessment can be better. Glass/amorphous/other content of fly ashes from the same source generally provided an indication of their reactivity, but this may not apply for materials obtained from different sources. Reactions of fly ash with quick lime were found to be insensitive for distinguishing between reactivity of different fly ashes.

Overall, fly ash fineness was found to be a good means of rapidly assessing its reactivity considering its simplicity and required test period. Several other, more involved, methods also indicated good relationships with activity index but these require special instrument/test conditions. It is suggested that in addition to 45 μm sieve residue, other methods of fineness measurement, e.g. by LASER analysis (sub 10 μm quantities, d_{50} and d_{90}) could also be considered for this. Therefore, the current test methods of testing fly ash (fineness, LOI, water requirement), with activity index, appear to be the best available means of assessing reactivity.

Given the relationships obtained between mortar and other assessment test results and concrete tests, it might be possible to estimate the fly ash behaviour in the later. However, it should be noted that relative strength gain in concrete would be less than that of mortar and the behaviour would be more consistent for fly ashes from the same source than between sources. It should also be noted that the general behaviour observed during the study did not apply to all fly ashes. For example, in some cases, those with carbon removed by STI technology or produced using oxy-fuel combustion were, not considered in some of the correlations. Further study has been initiated at the CTU, University of Dundee, to consider these issues.

9.2.3 Fly ash/AEA interaction study

Foam index tests

The study has established that the foam index test may be prone to significant variability if the procedure is carried out by different operators using manual shaking. This appears to be due to a combination of operator influences on the shaking applied to the AEA/PC/fly ash/water mixture and visual identification of the end point. The adoption of a standard method of shaking (automatic shaker) was found to give a more uniform foam during the test than with manual shaking, making observation of the end point easier. Furthermore, this reduced the variability between operators to acceptable levels, with slight improvements noted for that of a single operator.

It has also been demonstrated that the foam index determined with the automatic shaker gave very good correlations with the required quantity of AEA to achieve target air contents in both fly ash mortars and concretes. This behaviour applied for fly ashes with fineness (45 μm sieve residue) and LOI up to 29.1% and 14.2%, respectively, and where different admixtures were used, i.e. commercial AEAs and standard reagent.

Given the effects noted, the research suggests that there is potential to develop a standard foam index test for fly ash, with an automatic shaker and a standard reagent. This could then be used as a physical requirement test to enable this property of fly ash to be evaluated. Similarly, it has potential to be applied in concrete production control with the actual AEAs to detect the influence of fly ash property changes on admixture demand.

AB80 adsorption tests

Given the issues noted with evaluating fly ash/AEA interaction, the study examined the feasibility of adopting an approach used to test the adsorption properties of activated carbon. The colorimetric method provides an instrumental measure (eliminating operator influence) of dye adsorption by fly ash, enabling a quantitative assessment of the uptake of AEA by the material to be made. A number of issues associated with the test procedure have been investigated and suitable operating conditions identified as follows:

- 2.0 g fly ash with 100 ml of 100 mg/l AB80
- Fly ash/AB80 contact time, 30 minutes
- Correction for adsorption by filter paper, 0.5 – 6.2%

In addition to its quantitative approach, the technique could offer benefits compared to other test options in terms of economics (e.g. N₂ adsorption for specific surface area), and known test time-scale (foam index test time varies depending on the fly ash being considered). The method, therefore, also has potential as a physical requirement test for use during fly ash production, as suggested for the foam index test. For example, with further work, a classification scheme based on AB80 adsorption could be established to define fly ash suitability for air-entrained concrete. Similarly, in concrete production, relationships of the type given in Figure 8.26 could be developed for particular materials and target air contents, and used to modify admixture doses in relation to changes in fly ash adsorption, identified by the AB80 test.

Methylene blue tests

The results obtained from these tests were comparable with those obtained from foam index and AB80 adsorption. Indeed, the AEA doses required to achieve the target air content in mortar and concrete also correlated well with the MB value. However, the test results were not very precise for low LOI fly ash, which indicates that without having a specialized instrument it can be used for regular bulk quality control in fly ash production as with fine aggregate testing (originally in the standard BS EN 933-9 (BSI, 1999a)).

9.3 Recommendations for Further Study

This study investigated suitable assessment methods for testing fly ash reactivity and interaction with AEA in a cementitious system. For these purposes several promising methods were identified through an extensive experimental programme and their feasibility has been studied. In light of the research programme carried out, the following areas could be explored further:

9.3.1 Materials properties

It was noted that air-classification was effective for processing fly ash into various size fractions, and with coarse particles the carbon present in these fractions was also removed. However, carbon present in finer fraction still remained. On the other hand, carbon removal technology effectively removed carbon, but coarse mineral particles (lower reactivity) may still exist. Therefore, it might be possible to yield best quality material by carbon removal and thereafter size classification.

9.3.2 Reactivity assessment

- The study demonstrated accelerated curing could be a promising method. Limited work using maturity concepts suggests this may have potential for incorporating the above in the reactivity estimation process, but further work would be needed considering the response of different size fly ash particles to thermal action.
- In general, mortar tests with hydrated lime gave promising results but the high humidity curing system in a closed container might not be the best option for strength gain development. If the strength gain situation improved, this method could give a better assessment, eliminating PC effects from mortar tests. Further tests with underwater, high temperature, curing might provide a solution for this and to prevent lime leaching out from mortar, a saturated lime solution is recommended for curing.
- Limited tests were carried out with fly ash from a trial burner using oxy-fuel combustion technology and this might not represent the materials from full-scale combustion. Therefore, further work is needed to assess the properties of fly ash from full-scale combustion using this technology.
- For rapid assessment of reactivity, fly ash can be activated chemically to produce early reactivity results, but effectiveness of various activators needs to take into account for this.
- TGA analysis could be carried out with paste samples cured at high temperature.

9.3.3 Fly ash/AEA interaction study

- This study successfully demonstrated the assessment of fly ash/AEA interaction using foam index and the AB80 adsorption tests. The methylene blue dye

adsorption test could be another potential method, but needs further work to refine its dose increment.

- The study established relationships between the foam index, AB80 adsorption and required admixture doses to entrain target air contents in fresh mortar and concrete. As per Dhir *et al.* (1999), the air content varied with measurement time in fresh concrete but there was no significant difference between PC reference and fly ash concrete. However, a recent study by Sporel *et al.* (2009) indicates high specific surface area fly ashes are more prone to potential air loss with time. Therefore, further tests of varying duration on fresh concrete could be initiated to examine the effect of specific surface area on air-loss. In addition, a compensation dose may apply for this and further relationships may be developed to estimate AEA dose requirement to maintain a certain quantity of air at a given time after mixing.
- The study found no significant effect of air-entrainment on the permeation properties of concrete, which appears to relate how the air-void distributed in air-entrained concrete (i.e. discrete and not contributing to continuity of capillary pores). However, further work may be carried out with air-void parameter (e.g. spacing factor) in hardened concrete to verify this.
- In addition to the air-void parameters, further tests can be carried out to examine effectiveness of air-entrainment on freeze-thaw durability.
- Limited number of between-laboratory tests indicated a good agreement of LOI, fineness (PSD or 45 μm sieve residue) and activity index. Further work could be carried out with the tests for fly ash/AEA interaction (i.e. foam index and AB80 test). Thereafter, these tests could be verified with industry to establish suitability for use in fly ash and concrete production control.

REFERENCES

- Adamiec P, Benezet J C and Benhassaine A (2008). Pozzolanic reactivity of silico-aluminous fly ash. *Particuology*, Vol. 6, No. 2, pp. 93-98.
- Adonyi Z and Szécsényi K M (1996). Thermal analysis of some fly ashes. II. Self-hardening activity of fly ashes. *Journal of Thermal Analysis*, Vol. 46, No. 1, pp. 139-150.
- Agarwal S K (2006). Pozzolanic activity of various siliceous materials. *Cement and Concrete Research*, Vol. 36, No. 9, pp. 1735-1739.
- Al-Mansour F and Zuwal J (2010). An evaluation of biomass co-firing in Europe, *Biomass and Bioenergy*, Vol. 34, No. 5, pp. 620-629.
- Amer A A (1998). Thermal analysis of hydrated fly ash-lime pastes. *Journal of Thermal Analysis and Calorimetry*, Vol. 54, No. 3, pp. 837-843.
- The American Coal Ash Association (ACAA) (2011). 2010 coal combustion product (CCP) production & use survey report, available at: http://acaa.affiniscap.com/associations/8003/files/2010_CCP_Survey_FINAL_102011.pdf (accessed May 2012).
- Antiohos S K, Papageorgiou A, Papadakis V G and Tsimas S (2008). Influence of quicklime addition on the mechanical properties and hydration degree of blended cements containing different fly ashes. *Construction and Building Materials*, Vol. 22, No. 6, pp. 1191-1200.
- Antiotios S K and Tsimas S (2006). Reactive silica of fly ash as an indicator for the mechanical performance of blended cements. *Measuring, Monitoring and Modeling Concrete Properties*, Konsta-Gdoutos M S Eds., Springer, the Netherlands, ISBN: 1-4020-5103-4, pp. 403-409.
- Antiohos S and Tsimas S (2005). Investigating the role of reactive silica in the hydration mechanisms of high-calcium fly ash/cement systems. *Cement and Concrete Composites*, Vol. 27, No. 2, pp. 171-181.
- Antiohos S and Tsimas S (2004). Activation of fly ash cementitious systems in the presence of quicklime Part I. Compressive strength and pozzolanic reaction rate. *Cement and Concrete Research*, Vol. 34, No. 5, pp. 769-779.
- Asadi M (2007). Beet-sugar handbook. *Wiley-Interscience, John Wiley & Sons Inc.*, ISBN: 0-471-76347-0, Hoboken, NJ, USA.

AMERICAN SOCIETY FOR TESTING AND MATERIALS (ASTM)

- ASTM C311 (2011a). Standard test methods for sampling and testing fly ash or natural pozzolans for use as a mineral admixture in Portland-cement concrete. ASTM International, West Conshohocken, PA, USA.

ASTM C593 - 06(2011b) Standard specification for fly ash and other pozzolans for use with lime for soil stabilization. ASTM International, West Conshohocken, PA, USA.

ASTM C618 (2012). Standard specification for coal fly ash and raw or calcined natural pozzolan for use in concrete. ASTM International, West Conshohocken, PA, USA.

ASTM C1240 (2011c). Standard Specification for Silica Fume for Use in Hydraulic-Cement Concrete and Mortar. ASTM International, West Conshohocken, PA, USA.

ASTM D2799 (2011d). Standard test method for microscopical determination of the maceral composition of coal. ASTM International, West Conshohocken, PA, USA.

ASTM D3860 (2008). Standard practice for determination of adsorptive capacity of activated carbon by aqueous phase isotherm technique. ASTM International, West Conshohocken, PA, USA.

ASTM C260M (2010). Standard specification for air-Entraining admixtures for concrete. ASTM International, West Conshohocken, PA, USA.

Aydin S, Karatay C and Baradan B (2010). The effect of grinding process on mechanical properties and alkali-silica reaction resistance of fly ash incorporated cement mortars. *Powder Technology*, Vol. 197, No. 1-2, pp. 68-72.

Baert G, Hoste S, De Schutter G and De Belie N (2008). Reactivity of fly ash in cement paste studied by means of thermogravimetry and isothermal calorimetry. *Journal of Thermal Analysis and Calorimetry*, Vol. 94, No. 2, pp. 485-492.

Ball M C and Carroll R A (1999). Studies of hydrothermal reactions of UK pulverized fuel ashes. Part 1. Reactions between pulverized fuel ash and calcium hydroxide. *Advances in Cement Research*, Vol. 11, No. 2, pp. 53-61.

Baltrus J P and LaCount R B (2001). Measurement of adsorption of air-entraining admixture on fly ash in concrete and cement. *Cement and Concrete Research*, Vol. 31, No. 5, pp. 819-824.

Benezet J-C and Benhassaine A (2009). Contribution of different granulometric populations to powder reactivity. *Particuology*, Vol. 7, No. 1, pp. 39-44.

Bentz D P and Remond S (1997). Incorporation of fly ash into a 3-D cement hydration microstructure model. Building and Fire Research Laboratory, *National Institute of Standards and Technology (NIST)*, Gaithersburg, Maryland 20899, USA. Report No. NISTIR 6050, 55p.

Biernacki J J, Williams P J and Stutzman P E (2001). Kinetics of reaction of calcium hydroxide and fly ash. *ACI Materials Journal*, Vol. 98, No. 4, pp. 340-349.

Bijen J and van Selst R (1993). Cement Equivalence Factors for Fly-Ash. *Cement and Concrete Research*, Vol. 23, No. 5, pp. 1029-1039.

Blanco F, Garcia M P, Ayala J, Mayoral G and Garcia M A (2006). The effect of mechanically and chemically activated fly ashes on mortar properties. *Fuel*, Vol. 85, No. 14-15, pp. 2018-2026.

Brown R C and Dykstra J (1995). Systematic errors in the use of loss-on-ignition to measure unburned carbon in fly ash. *Fuel*, Vol. 74, No. 4, pp. 570-4.

Brunauer S, Emmett P H and Teller E (1938). Adsorption of Gases in Multimolecular Layers. *Journal of the American Chemical Society*, Vol. 60, No. 2, pp. 309-319.

BRITISH STANDARD INSTITUTION (BSI)

BS EN 196-1 (2005a). Methods of testing cement: Determination of strength. BSI, London, UK.

BS EN 196-2 (2005b). Methods of testing cement: Chemical analysis of cement. BSI, London, UK.

BS EN 196-5 (2011a). Methods of testing cement. Pozzolanicity test for pozzolanic cement. BSI, London, UK.

BS EN 196-6 (2010a). Methods of testing cement. Determination of fineness. BSI, London, UK.

BS EN 197-1 (2011b). Cement: Composition, specifications and conformity criteria for common cements. BSI, London, UK.

BS EN 450-1 (2005c). Fly ash for concrete: Definition, specifications and conformity criteria. BSI, London, UK.

BS EN 451-2 (1995). Method of testing fly ash: Determination of fineness by wet sieving. BSI, London, UK.

BS EN 459-2 (2010b). Building lime: Test methods. BSI, London, UK.

BS EN 933-9 (1999a). Tests for geometrical properties of aggregates: Assessment of fines - Methylene blue test. BSI, London, UK.

BS EN 934-2 (2009a). Admixtures for concrete, mortar and grout: Concrete admixtures - Definition, requirements, conformity, marking and labelling. BSI, London, UK.

BS EN 1015-3 (1999b). Methods of test for mortar for masonry: Determination of consistence of fresh mortar (by flow table), BSI, London, UK.

BS EN 1015-7 (1999c). Methods of test for mortar for masonry: Determination of air content of fresh mortar. BSI, London, UK.

BS EN 1097-6 (2000). Tests for mechanical and physical properties of aggregates: Determination of particle density and water absorption. BSI, London, UK.

BS 1881 – 208 (1996). Testing concrete: Recommendations for the determination of initial surface absorption of concrete. BSI, London, UK.

BS 3892-1 (1997). Pulverised-fuel ash: specification for pulverised fuel ash for use with Portland cement, BSI, London, UK.

BS 3892-1 (1982). Pulverized-fuel ash: Specification for pulverized-fuel ash for use as a cementitious component in structural concrete. BSI, London, UK.

BS EN 12350-7 (2009b). Testing fresh concrete: Air content – Pressure methods. BSI, London, UK.

BS EN 12390 – 8 (2009c). Testing hardened concrete: Depth of penetration of water under pressure. BSI, London, UK.

BS EN 12620 (2002). Aggregates for concrete. BSI, London, UK.

Burriss S C, Li D and Riley J T (2005). Comparison of heating losses and macro thermogravimetric analysis procedures for estimating unburned carbon in combustion residues. *Energy Fuels*, Vol. 19, No. 4, pp. 1493–502.

Cameron F K and Patten H E (1911). The solubility of lime in aqueous solutions of sugar and glycerol. *The Journal of Physical Chemistry*, Vol. 15, No. 1, pp. 67–72.

Cheary R W and Coelho A A (1994). Synthesising and fitting linear position sensitive detector step-scanned line profile. *Journal of Applied Crystallography*, Vol. 27, pp. 673-681.

Chaipanich A and Nochaiya T (2010). Thermal analysis and microstructure of Portland cement-fly ash-silica fume pastes. *Journal of Thermal Analysis and Calorimetry*, Vol. 99, No. 2, pp. 487-493.

Choy K K H, Porter J F and McKay G (2000). Langmuir isotherm models applied to the multicomponent sorption of acid dyes from effluent onto activated carbon. *Journal of Chemical and Engineering Data*. Vol. 45, No. 4, pp. 575–584.

Christensen B J, Coverdale R T, Olson R A, Ford S J, Garboczi E J, Jennings H M and Mason T O (1994). Impedance spectroscopy of hydrating cement-based materials: measurement, interpretation, and application. *Journal of the American Ceramic Society*, Vol. 77, No. 11, pp. 2789-2804.

Chun X, Wang B J and Song Q L (2006). Study pozzolanic activity of mineral admixtures in forms of Li-salt industrial residue and fly ash, *Environmental Ecology and Technology of Concrete*, Book Series: Key Engineering Materials, Vol. 302-303, pp. 162-166.

Clendenning T G and Durie N D (1962). Properties and use of fly ash from a steam plant operating under variable load. *Proceeding of the American Society for Testing Materials*, Vol. 62, pp. 1019–37.

Concrete Society (2011). Cementitious materials: the effect of GGBS, fly ash, silica fume and limestone fines on the properties of concrete. Technical Report 74. *The Concrete Society*, Camberley, Surrey, UK, 57p.

Construction Industry Research and Information Association (CIRIA) (2001). Freeze/thaw resisting concrete – its achievement in the UK. CIRIA, London, UK.

Davis R E, Carlston R W, Kelly J W, and Davis H E (1937). Properties of cements and concretes containing fly ash. *Journal of the American Concrete Institute*, Vol. 33, pp. 577-612.

de Rojas M I S and Frías M (1996). The pozzolanic activity of different materials, its influence on the hydration heat in mortars. *Cement and Concrete Research*, Vol. 26, No. 2, pp. 203-213.

Department of Energy and Climate Change (DECC) (2010) UK Energy in brief 2010. A National Statistics Publication, available at: www.decc.gov.uk/en/content/cms/statistics/publications/publications.aspx (accessed May 2012).

Department of Trade and industry (DTI) (1999). Supercritical steam cycles for power generation applications. *Technology Status Report 009*, 13p.

Dhir R K, McCarthy M J, Limbachiya M C, Zhang D S and El-Sayed H I (1999). PFA concrete: air entrainment and freeze/thaw durability. *Magazine of Concrete Research*, Vol. 51, No. 1, pp. 53-64.

Dhir R K, Hewlett P C and Chan Y N (1987). Near-surface characteristics of concrete: assessment and development of test methods. *Magazine of Concrete Research*, Vol. 39, No. 141, pp. 183-195.

Dodson V H (1990). Concrete Admixtures. *Van Nostrand Reinhold*, New York, NY, USA, pp. 140-143.

Dodson V H (1980). Foam Index Test. *Presentation at the Transportation Research Board*, Washington, DC, USA.

Donatello S, Tyrer M and Cheeseman C R (2010). Comparison of test methods to assess pozzolanic activity. *Cement and Concrete Composites*, Vol. 32, No. 2, pp. 121-127.

ELTRA (2012). CS-800: Carbon/Sulfur determinator, *ELTRA GmbH* (Online at: www.eltragmbh.com/cs800/information.shtml, last accessed in 2012).

Environment Canada (2008). Screening assessment for the challenge – Benzene-sulfonic acid, 3,3'-[(9,10-dihydro-9,10-dioxo-1,4-anthracenediyl) diimino]bis [2,4,6-trimethyl] disodium salt (Acid Blue 80, CAS RN 4474-24-2), Ottawa, 27 p.

European Coal Combustion Products Association (ECOBA) (2010). Production and utilisation of CCPs in 2009 in Europe (EU 15). Available at: www.ecoba.com/evjm/media/ccps/ecoba_statistics_2009.pdf (last accessed: May 2012).

European Commission (EC) (2012). Electricity production, consumption and market overview, Eurostat, available at: http://epp.eurostat.ec.europa.eu/statistics_explained/index.php/Electricity_production,_consumption_and_market_overview (last accessed May 2012)

Fainerman V B, Miller R and Joos P (1994). The measurement of dynamic surface-tension by the maximum bubble pressure method. *Colloid and Polymer Science*, Vol. 272, No. 6, pp. 731–739.

Fan M and Brown R C (2001). Comparison of the loss-on-ignition and thermogravimetric analysis techniques in measuring unburned carbon in coal fly ash. *Energy Fuels*, Vol. 15, No. 6, pp. 1414–1417.

Fan Y M, Yin S H, Wen Z H and Zhong J Y (1999). Activation of fly ash and its effects on cement properties. *Cement and Concrete Research*, Vol. 29, No. 4, pp. 467–472.

Feng Q G, Yamamichi H, Shoya M and Sugita S (2004). Study on the pozzolanic properties of rice husk ash by hydrochloric acid pretreatment. *Cement and Concrete Research*, Vol. 34, No. 3, pp. 521–526.

FERCo (2012). HOT FOIL™ LOI Instrument, *Fossil Energy Research Corp.*, online at: www.ferco.com/LOI.html, (last accessed April 2012).

Folagbade S O (2011). Carbonation and permeation properties of cement combinations using CEM I, fly ash, silica fume and metakaolin. *PhD thesis*, Concrete Technology Unit, University of Dundee, UK, 290p.

Folliard K, Hover K, Harris N, Ley M T and Naranjo A (2009). Effects of Texas fly ash on air-entrainment in concrete: Comprehensive report. Report No. FHWA/TX-08/0-5207-1, Center for Transportation Research, The University of Texas at Austin, Austin, TX, USA, 577p.

Font O, Moreno N, Querol X, Izquierdo M, Alvarez E, Diez S, Elvira J, Antenucci D, Nugteren H, Plana F, López A, Coca P and Peña F G (2010). X-ray powder diffraction-based method for the determination of the glass content and mineralogy of coal (co)-combustion fly ashes. *Fuel*, Vol. 89, No. 10, pp. 2971–2976.

Freeman E, Gao Y-M, Hurt R and Suuberg E (1997). Interactions of carbon-containing fly ash with commercial air-entraining admixtures for concrete. *Fuel*, Vol. 76, No. 8, pp. 761–765.

Frias M, Villar-Cocina E, de Rojas S M I, Valencia-Morales E (2005). The effect that different pozzolanic activity methods has on the kinetic constants of the pozzolanic reaction in sugar cane straw-clay ash/lime systems: Application of a kinetic–diffusive model. *Cement and Concrete Research*, Vol. 35, No. 11, pp. 2137–2142.

Gao Y, Külaots I, Chen X, Suuberg E M, Hurt R H and Veranth J M (2002). The effect of solid fuel type and combustion conditions on residual carbon properties and fly ash quality. *Proceedings of the Combustion Institute*, Vol. 29, pp. 475–83.

Gao Y, Külaots I, Chen X, Aggarwal R, Mehta A, Suuberg E M and Hurt R H (2001). Ozonation for the chemical modification of carbon surfaces in fly ash, *Fuel*, Vol. 80, No 5, pp. 765-768.

Gao Y-M, Shim H-S, Hurt R H, Suuberg E M and Yang N Y C (1997). Effects of carbon on air entrainment in fly ash concrete: the role of soot and carbon black. *Energy & Fuels*, Vol. 11, No. 2, pp. 457-462.

Gava G P and Prudencio Jr. L R (2007b). Pozzolanic activity tests as a measure of pozzolans' performance. Part 2. *Magazine of Concrete Research*, Vol. 59, No. 10, pp. 735-741.

Gava G P and Prudencio Jr. L R (2007a). Pozzolanic activity tests as a measure of pozzolans' performance. Part 1, *Magazine of Concrete Research*, Vol. 59, No. 10, pp. 729-734.

Gayathri T (2008). Feasibility of recovery and processing long-term stored PFA for use as a cement addition in concrete. *PhD thesis*, Concrete Technology Unit, University of Dundee, UK, 276p.

Gebler S H and Klieger P (1983). Effect of fly ash on the air-void stability of concrete. *Portland Cement Association*, Skokie, IL, USA, Report No. RD085.01T, 40p.

Giergiczny Z (2004). Effect of some additives on the reactions in fly ash-Ca(OH)₂ system. *Journal of Thermal Analysis and Calorimetry*, Vol. 76, No. 3, pp. 747-754.

GmbH (2012). UV-Vis spectrometer. *UV-Elektronik GmbH*, Online at: www.uv-groebel.com/pdf_enu/E_PCSpektrometer.pdf. (last accessed May 2012).

Goni S, Guerrero A, Luxan M P and Macias A (2003). Activation of the fly ash pozzolanic reaction by hydrothermal conditions. *Cement and Concrete Research*, Vol. 33, No. 9, pp. 1399-1405.

Grace W R and Co. (Conn.) (2006). The foam index test: A rapid indicator of relative AEA demand, *Technical Bulletin TB-0202* (www.graceconstruction.com, last accessed April 2011)

Guerrero A, Hernandez M S and Goni S (2000). The role of the fly ash pozzolanic activity in simulated sulphate radioactive liquid waste. *Waste Management*, Vol. 20, No. 1, pp. 51-58.

Hachman L, Burnett A, Gao Y, Hurt R and Suuberg E (1998). Surfactant adsorptivity of solid products from pulverized-coal combustion under controlled conditions, *27th International Symposium on Combustion*, The Combustion Institute, Pittsburgh, USA, pp. 2965-2971.

Hameed B H, Din A T M and Ahmad A L (2007). Adsorption of methylene blue onto bamboo-based activated carbon: Kinetics and equilibrium studies. *Journal of Hazardous Materials*, Vol. 141, No. 3, pp. 819-825.

Hang P T and Brindley G W (1970). Methylene blue absorption by clay minerals. Determination of surface areas and cation exchange capacities (Clay-organic studies XVIII). *Clays and Clay Minerals*, Vol. 18, No. 4, pp. 203-212.

-
- Harrison T A (1995). Formwork striking times – criteria, prediction and methods of assessment. *Construction Industry Research and Information Association (CIRIA) Report 136*, Westminster, London, UK, 73p.
- Heikal M, El-Didamony H, Helmy I M and El-Raouf A F (2003). Pozzolanic activity of fly ash. *Silicates Industriels*, Vol. 68, No. 9-10, pp. 111-117.
- Heinz D, Göbel M, Hilbig H, Urbonas L and Bujauskaite G (2010). Effect of TEA on fly ash solubility and early age strength of mortar. *Cement and Concrete Research*, Vol. 40, No. 3, pp. 392-397.
- Helmuth R (1987). Fly ash in cement and concrete. *Portland Cement Association*, Skokie, IL, USA, 203 pp.
- Hill R, Rathbone R, and Hower J C (1998). Investigation of fly ash carbon by thermal analysis and optical microscopy, *Cement and Concrete Research*, Vol. 28, No. 10, pp. 1479-1488.
- Hill R L, Sarkar S L, Rathbone R F and Hower J C (1997). An examination of fly ash carbon and its interaction with air entraining agent, *Cement and Concrete Research*, Vol. 27, No. 2, pp. 193-204.
- Hower J C and Mastalerz M (2001). An Approach toward a Combined Scheme for the Petrographic Classification of Fly Ash. *Energy & Fuels*, Vol. 15, pp. 1319-1321.
- Hower J C, Robl T L and Thomas G A (1999a). Changes in the quality of coal combustion by products produced by Kentucky Power Plants, 1978 to 1997: Consequences of Clean Air Act Directives. *Fuel*, Vol. 78, No. 6, pp. 701-712.
- Hower J C, Thomas G A and Palmer J (1999b). Impact of the conversion to low-NO_x combustion on ash characteristics in a utility boiler burning Western US coal. *Fuel Processing Technology*, Vol. 61, No. 3, pp. 175-195.
- Hower J C, Rathbone R F, Robl T L, Thomas G A, Haeberlin B O and Trimble A S (1997). Case study of the conversion of tangential- and wall-fired units to low-NO_x combustion: Impact on fly ash quality. *Waste Manage*, Vol. 17, No. 4, pp. 219-229.
- Hower J C, Rathbone R F, Graham U M, Groppo J G, Brooks S M, Robl T L and Medina S S (1995). Approaches to the petrographic characterization of fly ash. *11th International Coal Testing Conference*, Lexington, KY, pp. 49-54.
- Hubbard F H and Dhir R K (1984). A compositional index of the pozzolanic potential of pulverized-fuel ash. *Journal Material Science Letters*, Vol. 3, No. 11, pp. 958-960.
- Hwang K, Noguchi T and Tomosawa F (2004). Prediction model of compressive strength development of fly-ash concrete. *Cement and Concrete Research*, Vol. 34, No. 12, pp. 2269-2276.

Institute of Technological Research of São Paulo (1997). Pozzolanic Activity: Modified Chapelle Method. *IPT*, São Paulo, Brazil. (In Portuguese.)

ISO 10694 (1995). Soil quality – Determination of organic and total carbon after dry combustion (elementary analysis). *ISO*, ISO Central Secretariat, Geneva, Switzerland.

JCAS I-61 (2008). Measurement of the amount of methylene blue absorption by fly ash. *Japan Cement Association*, Test manual – IV, pp. 42-45, Japan (In Japanese).

Jing Z, Matsuoka N, Jin F, Yamasaki N, Suzuki K, Hashida T (2006). Solidification of coal fly ash using hydrothermal processing method. *Journal of Materials Science*, Vol. 41, pp. 1579–1584.

Jolocieur C, To T C, Benoit E, Hill R, Zhang Z Z and Page M (2009). Fly ash carbon effects on concrete air-entrainment: fundamental studies on their origin and chemical mitigation. *World of Coal Ash (WOCA)*, Lexington, KY, 4-7 May 2009.

Joshi R C and Lohtia R P (1997). Fly ash in concrete, production, properties and uses. *Advances in Concrete technology Volume 2*, Gordon and Breach Science Publishers, Amsterdam, the Netherlands, ISBN: 90-5699-579-0, 269p.

Külaots I, Hurt R H and Suuberg E M (2004). Size distribution of unburned carbon in coal fly ash and its implications. *Fuel*, Vol. 83, No. 2, pp. 223-230.

Külaots I, Hsu A, Hurt R H and Suuberg E M (2003). Adsorption of surfactants on unburned carbon in fly ash and development of a standardized foam index test. *Cement and Concrete Research*, Vol. 33, No. 12, pp. 2091-2099.

LaCount R B and Kern D G (2005). Economical treatment of high carbon fly ash to produce a low foam index product with carbon content retained. *Technical Report DE-FC26-98FT40028*, Waynesburg College, Waynesburg, PA, USA, 28p.

LECO Corporation (2012). CS844 Series: Carbon and sulfur in inorganic materials by the combustion infrared detection technique, online at: www.leco.com/products/inorganic/carbon_sulfur/cs844/cs_844.html, (last accessed April 2012)

Lee C Y, Lee H K and Lee K M (2003). Strength and microstructural characteristics of chemically activated fly ash–cement systems. *Cement and Concrete Research*, Vol. 33, No. 3, pp. 425–431.

Lei S, Miyamoto J, Kanoh H, Nakahigashi Y and Kaneko K (2006). Enhancement of the methylene blue adsorption rate for ultramicroporous carbon fiber by addition of mesopores. *Carbon*, Vol. 44(10), pp. 1884–1890.

Li H J, Sun H H, Tie X C and Xiao X J (2008). A new method to evaluate the hydraulic activity of Al-Si materials. *Science in China Series E: Technological Sciences*, Vol. 51, No. 2, pp. 113-120.

Li D X, Xu Z Z, Luo Z M, Pan Z H and Cheng L (2002). The activation and hydration of glassy cementitious materials. *Cement and Concrete Research*, Vol. 32, No. 7, pp. 1145-1152.

-
- Li D X, Chen Y M, Shen J L, Su J H and Wu X Q (2000a). The influence of alkalinity on activation and microstructure of fly ash. *Cement and Concrete Research*, Vol. 30, No. 6, pp. 881-886.
- Li D X, Chen Y M, Shen J L and Luo Z M (2000b). The influence of temperature and admixtures on activation of low calcium fly ash. *Journal of Wuhan University of Technology-Materials Science Edition*, Vol. 15, No. 3, pp. 13-18.
- Liu B J, Xie Y J and Li J (2005). Influence of steam curing on the compressive strength of concrete containing supplementary cementing materials. *Cement and Concrete Research*, Vol. 35, No. 5, pp. 994-998.
- Luxan M P, Madruga F and Saavedra J (1989). Rapid evaluation of pozzolanic activity of natural products by conductivity measurement. *Cement and Concrete Research*, Vol. 19, No. 1, pp. 63-68.
- Ma W P and Brown P W (1997). Hydrothermal reactions of fly ash with $\text{Ca}(\text{OH})_2$ and $\text{CaSO}_4 \cdot 2\text{H}_2\text{O}$. *Cement and Concrete Research*, Vol. 27, No. 8, pp. 1237-1248.
- Majumdar A J and Larner L J (1977). The measurement of Pozzolanic Activity. *Cement and Concrete Research*, Vol. 7, No. 2, pp. 209-210.
- Malhotra V M (1993). Fly ash, slag, silica fume, and rice husk ash in concrete: A review. *Concrete International*, Vol. 15, No. 4, pp. 23-28.
- Manz O E (1999). Coal fly ash: a retrospective and future look, *Fuel*, Vol. 78, No. 2, pp. 133-136.
- Maroto-Valer M M, Taulbee D N and Hower J C (2001). Characterization of differing forms of unburned carbon present in fly ash separated by density gradient centrifugation. *Fuel*, Vol. 80, No. 6, pp. 795-800.
- McCarter W J and Tran D (1996). Monitoring pozzolanic activity by direct activation with calcium hydroxide. *Construction and Building Materials*, Vol. 10, No. 3, pp. 179-184.
- McCarthy M J and Dhir R K (2005). Development of high volume fly ash cements for use in concrete construction. *Fuel*, Vol. 84, No. 11, pp. 1423-1432.
- Mehta P K (1986). Standard specifications for mineral admixtures - an overview. *American Concrete Institute*, Special publication, Vol. 91, No. SP91-30, pp. 637-658.
- Mielenz R C, Wolkodoff V E, Backstrom J E and Flack H L (1958). Origin, evolution, and effects of the air void system in concrete. Part 1 - Entrained air in unhardened concrete. *Journal of the American Concrete Institute*, Vol. 30, No. 1, pp. 95-212.
- Moropoulou A, Bakolas A and Aggelakopoulou E (2004). Evaluation of pozzolanic activity of natural and artificial pozzolans by thermal analysis. *Thermochimica Acta*, Vol. 420, No. 1-2, pp. 135-140.

BRAZILIAN ASSOCIATION OF TECHNICAL STANDARDS (NBR)

NBR 5751 (1992a). Pozzolanic materials: Determination of the pozzolanic activity: Pozzolanic activity index with lime. *NBR*, Rio de Janeiro, Brazil. (In Portuguese).

NBR 5752 (1992b). Pozzolanic materials: Determination of the pozzolanic activity index. *NBR*, Rio de Janeiro, Brazil. (In Portuguese).

Neville A M (2011). *Properties of Concrete*. 5th Edition, Pearson Education Limited, ISBN: 978-0-273-75580-7, Harlow, UK.

Normann F, Andersson K, Leckner B and Johnsson F (2008). High-temperature reduction of nitrogen oxides in oxy-fuel combustion, *Fuel*, Vol. 87, No. (17-18), pp. 3579-3585.

Pacewska B, Blonkowski G and Wilinska I (2008a). Studies on the pozzolanic and hydraulic Properties of fly ashes in model systems. *Journal of Thermal Analysis and Calorimetry*, Vol. 94, No. 2, pp. 469-476.

Pacewska B, Wilinska I and Blonkowski G (2008b). Investigations of cement early hydration in the presence of chemically activated fly ash - Use of calorimetry and infrared absorption methods. *Journal of Thermal Analysis and Calorimetry*, Vol. 93, No. 3, pp. 769-776.

Panagiotopoulou C, Perraki T, Tsvivilis S, Skordaki N and Kakali G (2009). A study on alkaline dissolution and geopolymerisation of hellenic fly ash. *Ceramic Engineering and Science Proceedings* (Lin *et al.* Eds.), Vol. 29, No. 10, pp. 165-173

Panagiotopoulou C, Kontori E, Perraki T and Kakali G (2007). Dissolution of aluminosilicate minerals and by-products in alkaline media. *Journal of Materials Science*, Vol. 42, No. 9, pp. 2967-2973.

Pang J (2012). Fly ash property influences on bubble formation in air-entrained concrete. *Undergraduate project*, Concrete Technology Unit, University of Dundee, UK, 80p.

Papadakis V G, Antiohos S and Tsimas S (2002). Supplementary cementing materials in concrete Part II: A fundamental estimation of the efficiency factor. *Cement and Concrete Research*, Vol. 32, No. 10, pp. 1533–1538.

Paya J, Borrachero M V, Monzo J, Peris-Mora E and Amahjour F (2001). Enhanced conductivity measurement techniques for evaluation of fly ash pozzolanic activity. *Cement and Concrete Research*, Vol. 31, No. 1, pp. 41-49.

Paya J, Monzo J, Borrachero M V, Peris-Mora E and Amahjour F (2000). Mechanical treatment of fly ashes Part IV. Strength development of ground fly ash-cement mortars cured at different temperatures. *Cement and Concrete Research*, Vol. 30, No. 4, pp. 543-551.

Paya J, Monzo J, Borrachero M V, Perris E and Amahjou F (1998). Thermogravimetric methods for determining carbon Content in fly ashes. *Cement and Concrete Research*, Vol. 28, No. 5, pp. 675-686.

Paya J, Monzo J, Peris-Mora E, Borrachero M V, Tercero R and Pinillos C (1995). Early-strength development of portland cement mortars containing air classified fly ashes. *Cement and Concrete Research*, Vol. 25, No. 2, pp. 449-456.

Pedersen K H, Jensen A D and Dam-Johansen K (2010). The effect of low-NO_x combustion on residual carbon in fly ash and its adsorption capacity for air entrainment admixtures in concrete. *Combustion and Flame*, Vol. 157, No. 2, pp. 208-216.

Pedersen K H, Jensen A D, Skjøth-Rasmussen M S and Dam-Johansen K (2008). A review of the interference of carbon containing fly ash with air entrainment in concrete. *Progress in Energy and Combustion Science*, Vol. 34, No. 2, pp. 135-154.

Pedersen K H, Andersen S I, Jensen A D and Dam-Johansen K (2007). Replacement of the foam index test with surface tension measurements, *Cement and Concrete Research*, Vol. 37, No. 6, pp. 996-1004.

Pheeraphan T, Cayliani L, Dumangas Jr. M I and Nimityongskul P (2002). Prediction of later-age compressive strength of normal concrete based on the accelerated strength of concrete cured with microwave energy. *Cement and Concrete Research*, Vol. 32, No. 4, pp. 521-527.

Qiao X C, Poon C S and Cheung E (2006). Comparative studies of three methods for activating rejected fly ash. *Advances in Cement Research*, Vol. 18, No. 4, pp. 165-170.

Rosell-Lama M, Villar-Cociña E and Frias M (2011). Study on the pozzolanic properties of an atural Cuban zeolitic rock by conductometric method: Kinetic parameters. *Construction and Building Materials*, Vol. 25, No. 2, pp. 644-650.

Roszczynialski W (2002). Determination of pozzolanic activity of materials by thermal analysis. *Journal of Thermal Analysis and Calorimetry*, Vol. 70, No. 2, pp. 387-392.

Rowles M and O'Connor B (2003). Chemical optimisation of the compressive strength of aluminosilicate geopolymers synthesised by sodium silicate activation of metakaolinite. *Journal of Materials Chemistry*, Vol. 13, No. 5, pp. 1161-1165.

Rowles M R, Hanna J V, Pike K J, Smith M E and O'Connor B H (2007). ²⁹Si, ²⁷Al, ¹H and ²³Na MAS NMR study of the bonding character in aluminosilicate inorganic polymers. *Applied Magnetic Resonance*, Vol. 32, No. 4, pp. 663-689.

Sadgrove B M (1975). Prediction of strength development in concrete structures. In: *54th Annual meeting of the Transport Research Board, Washington DC, January 1975* (Cited by Harrison, 1995).

Saperstein D D (1987). IR spectrophotometric method for the measurement of toluene adsorptivity in activated carbon. *Langmuir*, Vol. 3, No. 1, pp. 81-85.

- Schwarz N and Neithalath N (2008). Influence of a fine glass powder on cement hydration: Comparison to fly ash and modeling the degree of hydration. *Cement and Concrete Research*, Vol. 38, No. 4, pp. 429-436.
- Scott A N and Thomas M D A (2007). Evaluation of fly ash from co-combustion of coal and petroleum coke for use in concrete. *ACI Materials Journal*, Vol. 104, No. 1, pp. 62-69.
- Sear L K A (2011), Future trends for PFA in cementitious systems. *Future Cement Conference and Exhibition*, 8 February 2011, London Chamber of Commerce, London UK (Online at: www.ukqaa.org.uk, last accessed May 2012).
- Sear L K A (2001). The properties and use of coal fly ash. *Thomas Telford*, London, UK, ISBN: 0-7277-3015-0, 261p.
- Serway R A, Faughn J S and Vuille C (2011). College Physics. Vol. 1, Ninth edition, *Brooks/Cole*, Boston, MA, USA, ISBN: 0-8400-6848-4, 512p.
- Sharma R C, Jain N K and Ghosh S N (1993). Semitheoretical method for the assessment of reactivity of fly ashes. *Cement and Concrete Research*, Vol. 23, No. 1, pp. 41-45.
- Shehata M H and Thomas M D A (2006). Alkali release characteristics of blended cements. *Cement and Concrete Research*, Vol. 36, No. 6, pp. 1166-1175.
- Shi C J, Wu Y Z, Riefler C and Wang H (2005). Characteristics and pozzolanic reactivity of glass powders. *Cement and Concrete Research*, Vol. 35, No. 5, pp. 987-993.
- Shi C and Day R L (2001). Comparison of different methods for enhancing reactivity of pozzolans. *Cement and Concrete Research*, Vol. 31, No. 5, pp. 813-818.
- Shvarzman A, Kovler K, Schamban I, Grader G S and Shter G E (2002). Influence of chemical and phase composition of mineral admixtures on their pozzolanic activity. *Advances in Cement Research*, Vol. 14, No. 1, pp. 35-41.
- Sinthaworn S and Nimityongskul P (2009). Quick monitoring of pozzolanic reactivity of waste ashes. *Waste Management*, Vol. 29, No. 5, pp. 1526-1531.
- Speight J G (2005). Handbook of coal analysis. *John Wiley & Sons*, New Jersey, USA, ISBN: 0-471-52273-2, 222p.
- Sporel F, Uebachs S and Brameshuber W (2009). Investigations on the influence of fly ash on the formation and stability of artificially entrained air voids in concrete. *Materials and Structures*, Vol. 42, No. 2, pp. 227-240.
- Stencel J M, Song H and Cangialosi F (2009). Automated foam index test: Quantifying air entraining agent addition and interactions with fly ash-cement admixtures. *Cement and Concrete Research*, Vol. 39, No. 4, pp. 362-370.

-
- Stone W E and Scheuch F C (1894). A method for determining calcium oxide in quicklime. *The Journal of the American Chemical Society*. Vol. 16, No. 2, pp. 721 – 725.
- Swamy R N (1993). Fly ash and slag: standards and specifications: help or hindrances? *Materials and Structures*, Vol. 26, No. 164, pp. 600–613.
- Swamy R N (Eds.) (1986). Cement replacement materials. *Concrete technology and design: Volume 3*, ISBN: 0-903384-52-3, Surrey University Press, London, UK, 255p.
- Sybertz F (1989). Comparison of different methods for testing the pozzolanic activity of fly ashes. *American Concrete Institute*, Detroit, MI, USA, Vol. 114, No. SP114-22, pp. 477–497.
- Tangpagasit J, Cheerarot R, Jaturapitakkul C and Kiattikomol K (2005). Packing effect and pozzolanic reaction of fly ash in mortar. *Cement and Concrete Research*, Vol. 35, No. 6, pp. 1145-1151.
- Tashiro C, Ikeda K and Inoue Y (1994). Evaluation of pozzolanic activity by the electric-resistance measurement method. *Cement and Concrete Research*, Vol. 24, No. 6, pp. 1133-1139.
- Taylor P C, Johansen V C, Graf L A, Kozikowski R L, Zemajtis J Z and Ferraris C F (2006). Identifying incompatible combinations of concrete materials: Volume II-Test protocol, *Federal Highway Administration*, Report No. HRT-06-080, McLean, VA, USA, 86p.
- Teychenné D C, Franklin R E and Erntroy H C (1997). Design of normal concrete mixes, 2nd revised edition, BRE report 331, *BRE press*, Watford, UK, 45p.
- Thompson A (2008). The current and future nature of combustion ashes. In Cox M, Nugteren H and Janssen-Jurkovicova M (Eds.), *Combustion residue: current, novel and renewable applications*. John Wiley & Sons, Ltd, West Sussex, England, ISBN: 978-0-470-09442-6, 5p.
- Topcu I B, Toprak M U and Akdag D (2008a). Early estimation of concrete strength with microwave curing method, *Teknik Dergi*, Vol. 19, No. 4, pp. 4539-4544.
- Topcu I B, Toprak M U and Akdag D (2008b). Determination of optimal microwave curing cycle for fly ash mortars. *Canadian Journal of Civil Engineering*, Vol. 35, No. 4, pp. 349-357.
- Tumidajski P J, Gong B and Baker D (2003). Correlation between 28-day and 6-hour compressive strengths. *Cement and Concrete Research*, Vol. 33, No. 9, pp. 1491-1493.
- Ubbriaco P, Bruno P, Traini A and Calabrese D (2001). Fly ash reactivity. Formation of hydrate phases. *Journal of Thermal Analysis and Calorimetry*, Vol. 66, No. 1, pp. 293-305.
- U S Department of Energy (USDOE) (2012). Electric Power Monthly, Report No. DOE/EIA-0226 (2012/04), U S Energy Information Administration, *Office of Electricity, Renewables & Uranium Statistics*, Washington, DC 20585, USA, (online at: www.eia.gov/cneaf/electricity/epm/epm_sum.html, last accessed May 2012)

- Valix M, Cheung W H and McKay G (2004). Preparation of activated carbon using low temperature carbonisation and physical activation of high ash raw bagasse for acid dye adsorption. *Chemosphere*, Vol. 56, No. 5, pp. 493-501.
- Venter J J and Vannice M A (1987). A diffuse reflectance FTIR spectroscopic (DRIFTS) investigation of carbon-supported metal carbonyl clusters. *Journal of American Chemical Society*, Vol. 109, No. 20, pp. 6204-6205.
- Vorres K (1979). Coal. In: *Kirk-Othmer Encyclopedia of Chemical Technology*, 3rd Edition, John Wiley & Sons Inc., New York, USA, Vol. 6, pp. 224-282.
- Wang A Q, Zhang C Z and Sun W (2004). Fly ash effects - II. The active effect of fly ash. *Cement and Concrete Research*, Vol. 34, No. 11, pp. 2057-2060.
- Wang X Y and Lee H S (2009). Simulation of a temperature rise in concrete incorporating fly ash or slag. *Materials and Structures*, Vol. 43, No. 6, pp. 737-754.
- Ward C R and French D (2006). Determination of glass content and estimation of glass composition in fly ash using quantitative X-ray diffractometry. *Fuel*, Vol. 85, No. 16, pp. 2268-2277.
- Wei X and Li Z (2005). Study on hydration of Portland cement with fly ash using electrical measurement. *Materials and Structures*, Vol. 38, No. 277, pp. 411-417.
- Wesche K (Eds.) (2005). Fly ash in concrete, Properties and performance. Report of Technical Committee 67-FAB Use of Fly Ash in Building RILEM, Report 7, *Taylor & Francis e-Library*, Master e-book ISBN 0-203-62641-9, 284p.
- Wilmoth K (2011). Rapid assessment methods to predict fly ash performance in concrete. *M Sc dissertation*. Concrete Technology Unit, University of Dundee, Dundee, UK.
- Winnefeld F, Leemann A, Lucuk M, Svoboda P and Neuroth M (2010). Assessment of phase formation in alkali activated low and high calcium fly ashes in building materials. *Construction and Building Materials*, Vol. 24, No. 6, pp. 1086-1093.
- World Business Council for Sustainable Development (WBCSD) (2002). The cement sustainability initiative – our agenda for action. ISBN 2-940240-24-8, July 2002, Switzerland.
- Xu H and van Deventer J S J (2003). Effect of source materials on geopolymerization. *Industrial & Engineering Chemistry Research*, Vol. 42, No. 8, pp. 1698-1706.
- Yamamoto T, Kanazu T, Nambu M and Tanosaki T (2006). Pozzolanic reactivity of fly ash-API method and K-value. *Fuel*, Vol. 85, No. 16, pp. 2345-2351.
- Yang X G, Ni W, Zhang X F and Wang Y L (2008). Effect of alkali-activation on aluminosilicate-based cementitious materials. *Journal of University of Science and Technology Beijing*, Vol. 15, No 6, pp. 796-801.

Yool A I G, Lees T P and Fried A (1998). Improvements to the methylene blue dye test for harmful clay in aggregates for concrete and mortar. *Cement and concrete research*, Vol. 28, No. 10, pp. 1417-1428.

Yu J, Külaots I, Sabanegh N, Gao Y, Hurt R H, Suuberg E S and Mehta A (2000). Adsorptive and optical properties of fly ash from coal and petroleum coke co-firing. *Energy & Fuels*, Vol. 14, No. 3, pp. 591-596.

Zhang X, Yang Y, Wong C L and Ong C K (1998). Study of hydration of OPC/PFA blend with various activators using microwave technique. *Journal of Materials Science*, Vol. 33, No. 16, pp. 4191-4199.

Zhang Y and Nelson Jr. (2007). Development of a new method to replace the foam index test. World of Coal Ash (WOCA), 7-10 May 2007, Northern Kentucky, KY, USA.

Zhu B R and Yang Q B (2006). Pozzolanic reactivity and reaction kinetics of fly ash. Proceedings of the 6th International Symposium on Cement & Concrete and CANMET/ACI International Symposium on Concrete Technology for Sustainable Development. Vol. 1-2, pp. 1446-1451.

APPENDIX – A

Table A – 1. Codes for monthly fly ash samples

CODE	DETAILS	CODE	DETAILS
A S Jul	Monthly samples from Source A conforming to BS EN 450 fineness Category S	C S Jul	Monthly samples from Source C conforming to BS EN 450 fineness Category S
A S Aug		C S Aug	
A S Sep		C S Sep	
A S Oct		C S Oct	
A S Nov		C Nov S	
A S Dec		C S Dec	
A S Jan		C Jan S	
A S Feb		C S Feb	
A S Mar		C S Mar	
A S Apr		C S Apr	
A S May		C S May	
A S Jun		C S Jun	

Table A – 2. Codes for of fly ash samples from various sources

CODE	DETAILS
A N Jul	Source A , sampling period July 2009 , BS EN 450 fineness Category N
B N Jul	Source B , sampling period July 2009 , BS EN 450 fineness Category N
B S Jul	Source B , sampling period July 2009 , BS EN 450 fineness Category S
C LLHF	Source C , low LOI, high fineness fly ash, sampling period June 2010
C ROS	Source C , Run-of-Station fly ash, sampling period July 2011
D STI	Source D , STI separated fly ash, Sampling period January 2010
D NSTI	Source D , Non STI , Sampling period September 2010
E UF	Source E , Ultra-fine fly ash, Sampling period May 2009
E EN1	Source E , confirming BS EN 450 fineness Category N , May 2009
E EN2	Source E , for use in EN 13055 products, May 2009
F CC	Source F , Petroleum coke co-combustion , Run-of-Station , February 2010
F Oxy1	Source F , Oxy-fuel trial combustion, August 2010
F Oxy2	
F Oxy3	
G	Source G , July 2010
H	Source H , January 2010
BD W1	Source Bangladesh (Bituminous) , sampling period January 2011 , BS EN fineness Category N
BD W2	
BD S	Source Bangladesh (Bituminous) , sampling period July 2010 , very coarse

Table A-3. Surface area of finer and coarser fraction (above/below 45 μm) fly ash

SAMPLE	SSA* (fine) m ² /g	SSA* (coarse) m ² /g	Total ¹ SSA* m ² /g	Combined ² SSA* m ² /g
A S Jul	2.10	0.46	2.57	2.45
C S Jul	1.49	0.45	1.94	2.52
A N Jul	1.77	0.84	2.61	2.64
B N Jul	1.76	0.62	2.38	1.54
C LLHF	1.78	0.52	2.30	2.10
C ROS	5.46	1.27	6.73	5.79
D NSTI	1.98	2.12	4.11	4.84
E UF	3.55	0.12	3.67	2.46
E EN2	3.31	2.96	6.27	5.20
G	3.29	2.34	5.62	5.50

*SSA, *Specific Surface Area*,

¹ *Sum of fine and coarse fraction*,

² *raw samples tested without separation*

Table A – 4. Chemical composition of monthly fly ashes received from Source A

	A-S Jul	A-S Aug	A-S Sep	A-S Oct	A-S Nov	A-S Dec	A-S Jan	A-S Feb	A-S Mar	A-S Apr	A-S May	A-S Jun
CaO	3.2	3.3	3.3	4.0	4.3	4.3	3.7	3.5	4.1	4.0	4.6	4.5
SiO ₂	48.6	49.9	48.7	44.5	44.2	47.6	50.8	50.7	48.2	47.1	43.9	44.8
Al ₂ O ₃	19.9	20.8	19.7	19.3	20.4	21.9	21.1	21.3	23.1	23.0	22.8	23.8
Fe ₂ O ₃	10.2	8.7	9.3	9.6	9.2	9.0	8.7	8.2	8.5	8.7	9.6	8.8
MgO	1.7	1.6	1.8	2.0	1.9	1.9	1.9	1.7	1.8	1.7	1.7	1.9
MnO	0.1	0.1	0.1	0.1	0.1	0.1	0.1	0.1	0.1	0.1	0.1	0.1
TiO ₂	1.1	1.1	1.0	1.1	1.1	1.1	1.0	1.0	1.1	1.1	1.2	1.2
K ₂ O	2.8	2.6	3.3	2.9	2.8	3.0	2.8	3.0	2.8	2.7	2.9	3.2
Na ₂ O	1.7	1.3	1.6	1.7	1.2	1.6	1.6	1.4	1.3	1.2	1.1	1.0
P ₂ O ₅	0.5	0.5	0.5	0.6	0.7	0.5	0.4	0.4	0.5	0.4	0.6	0.6
Cl	0.0	0.0	0.0	0.0	0.0	0.0	0.0	0.0	0.0	0.0	0.0	0.0
SO ₃	1.9	1.0	1.5	1.5	1.0	1.0	1.0	0.9	0.8	1.0	0.9	0.8
Mullite	12.2	13.2	11.3	10.8	12.0	11.0	9.7	11.4	13.0	13.7	14.3	15.4
Quartz	13.0	11.2	12.6	10.1	8.1	10.4	14.1	15.5	10.5	10.0	8.2	8.4
Hematite	3.2	2.7	3.4	3.3	3.1	3.4	2.8	3.1	2.9	3.1	4.5	4.9
Magnetite	0.3	0.3	0.4	0.4	0.3	0.2	0.2	0.1	0.2	0.2	0.1	0.2
Others	71.3	72.6	72.3	75.5	76.5	75.0	73.2	69.9	73.3	73.0	72.9	71.1

Table A – 5. Chemical composition of monthly fly ashes received from Source C

	C-S Jul	C-S Aug	C-S Sep	C-S Oct	C-S Nov	C-S Dec	C-S Jan	C-S Feb	C-S Mar	C-S Apr	C-S May	C-S Jun
CaO	2.8	2.9	2.7	3.4	3.7	3.3	2.7	2.8	3.0	2.8	2.1	2.4
SiO ₂	49.6	47.4	46.2	47.2	44.3	48.8	48.8	48.9	48.7	47.8	47.3	46.4
Al ₂ O ₃	22.4	21.9	21.2	21.4	21.3	22.5	23.0	24.0	23.5	22.8	21.8	21.7
Fe ₂ O ₃	7.9	7.9	10.3	8.3	8.7	7.4	8.0	7.2	7.4	7.8	9.5	10.3
MgO	1.7	1.8	1.7	1.6	1.6	1.8	1.5	1.6	1.6	1.7	1.4	1.5
MnO	0.1	0.1	0.1	0.1	0.1	0.1	0.1	0.1	0.1	0.1	0.1	0.1
TiO ₂	1.1	1.2	1.1	1.1	1.2	1.1	1.1	1.1	1.1	1.1	1.1	1.0
K ₂ O	2.4	2.6	2.8	2.8	2.7	2.9	2.8	2.6	2.5	3.1	3.3	3.2
Na ₂ O	1.2	1.8	1.1	1.7	1.2	1.4	1.2	1.4	1.0	1.3	1.7	1.5
P ₂ O ₅	0.6	0.6	0.4	0.7	0.9	0.5	0.4	0.4	0.5	0.5	0.3	0.3
Cl	0.0	0.0	0.0	0.0	0.0	0.0	0.0	0.0	0.0	0.0	0.0	0.0
SO ₃	1.1	1.2	1.0	1.2	1.1	0.8	0.7	0.9	0.6	0.7	0.8	0.9
Mullite	15.6	15.3	12.5	11.6	15.0	11.5	13.2	13.8	16.7	9.3	6.8	7.1
Quartz	8.9	10.0	8.7	9.1	10.5	8.4	9.4	8.8	10.6	7.4	7.3	7.2
Hematite	3.4	3.3	2.9	2.7	2.7	2.0	2.4	2.0	2.7	2.2	2.8	4.7
Magnetite	0.4	0.2	0.3	0.2	0.2	0.1	0.3	0.2	0.2	0.1	0.1	0.2
Others	71.9	71.3	75.7	76.4	71.5	77.9	74.7	75.2	69.8	81.1	83.0	80.7

Table A – 6. Chemical composition of other fly ashes received from various sources

	A-N Jul	B-N Jul	B-S Jul	C LLHF	C ROS	D STI	D NSTI	E UF	E EN1	E EN2
CaO	4.3	2.6	2.6	2.0	2.9	2.6	3.2	4.9	5.2	6.6
SiO ₂	48.1	49.7	47.5	46.5	44.7	53.5	39.0	56.2	52.2	53.8
Al ₂ O ₃	22.9	20.2	20.2	21.4	21.7	24.0	20.2	19.2	18.8	21.4
Fe ₂ O ₃	7.1	8.4	9.1	10.4	8.4	4.4	5.5	5.0	5.1	5.2
MgO	1.7	1.6	1.5	1.3	1.4	0.9	1.2	1.5	1.5	1.4
MnO	0.1	0.1	0.1	0.1	0.1	0.1	0.1	0.1	0.1	0.0
TiO ₂	1.2	1.1	1.1	1.0	1.1	0.9	1.0	1.0	1.0	1.2
K ₂ O	2.3	3.4	3.0	3.3	2.4	2.3	2.4	1.9	2.1	1.4
Na ₂ O	1.5	1.5	0.9	1.7	1.0	0.8	0.4	0.9	1.1	1.2
P ₂ O ₅	0.6	0.4	0.5	0.2	0.5	0.5	0.6	1.8	0.9	0.6
Cl	-	-	-	-	-	-	-	-	-	-
SO ₃	1.3	1.4	1.2	0.9	1.4	0.3	1.0	0.5	0.6	0.6
Mullite	16.0	10.1	14.0	5.7	13.5	12.5	8.6	13.0	18.6	11.6
Quartz	9.7	7.1	12.6	6.7	7.8	4.3	2.2	16.2	19.4	11.1
Hematite	2.7	2.8	3.6	3.4	3.5	0.0	1.8	1.5	0.9	1.4
Magnetite	0.4	0.2	0.2	0.0	0.1	0.1	0.1	0.1	0.1	0.2
Others	71.3	79.8	69.7	84.2	75.0	83.1	87.2	69.2	61.0	75.7

(Continued on next page)

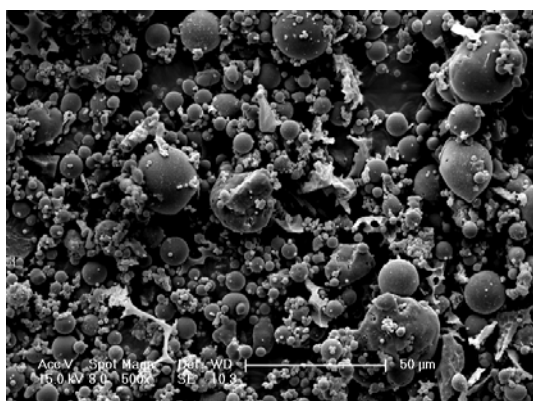
Table A – 7. Chemical composition of other fly ashes received from various sources

	F CC	F Oxy 1	F Oxy 2	F Oxy 3	G	H	BD W1	BD W2	BD S
CaO	4.0	4.2	4.4	4.1	6.8	4.2	0.7	0.7	1.1
SiO ₂	45.8	49.3	46.6	48.5	46.6	46.0	50.5	51.5	59.2
Al ₂ O ₃	25.2	19.7	17.7	18.3	18.3	25.5	32.0	31.6	25.6
Fe ₂ O ₃	7.4	13.4	12.4	11.8	6.9	5.8	2.8	2.8	2.9
MgO	1.5	1.1	0.8	0.9	2.3	1.3	0.6	0.3	0.3
MnO	0.1	0.1	0.1	0.1	0.1	0.1	0.0	0.0	0.0
TiO ₂	1.2	1.1	1.2	1.3	0.9	1.5	2.9	3.1	2.2
K ₂ O	2.2	2.3	2.3	2.3	2.4	1.3	0.8	0.9	0.9
Na ₂ O	0.7	0.8	1.0	0.8	1.9	0.5	0.3	0.2	0.2
P ₂ O ₅	0.4	0.2	0.1	0.1	0.7	0.7	0.5	0.6	0.6
Cl	-	0.3	0.2	0.2	-	-	-	-	-
SO ₃	0.9	2.8	2.5	1.9	1.5	1.0	1.0	0.2	0.3
Mullite	17.1	17.9	15.3	15.1	23.4	5.1	42.4	43.5	29.0
Quartz	6.3	12.8	14.9	15.1	11.7	5.2	10.7	10.9	36.2
Hematite	2.0	4.5	3.9	3.5	1.8	1.4	1.4	1.5	0.7
Magnetite	0.2	0.1	0.4	0.3	0.0	-	-	-	0.1
Others	74.3	64.6	65.7	66.1	63.0	88.2	45.4	44.1	34.0

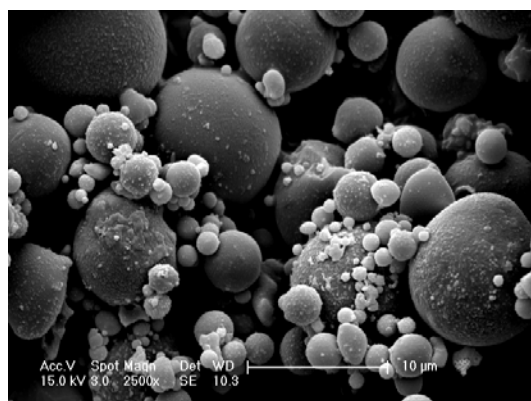
(Continued from previous page)

Table A – 8. Chemical composition of air-classified fly ashes from Sources C and L

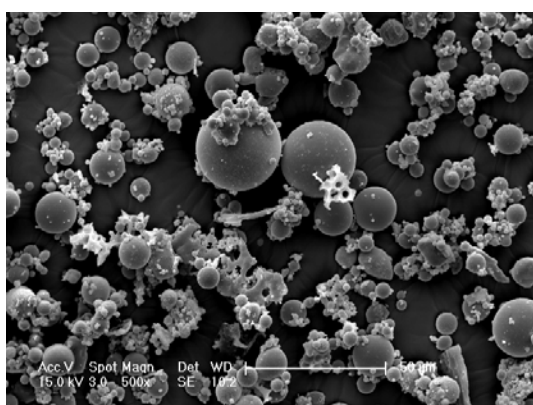
	C5	C10	C20	C30	C40	C50	CFD	L5	L10	L20	L30	L40	L50	LFD
CaO	2.3	2.1	2.1	2.2	2.3	2.3	2.6	6.1	7.0	7.5	6.6	6.9	6.0	6.5
SiO ₂	49.2	50.1	49.5	48.3	49.2	47.8	46.2	46.7	45.5	46.7	47.9	48.3	49.6	49.9
Al ₂ O ₃	22.5	22.5	22.7	21.7	20.9	20.8	20.0	23.3	23.5	23.2	22.9	22.6	22.9	22.1
Fe ₂ O ₃	6.5	6.6	6.9	7.4	7.2	7.7	8.7	6.8	7.8	7.5	7.4	7.3	7.2	7.1
MgO	2.1	1.6	1.6	1.5	1.4	1.4	1.4	1.8	1.8	1.8	1.7	1.7	1.7	1.6
MnO	0.1	0.1	0.1	0.1	0.1	0.1	0.1	0.1	0.1	0.1	0.1	0.1	0.1	0.1
TiO ₂	1.1	1.1	1.1	1.1	1.1	1.1	1.0	1.1	1.2	1.2	1.2	1.1	1.1	1.1
K ₂ O	3.0	3.1	3.1	3.1	2.8	2.8	2.6	2.0	1.9	1.8	1.7	1.7	1.7	1.6
Na ₂ O	1.6	1.2	1.2	1.1	1.0	1.0	0.9	1.1	1.3	1.2	1.1	1.3	1.3	1.2
P ₂ O ₅	0.6	0.6	0.6	0.5	0.5	0.5	0.4	0.7	0.5	0.5	0.5	0.4	0.4	0.4
Cl	-	-	-	-	-	-	-	-	-	-	-	-	-	-
SO ₃	1.3	0.8	0.9	1.1	0.9	1.0	0.9	0.8	0.9	0.9	0.8	0.9	0.9	1.0
Mullite	10.1	11.6	10.6	10.5	9.7	10.4	9.3	13.9	14.0	14.8	16.3	13.8	16.6	16.7
Quartz	5.7	6.8	5.7	7.6	9.2	7.5	9.4	7.5	7.7	9.3	12.9	14.8	16.5	21.4
Hematite	1.1	1.5	1.8	2.4	2.0	2.3	2.8	1.7	2.2	4.1	2.6	2.8	2.3	2.5
Magnetite	0.1	0.0	0.0	0.1	0.0	0.0	0.2	0.0	0.0	0.0	0.0	0.0	0.0	0.1
Others	82.9	80.1	81.9	79.4	79.1	79.8	78.3	76.9	76.1	71.7	68.2	68.7	64.6	59.3



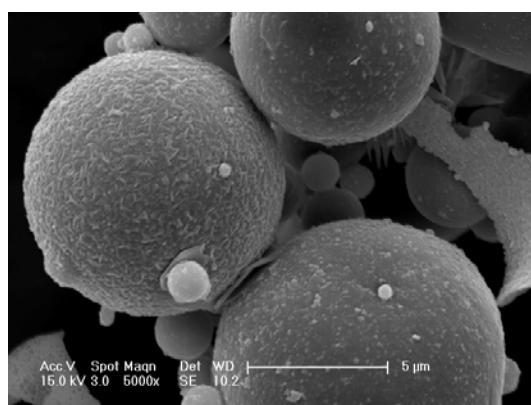
(a) A-S Jul (500x magnification)



(a) A-S Jul (2500x magnification)

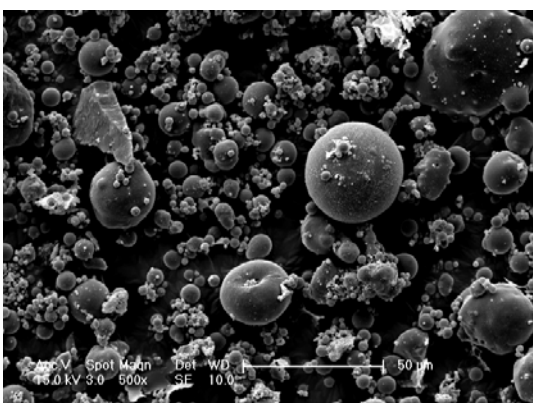


(b) A-S Jan (500x magnification)

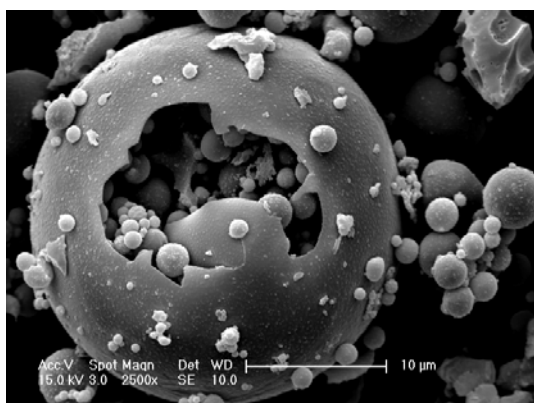


(b) A-S Jan (5000x magnification)

Figure A – 1. SEM images of monthly fly ashes from Source A (Category S)
(a) July 2009; and (b) January 2010



A-N Jul (500x magnification)



A-N Jul (2500x magnification)

Figure A – 2. SEM images of fly ashes from Source A
(Category N, sampling period July 2009)

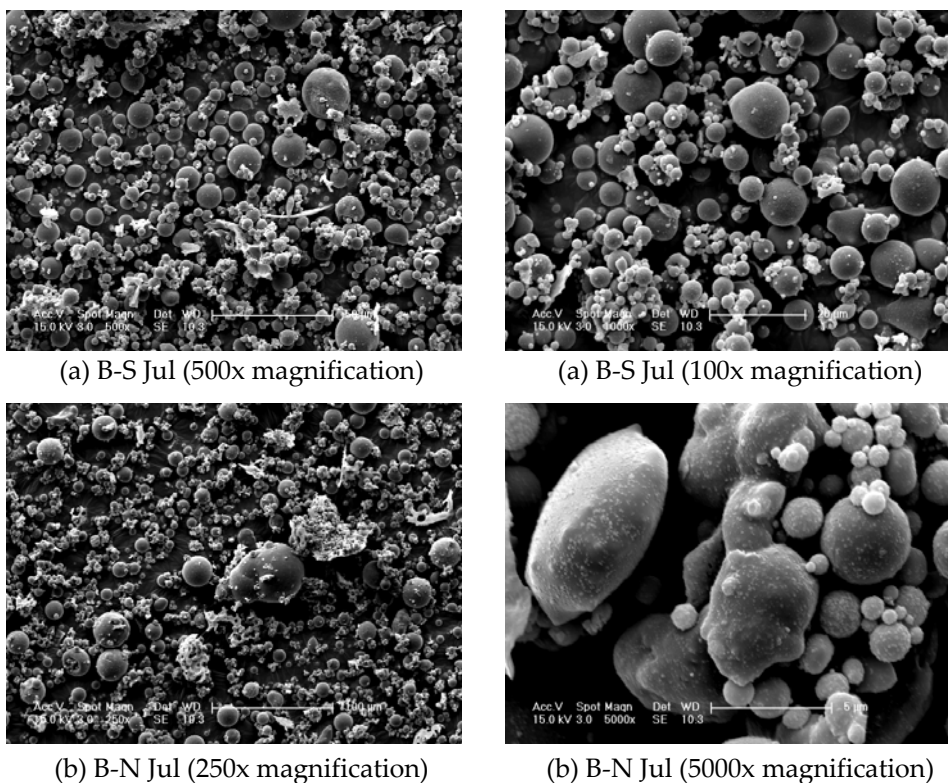


Figure A – 3. SEM images of fly ashes from Source B (sampling period July 2009) a) Category S; and b) Category N

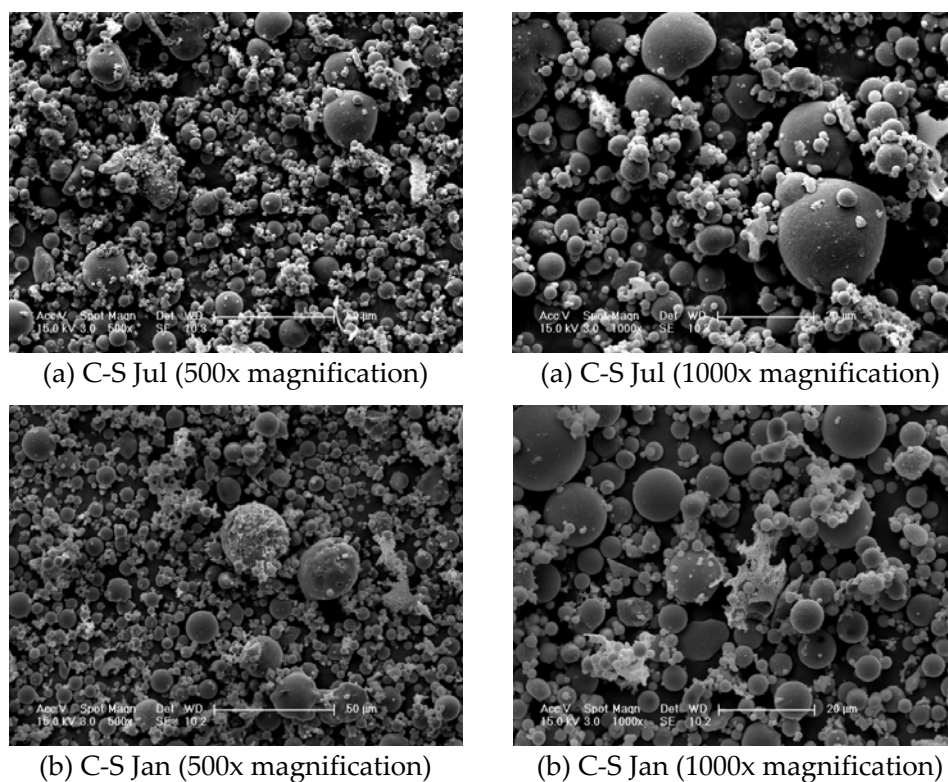


Figure A – 4. SEM images of monthly fly ashes from Source C (Category S) (a) July 2009; and (b) January 2010

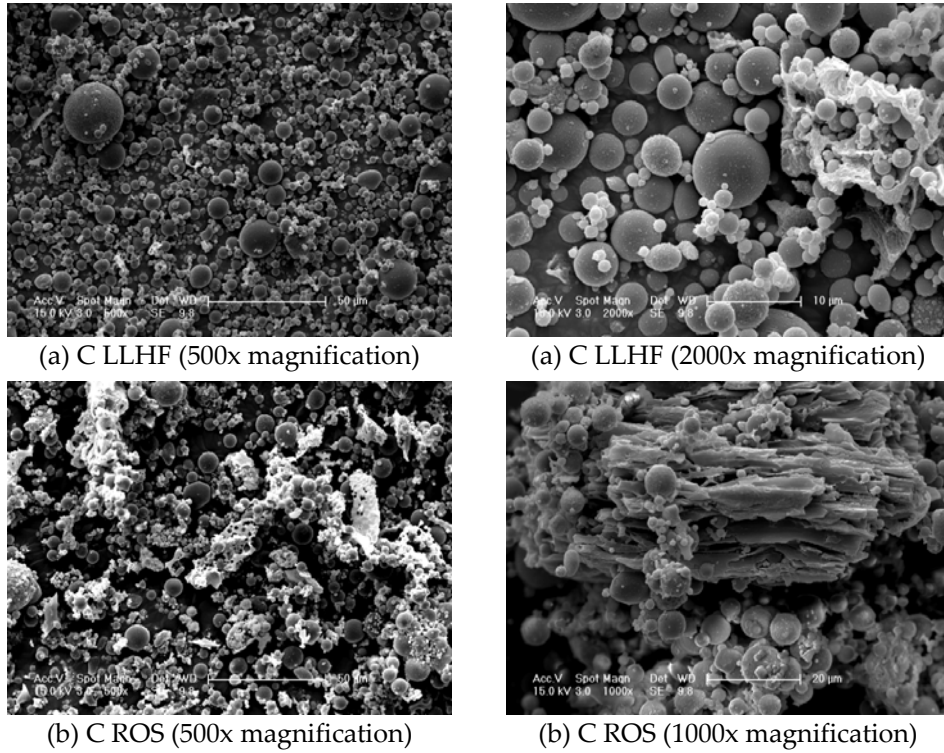


Figure A – 5. SEM images of fly ashes from Source C (Category N)
 (a) low LOI and high fineness (sampling period, July 2009); and
 (b) run-of-station (sampling period, June 2010)

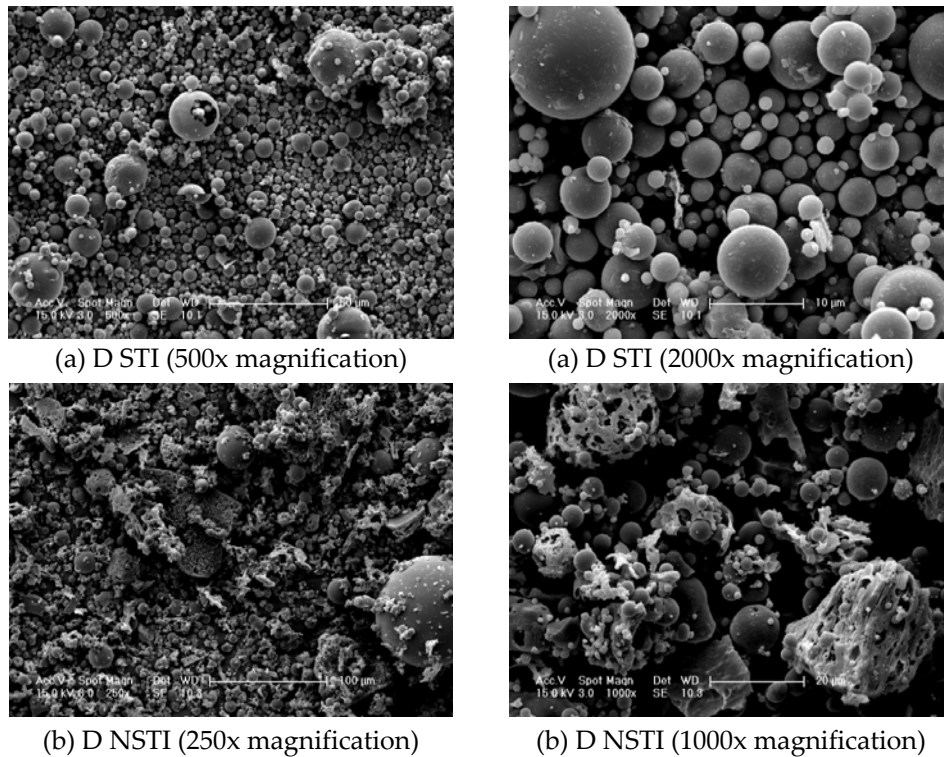
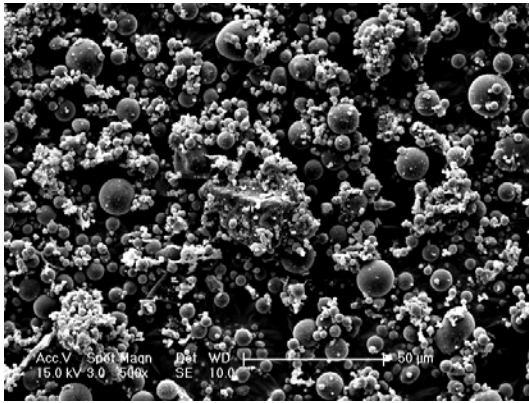
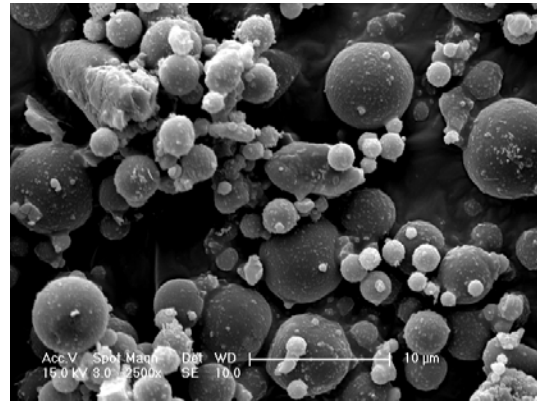


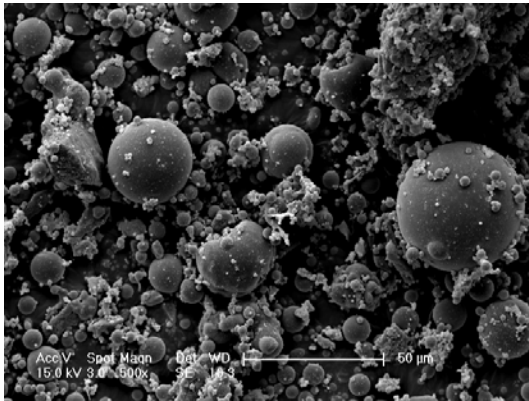
Figure A – 6. SEM images of fly ashes from Source D (Category N)
 (a) STI carbon removed (sampling period, January 2010); and
 (b) without STI application (sampling period, September 2010)



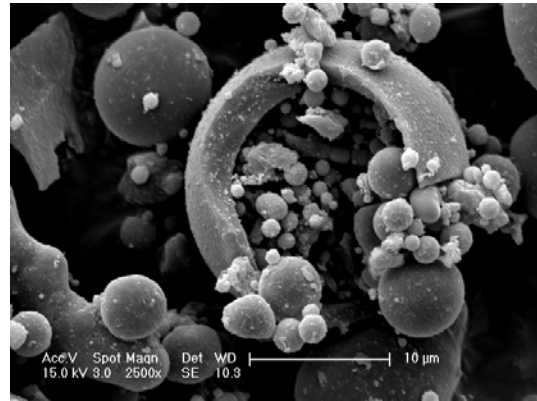
(a) E UF (500x magnification)



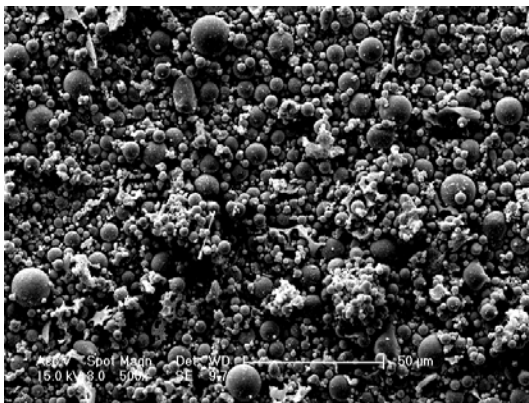
(a) E UF (2500x magnification)



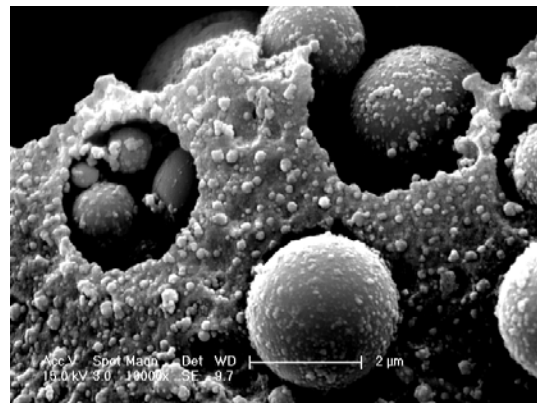
(b) E EN1 (500x magnification)



(b) E EN1 (2500x magnification)

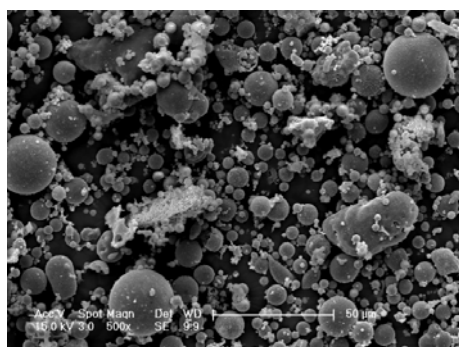


(b) E EN2 (500x magnification)

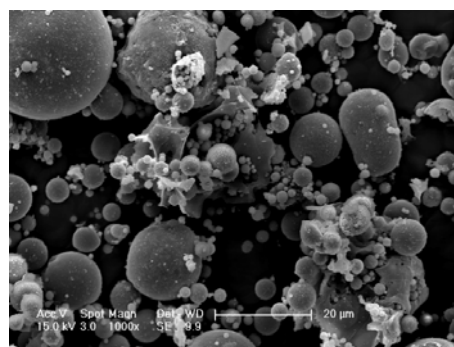


(b) E EN2 (1000x magnification)

Figure A – 7. SEM images of fly ashes from Source E (sampling period May 2009) (a) ultra-fine (Category S), (b) EN 450 (Category N); and (c) EN 13055 (Category N)

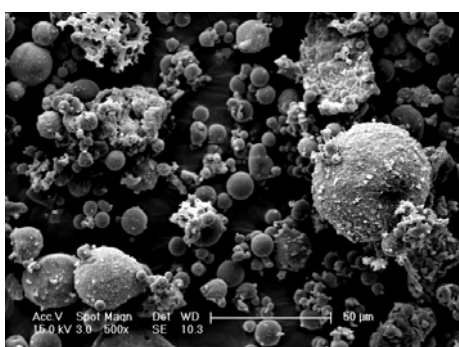


(a) F CC (500x magnification)

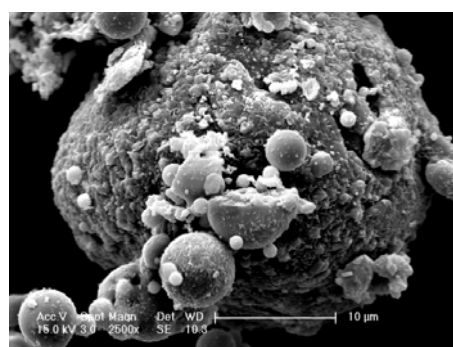


(a) F CC (1000x magnification)

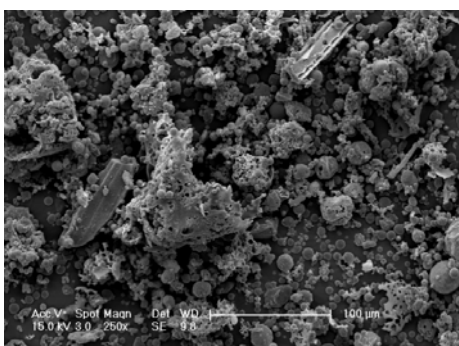
Figure A – 8. SEM images of petroleum coke co-combustion run-of-station fly ash from Source F (sampling period February 2010)



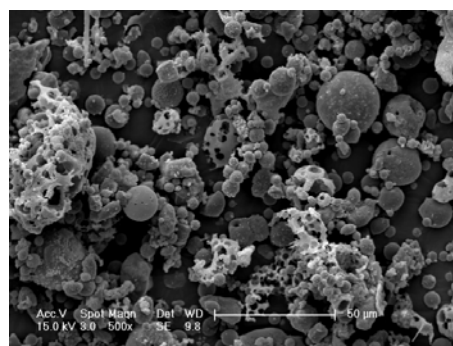
(a) F Oxy1 (500x magnification)



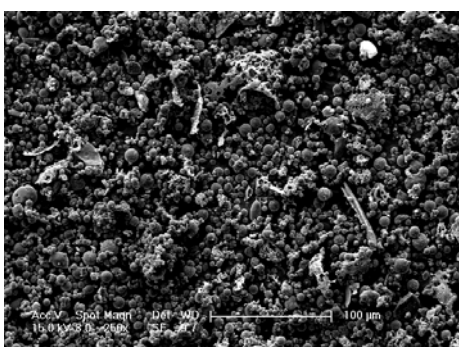
(a) F Oxy1 (2500x magnification)



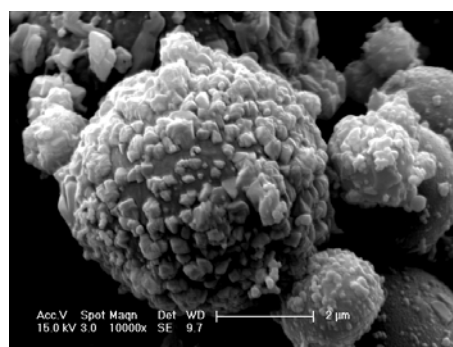
(b) F Oxy2 (250x magnification)



(b) F Oxy2 (500x magnification)

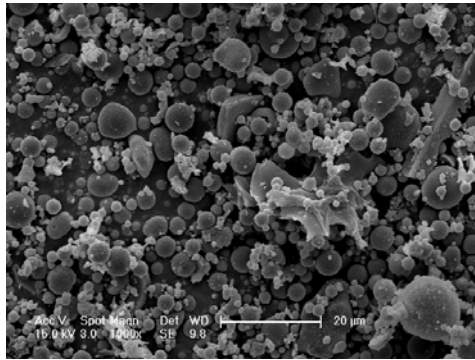


(b) F Oxy3 (250x magnification)

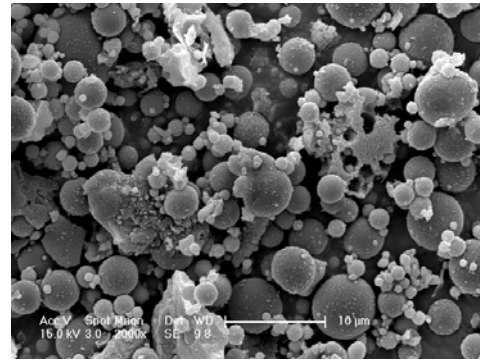


(b) F Oxy3 (10000x magnification)

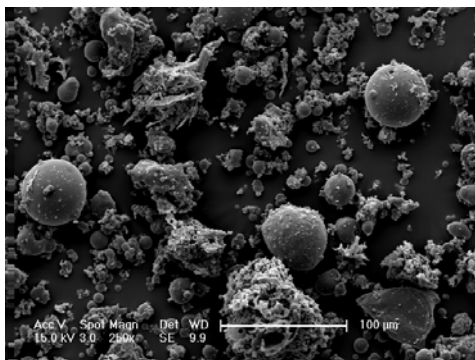
Figure A – 9. SEM images of oxy-fuel fly ashes from trial burning (Source F, sampling period August 2010) (a) Category N, (b) Category S; and (c) Category S



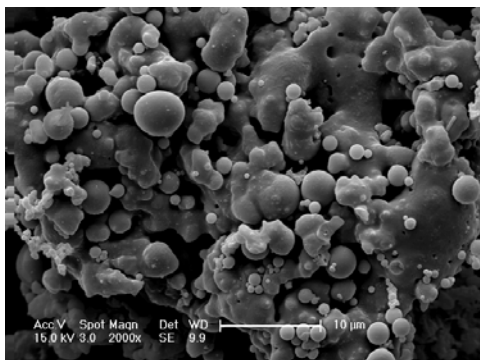
(a) G (1000x magnification)



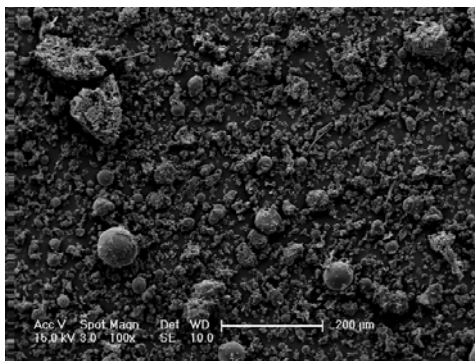
(a) G (2000x magnification)

Figure A – 10. SEM images of fly ash from Source G (Category N)

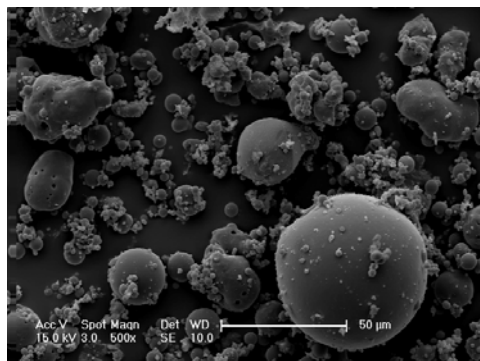
(a) BD W1 (250x magnification)



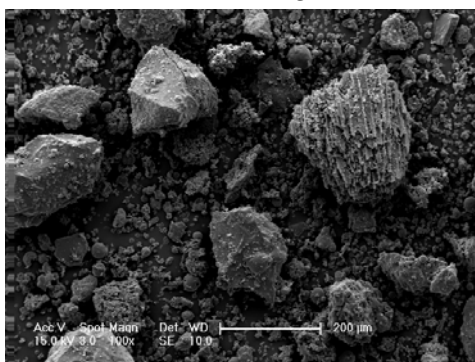
(a) BD W1 (2000x magnification)



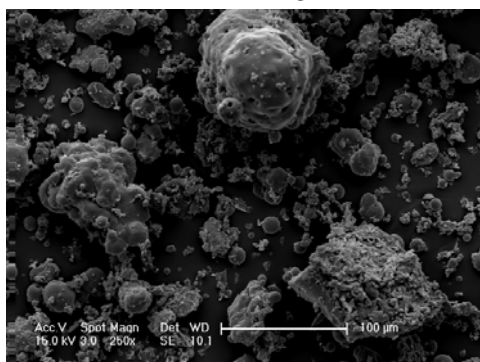
(b) BD W2 (100x magnification)



(b) BD W2 (500x magnification)

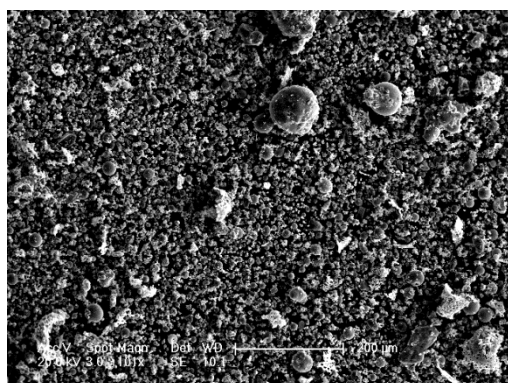


(b) BD S (100x magnification)

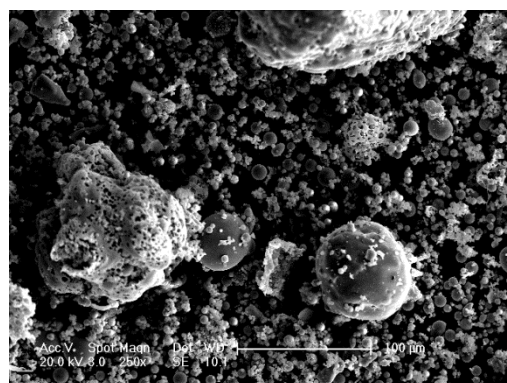


(b) BD S (250x magnification)

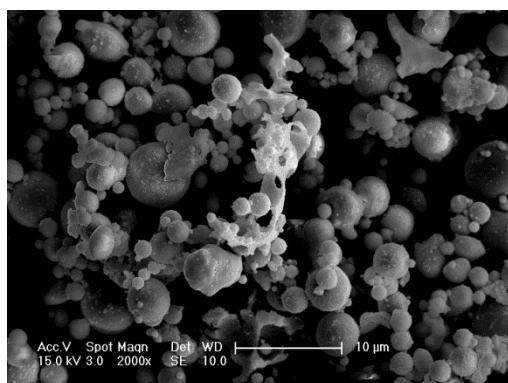
Figure A – 11. SEM images of fly ash obtained from Bangladesh (a), (b) January 2011, and (c) July 2010



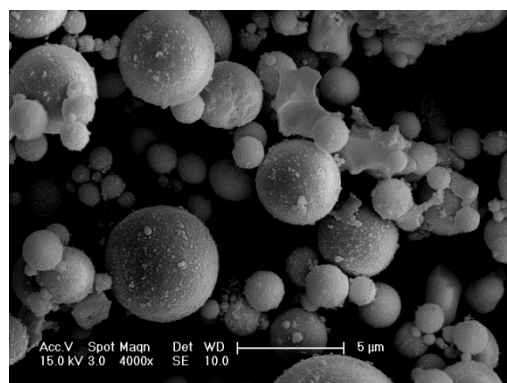
(a) CFD (101x magnification)



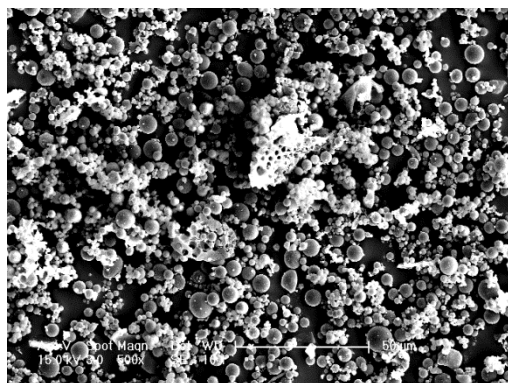
(b) CFD (250x magnification)



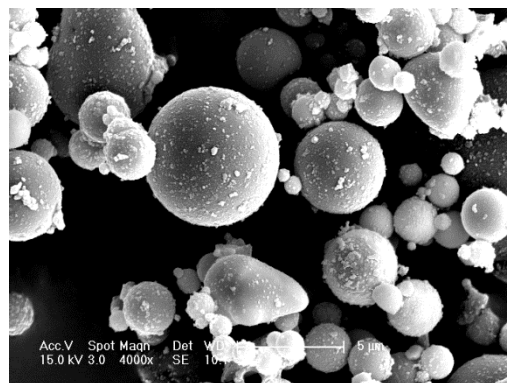
(c) C5 (2000x magnification)



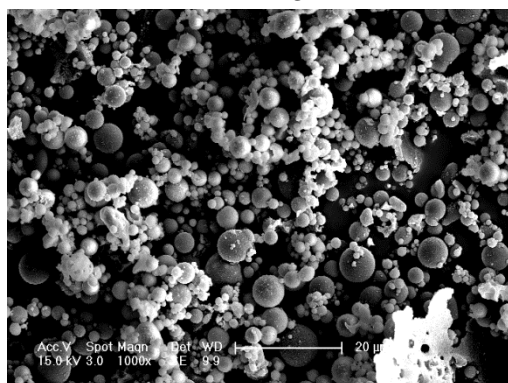
(d) C5 (4000x magnification)



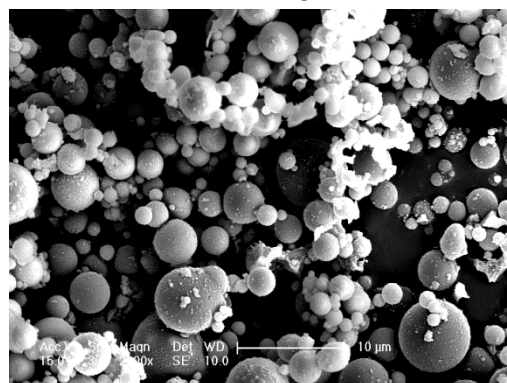
(e) C10 (500x magnification)



(f) C10 (4000x magnification)

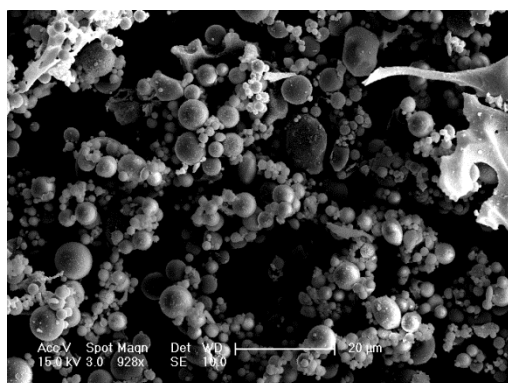


(g) C20 (1000x magnification)

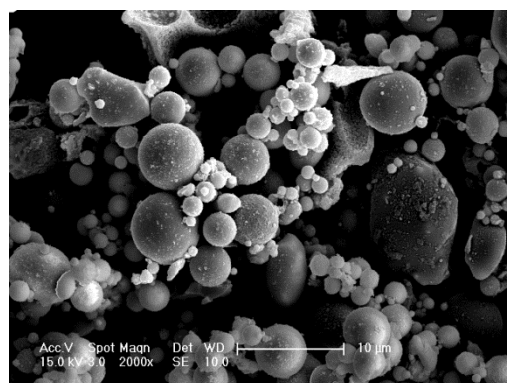


(h) C20 (2000x magnification)

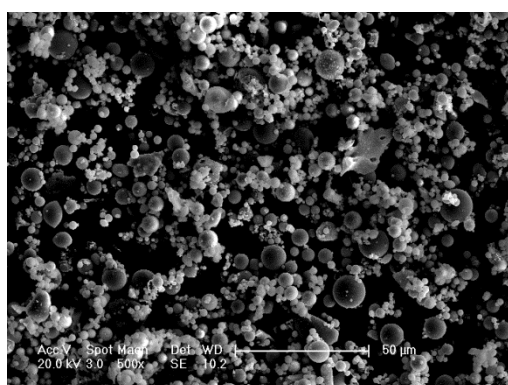
Continued to next page



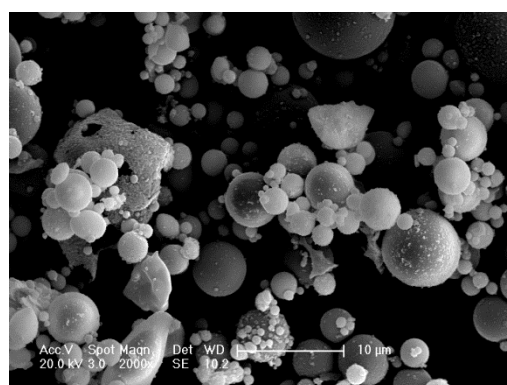
(c) C30 (928x magnification)



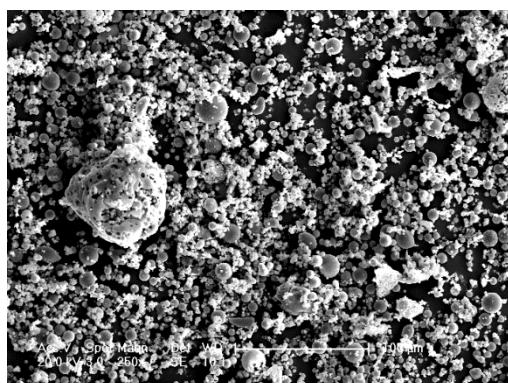
(d) C30 (2000x magnification)



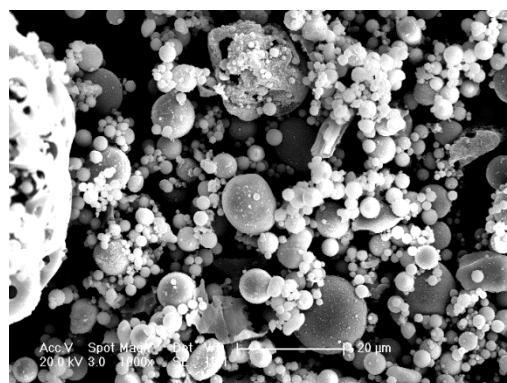
(e) C40 (500x magnification)



(f) C40 (2000x magnification)

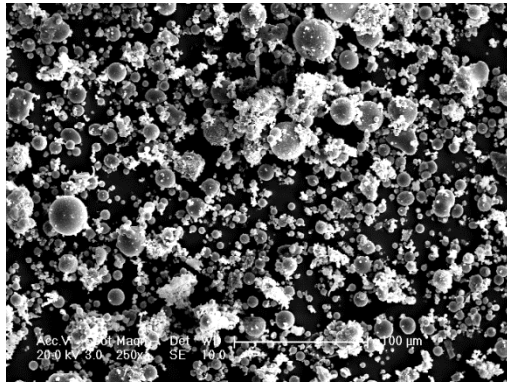


(e) C50 (250x magnification)

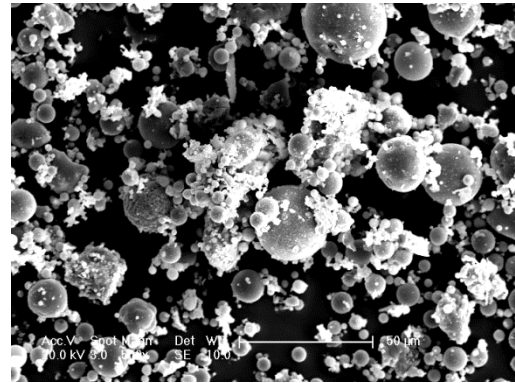


(f) C50 (1000x magnification)

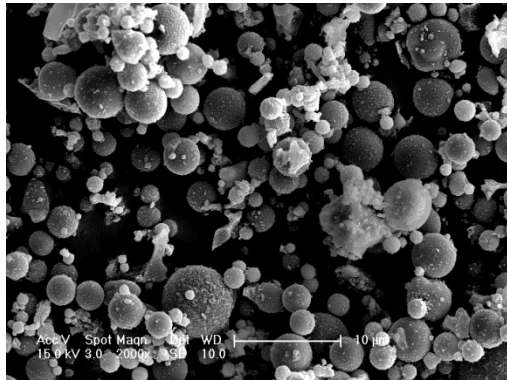
Figure A – 12. SEM images of air-classified fly ashes from Source C



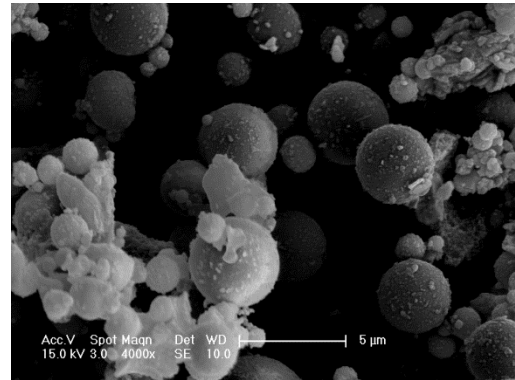
(a) LFD (250x magnification)



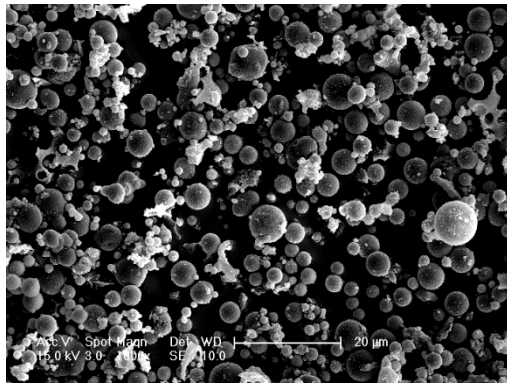
(b) LFD (500x magnification)



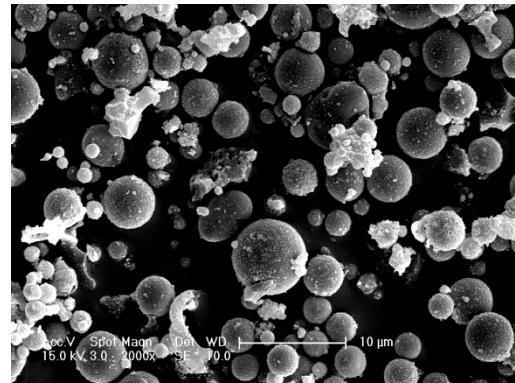
(c) L5 (2000x magnification)



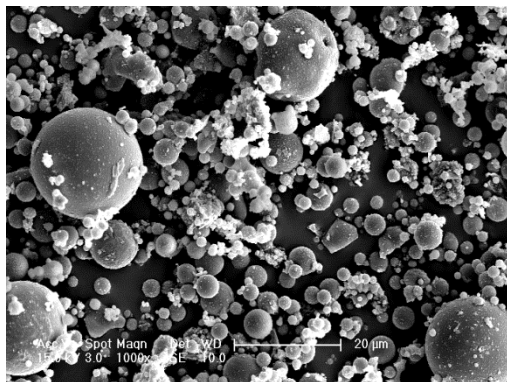
(d) L5 (4000x magnification)



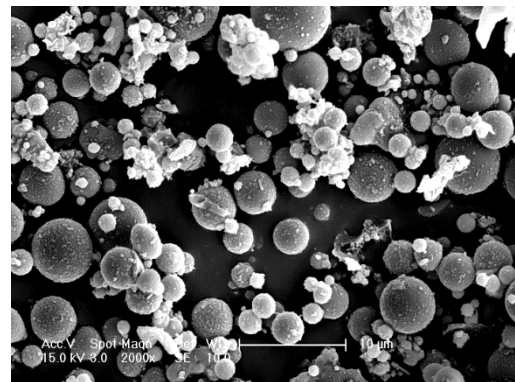
(e) L10 (1000x magnification)



(f) L10 (2000x magnification)

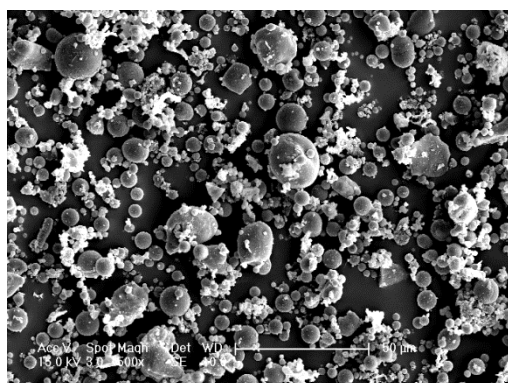


(e) L20 (1000x magnification)

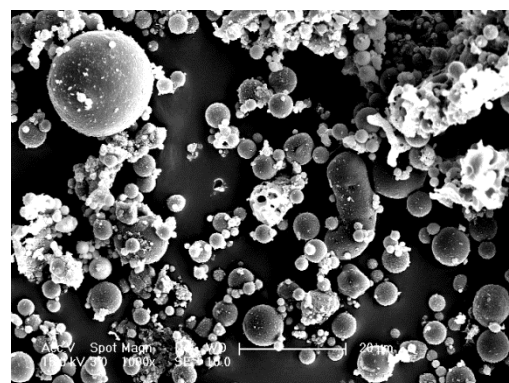


(f) L20 (2000x magnification)

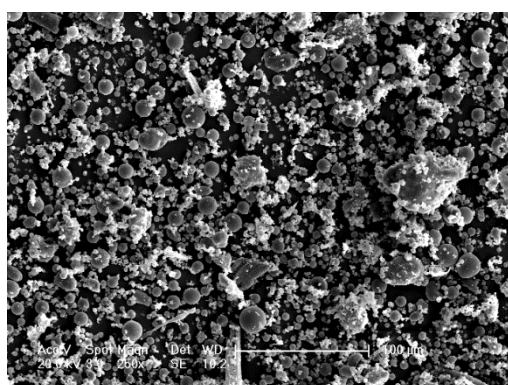
Continued to next page



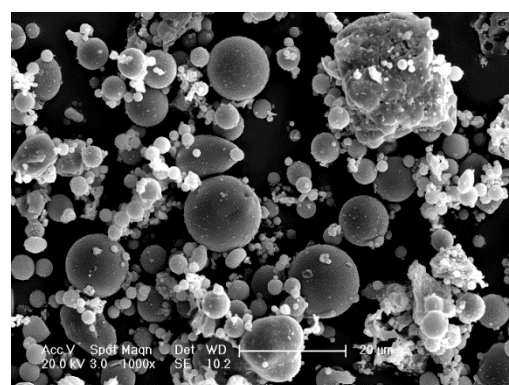
(c) L30 (500x magnification)



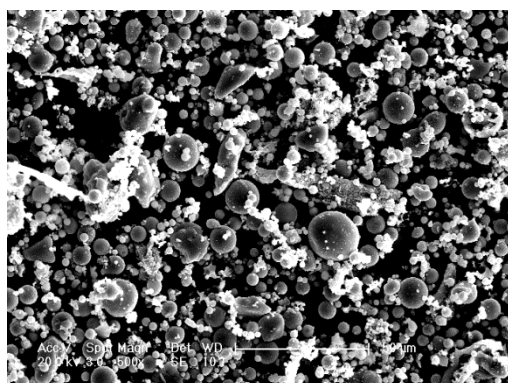
(d) L30 (1000x magnification)



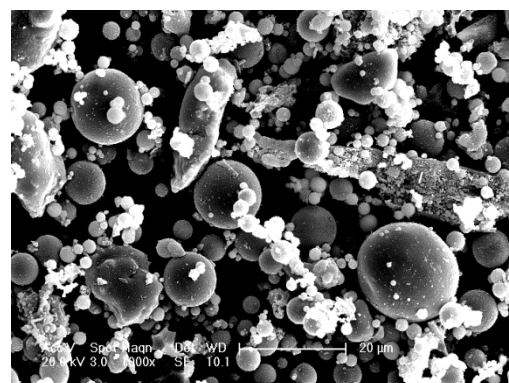
(e) L40 (250x magnification)



(f) L40 (1000x magnification)



(e) L50 (500x magnification)



(f) L50 (1000x magnification)

Figure A – 13. SEM images of air-classified fly ashes from Source L

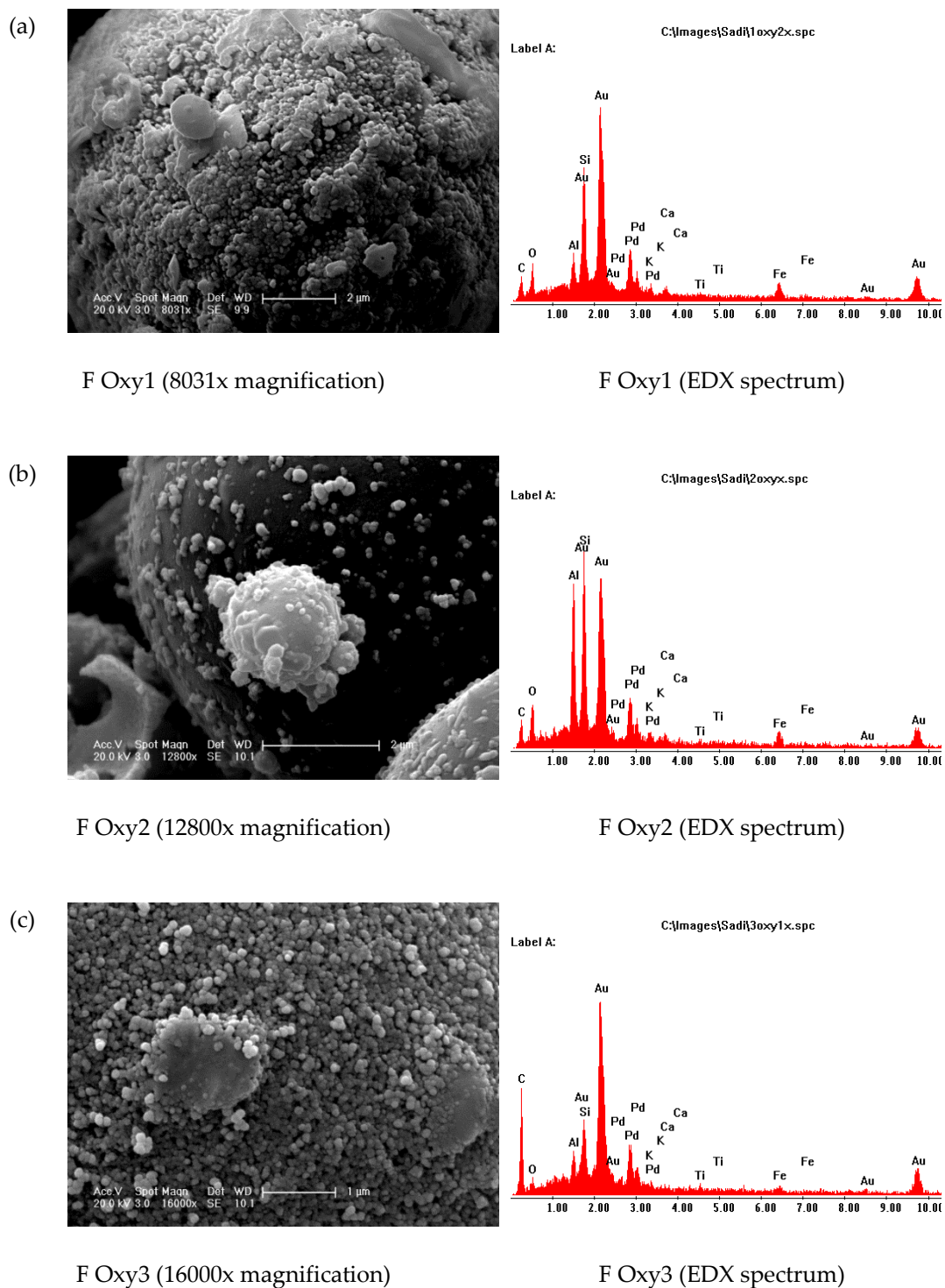


Figure A – 14. EDX analysis of the deposits on oxy-fuel fly ashes

APPENDIX – B

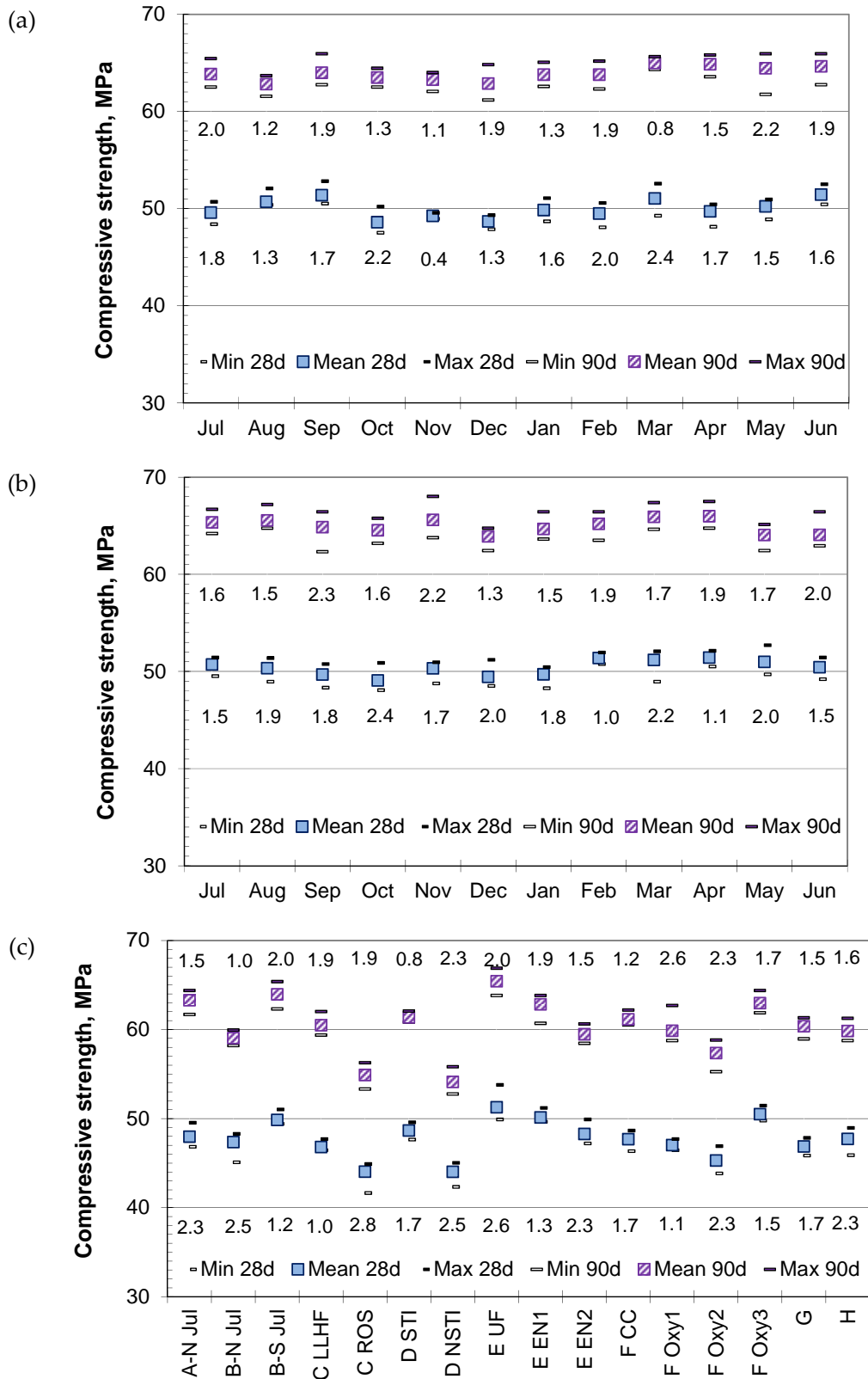


Figure B-1. BS EN 450 mortar compressive strength ranges (PC, HR52) of fly ashes from (a) Source A, monthly; (b) Source C, monthly; and (c) other sources. Numbers indicate coefficient of variation

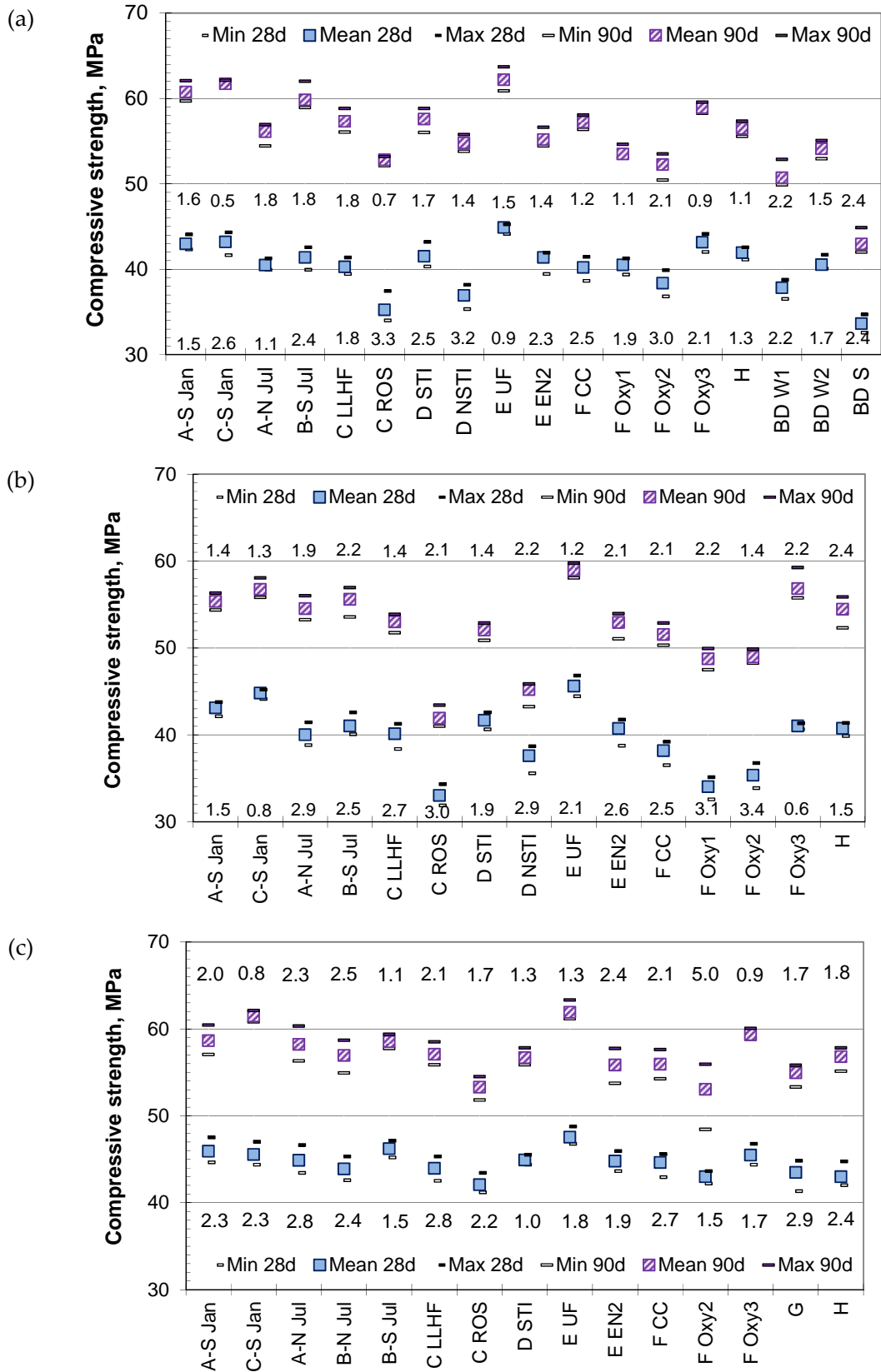


Figure B-2. BS EN 450 mortar compressive strength ranges of fly ashes from various sources using PC (a) HK42; (b) LD32; and (c) LD52. Numbers indicate coefficient of variation

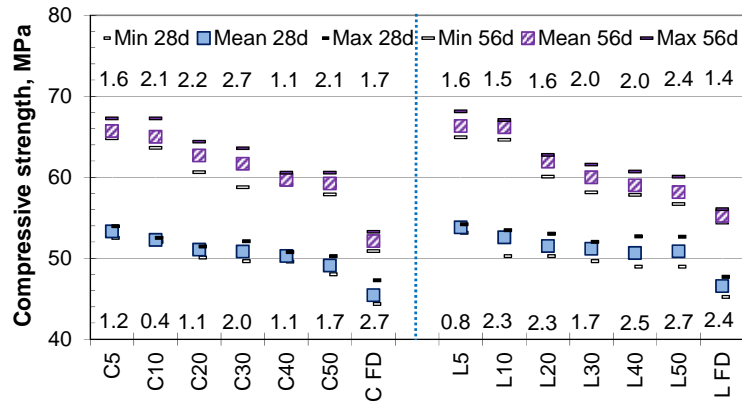


Figure B-3. BS EN 450 mortar strength ranges of air-classified fly ashes using PC HR52

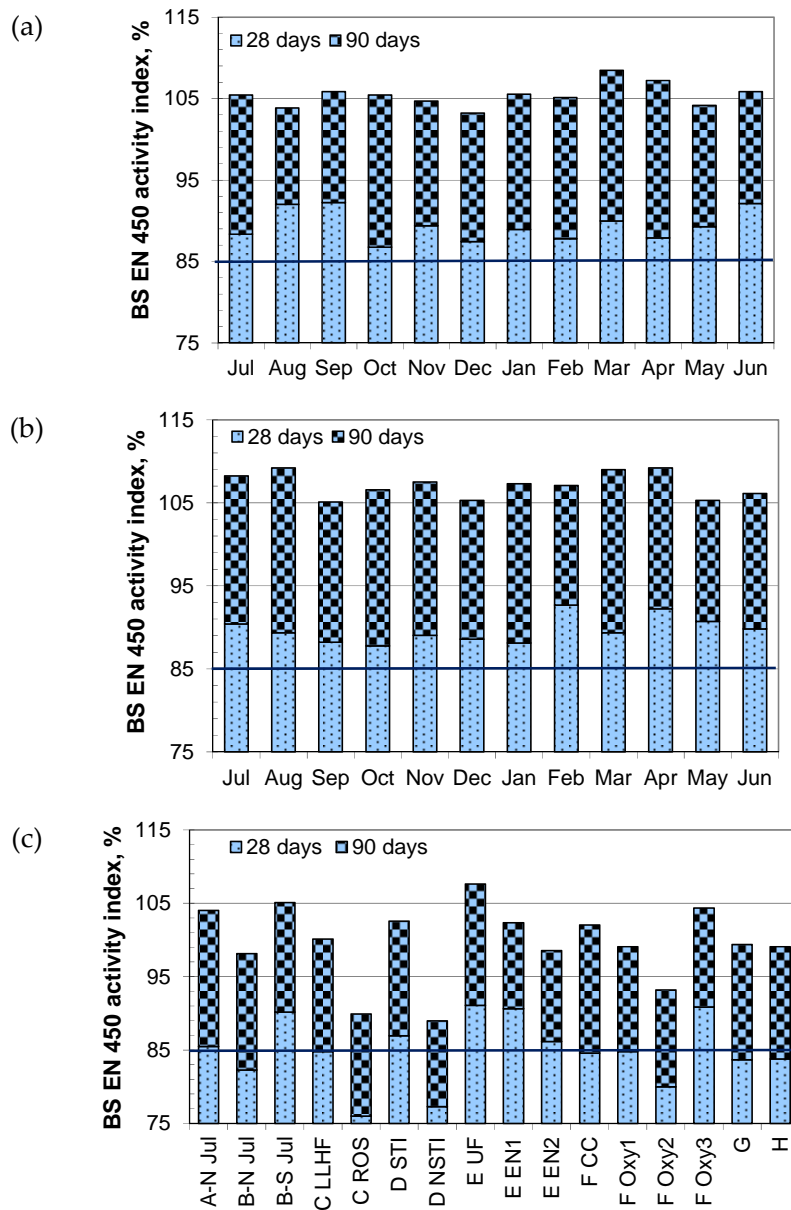


Figure B-4. BS EN 450 (minimum) activity index (PC, HR52) of fly ashes from (a) Source A, monthly; (b) Source C, monthly; and (c) other sources

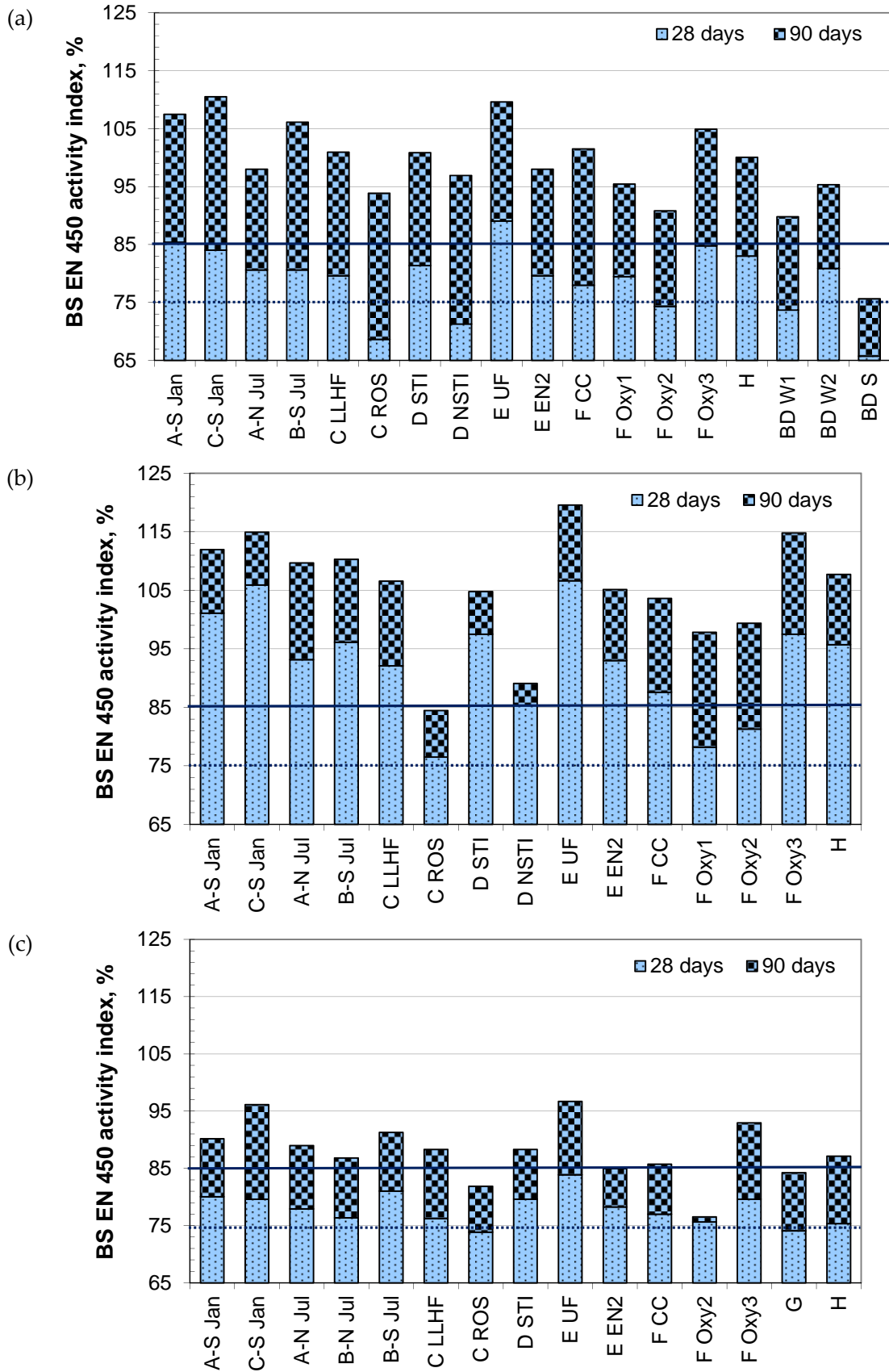


Figure B-5. BS EN 450 (minimum) activity index of fly ashes from various sources using PCs (a) HK42; (b) LD32; and (c) LD52

APPENDIX – C

Table C-1. Foam index results obtained by manual shaking

	SAMPLE	AEA S (0.01 M)	AEA C1	AEA C2	AEA C3
Monthly fly ash from Source A	Jul	90	7	115	10
	Aug	110	-	115	10
	Sep	80	-	105	12
	Oct	80	-	110	12
	Nov	120	-	95	6
	Dec	120	5	100	7
	Jan	150	4	110	8
	Feb	200	-	115	11
	Mar	120	-	110	11
	Apr	140	4	80	8
	May	130	-	-	-
	Jun	180	-	-	-
Monthly fly ash from Source C	Jul	90	5	120	10
	Aug	70	-	120	10
	Sep	110	-	145	13
	Oct	100	-	140	14
	Nov	290	-	135	9
	Dec	190	7	130	10
	Jan	140	8	125	9
	Feb	160	-	105	9
	Mar	170	-	100	10
	Apr	150	6	90	9
	May	170	-	-	-
	Jun	320	-	-	-
Fly ash from various sources	A N Jul	135	-	140	11
	B N Jul	80	-	75	8
	B S Jul	80	-	110	11
	C ROS	440	-	-	-
	C LLHF	180	-	-	-
	D STI	70	3	45	4
	D NSTI	-	-	-	-
	E UF	196	6	65	-
	E EN1	140	12	95	-
	E EN2	330	-	-	-
	F CC	560	18	220	21
	F Oxy1	220	-	-	-
G	840	-	-	-	
H	1260	40	425	31	

Foam index values for commercial AEAs given correspond to their original concentrations.

- Not tested